The Role of Hydrogen Sulfide in Ageing

Stephen E. Wilkie
BSc(Hons) MSc

SUBMITTED IN FULFILMENT OF THE REQUIREMENTS FOR THE DEGREE OF DOCTOR OF PHILOSOPHY

SCHOOL OF LIFE SCIENCES
COLLEGE OF MEDICAL, VETERINARY AND LIFE SCIENCES UNIVERSITY OF GLASGOW
NOVEMBER 2021

Table of Contents

List of Tables

List of Figures

Acknowledgements

I have been very lucky to have had a wonderful experience throughout my PhD. This was in large part due to the incredibly kind and helpful people I have worked with. Colin as my primary supervisor has been an enormous source of support, kindness, and guidance throughout my studies. He has been both a friend and a role model for me the past four years and I know we will find some excuse to work together again in the future. My other supervisors have also been instrumental in guiding me. Nik is a very generous and knowledgeable person, and I am incredible grateful to Asia for all the work she put in when hosting me at the Karolinska Institute in 2019. I have learned a lot from working with all of them and I am looking forward to working alongside Asia again during my post-doc. I would not have been able to get my PhD through the pandemic anywhere near as successfully without the encouragement and good will of Gillian - and it wouldn't have been half as fun either. Every one of my colleagues were a delight to work with and always willing to give advice and support, especially Jackie, Kate, Julie, Neal, Caroline, Diana, Gemma, Jenny, Shazia, Scott, Natalie and Rod. Billy was there too. I have also met some lifelong friends thanks to my experiences during this PhD and I'm looking forward to our futures as fully-fledged doctors together. Rosie, Keira, Kirstin, Felix, Emily, and Sarah I'll be seeing you all soon to celebrate. And finally, I have to thank both my Mum and my partner Gina. Both of you have given me more than I can ever return and I wouldn't even have thought I was capable of achieving this without either of you. You make me believe in myself and for that I am forever grateful.

Author's Declaration

I declare that work recorded in this thesis is entirely my own composition and that research described herein was carried out by me unless otherwise stated or acknowledged. No part of this thesis has been submitted for another degree. I hereby give my consent, for my thesis, if accepted, to be available for photocopy and interlibrary loan.

Stephen Wilkie
November 2021

Abbreviations

Abbreviation	Full Name
28S	28S ribosomal RNA
3-MP	3-Mercaptopyruvate
5S	5S ribosomal RNA
7SL	Signal recognition particle RNA
a-KB	alpha ketobutyrate
a-KG	Alpha ketoglutarate
ACN	Acetonitrile
AKI	Acute kidney injury
Akt	Protein kinase B
AL	Ad libitum
AMPK	AMP-activated protein kinase
APOE	Apolipoprotein E
ATP	Adenosine triphosphate
AUC	Area under the curve
b2M	Beta-2 microglobulin
BDP1	B double prime
BHMT	Betaine-Homocysteine S-Methyltransferase
BRF1	TFIIIB-related factor 1
CAT	L-cysteine:2-oxoglutarate aminotransferase
CBS	Cystathionine-beta-synthase
cGMP	Cyclic guanosine monophosphate
CLI	Critical limb ischemia
CO	Carbon monoxide
Complex I	NADH-coenzyme Q oxidoreductase
Complex II	Succinate-Q oxidoreductase
Complex III	Q-Cytochrome c oxidoreductase
Complex V	ATP synthase
Cox	Oxidised cytochrome C
COX	Cytochrome oxidase
CR	Caloric restriction
Cred	Reduced cytochrome C
CSE, CGL	cystathionine-gamma-lyase
CVD	Cardiovascular disease
Cys-S-SH	Cysteine persulfide
DESI	Desorption electrospray ionization
DR	Dietary restriction
DSE	Distal sequence element
EEA	Essential amino acid
eNOS	Endothelial NO synthase
EOD	Every other day
Erk	Extracellular-signal-regulated kinase

ETHE1	Ethylmalonic encephalopathy protein 1
FA	Formic acid
Foxo1/3a	Forkhead box type O 1/3a protein
Ftase	Farnesyl transferase
G609G	Heterozygous $LMNA^{G609G-/-}$ mice
GLUT4	Glucose transporter 4
GOT1	Glutamic-oxaloacetic transaminase 1
Grb2	Growth factor receptor-bound protein 2
GSH	Glutathione
GSSH	Glutathione persulfide
GTT	Glucose tolerance test
GWAS	Genome wide association study
H2S	Hydrogen sulfide
HFD	High fat diet
HGPS	Hutchinson Gilford Progeria Syndrome
HO	Heme oxygenase
HOMA-IR	Homeostatic model assessment of insulin resistance
HS-	Bisulfite
ICMT	ICMT, isoprenylcysteine carboxyl methyltransferase
ICR	Internal control region
ILS	Inbred long sleep
ILSXISS	ILS x ISS cross
IRI	Ischemia-reperfusion injury
IRS	Insulin recpetor substrate
IS	Internal standard
ISS	Inbred short sleep
Keap1	Kelch-like ECH-associated protein 1
KO	Knock-out
LC	Liquid chromatography
LOD	Limit of detection
LTP	Long term potentiation
MAT	Methionine adenosyl-transferase
MEK	Mitogen-activated protein kinase kinase
MPST, TUM1	3-mercaptopyruvate sulfurtransferase
MRM	Multiple reaction monitoring
MS	Mass spectrometry
MSBT	Methylsufonylbenzothiazole
MT	Methyltransferase
mTOR	Mammalian target of rapamycin

mTORC1	Mammalian target of rapamycin complex 1
N3-Methyl THF	Trimethylglycine betaine
NaHS	Sodium hydrosulfide
NH3	Amine
NMDA	N-Methyl-D-aspartic acid
NMN	Nicotinamide mononucleotide
NO	Nitric oxide
NOH	Nitroxyl
NRF2	Nuclear factor erythroid 2-related factor 2
OSHA	United States Occupational Safety and Health Administration
OXPHOS	Oxidative phosphorylation
PDK1	Phosphatidylinositol dependent kinase 1
PGC1a	PPARγ coactivator-1α
PI3K	Phosphatidylinositol 3 kinase
PIP2	Phosphatidylinositol (4,5)-bisphosphate
PIP3	Phosphatidylinositol (3,4,5)-triphosphate
PKC	Protein kinase C
PKG	Protein kinase G
PLP	Pyridoxal-5'-phosphate
Pol III	RNA Polymerase III
Polr3b Het KO	C57BL/6N-Polr3bem7(IMPC)Tcp mice
PPARγ	Peroxisome proliferator-activated receptor-γ
PPi	Inorganic pyrophosphate
PSE	Proximal sequence element
PTEN	Phosphatase and tensin homolog detected on chromosome 10
Qox	Oxidised co-enzyme Q
Qred	Reduced co-enzyme Q
R-S-S-R	Disufide bond
R-S-SH	Persulfide group
R-SH	Thiol group
R-SNO	S-nitrosothiol
R-SOH	Sulfenic acid
Raf	Rapidly accelerated fibrosarcoma protein
RAGE	Receptor for advanced glycation end-products
Ras	Rat sarcoma virus protein
RBC	Red blood cells
RC	Regular chow

RCE1	Ras Converting CAAX Endopeptidase 1
REDD1	Regulated in development and DNA damage response 1
Rheb	Ras homolog enriched in brain
RI	Recombinant inbred
RNS	Reactive nitrogen species
ROS	Reactive oxygen species
rRNA	Ribosomal RNA
RSK	Ribosomal S6 kinase
RSS	Reactive sulfur species
S^{2-}	Sulfide
S6K	Ribosomal protein S6
SAA	Sulfur-containing amino acids
SAAR	Sulfur-containing amino acid restriction
SAHH	S-adenosyl homocysteine hydrolase
SAM	S-adenosylmethioine
SEM	Standard error of the mean
sGC	Soluble guanylate cyclase
SGK	Serum and glucocorticoid-regulated kinase
SNOH	Thionitrous acid
SOD	Superoxide dismutase
SOS	Son of sevenless
SOU	Sulfide oxidation unit
SQR	Sulfur:quinone oxidoreductase
SRB	Sulfate reducing bacteria
SUOX	Sulfite oxidase
TBP	TATA binding protein
TBST	Tris-Buffered Saline Tween[20]
TFIIIA	Transcription factor for RNA polymerase A
TFIIIB1	Transcription factor for pol III B1
TFIIIB2	Transcription factor for pol III B2
TFIIIC	Transcription factor for pol III C
THF	Betaine
tRNA	Transfer RNA
Trx-S	Thioredoxin
TSC	Tuberous sclerosis protein
TST	Thiosulfate sulfurtransferase
ULK	Unc-51 link autophagy activating kinase
Vit B6	Vitamin B6
WS	Werner Syndrome
WT	Wild-type
ZMPSTE24	Zinc metalloproteinase STE24

Chapter 1 Introduction

1.1 Understanding ageing: then, now and future

Our understanding of the ageing process has developed dramatically since early civilisation. Across many ancient cultures, the lifespan of an individual was thought to be determined by divine beings. Perhaps the most well-known of these deities are the three sisters of fate in Greek mythology known collectively as the Moirai [1]. Each of the sisters was said to play a part in spinning, allocating, and cutting the thread of life, essentially determining the lifespan for all individuals. Equivalents to these sisters of fate are found in early Roman, Norse, Celtic, and Baltic belief systems [2]–[5]. This interpretation of lifespan as rigid and pre-determined as also found in the Christian bible, wherein it is stated that "A person's days are determined; you have decreed the number of his months and have set limits he cannot exceed", Book of Job 14:5. Despite these beliefs, modern societies have arrived at the consensus that human ageing and lifespan are in fact pliable to a variety of external factors. It is difficult to point to any specific moment where the collective wisdom shifted. Perhaps it was already present in ancient cultures, indeed the influence of a version of the fountain of youth myth across cultures [6] suggests a willingness to believe in longevity-boosting interventions. In the 4th Century BC the Greek philosopher Aristotle looked to the extreme variance in animal lifespan and attempted to rationalise these observations by examining the influence of sex, lifestyle, size, habitat, and breeding status on longevity [7]. This comparative biology approach to gerontology has grown since the time of Aristotle and remains a central pillar in ageing research to this day [8].

Some of the most compelling evidence that ageing is plastic has emerged from ecological studies of extremely long-lived organisms that appear to elude the ageing process almost entirely. For instance, it was discovered in 1998 that *Lomatia tasmanica,* a Tasmanian shrub that exists as a population of single clonal origin spreading over 1.2 km is at least 43600 years old [9]. Other organisms that helped expand our understanding of ageing are those of the genus *hydra*, a collection of cnidarian polyps that generated much intrigue in 1744 when their extensive regenerative capabilities were first reported by Abraham Trembley [10]. It was not until the work of Paul Brien in 1953 that the

utility of this incredible regenerative capacity was tested in the context of ageing, work that cemented *hydra* as a powerful model for understanding ageing ever since [11], [12]. With regard to vertebrates, the Greenland shark (*Somniosus microcephalus*) is reportedly the most long-lived, with an estimated maximum lifespan as high as 400 years, as calculated through radiocarbon dating of eye lens nuclei from 28 female sharks [13]. Several mammalian species also display extraordinary longevity, such as the naked mole rat (*Heterocephalus glaber*), a rodent native to east African countries with a maximum lifespan of over 30 years in captivity, more than 9 times the maximum lifespan of laboratory rats [14]. In fact, the naked mole rat's longevity is so extraordinary that it is the only mammal to violate Gompertzian mortality law i.e. they have no increase in age-specific hazard mortality with age, irrespective of sex or breeding status [15].

Given these examples of extreme longevity across taxa, it is natural to question the maximum lifespan for humans. Jeanne Calment was born in Provence, France in 1875 and lived to be 122 years and 164 days of age [16]. She was the oldest person to have ever lived and represents the maximum achievable human lifespan as we know it. Globally, maximum life expectancy has increased at a rate of 2.5 years per decade in a near-linear fashion since 1840 [17]. The driver of this increase over the past 4 decades appears to be primarily through reductions in mortality arising from cardiovascular disease [18]. A 2012 report published by the United Nations Population Fund and HelpAge International estimated that the proportion of the global population that is over the age of 60 will rise from 11% to 20% by 2050, in light of improvements in healthcare, sanitation, education, and nutrition [19]. However, it should also be noted that the yearly increase in life expectancy in several high-income countries has slowed in recent years and some countries have even seen a small reduction in average life expectancy [20]. This stagnation in life expectancy appears to be driven by elevated mortality in people over 65 years of age due to cardiovascular, respiratory, and nervous system diseases [21]. Additionally, social inequality in lifespan has become an area of particular focus in recent years, with multidisciplinary approaches being developed to address the socioeconomical conditions that cause those in low-income areas to have a shorter than average lifespan [20].

The next development in our modern understanding of ageing was our appreciation of the importance of intrinsic and extrinsic factors in modulating lifespan. Through extensive data collection and international collaboration, scientists have been able to establish the existence of 5 'blue zones', regions where the local populace have abnormally long lifespans and improved late-life health when compared to other nearby populations and global averages [22], [23]. Studies of these populations have identified specific dietary, lifestyle, and genetic factors that appear to drive the observed longevity across these populations [23]. For instance, diets in 'blue zones' are often rich in plant-based nutrition, meat is eaten less than 6 times a month, portion sizes are small, and people do not eat to full satiety [23]–[25]. By definition, these 'blue zones' contain an abnormally high concentration of centenarians and supercentenarians (people >100 or >110 years old, respectively), however centenarians also occur in regions other than the 'blue zones'. The occurrence of centenarians outside of 'blue zones' allows us to examine their longevity without the confounding factors of a shared lifestyle and environment. Interestingly, genetic studies of centenarians have identified several mutations that are consistent in both 'blue zones' and the general population including mutations in the genes *FOXO3A*, *APOE*, *IGF1*, *IGF1R*, and *PARP1* [26]. Other epidemiological studies have also identified 7 genes within the mammalian target of rapamycin (mTOR) signalling pathways to be associated with human longevity and late-life health [27]. However, epidemiological studies in twins have estimated that heritable traits account for less that 27% of longevity in both males and females [28]. The implication from these studies is that there is contribution from both intrinsic genetic traits and extrinsic lifestyle factors that consistently improve human longevity [29].

This brings us to the present moment, where we are equipped with the knowledge that extreme longevity is evident in several organisms, and that human lifespans are subject to influence from multiple factors. However, researchers in the field of ageing are divided into broadly three categories of thought regarding the future of human longevity [30]. The first group believe that while the 20th and 21st centuries have seen extraordinary increases in the mean and maximum lifespan in humans, we are already close to the limit of human longevity or may have already achieved it [31], [32]. The second group

believe that while improvements in infant and maternal mortality rates have brought us to our current average human lifespan, there remain many unexploited interventions that will propel human lifespan further, potentially to several hundred years of age [33]. While these first two groups are essentially at odds with one another, a third group has emerged that contains members of both. This group proposes that extension in lifespan is either unnecessary or suboptimal without a concomitant increase in healthspan, which is defined as the proportion of time that an individual spends free from disease across their lifetime [34]–[36]. Irrespective of which group(s) one is a member of, the progress towards these goals is dependent on a greater understanding of the fundamental biology that underpins ageing.

1.2 Biological roles for Hydrogen Sulfide

This thesis considers the potential role of hydrogen sulfide (H_2S) as a biological signalling molecule that exhibits control over many aspects of the fundamental biology of ageing. The following section describes the history, chemistry, and biology of H_2S, and collects the evidence for its role in ageing and age-related diseases.

1.2.1 A history of H_2S

Our understanding of H_2S was originally developed in the context of occupational medicine as a potent hazardous gas. Many species of bacteria produce H_2S as they putrefy decaying organic matter, this can result in toxic concentrations of the gas in enclosed spaces [37]. Sewer workers in the 1700s would disturb decaying matter as they worked, causing the gas to escape and resulting in irritation of their eyes and even blindness in some cases [38]. These accounts were collected by Bernardino Ramazzini in his seminal treatise on occupational medicine *De Morbis Artificum Diatriba,* which was translated to English in 1940 [38]. Describing the exposure of sewer workers to H_2S he evocatively details that “these foul exhalations wage ruthless war, and they attack so cruelly with their piercing stings that they rob them of life, that is to say of light”. By the 1770s, the volume of H_2S gas exuded by the antiquated sewage system in Paris, France caused eye irritation and rapid asphyxiation in members of the public [39]. As H_2S is a by-product of several modern chemical processes, the occupational risk of H_2S has only increased. In 1950, an accident at a gasoline production plant in Poza Rica, Mexico caused the release of H_2S gas into the atmosphere, resulting in the death of 22 people and hospitalizing 320 others within 20 minutes of release [40]. 52 American workers lost their lives due to H_2S-poisoning in the workplace in the years 1993-1999 and deaths occur to this day [41]. The symptoms associated with exposure to various concentrations of H_2S are summarised in **Table 1**. Most dramatically, the accumulation of H_2S in the upper levels of the ocean and subsequent expulsion into the atmosphere is a proposed mechanism for the end-Permian extinction event 250 million years ago [42], [43]. Considering this well-characterised toxicity, reports of endogenous H_2S production in mammalian systems seem at first counterintuitive. Such observations existed as early as the 1942 [44],

however no attempt to interrogate or understand the implications of this observation were made until the 1990s. Our understanding of the functional role of H_2S in normal physiology was actuated upon publication of work by Abe & Kimura in the mid-nineties which described three major findings: H_2S is produced in healthy human brains, the enzyme cystathionine-β-synthase (CBS) is the major producer of H_2S in this tissue, and neurons exposed to a specific concentrations of H_2S had improved neuronal function [45]. With a functional role for H_2S established in neural tissue several key findings over the subsequent decades have matured our appreciation of functional H_2S in several organs including stimulation of smooth muscle relaxation and vasorelaxation [46], [47], modulation of the inflammatory response [48], stimulation of angiogenesis [49], and interaction with other gaseous neurotransmitters [50], [51]. An exhaustive timeline detailing advances in this field was compiled by Szabo in 2017 [52].

Table 1 Health impact of exposure to various concentrations of H_2S
Adapted from OSHA guidelines, United States Department of Labor [53]

Concentration (ppm)	Symptoms/Effects
0.00011-0.00033	Typical background concentrations
0.01-5	Odour threshold, becoming more offensive at 3-5 ppm. Prolonged exposure may cause nausea, tearing of the eyes, headaches, or loss of sleep. Airway problems (bronchial constriction) in some asthma patients.
20	Possible fatigue, loss of appetite, headache, irritability, poor memory, dizziness.
100	Coughing, eye irritation, loss of smell after 2-15 minutes (olfactory fatigue). Altered breathing, drowsiness after 15-30 minutes. Gradual increase in severity of symptoms over several hours. Death may occur after 48 hours.
500-700	Collapse in 5 minutes. Serious damage to the eyes in 30 minutes. Death after 30-60 minutes.
700-1000	Rapid unconsciousness within 1 to 2 breaths, death within minutes. Near instant death at concentrations above 1000 ppm

1.2.2 Chemical properties of H_2S

H_2S is a colourless, toxic, corrosive gas, which is denser than air and has a potent odour of rotten eggs. This toxicity arises from inhibition of cytochrome C oxidase (complex IV of the electron transport chain) resulting in a shutdown of cellular aerobic respiration [54]. H_2S is a member of the dihydrogen chalcogenide family of compounds, which comprise two hydrogen atoms bound to a chalcogen atom. These compounds are polar molecules with bent geometry [55]. Whilst water is another dihydrogen chalcogenide compound, its chemistry is highly influenced by hydrogen bonding between molecules that is not present in other members of the family, giving water highly anomalous properties [56]. As such, the chemical properties of H_2S are closer to those of the other members of the dihydrogen chalcogenides, including hydrogen selenide, hydrogen telluride and hydrogen polonide [57]. As a discreet, uncharged molecule H_2S is lipid-soluble and can easily pass through plasma membranes, especially when dissolved in lipophilic solvents [58]. H_2S readily acts as a reducing agent, forming HS^- which can react to form many chemical species in biological tissues with a broad range of oxidation states [59]. The oxidation state of sulfur atoms across compounds present in biological settings is summarised in **Table 2**. The best studied sulfide species in biology are broadly described by three groups: free sulfides (including H_2S gas and acid-labile sulfide), metal-sulfide clusters (most commonly sulfur atoms bound to iron centres), and sulfane sulfide (sulfur atoms bound to at least one other sulfur in a chain) [60]. Upon reaction with metal ions, H_2S commonly forms insoluble, solid precipitates which have been exploited to measure H_2S for decades; most notably in the use of paper impregnated with lead (II) acetate which reacts to form lead (II) sulfide [61], [62].

Table 2 Formal oxidation state of sulfur atom(s) in common biological sulfur species. Based on [59].

Formal Oxidation State of Sulfur Atom(s)						
-2	**-1**	**0**	**+2**	**+4**	**+6**	**Multiple**
H_2S Hydrogen Sulfide	R-S-S-R Disulfide bonds	S^0 or S_8 Elemental Sulfur	S=O Sulfur Monoxide	SO_2 Sulfur Dioxide	SO_3 Sulfur Trioxide	$H\text{-}S^{-2}\text{-}S^0\text{-}S^{-2}\text{-}H$ Poly Sulfides
HS^- Hydrosulfide Anion		R-S-OH Sulfenic Acid	H_2SO_2 Sulfoxylic Acid	H_2SO_3 Sulfurous Acid	H_2SO_4 Sulfuric Acid	$[S^0\text{-}S^4O_3]^{2-}$ Thiosulfate
R-S-H Thiol				SO_3^{2-} Sulfite	SO_4^{2-} Sulfate	

1.2.3 Endogenous Production of H_2S

Enzymatic production of H_2S in mammalian tissues requires sulfur-containing amino acids (SAA), specifically methionine and cysteine, as substrates [63], [64]. Methionine cannot be synthesised *de novo* in mammals and must be consumed in the diet. In contrast, cysteine can be synthesised from methionine *via* conversion to homocysteine and also consumed through diet. Homocysteine conversion into cysteine is referred to as the transsulfuration pathway (first described in the context of plant metabolism, in which cysteine is converted to homocysteine [65]). From cysteine, H_2S is produced by two distinct canonical enzymatic pathways: directly through activity of two pyridoxal-5'-phosphate (PLP)-dependent enzymes, cystathionine-γ-lyase (CSE, or CGL) and cystathionine-beta-synthase (CBS), or indirectly through stepwise conversion into 3-mercaptopyruvate by L-cysteine:2-oxoglutarate aminotransferase (CAT) and then H_2S by 3-mercaptopyruvate sulfurtransferase (MPST, or TUM1) [66]. The latter pathway is referred to the PLP-independent pathway as although CAT is PLP-dependent, MPST is not. These pathways are further distinguished by their sub-cellular localisation. CSE and CBS operate predominately within the cytosol, although both can translocate to the mitochondria under certain stress conditions [67]. For instance, CSE translocates to the mitochondria during hypoxia, promoting H_2S production within mitochondria and subsequently increasing ATP production [68]. Human MPST exists in two distinct isoforms, TUM1-Iso1 which is exclusively found within the cytosol and TUM1-Iso2, a splice variant encoding an additional 20 amino acid mitochondrial-targeting sequence [69]. Specific activity of mitochondrial MPST is two to three times higher than cytosolic MPST in rat liver [70]. While the pathways described above exclusively use the L-enantiomer of cysteine as a substrate, Kimura *et al*. discovered a PLP-independent pathway for the production of H_2S from D-cysteine (mainly in cerebellum and kidney homogenates) through the action of MPST and D-Amino acid oxidase in mitochondria and peroxisomes, respectively [71]. While L-cysteine is the predominant, naturally occurring enantiomer of cysteine, common food processing practices rapidly racemise L-cysteine through heat and alkaline treatments, resulting in up to 44% conversion to D-cysteine [71]. The biologically relevant extent of this D-cysteine pathway remains unclear but

presents an interesting alternative to the canonical mammalian production of H_2S.

1.2.4 Endogenous Disposal of H_2S

Supraphysiological concentrations of H_2S can be toxic, so efficient removal of H_2S is performed by a suite of mitochondrial enzymes, collectively termed the sulfide oxidation unit (SOU) [72]. It has been shown that SOU actively catabolises H_2S when intracellular concentrations exceed 10 nM in intact cells, with more restrictive thresholds observed in proximity to mitochondria [73]. However, determining a precise definition of supraphysiological H_2S levels remains challenging due to limitations in detection methods and tissue and species specificity [74]. While the precise order of events and sulfur species involved in H_2S oxidation is still unclear, the disposal of H_2S consists of a series of oxidative reactions coupled to components of the electron transport chain within the mitochondria, ultimately yielding sulfate which is excreted in the urine. The first step in this pathway is the oxidation of H_2S by the flavoprotein sulfur:quinone oxidoreductase (SQR) catalytic cycle whereby the flavin co-factor is cyclically reduced by H_2S and oxidized by ubiquinone, with coenzyme Q acting as an electron acceptor [75]. It is through coenzyme Q that H_2S metabolism is coupled to ATP generation by oxidative phosphorylation, making H_2S a rare example of an inorganic compound capable of fuelling mammalian oxidative phosphorylation [76]. The product of this enzymatic cycle is the generation of SQR-persulfide intermediates, which are transferred primarily to glutathione (GSH) in human tissues, generating glutathione persulfide (GSSH) [77]. SQR is also capable of catabolising H_2S to produce thiosulfate from sulfite, although low tissue levels of sulfite makes it unclear whether this reaction accounts for a substantial proportion of physiological SQR activity in mammals, despite SQR having orders of magnitude greater reactivity with sulfite compared to GSH [78]. GSSH is oxidized by ethylmalonic encephalopathy 1 (ETHE1) or thiosulfate sulfurtransferase (TST) to form sulfite or thiosulfate, respectively. ETHE1 is a sulfur dioxygenase, consuming O_2 and water as substrates to oxidise H_2S [79]. TST may then reversibly convert thiosulfate to sulfite which is irreversibly oxidised into sulfate by sulfite oxidase (SUOX). Both sulfate and thiosulfate are removed *via* the circulatory system and then ultimately excreted in the urine [80]. Overall, disposal of 1 H_2S molecule requires consumption of 0.75 O_2 molecules: 0.5 by ETHE1 and 0.25 by Complex III [72]. The enzymatic generation of H_2S from SAAs and its subsequent removal are detailed in **Figure**

1. Of note, as mature red blood cells typically lack mitochondria, they utilize a methemoglobin pathway for the disposal of H_2S by conversion of H_2S into thiosulfate and polysulfides [81]. It remains an open question as to whether the methemoglobin pathway for H_2S oxidation found within red blood cells is utilised in other tissues in mammals.

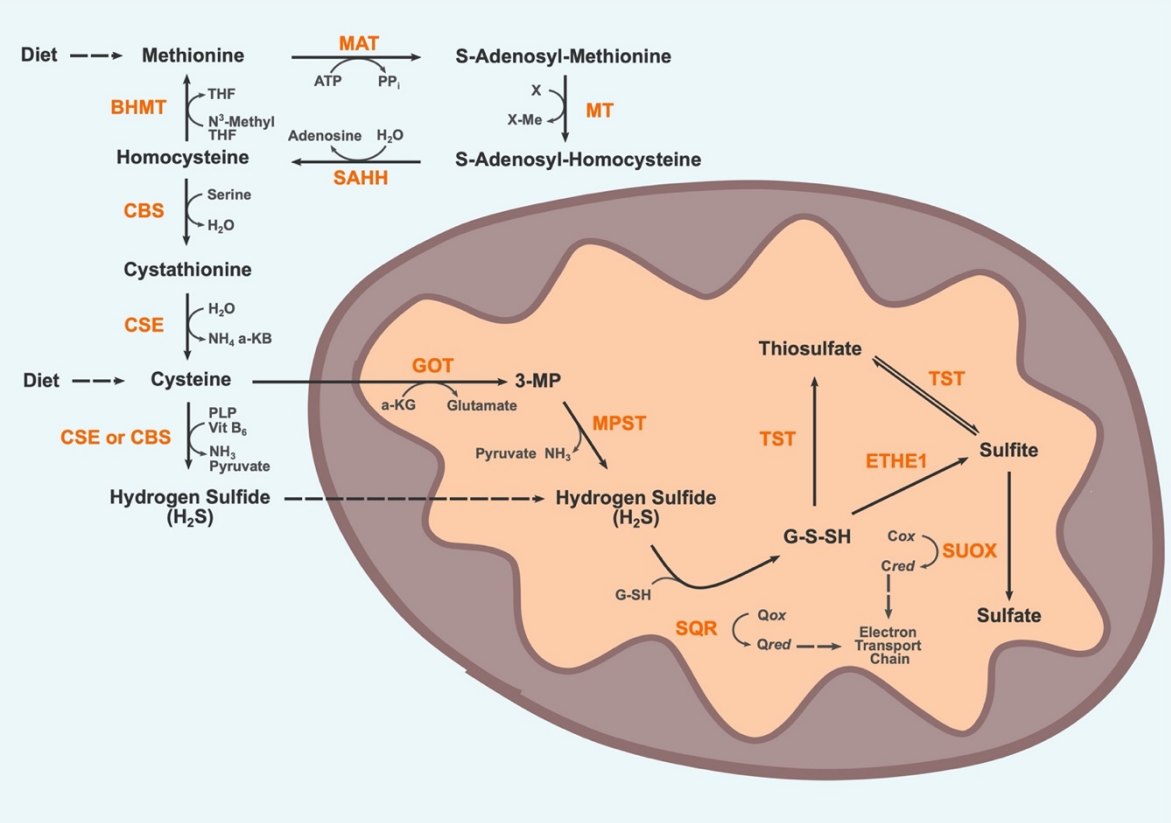

Figure 1 Substrate, intermediates, and enzymes involved in the endogenous production and disposal of H_2S.

The blue region represents the cytosol, the orange region represents the matrix of a mitochondrion. The transsulfuration pathway cycles methionine into homocysteine first, followed by enzymatic conversion of homocysteine into cysteine. From cysteine, H_2S is generated in the cytosol by CSE and CBS. H_2S can also be generated within mitochondria by the action of MPST on 3-MP, a metabolite of cystine. H_2S can freely permeate membranes including the mitochondrial membranes. H_2S disposal is carried out in mitochondria by several enzymes that comprise the sulfide oxidation unit (SOU). The precise mechanism of the SOU remains a subject of active research, the species and steps shown here represent just one proposed mechanism. Ultimately H_2S is oxidised into sulfate which is subsequently excreted in urine.
MAT: Methionine adenosyl-transferase, ATP: Adenosine triphosphate, PPi: Inorganic pyrophosphate, X: Methyl group acceptor, MT: Methyltransferase, SAHH: S-adenosyl homocysteine hydrolase, BHMT: Betaine-Homocysteine S-Methyltransferase, N3-Methyl THF: Trimethylglycine betaine, THF: Betaine, CBS: Cystathionine-β-synthase, CSE: Cystathionine-γ-lyase, NH3: Amine, a-KB: alpha ketobutyrate, PLP: pyridoxal 5'-phosphate, Vit B6: Vitamin B6, GOT: Glutamic-Oxaloacetic Transaminase, a-KG: alpha ketoglutarate, 3-MP: 3-Mercaptopyruvate, MPST: 3-Mercaptopyruvate Sulfurtransferase, SQR: Sulfur-Quinone oxidoreductase, Qox: Oxidised co-enzyme Q, Qred: Reduced co-enzyme Q, G-S-SH: Glutathione persulfide, ETHE1: Ethylmalonic encephalopathy 1 protein, TST: Thiosulfate Sulfurtransferase, SUOX: Sulfite Oxidase, Cox: Oxidised cytochrome C, Cred: Reduced cytochrome C.

1.2.5 Bacterial Production of H_2S

Putrefaction of decaying organic matter in anaerobic conditions results in the production of H_2S [82]. This is due to the action of a wide range of sulfate reducing bacteria (SRB) which utilize sulfate as a terminal electron acceptor for respiration, with the concomitant production of H_2S [83]. There is a wide range of such SRB within the microbiome of the human colon, primarily of the genus *Desulfovibrio* in the class d-Proteobacteria [84]. Endogenous production of H_2S in bacteria is catalysed by orthologs of CSE, CBS, and MPST [85]. The interactions between groups of bacteria are complex and poorly understood. SRB use a wide range of substrates including lactate, hydrogen, short-chain fatty acids, and amino acids, which places them in direct competition with other bacterial species such as hydrogenotrophic bacteria, methanogens and acetogens. However, SRB appear to dominate the use of hydrogen in the microbiome as they are capable of catabolizing hydrogen at concentrations far lower than other hydrogenotrophic species [86]. It is difficult to directly measure the proportion of H_2S produced by bacteria compared to endogenous enzymatic production in tissues. Germ-free mice have 50% less measurable H_2S in faecal samples compared to control mice and are capable of altering SRB-activity to compensate for the impairment in enzymatic H_2S production following a PLP-deficient diet [87]. H_2S gas produced by the microbiome in the gut can enter proximal human tissues or the bloodstream [88]. For instance, high levels of SRB-derived H_2S inhibits butyrate oxidation, the major source of energy production in intestinal colonocytes [89]. Furthermore, there is evidence that bacterial-derived H_2S can reduce arterial blood pressure in rats [90], and contradictory evidence points to either a therapeutic or causative role of H_2S in inflammatory bowel disease and colorectal cancer [91]. Additionally, there is potential for diet to influence the relative abundance of SRB, as diet has been shown to modify microbiome composition in general [92]. However, no significant effect of short-term adoption of diets either enriched for or deficient in SAAs was observed on relative SRB populations in stool samples from healthy human volunteers [93], and future studies employing longer term dietary interventions and greater statistical power are required to further clarify this question. Finally, it has been proposed that bacterial production of H_2S protects the bacteria against oxidative stress and may contribute to antibacterial resistance [94]. For example, Shatalin

et al. developed novel small molecule inhibitors of bacterial CSE and found these inhibitors improved antibiotic potency against *Staphylococcus aureus* and *Pseudomonas aeruginosa in vitro* and in mice [94], supporting the theory that endogenous production of H_2S in bacteria might contribute to antibacterial resistance. Research using germ-free mice is one approach that may help provide more information regarding the relevance of SRB-derived H_2S in whole-animal metabolism and physiology.

1.2.6 Signalling Modalities of H_2S

1.2.6.1 Post-Translational Modification (Persulfidation)

Protein modification by H_2S is a reversible post-translational modification that can occur on any cysteine residue. Overall, the thiol group (R-SH) present in cysteine is indirectly changed to a persulfide group (R-S-SH), a process known as persulfidation or sulfhydration. The thiol group must first be oxidised to form thiol derivatives such as sulfenic acid (R-SOH), a disulfide (R-S-S-R) or S-nitrosothiol (R-SNO), which can then react with H_2S to create a persulfidated protein residue. A schematic showing the various thiol derivatives H_2S can react with and their subsequent products are shown in **Figure 2**, adapted from [95]. Persulfides are highly reactive, with a nucleophilic terminal sulfur atom and an electrophilic inner sulfane sulfur atom [96]. Persulfidation of cysteine residues causes conformational changes in protein structure that alter protein activity such as the regulation of Kelch-like ECH-associated protein 1 (Keap1), which has well characterised conformational regulation through alterations of cysteine residues [97], [98]. Keap1 is the major inhibitor of the nuclear factor erythroid 2-related factor 2 (NRF2)-mediated antioxidant response element. *In vitro* approaches have shown alteration of cysteine residues on Keap1 following exposure to H_2S leading to inactivation of KEAP1, but currently there is no agreement on the precise residue(s) persulfidated in this process [97], [98]. Another established persulfidation target is the Kir6.1 subunit of K_{ATP} channels which confer cardioprotective effects when activated by H_2S [99]. An extensive review of the chemistry of persulfides, their molecular targets, and role in various tissues and diseases was compiled by Filipovic and colleagues in 2017 [100]. Persulfides decay under biologically relevant conditions, which poses a challenge in the identification, measurement, and characterisation of persulfidated species in biological contexts. The half-life of Cys-S-SH is approximately 35 min at 37°C [101]. Spontaneous removal of persulfides is caused by a disproportionation reaction between two persulfides to form a number of sulfur-containing species including: elemental sulfur, thiols, polysulfanes and/or H_2S [101]–[103]. Additional processes that can break down persulfides include homolysis by heat or light and enzymatic removal by the thioredoxin system. Given these constraints it is difficult to achieve a full understanding of the dynamics of protein persulfidation as most methods take a

"snap-shot" of global persulfidation at one time. Despite these limitations, our understanding of the extent of protein modification by persulfidation, collectively termed the persulfidome, is growing. In *Arabidopsis thaliana*, for example, 5% of the proteome was found to be persulfidated using modified tag-switching protocol that employed methylsufonylbenzothiazole (MSBT) to block both thiol and persulfide groups within the sample [104]. This was then followed by addition of CN-biotin which does not react with MSBT adducts of thiol origin and therefore allows for streptavidin-based pull-down of persulfidated proteins [104]. Additionally, proteomic studies in wild-type mice have found 10-25% of hepatic proteins to be persulfidated under physiological homeostasis [105]. Comprehensive work by Zivanovic *et al*. showed that a high degree of hepatic protein persulfidation is associated with extended lifespan, augmented by dietary restriction, and diminished with age; these trends were conserved across model organisms [106]. Bithi *et al*. described tissue-specific changes in the persulfidome of mice exposed to 50% dietary restriction and in mice homozygous null for CSE [107]. As persulfidation can in principle occur on any cysteine residue, and is a highly dynamic, reversible post-translational modification, there is enormous scope for H_2S to modify proteins in a variety of biological settings.

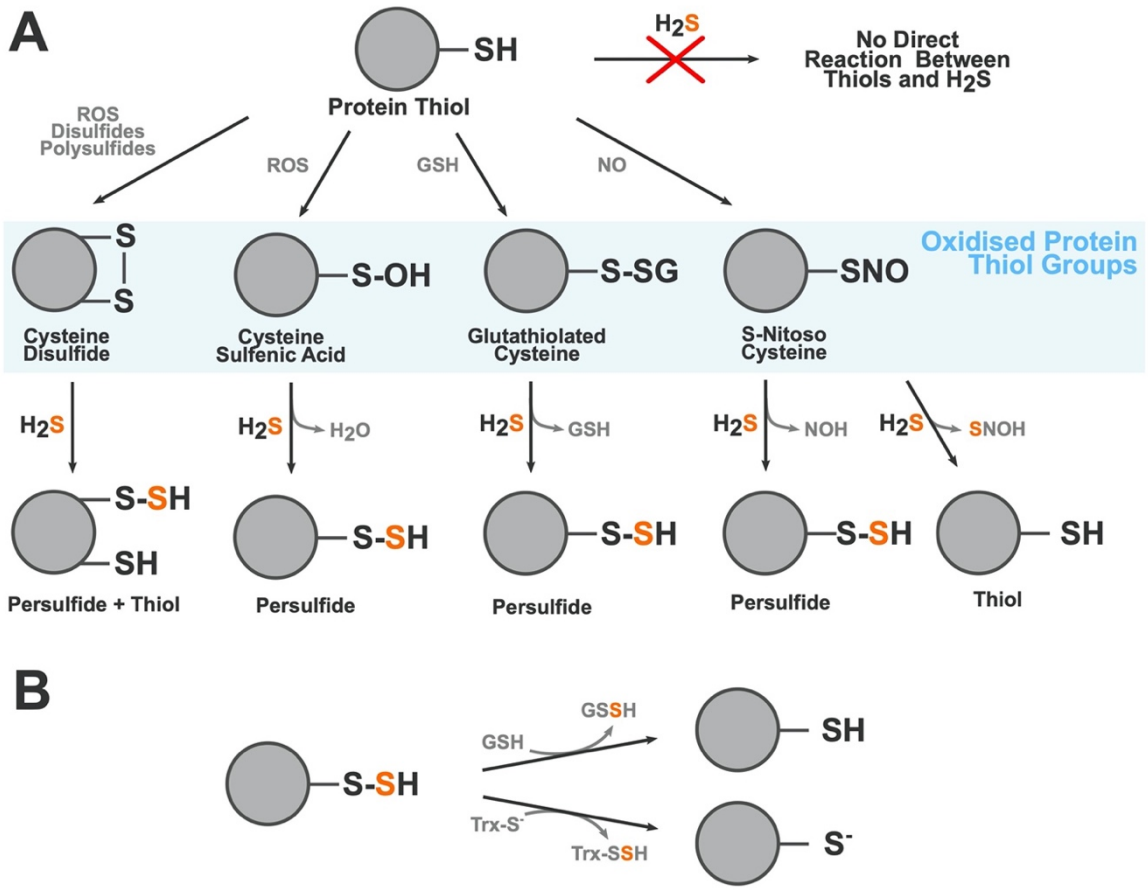

Figure 2 A Modification of cysteine residues by H_2S.

A H_2S cannot directly modify thiol groups (i.e. cysteine residues). The thiol group must first be oxidised into a disulfide (disulfide bond formation), sulfenic acid (S-Sulfenylation), glutathiolated cysteine (S-Glutathiolation), or a S-Nitroso Cysteine (S-Nitrosation). From these oxidised thiol groups H_2S can react to form persilfides, thiols, and a variety of by-products dependent on the type of oxidized thiol it is reacting with. The sulfur atom from the H_2S molecule is highlighted in orange to show where in the product it incorporates. **B** Persulfidation is a reversible post-translational modification and can be readily removed by action of glutathione and thioredoxin.
ROS: Reactive oxygen species, GSH: Glutathione, NO: Nitric oxide, NOH: Nitroxyl, SNOH: Thionitrous acid, GSSH: Glutathione persulfide, Trx-S-: Thioredoxin.

1.2.6.2 Binding with Metal Centres

H_2S is capable of binding to multiple metal ions, the most direct signalling modality in its repertoire. Upon binding, the coordination, charge, and oxidation states of the metal ion may be altered [108]. Such reactions become biologically relevant in the context of metalloproteins which contain metal centres in their quaternary structure. Metalloproteins represent a significant percentage of all mammalian proteins, with recent estimates suggesting that approximately 6,600 human proteins are metalloproteins [109], or approximately a third of all protein products. H_2S reaction with haemeproteins is well established, particularly with ferric haemoglobins but also metmyoglobins, methemoglobins, and peroxidases [110]. In fact, the much-discussed toxicity of H_2S is a result of its highly efficient inhibition of cytochrome c oxidase (COX, also known as Complex IV in the electron transport chain). COX is a dimer formed of subunits that include two heme, two copper, one magnesium and one zinc centre [111]. Inhibition of COX by H_2S occurs in a biphasic manner under a complex series of reactions with the haem and copper centres, forming intermediates that are currently unresolved [112]. Furthermore, H_2S inhibits angiotensin converting enzyme by binding to a zinc atom at the active site, with dose-dependent inhibition of this enzyme demonstrated in protein lysates from human endothelial cells [113]. Interestingly, binding with haem centres in haemoglobin may be the major H_2S clearance pathway in red blood cells (RBCs) [81]. It is established that RBCs do produce endogenous H_2S, primarily through MPST, but as most mammals lack mitochondria within their RBCs, they then do not possess the canonical clearance mechanisms (*see section 1.2.4*). Unchecked, H_2S production in the trillions of RBCs within the circulation would inevitably result in a lethal build-up of H_2S. However, it appears that a cycle of reactions between H_2S species and haemoglobin results in oxidation of H_2S into reactive sulfur species (RSS) such as thiosulfate and hydropolysulfides [81]. A similar process appears to occur between H_2S and myoglobin in cardiac and skeletal muscle [114].

1.2.6.3 Interaction with Other Gasotransmitters

H_2S is not alone as a gasotransmitter. Other compounds with similar properties are carbon monoxide (CO) and nitric oxide (NO). These gases are also toxic at high concentrations, are produced endogenously, and can freely permeate plasma membranes to exert biological effects. All three gasotransmitters are highly reactive producing various metabolites that are collectively termed RSS, reactive oxygen species (ROS), and reactive nitrogen species (RNS). It has become clear that these reactive chemical species can react with metabolites and derivatives of the other gasotransmitter molecules to form a densely interconnected web of products sometimes collectively termed the reactive species interactome. For instance, H_2S, NO and their derivatives react to form a family of nitrothiol compounds, resulting in modulation of signalling pathways [115]. Furthermore, each gasotransmitter can regulate the production of the other two gasotransmitters (**Figure 3)**. H_2S stimulates NO production through transcriptional, translational, and post-translational interventions in the NO synthesis pathway, with reports of both elevation and suppression of NO production [116]. The mechanism by which H_2S elevates CO production is still an area of active research but appears to involve activation of the Nrf2-mediated response (*see section 1.2.6.1*) upregulating heme oxygenase isoforms which generate CO [117]. These chemical species and intermediates are highly dynamic which makes measuring and understanding the exact processes involved in H_2S-NO-CO crosstalk challenging. What is clear is that such cross-talk is an important signalling modality across a diverse range of organisms, influencing plant growth and ripening for example [118], [119]. In mammals, the dynamics and functions of H_2S-NO-CO cross-talk are best understood in the cardiovascular system where they exert control over inflammation, angiogenesis, vasodilation and protection from ischemia-reperfusion injury [120], [121]. An interesting case study in the complexity of gasotransmitter crosstalk is demonstrated by the regulation of the activity of soluble guanylate cyclase (sGC), a hemeprotein. Overall, the three gasotransmitters all increase sGC activity, but the biochemistries involved in this outcome are distinct. NO is an exceptionally strong activator of sGC, augmenting sGC activity over one hundred-fold [122]; in contrast, CO is a far weaker activator of sGC [123]. Due to this disparity in potency and binding strength, NO and CO compete for dominance in their interaction with sGC: when NO concentrations are low CO is

the predominant activator of sGC; but when NO concentrations are high CO actually inhibits NO-induced elevation of sGC activity [121]. Distinct from this, H_2S does not directly activate sGC but instead has been shown to reduce the heme moiety from Fe^{3+} to Fe^{2+}in human recombinant sGC. CO and NO only interact with Fe^{2+} sGC, thus H_2S facilitates the activity of the other two gases by increasing the available pool of Fe^{2+} sGC [124]. Thus, all three gases work to elevate sGC activity but there is considerable nuance in how this is achieved. The remainder of this introduction will focus on the effects of just one gasotransmitter, H_2S, in health, disease and ageing. However, considering the intricate and overlapping effects of all three gasotransmitters, we must be mindful of the possibility that any effects attributed to H_2S may in reality belong to the unity of all three gasotransmitters.

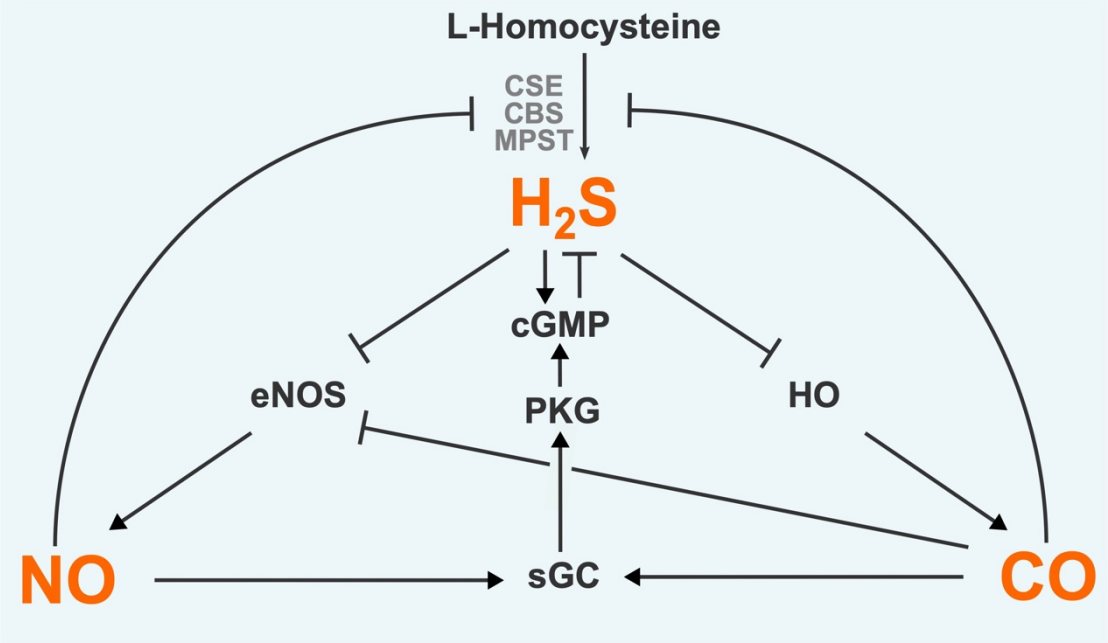

Figure 3 Established interactions between H_2S, CO, and NO signalling pathways.

Each gasotransmitter is capable of regulating the other two. Pointed arrows represent a stimulatory effect. Flat headed arrows indicate an inhibitory effect. H_2S: Hydrogen sulfide, NO: Nitric oxide, CO: Carbon monoxide, CBS: Cystathionine-β-synthase, CSE: Cystathionine-γ-lyase, MPST: 3-Mercaptopyruvate sulfurtransferase, eNOS: Endothelial NO synthase, HO: Heme oxygenase, sGC: Soluble guanylyl cyclase, PKG: Protein kinase G, cGMP: Cyclic guanosine monophosphate

1.3 H_2S and Ageing

1.3.1 Role of H_2S in Normative Ageing

Exploration of the processes that underlie ageing is most easily understood under the guidance of the hallmarks of ageing [125], a landmark review that proposed nine discrete categories of biological processes that are conserved in organismal ageing. A recent review by Perridon *et al*. considered the impact of H_2S on each of these hallmarks in turn and collected evidence showing direct, H_2S-mediated protection from all ageing hallmarks except for telomere attrition, for which no studies had been published [66]. This introduction will not aim to repeat the work previously published but instead assess subsequent publications concerning the effect of H_2S on specific tissue ageing. Whilst it is probable that the dynamics of H_2S production and activity are altered throughout age in most tissues of the body, recent papers have focussed on a few select organ systems including the heart, brain, and kidneys.

1.3.1.1 Cardiovascular Ageing

The typical progression of cardiovascular ageing is initiated by endothelial dysfunction, leading to vascular dysfunction, increased severity of atherosclerosis, and subsequently cardiovascular diseases (CVDs) including stroke, hypertension, and coronary heart disease [126]. Key molecular mechanisms that drive this pathological progression are under the influence of H_2S including: signalling through Nrf2, SIRT1, and AMP-activated protein kinase (AMPK)/mTOR; activation of potassium channels; and regulation of mitochondrial biogenesis by the peroxisome proliferator-activated receptor-γ (PPARγ) coactivator-1α (PGC-1a) [127]. Furthermore, exposing cells and mice to H_2S can ameliorate age-associated vascular ageing [128]. Treatment of cultured endothelial cells with nicotinamide mononucleotide (NMN, an NAD^+-elevating supplement) improves vascular remodelling in response to ischemic injury and enhances endurance and capillary density in old mice, effects that are augmented by co-treatment with H_2S-donating compounds [128]. The augmentation of vascular health by NAD^+ and H_2S boosting treatment is unsurprising due to the convergence of these signalling pathways through SIRT1. However, the same authors also reported that treatment with H_2S in isolation

enhanced basal mitochondrial respiration levels in HUVEC cultures, an effect not seen when using NMN [128]. This indicates that H_2S has protective effects independent of NAD. Other evidence for a protective role for H_2S in cardiac cell culture models include improved glucose utilization, improved metabolic efficiency of glycolysis and the citric acid cycle, and protection against induced cardiomyocyte hypertrophy [129]. Furthermore, CSE expression and H_2S production were found to be reduced in a model of aged primary rat cardiomyocytes [130]. Treatment of these cells with sodium hydrosulfide (NaHS, a H_2S-donating compound) improved cardioprotection in response to ischemia-reperfusion events *via* inhibition of mitochondrial permeability transition pore opening and improved mitochondrial membrane potential [130]. Peleli *et al.* used a mouse model with knock-out (KO) of MPST, one of the three enzymatic producers of H_2S (*see section 1.2.3*), to study the effect on sulfur-containing chemical species [131]. In these MPST KO mice there was no significant effect on H_2S, polysulfides, or sulfane sulfur level in heart tissue, nor did it affect blood pressure or vascular reactivity relative to wild-type controls, but elevation of several cardiac ROS markers was seen [131]. However, while some positive cardioprotective phenotypes were observed in these mice at 2-3 months of age (including protection from ischemia-reperfusion injury, IRI), deleterious phenotypes (including hypertension, cardiac hypertrophy, reduced myocardial nitric oxide production) were reported at 18 months of age [131]. The authors suggest that the cardioprotective effects in young mice could be explained by increased cardiac ROS levels providing a pre-conditioning against IRI, whereas at old age it appears that ablation of MPST is deleterious to heart function. This study is the first to investigate the cardiovascular phenotype in MPST KO mice and further studies should aim to extend understanding in the role and pathophysiology of MPST in the onset of age-related heart disease.

1.3.1.2 Neurological ageing

As neuromodulation was the first functional role described for endogenous H_2S in humans [45], it is unsurprising that H_2S is implicated as a key player in brain ageing. One conduit for multiple neuropathological processes is the receptor for advanced glycation end-products (RAGE). RAGE is among several receptors that bind to advanced glycation end-products, proteins and lipids that have been modified by reaction with sugar molecules in a non-enzymatic manner that accumulate in tissue with age, including the brain [132]. It should be noted that while the transmembrane forms of RAGE are implicated in neurotoxic signalling, soluble forms of RAGE have instead been shown to confer neuroprotective effects, in part due to inhibition of membrane-associated RAGE [133]. RAGE also binds to beta-amyloid, engendering deleterious effects and, as such, has drawn interest as a potential target in the treatment of Alzheimer's disease [134]. Treatment with exogenous H_2S in cells has been shown to inhibit stabilisation of membrane-associated RAGE dimers; the modality for this inhibition was direct persulfidation of a cysteine residue on RAGE [135]. Beyond RAGE signalling, other ageing processes are subject to H_2S regulation in neural cell systems. In a cell culture model of hyperglycaemia-induced hippocampal senescence, treatment of cells with a H_2S donor resulted in a reduction of senescence markers and improved autophagic flux in a SIRT1-dependent manner [136]. H_2S also influences synaptic plasticity, as shown by Abe & Kimura's work on H_2S-facilitated long term potentiation (LTP) [45]. Thus, stimulation of N-Methyl-D-aspartic acid (NMDA) receptors in active rat hippocampal synapses was augmented by AdoMet, a CBS activating compound [45]. More recently, Lu and colleagues [137] screened a group of aged mice on cognitive ability and showed CBS protein levels were significantly lower in the group with impaired cognition and that the cognitive impairment in these mice was rescued following administration of a H_2S donor (NaHS). These effects were associated with altered sensitivity of metabotropic glutamate receptors to local calcium levels [137], likely due to H_2S modulation of neuronal calcium homeostasis [138]. Similarly, the ability of rats to learn an adaptive associative response to fear conditioning was dependent on endogenous H_2S production by CBS [139]. When CBS was inhibited by hydroxylamine or amino-oxyacetate, amygdalar and hippocampal H_2S levels were reduced, NMDA-receptor mediated LTP was significantly impaired, and cued fear conditioning responses were dampened. All these

effects were rescued by application of H_2S donor compounds, even in the presence of CBS inhibitors, indicating that the loss of H_2S production is what mediates these effects. In agreement, a similar reduction in fear conditioning-stimulated LTP due to reduced tissue H_2S production and reversal of this effect by application of a sulfide donor was observed in synaptic plasticity in aged rats [140]. H_2S also modulates the biological response to ischemic stroke, which accounts for over 80% of all strokes [141]. Both endogenous and exogenous sources of H_2S confer neuroprotective effects at low doses and deleterious effects at higher doses. For instance, H_2S production *via* CBS is greatly elevated following stroke and inhibitors of CBS activity reduced infarct volume in rat models of stroke, whereas administration of H_2S donating compounds increased infarct volume [142]. However, elevated H_2S activity ameliorated deleterious pro-inflammatory response coordinated by microglia, a major contributor to the cerebral IRI pathology. Inhalation of a low dose of H_2S for 3 hours immediately after induced cerebral IRI in rats resulted in suppression of this inflammation response through protein kinase C-dependent reduction in aquaporin 4 protein expression, resulting in a reduction in ischemia infarct size and improved neurobehavioral outcomes [143].

1.3.1.3 Renal ageing

H_2S production in the kidney is driven by CSE and CBS activity with expression of these enzymes concentrated particularly in the proximal tubule [144]. As H_2S production through these enzymes is part of the transsulfuration pathway there is overlap with homocysteine metabolism which is associated with mortality in late-stage kidney disease [145]. Given the kidney's role in filtering blood content, it is unsurprising that they are sensitive to nutritional intake. Various studies demonstrated a link between diet composition and renal ageing, with amino acid content emerging as a key driver. Dietary restriction (DR) is the most well characterised intervention for improving health and lifespan (*see section* 1.3.2.1) and typically involves a reduction in gross calories consumed within a set period [146]. However, recent studies have highlighted a specific requirement for restriction of essential amino acids (EAA) in DR protocols for renal protective effects to occur [147]. In a study by Yoshida *et al*. mice were placed under 'simple DR' (40% reduction in calorie intake) and DR with supplementation of EAAs (DR+EAA) or non-essential amino acids (DR+NEAA)

[148]. They found that while DR and DR+NEAAs groups displayed extended lifespan and protection from tubulointerstitial lesions, these effects were lost in groups subjected to DR+EAA supplementation. More specifically, they found that excluding methionine from the EAA supplementation was sufficient to restore DR-induced benefits in longevity, kidney aging and oxidative stress, and was correlated with an increase in tissue H_2S levels and increased CSE gene expression. Wang *et al.* similarly found that methionine restriction alone was sufficient to extend lifespan and improve markers of renal ageing in mice. Their mechanistic investigations suggest that AMPK-dependent H_2S signalling protected kidney tissue from onset of senescence [149]. Additionally, various histological and functional markers of renal ageing were described in both male and female marmosets between ~3 and 16 years of age, with these changes correlating with an age-associated reduction in CBS protein levels across both sexes, although a significant reduction in H_2S production was observed only in male marmosets [150]. Another major consequence of renal ageing is acute kidney injury (AKI), which is driven in part by IRI [151]. A single incidence of AKI has profound implications for mortality; hospital patients with AKI commonly have 30-40% mortality rates and as high as 60% for AKI patients admitted to intensive care units [152]. Renal IRI can be ameliorated by the action of H_2S and NO signalling which improve blood flow by causing local vasodilation, inhibiting inflammatory cytokines, and reducing ROS production [153].

1.3.2 H_2S in Lifespan Extension

Ageing is plastic and modifiable by a variety of environmental, genetic, and pharmaceutical interventions [146]. This section will consider established lifespan extension interventions and assess the potential mechanistic role of H_2S in their modulation of biological ageing.

1.3.2.1 H_2S in Dietary Restriction

Dietary restriction (DR) is an umbrella term for a panel of interventions that have been known to consistently improve longevity across taxa for more than 100 years [154]–[156]. The conservation of this response suggests an evolutionary origin of longevity through DR, best understood through the framework of the disposable soma, mutation accumulation, and antagonistic pleiotropy theories of ageing, among others [157], [158]. A summary of common dietary restriction protocols is given in **Table 3.** In addition, DR typically confers significant health benefits, and improves late-life health by reducing the incidence and/or trajectory of a number of age-related pathologies, including cognitive decline, metabolic syndrome, cardiovascular disease and many cancers [154], [159]. Many of these health benefits are also observed in non-human primates exposed to life-long DR [159]. However, longevity gained by long term DR comes at the cost of neurological health, with cognitive defects found in rats and atrophy of grey matter volume in primates [160], [161]. Critically, many of the positive health benefits found in model organisms under DR are replicated in humans under DR protocols that carefully supply 100% of essential daily nutrients, but the impact on lifespan is currently unknown [154], [155]. The application of DR as a preventive therapeutic tool in humans is promising [162] but remains a challenge, largely due to the difficulty in avoiding accidental malnutrition. Additionally, DR is known to come at a cost in humans with not inconsiderable drawbacks including infertility, sarcopenia, osteoporosis, and reduced immunity [163]. As such, the challenges of applying DR in the wider human population are prohibitive and we may be better served by gaining an understanding of the mechanisms that underlie DR and designing therapeutics targeting them more selectively.

Table 3 Description of common dietary restriction protocols

Method	Abbreviation	Description
Ad Libitum	AL	Food freely available, potential for overeating and onset of obesity. Often used as a control group.
Weight Maintenance	WM	Animals given small (5-10%) reduction in food to prevent onset of obesity
Dietary Dilution	DD	Inert indigestible component forms part of dietary intake, maintains feed volume but reduces calories
Calorie Dilution	CD	Overall calorific content is reduced, often offset by an increase in dietary proteins
Protein Dilution	PD	Overall protein content reduced. Sometimes limited to essential amino acids
Calorie Restriction	CR	Reduction in overall calorie intake with same food volume. Animal is incapable of meeting total daily energy requirements
Dietary Restriction	DR	Reduction in overall food intake volume, feed composition is same as AL. Animal is incapable of meeting total daily energy requirements
Protein Restriction	PR	Reduction in overall protein intake with same food volume. Sometimes limited to essential amino acids
Methionine Restriction	MR	Restriction of essential amino acid Methionine exclusively. Total calorie and other amino acid intake is the same as AL
Intermittent Fasting	IF	Fasting periods of 24 hours without access to food. Number of fasting periods is 50% or less of the total days in the protocol
Every-Other-Day Feeding	EOD	Fasting periods of 24 hours without access to food every second day.

Our understanding of the mechanisms that underpin the effect of DR on lifespan remain imprecise despite decades of investigations. Several studies identified H_2S as a potentially conserved mechanism underlying DR-induced longevity and healthspan improvements. In a series of seminal papers led by Dr James Mitchell, the positive effects of multiple DR regimes were dependent on elevated H_2S production in yeast, worms, fruit flies and mice [164]–[168]. It is also clear that the effects attributed to DR can largely be recapitulated by the excision of specific dietary components from the diet, even if total calorific intake is maintained [169]. Such interventions include restriction of total protein or tryptophan intake, but perhaps the best studied is methionine restriction, which appears to be closely tied to the transsulfuration pathway and H_2S homeostasis [154]. Lifelong methionine restriction in mice protected against renal senescence and elevated endogenous H_2S production, with complementary *in vitro* assays indicating a mechanistic role for H_2S in this protection [149]. Given that the sulfur-containing amino acids (methionine and cysteine) are the canonical sources for endogenous *de novo* H_2S production, it is perhaps unsurprising that restriction of methionine modulates H_2S production. However, it is counterintuitive that restriction of the dietary source for *de novo* H_2S synthesis ultimately results in elevation of H_2S levels; a conundrum that has several possible solutions but no concrete answer to date [165]. One resolution to this apparent contradiction is that DR reduces hypothalamic-pituitary signalling, which functions partly through the inhibition of H_2S production by growth hormone and thyroid hormone at the transcriptional and protein levels respectively [170]. As such, DR-mediated reduction in growth and thyroid hormone release may reduce inhibition of H_2S production enzymes. One alternative explanation for the observation that reduced calorie intake elevates H_2S levels despite reduced pools of SAAs is that elevation of autophagic processes under nutrient-limiting conditions generates the substrate pool for H_2S biogenesis. DR and fasting interventions have been shown to elevate autophagy processes across tissues in mice and humans [171]. Indeed, induction of H_2S biogenesis under DNA damage stress has been demonstrated to be a autophagy-dependent response *in vitro* [172], and cysteine pools are maintained through autophagic processes in pancreatic cancer [173]. Methionine has also been shown to indirectly inhibit induction of autophagy by elevating S-adenosylmethioine (SAM) levels, which in turn promotes methylation of protein

phosphatase 2A, leading to autophagy inhibition[174]. Together, these studies support the premise that elevated autophagy replenishes the cellular cysteine pool, allowing for the generation of H_2S under nutrient-limiting conditions. More studies that directly measure H_2S levels under such conditions are required to definitively support this.

1.3.2.2 H_2S in Dwarf Mouse Models

Beyond dietary interventions, various mutations in model organisms confer significant longevity and healthspan benefits. In fact, the Ames dwarf mouse has the longest extension in lifespan achieved by genetic, dietary, or pharmaceutical intervention with mean and maximal lifespan increase of over 45% in both sexes [175]. The dwarf mouse models have genetic disruption of anterior pituitary gland function either through mutations in transcription factors like Pit1 and Prop1 (as in the Snell and Ames dwarf mice models, respectively) or in growth hormone signalling receptors such as growth hormone receptor and growth hormone releasing hormone receptor, both of which result in long lived dwarf mice [175]–[177]. There have been relatively few studies that tie the reduced pituitary signalling phenotype to the action of H_2S, with the notable exception of Hine *et al*. who showed that both the Snell and Ames dwarf models had upregulation of H_2S production pathways [170]. This is in part due to ablation of the transcriptional regulation of CSE and CBS expression by thyroid hormone signalling and through substrate availability control by autophagic processes respectively, in Dwarf mice [170]. This correlates well with previous research that used labelled metabolites to demonstrate an increase in flux of methionine through the transsulfuration pathway in Ames mice [178]. These studies unveiled a rerouting of metabolism through transsulfuration in the liver, brain, and kidneys of the mice with a concomitant, but non-significant, increase in hepatic CSE gene expression compared to wild type controls [178]. Hepatic CSE specific activity is also elevated in Ames mice [179]. The expected result of this altered metabolism is that the Ames mice will have an elevated pool of cysteine from which H_2S can be generated, which may contribute to the findings of Hine *et al*. that these mice have improved H_2S production capacity [170]. Interestingly, while restriction of dietary methionine extended lifespan and increased hepatic H_2S levels in many models, the Ames models showed no increased lifespan on a methionine-restricted diet [180]. H_2S levels have not

been measured in Ames mice under methionine-restricted conditions, however Brown-Borg *et al*. showed that much of the rerouting of metabolic processes through transsulfuration observed in Ames mice was unaffected by methionine restriction [181]. This was opposed to the expected upregulation of transsulfuration as seen in wild-type animals on methionine restriction [181]. From this we could infer that intact growth hormone signalling is essential for 'sensing' dietary amino acid abundance and plays an important role in coordinating altered metabolism in response to differential methionine abundance. Further work is required to assess if H_2S plays a role in this proposed mechanism for growth hormone regulation of methionine metabolism as well as in the extraordinary lifespan extension of growth hormone mutant mice.

1.3.3 H_2S in Longevity through Pharmaceutical Intervention

Longevity is plastic in response to a variety of pharmaceutical interventions, and chief among these are inhibitors of nutrient sensing pathways such as Rapamycin (targets mTOR signalling), and the anti-diabetic drugs Metformin (targets AMPK signalling) and Acarbose (targets IIS signalling) [154]. H_2S signalling overlaps with all of these mechanisms.

1.3.3.1 Rapamycin and mTOR Signalling

Within the context of mTOR signalling, H_2S can be either stimulatory or inhibitory, as recently reviewed [182]. This is counterintuitive as both H_2S and Rapamycin were implicated as pro-longevity molecules and therefore we might anticipate they would both act upon the mTOR pathway in a similar manner i.e. suppression of mTOR activity. This is the case in some instances, such as a study in brain tissue from diabetic mice where treatment with a H_2S donor elevated protein synthesis by inhibiting mTOR signalling and increasing autophagic processes [183]. Further, exogenously increased H_2S concentration induces autophagy in cells and is associated with inhibition of TOR activity [184], [185]. However, contradictory studies showed an anti-autophagic role for H_2S *via* mTOR signalling with myriad effects ranging from rescuing high-fat diet induced liver disease, protecting against diabetic myopathy, stimulating angiogenesis, and stimulating osteoclastogenesis [186]–[189]. Along with conflicting results in mTOR signalling, we lack a full appreciation of the effect of Rapamycin on H_2S production pathways. To date only one study has investigated this, using Rapamycin in *Saccharomyces cerevisiae* and human cells [190]. The authors found that Rapamycin inhibited H_2S production through depression of CSE and CBS gene transcription in both cell models, indicating a conserved role of Rapamycin in regulating H_2S generation [190]. More work is required to test how conserved this response to Rapamycin treatment is across tissues and species. There also remains a lack of studies that combine Rapamycin and H_2S-donors. Such approaches offer an additional understanding of how these compounds co-interact with mTOR signalling. One example of such an approach used a human hepatocellular carcinoma cell line and treatment with Rapamycin and a H_2S-donor separately or in combination [191]. Wang *et al.* also found that both treatments inhibited mTOR signalling and stimulated anti-tumour autophagic and

pro-apoptotic pathways and were additive when used in combination. The sum of work performed by researchers has confirmed the theory that longevity through Rapamycin inhibition of mTOR is subject to regulation by H_2S. However, further studies are required to dissect out the precise conditions where H_2S modulates mTOR in alignment with Rapamycin, in opposition, or whether there is a more nuanced interaction between these molecules.

1.3.3.2 Metformin and AMPK signalling

Metformin is another putative lifespan-extending drug that interacts with H_2S signalling. Metformin's mechanism of action remains only partially resolved, but appears to operate largely through activation of AMPK (which in turn inhibits mTOR and IIS signalling pathways) [192]. Early studies showed that there was a correlational link between metformin treatment in mice and elevation of H_2S levels in brain, heart, kidney, and liver tissues [193]. Following this discovery, the role of H_2S in the pharmacological activity of AMPK signalling and metformin treatment was studied in earnest and this body of work was collected in a 2017 review [194]. How metformin increases H_2S levels is becoming increasingly apparent and appears related to the ability of metformin to remodel DNA methylation patterns [195]. Work by Ma *et al*. showed that a high methionine diet (methionine forming 2% of diet) resulted in elevation of plasma homocysteine levels and a reduction in plasma H_2S levels, effects that were rescued by metformin treatment [196]. Complementary cell culture assays suggest that metformin treatment removes homocysteine-stimulated hypermethylation of the *CSE* promotor region, resulting in greater mRNA and protein expression of CSE and elevation of H_2S production [196]. Similarly, a metabolomics study in rats found that metformin treatment ameliorated oxidative liver damage caused by exposure to bisphenol A through elevation of CSE and CBS levels [197]. Our emerging understanding of the transcriptional control of H_2S producing genes presents a clear connection between metformin and H_2S production. However, as the modes of action of metformin remain only partially understood, more work is required to fully understand the interplay between H_2S, AMPK signalling, and metformin.

1.3.3.3 IIS signalling

Acarbose inhibits carbohydrate digestion and glucose absorption and is known to extend maximum lifespan in male and female mice, but only extends median lifespan in males [198]. There is currently a lack of studies interrogating the interaction of Acarbose with H_2S. This presents a potentially fruitful area of novel research as H_2S is already known to modulate insulin signalling and whole-animal glucose metabolism across tissues, cellular processes that appear intimately linked with longevity [199]. As with other signalling pathways, the effects of H_2S are complex, with independent studies reporting either protective or deleterious effects [200]. The endogenous production of H_2S in adipose cells was first described by Feng *et al.* who showed that elevated CSE expression and H_2S production was correlated with insulin resistance in rats, suggestive of a deleterious diabetic phenotype associated with H_2S expression in adipocytes [201]. Similar results were found in a hepatocyte cell line and primary mouse hepatocyte studies which showed that supraphysiological levels of H_2S, either through H_2S donor compounds or adenovirus-induced overexpression of CSE, negatively impacted glucose uptake and storage as glycogen [202]. These effects were attributed in part to inhibition of both the AMPK and IIS signalling pathways [202]. Finally, pancreatic beta-cells under chronic exogenous H_2S treatment exhibited suppression of insulin secretion and were protected against oxidative stress-induced apoptosis *via* elevated glutathione content and reduced ROS [203]. The authors suggest that this cytoprotection may constitute a homeostatic response to maintain islet beta-cell numbers in the presence of cytotoxic extracellular glucose concentrations (which is common in patients with uncontrolled Type 1 diabetes), but at the cost of reduced insulin secretion [203]. However, many other studies implicate a protective role of H_2S in insulin signalling pathways. Studies in a mouse myoblast cell model of insulin resistance found a reduction of H_2S production, despite elevation in CSE protein levels [204]. Treatment of these cells with exogenous H_2S improved insulin sensitivity and mitochondrial function in part through phosphorylation and activation of the insulin receptor pathway [204]. CSE activity and H_2S production in adipocytes also mediated translocation of glucose transporter 4 (GLUT4), an essential step in the effective uptake and utilisation of glucose [205]. Work by Xue *et al.* showed that H_2S donor treatment increased activation of insulin receptor and improved glucose uptake in adipocytes and myocytes and that chronic H_2S donor

treatment decreased blood glucose, improved insulin sensitivity and glucose tolerance, and elevated phosphorylation of insulin signalling pathway enzymes in a diabetic rat model [206]. However, the beneficial effect of H_2S donors on whole animal carbohydrate metabolism is contradicted by Gheibi *et al.* who showed that chronic administration of H_2S donor compounds in a type 2 diabetic rat model resulted in dose-dependent impairment of glucose tolerance, pyruvate tolerance, and insulin secretion [207]. These two rat studies underline the importance of H_2S donor concentration in interpretation of the biological effects of H_2S. The Xue *et al.* paper used NaSH over the range of 168-670 μg/Kg/day for 10 weeks, whereas the Gheibi *et al.* study used a higher range of 280-5600 μg/Kg/day for 9 weeks. The majority of the deleterious effects of chronic NaHS treatment reported by Gheibi *et al.* were found in the highest dosage groups, indicating that their treatment range may well approach the dosage at which NaHS begins to confer deleterious or toxic side-effects. The often-contradictory work compiled to date shows that the interaction between H_2S and the molecular, cellular, and physiological role of insulin signalling remains poorly understood and contradictory. As such, any potential overlap between H_2S and Acarbose in improving longevity and late-life health remains unresolved and more work is required to investigate this potentially lucrative signalling commonality.

1.4 The Potential for H_2S Therapeutics against Ageing

With the accumulated evidence that H_2S is central to physiology and pathology across species and tissues, the inevitable question is whether we can leverage our understanding of H_2S to design translational interventions, potentially even as a treatment against ageing [208]. Studies that show clinically relevant roles for H_2S in age-related diseases have fuelled this discussion. One such example is critical limb ischemia (CLI), the end stage of peripheral arterial disease which is fast becoming a major morbidity in the aging population, with incidence increasing at twice the rate of global population growth and a higher global incidence than cancer, dementia, HIV/AIDs, and heart failure [209]. Islam *et al.* examined gastrocnemius tissues sampled from post-amputation limbs of patients with CLI to interrogate regulation and signalling of H_2S in these patients [210]. CLI patients showed decreased transcription of CSE, CBS, and MPST mRNAs, reduced H_2S and sulfane sulfur levels, a reduction in NRF2 activity and transcription of its target genes such as catalase and glutathione peroxidase and an increase in markers of oxidative stress such as malondialdehydes and protein carbonyls [210]. While their study was limited by the difficulty in obtaining human control samples from amputees without CLI, the results show a potentially pathological role of dysregulated H_2S production and signalling in a clinical setting. Further work is required to develop this understanding and attempt H_2S-based therapies for this growing clinical population. Another major clinical presentation in the ageing population is the increased risk of osteoporosis. A genome wide association study (GWAS) identified nonsynonymous single nucleotide polymorphisms in the H_2S oxidising enzyme gene SQR as a susceptibility variant in postmenopausal osteoporosis in Korean women [211]. Validation studies in a preosteoblast cell line found overexpression of this variant improved markers of osteoblast differentiation [211]. The study did not have a direct measure of H_2S in individuals with this variant and so could not determine for certain if the variant resulted in an increase or decrease in the H_2S oxidation activity of SQR. Nonetheless, this implicates H_2S in osteoblast maintenance. This is supported by other studies that have described conflicting roles for H_2S in bone remodelling [212], [213]. Further, a GWAS meta-analysis of age-related hearing impairment identified CSE as one of the 7 loci that was reproducibly identified as a candidate in the onset of hearing loss [214], while

another identified a variant in the promotor region of CBS in peripheral neuropathy caused by chemotherapy treatment of multiple myeloma [215]. These studies help foster the potential for H_2S-based therapies as they suggest a role for H_2S in many age-related pathologies and provide novel targets for drug development.

The emerging understanding of how H_2S exerts influence over clinically relevant biological processes raises hopes for the development of a new class of therapeutics. However, several major obstacles prevent this from being immediately achievable. The chemical nature of H_2S itself poses the greatest challenge to its use as a therapy. The volatility of H_2S impedes its study in basic research as H_2S gas readily escapes into the air on the bench. Further, as H_2S reacts so readily with a wide range of other chemical species, it would prove challenging to control off-target effects in a potential H_2S-based therapy. Of greatest concern, however, is the powerful inhibition of COX by H_2S. It has been proposed that the regulation of H_2S production and oxidation is so well conserved across species largely due to the necessity to precisely modulate intracellular H_2S levels to avoid toxicity by COX inhibition. There may be some hope, however, that chronic administration of H_2S need not be toxic. Reed *et al.* investigated cognitive outcomes in the urban population of Rotorua, New Zealand where residents have been exposed to unusually high atmospheric concentrations of volcanic H_2S for decades [216]. As H_2S is a known environmental toxin, they spilt the study population into quartiles based on estimated H_2S exposure, with the hypothesis that the highest exposure quartile (31-64 ppb) would have reduced cognition compared to the lowest quartile (0-10 ppb). However, they found that areas of the city with the lowest exposure to ambient H_2S had no significant reduction in measures of cognition while those exposed to the highest levels of ambient H_2S actually showed better performance in reaction time and the digit symbol tests [216]. Related studies on the population of Rotorua found no association between H_2S exposure and asthma risk, peripheral neuropathy, cancer incidence, and actually indicated a potential protective effect against Parkinson's disease [217]–[220]. While these studies are indicative of safe, long-term exposure to H_2S in humans, there are limitations in their design including the difficulties in estimating the ambient H_2S levels throughout the decades, misclassification of individuals into the wrong

exposure group, and it is impossible to confirm causality for any of the observed effects as the studies were epidemiological in nature. These limitations necessitate further study to best understand the therapeutic window for safe and effective H_2S exposure. The challenges of H_2S therapies and the positive and negative considerations for each of the established H_2S-donating compounds was reviewed recently [221]. Given these challenges, any progress in the development of H_2S therapies is contingent on better measurements of tissue H_2S concentrations *in vivo*, improved resolution of flux through H_2S production, oxidation, and signalling, establishment of the therapeutic window for H_2S compounds, and innovations in the administration and targeting of H_2S in therapies. These are not insubstantial open questions for the field but given the rapid rise in interest of H_2S biology in recent years, our understanding of these questions is likely to expand greatly.

1.5 Future Directions and Conclusions

Increasing evidence shows that H_2S is integral to multiple healthspan- and lifespan-extending interventions, whether dietary, pharmacological, or genetic in nature. This is due to the capability of H_2S to participate in a multitude of biological processes by virtue of its diverse signalling modalities. There is a high degree of evolutionary conservation across taxa to produce H_2S itself through the transsulfuration pathway and in the signalling pathways it interacts with. Together, these attributes implicate H_2S as a powerful modulator of healthspan, severity of disease, and longevity. However, there are many aspects of our understanding that remain vague. Most prominently, due to the short half-life and chemical promiscuity of H_2S it is extremely challenging to obtain accurate measures of H_2S and related chemical species *in vivo*. This limitation means that while we are increasingly certain of a correlation between H_2S and various markers of longevity, it is difficult to ascertain which specific chemical species confers the observed effects and where these effects are occurring at the tissue, cellular or even sub-cellular level. In addition, while this review has focussed on the many beneficial effects of H_2S, it should not be forgotten that excessive levels of H_2S are extremely toxic in biological systems. As such, future research should focus on better understanding the precise mechanisms by which H_2S operates and the development of more sophisticated methods for measuring *in vivo* H_2S levels. Only once these advancements are made can we begin in earnest to work towards H_2S-based therapeutics.

Chapter 2 Methods and Materials

2.1 Mouse models

2.1.1 ILSXISS recombinant inbred mouse strains, dietary restriction and experimental design

The ILSXISS strains TejJ89, TejJ48 and TejJ114 were purchased from the Jackson Laboratory (Bar Harbour, Maine, URL: http://www.informatics.jax.org) as breeding pairs and experimental cohorts subsequently bred at The University of Glasgow. As previously discussed [222], female mice from strains TejJ89, TejJ48 and TejJ114 showed repeatable directional effects (TejJ89 lifespan extension under DR, TejJ48 lifespan unaffected under DR, TejJ114 lifespan shortening under DR) on lifespan following 40% dietary restriction (DR) across 2 independent studies, but that no strain-specific differences in lifespan were reported when these mice were maintained on an *ad libitum* (AL) diet [223], [224]. It should be noted that several potential shortcomings to experimental design of these original studies have been identified [225], not least that 40% DR may simply be sub-optimal in TejJ48 and TejJ114, and that lifespan extension in these strains is likely to be seen at a higher or lower level of DR; these dose-response experiments are still to be undertaken [225]. However, for the purposes of this study I was interested in whether there was a relationship between H_2S production and reported lifespan under 40% DR. Female mice were used for all experiments because lifespan was only determined in females across both original studies [223], [224]. In addition, I also examined components of the H_2S signaling network in female C57BL/6J mice that followed a similar long-term 40% DR protocol, to further examine potential strain-specific effects. It has previously been shown that hepatic H_2S production is increased female C57BL/6J mice under 40% DR [226]. All mice were maintained from weaning onwards at 22±2°C and on a 12L/12D cycle (lights on 0700–1900h) in groups of 4 mice within shoebox cages (48cm×15cm×13 cm), with AL access to water and standard chow (CRM(P), Research Diets Services, LBS Biotech, UK; Atwater Fuel Energy-protein 22%, carbohydrate 69%, fat 9%). 10% DR was introduced in a graded fashion from 10 weeks of age and then held at 40% DR from 12 weeks onwards, with the food intake of the DR cohorts was adjusted on a weekly basis relative to the average weekly AL food intake of the appropriate (strain-specific) AL controls [222],

[227]. Following 10 months of 40% DR (13 months of age) female mice were fasted overnight and culled using cervical dislocation under a UK Home Office Project Licence (60/4504) and following the “principles of laboratory animal care” (NIH Publication No. 86-23, revised 1985). Tissues were immediately dissected out, snap-frozen in liquid nitrogen and stored at −80°C until use.

2.1.2 Hutchinson Gilford Progeria Syndrome (HGPS) animal model, high-fat diet, and experimental design

Mice carrying the human HGPS single-base mutation ($LMNA^{G609G-/+}$) were generated on a C57BL/6N background by Prof. Carlos López-Otin (Universidad de Oviedo, Spain) [228]. Heterozygous $LMNA^{G609G-/+}$ female and male mice were obtained from the Otin lab and subsequently bred in the laboratory of Prof. Susana Gonzalo (Saint Louis University, MO, US) to generate wild type (WT) control mice and homozygous $LMNA^{G609G+/G609G+}$ mice, referred to simply as G609G mice hereafter [229]. All animal studies were approved (protocol #2299) and conducted in accordance with the Animal Studies Committee at Saint Louis University. Mice were housed at a constant temperature of 23°C with food and water provided *ad libitum* under a 12:12 light-dark cycle. Litter mates of G609G genotype were randomly assigned into one of two diet groups and fed either regular chow (RC) or high fat diet (HFD) immediately post-weaning (approximately 3 weeks of age)- diet composition for diets is provided in **Table 4**. Mice were culled by cervical dislocation at either 70 days (WT, males, n=4), 100 days (G609G RC, females, n=4) or 150 days (G609G HFD, females, n=4). Immediately following death, the liver was collected, snap-frozen in liquid nitrogen and stored at -80°C. Tissue samples were subsequently shipped to University of Glasgow for analysis.

Table 4 Composition of regular chow and high fat diet [229]

	Regular Chow (RC)	High fat diet (HFD)
Supplier	LabDiet	ResearchDiets
Diet Reference Number	5053	D12492
kcal/g	3	5.2
Protein (% kcal)	24.5	20
Carbohydrates (% kcal)	62.4	20
Fat (% kcal)	13.1	60

2.1.3 RNA Polymerase III heterozygous knock out animal model

2.1.3.1 Dietary restriction and experimental design

C57BL/6N-Polr3bem7(IMPC)Tcp mice (henceforth referred to as Polr3b Het KO mice) were generated by The Centre for Phenogenomics (Toronto, Canada) as breeding pairs and experimental cohorts subsequently bred at The University of Glasgow. Mice were maintained from weaning onwards at 22±2°C and on a 12L/12D cycle (lights on 0700–1900h) within individually ventilated cages (48cm×15cm×13 cm), with AL access to water and standard chow (CRM(P), Research Diets Services, LBS Biotech, UK; Atwater Fuel Energy-protein 22%, carbohydrate 69%, fat 9%). For mice in the dietary restriction experiment, n = 8 mice from WT or Het genotypes were assigned into DR or AL groups at 7 months of age such that there was no difference between mean body weights in each group. 1 mouse in the Het DR group was culled due to recurrent severe dermatitis and genital ulceration before onset of DR feeding. The DR groups were kept individually housed for an adjustment period of 4 weeks. DR groups were fed daily a fraction of the daily intake of their AL control cohorts. Specifically, DR groups were fed a 10% reduction in food intake by weight compared to AL control groups for 1 week, followed by a 20% reduction in food intake by weight compared to AL control groups for 1 week, and finally a 40% reduction in food by weight compared to AL control groups for 4 weeks. The food intake of the AL groups was measured weekly. Prior to culling all mice were fasted overnight and their body weight and recorded. Body temperature was also recorded by restraining mouse and measuring body temperature just above genitals using a TZP No Touch infrared thermometer (The Packaging Zone, England, UK). Mice were culled using cervical dislocation under a UK Home Office Project Licence (PDBDC7568) and following the “principles of laboratory animal care” (NIH Publication No. 86-23, revised 1985). Tissues were immediately dissected out, snap-frozen in liquid nitrogen and stored at −80°C until use.

2.1.3.2 Genotyping

The Polr3b Het KO mice have an 8bp insertion in the Polr3b gene, close to the start of exon 6 (TCCAGTGT at Chromosome 10 positive strand 84632456 bp, GRCm38) which is predicted to cause a frameshift mutation with early truncation (c.305_306insTCCAGTGT; p.R103Pfs*3). Primers were designed to carry out PCR specific for the WT or mutant allele (**Table 5**). The forward primers for both WT and mutant sequences recognise a site present in both the WT and Het alleles, while the reverse primers are specific for either WT or Het allele but should not bind to both. Some non-specific bands are produced by the Het primers in WT samples, but these are bigger than the expected PCR product. DNA was isolated from mouse ear samples by digestion in 500 uL lysis buffer (100 nM Tris, 5 mM EDTA, 0.2% SDS, 200mM NaCl, pH 8.5) supplemented with 10 uL proteinase K (25 mg/mL) for 3 hours at 55ºC. Solutions were centrifuged at 13,000 g for 20 min at 4ºC. The supernatant was reserved to a fresh tube containing 500 uL chilled isopropanol and inverted gently three times. This solution was centrifuged at 13,000 g for 20 min at 4ºC to produce a DNA-containing pellet. The supernatant was discarded, and the pellet was resuspended in 500 μL of 70% ethanol. The solution was centrifuged again at 13,000 g for 5 min at 4ºC, the supernatant was discarded, and the pellet was allowed to air dry for 3 hours. The pellet was resuspended in 100 μL TE buffer (10mM Tris, 1 mM EDTA, pH 8.0), incubated at 37ºC for 30 min, and then stored at 4ºC. The DNA sample was diluted 1:10 before PCR genotyping. Cycling conditions for PCR were: initial denaturing at 95ºC for 10 mins, followed by 35 cycles at 95ºC for 30 sec, 53ºC for 35 sec, 72ºC for 65 sec. After cycling a final extension at 72ºC for 5 min was performed and samples were stored at 4ºC until run on a 2% agarose gel for 90 min with 100 bp ladder and visualised by ultraviolet transillumination in a ChemiDoc imager (BioRad, CA, US). Representative images of PCR products are shown in **Figure 4**. Ear samples were taken from all experimental mice at time of cull and genotype confirmed by this method.

Table 5 Primer sequences for genotyping WT and Polr3b Het KO mice

Target Allele	Forward Primer	Reverse Primer	Expected band size (bp)
WT	AGGCTGCTGTGCACTGTATT	GACGGCACTGGAGCAGAAT	82
Polr3b HET KO	TCAGTGGGGAAAGTTCAGGC	TCAGACGGACACTGGACACT	110

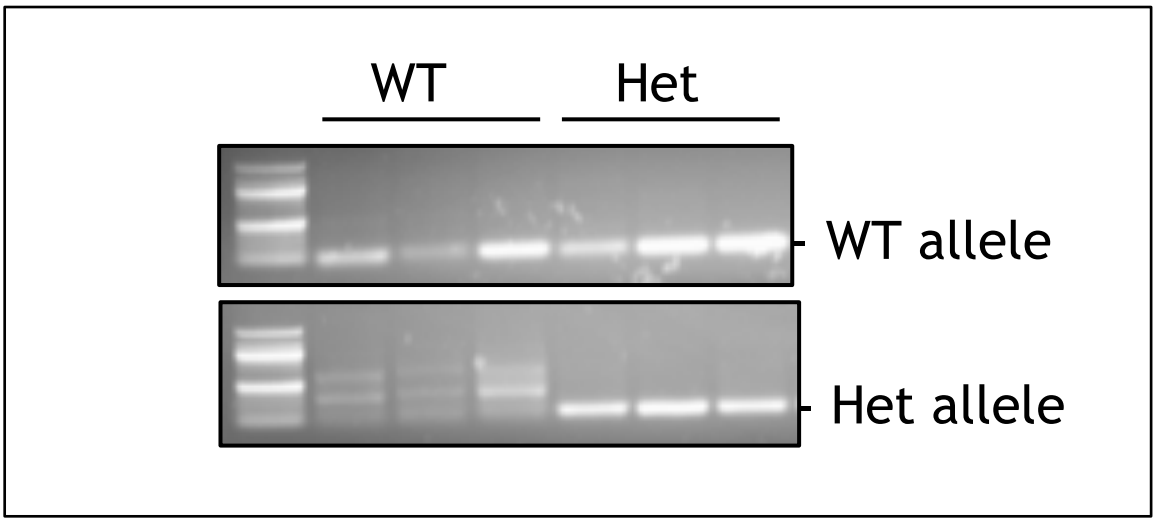

Figure 4 Genotyping of Polr3b Het KO mice

Representative genotyping PCR of WT and Het mouse DNA derived from ear samples. The top panel shows results for PCR amplification of the WT *Polr3b* allele. The bottom panel shows PCR amplification for the mutant *Polr3b* allele.

2.1.1 Assignment of mice into experimental groups

Prior to dietary restriction (DR), wild-type (WT) and Polr3b heterozygous knock-out (Polr3b Het KO) mice were assigned into experimental groups at 7-months of age and individually housed. These experimental groups were WT mice on *ad libitum* (AL) diet (WT AL), WT mice on DR (WT DR), Polr3b Het KO mice on AL (Het AL), and Polr3b Het KO mice on DR (Het DR). Mice were allocated into each experimental group within a genotype such that there was no difference in mean body weight between groups (Error! Reference source not found.**a**) at the start of the experiment. Two-way ANOVA analysis found no significant diet ($F(1,28) = 0.060$, $p = 0.808$) or genotype ($F(1,28) = 0.051$, $p = 0.823$) effect on mean initial body weight prior to onset of the experiment. Food intake over 1 week was measured for each mouse on AL diet and the average daily food intake was calculated (Error! Reference source not found.**b**). An unpaired t-test found no significant difference between the average daily food intake of WT AL mice compared to Het AL mice ($p = 0.326$) over a 1-week monitoring period prior to onset of DR protocol.

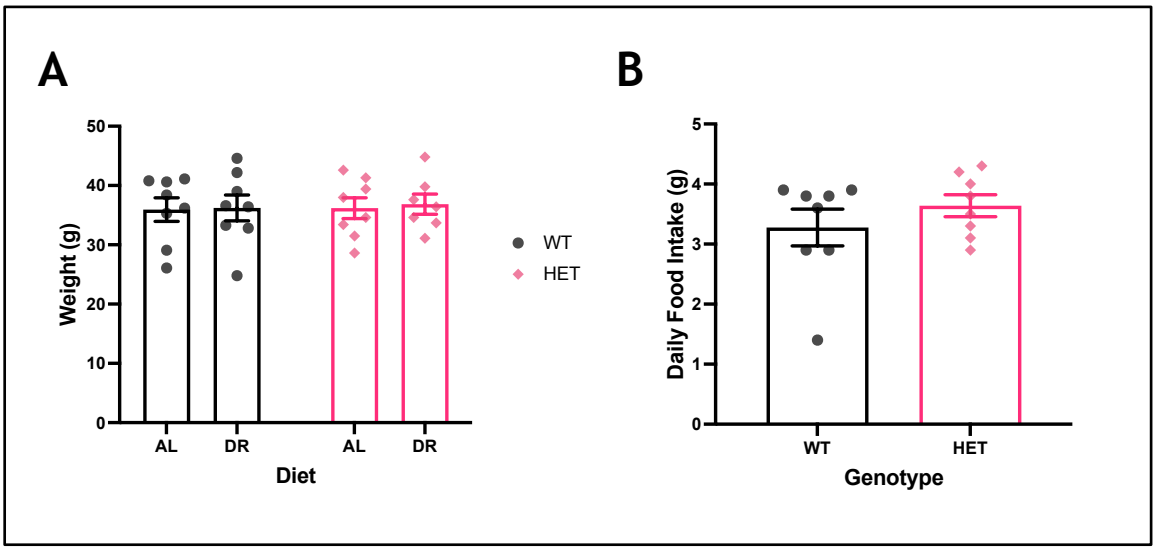

Figure 5 Experimental groups were assigned so there was no difference in mean body weight prior to onset of DR protocol

A Mean body weight prior to onset of DR protocol. B Average daily food intake of AL-fed mice measured over 1-week prior to onset of DR protocol. WT data in black, Het data in pink. Bars represent mean values. Error bars represent standard error of the mean.

2.2 Hydrogen sulfide (H_2S) measurements

2.2.1 Lead acetate assay of H_2S production capacity

Measurement of H_2S levels was performed in liver homogenates according to the previously described method [230]. Briefly, 100 mg of flash-frozen liver tissue was lysed in passive lysis buffer. Protein concentration was determined by BCA assay (G Biosciences, MO, USA) and 100 ug of protein was loaded into a 96-well plate. 150 uL of reaction solution containing 10 mM L-cysteine and 1 mM pyridoxal-5'-phosphate was added to the protein. Filter paper that had previously been cut to the size of the plate, soaked in 20 mM lead(II)acetate trihydrate for 20 min, then dried under vacuum, was then securely attached to the plate. The assembled plate was incubated at 37°C for 1 hr. H_2S sulfide gas produced during this time collects in the head space between the top of the solution in the well and the lead(II)acetate paper, forming a brown-black substrate on the paper. The amount of H_2S generated in each sample was quantified by densitometry analysis of the brown-black substrate (ImageJ).

2.2.2 Mito A measurement of mitochondrial H_2S Level

MitoA and MitoN were quantified in mouse blood using liquid chromatography tandem mass spectrometry (LC-MS/MS). Mice received a tail vein IV injection of 50 nM mitoA in 0.9% saline (100 µL). MitoA was given 1.5 hr to distribute into mitochondria. Mice were culled by cervical dislocation 90 min after administration. Liver was excised and flash frozen in liquid nitrogen. MitoA and MitoN were extracted from tissue by homogenization of liver (50 mg) enriched with 5 pg d15-MitoN (95% ACN, 210 µL) which was used as an internal standard (IS). Homogenates were centrifuged (16,000 g, 10 min, RT) and the supernatant was transferred to a clean tube and stored on ice. The pellet was re-extracted (95% CAN, 210 µL), spun down again (16,000 g, 10 min, RT) and the supernatants were combined and incubated at 4°C for 30 min. Calibration standards comprise MitoA and MitoN standards ranging from 0.01 to 10 pg in 500 µL 95% ACN. 500 µL of the supernatants and calibration standards were loaded onto an ISOLUTE PLD+ protein and phospholipid removal plate (Biotage, Sweden). Samples and standards were pulled through the plate under vacuum into a 2 mL deep-well 96-well plate. Wells were dried completely at 40°C under N_2 and resuspended in 100 uL 20% ACN, 0.1% FA. The plate was shaken at (250 rpm, 20 min) to ensure reconstitution. Liquid chromatography-Mass Spectrometry was performed on an I-class Acquity LC system-Xevo TQS triple quadrupole mass spectrometer (Waters, Warrington, UK). Samples were kept at 10°C and injected onto an Acquity UPLC BEH C18 column fitted with a 0.2 µm filter (1 x 50 mm, 1.7 µm, Waters). Chromatographic separation of mitoA and mitoN was achieved using mobile phase A composition: water:ACN, (95:5, 0.1% FA), mobile phase B: ACN:water (90:10, 0.1% FA). LC mobile phases were infused at 200 µL/min using the gradient: 0– 0.3 min, 5% B; 0.3–3 min, 5–100% B; 3– 4 min, 100% B, 4.0– 4.10, 100–5% B; 4.10– 4.60 min, 5% B. MS/MS analysis was performed under positive ion mode (Source spray voltage, 3.2 kV; cone voltage, 125 V; ion source temperature, 100 °C). Curtain and collision gas were nitrogen and argon, respectively. Analytes were detected by multiple reaction monitoring (MRM). MitoA undergoes neutral loss of N_2 to a nitrene (precursor ion). For quantification the following transitions were used: MitoA, m/z 437.2 →183.1; MitoN, m/z 439.2 → 120.0; d15-MitoN, 454.2 → 177.1 m/z. MassLynx 4.1 software was used to integrate the peak area of the analytes MitoA, MitoN and

the d15-MitoN internal standard. Response was calculated by normalizing sample peak areas to the IS peak area. By comparison of sample responses to calibration standard responses the mass of each analyte in the tissue sample was calculated. The mass of analyte was normalised to the mass of tissue homogenizer and MitoN/MitoA ratio was calculated.

2.3 Reverse Transcriptase quantitative-PCR

RNA was isolated from liver tissue by addition of 500 µL TRIzol (Life Technologies, USA) to sections of liver tissue and homogenized using a glass-glass homogeniser. Samples were moved to screw top Eppendorf and 150 µL chloroform added. Samples were then spun by centrifuge at over 8000 g and the supernatant containing the RNA isolate was taken to a fresh Eppendorf. RNA cleanup was performed according to instructions provided in RNAeasy Mini Kit (Qiagen, Germany), including the optional DNase digestion step. First strand synthesis of cDNA was performed by incubating 2 µg of RNA (quantified by spectrophotometry using Nanodrop 1000 UV-Vis spectrophotometer, ThermoScientific, MA, US) with 0.333 µL 3 µg/µL Random Primer Mix (Invitrogen) in a total volume of 15 µL with RNAse-free water at 70°C for 5 min using a MJ research PTC-200 Peltier Thermal Cycler (Biorad, CA, US). Synthesis of cDNA was then performed by adding 10 µL master mix (1 µL Promega M-MLV reverse transcriptase, 5 µL Promega M-MLV 5x buffer, 5 µL pooled 10mM dNTPs, and 0.625 µL RNAseOUT 40 units/µL) to the first stand sample and heating to 37°C for 1 hour. Samples were then diluted 1:1 with PCR-grade water and used directly for RT-qPCR. RT-qPCR was performed in a 384-well PCR plate. Each well contained 1 µl cDNA, 0.25 µL 10mM upper primer, 0.25 µL 10mM lower primer, 3.5 µL PCR-grade water and 5 µL QuantiFast SYBR green PCR master mix (Qiagen, UK). PCR reaction was performed using a 7900HT Fast Real-Time PCR System (Applied Biosystems, CA, US). PCR profile was as follows: 95°C for 5 minutes; 94°C for 30 seconds, 60°C for 30 seconds, 72°C for 30 seconds for 40 cycles; 72°C for 5 mins. Fold change was calculated following the $\Delta\Delta$Ct method and expressed as $2^{-\Delta\Delta Ct}$. The endogenous control gene was β2M, which has been previously shown to be an appropriate housekeeping control gene for studies that alter diet [231]. Primers were designed using the UPL Library Assay Design Centre (Roche) and BLASTn (NCBI) and primer sequences are provided in **Table 6**.

Table 6 Primer sequences used in RT-qPCR experiments

CBS: Cystathionine-β-synthase, CSE: Cystathionine-γ-lyase, TST: Thiosulfate Sulfurtransferase, MPST: 3-Mercaptopyruvate Sulfurtransferase, ETHE1: Ethylmalonic encephalopathy 1 protein, SUOX: Sulfite Oxidase, 28S: 28S rRNA, 5S: 5S rRNA, 7SL: Signal recognition particle RNA, B1 consensus: primer that binds to approximately 100 B1 family genes, β2M: beta-2 microglobulin

Gene Name	Amplicon (nt)	Length of Intron spanned (nt)	Forward Primer Sequence	Reverse Primer Sequence
CBS	84	903	gctgggcacactctctcac	caggcctggtctcgtgat
CSE	78	985	catgctaaggccttcctcaa	ctcagccagactctcatatcctc
TST	82	5208	ccagctggtggactctcg	gtggcccgagtctagtcct
MPST	85	2772	cttgccgagtgccttcac	gcctaggagatgctcagattg
ETHE1	88	11056	gattccatccgctttggac	ggtcgttcaggacaaaggtg
SUOX	131	257	ttccacaggccatcagagt	ccatctccgagtccttgagt
28s			cccgacgtacgcagttttat	ccttttctggggtctgatga
5S			ggccataccaccctgaacgc	cagcacccggtattcccagg
7SL			gtgtccgcactaagttcggcatcaatatgg	tattcacaggcgcgatcccactactgatc
Pre-tRNA Leu			gtcaggatggccgagtggtctaaggcgcc	ccacgcctccatacggagaccagaagaccc
Pre-tRNA Tyr			ccttcgatagctcagctggtagagcggagg	cggaattgaaccagcgacctaaggatctcc
B1 Consensus			tggtggtgcatgcctttaat	cctggtgtcctggaactcact
β2M	75	-	acagttccacccgcctcacatt	tagaaagaccagtccttgctgaag

2.4 Western blotting

Protein lysate was obtained by homogenisation of liver tissue in 1 mL ice cold RIPA buffer (Radio Immunoprecipitation Assay Buffer; 150 mM sodium chloride, 1% NP-40 or Triton X-100, 0.5% sodium deoxycholate, 0.1% sodium dodecyl sulphate, 50 mM Tris, pH 8) containing protease and phosphatase inhibitors (Halt™ Protease and Phosphatase Inhibitor Cocktail, Thermo Fisher Scientific, UK; phenylmethylsulfonyl fluoride, Sigma Life Sciences, Germany; cOmplete Mini EDTA-free protease inhibitor cocktail, Merck, NJ, US) using a glass-glass homogeniser. Homogenate was left on ice for 40 min and then spun by centrifuge at over 8000 g for 10 minutes at 4°C. The supernatant was collected and used as protein lysate. Protein concentration was assessed by BCA assay (G Biosciences, MO, USA) and 20 ug of protein was loaded per well into homemade 4-12% bis-tris polyacrylamide gels. Precision Plus Protein™ Dual Xtra Standards protein marker (BioRad, CA, US) were added to a well on each gel. Proteins were separated by electrophoresis at 90 V for 90 mins and then transferred onto nitrocellulose membrane at 0.25 V for 1 hour. Membranes were stained with Ponceau-S (Sigma Life Sciences, Germany), briefly washed in deionised water and the resulting total protein stain was captured using a Chemidoc™ XRS System (BioRad, CA, US). The Ponceau-S stain was removed by 1xTBST (Tris-Buffered Saline Tween^{20}) and the membrane was blocked with 5% milk in 1xTBST for 40 min. The membrane was washed 5 times with 1xTBST for 5 mins under constant shaking. Primary antibodies (AbCam, Cambridge, UK) were added to the membrane in 5% BSA in 1xTBST. CSE (ab151769) and ETHE1 (ab174302) primary antibodies were used at 1:1000 dilution, CBS (ab135626), MPST (ab85377), and SQR (ab155320) were used at 1:500 dilution and total OXPHOS rodent cocktail (ab110413) was used at 1:10000 dilution. Phospho-IR/IGF1R (Tyr1162, Tyr1163) Polyclonal Antibody (44-804G, Invitrogen, MA, US) was used at 1:1000 dilution. Primary antibodies were allowed to incubate with the membrane overnight at 4°C, under constant shaking. Anti-rabbit secondary antibody (Anti-rabbit IgG Alexa Fluor 680 conjugate, Abcam ab186696) was used at 1:10000 dilution in 5% BSA in 1xTBST as the secondary antibody for all blots. The secondary was allowed to incubate with the membrane for 1 hour, under constant shaking. The membrane was washed 5 times with 1xTBST for 5 mins, under constant shaking before addition of all antibodies and before imaging by

an Odyssey M Fluorescent imager (LiCor, NE, US). Protein signals were quantified using densitometry software (ImageStudio; LiCor, NE, US) and normalised to the total protein signal of their respective lane.

2.5 Activity assays

2.5.1 MPST activity assay

3-Mercaptopyruvate sulfurtransferase (MPST) activity was determined by measuring thiocyanate production capacity as described previously for Thiosulfate sulfurtransferase (TST) rhodanese activity [232], except that sodium 3-Mercaptopyruvate (3-MP) was used as a substrate instead of sodium thiosulfate. In a 96-well plate, 20 µg of protein lysate in RIPA was mixed with 10 µL 200 mM 3-MP (Santa-Cruz, UK) and taken to 90 µL with 500mM potassium phosphate pH 5.5 buffer. Samples were incubated at 37°C for 2 min before addition of 10 µL 500 mM potassium cyanide. A calibration curve of 50, 25, 10, 5, 2.5, 1, 0.5, 0.25, 0.1 mM potassium thiocyanate solutions was also prepared and exposed to the same conditions as above excluding the addition of potassium cyanide. The reaction was allowed to occur for 5 minutes at 37°C before termination by addition of 11 µL of 38% formaldehyde to all wells. Thiocyanate production was visualised by addition of 125 µL $Fe(NO_3)_3$/26% HNO_3 where an orange-brown solution formed. Results were quantified by measuring absorbance for 460 nm light in a spectrophotometer (Multiscan GO Microplate Spectrophotometer, Thermo Scientific, MA, USA). All samples were performed in duplicate and the average 460 nm absorbance was calculated.

2.5.2 TST activity assay

Thiosulfate sulfurtransferase (TST) rhodanese activity was determined by measuring thiocyanate production capacity as previously described [233]. The assay was performed in a 96-well plate, where 20 µg of protein lysate was added. The reaction was initiated by the addition of 10 µL 500 mM thiosulfate and taken to 90µL with 500mM potassium phosphate pH 5.5 buffer. After a 2 min incubation at 37ºC 10µL 500mM potassium cyanide was added to each sample. A standard curve of 0.1, 0.25, 0.5, 1, 2.5, 5, 10, 25, 50 mM potassium thiocyanate solutions was also prepared following the same conditions as above but without the addition of potassium cyanide. The reaction proceeded for 5 min at 37ºC and was stopped by the addition of 11µL of 38% formaldehyde. Lastly, 125 µL $Fe(NO_3)_3$/26% HNO_3 was added which produced a colorimetric change. Results were quantified by spectrophotometry, measured at 460 nm absorbance. All samples were performed in duplicate, calculating the average absorbance.

2.6 Glucose homeostasis measurements

2.6.1 Blood glucose, insulin, and insulin resistance measurements

Fresh blood was collected from mice at cull following a 15-hour fasting period. Blood glucose measurements were taken immediately from whole blood by OneTouch Ultra Easy blood glucose monitor (LifeScan, CA, US). Plasma was collected from whole blood to determine insulin levels. Plasma was isolated by centrifugation of whole blood at 3000 g for 7 min. Plasma samples were stored at -20^{o}C until insulin concentration was determined by Rat/Mouse Insulin ELISA (Merck Millipore, Sigma Aldrich, EZRMI-13K) following manufactures instructions. Insulin resistance (IR) is estimated using the homeostatic model assessment (HOMA) methodology, HOMA-IR index = [fasted glucose (mmol/L) x fasted insulin (mIU/L)]/22.5) [234].

2.6.2 Glucose tolerance test

Glucose tolerance test (GTT) was performed as described previously [235]. Briefly, 1 week prior to cull, mice were fasted overnight by transferring mice to clean cages with no food or faeces in cage and AL access to drinking water. Mice were weighed and baseline (t = 0) fasted blood glucose (mM) was recorded by blood samples (<5 uL) from caudal vein venesection by scalpel blade. From a 20% D-glucose solution, 2g of glucose/kg body mass was injected intraperitoneally. Blood glucose levels were measured at 15, 30, 60, and 120 minutes after glucose injection by gently reopening caudal vein cut and taking sequential blood samples (<5 uL). At the end of the GTT experiment the mice were provided food and water in their home cage and were observed for any abnormal behaviour. The area under the curve (AUC) of the blood glucose trace for each mouse was calculated using the trapezoid rule and a linear interpolation method from Prism Software (GraphPad, CA, US).

2.7 Statistical Analysis

Unless otherwise stated, all statistical analyses were performed using Prism 6 (GraphPad Inc., La Jolla, CS, USA) software. Data were first analysed by Grubbs outlier test with alpha set to 5%. Any removed outliers are noted in figure legends. Statistical significance was determined by performing 2-way ANOVA analysis with Tukey's correction for *post-hoc* multiple comparison tests. * denotes a *post-hoc* p value of < 0.05, ** denotes a p value of < 0.01, and *** denotes a p value < 0.001, and **** denotes a p value < 0.0001.

Chapter 3 The impact of dietary restriction on hydrogen sulfide levels in female recombinant inbred ILSXISS mice

3.1 Abstract

Modulation of the aging process by dietary restriction (DR) across multiple taxa is well established. While the exact mechanism through which DR acts remains elusive, the gasotransmitter hydrogen sulfide (H_2S) may play an important role. I employed a comparative-type approach using females from three ILSXISS recombinant inbred mouse strains previously reported to show differential lifespan responses following 40% DR. Following long-term (10 months) 40% DR, strain TejJ89 — reported to show lifespan extension under DR — exhibited elevated hepatic H_2S production relative to its strain-specific *ad libitum* (AL) control. Strain TejJ48 (no reported lifespan effect following 40% DR) exhibited significantly reduced hepatic H_2S production, while H_2S production was unaffected by DR in strain TejJ114 (shortened lifespan reported following 40% DR). These differences in H_2S production were reflected in highly divergent gene and protein expression profiles of the major H_2S production and disposal enzymes across strains. Increased hepatic H_2S production in TejJ89 mice was associated with elevation of the mitochondrial H_2S-producing enzyme 3-mercaptopyruvate sulfurtransferase (MPST). These findings further support the potential role of H_2S in DR-induced longevity and indicate the presence of genotypic-specificity in the production and disposal of hepatic H_2S in response to 40% DR in mice.

3.2 Introduction

3.2.1 DR, Hydrogen Sulfide, and Aging

Empirical evidence has existed for over a century that dietary restriction (DR) increases lifespan and healthspan across multiple species [154]–[156]. In mice, significant strain-specific differences in lifespan exist [236], [237] and genetic background may consequently play an important but under-appreciated role in how particular strains respond to DR [225], [226], [238]–[240]. For example, two independent studies have reported that recombinant inbred ILSXISS mice show significant strain-specificity in longevity following 40% DR [223], [224], and phenotypic parameters linked to the ageing process, such as in mitochondrial function and adiposity, have been shown to differ between ILSXISS strains under 40% DR [222], [241]. Precisely how DR facilitates its beneficial effects on lifespan and healthspan have proved challenging to elucidate, although many mechanisms have been proposed [154], [165], [242]–[244]. One such putative mechanism is the gasotransmitter hydrogen sulfide (H_2S). Direct manipulation of H_2S levels through genetic, pharmacological or environmental means can modulate lifespan in invertebrate models [165], [245]–[248] and elevated hepatic H_2S production appears to be a conserved phenotype in long-lived mouse models, including DR and various genetic mutants [170], [226]. Pharmacological elevation of H_2S also ameliorates age-associated atherosclerosis, fibrosis, cognitive decline and kidney dysfunction in rodents [128], [249], [250], partially ameliorates the progeroid phenotype in Werner syndrome fibroblasts [251] and senescence in endothelial cells [252]. Furthermore, DR-induced protection from ischemia-reperfusion injury was abrogated in mice treated with an inhibitor of cystathionase-γ-lyase (CSE), the major hepatic H_2S-producing enzyme [253], and longevity in mice following methionine restriction was associated with increased H_2S production and a reduction in various senescence markers within the kidney [149]. Consequently, it has been proposed that elevation of endogenous H_2S may play a prominent role in the lifespan and healthspan effects of DR [165].

Here, I employed a comparative-type approach [222] in which I determined hepatic H_2S production and levels of key enzymes involved in H_2S metabolism (see **Figure 6**) in female mice from three genetically distinct

recombinant inbred ILSXISS strains exposed to long-term (10 months) 40% DR. These strains have previously been reported to show variable lifespan responses to 40% DR ranging from life-extension to life-shortening relative to strain-specific *ad libitum* controls [223], [224]. The work comprising this thesis chapter has been published in a peer-reviewed journal [254], the published version is included in **Appendix II.**

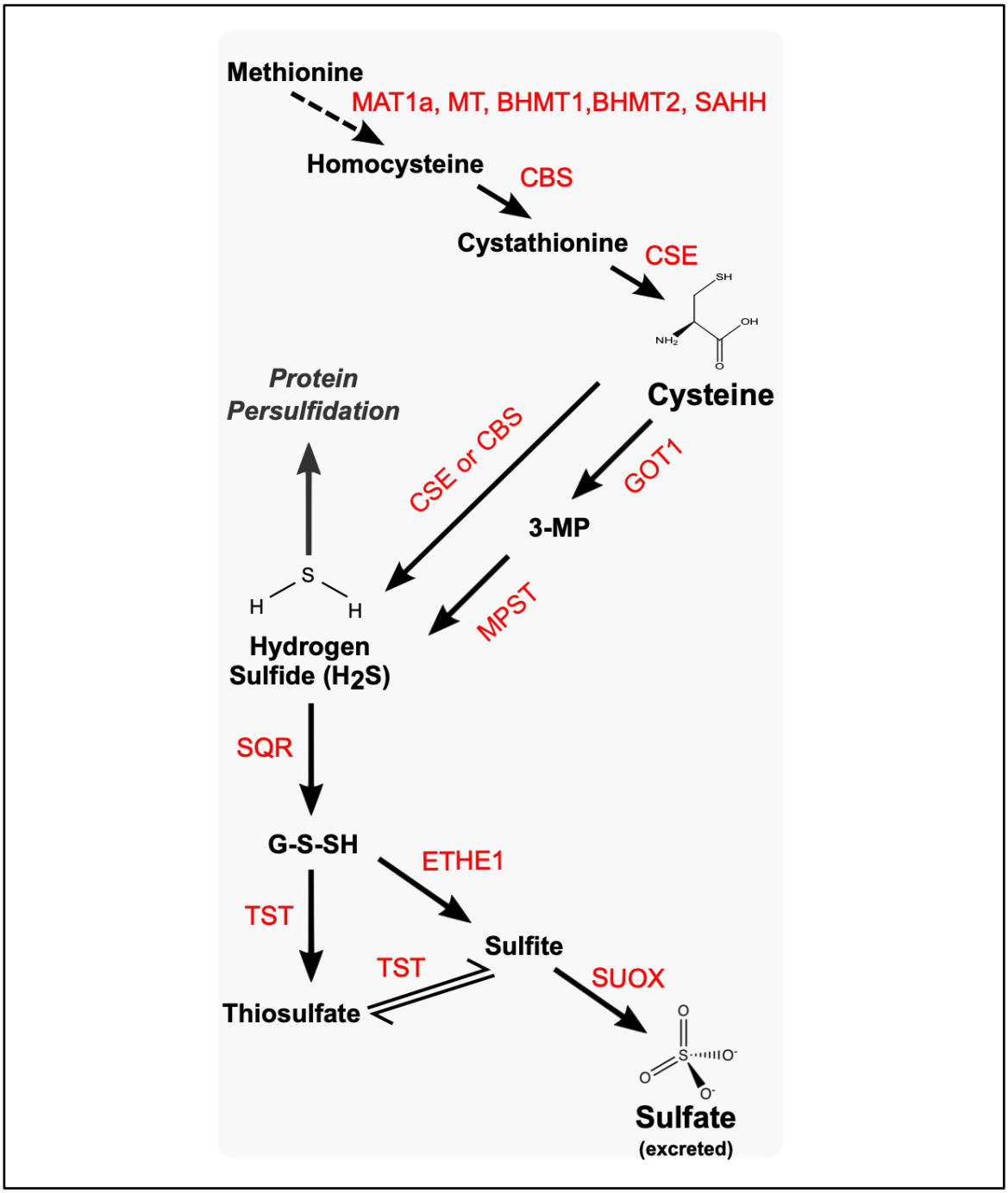

Figure 6 Molecular pathways involved in the production and elimination of H_2S.

Molecular pathways involved in the enzymatic production of H_2S from amino acid metabolism and subsequent elimination of H_2S by components of the sulfide disposal unit. Enzymes in red. MAT1a: Methionine Adenosyltransferase 1A, MT: Methyl transferase, SAHH: S-Adenosylhomocysteine hydrolase, BHMT1: Betaine-Homocysteine S-Methyltransferase 1, BHMT2: Betaine-Homocysteine S-Methyltransferase 2, CBS: Cystathionine-β-synthase, CSE: Cystathionine-γ-lyase, GOT1: Glutamic-oxaloacetic transaminase 1, MPST: 3-Mercaptopyruvate Sulfurtransferase, SQR: Sulfide:Quinone oxidoreductase, TST: Thiosulfate Sulfurtransferase, ETHE1: Ethylmalonic encephalopathy 1 protein, SUOX: Sulfite Oxidase.

3.2.2 ILSXISS Recombinant Inbred Mouse Strains

Breeding of the ILSXISS recombinant inbred (RI) mouse strains was initially developed to aid quantitative trait loci analysis experiments. An eight-way cross of several mouse strains (A, AKR, BALB/c, C3H/2,C57BL, DBA/2, IsBi and RIII) were selective bred for their sensitivity to ethanol [255]. This led to the establishment of two highly inbred strains, inbred long sleep (ILS) and inbred short sleep (ISS). The ILS and ISS strains were cross bred for over twenty generations leading to establishment of a panel of 71 RI ILSXISS strains [255]. This breeding strategy ensured that each sub-strain would possess a unique combination of ILS or ISS haplotype at each genetic loci. For the purposes of this study, ILSXISS strains were exploited for their highly unusual responses to DR regimes. In two independent studies, it was discovered that the majority of the ILSXISS sub-strains were either unresponsive to DR in terms of lifespan or experienced a significant shortening of lifespan under DR [223], [224]. This divergence in response from mice of a distinct yet comparable genetic background presents an invaluable tool to dissect the nature of DR-responses with respect to longevity. This study employed the use of three female ILSXISS mouse strains on 10-month 40% DR: TejJ89 (increased lifespan on DR), TejJ48 (no effect of DR on lifespan) and TejJ114 (decreased lifespan on DR). These strains were selected as they showed reproducible response in lifespan between the two studies and there was no significant difference in lifespan on DR in free-fed *ab libitum* controls. Female mice were used as male ILSXISS lifespan had only been studied in one DR experiment.

3.3 Aims and hypothesis

Hypothesis

Hydrogen sulfide (H_2S) production is essential for dietary restriction (DR) benefits to manifest in ILSXISS strains. As previous reports have found that ILSXISS strains experience divergent responses to DR with respect to lifespan, I hypothesis they will differentially metabolise H_2S. As DR-induced longevity only occurs in TejJ89 mice, I predicted that DR causes an increase in H_2S levels in Tej89 mice and either be unaffected or decreased in TejJ48 and TejJ114 mice. I expect there will be divergent regulation of H_2S production and clearance on DR in these mouse strains.

Aims

1. Determine hepatic H_2S production capacity in TejJ89 and TejJ114 mice on 10-month 40% DR in ILSXISS mouse strains

2. Evaluate the effect of 10-month 40% DR on the transcriptional and translational regulation of enzymes central to H_2S production and elimination in ILSXISS mouse strains

3.4 Results

3.4.1 Genotype-specific hepatic H_2S production following 40% DR in female ILSXISS mice

Using the lead acetate method to determine hepatic H_2S production [164], [230], I observed a significant genotype effect ($F=12.243$, $p<0.001$) but no treatment effect ($F=0.150$, $p=0.701$) (**Figure 7**). However, a significant genotype*treatment interaction was detected ($F=13.833$, $p<0.001$) across the ILSXISS mice. *Post-hoc* analysis indicated that H_2S production was significantly elevated by 40% DR in strain TejJ89 ($p=0.005$), but significantly reduced by 40% DR in strain TejJ48 ($p=0.031$) relative to their strain-appropriate AL controls (Fig. 1a and 1b). In addition, H_2S production was significantly elevated in strain TejJ89 relative to strains TejJ48 ($p=0.022$) and TejJ114 ($p<0.001$). This genotype effect was primarily driven by significantly elevated H_2S production in TejJ89 under 40% DR compared to all other groups, with no differences in H_2S production detected between ILSXISS strains under AL feeding (**Figure 7a and Figure 7b**). I also determined H_2S production within the kidneys of these mice (**Figure 7c**). No significant treatment effect was detected ($F=1.540$, $p=0.0221$). but a significant genotype effect on kidney H_2S production was seen ($F=3.294$, $p=0.047$), being significantly elevated in strain TejJ89 relative to strain TejJ48 ($p=0.050$).

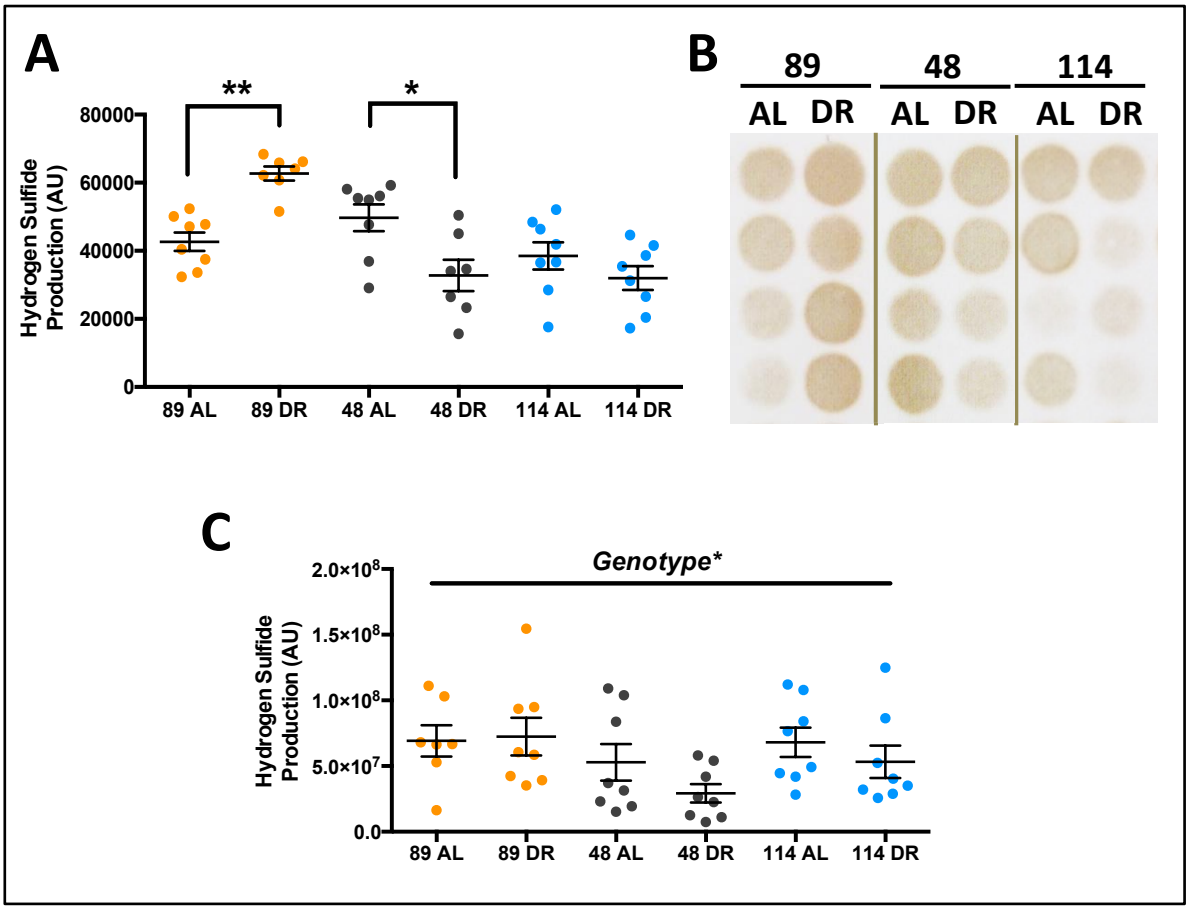

Figure 7 Strain-specificity exists in hepatic H2S production following 40% dietary restriction in female ILSXISS mice

A Hepatic H_2S production levels in TejJ89, TejJ48 and TejJ114 mice on AL or 40% DR, as quantified by densitometry analysis of lead acetate assay results. **B** Representative photos of lead acetate precipitates formed in the assay; darker precipitates indicate higher hepatic H_2S production capacity. TejJ89 data in orange, TejJ48 data in grey, TejJ114 data in blue. Error bars represent SEM. *p<0.05, **p<0.01. **D** Renal H_2S production levels in AL and DR TejJ89, TejJ48 and TejJ114 mice as quantified by densitometry analysis of lead acetate assay results. Error bars represent SEM. *p < 0.05. Genotype (TejJ89, TejJ48 or TejJ114).

3.4.2 Transcript levels of H_2S-production and -elimination proteins in ILSXISS mice following 40% DR

In order to better understand the enzymatic pathways regulating endogenous H_2S (see **Figure 6**) across different ILSXISS strains maintained under AL or 40% DR, I determined gene expression levels of a suite of H_2S-producing and -eliminating proteins (**Figure 8a-k**). *Cse*, *Cbs* and *Mpst* transcript levels (**Figure 8a-c**) were unaffected by both genotype and treatment (see **Table 7** for all statistical output). However, a significant genotype*treatment interaction effect was observed for both *Cbs* (**Figure 8b**, F=4.737, p=0.017) and *Mpst* (**Figure 8c**, F=6.734, p=0.004), with lower expression in strain TejJ89 under AL feeding relative to strain TejJ114 under Al feeding (p=0.008 and p=0.024 for *Cbs* and *Mpst* respectively). *Got 1* (**Figure 8d**) and *Ethe1* expression (**Figure 8e**) differed significantly with genotype (F= 7.185, p=0.003 and F=10.445, p<0.001 for *Got 1* and *Ethe1* respectively) but not by treatment, with strain TejJ48 having significantly lower *Got1* and *Ethe1* expression relative to strains TejJ89 and TejJ114 (p<0.01, in all cases). *Tst* expression levels (**Figure 8f**) showed a significant genotype (F=6.659, p=0.004), but no treatment effect, but with reduced expression in TejJ89 mice compared to TejJ114 mice (p=0.003). A significant *Tst* genotype*treatment interaction was also detected (F=6.745, p=0.004), with AL TejJ89 mice having significantly lower *Tst* expression levels compared to AL TejJ114 mice (p<0.001), and 40% DR reducing *Tst* expression in Tej114 mice (p=0.007) relative to TejJ114 controls (**Figure 8f**). While no significant genotype nor treatment effect on *Suox* expression was detected (**Figure 8g** and **Table 7**), a significant genotype*treatment interaction effect was observed (F=5.694, p=0.008), again with AL TejJ89 mice having significantly reduced expression relative to AL TejJ114 mice (p=0.035), and 40% DR significantly reducing *Suox* expression in Tej114 mice relative to AL TejJ114 mice (p=0.008). *Mat1a* (**Figure 8h**) did not show any significant genotype effect (F=1.069, p=0.356) but a significant treatment effect was detected (F=5.3183, p=0.030), being significantly decreased by 40% DR across all ILSXISS strains. No significant genotype or treatment effects were detected for *Bhmt1*, *Bhmt2* or *Sahh* (**Figure 8i-k**, **Table 7**).

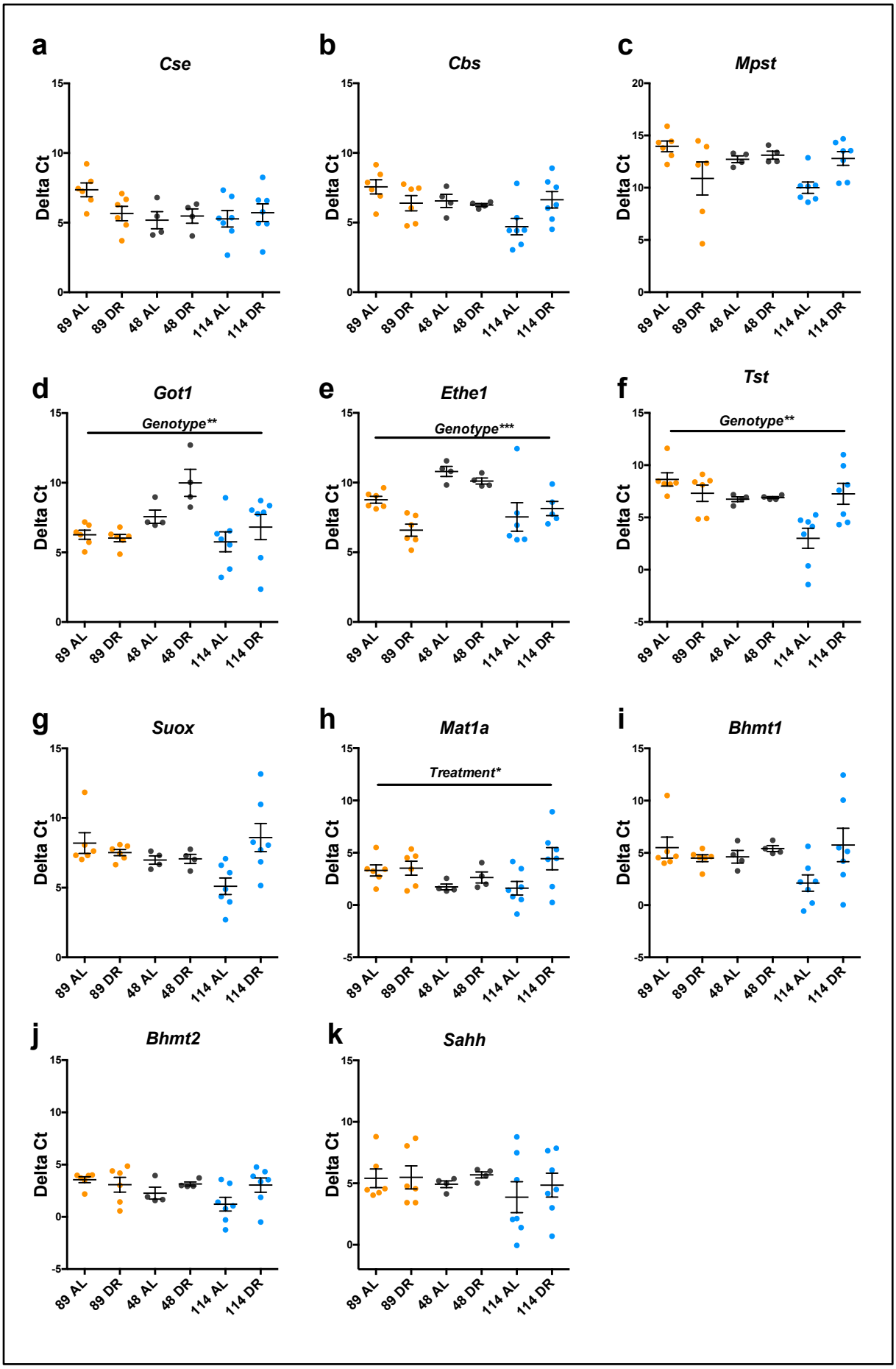
a
Cse
b
Cbs
c
Mpst
d
Got1
Genotype**
e
Ethe1
Genotype***
f
Tst
Genotype**
g
Suox
h
Mat1a
Treatment*
i
Bhmt1
j
Bhmt2
k
Sahh
Delta Ct
89 AL
89 DR
48 AL
48 DR
114 AL
114 DR

Figure 8 ILSXISS mouse strains exhibit differential transcriptional regulation of H2S-production and elimination enzymes following 40% DR.

Hepatic mRNA gene expression (presented as Delta Ct values, a lower DeltaCt indicates a higher number of mRNA transcripts for that gene) of H_2S-producing (**A-D**), H_2S-eliminating (**E-G**), and methionine to cysteine conversion (**H-K**) genes in TejJ89, TejJ48 and TejJ114 in AL and DR mice measured by RT-qPCR. TejJ89 data in orange, TejJ48 data in grey, TejJ114 data in blue, Error bars represent SEM. *p<0.05, **p< 0.01, ***p<0.001. Genotype (TejJ89, TejJ48 or TejJ114) and Treatment (AL or DR). See Table S1 for statistical output from GLM. Cse: Cystathionine-γ-lyase, Cbs: Cystathionine-β-synthase, Mpst: 3-Mercaptopyruvate Sulfurtransferase. Got1: Glutamic-oxaloacetic transaminase 1, Ethe1: Ethylmalonic encephalopathy 1 protein, Tst: Thiosulfate Sulfurtransferase, Suox: Sulfite Oxidase, Mat1a: Methionine Adenosyltransferase 1A, Bhmt1: Betaine-Homocysteine S-Methyltransferase 1, Bhmt2: Betaine-Homocysteine S-Methyltransferase 2, Sahh: S-Adenosylhomocysteine hydrolase.

3.4.3 Protein levels of H_2S-production enzymes in ILSXISS and C57BL/6J mice following 40% DR

Studies in C57BL/6J mice have repeatedly shown that generation of hepatic H_2S is driven primarily through CSE and CBS, with CSE appearing to be the predominant enzymatic source (e.g. [256]). I subsequently compared hepatic protein levels of CSE, CBS and MPST in TejJ89, TejJ48 and TejJ114 mice to levels in C57BL/6J mice under AL and 40% DR. CSE protein levels (**Figure 9a**) were significantly affected by genotype ($F=14.845$, $p<0.001$) and treatment ($F=5.559$, $p=0.024$), with a significant treatment*genotype interaction also present ($F=5.990$, $p=0.002$). CSE levels were significantly higher in C57BL/6J mice relative to all ILSXISS strains ($p<0.001$, in all cases), with no strain-specific differences in CSE levels observed between ILSXISS strains. CSE protein levels were elevated by 40% DR but only significantly so in C57BL/6J mice ($p=0.002$). Hepatic CBS levels were also affected by genotype ($F=6.451$, $p=0.001$) but not by treatment ($F=0.037$, $p=0.848$), with TejJ89 mice having increased levels relative to both TejJ114 ($p=0.002$) and C57BL/6J ($p=0.016$) mice (**Figure 9b**). MPST levels were significantly altered by both genotype ($F=12.984$, $p<0.001$) and treatment ($F=8.812$, $p=0.005$), with a significant genotype*treatment interaction ($F=9.848$, $p<0.001$) also observed (**Figure 9c**). Hepatic MPST levels were significantly elevated in TejJ89 mice compared to all other genotypes ($p<0.001$, in all cases). The elevated H_2S levels observed in TejJ89 mice under 40% DR was associated with a significant elevation in hepatic MPST levels relative to TejJ89 AL mice (**Figure 9c**, $p<0.001$), but 40% DR did not alter MPST levels significantly in any other genotype compared to their appropriate AL controls. I subsequently determined hepatic MPST activity within the ILSXISS mouse strains (**Figure 9d**), but no genotype ($F=0.144$, $p=0.707$) nor treatment ($F=2.755$, $p=0.081$) effect was observed. These findings show that genotype-specific differences exist in protein levels of the primary cellular H_2S generating enzymes CSE, CBS and MPST within mouse liver (**Figure 9a-c**). The increased H_2S levels following 40% DR in strain TejJ89 was associated with an increase in MPST protein levels, but not in CSE (significantly elevated in C57BL/6J mice under 40% DR) or CBS levels, and that protein levels of these enzymes were unresponsive to 40% DR in both strain TejJ48 and TejJ114.

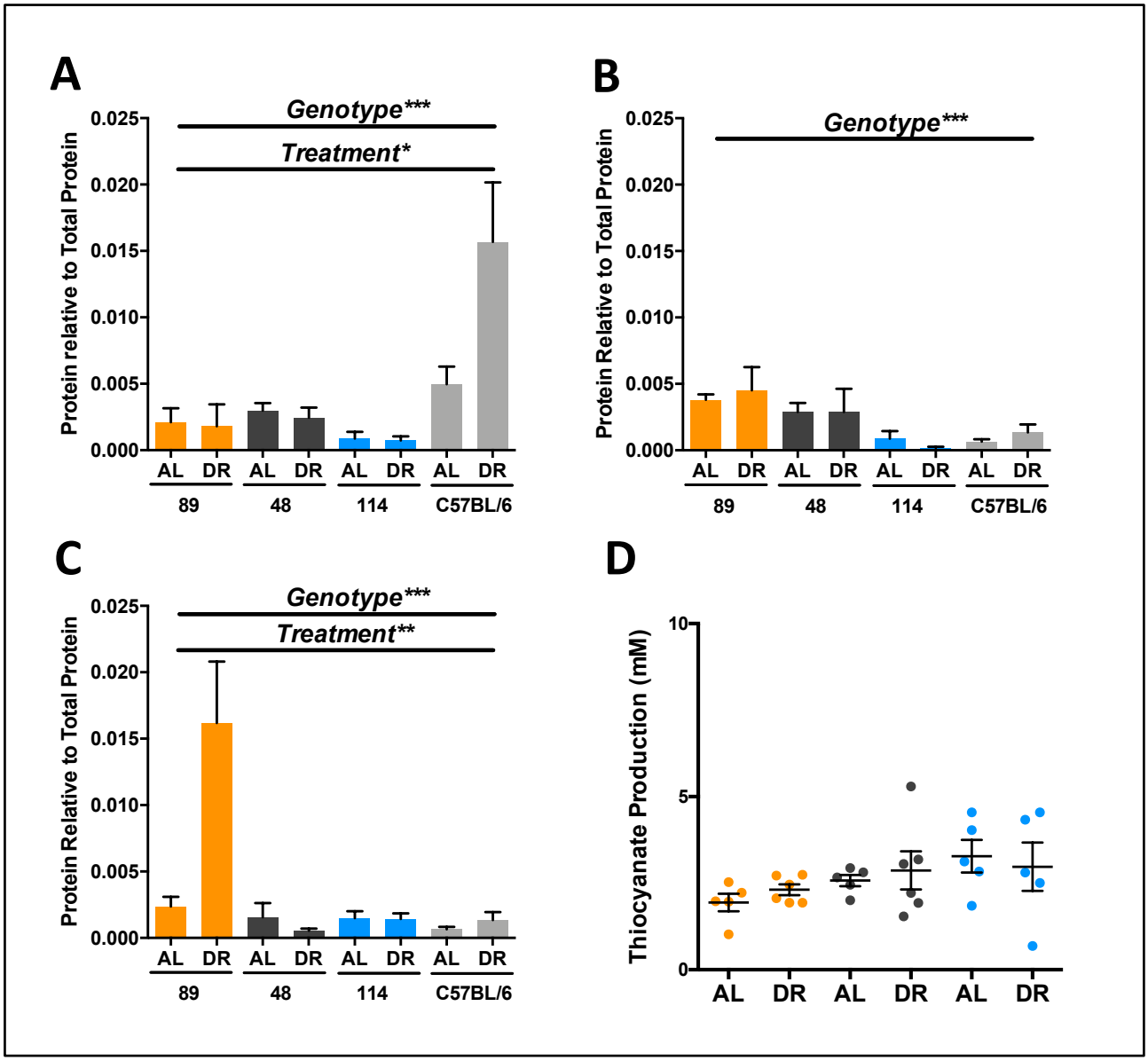

Figure 9 40% DR significantly increases Cystathionine gamma-lyase (CSE) within the liver of C57BL/6J mice but significantly increases 3-Mercaptopyruvate sulfurtransferase (MPST) within the liver of TejJ89 mice.

Hepatic protein levels of CSE (**A**), Cystathionine-β-synthase (CBS, **B**) and MPST (**C**) in TejJ89 (n=6), TejJ48 (n=4), TejJ114 (n=6) and C57BL/6J (n=4) AL and 40% DR mice. TejJ89 data in orange, TejJ48 data in grey, TejJ114 data in blue, C57BL/6J data in light grey. Error bars represent SEM. *p<0.05, **p< 0.01, ***p<0.001. Genotype (TejJ89, TejJ48, TejJ114 or C57BL/6J) and Treatment (AL or DR). **D** 3-Mercaptopyruvate sulfurtransferase (MPST) activity in liver as determined by thiocyanate production capacity in AL and DR TejJ89, TejJ48 and TejJ114 mice. *p<0.05 Genotype (TejJ89, TejJ48 or TejJ114).

3.5 Discussion

A reduction in the intake of calories or in the intake of macro- or micronutrients, termed here as dietary restriction (DR), is currently the most widely employed experimental intervention to modulate ageing. Indeed, DR has been shown to extend lifespan and healthspan in an evolutionary diverse group of organisms [154], [257] and has also been shown to provide a number of beneficial effects in humans [258], [259]. However, it is still not understood how DR mechanistically elicits its beneficial effects. In addition, a number of studies, particularly in mice, report that the DR-response on lifespan and healthspan can vary across different mouse strains [223], [224], [226], [227], [236], [240], [260], [261]. Better understanding of the basis of this genetic variation to DR is important if I hope to translate experimental findings from (typically) highly inbred mouse models to highly genetically heterogenous humans [225].

In this study I investigated the potential relevance of H_2S in DR-induced lifespan by comparing genetically distinct ILSXISS recombinant inbred mouse strains that have been reported to show significant variation in their lifespan under 40% DR, from life extension to no response, through to life shortening [223], [224]. A number of studies have now reported genetic or pharmacological interventions that modulate H_2S levels can profoundly impact longevity in model organisms [165], [245]–[248] and protect against age-associated dysfunction [149], [250], [252]. In addition, increased hepatic H_2S is a conserved phenotype in long-lived mouse models [170], is increased significantly by DR in C57BL/6J and DBA/2 mice [164], [226] and is essential for mediating the beneficial effects of DR [164]. I found that hepatic H_2S was only elevated in female mice from strain TejJ89 under long-term 40% DR; TejJ89 is the single ILSXISS strain in this study reported to show DR-induced longevity [223], [224]. In contrast, strain TejJ48 - reported to be refractory to 40% DR [223], [224] - showed a significant reduction in hepatic H_2S when exposed to 40% DR. In strain TejJ114 - reported to show lifespan shortening under 40% DR [223], [224] - I observed no DR-associated difference in hepatic H_2S production relative to AL mice. However, no treatment nor interaction effect was observed in kidney H_2S production, suggesting tissue-specificity exists in the impact of DR on H_2S production in mice in contrast to findings (H_2S concentration) previously reported in following DR in F344 rats [262]. In addition, significant strain-specificity in H_2S production was also

observed, being elevated in strain TejJ89 relative to both TejJ48 and TejJ114 for liver and elevated in TejJ89 compared to TejJ48 for kidney. These findings indicate that TejJ89 mice show a similar correlation between increased hepatic H_2S production and significantly extended lifespan that has been reported in other mouse strains such as C57BL/6J and DBA/2 [226]. Consequently, these findings do further support the premise that elevated hepatic H_2S levels may be an important mediator of the beneficial effects of DR [164], [165].

To further investigate the potential processes underlying these strain-specific differences in H_2S following 40% DR, I examined a suite of H_2S–producing and –degrading enzymes at the protein and transcript level within the ILSXISS mice. The predominately cytosolic enzymes cystathionine γ-lyase (CSE or CGL) and cystathionine ß-synthase (CBS) are the main sources of H_2S within cells [263], and mice carrying genetic defects in these enzymes are prone to a number of pathologies [166]. In particular, elevated hepatic H_2S following DR correlates with transcript and protein levels of CSE [264], [265], and similarly CSE levels are elevated in several long-lived mouse mutants [170]. Perhaps surprisingly, I did not observe any genotype or treatment effects on transcript levels of *Cse*, *Cbs* or *Mpst*, although several significant genotype and genotype by treatment interaction effects (*Cbs*, *Mpst*, *Tst*, *Suox*) were detected, typically with TejJ89 AL mice having significantly reduced expression compared to TejJ114 AL mice. At the protein level, CSE was significantly elevated in C57BL/6J mice compared to all ILSXISS strains, with 40% DR further increasing CSE levels within the liver of C57BL/6J mice but DR not having any effect on CSE levels in ILSXISS mice. Hepatic CBS protein levels were unaffected by 40% DR across all genotypes studied. Given that both CSE and CBS levels were unaffected by 40% DR in strain TejJ89 despite the DR-associated increased in H_2S production, I subsequently investigate 3-mercaptopyruvate sulfurtransferase (MPST). This is the he third H_2S-producing enzyme within cells but that has been much less characterised compared to CSE and CBS, particularly in the context of ageing and DR. CSE and CBS primarily remain cytoplasmic under normal physiological conditions, whereas MPST can localise to mitochondria and exhibits a profound influence over mitochondrial-specific metabolism and H_2S levels [266]. Further, while CSE and CBS work in concert to convert homocysteine into H_2S via step-wise reactions, MPST generates H_2S from a distinct substrate, 3-

mercaptopyruvate [267], [268]. I found MPST to be significantly increased in the liver of TejJ89 mice under 40% DR, although unaffected by DR in strains TejJ48, TejJ114 or in C57BL/6J mice, graphically represented in **Figure 10**. Precisely why C57BL/6J mice and TejJ89 mice appear to have distinct mechanistic routes (elevated CSE or MPST respectively) to achieve the same outcome of elevated hepatic H_2S under DR still needs to be determined.

There are of course some caveats to these findings, not least that this work is highly correlational. As discussed elsewhere, the variation in phenotypic responses to DR is quite broad [225], [226], [240] and I only examined one sex and only three strains of ILSXISS mice, albeit strains that represent the variety of lifespan responses reported in the original studies [223], [224]. I was vigilant in the choice of strains in this comparative study, choosing those that showed a similar direction of response across both studies. In addition, and as discussed in detail elsewhere [225], significant differences in experimental design and husbandry practices existed between the original studies. Consequently, a fuller investigation of the lifespan response to DR in ILSXISS mice, particularly under graded levels of DR is warranted, but will be a major undertaking [225]. In addition, it will also be interesting to investigate precisely how H_2S production varies in different tissues and in different cellular locations following DR, which may be made more feasible with the advent of novel chemical probes to determine H_2S *in vivo* [269], [270]. However, irrespective of these caveats I have importantly shown that endogenous H_2S levels and associated signalling pathways differ significantly across particular mouse genotypes when exposed to long-term 40% DR. These data suggest that, similar to previous reports, increased H_2S production and/or metabolism is a conserved mechanism through which DR acts to increase lifespan in mice [165], [170], but the precise cellular processes that regulate H_2S production and elimination under DR appear highly strain- (and potentially tissue-) specific.

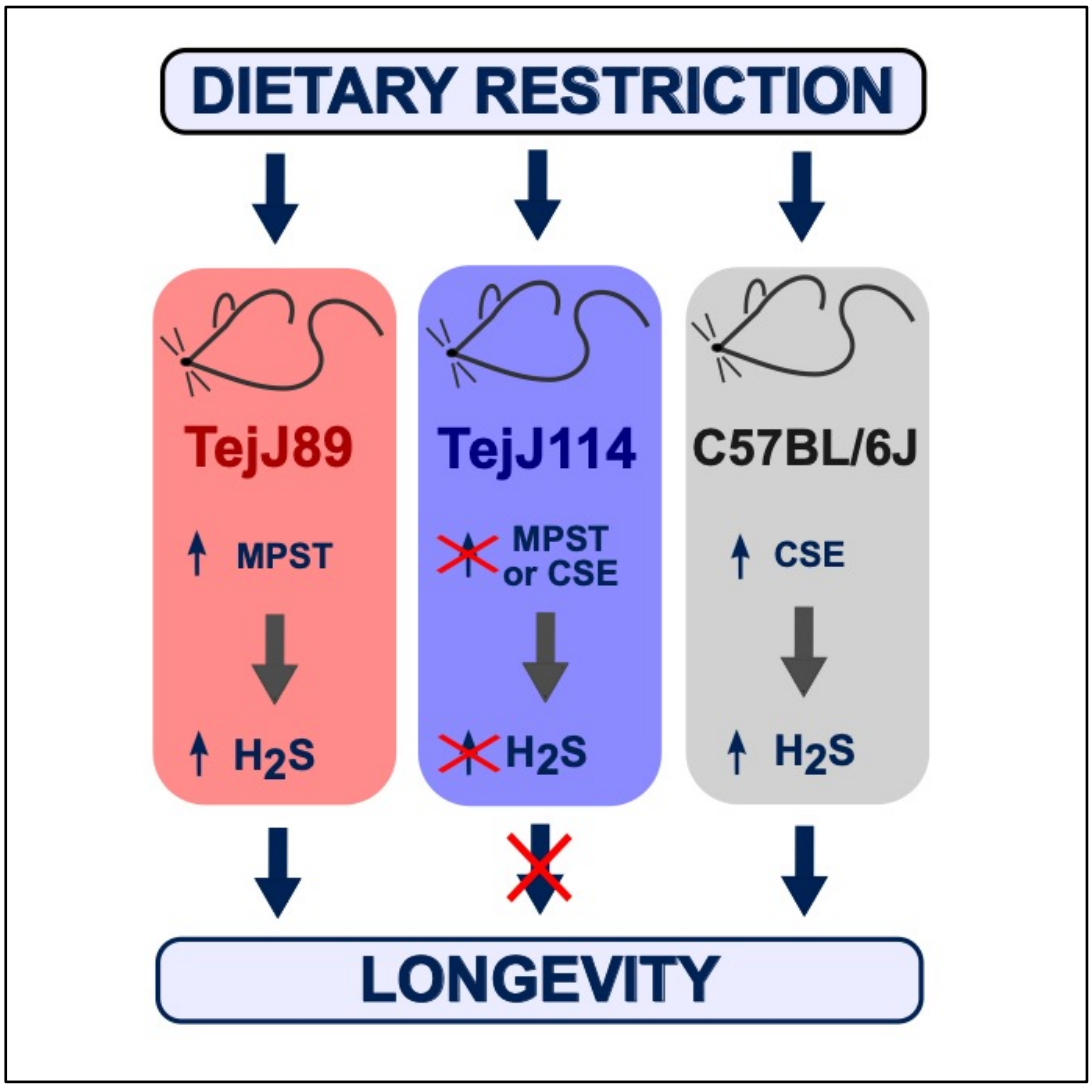

Figure 10 Proposed mechanism to account for differential responses to DR in ILSXISS recombinant inbred and C57BL/6J mouse strains

TejJ89 and C57BL/6J mice experience lifespan extension on DR, TejJ114 have shorter lifespans on DR. DR increases hepatic H_2S levels in Tej89 and C57BL/6J mice, through elevation of MPST and CSE respectively. Tej114 mice do not exhibit elevated H_2S levels following DR. Therefore, DR-induced longevity appears to correlate with increased H_2S production across mouse strains but the precise enzymatic production is strain-specific.

3.6 Conclusions

In summary, I have demonstrated that ILSXISS strains that demonstrate different lifespan response to DR also show divergent hepatic H_2S metabolism profiles. This is mirrored by differential transcriptional and translational expression of major H_2S-producing and elimination enzymes on 10-month 40% DR. While the most common driver of hepatic H_2S production in c57BL/6J mice is CSE, I have identified upregulation of MPST as the major enzymatic source of H_2S in ILSXISS mice following 10-month 40% DR. TejJ114 mice, which have shorter lifespans on DR, display evidence of decreased beta-oxidation and an increase in senescence on DR, effects not present in TejJ89 mice. These data suggest that, similar to previous reports, increased H_2S production and/or metabolism is a general mechanism through which DR acts to increase lifespan in mice [165], [166] but the precise cellular processes that regulate H_2S production and elimination are species, strain, and tissue specific.

3.7 Supplemental tables

Table 7 RT-qPCR data analysis output.

All data (raw delta CT values) were analysed using a general linear modelling (GLM) approach with genotype (TejJ89, TejJ48 and TejJ114) and treatment (AL or DR) introduced as fixed factors, and a post-hoc Bonferroni test employed for multiple comparisons. In all cases, non-significant interactions ($p>0.05$) within the GLM analyses were removed in order to obtain the best-fitting model. Significant ($p<0.05$) p values are indicated in bold. Cse: Cystathionine-γ-lyase, Cbs: Cystathionine-β-synthase, Mpst: 3-Mercaptopyruvate Sulfurtransferase, Got1: Glutamic-oxaloacetic transaminase, Ethe1: Ethylmalonic encephalopathy 1 protein, Tst: Thiosulfate Sulfurtransferase, Suox: Sulfite Oxidase, Mat1a: Methionine adenosyltransferase, Bhmt1: Betaine-homocysteine methyl transferase-1, Bhmt2: Betaine-homocysteine methyl transferase-2, Sahh: S-adenosyl homocysteine hydrolase.

Gene name	Genotype effect	Treatment effect	Genotype*treatment interaction
Cse	F=2.159, p=0.133	F=0.492, p=0.488	–
Cbs	F=3.193, p=0.056	F=0.110, p=0.743	F=4.737, p=0.017
Mpst	F=1.619, p=0.216	F=0.003, p=0.958	F=6.734, p=0.004
Got1	F=7.185, p=0.003	F=2.608, p=0.117	–
Ethe1	F=10.445, p<0.001	F=2.405, p=0.133	–
Tst	F=6.659, p=0.004	F=2.142, p=0.154	F=6.745, p=0.004
Suox	F=1.281, p=0.294	F=2.707, p=0.111	F=5.694, p=0.008
Mat1a	F=1.069, p=0.356	F=5.183, p=0.030	–
Bhmt1	F=0.684, p=0.512	F=2.172, p=0.151	–
Bhmt2	F=2.008, p=0.152	F=2.325, p=0.138	–
Sahh	F=0.865, p=0.431	F=0.614, p=0.440	–

Table 8 RT-qPCR primer sequences

Primers were designed using the UPL Library Assay Design Centre (Roche) and BLASTn (NCBI). Cbs: Cystathionine-β-synthase, Cse: Cystathionine-γ-lyase, Got1: Glutamic-oxaloacetic transaminase 1, Tst: Thiosulfate Sulfurtransferase, Mpst: 3-Mercaptopyruvate Sulfurtransferase, Ethe1: Ethylmalonic encephalopathy 1 protein, Suox: Sulfite Oxidase, Mat1a: Methionine adenosyltransferase, Bhmt1: Betaine-homocysteine methyl transferase-1, Bhmt2: Betaine-homocysteine methyl transferase-2, Sahh: S-adenosyl homocysteine hydrolase.

Gene Name	Amplicon (nt)	Intron Spanning	Intron span (nt)	Forward Primer Sequence	Reverse Primer Sequence
Cbs	84	Y	903	gctgggcacactctctcac	caggcctggtctcgtgat
Cse	78	Y	985	catgctaaggccttcctcaa	ctcagccagactctcatatcctc
Got1	97	Y	2350	ttcagtttcaccggcttga	agccgcacatgttgatcc
Tst	82	Y	5208	ccagctggtggactctcg	gtggcccgagtctagtcct
Mpst	85	Y	2772	cttgccgagtgccttcac	gcctaggagatgctcagattg
Ethe1	88	Y	11056	gattccatccgctttggac	ggtcgttcaggacaaaggtg
Suox	131	Y	257	ttccacaggccatcagagt	ccatctccgagtccttgagt
Mat1a	74	Y	5133	tctgaggcgctctggtgt	cctgcatgtactgaactgttacct
Bhmt1	96	Y	2419	cggcttcagaaaaacatgg	gattctgccagtattccctttctg
Bhmt2	83	Y	1758	gacaagctggaaaacagagga	cgtgcaatgtcacaagcag
Sahh	95	Y	1568	acccagataaataccctgttgg	cagcttcacattcagcttgc

Chapter 4 Optimisation of Mass Spectrometry-Based Methods for Detecting H_2S Levels *in vivo* using the MitoA Probe

4.1 Abstract

Hydrogen sulfide (H_2S) is a gasotransmitter molecule that has profound influence over a diverse panel of biological processes. However, there is currently an absence of assays that specifically and accurately measure H_2S levels *in vivo*. One novel approach to measuring H_2S *in vivo* is a molecular probe called MitoA designed by Prof. Richard Hartley (University of Glasgow, UK). This probe is injected intravenously into the bloodstream and within hours it passively localises to the mitochondrial compartment of cells across nearly all tissues. The MitoA compound reacts irreversibly with H_2S, to form a new compound, MitoN. Tissue samples are then analysed by liquid chromatography tandem mass spectrometry (LC/MS/MS). The ratio of MitoN to MitoA is a precise and specific proxy measurement of the amount of H_2S that was present *in vivo*. When attempting this method in mice, I found that extensive method development was required to optimise the sample preparation and analysis of MitoA in liver samples by LC/MS/MS. Further, I sought to design a desorption electrospray ionization (DESI) imaging method using MitoA in liver tissue sections which would allow spatial resolution of H_2S concentration across tissue sections.

4.2 Introduction

4.2.1 Why Measure Hydrogen Sulfide?

The gas hydrogen sulfide (H_2S) is now well established as a major signalling molecule in mammalian systems [52], [256], [266]. H_2S is a small gaseous molecule that can freely permeate through membranes, is endogenously produced, and has defined functions at physiological concentrations [58]. Due to these characteristics, H_2S is widely regarded as the third 'gasotransmitter' alongside nitric oxide (NO) and carbon monoxide [271]. Primarily, H_2S operates through posttranslational modification of proteins – specifically by persulfidation of cysteine residues [95]. Other modes of action include complex interaction with NO signalling [51], [121], and direct bonding to metal centres such as iron atoms within metalloproteins, which are ubiquitous in biology [99]. Through these modes of signalling, H_2S activity can influence a variety of biological processes. For instance, application of exogenous H_2S-donor compounds confers cardioprotective effects again ischemia-reperfusion injury in rats, induce a suspended-animation state in mice, and can ameliorate dysregulated proteostasis in human fibroblast derived from Werner Syndrome patients [185], [251], [272], [273].

Within the context of ageing research, H_2S has received particular attention due to its potential role in the healthspan and lifespan-extending intervention of dietary restriction (DR) [208], [274]. DR typically results in sizeable extension of lifespan and healthspan across taxa from yeast to non-human primates [154], but despite decades of investigation, the precise molecular mechanism(s) that underlie the beneficial effects of DR remain elusive[275]. DR protocols are often a simple percentage reduction in available food compared to *ab libitum* (AL) fed controls, this is known as calorie restriction (CR) and commonly involves a 20-40% reduction in gross daily calorie intake. One alternative DR protocol is sulfur-containing amino acid (SAA) restriction (SAAR), wherein gross calorific intake is maintained between experimental and control groups, but the SAAR group have depleted methionine and cysteine amino acid in their diet. Critically, it has been shown that most DR protocols including SAAR result in elevated endogenous H_2S production, and genetical modified mice that cannot endogenously produce H_2S do not

experience any health benefit from DR diets [164]. Therefore, it is likely that reduced metabolism of SAAs is in part are causative of CR health benefits. One such metabolic process that is SAA dependent is the endogenous enzymatic production of H_2S from cysteine and methionine [63], [64]. However, the precise nature of the role H_2S plays in DR interventions is poorly understood. As such, studies of H_2S levels in DR experiments are of critical need and may help elucidate the mechanisms by which DR modulated lifespans. One key outstanding question is the mechanism by which a reduction in dietary SAAs, the substrate for endogenous H_2S generation, results in elevated H_2S levels. Several explanations for this unintuitive observation have been proposed. For instance, DR protocols reduce hypothalamic-pituitary signalling through growth hormone and thyroid hormone, both of which both of which inhibit the activity of H_2S-generating enzymes *via* through post-translational restriction of essential substrates and post-transcriptional regulation of H_2S production enzymes, respectively [170]. Another potential explanation is that DR and fasting interventions elevate autophagy in tissues in mice and humans, which provides the pool of SAAs needed for H_2S generation despite a reduction in dietary SAA intake [171]. The development of improved H_2S detection methods will be crucial to determine the precise mechanisms by which nutrient-limiting diets elevate H_2S production and could yield valuable novel targets for improving health and longevity.

4.2.2 Challenges in Measuring Hydrogen Sulfide

Measuring tissue H_2S levels using currently established methods is challenging because it is a highly reactive compound and physiological sulfur species are highly dynamic [276]. A summary of common biological sulfur redox states is presented in **Table 2**. Sulfur pools in biological systems can be broadly grouped into three categories: free sulfide i.e. H_2S, acid labile sulfide i.e. Fe-S clusters, and sulfane sulfur i.e. persulfides [277]. Depending on the sample preparation conditions any combination of these sulfur pools may be excluded from analysis. For instance, the pool of free sulfide compounds includes H_2S, bisulfite (HS^-), and sulfide (S^{2-}), three chemical species which have some common reactivities but are distinct in others [278]. The chemical composition of the free sulfide pool is shifted towards H_2S in acidic conditions and S^{2-} in alkaline conditions [278]. Therefore, detection method that alters sample pH or is more sensitive for one sulfide species than the others may inaccurately report the biological sulfide levels [278]. Furthermore, aqueous solutions of H_2S are highly volatile and passive loss of H_2S during sample preparation is unavoidable [279]. Therefore, simply measuring H_2S levels in blood samples may poorly represent the sulfur status within organs of an animal. Combined, these factors make detection methods for H_2S highly influenced by experimental condition. For instance, quantification of H_2S levels by monobromobimane derivation is sensitive to pH, oxygen concentration, reaction vessel, and presence of trace metals [276]. In addition, all sample preparation techniques must account for the rapid loss of H_2S from samples through oxidation and volatilization [276]. As such, careful consideration must be given in experimental design to ensure the desired sulfide measurement is being recorded. A summary of the selected methods to measure H_2S levels in animal tissues and their associated advantages and disadvantages are presented in **Table 9.** A comprehensive review of emerging H_2S detection methods was compiled recently by Ibrahim *et al*. [280].

Table 9 Summary of current methods to detect H_2S in biological samples and their advantages and disadvantages

Method	Advantages	Disadvantages	Reference
Lead Acetate Reaction Formation of lead-sulfur precipitate	Simple, medium throughput, can be used with variety of tissue types, simple methodology	Measurement of H_2S production capacity rather than H_2S levels	[230]
Monobromobimane Reaction Generates sulfur diamine, measured by HPLC	Medium throughput, can be used with variety of tissue types, simple methodology	Low specificity for H_2S	[281]
Amperometric/Polarographic Probe H_2S Specific Membrane	Specific for H_2S, also measures O_2 levels, can be used with variety of tissue types	Low throughput	[282]
N,N-dimethyl-p-phenylenediamine Sulfate Reaction Colourimetric generation of methylene-blue	Medium throughput, can be used with variety of tissue types, simple methodology	Can be used with plasma samples only	[283]
Fluorescent Sensors Sulfide-specific Fluorescent dyes	Cell permeable, high sensitivity, capable of in vivo measurements	Limited by specificity for H_2S as opposed to other sulfur-containing compounds, low throughput	[284]
Ion-Selective Electrode Specific detection of S^{2-} ions in solution using a crystalline membrane	Good selectivity for S^{2-} ions	Low sensitivity, required pH > 11 to generate S_{2-} ions but this also frees sulfide from bound cysteine groups, artificially inflating results, low throughput	[285]

4.2.3 MitoA, A Novel *in vivo* Exomarker for Hydrogen Sulfide

Here, I report the optimisation and use of the recently developed MitoA exomarker probe, designed by Prof. Richard Hartley (University of Glasgow, Scotland, UK) [269]. The MitoA compound reacts with H_2S in a highly specific manner to form a new compound termed MitoN **(Figure 11a)**. MitoA rapidly localises to mitochondria without requiring enzymatic import by taking advantage of the existing membrane potential differences across plasma and mitochondrial membranes **(Figure 11b)** [286]. As such, a tail vein injection of MitoA into a mouse leads to the MitoA compound rapidly accumulating in the mitochondria of the liver, heart, brain and kidney within 20 min, upon which the local H_2S concentration will result in a proportion of the MitoA reacting to form MitoN [269]. Subsequently, by extracting the compounds from tissues and analysing them via mass spectrometry the relative abundance of MitoA and MitoN can be calculated. In addition, deuterated versions of both compounds have been synthesised (termed d15-MitoA and d15-MitoN) in which the 15 hydrogens on the triphenyl phosphonium group have been exchanged for deuterium [269]. By spiking in a known concentration of these deuterated internal standard (IS) into the samples and preparing a standard curve of known concentrations of MitoA and MitoN, the absolute concentration of each analyte can be determined and used as a proxy measure for the mitochondrial H_2S level *in vivo* [269]. This approach has been used to measure mitochondrial H_2S levels in gill, liver, brain, and muscles tissue samples from Atlantic Molly (*Poecilia mexicana*) [287], and in brain tissue from mice, rats and squirrels (*Ictidomys tridecemlineatus*) [288].

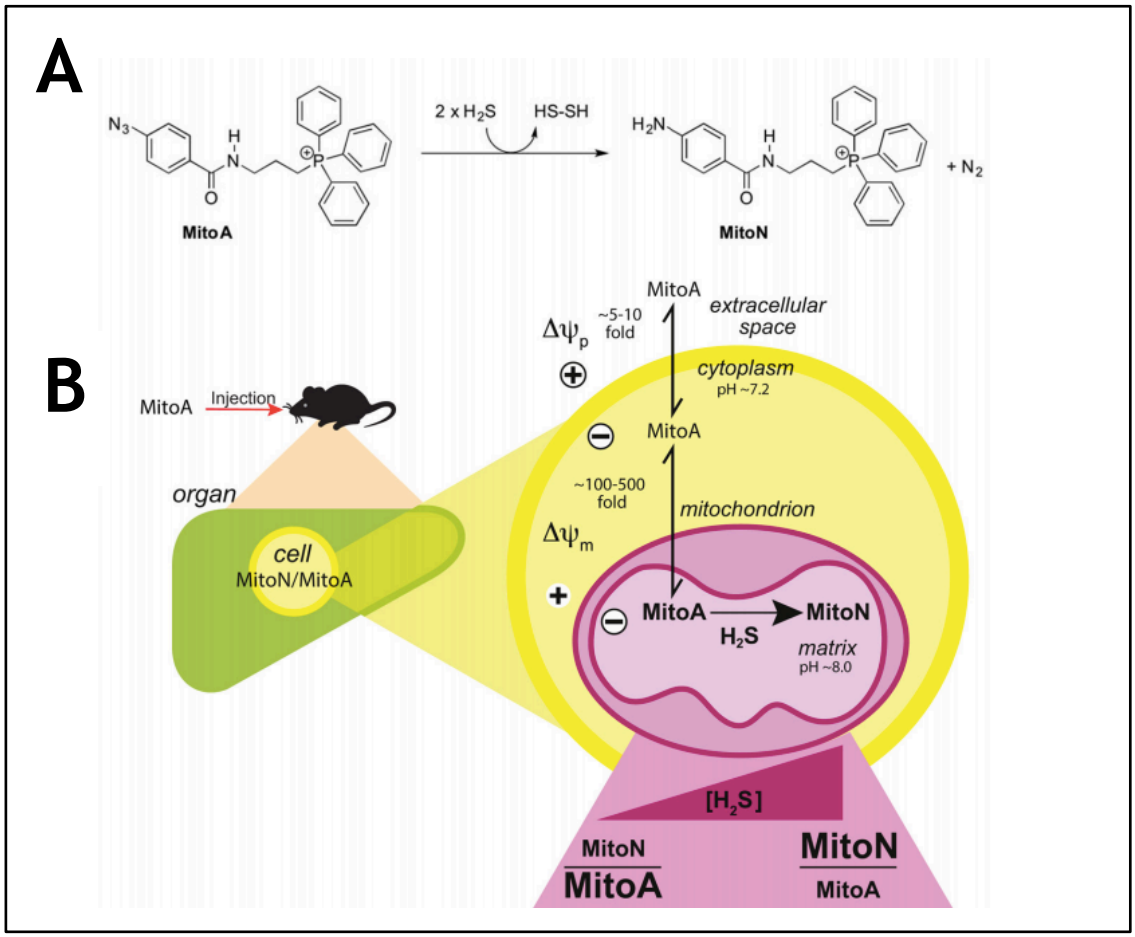

Figure 11 Biochemical basis of MitoA

A Schematic showing the reaction between MitoA and H_2S to form MitoN. **B** Diagram detailing the localisation of MitoA to the mitochondria in mammalian tissues. Figure source: Arndt et al., 2017.

4.2.4 Thiosulfate sulfurtransferase knock out (TST KO) mouse model

Thiosulfate transferase (TST, also known as Rhodanese) is a nuclear encoded mitochondrial protein that detoxifies cyanide by transferring a sulfur group from thiosulfate onto cyanide, producing thiocyanate and sulfite [289]. However, it has also emerged that TST has a role in the metabolism of H_2S. The first stage H_2S oxidation it catalysed by the mitochondrial enzyme sulfide:quinone oxidoreductase which transfers the sulfur atom primarily to glutathione, generating glutathione persulfide (GSSH) [77]. TST then uses GSSH as a substrate for the transfer of a sulfane sulfur to a sulfite molecule, generating thiosulfate which is ultimately excreted in the urine [80]. TST has drawn recent attention when Morton *et al*. identified it as an adipose-specific antidiabetic gene [232]. This was achieved using polygenic mouse strains divergently selected over 60 generations for either a fat (F) or lean (L) phenotype with regards to adiposity and lean body mass, resulting in F and L mouse strains that have the same lean body mass but a large difference in body fat percentage (23% body fat in F mice compared to 4% body fat in L mice) [290], [291]. Using these F and L strains, Morton *et al*. found that expression of TST in adipocytes was correlated with lower fat mass and lower fasted blood glucose levels, and transgenic adipocyte TST overexpression in mice was protective against high fat diet induced obesity and insulin resistance [232]. TST has several molecular functions that may underpin its promotion of a lean phenotype, chiefly in the modulation of mitochondrial function, where it localises. This includes alteration of mitochondrial oxidative phosphorylation complexes I and II [292], [293], the degradation of reactive oxygen species in mitochondria [294], and unfolded TST may potentially be involved in the mitochondrial import of 5S ribosomal RNA [295]. The role of TST in managing H_2S levels is complicated. It is known that TST forms part of the sulfide oxidation unit, however the precise mechanistic sequence involved remains an area of active research. Morton *et al*. found that whole blood H_2S levels were greatly elevated in $TST^{-/-}$ mice compared to controls by a monobromobimane derivisation method [232], however hepatic H_2S levels were unaffected by transgenic TST knock out across multiple H_2S detection methods [296]. To further elucidate the production of H_2S in the context of TST null mice, I optimised an LC/MS/MS method for the analysis of tissue samples from $TST^{-/-}$ mice injected with MitoA and attempted an imaging

mass spectrometry method to spatially resolve H_2S levels in hepatic tissue samples.

4.3 LC/MS/MS Method Development

Analysis of MitoA, MitoN and their deuterated ISs in murine liver has been reported in the initial proof-of-concept paper describing the functionality of MitoA by Arndt *et al.* [269]. However, this approach had not yet been replicated by any other group. I received lab-synthesised MitoA, MitoN, d15-MitoA, and d15-MitoN compounds from Prof. Richard Hartley's group (University of Glasgow, UK), to enable me to apply the same methodology in the detection of mitochondrial H_2S levels in hepatic samples from a transgenic TST KO mouse model. The analysis of these compounds by liquid chromatography tandem mass spectrometry (LC/MS/MS) was performed at the Mass Spectrometry core facility at the Queen's Medical Research Institute (University of Edinburgh, UK) with help and support from Natalie Homer, Ruth Andrew, Scott Denham, and Shazia Khan. The analysis used the same liquid chromatography (LC) parameters but required optimisation and validation of the mass spectrometry (MS) parameters and sample preparation methodology. This chapter will detail the method development for the optimized LC/MS/MS analysis of MitoA in hepatic tissues. Additionally, I attempted to use MitoA-injected liver tissue sections in an imaging MS experiment. The imaging experiment was ultimately unsuccessful, but the method development is described in **section 4.4**.

The following experimental parameters were consistent across all experiments described in this chapter. Analytes and tissue samples were analysed in positive ion mode using an Acquity UPLC BEH C18 column (1 x 50 mm, 1.7 μm; Waters, Wilmslow, UK) with a Waters UPLC filter (0.22 μm) in a Waters I-Class HPLC in tandem with a triple-quadropole mass spectrometer (Waters, Xevo TQ-S). Specific settings for LC/MS/MS analysis are detailed in **Table 10**.

Table 10 MS Settings for all LC/MS/MS analysis

Parameter	Setting
LC Program Time	4.5 min
LC Solvent A	95% water, 5% ACN, 0.1% FA
LC Solvent B	90% ACN, 10% water, 0.1% FA
Solvent Gradient	0.2 L/min, gradient: 0– 0.3 min, 5% B; 0.3–3 min, 5–100% B; 3– 4 min, 100% B, 4.0– 4.10, 100–5% B; 4.10– 4.60 min, 5% B
Injection Volume	10 μL
Source Spray Voltage	3.2 kV
Cone Voltage	125 V
Ion Source	100 °C
Collision Energy	75 V

4.3.1 MS Tuning of Analytes

Tuning of a mass spectrometer to specific analytes allows for optimisation of experimental parameters to improve detection of those analytes [297]. Parameters that commonly require optimization include cone voltage, collision energy, and source spray voltage [297]. I used Intellistart™ software (Waters, Wilmslow, UK) to tune the MS system to all four analytes: MitoA, MitoN, d15-MitoA, and d15-MitoN. Standards of each analyte were prepared at 5 nM in 20% ACN 0.1% FA directly infused into the MS. The Intellistart™ software optimised experimental parameters for the detection of these analytes and determined the most prevalent mass transitions for each compound **(Table 11)**. These mass transitions are a characteristic pattern of masses produced by the ionized analyte fragmenting down into daughter ions [297]. The mass transitions highlighted in bold indicate the transitions I selected to identify each compound in all downstream analyses, these transitions were from different masses to those utilized by Arndt *et al* in their analysis [269]. The chromatograms for each analyte and the associated transitions are shown in **Figure 12**. Chromatograms for MitoA, MitoN and d15-MitoN demonstrate that these compounds have peaks arising from the desired transitions only i.e. when tuning the MitoA analyte, peaks were only detected from a parent ion of the correct mass for MitoA (437.16 m/z) and not from any other mass. I found strong signals for all mass transitions that were identified by the MS Tune software for each analyte. However, for d15-MitoA, peaks were observed for transitions relating to the d15-MitoA transition but also from MitoA transitions **Figure 12**. The relative signal intensity of these peaks were $2.02x10^5$ and $1.09x10^4$ respectively. This is indicative of contamination of the d15-MitoA compound with MitoA, likely due to impurities in the chemical synthesis of the d15-MitoA compound. The d15-MitoA compound was a viscous, oily substance of yellow-brown colour and visually appeared less pure than the d15-MitoN compound which was a fine power of one consistent colour. The d15-MitoN compound only had one strong peak for the expected d15-MitoN transition **Figure 12**. As the contamination peak in d15-MitoA is approximately 20x smaller than the desired peak and the compound is used at a much lower concentration in sample analysis (100 pM for analysis compared to 5 nM in this experiment), it is not expected that the impurity of this IS will significantly affect downstream analysis. LC retention times for MitoA

and its deuterated IS were identical at 2.02 min while MitoN and d15-MitoN both had a retention time of 1.66 min. These retention times were maintained across all transitions recorded for all four compounds.

Table 11 Summary of parent and daughter ions for each compounds as identified by MS Tune software

Daughter ions highlighted in bold are the ones selected as the characteristic transition for each compound in all downstream analysis. All values reported as m/z.

MitoA		MitoN		d15-MitoA		d15-MitoN	
Parent Ion	**Daughter Ions**	**Parent Ion**	**Daughter Ions**	**Parent Ion**	**Daughter Ions**	**Parent Ion**	Daughter Ions
437.16	**183.06**	439.16	**120.06**	452.22	**191.11**	454.22	**120.06**
	346.22		177.20		361.29		177.13
	175.13		183.11		113.11		191.17
			92.11				92.11
			65.13				65.13

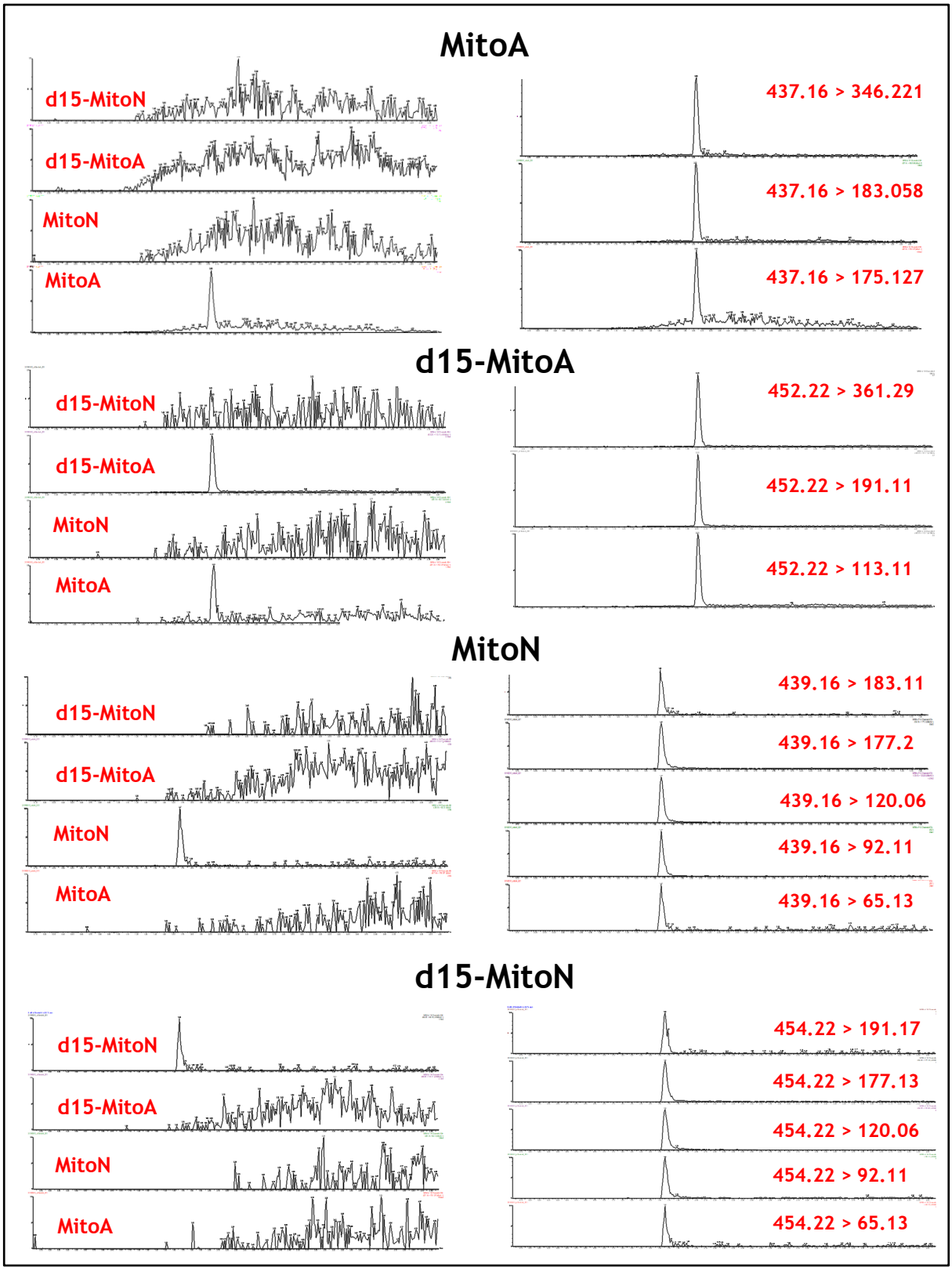

Figure 12 MS Tuning chromatograms for the Mito A and Mito N analytes and the d15-MitoA and d15-MitoN internal standards
Chromatograms on the left shown peaks arising from direct infusion of each analyte into the mass spectrometer (top to bottom: MitoA, d15-MitoA, MitoN, d15-MitoN). Each compound should only display strong peaks for itself. On the right chromatograms are shown for each of the transitions identified by the MS Tune programs for each compound. Analytes were prepared at 5 nM in 20% ACN 0.1% FA. The x-axis in all graphs represents retention time, with the y-axis representing signal intensity.

4.3.2 Analyte Calibration Curves

Next the preparation of a calibration curve for each analyte in the presence of IS was assessed. Good linearity is required for quantification of analytes in tissue samples and generation of a calibration curve allows for determination of the limit of detection (LOD) for each analyte [298]. MitoA and MitoN compounds were prepared from 0.025 – 100 ng/100 μL in 95% acetonitrile (ACN) 0.1% formic acid (FA). All calibration curve standards included 2 ng of both the IS compounds, d15-MitoA and d15-MitoN. The signal arising from each analyte is determined by measuring signals arising from the mass transitions highlighted in **Table 11**. Response of MitoA is normalised to the d15-MitoA signal and MitoN relative to d15-MitoN. Calibration curves, retention times, signals achieved from analytes and ISs and the calculated responses are detailed for MitoA **(Figure 13)** and MitoN **(Figure 14).** Both curves exhibited good linearity (R^2 = 0.9992 for MitoA and 0.9986 for MitoN). Both MitoA and MitoN were detectable at the lowest concentration used in this experiment of 0.025 ng/100 μL. As such, the LOD of each compound was found to be sub 0.025 ng/100 μL. However, this LOD is determined from analytes prepared in pure solution and without the confounding components that arise in samples prepared from tissue homogenate. As such the next step was to assess if the compounds are detectable after extraction from hepatic tissue samples.

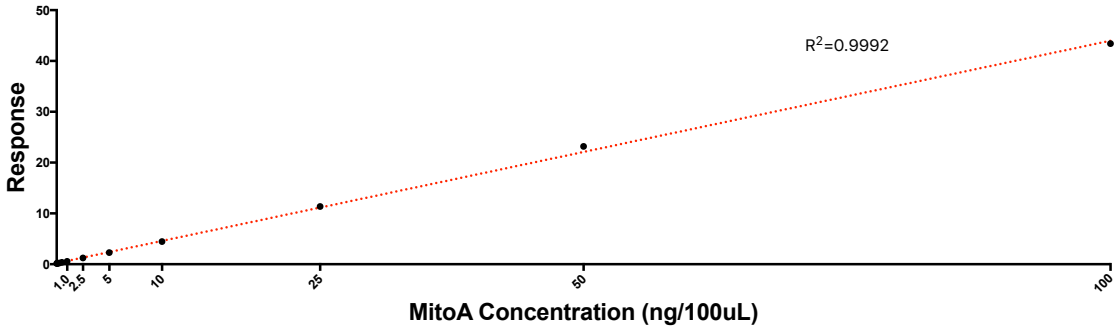

Standard Conc. (ng/100µL)	Area	RT	IS Area	IS RT	Response	Calculated Conc. (ng/100µL)	%Dev	S/N
0.025	14397.756	2.01	91806.594	1.99	0.157	0.0	10.5	320.509
0.050	15550.067	2.01	92704.223	1.99	0.168	0.1	4.6	277.892
0.100	16925.090	2.01	91451.810	1.99	0.185	0.1	-8.5	386.759
0.250	24915.221	2.01	100012.985	1.99	0.249	0.2	-5.4	724.156
0.500	35879.922	2.01	95480.299	1.99	0.376	0.5	4.6	914.213
1.000	55175.000	2.01	96851.023	1.99	0.570	1.0	-3.8	1519.229
2.500	122367.047	2.01	98919.258	1.99	1.237	2.5	-1.1	2355.841
5.000	218791.234	2.01	95067.711	1.99	2.301	4.9	-2.4	5419.872
10.000	414987.969	2.01	92935.035	1.99	4.465	9.8	-2.2	6593.480
25.000	1067721.000	2.01	93958.054	1.99	11.364	25.4	1.5	10731.647
50.000	2009589.875	2.01	86670.067	1.99	23.187	52.1	4.3	9261.728
100.000	3666611.750	2.01	84471.274	1.99	43.407	97.9	-2.1	16367.178

Figure 13 Calibration curve and supporting table for MitoA standards

Standards were prepared from 0.025-100 ng/100 µL in a deep-well 96-well plate containing 100 µL 20% ACN 0.1% FA and analysed by LC/MS/MS. RT: Retention time, IS: Internal standard, %Dev: Percentage relative standard deviation, S/N: Signal to noise ratio, ACN: Acetonitrile, FA: Formic acid.

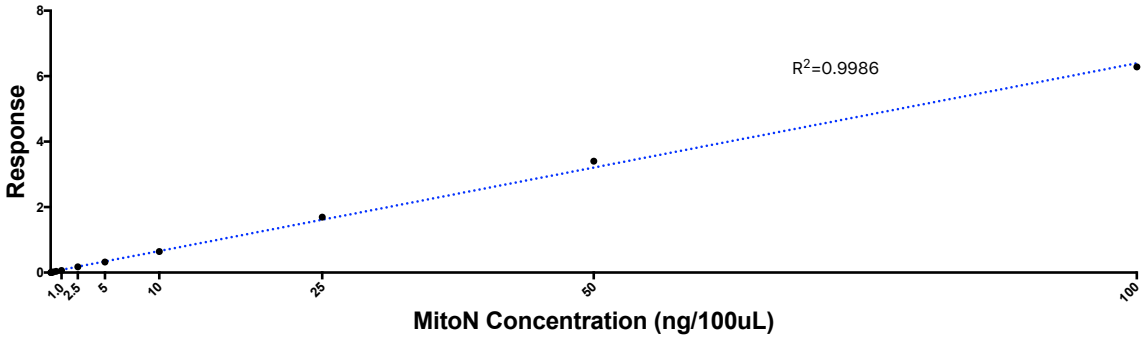

Standard Conc. (ng/100uL)	Area	RT	IS Area	IS RT	Response	Calculated Conc. (ng/100uL)	%Dev	S/N
0.025	183.267	1.67	91806.594	1.64	0.002	0.0	-23.6	3.664
0.050	372.356	1.66	92704.223	1.64	0.004	0.1	0.3	9.011
0.100	613.379	1.66	91451.810	1.64	0.007	0.1	-8.5	19.179
0.250	1928.889	1.66	100012.985	1.64	0.019	0.3	14	52.953
0.500	3473.989	1.66	95480.299	1.64	0.036	0.5	9.6	126.398
1.000	6212.794	1.66	96851.023	1.64	0.064	1.0	-2.5	124.246
2.500	17340.246	1.66	98919.258	1.64	0.175	2.7	7.4	531.570
5.000	30797.764	1.66	95067.711	1.64	0.324	5.0	-0.6	526.281
10.000	59635.082	1.66	92935.035	1.64	0.642	9.9	-1.4	1660.293
25.000	159020.266	1.66	93958.054	1.64	1.692	26.0	4.1	3317.180
50.000	294879.281	1.66	86670.067	1.64	3.402	52.3	4.6	5757.737
100.000	530746.125	1.66	84471.274	1.64	6.283	96.6	-3.4	7705.985

Figure 14 Calibration curve and supporting table for MitoN standards

Standards were prepared from 0.025-100 ng/100 μL in a deep-well 96-well plate in 100 μL 20% ACN 0.1% FA and analyzed by LC/MS/MS. RT: Retention time, IS: Internal standard, %Dev: Percentage relative standard deviation, S/N: Signal to noise ratio, ACN: Acetonitrile, FA: Formic acid.

4.3.3 Analysis of Hepatic Tissue Samples

Next, I sought to determine if the MitoA and MitoN analytes could be detected after extraction from murine hepatic tissue samples. To do this, a 11-week old C57BL/6J male mouse was injected with 100 μL of 50 nM MitoA *via* a tail vein injection. After 1.5 hr the mouse was culled by schedule 1 cervical dislocation and cessation of circulation was confirmed by cutting the femoral artery. The liver was dissected and flash frozen in liquid nitrogen. Extraction of MitoA and MitoN and spiking of the solution with internal standards was performed as described in **Figure 15a**. Briefly, 50 mg of liver tissue was homogenized in 210 uL 95% ACN supplemented with the deuterated ISs. The homogenate was moved to a fresh Eppendorf tube and centrifuged at 16,000 g for 10 min at 4°C. The supernatant was reserved to a fresh Eppendorf tube and the pellet was resuspended in 50 uL 95% ACN, centrifuged at 16,000 g for 10 min at 4°C and the supernatant was pooled with the previous extraction. This was step was repeated one more time before the extracted solution was passed through a 0.2 μm filter, dried under vacuum, and finally resuspended in 100 μL 20% ACN 0.1% FA. The resuspended sample solution was added to a deep-well 96-well plate and analysed alongside a calibration curve of MitoA and MitoN standards **Figure 15b**. Both analytes were detectable in this extracted solution, with a calculated concentration of MitoA and MitoN of 0.025 and 0.095 ng/100 μL, respectively. From these data the [MitoN]:[MitoA] ratio in this hepatic sample is 0.095/0.025 = 3.748. This confirms that both analytes are detectable from hepatic tissue and can be quantified by use of spiked ISs in the sample preparation.

A

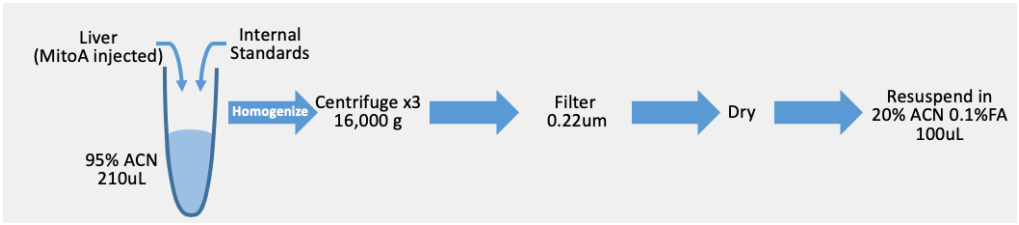

B

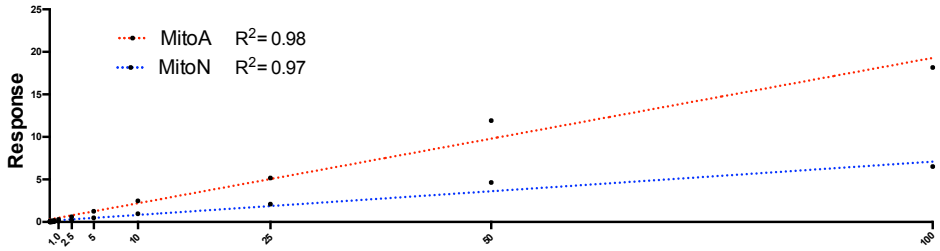

	Standard Conc. (ng/100uL)	Area	RT	IS Area	IS RT	Response	Calculated Conc. (ng/100uL)	%Dev	S/N
MitoA	0.025	46102.523	1.97	550100.875	1.96	0.084			976.882
	0.050	47755.004	1.97	497239.688	1.96	0.096	0.055594	11.2	2119.909
	0.100	60372.941	1.97	521205.219	1.96	0.116	0.152841	52.8	1438.199
	0.250	60513.258	1.97	450942.000	1.96	0.134	0.243045	-2.8	1349.475
	0.500	89502.719	1.97	470073.906	1.96	0.19	0.519206	3.8	1067.669
	1.000	138608.469	1.97	451028.406	1.96	0.307	1.093628	9.4	3166.438
	2.500	279485.531	1.98	456653.750	1.96	0.612	2.590731	3.6	5295.802
	5.000	548112.000	1.98	433039.938	1.96	1.266	5.802470	16.0	4604.582
	10.000	1086689.750	1.97	435626.031	1.96	2.495	11.839841	18.4	15579.533
	25.000	2408732.500	1.97	464722.563	1.96	5.183	25.049433	0.2	16194.231
	50.000	5594257.500	1.97	468735.844	1.96	11.935	58.221186	16.4	34602.577
	100.000	8145245.500	1.97	448251.250	1.96	18.171	88.861532	-11.1	23819.695
	Liver Sample	**18950.232**	**1.98**	**210792.609**	**1.96**	**0.09**	**0.025426**		**225.928**
MitoN	0.025	7453.576	1.63	1751663.500	1.61	0.004			263.353
	0.050	12495.171	1.63	1659098.500	1.61	0.008	0.039249	-21.5	352.706
	0.100	24631.729	1.63	1697724.000	1.61	0.015	0.129050	29.1	454.205
	0.250	39049.746	1.63	1669547.375	1.61	0.023	0.243348	-2.7	1389.730
	0.500	82545.219	1.62	1730247.750	1.61	0.048	0.556327	11.3	1738.583
	1.000	159405.781	1.63	1634802.875	1.61	0.098	1.197277	19.7	2875.507
	2.500	385047.219	1.63	1706655.750	1.61	0.226	2.846066	13.8	4604.587
	5.000	782240.313	1.63	1601661.125	1.61	0.488	6.228115	24.6	5985.674
	10.000	1521264.875	1.63	1547327.250	1.61	0.983	12.595899	26.0	6073.588
	25.000	3435282.000	1.63	1632576.375	1.61	2.104	27.024252	8.1	17952.071
	50.000	6834877.000	1.62	1470649.625	1.61	4.648	59.757616	19.5	13040.736
	100.000	9089187.000	1.63	1394817.750	1.61	6.516	83.810718	-16.2	24883.308
	Liver Sample	**5009.926**	**1.66**	**421463.75**	**1.65**	**0.012**	**0.095308**		**37.754**

Figure 15 Analysis of hepatic tissue sample

A Diagram showing sample preparation protocol for the preparation of the MitoA-injected hepatic tissue sample. **B** Calibration curve and supporting table for MitoA and MitoN standards. Standards were prepared from 0.025-100 ng/100μL in a deep-well 96-well plate in 100 μL 20% ACN 0.1% FA.

4.3.4 Matrix and Recovery Effects

Having confirmed that all four analytes were detectable after extraction from mouse liver tissue, I next sought to determine if it was possible to improve the detection of these analytes. The use of trace analysis techniques such as LC/MS/MS on tissue samples is often impeded by contaminants arising from the tissue sample (matrix effects) and the difficultly in extracting all of the analyte from the tissue (recovery effects) [299], [300]. I then undertook an experiment to determine the signal loss arising from each of these effects by preparing solutions containing the d15-MitoA and d15-MitoN ISs under three different protocols termed pre-spike, pure solution, and post-spike **(Figure 16a)**. Peak area for analytes prepared by each protocol was calculated **(Figure 16b, summarised in Table 12)** and used to evaluate the contribution of matrix and recovery effects to the overall loss of signal in tissue sample according to **equations 1 and 2 (Table 13)**.

$$Matrix\ effects\ (\%) = \left(\frac{Response_{Pure\ Solution}}{Response_{Post\ Spike}} - 1\right) x100 \quad -Equation\ 1$$

$$Recovery\ effects\ (\%) = \left(\frac{Response_{Post\ Spike}}{Response_{Pre\ Spike}}\right) x100 \quad -Equation\ 2$$

From these data it is apparent that there is highly efficient recovery of the analytes from tissue samples, 94.65% for MitoA and 98.25% for MitoN. These data indicate that the sample preparation method of homogenisation, centrifugation, filtration, drying, and then resuspension incurs only a modest loss of both MitoA and MitoN. However, there were significant matrix effects which result in a large reduction in signal for both MitoA (-46.16%) and MitoN (-61.21%). This indicates that filtration of the tissue homogenate through a 0.22 μm filter is insufficient to completely remove components of the tissue matrix, which results in ion suppression [301]. Less volatile components in the tissue matrix cause ion suppression of the analytes of interest (here, MitoA and MitoN) by impeding droplet formation and/or evaporation and thereby reducing the amount of ions that reach the MS detector [301].

Table 12 Peak areas of peaks arising from Mito A and Mito N in standards prepared by each method. All values given in arbitrary units.

	Sample Preparation Method		
	Pre Spike	**Post Spike**	**Pure Solution**
MitoA:	685062	723779	1272393
MitoN:	2595789	2641969	6692047

Table 13 Summary of calculated matrix and recovery effects

	MitoA	**MitoN**
Recovery Effects (%)	94.65	98.25
Matrix Effects (%)	-46.16	-61.21

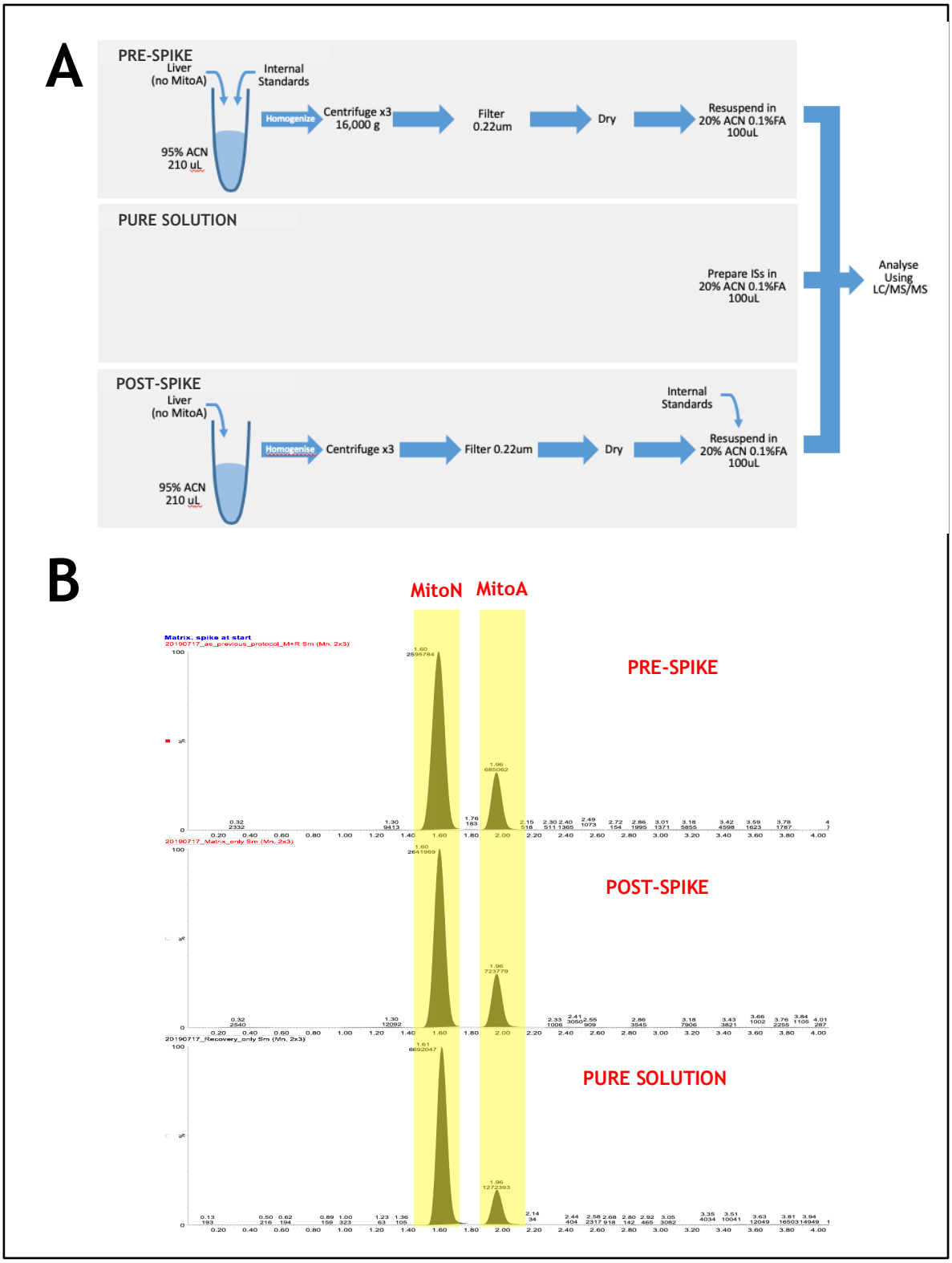

Figure 16 Determination of matrix and recovery effects

A Diagram showing standard preparation by three different protocols to determine recovery and matrix effects. **B** Integrated chromatographic peaks for MitoA and MitoN in each of the three standards. Peak areas for each compound are summarized in Table 12. The x-axis in all graphs represents retention time, the y-axis in all graphs represents signal intensity.

4.3.5 Impact of Resuspension on Recovery

One suspected source of reduced recovery was loss of analyte during the drying and final resuspension steps of sample preparation, which can often result in reduced analyte signal in LC/MS/MS analysis due to incomplete solubilisation of the dried analyte or sedimentation of analyte to the bottom of the sample well [302], [303]. To determine the reduction in signal from this process a solution containing 2ng of both d15-MitoA and d15-MitoN was prepared with or without the drying and resuspension steps **(Figure 17a)**. There was no significant change in signal intensity or retention time between the resuspended and non-resuspended standards, $2.7x10^7$ and $2.9x10^7$ respectively **(Figure 17b)**. This indicates that drying and resuspending the analytes has a very limited impact on recovery.

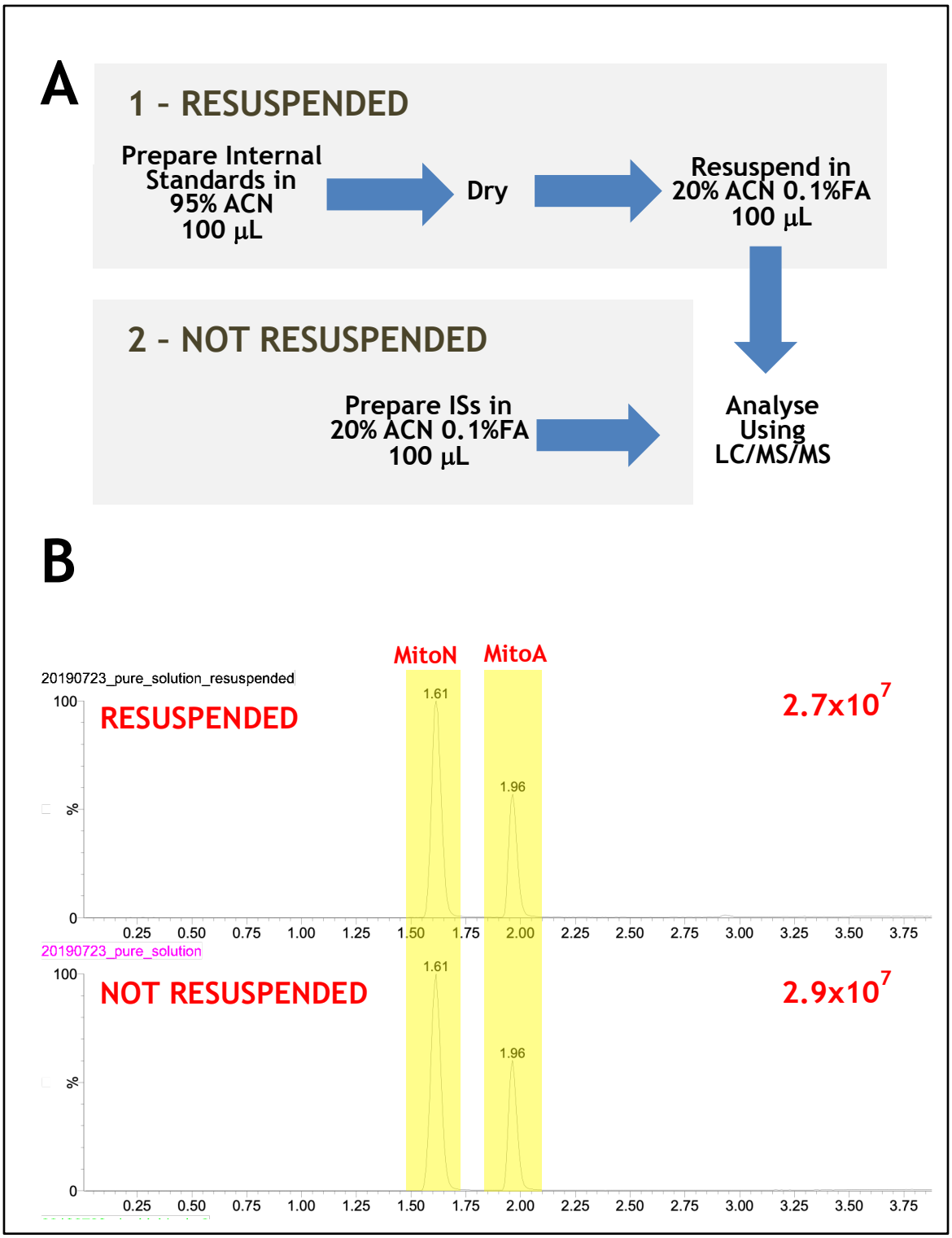

Figure 17 Impact on resuspension of standards and analytes on recovery

A Diagram showing standard preparation protocol for standards to determine the effect of drying and resuspending analytes for analysis. **B** Chromatographic peaks arising from MitoA and MitoN in standards either with or without a resuspension protocol. There is no significant change in signal intensities between methods. The numbers in red represent the maximum signal intensity recorded in each chromatogram. The x-axis in all graphs represents retention time, the y-axis in all graphs represents signal intensity.

4.3.6 Phospholipid Extraction

Due to the matrix effects quantified described in **section 4.3.4**, I then investigated the use of an Isolute PLD+ phospholipid removal plate (Waters, Wilmslow, UK) to extract phospholipids from sample solutions prior to analysis. Phospholipids are major constituents of biological membranes [304], and are the primary source of matrix effects in MS analysis of analytes extracted from tissue samples [305]. The PLD+ phospholipid extraction plate uses a protein crash and filtration method to removal phospholipid contaminant arising in tissue samples [306]. To observe the effect of phospholipid extraction, six standards of d15-MitoA and d15-MitoN were prepared. One group of three standards were prepared and analysed as described in **Figure 16a** (described as non PLD+ extracted in this experiment), and another group of three standards was prepared similarly except the standards were pulled through a Isolute PLD+ plate under vacuum, dried and resuspended in 100 μL 20% ACN 0.1% FA before injection into the LC/MS/MS (described as PLD+ extracted in this experiment). Chromatograms for all standards prepared are shown in **Figure 18**. There were no strong peaks found in the characteristic phospholipid mass range for the PLD+ phospholipid extracted pure solution standard or the non-extraction pure solution. This is as expected, as neither of these standards contain liver tissue and as such no phospholipids should be present to contaminate the standards. However, strong peaks in the characteristic phospholipid mass range were observed in the pre-spike and post-spike standards that were not PLD+ extracted. Phospholipid peaks were not detectable in pre-spike and post-spike standards that were PLD+ extracted. These data indicate that standards prepared from tissue samples are contaminated with phospholipids, even after filtration through 0.22 μm filters, but that this contamination is no longer detectable after use of an Isolute PLD+ extraction plate. The phospholipid extraction did result in a modest reduction in signal of the analytes (The pure solution had a signal intensity of 1.9×10^7 without Isolute PLD+ extraction and 1.0×10^7 after extraction). Given these findings, a PLD+ extraction step was included in all subsequent sample preparation methods for LC/MS/MS analysis.

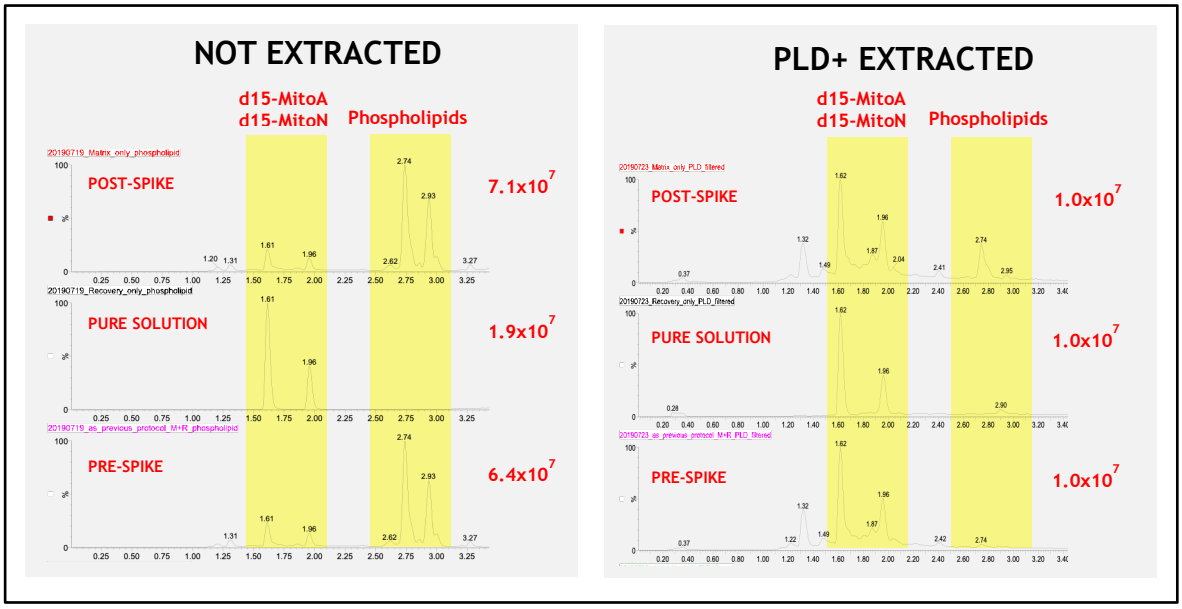

Figure 18 Comparison of chromatograms with or without PLD+ Extraction

LEFT: Chromatographic peaks arising from analytes of interest and phospholipid contaminants in standards without Isolute PLD+ extraction. Phospholipid peaks are only visible in the two standards that are prepared with the inclusion of hepatic tissue.

RIGHT: Chromatographic peaks arising from analytes of interest and phospholipid contaminants in standards following Isolute PLD+ extraction. No major phospholipid peaks are visible in any of the standards. All standards were prepared in 100 μL 20% ACN 0.1% FA. ACN: Acetonitrile, FA: Formic acid.

The numbers in red represent the maximum signal intensity recorded in each chromatogram. The x-axis in all graphs represents retention time, the y-axis in all graphs represents signal intensity.

4.3.7 Measurement of Hydrogen Sulfide Levels in Transgenic Mice Injected with MitoA

In order to determine the efficacy of the developed method, I applied the method to liver samples from transgenic mice with thiosulfate sulfurtransferase (TST) enzyme knocked out. Briefly, 11-week old C57BL/6J wild-type (n=6) or TST KO (n=6) male mice were injected with 100 μL of 50 nM MitoA via tail vein injection. After 1.5 hr the mice were culled by schedule 1 cervical dislocation and cessation of circulation was confirmed by cutting the femoral artery. Liver samples were dissected and flash frozen in liquid nitrogen. Extraction of MitoA and MitoN and spiking of the solution with internal standards was performed as described for the 'post-spike' method **(Figure 16a)**, with an additional PLD+ extraction step immediately prior to resuspension. The resuspended sample solution was added to a deep-well 96-well plate and analysed alongside a calibration curve of MitoA and MitoN standards (**Figure 19)**. Both analytes were detectable in this extracted solution for all samples except from one C57BL/6J wild-type sample (likely due to failed intravenous injection of MitoA) which was excluded from analysis.

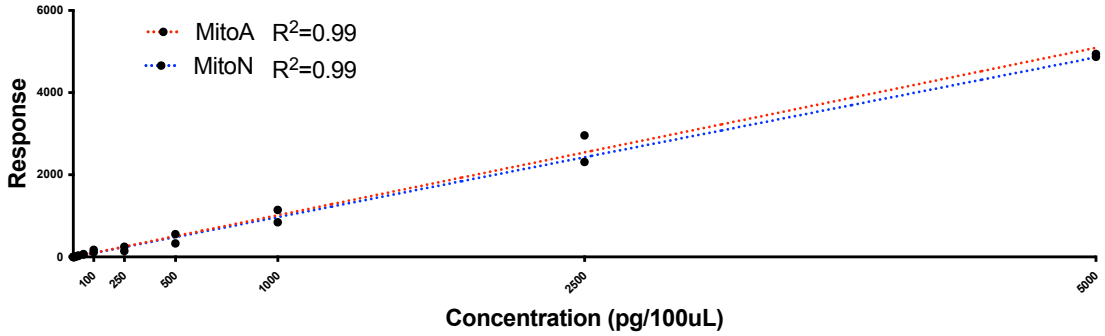

	Standard Conc. (ng/100uL)	Area	RT	IS Area	IS RT	Response	Calculated Conc. (ng/100uL)	%Dev	S/N
MitoA	1	13.98	1.95	16735.365	1.58	0.001	2.6949	169.5	1.254
	2	7.608	1.96	32815.355	1.57	0.000	0.427789	-82.9	0.787
	5	169.256	1.91	169182.938	1.57	0.001	3.315007	-33.7	13.907
	10	146.967	1.92	92414.977	1.58	0.002	5.530835	-44.7	9.844
	25	1434.077	1.92	186918.25	1.58	0.008	28.377674	13.5	82.226
	50	1876.124	1.92	120347.578	1.58	0.016	58.11801	16.2	129.973
	100	3753.729	1.91	120249.688	1.57	0.031	116.820761	16.8	287.240
	250	2111.627	1.92	54256.523	1.57	0.039	145.757954	-41.7	87.153
	500	8636.711	1.92	98056.211	1.57	0.088	330.427812	-33.9	644.447
	1000	20623.525	1.92	91726.281	1.57	0.225	844.163452	-15.6	1175.154
	2500	2524.604	1.92	3201.194	1.58	0.789	2962.113237	18.5	88.186
	5000	5251.846	1.92	3988.651	1.58	1.317	4945.752568	-1.1	336.678
MitoN	1	29.864	1.57	16735.365	1.58	0.002			2.348
	2	82.078	1.65	32815.355	1.58	0.003	2.76557	10.6	5.565
	5	383.774	1.59	169182.938	1.57	0.002	1.818666	-63.6	15.158
	10	369.407	1.59	92414.977	1.58	0.004	8.850441	-11.5	24.496
	25	1959.021	1.58	186918.25	1.58	0.010	35.220072	40.9	45.647
	50	2364.015	1.59	120347.578	1.58	0.020	72.486876	45.0	128.835
	100	5431.607	1.58	120249.688	1.57	0.045	176.308845	76.3	238.253
	250	3457.12	1.58	54256.523	1.57	0.064	251.751282	0.7	196.649
	500	13677.956	1.58	98056.211	1.57	0.139	559.940531	12.0	700.681
	1000	25998.705	1.58	91726.281	1.57	0.283	1145.412222	14.5	774.688
	2500	1827.033	1.59	3201.194	1.58	0.571	2313.927766	-7.4	66.370
	5000	4788.191	1.59	3988.651	1.58	1.200	4875.167266	-2.5	215.129

Figure 19 Calibration curve for final analysis of hepatic tissue samples

Calibration curve and supporting table for MitoA and MitoN standards. Standards were prepared from 1-5000 ng/100 μL in a deep-well 96-well plate in 100 μL 20% ACN 0.1% FA. ACN: Acetonitrile, FA: Formic acid.

From these data the concentration of each analyte in solution was calculated using TargetLynx (Waters, Wilmslow, UK) quantification software and normalising to the mass of tissue homogenized for analysis. The [MitoN]:[MitoA] ratio in each hepatic sample was calculated, these data are summarised in **Figure 20a**. For comparison, the same mouse liver samples were used in a lead acetate assay. This assay measures H_2S production capacity *ex vivo* and is the most commonly used method in the literature [230]. Briefly, protein homogenate was prepared in lysis buffer from flash-frozen liver samples and loaded into a 96-well plate. The protein lysates were mixed with a reaction solution containing 10 mM L-cysteine and 1 mM pyridoxal-5'-phosphate hydrate which are the substrate and co-factor for CSE and CBS-dependant H_2S production, respectively. The plate is tightly covered with filter paper that was soaked in 20 mM lead(II) acetate and dried. As H_2S accumulates in the head of the plate wells it reacts with the lead(II)acetate in the filter paper at 37^{o}C for 1-2 hr to produce a brown-black precipitate. The density of colour change produced in each well is a measurement of the H_2S produced in that well. TST wt and KO liver protein samples were prepared in triplicate with 20 ug of liver protein lysate per well, incubated for 2 hr at 37^{o}C and density of precipitate formed was quantified by LiCor Image Studio^{TM} (**Figure 20b**). The results presented in **Figure 20a and Figure 20c** show a similar upward trend in hepatic mitochondrial H_2S levels *in vivo* and H_2S production capacity *ex vivo*, with the latter being significantly upregulated. Simple linear regression analysis found a weak correlation (R^2 = 0.399) between these data (**Figure 20c**).

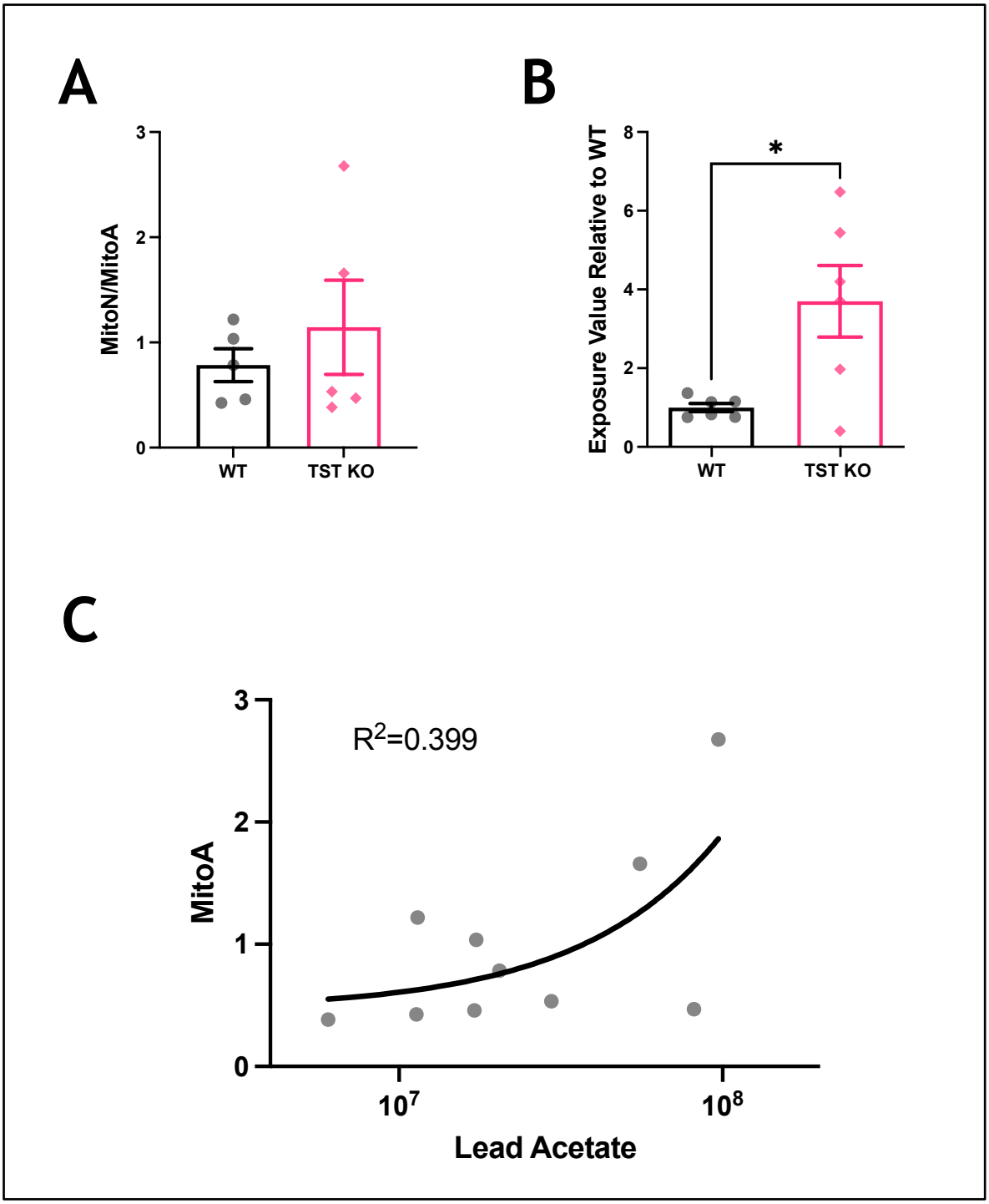

Figure 20 Hepatic H_2S production in hepatic mouse samples

A MitoN/MitoA ratio calculated from concentration of MitoA and MitoN in each sample. A higher MitoN/MitoA ratio indicates more H_2S was present in the tissue *in vivo*. **B** H_2S production capacity measured by lead acetate assay using the same liver samples used in LC/MS/MS analysis. **C** Correlation of H2S detected by lead acetate and MitoA methodologies. Error bars represent SEM. Statistical significant determined by two-sample unpaired t-test with alpha = 0.05. Grubbs outlier test with alpha = 0.05 identified no outliers. * = $p<0.05$.

There are several explanations for why the results presented here do not directly mirror one another. First, the lead acetate method employs supraphysiological concentrations of substrates for H_2S production [230]. This is intentional as the assay aims to determine the maximal production capacity of the sample [230]. By contrast, the MitoA method does not stimulate any H_2S generating enzymes but instead passively measures the concentration of mitochondrial H_2S in tissue [269]. Second, the substrates and co-factors employed in the lead acetate method selectively hyperactivate two H_2S-generating enzymes (Cystathionine-γ-lyase and Cystathionine-β-synthase) but do not stimulate 3-Mercaptopyruvate sulfurtransferase (MPST) activity [267]. As such, the assay is a measurement of the maximal enzymatic activity of two just two of the H_2S-generating proteins. Finally, MPST is the only H_2S-generating enzyme that can localise to mitochondria in normal physiological conditions and, as such, it is the activity of MPST that is being selectively measured by quantifying the extent of MitoA conversion into MitoN [307]. In this light, the two assays can be considered complimentary to one another: lead acetate assay to measure cytosolic maximal H_2S production, MitoA to determine absolute H_2S levels in mitochondria.

4.4 Imaging mass spectrometry method development

Given the successful development and optimisation of a LC/MS/MS method utilizing MitoA, I next examined the potential use of MitoA for MS imaging techniques. Such a method would allow spatial resolution of H_2S concentration across tissue sections. The liver is a major site of H_2S production, and H_2S directly influences hepatic lipid metabolism, ATP production, and disease pathogenesis [256]. It has also become clear that hepatocytes in the liver are functionally defined across the porto-central axis [308], [309]. Essentially, the liver is arranged into lobules with portal tracts at the periphery and a central vein at the centre, and hepatocytes have different functionality dependent on their location within the lobule. This paradigm is termed liver zonation and an increasing number of studies have defined the molecular functionality of hepatocytes dependent on their zonation in terms of glycolysis, β-oxidation, and iron homeostasis [308], [309]. To date, no studies had determined H_2S levels across the hepatocyte zonation axis. Thus, I attempted to combine the MitoA probe with imaging MS techniques to answer this unmet question, however, the method development was ultimately unsuccessful. I have detailed the method development and discussed potential reasons as to why this was the case.

4.4.1 Direct infusion of analytes

First, the MitoA and MitoN analytes were directly infused into the MS to establish if they were readily detected by the MS used for imaging experiments (Synapt G2-Si QToF (Waters Corporation, Manchester, UK). The analytes were prepared at 0.1 μg/mL in 50% ACN 0.1% FA and infused into the spectrometer at 2 μL/min flow rate. Mass spectra for each compound are presented in **Figure 21**. Strong, gaussian peaks were detected for both MitoA (at 465.1737 m/z) and MitoN (at 439.1864 m/z).

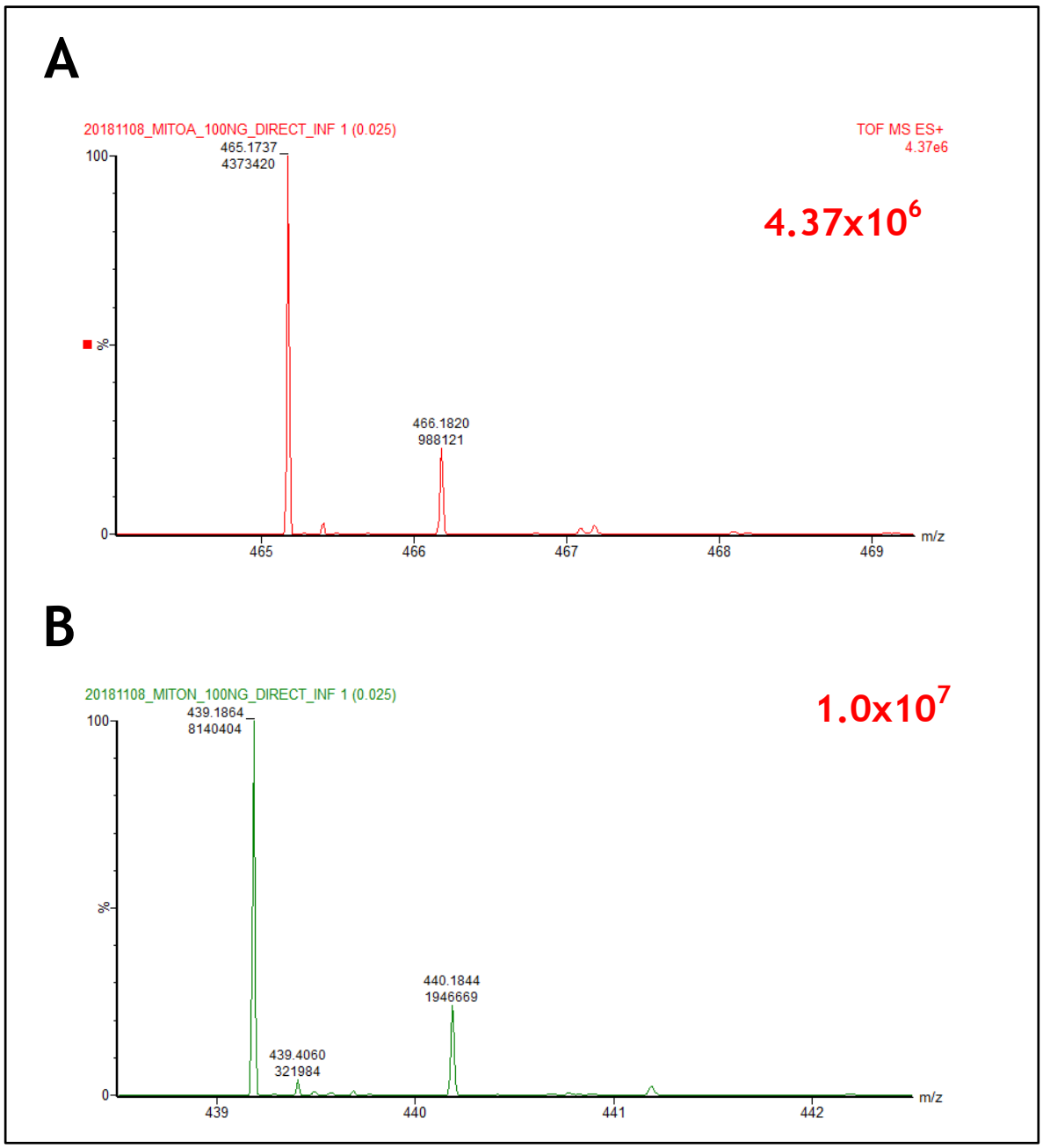

Figure 21 Mass spectra for direct infusion of MitoA and MitoN into MS

Mass spectra generated by direct infusion of MitoA (**A**) and MitoN (**B**) into mass spectrometer. Standards of each analyte were prepared at 0.1 μg/mL in 50% ACN and 0.1% FA and subsequently infused into the spectrometer at 2 μL/min flow rate. The numbers in red represent the maximum signal intensity recorded in each chromatogram. The x-axis represents retention time and the y-axis represents signal intensity.

4.4.2 Analyte spotting on glass slide

After establishing that the analytes were detectable on the MS, I next moved to imaging the analytes on a glass plate by desorption electrospray ionization (DESI) MS imaging. DESI imaging allows for label-free measurement of analytes from complex samples, including hepatic tissue sections [310]. For this initial investigation, analytes were spotted onto glass slides at 0.001-100 μg/mL and dried under vacuum. The slide was then imaged using a DESI platform (2D Prosolia DESI source) with DESI solvent of 98% MeOH 0.1% FA infused at 2.5 μL/min. MS resolution was set to 10000, mass window 0.02 m/z, and number of intense peaks selected was 100. Additionally lock mass was used with caffeine internal standard at mass 556.27 m/z. The images produced at both 100x100 and 200x200 μm resolution are shown in **Figure 22**. From these images we can see that the limit of detection (LOD) for MitoA is 0.01 μg/mL and 0.1 μg/mL for MitoN. This confirms that both analytes can be imaged using DESI MS, however the LOD is high compared to commonly reported LODs for detecting analytes in liver tissue by imaging MS techniques [311].

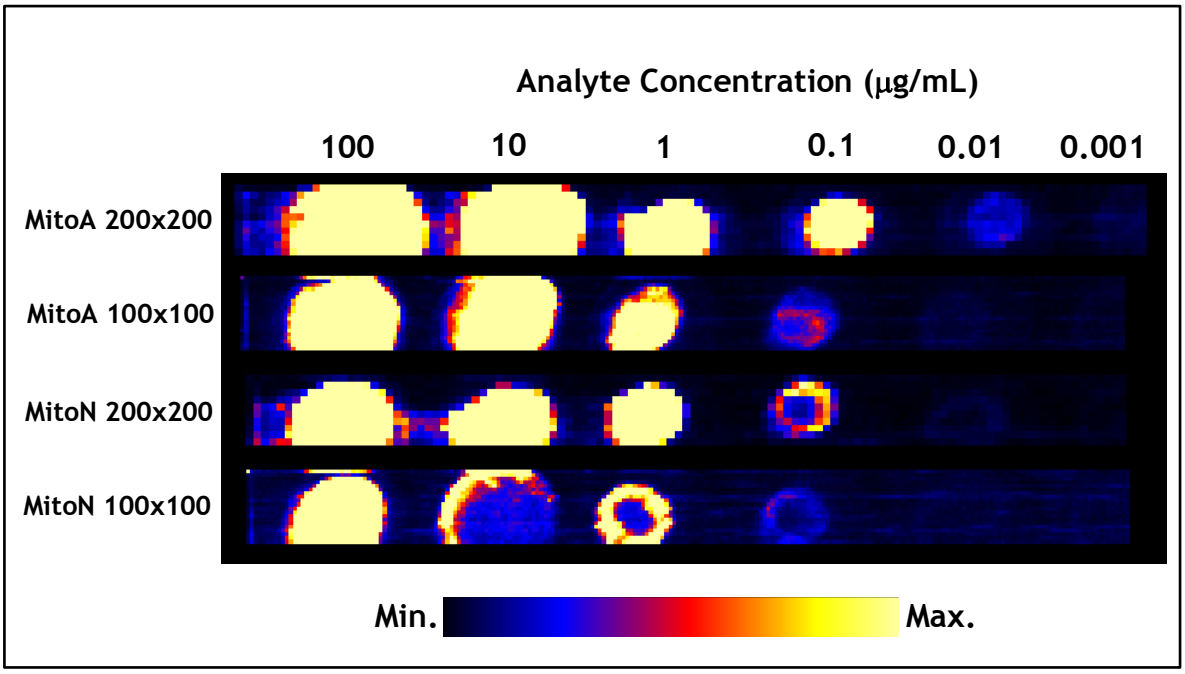

Figure 22 DESI MS imaging of MitoA and MitoN analytes on a glass slide

Image acquired by DESI MS imaging of a glass slide with MitoA and MitoN analytes spotted and dried onto the surface at 0.001-100 μg/mL. Resolution was set to 200x200 or 100x100 μm.

4.4.3 Analyte spotting on hepatic tissue

Next, I investigated whether the analytes were still detectable when spotted onto mouse hepatic tissue sections and established a LOD for each analyte on hepatic tissue. For this, flash-frozen mouse liver was sectioned to 10 μm thickness using a cryostat (Leica CM1520, Leica Biosystems) and adhered to a glass slide. Then 0.5 μL aliquots containing MitoA and MitoN in 98% MeOH 0.1% FA at 0.001-5 μg were spotted onto the liver section and then dried under vacuum. The location of each spot is shown in **Figure 23a**. The slide was then imaged using a DESI platform (2D Prosolia DESI source) with DESI solvent of 95% MeOH infused at 2.5 μL/min. MS resolution was set to 10000, mass window 0.02 m/z, and number of intense peaks selected was 100. Additionally lock mass was used with caffeine internal standard at mass 556.27 m/z. The images produced for MitoA and MitoN signals are shown in **Figure 23b** and **Figure 23c**, respectively. From these images we can see that the LOD on hepatic tissue sections is 0.1 μg/mL for both MitoA and MitoN.

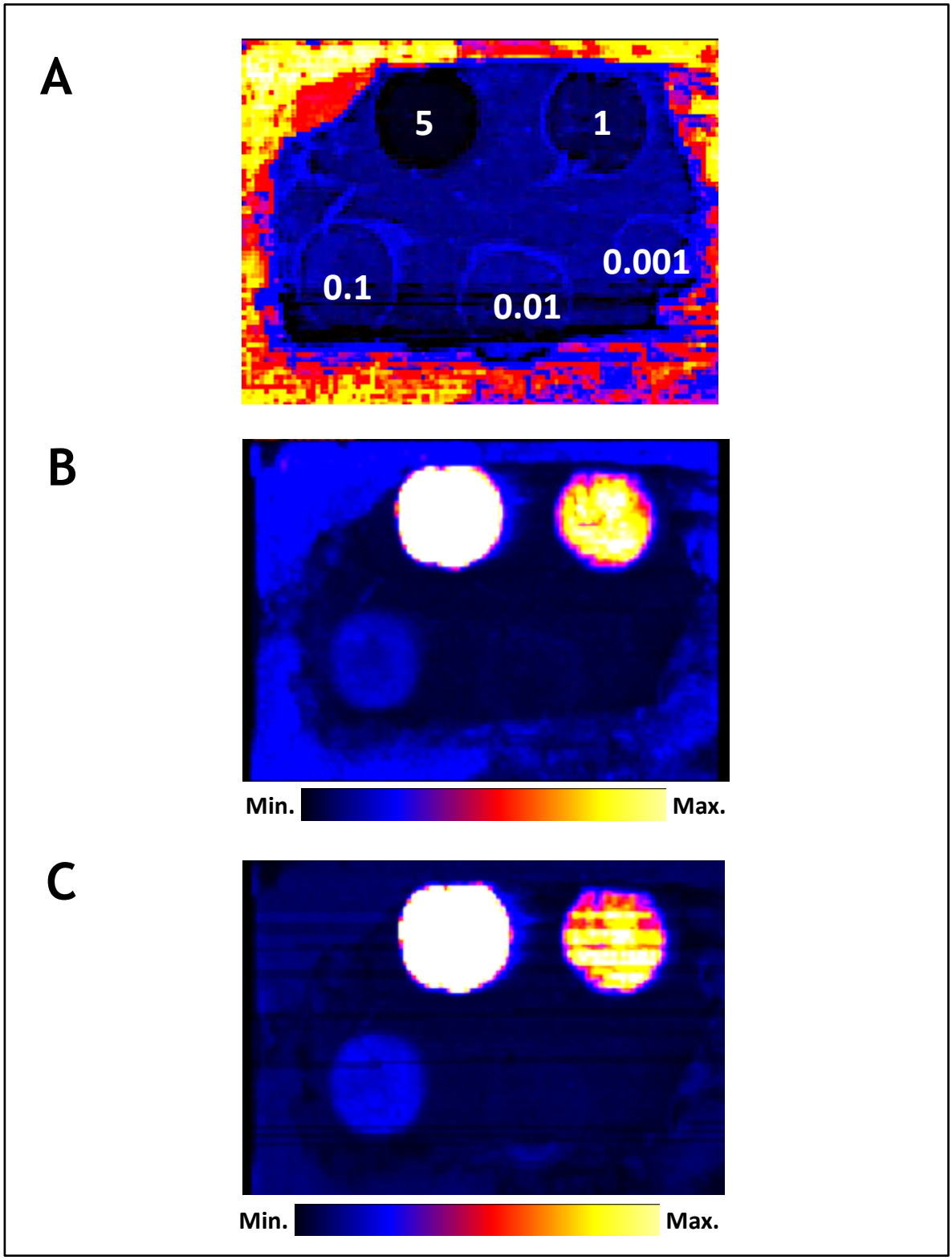

Figure 23 DESI MS imaging of MitoA and MitoN analytes on hepatic tissue section

A Location and concentrations of each analyte spot on the liver sample. Both MitoA and MitoN were included in each spot at the concentration indicated, 0.001-5 μg/mL. Standards were prepared in 98% MeOH 0.1% FA then dried under vacuum **B** DESI imaging of signals arising from MitoA. **C** DESI imaging of signals arising from MitoN.

4.4.4 Imaging of MitoA-injected hepatic tissue

Finally, the DESI MS method was applied to tissues sample from a mouse injected with MitoA. Briefly, 11-week old C57BL/6J wild-type (n=6) or TST KO (n=6) male mice were injected with 100 μL of 50 nM MitoA via tail vein injection. After 1.5 hr the mice were culled by schedule 1 cervical dislocation and cessation of circulation was confirmed by cutting the femoral artery. Liver samples were dissected and flash frozen in liquid nitrogen. A liver tissue section at 10 μm thickness was prepared by cryostat and adhered to a glass plate. Additionally, two other liver sections were adhered to the plate at the same thickness: one for optimisation of DESI machinery prior to analysis and another large tissue section to allow the spotting of a calibration curve of the MitoA and MitoN analytes. The layout of the slide is shown in **Figure 24a,** while the concentration of the seven calibration standards and their location on the tissue section are shown in **Figure 24b** and **Figure 24c**. As previously, 0.5 μL aliquots containing MitoA and MitoN standards in 98% MeOH 0.1% FA were spotted onto the liver section and then dried under vacuum. The slide was then imaged using the DESI platform with DESI solvent of 95% MeOH infused at 2.5 μL/min. MS resolution was set to 10000, mass window 0.02 m/z, and number of intense peaks selected was 100. Additionally, lock mass was used with caffeine internal standard at mass 556.27 m/z.

A

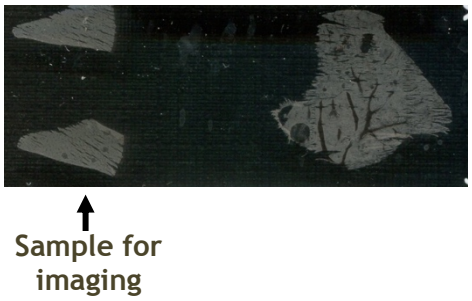

B

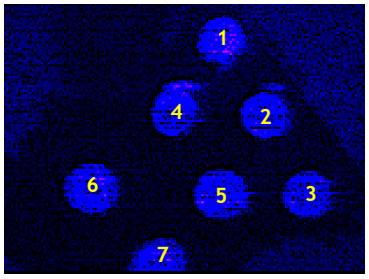

C

Spot #	Mito A (ng/ml)	Mito N (ng/ml)
1	500	0
2	400	100
3	350	150
4	250	250
5	150	350
6	100	400
7	0	500

Figure 24 Set up of slide and calibration standards for analysis of MitoA-injected hepatic tissue section

A Slide layout for analysis. **B** Layout of calibration curve standards on hepatic tissue sample. **C** Concentration of MitoA and MitoN standards in each spot. Standards were prepared in 98% MeOH 0.1% FA then dried under vacuum

Mass spectra for the detection of MitoA and MitoN in each standard curve spot are shown in **Figure 25a**. Images showing this data are also given for MitoA and MitoN in **Figure 25b** and **Figure 25c**, respectively. The calibration curve for these standards is given in **Figure 25d**. The calibration curve produced by this experiment has strong linearity (R^2 = 0.9985), indicating this is a robust method to quantify MitoA and MitoN signals on hepatic tissue sections without the need for infusion of deuterated standards.

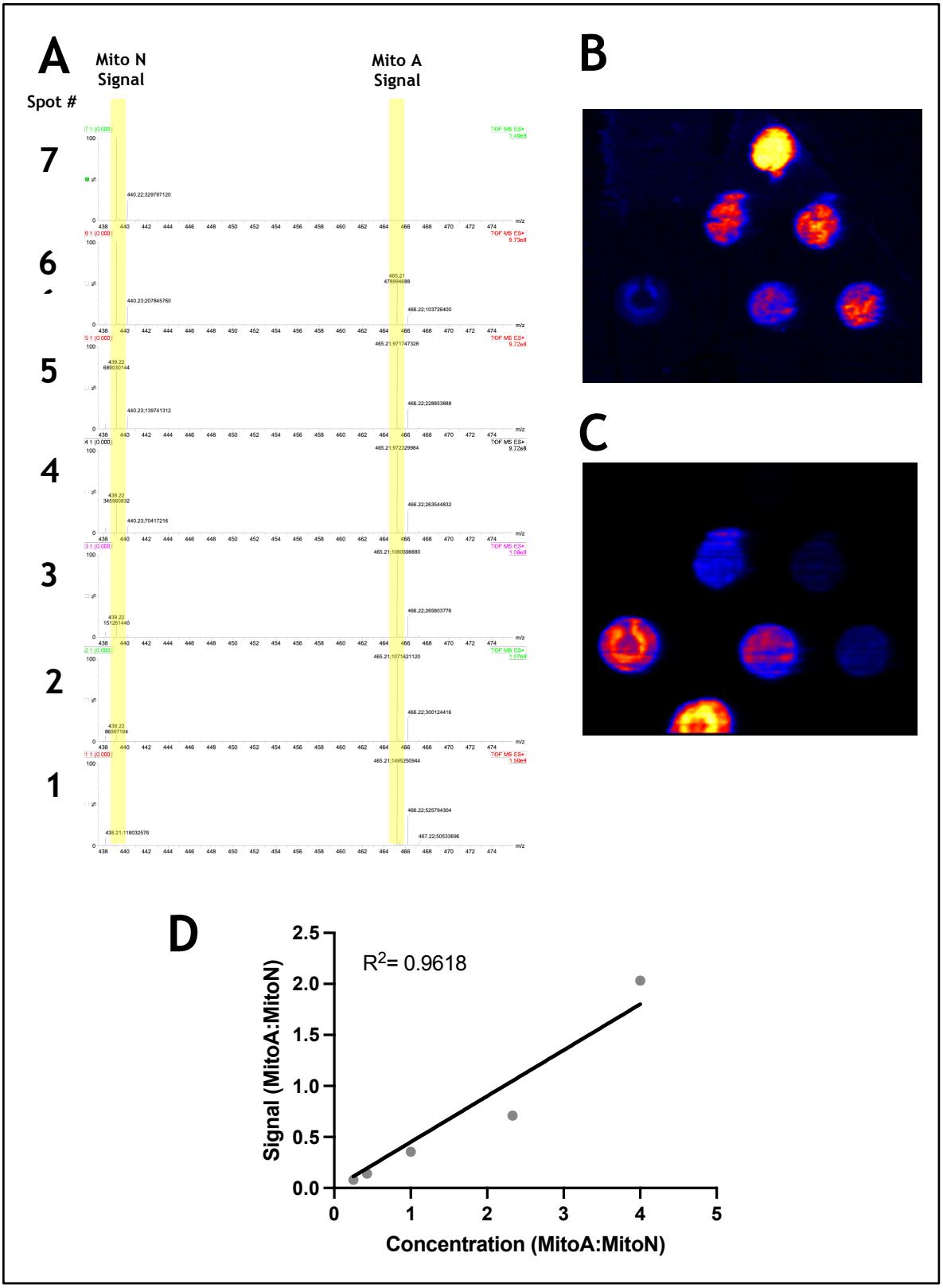

Figure 25 Calibration curve of MitoA and MitoN standards spotted onto hepatic tissue section for the quantification of MitoA-injected hepatic tissue section

A Mass spectra for MitoA and MitoN signals in each calibration standard curve. **B** DESI Imaging of signals arising from MitoA. **C** DESI imaging of signals arising from MitoN. **D** Calibration curve quantifying signals arising from MitoA and MitoN standards spotted onto hepatic tissue section.

Unfortunately, no signal was detected for MitoA or MitoN from the MitoA-injected tissue sample (**Figure 26**). It appears likely that MitoA is simply not detectable by DESI MS imaging at the concentration used in this experiment. As our lab is not licensed to attempt higher concentrations of a lab synthesized compound for animal welfare considerations the development of an imaging MS methodology using MitoA was suspended.

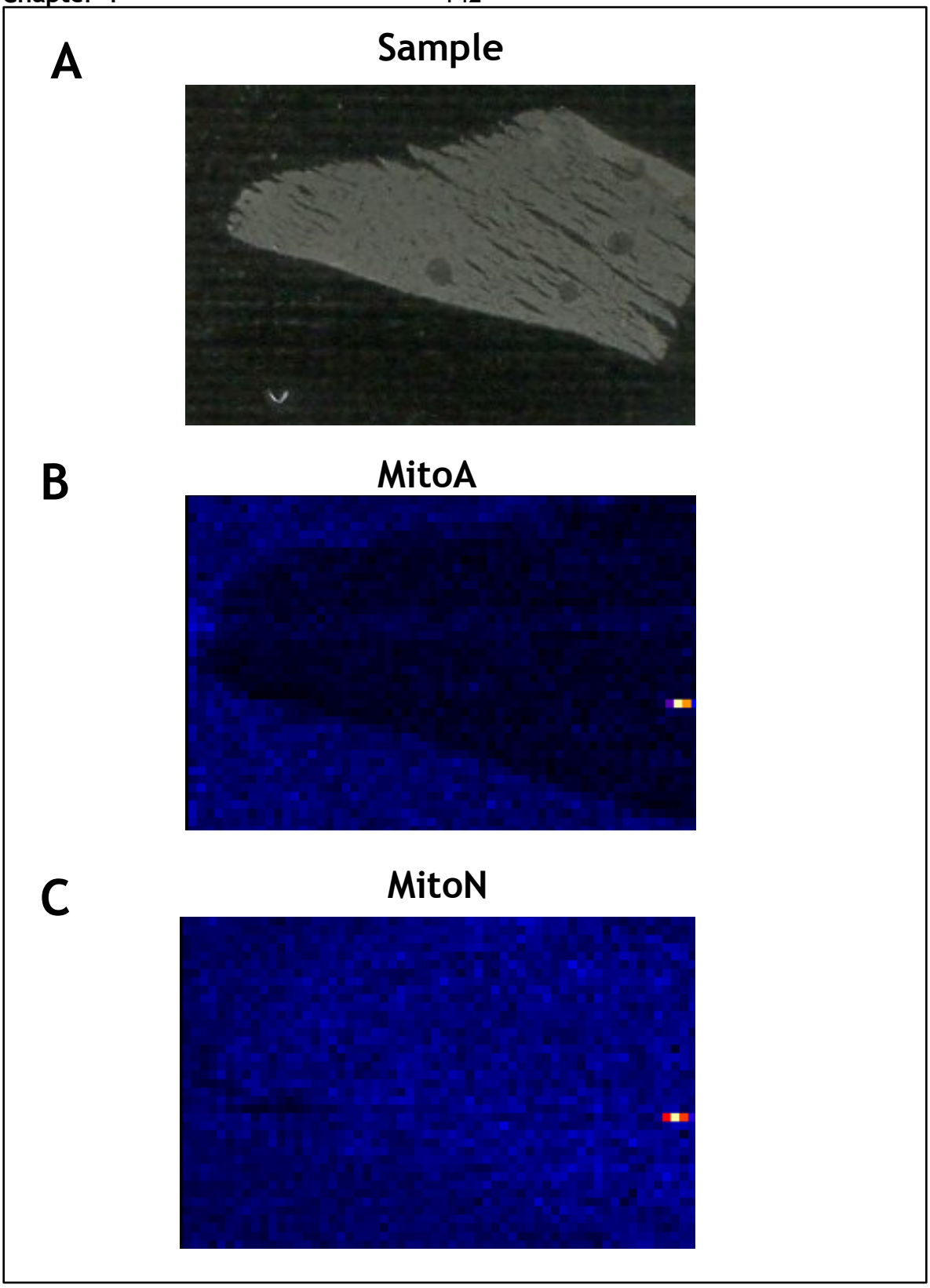

Figure 26 Attempted detection of MitoA and MitoN from MitoA-injected hepatic tissue section

A Digital image showing tissue section from mouse injected with MitoA prior to cull. **B** DESI imaging of signals arising from MitoA, none detectable. **C** DESI imaging of signals arising from MitoN, none detectable.

4.5 Summary

H_2S has emerged as a powerful modulator of many biological processes. As such, study of this molecule has attracted great interest. However, the main obstacle preventing a deeper understanding of the biological role of H_2S lies in the difficulty of accurately measuring H_2S levels in biological sample. As a reactive gaseous molecule, H_2S rapidly is degraded during sample preparation and readily diffuses into the atmosphere. Current methods for determining H_2S levels are limited to *ex vivo* measurements that may not accurately reflect the concentration within tissues of living organisms. To answer this unmet need a novel probe called MitoA was developed by Prof. Richard Hartley (University of Glasgow, UK) which allows for accurate measurements of *in vivo* mitochondrial H_2S levels by injection of the compound into an organism, extraction of compounds from tissue samples, and then determination of analyte concentration by mass spectrometry-based analysis. To date, the only previous study using this methodology in mice was a proof-of-concept study conducted by Hartley *et al*. I applied the MitoA probe to a mouse model with genetic knock out of thiosulfate sulfurtransferase (TST KO), a mitochondrial protein that improves insulin sensitivity under obesogenic stress and is involved in the oxidation and disposal of H_2S. The TST KO is a novel mouse model which has unresolved metabolism of H_2S compared to wild-type controls. In my analysis of MitoA-injected samples of TST KO mice I optimized the mass spectrometry and sample preparation protocols. The result was a working method that allowed measurement of *in vivo* mitochondrial H_2S levels and revealed subtle differences in reported H_2S levels as measured by MitoA and another commonly used cytosolic H_2S measurement technique. The results have clarified the metabolism of H_2S in this model and contributed to the understanding of the subcellular localisation of H_2S production and published as part of a study in Cell Reports [312]. Further to this, I attempted to develop an imaging mass spectrometry methodology to yield spatial resolution of H_2S across tissue sections. Unfortunately, the method development was unsuccessful due to the concentration of analytes in the sample being below the detection threshold of the mass spectrometer. Due to animal licensing limitations, I could not carry out the required dosing study to determine a detectable concentration for the analytes.

Chapter 5 Exploring the Role of Hydrogen Sulfide in a Mouse Model of Hutchinson-Gilford Progeria Syndrome

5.1 Abstract

Progeria syndromes are rare diseases characterised by greatly accelerated biological ageing, of which Hutchinson-Gilford progeria syndrome (HGPS) is the best studied. Current treatments are limited, and most patients die before 15 years of age. Hydrogen sulfide (H_2S) is an important gaseous mediator of mammalian physiology. H_2S interacts with several processes that appear to modulate ageing, and treatment with H_2S can ameliorate several hallmarks of ageing in model organisms. To date, the regulation of H_2S in HGPS has not been characterised. In this study I used the G609G mouse model, which has the equivalent causative mutation of human HGPS, maintained on either regular chow (RC) or high fat diet (HFD). HFD has been shown to dramatically extend lifespan in G609G mice. I examined transcript, protein and enzymatic activity levels of the pathways that regulate hepatic H_2S production and disposal. G609G mice on RC diet were found to have reduced H_2S production capacity within the liver, with a compensatory elevation in mRNA transcripts associated with H_2S production enzymes such as cystathionine-γ-lyase (CSE). However, both H_2S levels and CSE protein were rescued in G609G fed HFD relative to G609G RC mice. The study presented here provides further evidence that H_2S signalling has a role in ageing, in that a disease of accelerated ageing can be characterised by a marked reduction in hepatic H_2S production which is restored by HFD. As current treatment for patients with HGPS have failed to confer significant improvements to symptoms or lifespan, the need for novel therapeutic targets is acute and the regulation of H_2S through dietary means may be a promising new avenue for research.

5.2 Introduction

5.2.1 Progeria Syndromes

Progeroid syndromes are set of genetic disorders characterized by a shortened lifespan and development of biological alterations normally associated with advanced age such as hair loss, frailty, and atherosclerosis [313]. Studies of these progeroid diseases can yield valuable insight into the biology of healthy normative ageing [314]–[316]. While all diseases of Progeria are extremely rare, the most common human progeria is Hutchinson-Gilford progeria syndrome (HGPS), with a prevalence of 1 in 20 million [317]. HGPS is an example of a laminopathy, a set of diseases caused by mutations in the lamin A (LMNA) gene which encodes for Lamin proteins [318], [319]. Lamins are a class of fibrous filaments which provide vital structural support to the nucleus by lining and mechanically stabilising the inner nuclear membrane and anchoring chromatin and transcription factors to the nuclear periphery [320]. There are two types of lamins in the mammalian genome: A-type (Lamin A and Lamin C) which result from splicing of the LMNA gene, and B-type (Lamin B1 and Lamin B2) encoded by LMNB1 and LMNB2 genes, respectively [319]. Lamin-C is directly translated from the LMNA mRNA, while lamin-A is initially synthesised as a precursor that is post-translationally processed to produce mature lamin-A [319]. Canonically, maturation of pre-lamin A is initiated by farnesylation of the -CAAX by farnesyl transferase (FTase), with the three terminal amino acids subsequently cleaved by an endoprotease, leaving a terminal cysteine which is then methylated [321]. Finally, a metalloprotease (Zinc metalloproteinase STE24, ZMPSTE24) cleaves fifteen C-terminal residues, including the farnesylated and methylated cysteine, thus producing the mature lamin-A [321]. However, in HGPS, the canonical maturation of lamin proteins is derailed by a single-base mutation (GGC>GGT) in exon 11 of LMNA gene [320], [322]. This mutation activates a cryptic splice site and results in the deletion of 50 residues near the C-terminus of pre-lamin-A, including the ZMPSTE24 recognition site [321]. This leads to a permanently farnesylated and methylated lamin-A isoform, named progerin (**Figure 27)**. The expression of progerin disrupts the nuclear membrane by binding to lamin-A, and has been shown in mouse models to stimulate expression of senescence markers such as senescence-associated beta-galactosidase and is associated with dramatically reduced lifespan [323].

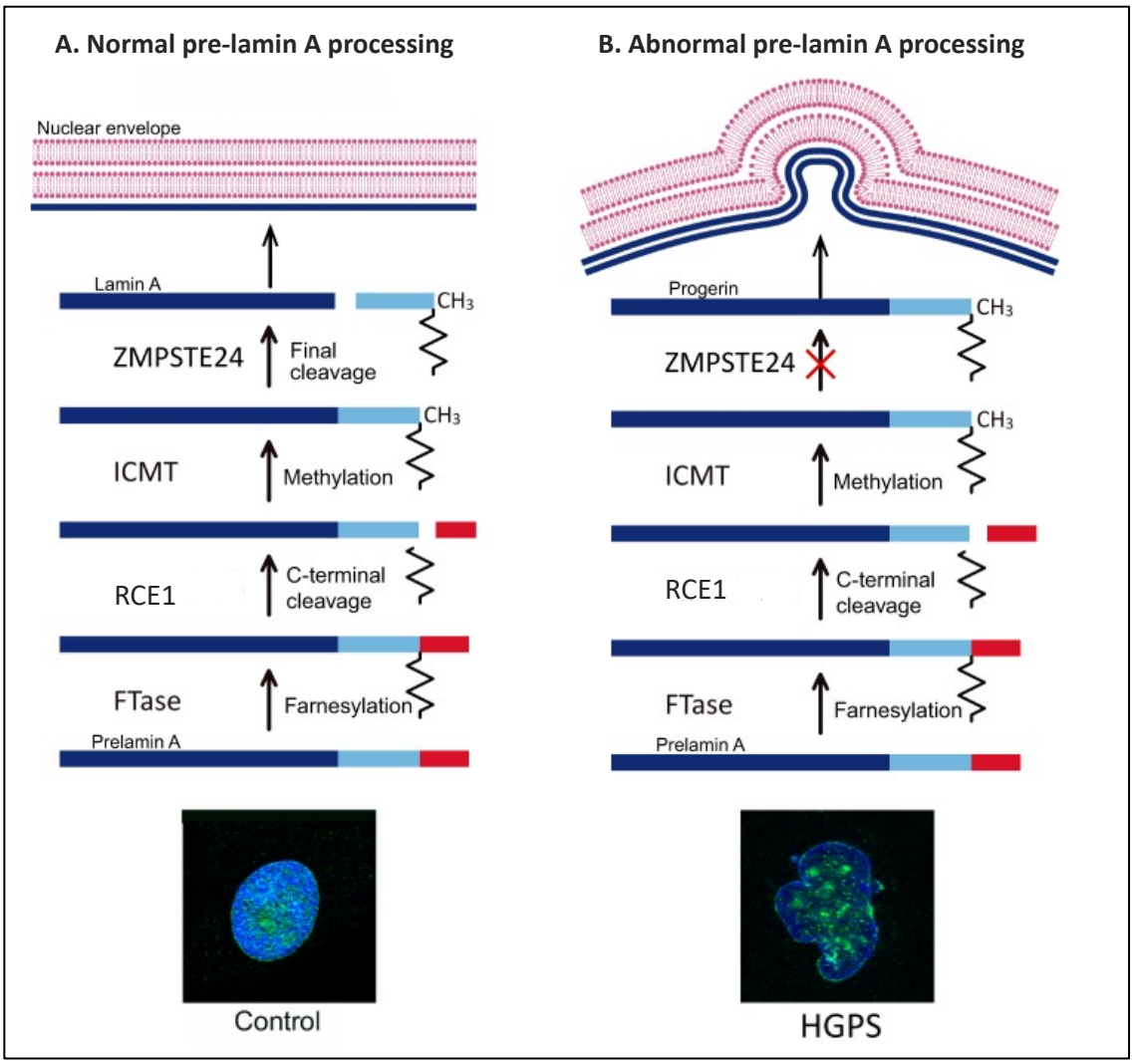

Figure 27 Physiological and pathological pre-lamin A processing and maturation.

A In healthy cells the pre-lamin A precursor protein undergoes several processing steps to produce mature lamin A which then associates with the nuclear envelope. **B** In patients with HGPS, a mutation in LMNA gene activates a cryptic splice site leading to aberrant splicing which ultimately results in the deletion of 50 amino acids near the C-terminus of pre-lamin A. This truncated protein product is farnesylated and methylated as with healthy pre-lamin A processing. However, the truncated pre-lamin A cannot undergo the final processing step of C-terminal cleavage. This results in accumulation of permanently farnesylated and methylated lamin A isoform, termed progerin. Progerin accumulation at the nuclear envelope disrupts the nuclear lamina network and is characterised by irregular nuclear morphology as seen by microscope images. ZMPSTE24, zinc metalloproteinase STE24; ICMT, isoprenylcysteine carboxyl methyltransferase; RCE1, Ras Converting CAAX Endopeptidase 1; FTase, farnesyltransferase; HGPS, Hutchinson-Gilford progeria syndrome (Adapted from [324]).

Other organelles that are altered in HGPS include mitochondria, which have been linked to changes to the metabolic profile of patients, including reduced fat stores and reduced ATP production [325]. Fibroblasts from patients with HGPS have reduced expression of cytochrome C, complex IV component cytochrome C oxidase subunit 1, and complex V [326]. These alterations are associated with reduced mitochondrial membrane potential, increased cytochrome c oxidase activity, and metabolic reprogramming from oxidative phosphorylation to glycolysis [327]. Examination of HGPS fibroblasts under high-resolution microscopy reveals an increase in swollen or fragmented mitochondria and a reduction in mitochondrial mobility in HGPS fibroblasts [328]. Many of these effects appear to be directly driven by the expression of progerin, which results in reduced expression of PGC-1a and elevated complex I activity which drives overproduction of superoxide anion [329]. Additionally, the reduction in mature Lamin A due to progerin production appears partially causative. This was demonstrated in lentiviral knockdown of the *LMNA* gene in healthy human fibroblasts which resulted in elevation of basal ROS levels and mitochondrial membrane potential depolarisation, leading to apoptosis [330]. Cellular disruption of mitochondrial dynamics is also a central driver of multiple ageing hallmarks across species [331]. Progerin also accumulates across tissue during physiological ageing due to spontaneous activation of the cryptic splice site in HGPS, which suggests that normal ageing and progeroid syndromes may share some common molecular processes [322]. Moreover, many of the hallmarks of physiological ageing are observed in HGPS patients such short stature, low body weight, hair loss, lipodystrophy, scleroderma, decreased joint mobility, and osteolysis [324]. Combined, the link between progerin accumulation and hallmarks of ageing, the manifestation of age-related diseases in HGPS patients, the expression of progerin during normal ageing, and the well-characterized genetic defects in HGPS make it an attractive model to help understand human ageing [332].

5.2.2 Progeria Mouse Models and Diet

As discussed, mutations in the *LMNA* gene cause the accumulation of progerin in the nuclear lamina, driving HGPS progression. The most common of these mutations is the point mutation c.1824C>T;p.Gly608Gly in the human *LMNA* gene and a mouse model exists with an equivalent 1827C>T;p.Gly609Gly mutation in the *Lmna* gene, known as $Lmna^{G609G+/G609G+}$ or simply G609G [228]. The G609G mouse model was created by Carlos Lopez-Otin and captures much of the human HGPS disease phenotype, including the mitochondrial dysfunction phenotype [326], [332], [333] and the aberrant splicing events associated with HGPS [228]. However, the G609G model does not fully capture the range of pathologies observed in patients with HGPS. One major phenotype of HGPS in humans alopecia and the leading cause of death (>90%) is myocardial infarction or other cardiovascular pathologies such as stroke [334]. In the G609G mouse model hair loss is incomplete and the major cause of death is cachexia and starvation [229]. One explanation for the lack of cardiovascular pathology in G609G mice is the highly atheroprotective profile of blood lipids in mice in general [335]. Most mouse models have a lower plasma cholesterol concentration and a higher ratio of high-density lipoprotein relative to low density lipoprotein, compared to humans [335]. This makes many mouse models resistant to high-fat diet (HFD) induced atherosclerosis, which necessitates transgenic inactivation of *Apoe* to induce pathology (this is true in G609G mice too [336]). Beyond genetic manipulation, diet has emerged as an intervention central to the progeroid phenotype. Therapeutically, a low methionine diet in G609G mice has been shown to extend lifespan and reprogram transcriptional regulation of DNA damage repair and the metabolism of bile lipid/acid levels to be more like non-HGPS control mice compared to G609G maintained on regular chow diet (RC) [337]. Interestingly, a low methionine diet is also an established intervention for the elevated of H_2S production in mice, conferring multiple health benefits and lifespan extension [165]. Consideration should also be given to the typical dietary intake of patients with HGPS. The Progeria Research Foundation (California, US) notes that patients with HGPS consume sufficient calories in small, frequent meals, and suggests the use of “nutritious and high calorie foods and supplements” [338]. Indeed, G609G mice on regular chow (RC, 24.5% protein, 62.4% carbohydrate, 13.1% fat, 3 kcal/g) diet have a mean

survival approximately 110 days, however when fed a high cholesterol diet (15.2% protein, 42.7% carbohydrate, 42.0% fat, 4.5 kcal/g) from 1 month of age onwards this was extended to 169 days [229]. More strikingly, G609G mice on a high-fat diet (HFD, 20.0% protein, 20.0% carbohydrate, 60.0% fat 5.2 kcal/g) had an average lifespan of 193 days. Surprisingly, G609G mice did not appear susceptible to the negative effects of HFD. Indeed, G609G HFD mice had significantly lower serum glucose and plasma insulin levels compared to WT HFD mice, with levels actually being more comparable to WT and G609G mice on RC [229]. Furthermore, glucose tolerance of G609G HFD was improved compared to G609G RC fed mice [229]. However, the HFD feeding in G609G mice, leading to a longer-life, more fully captured the phenotype of human HGPS, with onset of previously unseen pathologies including full body alopecia, skeletal dysplasia and aortic wall stiffening (**Figure 28**). As such, the application of HFD in G609G mice may be considered as therapeutic (as is greatly extends lifespan compared to RC controls) but also may prove useful if employed as standard animal care conditions for G609G to more fully recapitulate the disease phenotype seen in patients with HGPS.

Studies in mice have shown that *ex vivo* H_2S production is negatively affected across tissues under the stress of HFD feeding, with a correlated reduction in the protein levels of H_2S-generating enzyme cystathionine-γ-lyase (CSE) [339]. HFD mice that undergo 24 weeks of moderate exercise had increased hepatic H_2S production and *Cse* mRNA transcripts and amelioration of hepatic steatosis and fibrosis compared to non-exercised controls, which is suggestive of a relationship between H_2S and the protective effects of exercise against HFD-induced non-alcoholic fatty liver disease [265]. Additionally, intraperitoneal injection of the H_2S donating compound sodium hydrosulfide (NaHS) mitigated against markers of renal injury caused by HFD-induced obesity in mice [340]. Collectively, these data indicate that the deleterious effects of HFD in mice are associated with a reduction in H_2S production. However, given that HFD is beneficial for the health and lifespan of G609G mice compared to an RC diet, understanding the metabolism of H_2S within the unique context of G609G mice on HFD may help further our understanding of the role of diet and H_2S in progeria.

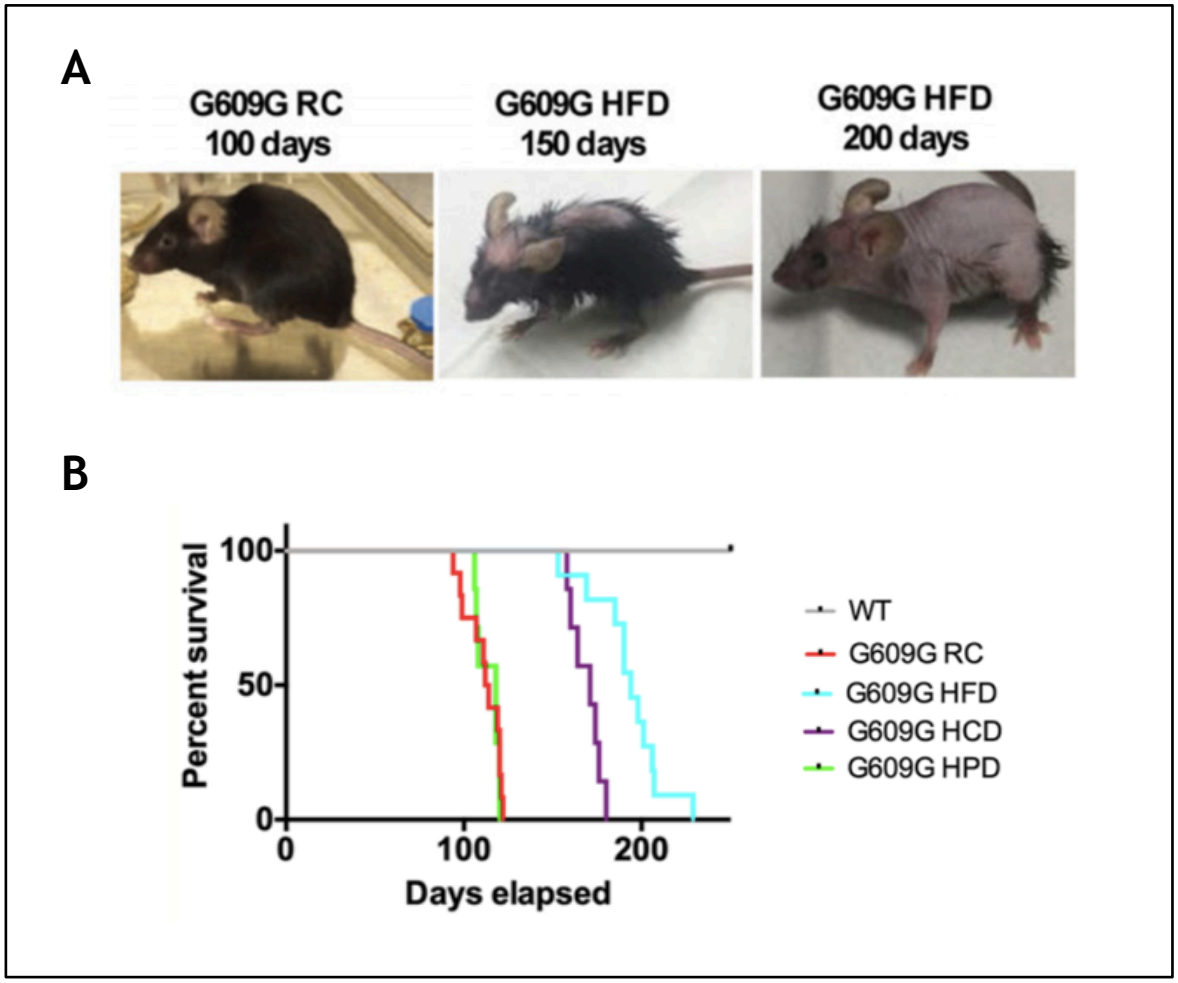

Figure 28 G609G mice maintained on high-fat diet have doubled lifespan and better mimic the phenotype of human HGPS than those fed regular chow (RC) diet

A LEFT, G609G RC-fed mice near death at 100 days old; MIDDLE, G609G HFD-fed mice at 150 days old; RIGHT, G609G HFD at 200 days of age. These representative pictures clearly demonstrate progressive alopecia across the whole animal, one of the major phenotype in HGPS patients that is not seen in RC fed G609G mice on RC diet. **B** Kaplan–Meier plots comparing survival curves between WT and G609G mice fed RC, HFD, HCD or HPD are shown. Note that while HFD has the most pronounced impact on survival (average lifespan of 111 days on RC compared to 193 days on HFD), HCD also produces a significant extension in maximal lifespan. HPD fails to alter lifespan. Regardless of diet, all G609G mouse groups have drastically shorter lifespans compared to WT controls (WT controls were fed a RC diet).
RC, regular chow; HFD, high-fat diet; HCD, high-cholesterol diet; HPD, high-protein diet; HGPS, Hutchinson-Gilford Progeria Syndrome. (Images and data from Kreienkamp *et al.*, 2019 [234].

5.2.3 H_2S in Progeria

Therapeutic treatments for patients with progeroid diseases remain lacking, with an average life expectancy of humans with HGPS typically being under 15 years [341]. Current treatments include farnesyltransferase inhibitors, rapamycin analogues, sulforaphane, and vitamin D analogues which all have clear impacts on disease symptoms but have yet to provide substantial improvements to patient lifespan or incidence of comorbidities [341]. While no studies have investigated the role of H_2S in HGPS to date, there is known overlap between H_2S and the mechanisms that underpin rapamycin, sulforaphane, and vitamin D treatment. In this section I will describe the known role for H_2S in the mechanisms of these treatments when studied in conditions other than HGPS. Whether H_2S has similar roles in the context of HGPS is currently unestablished.

Rapamycin is an inhibitor of mammalian target of rapamycin (mTOR) complex 1 (mTORC1), and H_2S can either stimulate or inhibit mTOR signalling [182]. This is counterintuitive as both H_2S and rapamycin are implicated as pro-longevity molecules and therefore we might anticipate they would both act upon the mTOR pathway in a similar manner i.e. suppression of mTOR activity. This has been found in some instances, such as studies in the Zucker diabetic rat model where culture of *ex vivo* brain slices with NaHS, a H_2S donor, decreased protein aggregation through inhibition of mTOR signalling and increased autophagy [183]. In addition, exogenous administration of several H_2S donors induced autophagy in rat pancreatic exocrine cells and was associated with inhibition of TOR phosphorylation at serine 2448 [184], [185]. In contrast, H_2S has also been shown to activate mTOR with myriad effects ranging from stimulating angiogenesis in vascular endothelial cells *via* the micro RNA miR-640, by stimulating osteoclastogenesis in monocyte/macrophage-like cells (Raw 264.7) by phosphorylating mTOR and inhibiting autophagy [187], [189]. Along with conflicting results on how H_2S influences mTOR signalling, we also lack a full appreciation of the effect of rapamycin on H_2S production pathways. To date only one study has investigated the effect of rapamycin on H_2S, this study did so in *Saccharomyces cerevisiae* and in human HeLa and 293T cell lines [190]. Rapamycin inhibited H_2S production through depression of cystathionase-γ-lyase (CSE) and cystathionine-β-synthase (CBS) gene transcription in both cell models and in the yeast homologs of these genes [190]. There is a lack of studies that

combine Rapamycin and H_2S-donors. Such studies would help develop our understanding of how these compounds may co-interact on the mTOR signalling pathway. One example of such an approach used a human hepatocellular carcinoma cell line and treatment with Rapamycin and a H_2S-donor separately or in combination [191]. They found that both treatments inhibited mTOR signalling and stimulated anti-tumour autophagic and pro-apoptotic pathways, with an additive effect when both were used in combination.

Sulforaphane is an isothiocyanate compound found naturally in cruciferous vegetables [342]. HGPS patient fibroblasts cultured in sulforaphane-rich media showed amelioration of the HGPS phenotype, with normalised nuclear morphology, enhanced proteostasis, and elevated proliferation [343]. The mechanism through which sulforaphane operates appears to involve the generation of H_2S when dissolved in a solution, with sulforaphane treatment elevating H_2S levels upon addition cell culture, and tissue homogenates [342], [344]. Given that sulforaphane is a compound that is essentially a naturally occurring H_2S donor there have been a surprisingly limited number of studies that directly monitor H_2S levels following sulforaphane treatment, and none in the context of HGPS. Treatment with or ingestion of sulforaphane-rich vegetable homogenates has been shown to be a promising treatment in Alzheimer's disease and boosts antiviral responses of natural killer cells in human clinical trials [344], [345]. Furthermore, sulforaphane treatment in a human prostate cancer cell line was found to impede cancer cell survival *via* H_2S-mediated JNK and MAPK signalling [342]. Finally, the activity of sulforaphane has been attributed largely to mechanisms that are also modified by H_2S, such as potent activation of nuclear factor erythroid 2-related factor 2 (NRF2) by modification of Kelch Like ECH Associated Protein 1 (KEAP1) [98], [346] and inhibition of insulin signalling [200], [347]. Indeed a diet rich in sulforaphane improves markers of skin health in young and aged mice through micro RNA34a-dependent activation of NRF2 response, the same microRNA that is elevated by H_2S and confers protection against hepatic ischemia-reperfusion injury in young and old rats by augmenting the NRF2 response [348], [349]. These data support the hypothesis that sulforaphane and H_2S sulfide operate through similar molecular pathways. As sulforaphane generates H_2S in solution, the sub-optimal treatment of HGPS with

sulforaphane may be improved by a greater understanding of the influence of H_2S in HGPS.

Vitamin D and related compounds have also been used in the treatment of HGPS [350], and some evidence exists for a commonality between vitamin D and H_2S in their modes of action. Vitamin D treatment in mice has been shown to elicit a dose-dependent elevation of tissue H_2S levels in kidney and brain [351]. Cell culture studies found that H_2S formation was central to Vitamin D-induced protection of adipocytes from inflammation and impaired glucose utilization due to high glucose culture conditions [205]. Finally, a population study found a correlation between reduced plasma H_2S and Vitamin D levels in African American type-II diabetics compared to Caucasians with type-II diabetes, and *in vitro* studies in monocyte culture also found an elevation of CSE expression and H_2S production following Vitamin D treatment [352].

Together, the strong overlap between proven treatments for HGPS and established molecular mechanisms under the influence of H_2S (mTOR signalling, NRF2 response, and vitamin D signalling) it is surprising there have been so few studies addressing the role of H_2S in the management of HGPS. While there has been no research directly linking H_2S to HGPS, there has been work published in another progeria syndrome, Werner Syndrome (WS). In human WS fibroblasts, it was shown that the cellular morphological phenotype, characterised by increased protein aggregation, high levels of oxidative stress and nuclear dysmorphology, was ameliorated by sodium hydrosulfide (NaHS) treatment [251].The beneficial effects of NaHS treatment were proposed to be due to inhibition of mTOR, as rapamycin treatment displayed similar effects to NaHS treatment with respect to protein aggregation, oxidative stress and nuclear morphology. Furthermore, the enzymes involved in endogenous production of H_2S were downregulated in WS cells, suggesting that reduced H_2S levels may play a role in WS phenotype [251]. Overall, this study hints to the importance of H_2S production in WS progeria and stresses the importance of further research across all progeroid diseases.

5.3 Aims and hypothesis

Hypothesis

In this chapter I examined tissue samples from a Hutchinson-Gilford Progeria Syndrome (HGPS) mouse model, referred to as G609G. G609G mice fed a high-fat diet (HFD) have a significant extension in lifespan compared to those fed a regular chow (RC) diet. As H_2S is associated with longevity, I expected hepatic production of H_2S to be reduced in the G609G mice compared to wild-type (WT) controls. I expected that G609G mice on HFD would have partial rescuing of their sulfide production mechanisms compared to RC fed mice, but that H_2S levels would still be lower than those found in WT control mice.

Aims

1. Investigate the production capacity of H_2S in hepatic tissue from G609G mice on RC and HFD, compared to WT controls.

2. Examine the transcriptional regulation of H_2S production and disposal enzymes on RC and HFD, compared to WT controls.

3. Investigate the protein abundance of H_2S production and disposal enzymes on RC and HFD, compared to WT controls.

4. Investigate the abundance of proteins essential of mitochondrial oxidative phosphorylation on RC and HFD, compared to WT controls.

5.4 Results

5.4.1 Hepatic H_2S capacity in progeroid and WT mice

To test the initial hypothesis that hepatic H_2S production capacity would be reduced in G609G mice and enhanced by HFD, I applied the lead acetate assay to hepatic tissue protein homogenates from all samples **(Figure 29)**. A representative image of this precipitate is shown in **Figure 29a.** A significant difference between groups was found ($H = 6.659$, $p = 0.020$) with Dunn's multiple comparisons determining a significant reduction in H_2S production capacity between WT and G609G RC samples ($p = 0.041$) but not between WT and G609G HFD ($p = 0.210$). There was no significant difference in H_2S production capacity between G609G mice on either diet ($p > 0.999$). The assay was performed using 100 ug of hepatic protein lysate per well in triplicate. The validity of loading each well with this mass of protein was assessed by measuring the linearity of signal intensity produced over a range of protein loadings, from 50 – 400 ug per well **(Figure 29b)**. A least squares fit regression model confirms a strong linearity in assay output compared to protein loading across the range studied ($R^2 = 0.94$) indicating the method is robust over this range.

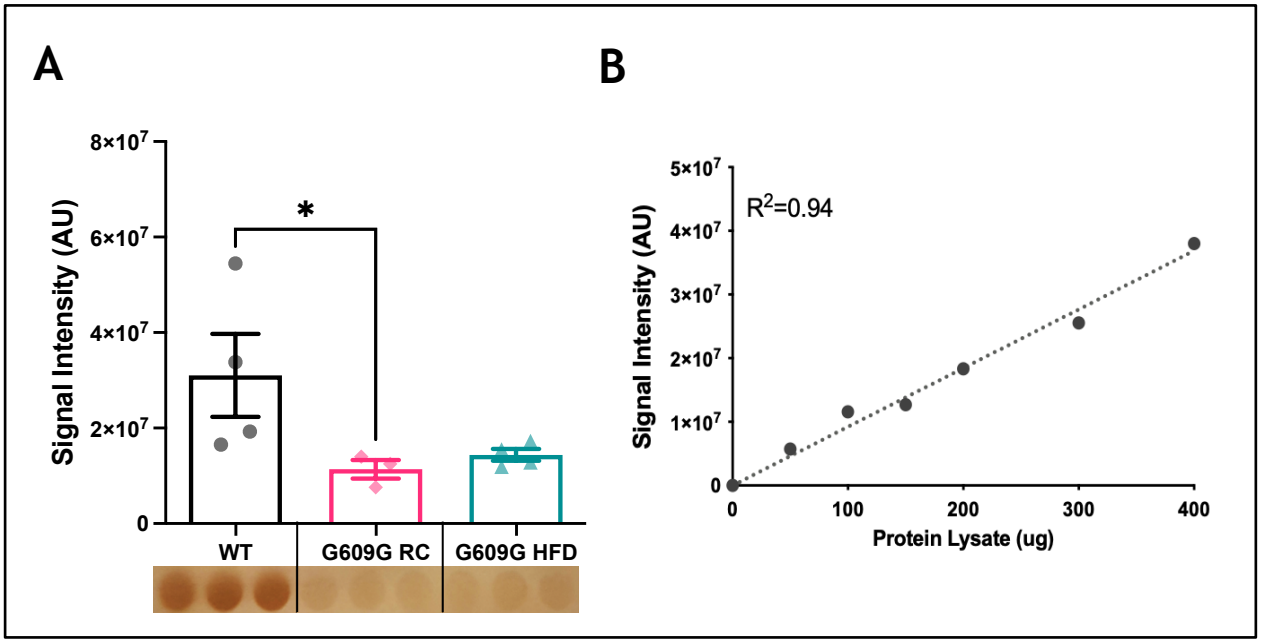

Figure 29 H_2S production is downregulated in G609G samples compared to WT

A Hepatic H_2S production capacity assay assessed in protein lysates from WT, G609G RC and G609G HFD mice. Data quantified by densitometry analysis of lead acetate assay results. A representative image of the lead sulfide precipitate that form as the output of the lead acetate assay is shown beneath the plot. Darker precipitates indicate higher hepatic H_2S production capacity in the tissue sample. WT data shown in black, G609G RC data shown in pink, G609G HFD data shown in green. **B** Calibration curve showing lead acetate assay output intensity across a range of protein loadings from the same WT RC liver tissue sample. Line of best fit generated by least-squares fit model demonstrates a strong linearity across different protein loadings. Statistical significance was determined by Kruskal-Wallis non-parametric ANOVA test with alpha = 0.05, with Dunn's correction for multiple comparison. Grubbs outlier test with alpha = 0.05 was performed; one outlier was removed in G609G RC group. Histograms denote mean values with error bars representing standard error of the mean (SEM). * = $p < 0.05$

5.4.2 Transcriptional regulation of H_2S-production and disposal enzymes

Given the significant reduction in hepatic H_2S production capacity in G609G RC mice compared to WT controls, I then investigated whether major components of the enzymatic H_2S production and disposal processed were altered **(Figure 30)**. Transcript levels of *Cse* were found to be significantly increased in G609G mice on both diets compared to WT controls ($p = 0.005$ and $p = 0.007$, respectively). *Cbs* expression was similarly elevated in G609G RC mice relative to WT controls ($p = 0.028$) but was not different between HFD-fed G609G mice relative to WT mice ($p = 0.558$). *Cse* and *Cbs* comprise the cytosolic endogenous H_2S production pathway in mammals, however, a distinct pathway for H_2S generation in mitochondria is mediated by *Mpst*. No difference in *Mpst* transcript levels were seen between WT and G609G RC mice ($p = 0.216$) but were significantly reduced in G609G HFD mice relative to WT controls ($p = 0.005$). There was no significant difference between G609G mice on RC compared HFD diet for *Cse*, *Cbs*, or *Mpst* gene expression. I also probed for genes that regulate the oxidation and disposal of H_2S. *Ethe1* expression was significantly reduced in G609G HFD mice ($p = 0.003$) compared to WT mice but not different in G609G RC mice relative to WT mice ($p = 0.525$). *Tst* expression was found to be significantly reduced in both G609G RC and G609G relative to WT mice ($p = 0.047$ and $p = 0.021$ for RC and HFD fed G609G mice, respectively). Finally, *Suox* expression was not different in G609G mice on either diet when compared to WT mice ($p = 0.128$ and $p = 0.340$ for RC and HFD fed G609G mice, respectively).

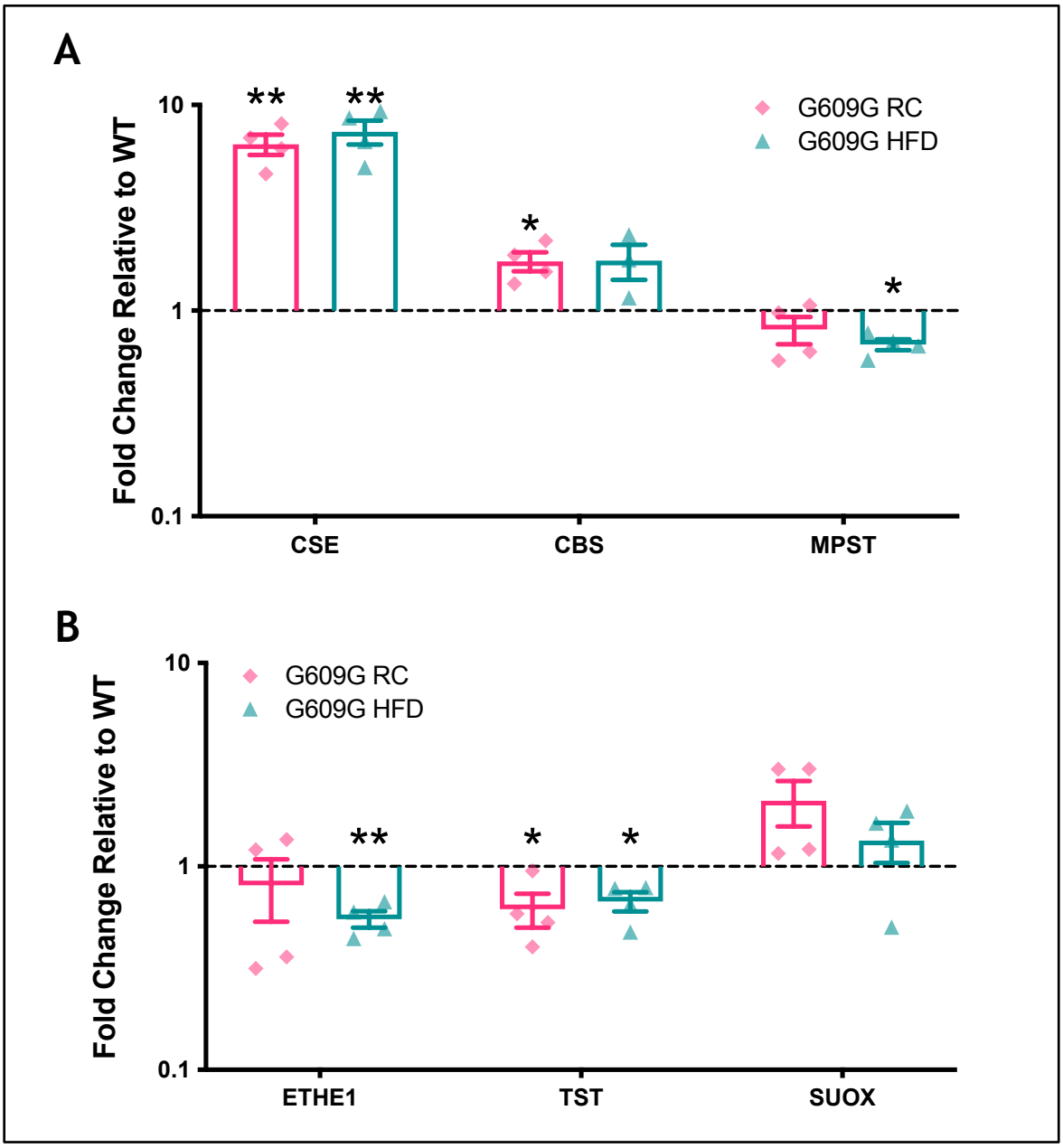

Figure 30 Gene expression of selected H_2S production and removal enzymes

Mean fold change in hepatic mRNA gene expression of H_2S producing enzymes *Cse*, *Cbs*, *Mpst* (**A**) and H_2S disposal enzymes *Ethe1*, *Tst* and *Suox* (**B**) as measured by RT-qPCR. Relative expression values were calculated using the $2^{-\Delta\Delta Ct}$ method. WT data shown in black, G609G RC in pink, G609G in Green. Statistical significance determined by one-sample t-test comparing the fold change to a theoretical mean of one. Grubbs outlier test with alpha = 0.05 was performed, no outliers removed. Bars show mean values with error bars representing standard error of the mean. Cse: Cystathionine-beta-lyase, Cbs: Cystathionine-Beta-synthase, Mpst: 3-Mercaptopyruvate Sulfurtransferase, Ethe1: Ethylmalonic encephalopathy 1 protein, Tst: Thiosulfate Sulfurtransferase, Suox: Sulfite Oxidase. * = $p < 0.05$, ** = $p < 0.01$

5.4.3 Protein abundance of H_2S-production and -disposal enzymes

The protein levels of major H_2S producing and disposal enzymes were also measured (**Figure 31** and **Figure 32**, respectively). A significant difference between groups in CSE protein levels was found ($H = 8.115$, $p = 0.003$), **Figure 31a**. Dunn's multiple comparisons determined a significant reduction in CSE protein levels between G609G RC and G609G HFD samples ($p = 0.0134$) but no significant difference between any other groups. No differences in protein levels were observed for either CBS ($H = 3.598$, $p = 0.1778$) or MPST ($H = 2.192$, $p = 0.370$) between groups as shown in **Figure 31b** and **Figure 31c**. As with CSE, protein levels of TST (**Figure 32a)** were found to be significantly different between groups ($H = 8.115$, $p = 0.0031$), with *post hoc* testing determining a significant difference between G609G RC and G609G HFD mice ($p = 0.0134$) only. ETHE1 levels (**Figure 32b)** did not differ between groups ($H = 0.7308$, $p = 0.7463$).

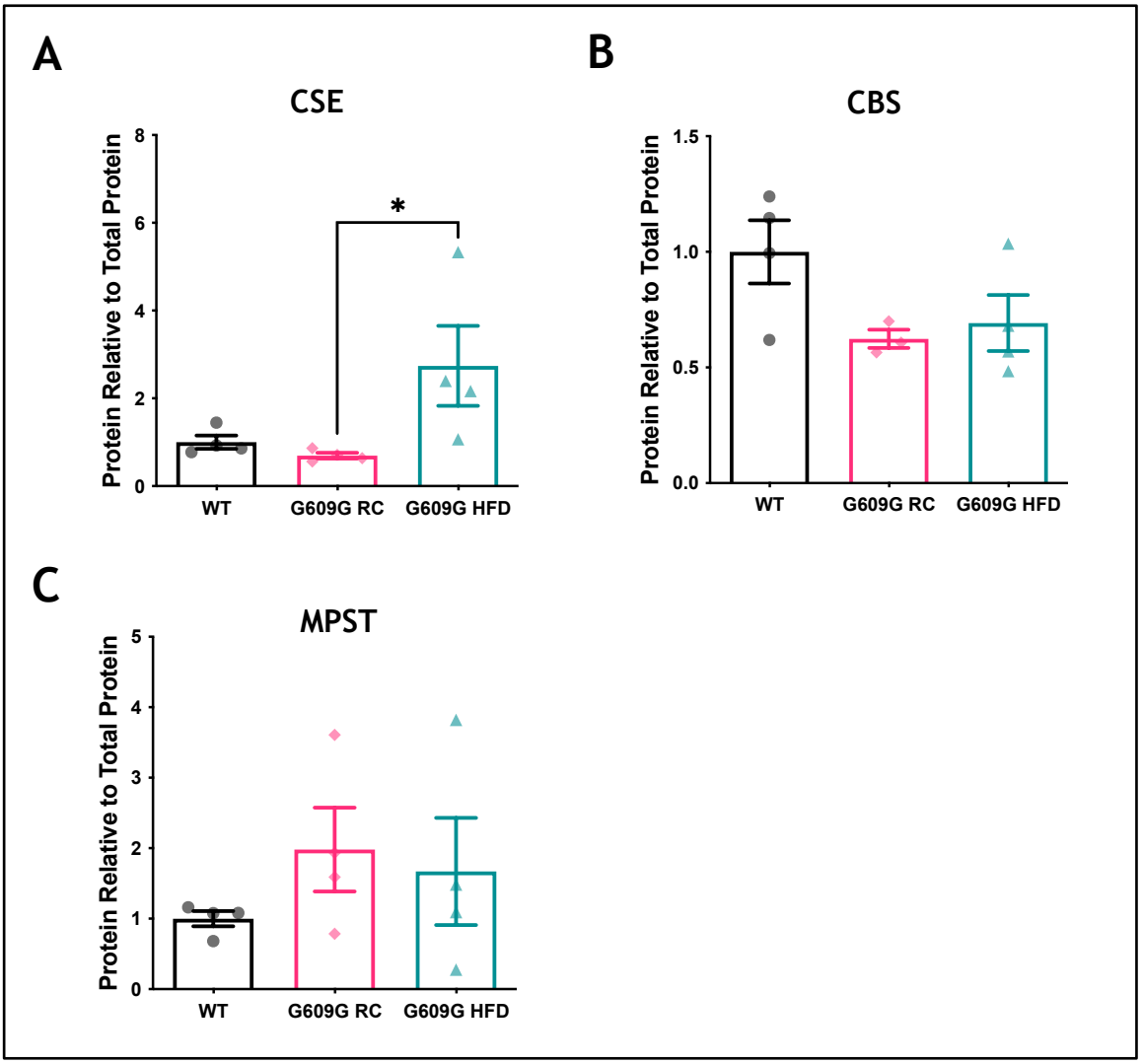

Figure 31 Hepatic protein levels of H_2S producing enzymes

Western blotting of hepatic protein lysates quantified by densitometry analysis and expressed relative to total protein loading for **A** CSE, **B** CBS, and **C** MPST. WT data shown in black, G609G RC in pink, G609G HFD shown in green. Statistical significance was determined by Kruskal-Wallis non-parametric ANOVA test with alpha = 0.05, with Dunn's correction for multiple comparison. Grubbs outlier test with alpha = 0.05 was performed, no outliers removed. Bars show mean values with error bars representing standard error of the mean (SEM). * = $p < 0.05$. CSE: Cystathionine-beta-lyase, CBS: Cystathionine-Beta-synthase, MPST: 3-Mercaptopyruvate Sulfurtransferase.

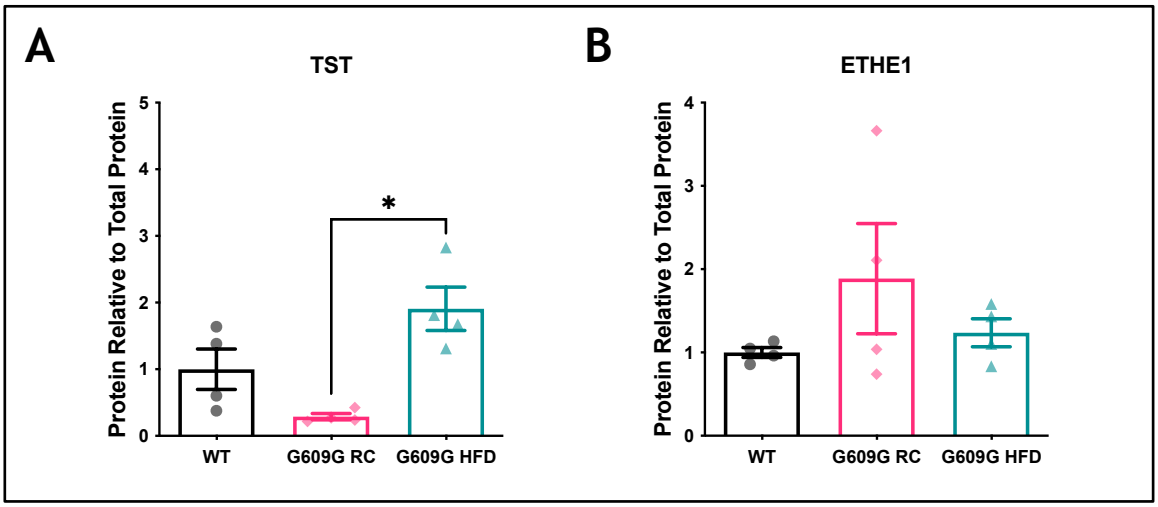

Figure 32 Hepatic protein levels of H_2S disposal enzymes

Western blotting of hepatic protein lysates quantified by densitometry analysis and expressed relative to total protein loading for **A** TST and **B** ETHE1. WT data shown in black, G609G RC in pink, G609G HFD shown in green. Statistical significance was determined by Kruskal-Wallis non-parametric ANOVA test with alpha = 0.05, with Dunn's correction for multiple comparison. Grubbs outlier test with alpha = 0.05 was performed, no outliers removed. Bars show mean values with error bars representing standard error of the mean (SEM). * = $p < 0.05$. ETHE1: Ethylmalonic encephalopathy 1 protein, TST: Thiosulfate Sulfurtransferase.

5.4.4 Determination of TST activity in hepatic protein lysates

Gene expression analysis showed that TST mRNA transcripts were significantly reduced in G609G mice on both diets compared to WT controls **(Figure 30b).** However, at the protein level there was a divergence in levels of TST protein between G609G groups, with TST significantly elevated in G609G HFD compared to G609G RC **(Figure 32a).** In light of these divergent results, I used a TST activity assay to interrogate the effect of genotype and diet on the rhodanese activity of TST (**Figure 33a)**. Statistical analysis determined no significant difference between groups ($H = 5.115$, $p = 0.074$), despite a modest downwards trend in G609G HFD TST activity compared to WT controls and G609G RC mice.

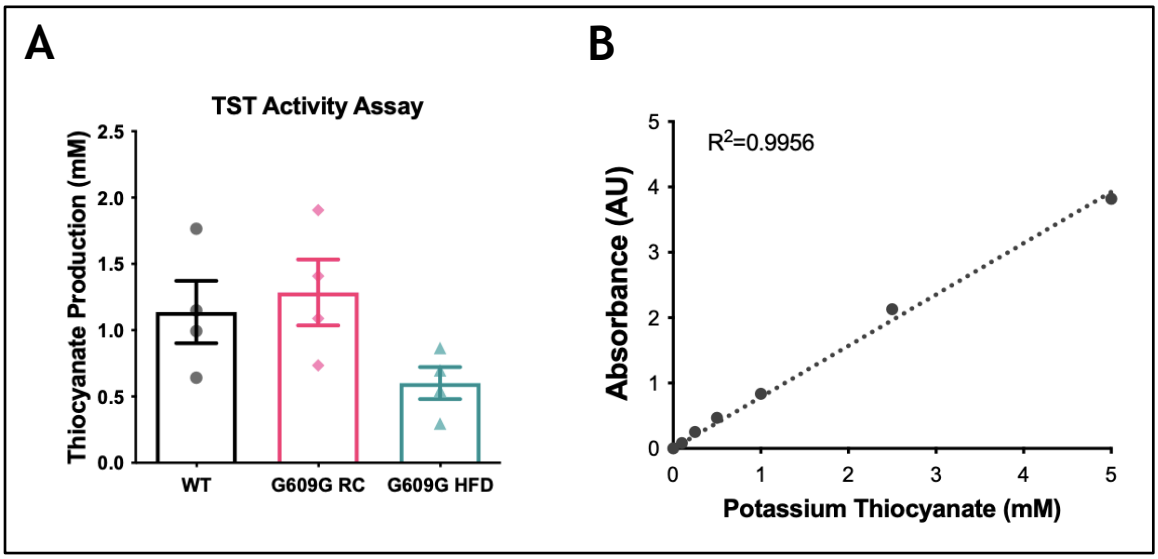

Figure 33 TST activity assay in hepatic fractions

A The activity of TST protein in hepatic protein lysates as measured by a thiocyanate production capacity assay. 20ug of liver protein lysates was loaded per well in triplicate. WT data shown in black, G609G RC in pink, G609G HFD in green. Bars represent mean thiocyanate production with error bars representing standard error of the mean (SEM). **B** Calibration curve using potassium thiocyanate standards. Linearity determined by least-squares fit model with R^2 = 0.9956. Statistical significance was determined by Kruskal-Wallis non-parametric ANOVA test with alpha = 0.05, with Dunn's correction for multiple comparison. Grubbs outlier test with alpha = 0.05 was performed, no outliers removed. TST: Thiosulfate Sulfurtransferase.

5.4.5 Protein levels of OXPHOS complexes in progeroid and WT mice

Finally, I blotted for components of the oxidative phosphorylation (OXPHOS) pathway: Complex I (NADH-coenzyme Q oxidoreductase), Complex II (succinate-Q oxidoreductase), Complex III (q-cytochrome c oxidoreductase) and Complex V (ATP synthase) as shown in **Figure 34**. No significant differences between groups in Complex I ($H = 2.000$, $p = 0.397$), Complex II ($H=2.192$, $p = 0.370$) or Complex III ($H=3.417$, $p = 0.195$) protein levels were observed, with significant variation within each group observed for these complexes (**Figure 34**). For Complex V however, there was a significant difference in protein levels between groups ($H = 7.636$, $p = 0.004$), with Complex V protein levels significantly elevated in HFD-fed compared to RC-fed G609G mice ($p = 0.017$), with non-significant differences between and G609G RC mice ($p=0.343$) or WT controls and G609G HFD mice ($p = 0.602$).

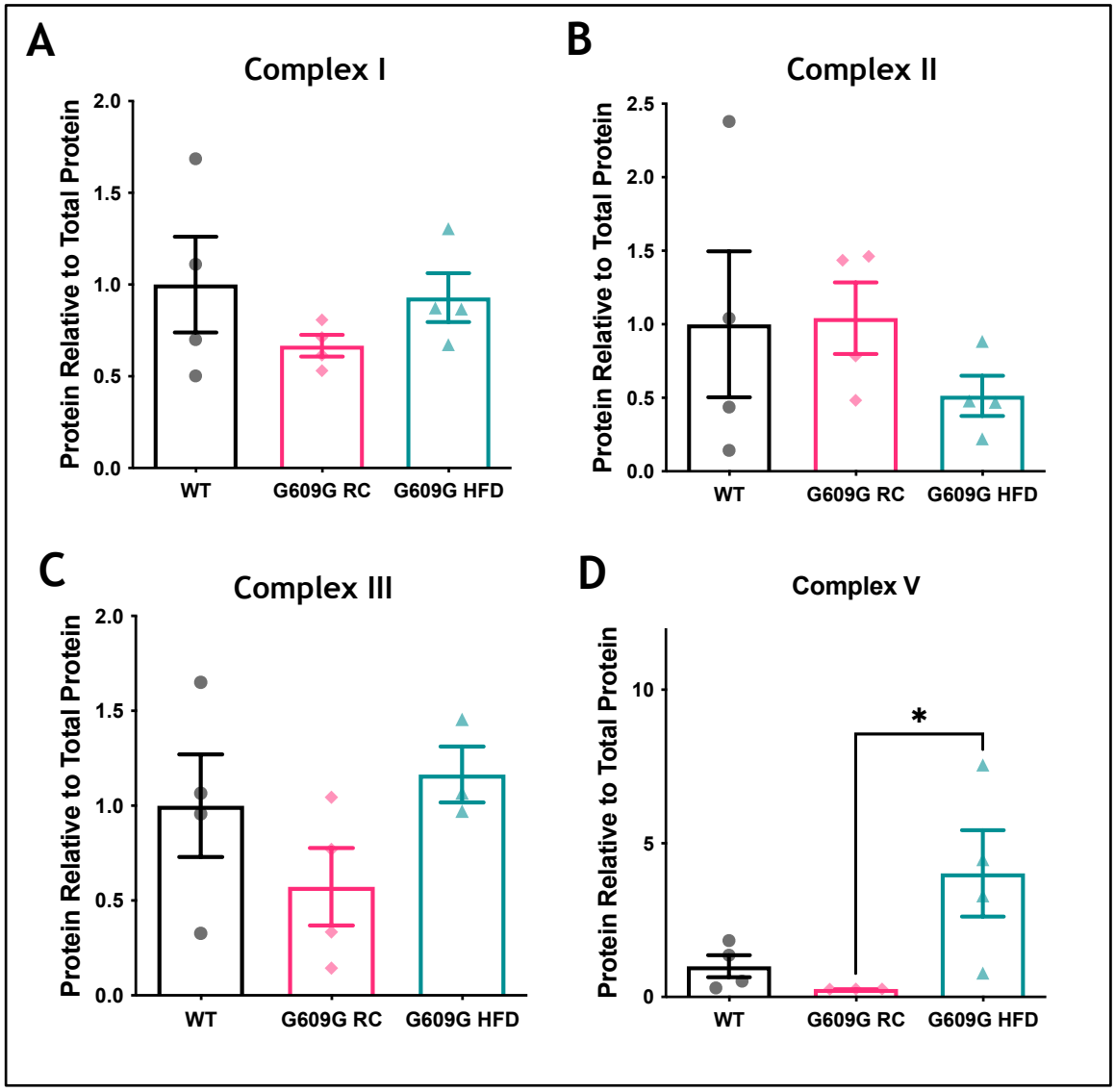

Figure 34 Western blot analysis of OXPHOS subunits in G609G RC, G609G HFD relative to WT mice

Western blotting of hepatic protein lysates quantified by densitometry analysis and expressed relative to total protein loading for **A** Complex I, **B** Complex II, **C** Complex III, **D** Complex V. WT data shown in black, G609G RC in pink, G609G HFD shown in green. Statistical significance was determined by Kruskal-Wallis non-parametric ANOVA test with alpha = 0.05, with Dunn's correction for multiple comparison. Grubbs outlier test with alpha = 0.05 was performed, no outliers removed. Bars show mean values with error bars representing standard error of the mean (SEM). * = $p < 0.05$. Complex I: NADH-coenzyme Q oxidoreductase; Complex II: succinate-Q oxidoreductase; Complex III: q-cytochrome c oxidoreductase; Complex V: ATP synthase.

5.5 Discussion

5.5.1 H_2S production is downregulated in a mouse model of HGPS

Recent studies investigating the role of hydrogen sulfide (H_2S) in ageing and age-related diseases have demonstrated that elevated H_2S levels appear essential for dietary restriction benefits [164], [170], [274], are a conserved phenotype in long-lived mouse models [164], [170], and that a reduction in tissue H_2S levels is observed with age across model organisms [127], [252]. To date no studies have directly measured H_2S production in Hutchinson-Gilford Progeria Syndrome (HGPS) despite the emerging understanding that H_2S may be central to longevity and healthy ageing, and despite commonalities in the signalling modalities of H_2S and several established HGPS treatments (see section 5.2.3).

To address this lack of understanding, this preliminary study used the HGPS mouse model G609G [353] to investigate regulation of H_2S level in the context of HGPS and test the hypothesis that a reduction in hepatic H_2S production underlies HGPS pathology. The G609G has a pronounced lifespan extension on high-fat diet (HFD) compared to regular chow (RC) [229]. As such both diets were investigated to determine if H_2S production was subject to dietary influence. I utilised the lead acetate method [230] to assay *ex vivo* H_2S production capacity, as this method provides a reliable measurement of cytosolic H_2S production, has been used extensively across model systems which allows for easy comparison with previous reports, and is easily modifiable to detect a high dynamic range of H_2S production capacities [230]. These data show a significant reduction in H_2S production capacity in G609G mice on RC compared to WT controls and a non-significant reduction in G609G HFD compared to WT controls. Broadly, these results are in line with the hypothesis that this HGPS model will have reduced H_2S production on RC diet, with a partial rescue in mice fed HFD. The lack of a significant reduction in the HFD fed mice is contrary to previous studies as HFD in WT mice has been shown to reduce plasma H_2S levels and lower activity of CSE, CBS and MPST in liver [354]. While these data do indeed show that the G609G HFD do not have a significant reduction in H_2S production capacity relative to WT controls, these data are derived from a low sample size and should be interpreted with caution. A repeat

of this experiment with sufficient power would support my findings that G609G on HFD have a partial rescue of H_2S production capacity compared to G609G RC. Indeed, post-hoc power analysis on my preliminary date suggests that a sample size of at least 11 is required to have the statistical power to determine a significant difference between groups (Prism 9 software, GraphPad Inc., La Jolla, CS, US; 2-sided test, $\alpha = 0.05$, desired power = 0.8), which is significantly more that the sample size of 4 used in this experiment. However, given the data available it is possible to say that hepatic H_2S production is reduced compared to WT control in a mouse model of progeria on RC but this is non-significant in HFD-fed G609G mice.

5.5.2 Progeria model mice exhibit a transcriptional compensation in response to reduced H_2S levels

Given the discovery that hepatic H_2S production is compromised in G609G mice, transcriptional control of H_2S production and disposal enzymes was assessed. The H_2S production gene *Cse* is canonically the major producer of H_2S in hepatic tissues [253], and was found to be significantly elevated in G609G mice on both RC and HFD compared to WT controls. *Cbs* is also expressed in liver tissue but far less than *Cse* (see [253]) and was found here to be significantly upregulated in G609G RC but not in G609G HFD. Similarly, *Mpst* gene expression was found to be significant reduced in G609G HFD mice compared to WT controls. Collectively, these data present a confounding transcriptional landscape in G609G mice. As H_2S production was shown to be significantly reduced in G609G RC livers, these data demonstrating elevated expression in some H_2S producing genes were unexpected. These data may point to a futile compensatory elevation of H_2S producing enzymes in response to reduced H_2S levels. A compensatory mechanism of this type has been reported in rats which were injected in the heart with a synthetic catecholamine (isoproterenol) to generate a model of human myocardial infarction [355]. Hearts treated with this compound had reduced H_2S content in myocardium and plasma sample compared with controls, however *Cse* gene expression was upregulated [355]. One potential explanation for these findings is that transcriptional regulation of *Cse* and *Cbs* expression can be altered by reactive oxygen species (ROS). Studies have shown that ROS, and hydrogen peroxide in particular, are capable of elevating expression of *Cse* [356]. This is likely an antioxidative mechanism that seeks to elevate H_2S so that H_2S can scavenge ROS, such a mechanism has been observed in rat livers which elevated H_2S to ameliorate oxidative damage [357]. Crucially, it has been demonstrated previously that G609G mice on RC have chronic elevated ROS production and as such this may stimulate upregulation of *Cse* [358]. Interestingly, this ROS-H_2S axis has been proposed as a potential component of the mitohormesis theory: low levels of stressors (e.g. ROS) result in upregulation of protective mechanisms (e.g. H_2S signalling) which in-turn results in long term improvements in cell function [359]. However, studies in human cells derived from patients with another progeria syndrome (Werner's Syndrome, WS) found that CSE and CBS mRNA expression was reduced compared to healthy controls [251], unlike the findings I have presented here. Similar to

the G609G model, cells from patients with WS are also characterised by a significant reduction in ROS detoxification components superoxide dismutase and glutathione [360], [361]. As this study in cells from WS patients is the only other study to measure H_2S levels in any progeria condition to date, there is no equivalent study in rodent models to compare my findings with. More studies are required to determine if this compensatory elevation in gene expression of H_2S-generating genes is found in any other models of progeria diseases, or if it is found in other animal models more generally. Within these G609G mice however, it appears that post-transcriptional processes prevent the elevation in transcription of H_2S production genes from elevating H_2S levels, precluding any beneficial effects of chronic elevated ROS in these mice.

5.5.3 Compensation of reduced H_2S levels in G609G mice is blocked at the protein level

To gain better understanding of the regulation of H_2S production I then quantified protein levels of H_2S producing and disposal enzymes. In contrast to my transcriptional data, no significant changes in CSE protein levels in G609G RC or G609G HFD mice were observed relative to WT controls, but there was a significant increase in G609G HFD mice compared to G609G RC mice. Previous studies have found that CSE protein levels may be controlled at the transcriptional level by repression of *Cse* gene expression [170]. However, such an explanation does not account for the data presented here, where *Cse* mRNA transcripts are significantly upregulated in G609G mice on both diets but protein abundance of CSE appears diet dependent, being elevated on HFD in G609G mice compared to RC G609G and WT controls. One potential explanation is that the extent of post-translational degradation of CSE was different between groups. Ubiquitination is an established mechanism by which CSE stability is controlled and it has been demonstrated that CSE ubiquitination and degradation is promoted by superoxide anions [362]. Indeed, the difference between RC and HFD-fed G609G mice in CSE protein stability could also be explained by the observation that, unlike most oxidative damage compounds, superoxide anion generation in rodent liver is reduced by HFD, [363]. As such, future studies should look to measure ROS production (in particular superoxide anion), superoxide dismutase (SOD) activity, or markers of oxidative damage as these may help understand both the transcriptional and post-translational regulation of CSE enzyme. To summarise, while HFD in WT mice has deleterious effects on H_2S metabolism and general metabolism [339], in G609G mice it appears to be beneficial [229]. This may reflect the importance of nutrient rich diets in human patients with HGPS, where “nutritious and high calorie foods and supplements” are recommended [338]. Moreover, increased CSE protein levels were shown to be positively corelated with increased lifespan in DR mice [170], a relationship that is mirrored in the data presented here for G609G mice on HFD. Consequently, the elevated CSE protein levels in G609G HFD support prior evidence suggesting that HFD is beneficial in this model of human HGPS, increasing their lifespan [320]. Protein levels of TST, a H_2S catabolising enzyme, followed the same pattern of abundance seen for CSE protein i.e. a significant increase in G609G HFD mice compared to G609G RC mice. However, when

assessing the activity of this enzyme no difference was found between groups, in fact a downwards trend in TST activity was found in G609G HFD mice despite an increase in TST protein levels in these mice. TST has recently emerged as a protein that protects against deleterious effects of type 2 diabetes and metabolic stressors, including HFD, by enhancing mitochondrial function and degrading ROS [232]. Given the maintenance of TST activity in G609G HFD mice compared to G609G RC and WT groups, it is unlikely that the beneficial effects of TST on mitochondrial function or oxidative damage will be felt in G609G HFD mice, despite their increase in TST protein levels.

In summary, G609G mice on RC diet have a significant reduction in H_2S production capacity which is associated with lower levels of CSE protein, despite transcriptional upregulation of *Cse*, coupled with a maintenance in H_2S disposal enzyme protein levels and activity. However, on HFD there was no significant reduction in H_2S production capacity compared to WT mice, an increase in both *Cse* expression and CSE protein levels and no alteration in the activity of TST, a key H_2S oxidation enzyme. One potential explanation for the effect of diet on H_2S metabolism is through HFD-induced elevation in oxidative damage [364], [365], which is capable of modifying both the transcriptional and post-translational regulation of enzymes in the H_2S metabolism pathway and ultimately modulated tissue H_2S levels [186], [265], [340]. This indicates that the atypical positive effect of HFD on lifespan in G609G mice is mirrored by an atypical elevation of H_2S metabolism pathways in response to HFD. These data are in agreement with the growing number of studies that have identified elevated H_2S production as correlated with, or essential for, lifespan extension [127], [164], [262], [366].

5.5.4 Mitochondrial oxidative phosphorylation (OXPHOS) protein abundance in G609G mice

Mitochondrial dysfunction, including decreased OXPHOS capacity and elevated oxidative damage, has emerged as one of the key hallmarks of ageing [367]. Furthermore, it has been shown previously that fibroblasts from patients with HGPS have a dramatic reduction in OXPHOS protein abundance such as subunits of complexes II and IV [326]. The data presented here shows that protein levels of OXPHOS complexes I, II, or III proteins were maintained relative to control mice in G609G mice on both diets. However, a significant difference between RC and HFD-fed mice was seen for complex V (ATP synthase), with a significant elevation in the HFD-fed mice. Interestingly, studies in HepG2 and HEK293 cell lines have shown that both endogenous and exogenous sources of H_2S directly modified complex V (*via* post-translational persulfidation on cysteine residues 244 and 294) to stimulate elevated ATP synthase activity [368]. Other studies have described an additional pathway *via* sirtuin signalling by which H_2S modifies complex V to improves mitochondrial function [369]. As HFD G609G mice have elevated expression of complex V compared to RC-fed G609G mice and no significant change in H_2S production capacity compared to WT mice, it is possible these effects combine to greatly elevated ATP synthase activity in G609G mice on HFD compared to RC-fed G609G mice. The data here give some indication that diet can alter the ATP generating capacity of G609G mice, however more studies are required to investigate the impact of these changes in protein on cellular respiration and ATP concentration.

5.6 Conclusions

This study demonstrates that H_2S metabolism is differentially regulated in a mouse model of HGPS, and the regulation of proteins central to the production and disposal of H_2S are responsive to dietary composition. Overall, HFD feeding appeared to partially rescue G609G mice from a phenotype of diminished H_2S production by elevating CSE expression at the protein and transcriptional level, while maintaining protein activity of H_2S disposal enzyme such as TST. This study was designed due to the lack of understanding in the mechanistic targets of known treatments against HGPS and the established mechanisms by which H_2S influences cellular processes. Furthermore, as we have increasing appreciation of the role of H_2S as a regulator of healthy ageing it is necessary to address the lack of studies directly measuring H_2S metabolism in the context of progeria. The pilot study presented here is the first to study H_2S metabolism in the context of HGPS and builds on the single study of H_2S in Werner's Syndrome [251]. The data acquired here confirms some aspects of the role of H_2S in HGPS but raises more questions about the mechanisms. Studies in primary cell culture and animal models that knock down/out or overexpress *CSE* would assist in proving a mechanistic role for H_2S in the first instance. Lentiviral constructs for the overexpression of progerin in mammalian cells are already established (see [370]) and could help clarify any direct relationship between progerin protein levels and a reduction in tissue H_2S. Subsequent application of H_2S donating compounds (such as NaHS and GYY4137 [371]) could then be used to investigate if exogenous H_2S treatment can rescue the progeroid phenotype, establish causation and a potential therapeutic window. Given my finding that OXPHOS complex V was significantly elevated in G609G mice on HFD compared to RC, high-resolution respirometry techniques in progerin overexpressing cell lines or primary cell cultures from G609G mice would allow determination of mitochondrial function [372]. Furthermore, the regulatory patterns observed in these samples could be explained by alterations in the oxidative stress experienced in each study group. Assays to measure the redox state of samples as well as their production of specific ROS species would provide insight into the dynamics in oxidative stress in these mice. As described previously, there is an established role for the superoxide anion in the transcriptional control of H_2S. Superoxide anion is a by-product of OXPHOS respiration, and as a ROS species

that is elevated in progeroid mice and reduced on HFD, experiments that monitor the generation and disposal of this compound are of particular interest in the context of G609G mice on RC or HFD. Indeed, exogenous delivery of superoxide would also be a vital experiment to elucidate the molecular patterns found in this work, but would require access to live G609G mice. Finally, a key limitation in this study was statistical power. This was due to the apparent difficulty in housing a colony of mice with the G609G mutation by my collaborators in the USA [353]. These mice are infertile, have an abundance of comorbidities, and due to their small size have limited tissue available. As such, the sample sizes available for this pilot study were very small. The statistical power of this study would be improved by having approximately 11 mice per group and including a WT HFD cohort to allow 2-factor ANOVA analysis of the results. Regardless, the work presented here addresses an area of research that remains critically understudied and provides new evidence that the accelerated ageing phenotype observed in HGPS may be partially explained by a reduction in hepatic H_2S levels.

Chapter 6 RNA Polymerase III and Dietary Restriction in the Regulation of Hydrogen Sulfide

6.1 Abstract

RNA Polymerase III (Pol III) is one of three mammalian RNA polymerases that together transcribe much of the cellular transcriptional and translational machinery. Knockdown of Pol III in flies and worms extends lifespan downstream of mammalian target of rapamycin (mTOR), an established highly conserved lifespan determinant. It is currently unknown whether knockdown of Pol III extends lifespan in mice. Given that the gasotransmitter H_2S correlates positively with longevity across taxa, and that hepatic H_2S is elevated in long-lived mice, I investigated H_2S in putative long-lived Pol III (Polr3b Het KO) mice and wild type (WT) mice of both sexes. H_2S production was elevated only in male Polr3b Het KO mice relative to WT controls. These mice were maintained on a C57BL/6N background, a strain not previously studied in the context of H_2S signalling or dietary restriction (DR). Male WT and Polr3b Het KO mice were exposed to 1-month 40% DR and then cytosolic and mitochondrial H_2S production and components of the H_2S signalling pathway were examined. I found that both DR and Polr3b Het KO elevated cytosolic hepatic sulfide production in an additive manner. However, mitochondrial H_2S levels were positively associated with Polr3b Het KO and negatively associated with DR. Together, my data indicate that DR has a specific effect on H_2S production that appears dependent on cellular location and that DR and Polr3b KO appear to work through distinct pathways to elevate cytosolic H_2S production.

6.2 Introduction

6.2.1 RNA Polymerase III

RNA polymerase III (Pol III) is responsible for the translation of several hundred noncoding RNAs in response to nutrient availability, growth signals and cellular stress [373], [374]. Chief among these are ribosomal RNA (rRNA) sub-units such as 5S rRNA and transfer RNAs (tRNA) [375]. Other translational products of Pol III include U6 splisosomal RNA, RNaseP/RNaseMRP, 7SL and 7SK RNA, vault RNA, y RNA, SINEs, many microRNAs, regulatory antisense RNAs and small nucleolar RNAs [376]. Collectively, these transcripts have significant influence over a number of cellular processes including ribosomal biogenesis, the translation of mRNA transcripts into proteins, and the splicing of mRNA transcripts [376], [377]. Global mediation of Pol III activity is performed by the transcription factor Maf1, a downstream signalling molecule at a terminus of the mammalian target of rapamycin (mTOR) signalling network (**Figure 35**). Maf1 inhibits RNA polymerase I and Pol III activity and can either activate or repress RNA polymerase II activity, dependant on the specific gene sequence [378], [379]. The activity of Maf1 is controlled by mTOR complex 1 (mTORC1) [380], [381]. When hyperphosphorylated during periods of nutritional surplus and mTORC1 activation, Maf1 is localised to the cytosol and Pol III activity is unimpeded [382]. Dephosphorylation of Maf1 results in it localising to the nucleus where it prevents Pol III gene transcription. This is achieved by directly binding to Pol III or through association with the Pol III transcription factor B (TFIIIB) subunit TFIIIB-related factor 1 (BRF1), preventing interaction between TFIIIB, Pol III and Pol III promotor sequences [382]–[385]. A summary of Pol III transcriptional machinery is presented in **Figure 36** [386]. Due to its role in essential cellular processes, Pol III is highly conserved in eukaryotes [375], [387]. Transcription of 5S rRNA and tRNAs account for approximately 15% of total cellular RNA synthesis and both profoundly influence cellular metabolism [388]. Pol III is expressed in most tissues in mammals to the extent that it is commonly used as a ‘housekeeping gene’ in cellular biology experiments [389], [390]. Indeed, numerous Pol III tRNA transcripts (including at least one tRNA isoform per amino acid residue) are also considered ‘housekeeping genes’ due to the consistency in Pol III expression and activity, even under environmental stressors [389], [390].

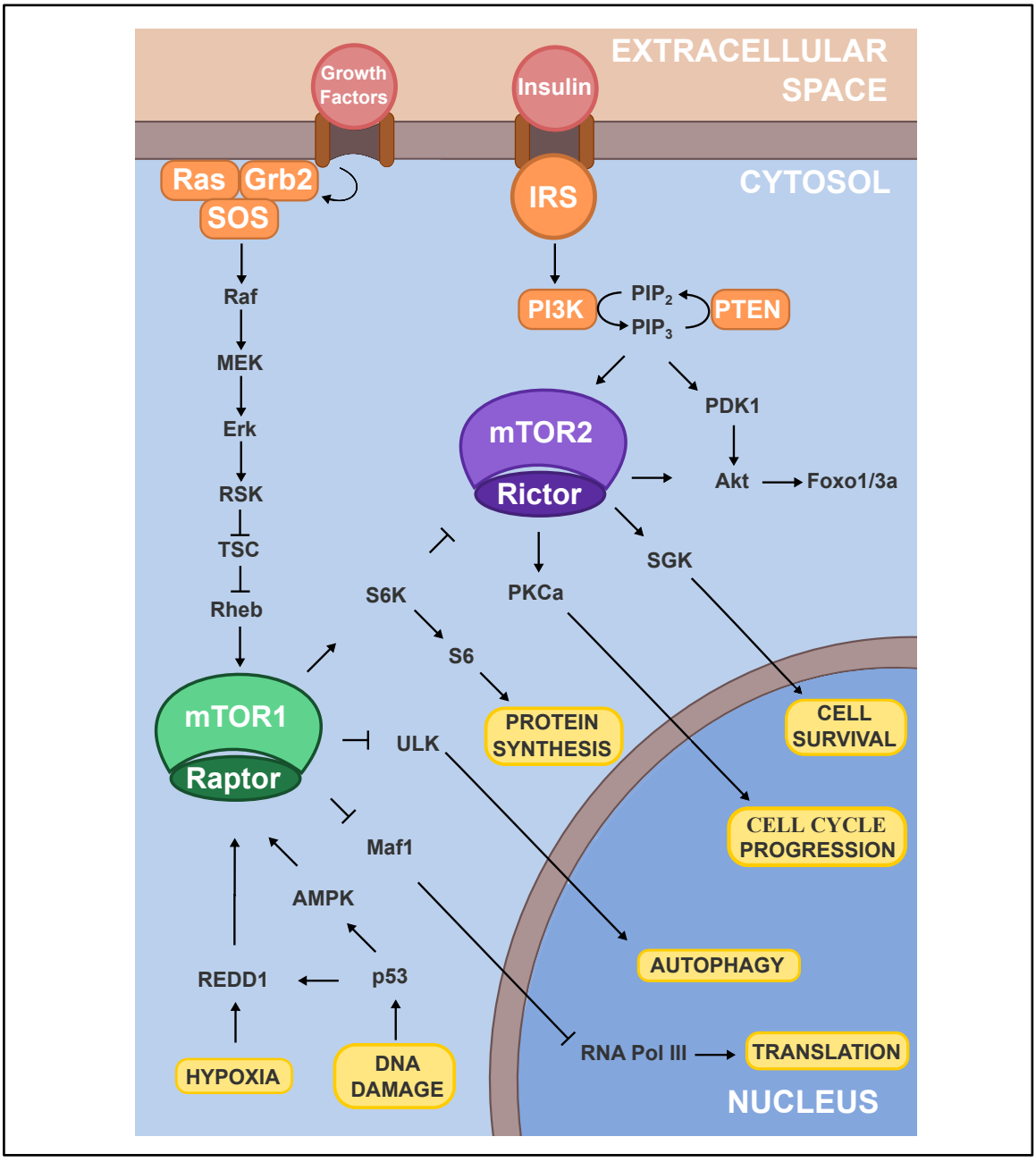

Figure 35 Diagram representing key sections of mTOR signalling pathways through mTOR complex 1 (mTORC1) and mTOR complex 2 (mTORC2)

mTORC1 and mTORC2 are activated through endothelial growth factor receptor signalling and Insulin/Insulin-like signalling pathways, respectively, as well as nutrient availability (not shown). Through inhibition of Maf1, mTORC1 senses growth factors and encourages greater translation of proteins and non-coding RNAs via RNA polymerase III and S6K. Other stimuli affecting mTORC1 activity include hypoxia and DNA damage. Ras: Rat sarcoma virus protein, Grb2: Growth factor receptor-bound protein 2, SOS: Son of sevenless, Raf: Rapidly accelerated fibrosarcoma protein, MEK: Mitogen-activated protein kinase kinase, Erk: extracellular-signal-regulated kinase, RSK: Ribosomal S6 kinase, TSC: tuberous sclerosis protein, Rheb: Ras homolog enriched in brain, IRS: Insulin receptor substrate, PI3K: Phosphatidylinositol 3 kinase, PTEN: Phosphatase and tensin homolog detected on chromosome 10, PIP_2: Phosphatidylinositol (4,5)-bisphosphate, PIP_3: Phosphatidylinositol (3,4,5)-triphosphate, PDK1: Phosphatidylinositol dependent kinase 1, Akt: Protein kinase B, Foxo1/3a: Forkhead box type O 1/3a protein, S6K: S6 kinase, S6: Ribosomal protein S6, PKCa: Protein kinase C, SGK: serum and glucocorticoid-regulated kinase, ULK: unc-51 like autophagy activating kinase, REDD1: regulated in development and DNA damage response 1, AMPK: adenosine monophosphate-activated protein kinase.

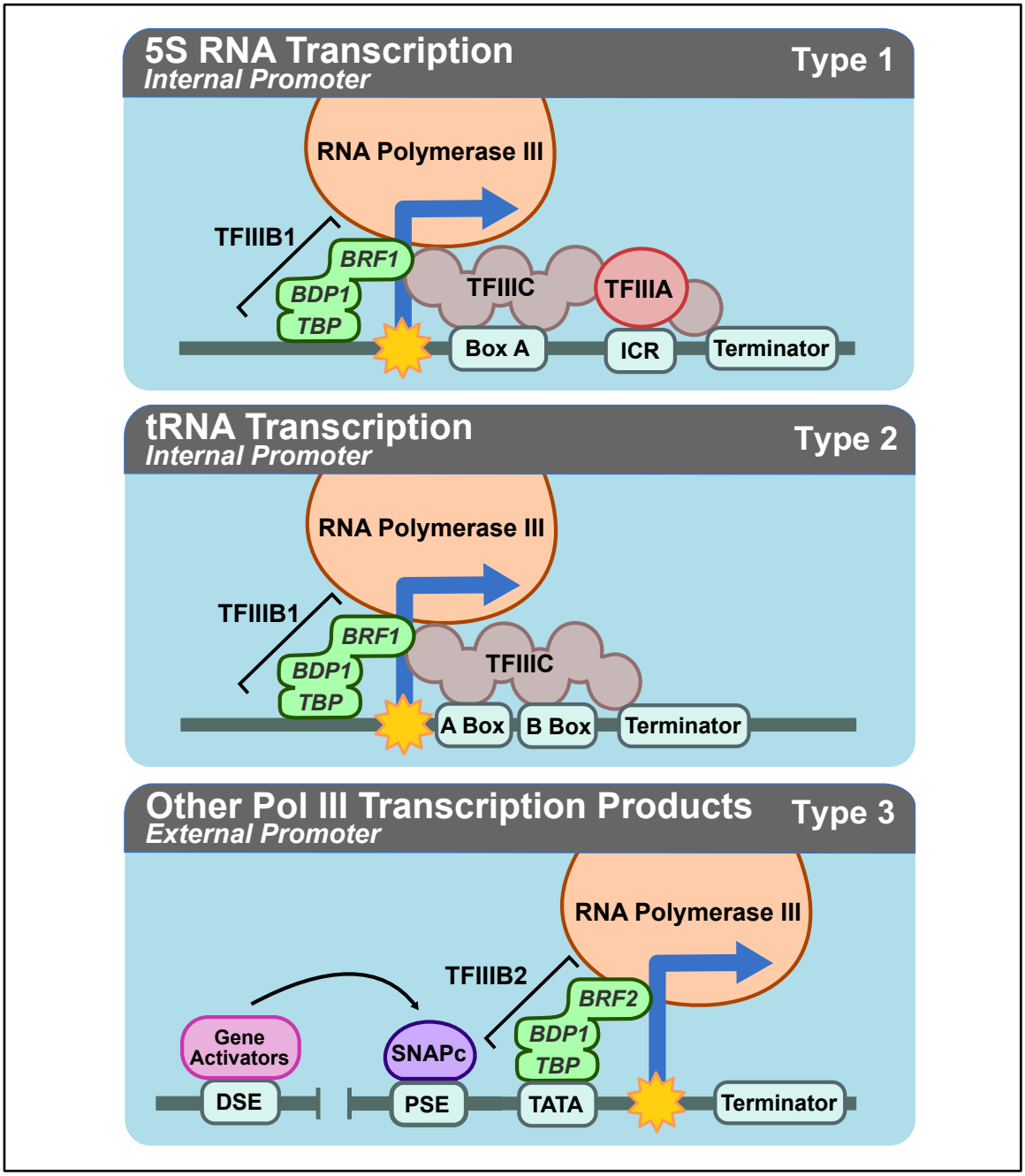

Figure 36 Transcription machinery for some Pol III gene products

Different transcriptional complexes are formed with Pol III depending on the target gene. TFIIIB1, Transcription factor for RNA polymerase III B1; BRF1, TFIIIB-related factor 1; BDP1, B double prime; TBP, TATA binding protein; TFIIIC, Transcription factor for RNA polymerase C; TFIIIA, Transcription factor for RNA polymerase A; ICR, Internal control region; DSE, Distal sequence element; PSE, proximal sequence element; TFIIIB2, Transcription factor for RNA polymerase B2; BRF2, TFIIIB-related factor 2. Adapted from Arimbasseri & Maraia, 2016.

6.2.2 RNA Polymerase III and Ageing

Beyond its central role in general cell maintenance, Pol III activity has emerged as a modulator of longevity [391]. This is perhaps unsurprising given that maintaining homeostasis in the translation of mRNA into proteins is a conserved longevity determinant across species [392], [393]. Protein synthesis rates and Pol III activity are also subject to regulation by mammalian target of rapamycin (mTOR) signalling [380], and reduced signalling through mTOR has been demonstrated as a longevity determinant [394]. Studies have shown that a reduction in mTOR signalling has a beneficial effect on lifespan in mice, and inhibition of mTOR orthologs extends lifespan in *S. cerevisiae*, *C. elegans*, and *Drosophila* [395][396]–[398]. Dietary restriction (DR) protocols limit availability of nutrients and can reduce mTOR activity [399], [400]. However, this reduction in mTOR activity on DR is tissue-specific [401], [402]. DR remains the most studied longevity intervention and produces pronounced extensions in lifespan and healthspan, although the precise mechanism/s underlying its effects has remained elusive. During DR, there is a significant reduction in the abundance of growth factors and nutrients available to the cell [403]. Signalling through mTOR senses this reduction and responds by reducing transcription of proteins that are involved in non-essential cellular activities related to anabolism, and encouraging catabolic processes such as autophagy and mitophagy [403]. Given this, it is expected that Pol III activity is reduced under DR but few studies have directly examined this. The inhibitory effect of short (19 hour) and medium (40 hour) term fasting on the activity of RNA polymerases I and II has been described [404], but not for Pol III. Modulation of Pol III itself, downstream of mTOR, has also been shown to influence longevity in model organisms [391]. Filer *et al* investigated tissue and cell-specific reductions in Pol III in yeast, flies and worms [405], showing that gut-specific reduction of Pol III in adult flies and worms resulted in extended lifespan and recapitulated many of the healthspan benefits observed with reduced mTOR signalling [405]. Pol III inhibition within intestinal stem cells of adult flies alone was sufficient to ameliorate age-associated gut pathology [405]. Together, these results indicate that Pol III itself may be a promising novel therapeutic target for longevity. However, no studies to date have examined the effect of Pol III deficiency on longevity in mice.

Longevity has been assessed in the context of reduced activity of the Pol III inhibitor protein MAF1. Unexpectedly, Maf1 KO female mice, but not male, were significantly longer lived when maintained on a chow diet [406]. Male Maf1 KO mice were leaner than WT mice and resistant to high-fat diet (HFD) induced obesity [407], HFD studies were not undertaken in female Maf1 KO mice. It was suggested that the HFD-resistant phenotype in males was due to inefficiency in energy usage caused by unchecked Pol III activity. Specifically, Maf1 KO mice displayed futile RNA cycling, a highly energy demanding process, due to enhanced Pol III activity [407]. The energy to support this futile RNA cycling was apparently provided through elevated autophagy and lipolysis, and this highly catabolic state protected against HFD-induced obesity [407]. However, the precise role of Maf1 in longevity appears complex. Studies in yeast have shown that *Maf1* deletion actually shortens lifespan, but that DR-induced longevity is dependent on *Maf1* expression [408]. Contrary to this, *Mafr1* KO in worms extends lifespan but had no influence on DR-induced longevity [409]. As MAF1 regulates the activity of all three RNA polymerases, it is unclear if the effects described above are due to modulated Pol III activity specifically. These results suggest that mediation of lifespan through Maf1 is complex and controlled by distinct regulatory mechanisms across species.

6.2.3 The role of hydrogen sulfide (H_2S) in ageing, dietary restriction, and RNA Polymerase III

As mentioned earlier within this thesis, H_2S is a gasotransmitter capable of influencing diverse biological processes including neuronal function [45], smooth muscle vasorelaxation [46], [47] modulation of the inflammatory response [48], and stimulation of angiogenesis [49]. This is achieved through diverse signalling modalities available to H_2S. These include post translational modification of protein cysteine groups (termed persulfidation) [95], binding to metal centres in metalloproteins [108], and interaction with the other gasotransmitters: carbon monoxide and nitric oxide [115]. H_2S is produced endogenously from enzymatic catabolism of the sulfur-containing amino acids, methionine and cysteine [63], [64]. Enzymes involved in this include cystathionine-gamma-lyase (CSE, or CGL), cystathionine-beta-synthase (CBS), and 3-mercaptopyruvate sulfurtransferase (MPST) [66]. CSE and CBS exist almost exclusively in the cellular cytoplasm, whereas MPST can localise to both the cytoplasm and mitochondria [69], where its H_2S-generating activity is greater [70]. Enzymatic catabolism of H_2S is performed by a suite of mitochondrial enzymes known as the sulfide oxidation unit (SOU) [72], as summarised in **Figure 1**. Ageing has been shown to be subject to regulation by H_2S, with accumulating evidence demonstrating H_2S-mediated protection against all hallmarks of ageing, except for telomere shortening for which no studies had been published [66].

It is through DR studies that our appreciation of the role of H_2S in ageing is most fully developed. It has been known for over 100 years that DR extends lifespan across taxa [154]–[156], confers significant health benefits, and improves late-life health by reducing the incidence and/or trajectory of a number of age-related pathologies, including cognitive decline, metabolic syndrome, cardiovascular disease and many cancers [154], [159]. While the benefits of DR in healthy ageing present an interesting therapeutic intervention [162], side effects such as infertility, sarcopenia, osteoporosis, and reduced immunity make applying DR protocols in humans untenable [163]. The need to understand the downstream mechanistic effectors of DR is pressing. H_2S could be one such effector of DR as the beneficial effects of DR have been shown to depend on elevated H_2S production in diverse models from yeast to mice [164]–[168] and H_2S production is also elevated in long-lived mouse mutants [170]. The

mechanism by which DR elevates H_2S is currently unresolved. One proposal is that the elevation of autophagy under nutrient-limiting conditions [171], generates the substrate pool for H_2S biogenesis. Additionally, H_2S itself can inhibit mTOR signalling to alter cellular metabolism and promote autophagy [183], [184], [185], and the mTORC1 inhibitor rapamycin inhibits H_2S production through depression of CSE and CBS gene transcription [190]. However, contradictory studies showed an anti-autophagic role for H_2S *via* mTOR signalling [186]–[189]. Together these studies paint a complex picture of DR/mTOR/H_2S signalling and further research is required to determine the precise conditions by which H_2S inhibits or stimulates mTOR. Beyond mTOR signalling, DR may also confer beneficial ageing effects through elevated activation of nuclear factor erythroid 2-related factor 2 (NRF2) [410]. H_2S can also modulate NRF2 activity through persulfidation of cysteine residues on Kelch-like ECH-associated protein 1 (Keap1) [97], [98], which is the major inhibitor of NRF2. This shared influence of NRF2 activity might by another mechanism by which H_2S acts as an effector of DR.

To date, no studies have investigated the effect of reduced Pol III expression on H_2S. Given that both Pol III and H_2S are regulated by DR and mTOR signalling, and both have an established role in healthy ageing, more research is required to elucidate if these powerful modulators of cellular processes are indeed causative of longevity. In this study I examined regulation of H_2S production in Polr3b Het KO mice, a putative long-lived mouse model. I found that hepatic H_2S production capacity was only elevated in male Polr3b Het KO mice. As I have previously published pronounced strain-specificity in H_2S production under DR (**Chapter 3,** [254]), and as the impact of DR on H_2S has not been measured in C57BL/6N mice, I placed male C57BL/6N wild-type (WT) and Polr3b Het KO mice under 1-month 40% DR and examined measures of H_2S production, gene transcription, protein levels, and the NRF2 antioxidant response. The WT DR group acted as a positive control to determine whether the effects of DR on H_2S reported in other WT mouse strains is replicated in C57BL/6N mice.

6.3 Aims and hypothesis

Background

Reduction in RNA polymerase III (Pol III) results in extension in lifespan in flies and worms. Dietary restriction (DR) has been shown to support healthy metabolism and extend lifespan across species. DR is sensed by mammalian target of rapamycin (mTOR) signalling, which controls the Pol III inhibitor Maf1. Hydrogen sulfide (H_2S) levels in tissues positively correlate with DR and longevity across species and stimulate protective antioxidant responses including NFE2-related factor (NRF2).

Hypothesis

In mice with heterozygous knock out of the Pol III sub-unit *Polr3b* (Polr3b Het KO mice), which is a putative long-lived model, I predicted that hepatic production of H_2S would be elevated relative to wild-type (WT) mice, but that this increase would not be additive with DR due to redundancy in molecular pathways. To this end I placed male WT and Polr3b Het KO mice under both *ad libitum* (AL) feeding and 1-month of 40% DR.

Aims

1. Investigate the impact of DR in mice in both WT and Polr3b Het KO mice on the production and disposal of hepatic H_2S in the cytosolic and mitochondrial compartments using both the lead acetate and MitoA approaches.

2. Determine the effect of DR in both WT and Polr3b Het KO mice on glucose homeostasis, body weight, body temperature (data in **Appendix I**), gene expression of Pol III target genes and in parameters linked to antioxidant protection and oxidative damage.

6.4 Results

6.4.1 Polr3b Het KO mice have the same physiological response to DR as WT

I placed WT and Het mice under 4-weeks of 40% dietary restriction (DR) to examine if the expected disruption of translational machinery in Polr3b Het KO mice shared molecular mechanisms with the reduced protein synthesis of mice under DR conditions. Body weight was measured in both DR and *ad libitum* (AL) groups weekly during the DR intervention period (10% reduction in food available compared to AL groups in week 1, 20% reduction in week 2, then 40% reduction in weeks 3-6) in male WT and male Polr3b Het KO mice (**Figure 37a**). No statistical difference in body weight was found between WT and Polr3b Het groups on the same diet. The body weights immediately prior to cull are presented in **Figure 37b**, showing a significant decrease in mice on DR compared to AL ($F(1, 26) = 23.250$, $p < 0.0001$), but no difference between genotypes ($F(1, 26) = 0.007$, $p = 0.939$). Post-hoc multiple comparison tests found a significant difference between WT DR and WT AL groups ($p = 0.0003$), and Het DR and Het AL groups ($p = 0.0003$).

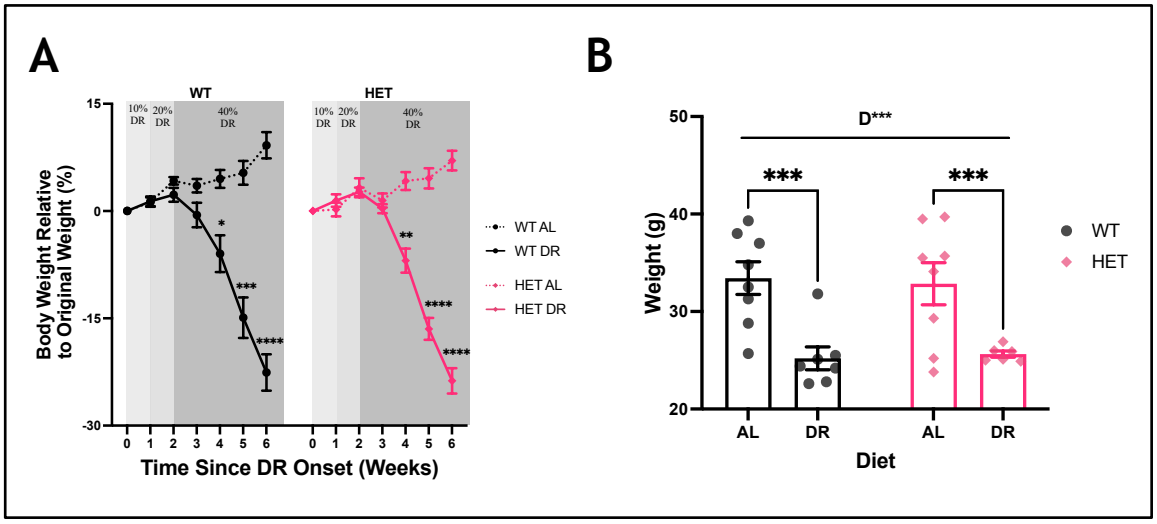

Figure 37 Changes in mouse weight under DR

A Changes in mean mouse body weight presented relative to initial bodyweight at onset of DR. **B** Mean body weight immediately prior to cull at end of DR protocol. Statistical significance determined by 2-way ANOVA with genotype and diet as factors and Tukey multiple comparisons with alpha = 0.05. Grubb's outlier test was performed with alpha = 0.05, no outliers removed. WT data in black, Het data in pink. Bars/lines/dots represent mean value and error bars represent standard error of the mean. AL: *ad libitum*, DR: Dietary restriction. * = $p < 0.05$, *** = $p < 0.001$, **** = $p < 0.0001$. D*** = two-way ANOVA main effect $p < 0.001$.

6.4.2 Pol III protein expression in Polr3b Het KO mice under DR

Hepatic protein levels of Pol III were assessed by blotting for the Polr3b subunit of Pol III, which is the sub-unit knocked-out in the Polr3b Het KO mouse model used in these experiments **(Figure 38a)**. A significant diet effect was found ($F(1, 26) = 12.300$, $p = 0.002$), with a reduction in Polr3b protein levels under DR diets compared to AL. There was no significant genotype effect ($F(1,26) = 3.015$, $p = 0.094$) on Polr3b protein levels. Pairwise comparisons found a significant reduction in Pol III protein between AL and DR fed animals of either genotype ($p = 0.009$ for WT mice, $p = 0.009$ for Het mice). I also blotted for Maf1 protein, an inhibitor of Pol III activity **(Figure 38b)**. No significant diet ($F(1,28) = 0.009$, $p = 0.924$) or genotype ($F(1,28) = 0.040$, $p = 0.843$) effects were found in MAF1 protein levels. Finally, I blotted for phosphorylated ribosomal protein S6 (pS6), a target of mTOR signalling upstream of Pol III (**Figure 38c)**. No significant diet ($F(1,12) = 1.330$, $p = 0.271$) or genotype ($F(1,12) = 1.270$, $p = 0.282$) effects were found for hepatic pS6 protein levels. However, hepatic *Ulk1* gene expression was found to be significantly increased by diet ($F(1,27) = 18.18$, $p = 0.0002$). Multiple comparisons found a significant difference between WT AL and WT DR groups ($p = 0.0012$), and Polr3b Het KO AL and Polr3b HetKO DR groups ($p = 0.0012$). No genotype effect was found for *Ulk1* gene expression ($F(1,27) = 0.124$, $p = 0.728$).

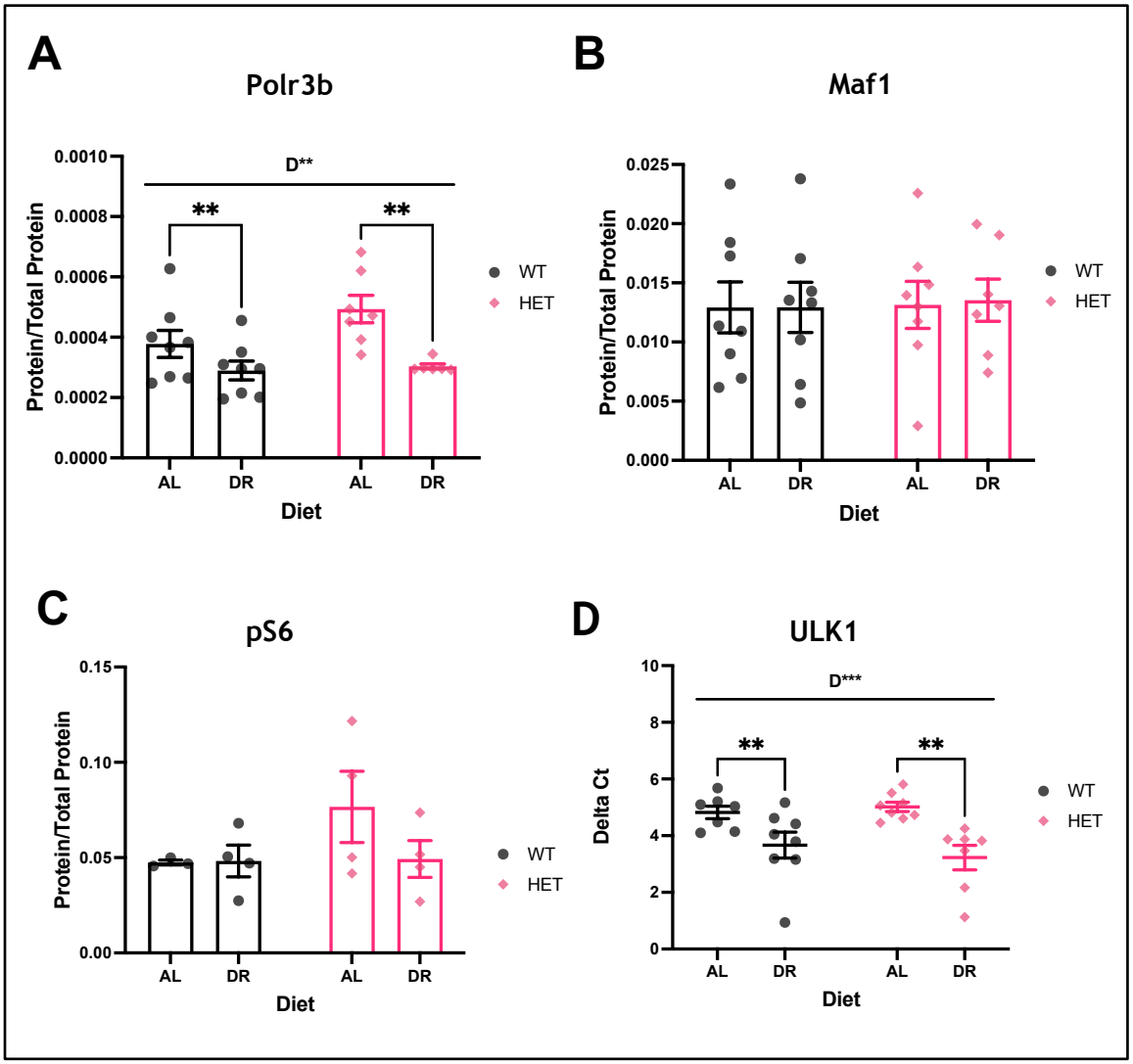

Figure 38 Hepatic protein levels of Pol III subunit Polr3b and Pol III inhibitor Maf1

Hepatic protein levels of the Pol III subunit Polr3b (**A**), Maf1 (**B**), and pS6 (**C**) as measured by western blotting. Data quantified by densitometry analysis and normalised to total protein loading. **D** Relative hepatic gene expression of ULK1 as measured by RT-qPCR. Data presented as raw Ct values of each gene. WT data in black, Het data in pink. Statistical significance determined by 2-way ANOVA with genotype and diet as factors and Tukey multiple comparisons with alpha = 0.05. Grubb's outlier test was performed with alpha = 0.05, one outlier removed in Het AL group. Bars represent mean value and error bars represent standard error of the mean. AL: *ad libitum*, DR: Dietary restriction, ULK1: Unc-51 Like Autophagy Activating Kinase 1. ** = $p < 0.01$. D* = two-way ANOVA diet main effect $p < 0.05$, D*** = two-way ANOVA diet main effect $p < 0.001$.

I measured hepatic gene expression of Pol III target genes by RT-qPCR to determine the effect of Polr3b Het KO and DR on Pol III activity. The ΔCt values for each individual gene studied are given in **Figure 39a-f** (Note that a higher ΔCt value indicates a lower expression of that mRNA transcript). For most of the genes probed in this study there was no significant genotype or diet effect (see **Table 14** for full results), except for the B1 consensus probe, for which a genotype x diet interaction was found ($F(1,24) = 7.103$, $p = 0.014$). Multiple comparisons revealed a significant reduction in B1 consensus transcripts in Het AL mice compared to WT AL ($p = 0.043$) and a reduction in WT mice on DR compared to AL controls ($p = 0.048$).

Table 14 Full results of two-way ANOVA analysis of hepatic gene expression of RNA polymerase III target genes

28S: 28S rRNA, 5S: 5S rRNA, 7SL: Signal recognition particle RNA, B1 consensus: primer that binds to approximately 100 B1 family genes. Results in bold are considered statistically significant. NS = non-significant.

	Diet Effect (D)		Genotype Effect (G)		D x G Interaction	
Gene Name	**F-Value**	**P-Value**	**F-Value**	**P-Value**	**F-Value**	**P-Value**
28S rRNA	(1,26) 1.621	0.214	(1,26) 1.400	0.2472	*NS*	*NS*
5S rRNA	(1,27) 0.103	0.750	(1,27) 1.762	0.195	*NS*	*NS*
7SL	(1,27) 1.486	0.233	(1,27) 0.206	0.653	*NS*	*NS*
pre-tRNA Leu	(1,26) 0.328	0.572	(1,26) 0.337	0.567	*NS*	*NS*
pre-tRNA Tyr	(1,26) 0.374	0.546	(1,26) 0.200	0.659	*NS*	*NS*
B1 Consensus	(1,24) 1.267	0.272	(1,24) 1.403	0.248	**(1,24) 7.103**	**0.014**

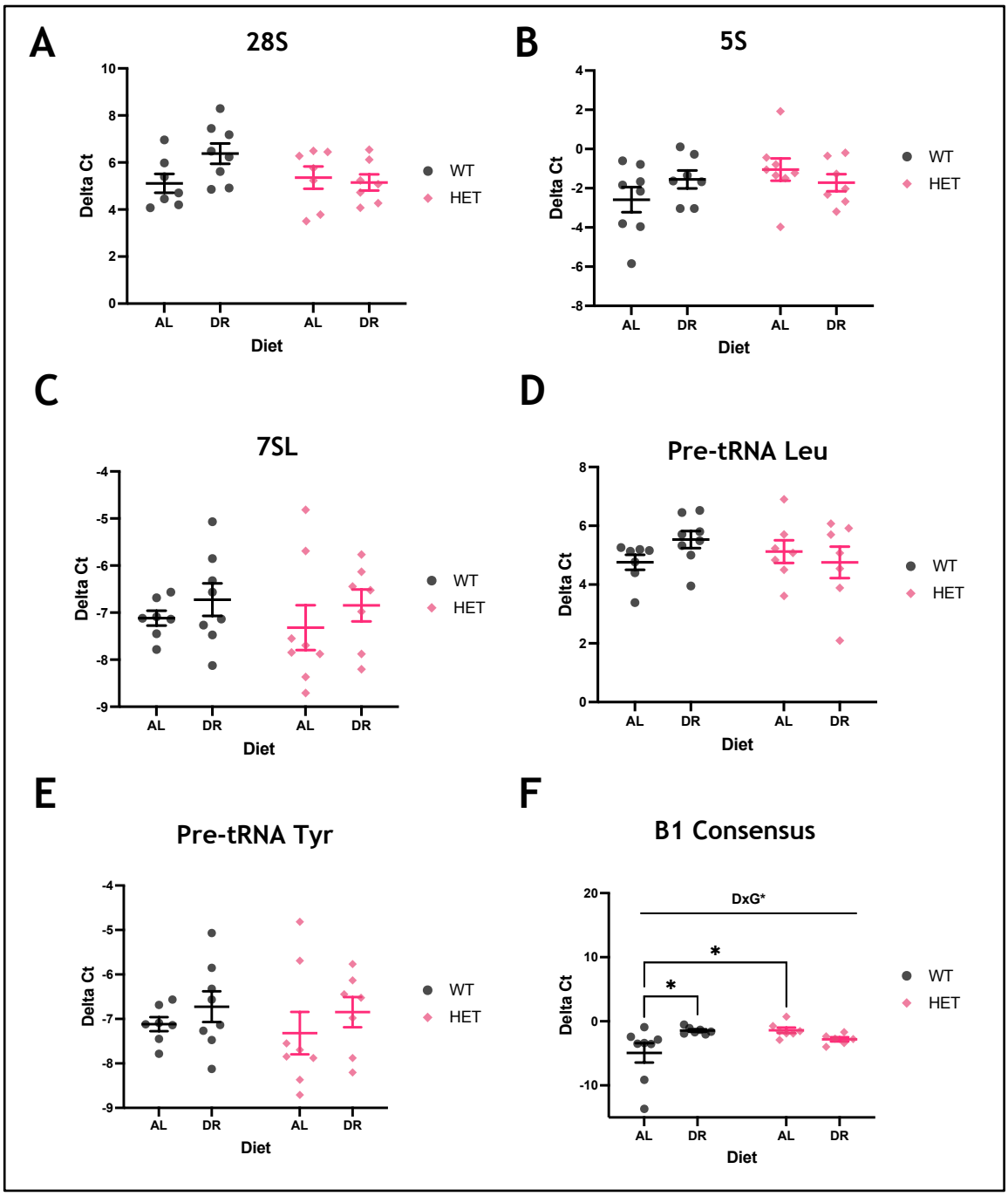

Figure 39 Hepatic gene expression of Pol III target genes

Relative hepatic gene expression of Pol III target genes measured by RT-qPCR. Data presented as raw ΔCt values for each gene (**A-F**). Statistical significance determined by 2-way ANOVA analysis of ΔCt values with genotype and diet as factors and Tukey multiple comparisons with alpha = 0.05. Grubb's outlier test was performed with alpha = 0.05, no outliers removed. WT data in black, Het data in pink. Bars/lines/dots represent mean value and error bars represent standard error of the mean. AL: *ad libitum*, DR: Dietary restriction. * = $p < 0.05$. 28S: 28S rRNA, 5S: 5S rRNA, 7SL: Signal recognition particle RNA, B1 consensus: primer that binds to approximately 100 B1 family genes. DxG* = two-way ANOVA DietxGenotype interaction effect $p < 0.05$.

6.4.3 Hydrogen sulfide (H_2S) production is elevated in male but not female Polr3b Het KO mice

As a novel mutant, H_2S metabolism has not been measured in Polr3b het KO mice. I used the lead acetate method to measure hepatic H_2S production capacity in 4-month male and female WT and Polr3b Het KO mice (**Figure 40a**). Neither a genotype ($F(1,20) = 4.066$, $p = 0.057$) nor sex ($F(1,20) = 0.739$, $p = 0.400$) effect was found on H_2S production capacity. However, there was a significant genotype x sex interaction effect ($F(1,20) = 5.580$, $p = 0.028$). Multiple comparison testing found that this interaction was driven by significantly higher H_2S production in male Het mice compared to male WT mice ($p = 0.027$). Given these results I investigated cross-sectional H_2S production capacity in liver samples from male Polr3b Het KO mice at 4, 9, 12, and 17 months of age (**Figure 40b**). Significant age ($F(3,30) = 4.899$, $p = 0.007$) and genotype ($F(1,30) = 4.487$, $p = 0.043$) effects were found, with multiple comparisons showing elevation in Polr3b Het KO mice compared to WT, and a significant decrease in H_2S production capacity from 9 to 17 months of age in both WT and Polr3b Het KO mice ($p = 0.014$ and $p = 0.014$, respectively).

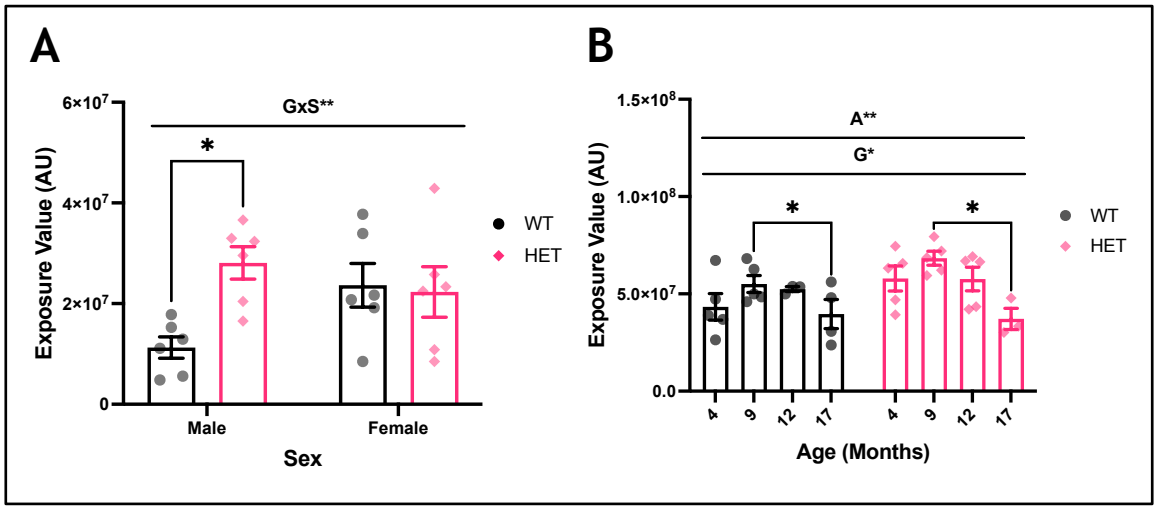

Figure 40 Hepatic H_2S levels are modified by Pol III expression in male mice and decline with age

A Hepatic H_2S production capacity as measured by lead acetate method in male and female mice. Statistical significance determined by 2-way ANOVA with genotype and diet as factors and Tukey multiple comparisons with alpha = 0.05. Grubb's outlier test was performed with alpha = 0.05, no outliers removed. **B** Hepatic H_2S production capacity as measured by lead acetate method in male mice at different age cross-sections. Statistical significance determined by 2-way ANOVA with genotype and age as factors and Tukey multiple comparisons with alpha = 0.05. Grubb's outlier test was performed with alpha = 0.05, no outliers removed. WT data in black, Het data in pink. Bars represent mean value and error bars represent standard error of the mean. AL: *ad libitum*, DR: Dietary restriction. * = $p < 0.05$ between indicated groups. DxS* = two-way ANOVA DietxSex interaction effect $p < 0.05$, A** = two-way ANOVA age main effect $p < 0.01$, G* = two-way ANOVA genotype main effect $p < 0.05$.

6.4.4 H_2S production is differentially modulated by DR and Polr3b Het KO dependent on cellular compartment

I next used the lead acetate assay to measure hepatic H_2S production capacity in WT and Polr3b Het KO mice under both AL and DR diets (**Figure 41a**). Two-way ANOVA analysis determined that there was both a significant diet ($F(1,27) = 26.870$, $p < 0.0001$) and genotype ($F(1,27) = 8.330$, $p = 0.008$) effect on H_2S production capacity, being elevated in DR mice relative to AL mice and being elevated in Polr3b Het KO mice relative to WT mice. Using a multiple comparison approach, I found that there was an elevation in H_2S production capacity in WT DR mice compared to WT AL mice ($p = 0.0001$), in Polr3b Het AL mice compared to WT AL mice ($p = 0.036$), in Polr3b Het DR mice compared to Polr3b Het AL mice ($p = 0.0001$), and in Polr3b Het DR mice compared to WT DR mice ($p = 0.036$). Consequently, there was an additive effect of diet and Polr3b Het KO on H_2S production capacity suggesting that both interventions elevate H_2S production capacity through distinct mechanisms.

I then examined *in vivo* mitochondrial H_2S levels by using the MitoA probe and LC-MS/MS analysis as described in **Chapter 4** (**Figure 41b)**. Two-way ANOVA analysis found a significant diet ($F(1,25) = 8.034$, $p = 0.009$) and genotype x diet interaction effect ($F(1,25) = 4.918$, $p = 0.036$), but a non-significant genotype main effect ($F(1,25) = 0.026$, $p = 0.872$). There appears to be a very modest reduction in mitochondrial H_2S levels in WT DR mice compared to WT AL, which *post-hoc* testing revealed to be non-significant ($p = 0.970$). In Polr3b Het KO mice under DR there is a significant reduction in mitochondrial H_2S levels ($p = 0.009$) compared to Polr3b Het KO mice on AL diet. As such, the main and interaction effects identified by two-way ANOVA analysis appear driven by a large reduction in Polr3b Het KO mice on DR relative to Polr3b Het KO mice on AL. These data are in contrast with the lead acetate results described above, where both diet and genotype elevated cytosolic H_2S production capacity.

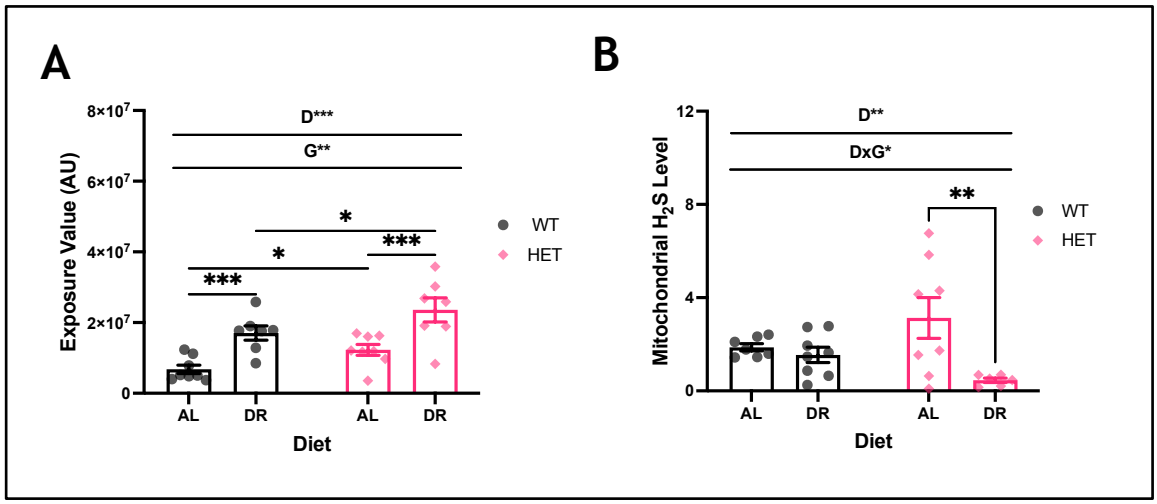

Figure 41 Regulation of hydrogen sulfide levels is modified by both DR and Polr3b Het KO, with divergence in regulation in the cytosolic and mitochondrial compartments

A Lead acetate assay measurements of hepatic cytosolic H_2S production capacity. **B** Mitochondrial H_2S levels as determined by analysis of MitoA and MitoN concentrations in liver samples. Statistical significance determined by 2-way ANOVA with genotype and diet as factors and Tukey multiple comparisons with alpha = 0.05. Grubb's outlier test was performed with alpha = 0.05, no outliers removed. WT data in black, Het data in pink. Bars represent mean value and error bars represent standard error of the mean. AL: *ad libitum*, DR: Dietary restriction. * = $p < 0.05$, ** = $p < 0.01$, *** = $p < 0.001$. D*** = two-way ANOVA diet main effect $p < 0.001$, G** = two-way ANOVA genotype main effect $p < 0.01$, D** = two-way ANOVA diet main effect $p < 0.01$, DxG* = two-way ANOVA DietxGenotype interaction effect $p < 0.05$.

I measured hepatic gene expression of H_2S metabolism genes by RT-qPCR to determine the effect of Polr3b Het KO and DR on transcriptional regulation of key H_2S production and disposal enzymes. The data is presented as ΔCt values for each individual gene studied (**Figure 42a-f**, note that a higher ΔCt value indicates a lower expression of that mRNA transcript). For most of the genes probed in this study there was no significant genotype or diet effect (see **Table 15** for full results). For the gene expression of the H_2S producing enzyme *Cbs*, a genotype x diet interaction was found ($F(1,26) = 9.386$, $p = 0.005$). Multiple comparisons revealed a significant elevation in *Cbs* transcripts in WT DR mice compared to WT AL ($p = 0.021$). Finally, a significant diet ($F(1,25) = 7.318$, $p = 0.012$) and diet x genotype interaction effect ($F(1,25) = 7.564$, $p = 0.011$) was found for *Ethe1* gene transcripts, no genotype main effect was found ($F(1,25) = 2.137$, $p = 0.016$). *Ethe1* encodes for a mitochondrial enzyme that comprises part of the H_2S disposal machinery. Multiple comparisons revealed a significant elevation in *Ethe1* transcripts in Polr3b Het KO mice under DR compared to Polr3b Het KO mice under AL feeding ($p = 0.006$).

Table 15 Full results of two-way ANOVA analysis of hepatic gene expression of H_2S production and disposal genes

Cse: Cystathionine-beta-lyase, *Cbs*: Cystathionine-Beta-synthase, *Mpst*: 3-Mercaptopyruvate Sulfurtransferase, *Tst*: Thiosulfate Sulfurtransferase, *Suox*: Sulfite Oxidase, *Ethe1*: Ethylmalonic encephalopathy 1 protein. Results in bold are considered statistically significant. NS = non-significant.

	Diet Effect (D)		Genotype Effect (G)		D x G Interaction	
Gene Name	**F-Value**	**P-Value**	**F-Value**	**P-Value**	**F-Value**	**P-Value**
CSE	(1,28) 3.096	0.089	(1,28) 0.341	0.564	*NS*	*NS*
CBS	(1,26) 1.494	0.233	(1,26) 0.393	0.536	**(1,26) 9.386**	**0.005**
MPST	(1,28) 3.485	0.072	(1,28) 1.011	0.323	*NS*	*NS*
TST	(1,26) 0.011	0.918	(1,26) 0.026	0.874	*NS*	*NS*
SUOX	(1,27) 0.491	0.490	(1,27) 0.307	0.584	*NS*	*NS*
ETHE1	**(1,25) 7.318**	**0.012**	(1,25) 2.137	0.156	**(1,25) 7.564**	**0.011**

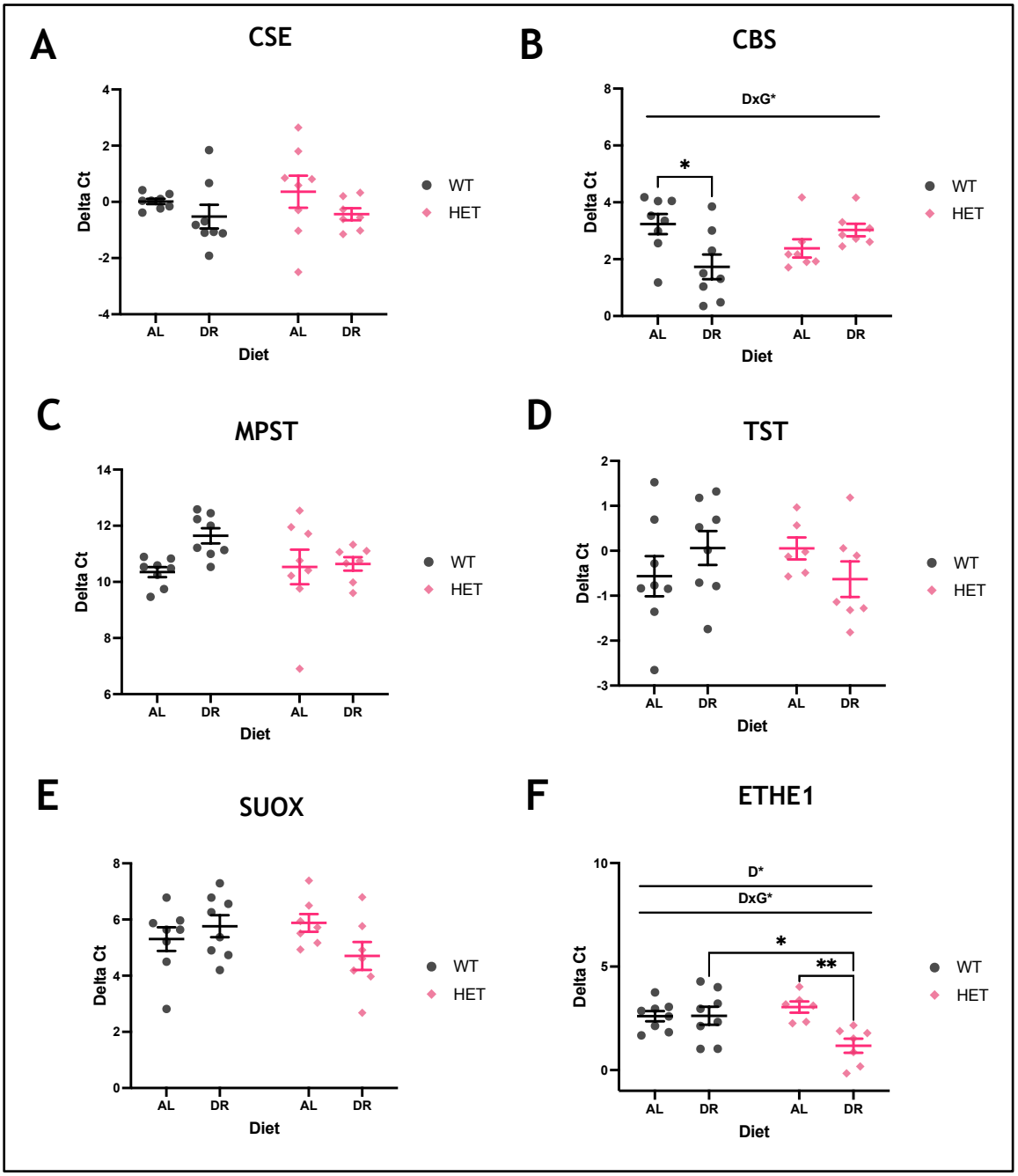

Figure 42 Hepatic gene expression of H_2S metabolism genes

Relative hepatic gene expression of H_2S metabolism genes measured by RT-qPCR. Data presented as raw ΔCt values for each gene (**A-F**). Statistical significance determined by 2-way ANOVA analysis of ΔCt values with genotype and diet as factors and Tukey multiple comparisons with alpha = 0.05. Grubb's outlier test was performed with alpha = 0.05, no outliers removed. WT data in black, Het data in pink. Bars/lines/dots represent mean value and error bars represent standard error of the mean. AL: *ad libitum*, DR: Dietary restriction. * = $p < 0.05$, ** = $p < 0.01$. Cse: Cystathionine-beta-lyase, Cbs: Cystathionine-Beta-synthase, Mpst: 3-Mercaptopyruvate Sulfurtransferase, Ethe1: Ethylmalonic encephalopathy 1 protein, Tst: Thiosulfate Sulfurtransferase, Suox: Sulfite Oxidase. DxG* = two-way ANOVA DietxGenotype interaction effect $p < 0.05$. D* = two-way ANOVA diet main effect $p < 0.05$,

I next blotted for protein levels of H_2S metabolism proteins by western blotting (**Figure 43**). There was no significant diet or genotype effect on the protein levels of hydrogen sulfide production enzymes CSE, CBS, or MPST (**Figure 43a-c,** full statistical results shown in **Table 16**). For ETHE1 a significant diet effect ($F(1,12) = 12.000$, $p = 0.005$) was found by two-way ANOVA analysis, but there was a non-significant genotype effect ($F(1,12) = 3.305$, $p = 0.094$). Multiple comparison analysis found a significant elevation in mean ETHE1 protein levels between WT AL and WT DR mice ($p = 0.021$), and Polr3b Het KO AL and Polr3b Het KO DR mice ($p = 0.021$). Finally, a significant genotype effect ($F(1,12) = 4.963$, $p = 0.046$) was found for protein levels of SQR, which was higher in Polr3b Het KO mice compared to WT mice. No significant diet effect was found ($F(1,12) = 1.543$, $p = 0.238$), and multiple comparisons found no significant difference in mean SQR protein levels between any specific experimental group.

Table 16 Full results of two-way ANOVA analysis of hepatic gene expression of H2S production and disposal proteins

Cse: Cystathionine-beta-lyase, Cbs: Cystathionine-Beta-synthase, Mpst: 3-Mercaptopyruvate Sulfurtransferase, Ethe1: Ethylmalonic encephalopathy 1 protein, SQR: Sulfur:quinone reductase. Results in bold are considered statistically significant. NS = non-significant.

	Diet Effect (D)		Genotype Effect (G)		D x G Interaction	
Protein Name	**F-Value**	**P-Value**	**F-Value**	**P-Value**	**F-Value**	**P-Value**
CSE	(1,28) 3.619	0.068	(1,28) 0.012	0.915	NS	NS
CBS	(1,28) 0.273	0.606	(1,28) 1.004	0.325	NS	NS
MPST	(1,28) 0.235	0.632	(1,28) 0.010	0.921	NS	NS
ETHE1	**(1,12) 12.000**	**0.005**	(1,12) 3.305	0.094	NS	NS
SQR	(1,12) 1.543	0.238	**(1,12) 4.96**	**0.046**	NS	NS

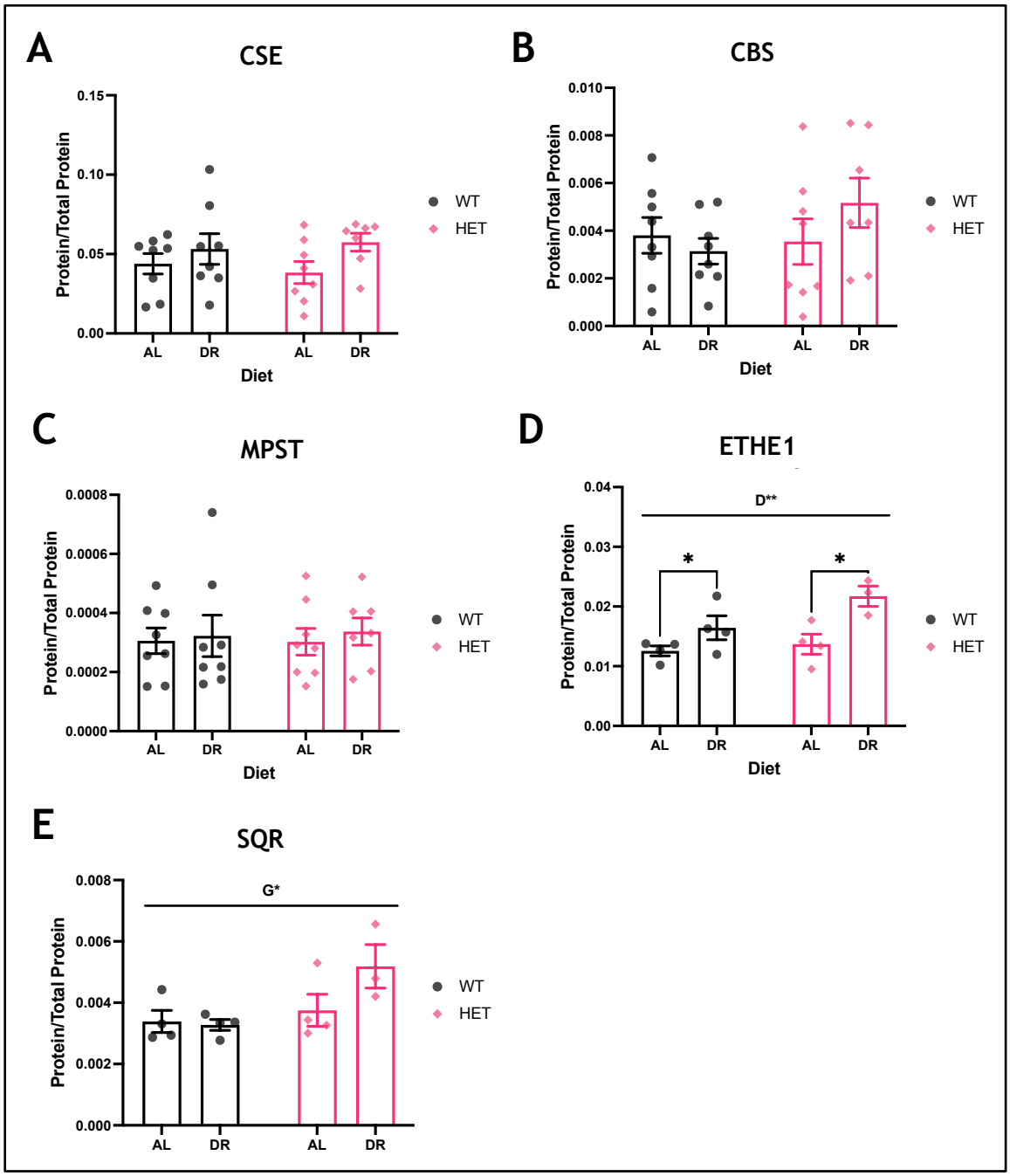

Figure 43 Hepatic protein levels of H_2S metabolism proteins

Hepatic protein levels of H_2S metabolism proteins measured by western blotting and normalised to total protein loading. Statistical significance determined by 2-way ANOVA analysis with genotype and diet as factors and Tukey multiple comparisons with alpha = 0.05. Grubb's outlier test was performed with alpha = 0.05, no outliers removed. WT data in black, Het data in pink. Bars represent mean value and error bars represent standard error of the mean. AL: *ad libitum*, DR: Dietary restriction. * = $p < 0.05$. Cse: Cystathionine-beta-lyase, Cbs: Cystathionine-Beta-synthase, Mpst: 3-Mercaptopyruvate Sulfurtransferase, Ethe1: Ethylmalonic encephalopathy 1 protein, SQR: Sulfur:quinone reductase. D** = two-way ANOVA diet main effect $p < 0.01$, G* = two-way ANOVA Genotype main effect $p < 0.05$.

6.4.5 Oxidative damage in Polr3b Het KO mice under DR

As H_2S is elevated in an additive manner by both DR and Polr3b Het KO, and H_2S confers antioxidative benefits, I examined markers of oxidative damage. Protein carbonyl content was measured as an established marker of oxidative damage (**Figure 44a**). Two-way ANOVA analysis found no diet effect ($F(1,18) = 2.145$, $p = 0.160$), although a significant genotype effect ($F(1,18) = 14.14$, $p = 0.001$) was seen, with protein carbonyl content lower in Polr3b Het AL mice compared to WT mice. Multiple comparisons found a significant difference between WT AL and Polr3b Het KO AL groups ($p = 0.007$), and WT DR and Polr3b Het KO DR groups ($p = 0.007$). Gene expression of *Nrf2* was measured by RT-qPCR, however no diet($F(1,25) = 2.251$, $p = 0.146$) or genotype ($F(1,25) = 0.011$, $p = 0.918$) effects were found (**Figure 44b**). Similarly, in *Sod1* gene expression no diet($F(1,27) = 1.452$, $p = 0.239$) or genotype ($F(1,27) = 0.458$, $p = 0.504$) effects were found (**Figure 44c**).

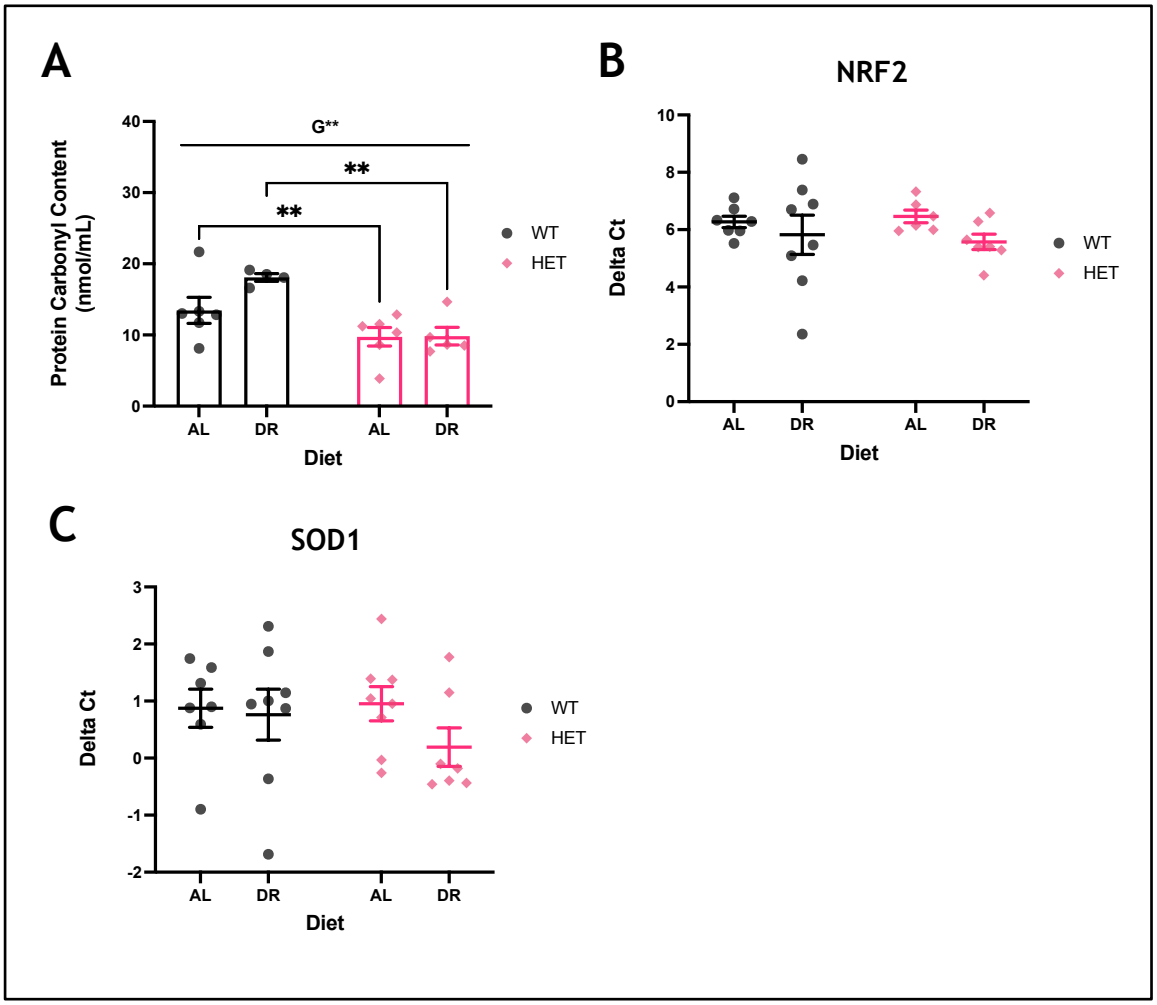

Figure 44 Evidence of reduced oxidative damage in Polr3b Het KO mice compared to WT is not related to improved NRF2 expression

A Protein carbonyl content as measured in hepatic protein lysate. Relative hepatic gene expression of NRF (**B**) and SOD1 (**C**) as measured by RT-qPCR. Data presented as raw Ct values of each gene. Statistical significance determined by 2-way ANOVA analysis of Ct values with genotype and diet as factors and Tukey multiple comparisons with alpha = 0.05. Grubb's outlier test was performed with alpha = 0.05. WT data in black, Het data in Pink. Bars/lines represent mean value and error bars represent standard error of the mean. AL: *ad libitum*, DR: Dietary restriction. ** = $p < 0.01$. NRF2: NFE2-related factor, SOD1: Superoxide dismutase. G** = two-way ANOVA genotype main effect $p < 0.01$.

6.5 Discussion

6.5.1 Polr3b Het KO results in incomplete reduction in Pol III activity

I examined Polr3b protein levels, as there are no published studies that have examined Pol III protein expression under DR in mice. I found that hepatic Polr3b protein levels were reduced under DR in both WT and Het mice. Under DR protein synthesis rates may be reduced, elevated, or maintained depending on the tissue studied, age of organism, severity of restriction, and duration of restriction [63], [411], [412]. Studies in 5-15 month old C57Bl/6 mice (specific sub-strain not given) found that 60% DR significantly elevated hepatic protein synthesis rates compared to AL controls [413]. Given that the Polr3b Het KO mice were of a similar age and DR severity, it was unexpected to see a reduction in Polr3b protein levels under DR feeding in both WT and Polr3b Het KO mice, as it is assumed that protein synthesis rates will be increased. Further, levels of the Polr3b sub-unit were not different in WT and Het mice. This was unexpected as our Polr3b Het KO mice were designed with the intention of knocking down Pol III activity. The *Polr3b* gene was edited in our Polr3b Het KO mice such that there was heterozygous insertion of an 8bp sequence (at a *locus* that encodes for the codon for cysteine 103 in the protein sequence) which results in early truncation of *Polr3b* transcripts. The insertion of this sequence was confirmed by genotyping all mice used in this experiment post-mortem. The antibody used in these experiments binds to an epitope that is downstream of the insertion codon (approximately between amino acids 120-220) and is therefore expected to not bind to *Polr3b* transcripts from the mutant allele. While protein levels of Polr3b appear to be unaffected in Polr3b Het KO mice compared to WT, it is possible that Polr3b protein transcribed from the mutant allele is inactive. To examine the activity of Pol III I measured gene expression levels of several Pol III target genes as well as transcription of 28S ribosomal RNA (rRNA) which is transcribed by RNA polymerase I as a control. Unexpectedly, most Pol III target genes are unaffected by Polr3b Het KO, except for B1 consensus genes which were reduced as hypothesised. This is not unprecedented: Vorländer *et al*. demonstrated that intestinal mutation of *Polr3b* in mice reduced expression of 5S rRNA and U6 snRNA but had no effect on expression of tRNAs [414]. Additionally, a variety of mutations in Polr3b have been described and confer myriad effects (such as

ataxia or neuropathy) dependent on which Pol III subunit interactions were ablated by the mutations [415]. This demonstrates that the phenotype of *Polr3b* mutants is dependent on the exact genetic alteration of the *Polr3b* locus and the resulting mutant protein product. I also found that DR reduced expression of B1 consensus genes in WT DR mice compared to WT AL, but there was no additional reduction in B1 gene transcription in Porl3b Het KO mice under DR compared to Polr3b Het KO mice on AL diet. Pol III activity under DR in mice has not been studied, although Pol III activity in yeast was reduced when changed from a rich medium (100% yeast peptone with 2% glucose) to a nutrient-deprived medium (15% yeast peptone with no glucose) for 12, 25, 75, or 180 min [416]. As such, this reduction in gene transcription for B1 genes is indicative of a reduction of Pol III transcription under DR in mice, but it is unclear why there is only a significant difference in B1 genes and not the other Pol III targets studies here. The B1 gene family is a type short interspersed elements (SINE), which evolved from 7SL RNA and is present in the genomes of all rodents [417], [418]. Some explanation for this finding may be found by examining the distinct transcriptional assemblies of the Pol III transcription machinery for different target genes, as illustrated in **Figure 36**. For example, the B1 consensus, tRNAs, and 7SL genes are transcribed by type 2 Pol III transcriptional machinery, whereas 5S rRNA is transcribed using type 1 Pol III transcriptional machinery [419]. These machineries recognised different promotor sequences and recruit different transcription factors dependent on the target gene [419]. It is possible that the specific machinery required for transcription of B1 consensus genes is dependent on POLR3B expression, whereas the other Pol III target genes examined here are not. However, the precise transcriptional complex components that POLR3B protein interacts with are poorly defined in the literature. Further resolution of the Pol III transcriptional machinery, with particular focus on POLR3B, is essential for the full understanding on the impact of Polr3b Het KO on Pol III transcriptional activity.

The effect of Polr3b Het KO and DR on physiology and glucose homeostasis was also measured in these mice. Results are given in **Appendix I**.

6.5.2 DR induced elevation of H_2S is independent of Pol III activity

Experiments in flies and worms have demonstrated that knock down of Pol III extends lifespan [405]; as such Polr3b Het KO in mice is a putative long-lived model. It is established that lifespan extension through dietary or genetic means is associated with increased endogenous H_2S levels [164], and so I examined H_2S production in male and female mice with this genetic modification. In mice, Polr3b Het KO in males resulted in a significant increase in hepatic H_2S production capacity, but there was no difference between female WT and Polr3b Het KO cohorts. While some reports have shown consistent responses in H_2S metabolism between male and female animals [226], sexual dimorphism in hepatic H_2S production has been described in other studies. For instance, C57BL/6 mice on every other day (EOD) diets exhibit sexual dimorphism, with elevated hepatic H_2S production capacity under EOD diet observed only in males [420]. The authors proposed that the lack of hepatic H_2S elevation in female mice may contribute to the diminished benefits of EOD diet on late-life frailty in females compared to males. Further, previous studies have described sexual dimorphism in hepatic transcription of Pol III target genes, with male C57BL/6 mice exhibiting altered methylation of U6 splisosomal RNA and an increase in U6 expression compared to female C57BL/6 mice [421]. As such, the observation presented here that Polr3b Het KO results in a sexually dimorphic elevation of hepatic H_2S production is not an unusual phenomenon. Cross-sectional analysis of male mice at 4, 9, 12, and 17 months of age confirms that Polr3b Het mice have elevated H_2S production and this declines with age in both WT and Het mice.

Pol III activity is downstream of the mTOR pathway, which itself is responsive to dietary restriction (DR). It is established in multiple mouse strains that DR elevates hepatic H_2S levels and, in fact, many of the benefits of DR appear dependent on hepatic H_2S [164]. However, the precise molecular mechanisms underpinning DR benefits remain unclear and no studies have measured H_2S levels in C57/BL6N mice under DR. With this observation that Polr3b Het KO is sufficient to elevate hepatic H_2S, I next investigated if reduced Pol III activity could form part of the mechanism by which DR elevates H_2S catabolism. To examine this, I placed WT and Polr3b Het KO mice under 4-weeks of 40% DR compared to *ad libitum* (AL) fed control mice under the hypothesis that Polr3b Het KO mice under DR would exhibit no further extension in hepatic

H_2S production compared to AL fed Het mice due to redundancy in their mechanisms for modifying H_2S metabolism. Unexpectedly, I found that both DR and Polr3b Het KO elevated hepatic H_2S production capacity in an additive manner. This finding suggests that, rather than Pol III activity operating downstream of DR, each of these interventions independently results in an elevation in H_2S levels. Here, I confirm that DR in male C57/BL6N mice is associated with increased hepatic H_2S levels but also that Polr3b Het KO (a putative lifespan extending genetic modification) is also independently capable of increasing H_2S levels in mice. Additionally, I used the Mito A *in vivo* probe to measure mitochondrial H_2S levels. Significant diet and diet x genotype interaction effects were found, with DR reducing mitochondrial H_2S levels modestly in WT mice and far more significantly in Het mice. The Polr3b Het KO mice on AL diet had an approximate 40% increase in mean mitochondrial H_2S levels compared to WT AL mice, however variation in the Het Al group is by far the largest of those studied here (coefficients of variation: WT AL 39.77%, WT DR 60.11%, Polr3b Het KO AL 78.99%, Polr3b Het KO DR 165.6%). The beneficial effects of H_2S in protecting mitochondrial function are well established [76], [252], [368], [369]. For instance, it has been shown that H_2S protects against ischemia-reperfusion injury through SQR-mediated transfer of electrons into the electron transport chain [164]. Despite this, no previous studies have measured the response of mitochondrial H_2S to DR. Here, I present a novel finding that unlike the cytosolic elevation in H_2S production seen in this study (and in **Chapter 3**) following DR, mitochondrial H_2S levels are in fact reduced under DR diet in both WT and Polr3b Het mice compared to AL controls. This uncoupling of cytosolic and mitochondrial H_2S metabolism could potentially be due to altered activity of the pyridoxal-5'-phosphate (PLP) and PLP-independent enzymatic H_2S production pathways. The PLP-dependent enzymes cystathionine-gamma-lyase (CSE) and cystathionine-beta-synthase (CBS) synthesise H_2S directly from cysteine whereas 3-mercaptopyruvate sulfurtransferase (MPST, or TUM1) synthesises H_2S indirectly through stepwise conversion into 3-mercaptopyruvate first by L-cysteine:2-oxoglutarate aminotransferase (CAT) and then into H_2S by MPST [66]. CSE and CBS operate predominately within the cytosol while mammalian MPST exists in two distinct isoforms, TUM1-Iso1 which is exclusively found within the cytosol and TUM1-Iso2, a splice variant encoding an additional 20 amino acid mitochondrial-targeting sequence [69]. I found no difference

between genotype or diet groups in the expression of mitochondrial *Mpst* mRNA or protein levels of MPST. This is unlike my findings in **Chapter 3**, where mRNA and protein levels of MPST were elevated on DR in the TejJ89 sub-strain from the ILSXISS panel of mouse strains. Alterations to expression of the enzymes that comprise the sulfur oxidising unit (SOU) are unlikely to explain the observed uncoupling of cytosolic and mitochondrial H_2S levels as the SOU is localised to mitochondria and catalyses the disposal of H_2S from both cytosolic and mitochondrial origin. Therefore, the divergence in mitochondrial H_2S levels from levels present in the cytosol under DR conditions could be due to reduced MPST activity despite maintenance of protein abundance, however there is no clear understanding of post-translational modification of MPST activity in the literature to date [422]. Putative regulators of MPST activity include phosphorylation sites at the N-terminus which may inhibit mitochondrial import of MPST [423], and inactivation of recombinant MPST protein by hydrogen peroxide (H_2O_2) [424]. However, it is unclear if MPST retains its N-terminus following mitochondrial import [307] and the physiological relevance of H_2O_2 inhibition of MPST generation of H_2S is disputed [425]. Future studies that measure MPST protein levels in both cytosolic and mitochondrial fractions of hepatic tissue homogenates may provide insight into the distribution of MPST protein between these cellular compartments. I also investigated the regulation of enzymes in the H_2S disposal pathway. Only transcription of *Ethe1* is differentially regulated in Polr3b Het KO DR mice compared to Polr3b Het KO AL, but at the protein level DR elevates ETHE1 levels in both WT and Het animals compared to AL-fed controls. Finally, protein levels of SQR were found to be elevated in Polr3b Het KO mice compared to WT. Interestingly, the metabolism of H_2S by SQR is coupled to oxidative phosphorylation across mammalian tissues, including liver [72], [426], [427]. Future studies could employ high-resolution respirometry techniques to ascertain if the alterations in H_2S production caused by Polr3b Het KO and DR impact on mitochondrial respiration. As present, this novel observation that mitochondrial H_2S is reduced under DR has no clear explanation.

6.5.3 Oxidative damage is reduced in Polr3b Het KO mice compared to WT

Given the antioxidative role of H_2S as a reactive oxygen species (ROS) scavenger and stimulator of the nuclear factor E2-related factor 2 (NRF2) response [428], I next investigated whether there was a difference in oxidative damage between experimental groups. Protein carbonyls are irreversible alterations to proteins under oxidative conditions and serve are useful markers of the extent of oxidative damage in a sample [429]. I found that Polr3b Het mice had lower hepatic protein carbonyl content compared to WT mice. This may in part be due to the antioxidative effect of H_2S, which directly scavenges ROS such as superoxide and hydrogen peroxide, and promotes the NRF2 response [355], [430]. However, if H_2S was driving the reduction in protein oxidation we would expect to see an additive effect of DR and genotype as previous data showed an additive effect of these on H_2S production capacity. Diet had no effect on protein carbonyl content in both WT and Porl3b Het KO mice. This is a common finding, as a majority of studies in the literature examining the effect of DR on hepatic protein carbonyl content also found no effect [431]. To help explain these findings I next examined hepatic *Nrf2* and *Sod2* expression. These comprise two major components of the antioxidative response to ROS. However, no effect was found for either DR diet or Polr3b Het KO in the expression of these genes. As such, the reduced hepatic protein carbonyl content in Polr3b Het KO may only be partially accounted for by the elevated H_2S production capacity in these mice. Future studies could measure other antioxidants such as glutathione and catalase in samples from these Polr3b Het KO mice to more fully characterise their antioxidative response compared to WT controls.

6.6 Conclusions

I hypothesised that Polr3bHet KO mice would have an improved metabolic phenotype but this would not be additive with DR due to shared molecular pathways. However, no effect of Polr3b Het KO was found on any measures of physiology or glucose homoeostasis measured here. Further, no additive effect of DR and Polr3b Het KO was found on these measures. This suggests that, despite being downstream of DR and mTOR signalling, reduced Pol III activity is not central to the effects of DR on these measures. As Polr3b Het KO mice are predicted to be long-lived, I also expected their production of H_2S to be elevated compared with WT controls. This was found in a measure of cytosolic H_2S production capacity and surprisingly was additive with DR, indicating the DR and Polr3b Het KO elevate H_2S production capacity *via* distinct mechanisms. I also report here the first measurement of *in vivo* mitochondrial H_2S under DR conditions. I found that mitochondrial H_2S was elevated in Het mice compared to WT but negatively regulated by DR in both genotypes. There was no clear explanation for this finding when examining the gene expression and protein levels of H_2S metabolising. Finally, I show here that protein oxidative stress is reduced in Polr3b Het KO mice compared to WT, which may be driven by elevated H_2S levels in these mice. However, while H_2S is elevated in an additive manner by DR and Polr3b Het KO, reduced protein oxidative damage was not additive. As such, the antioxidative properties of H_2S can only partially explain the improvement in antioxidative capacity. Exploration of other antioxidant mechanisms is required to contextualise these findings.

Chapter 7 General Discussion

H_2S is a gaseous molecule that has profound effects on many biological processes [432]. It shares three properties with nitric oxide and carbon monoxide that qualifies these gases as gasotransmitters: free permeation through membranes, endogenous production, and possession of specific functions and induced effects at physiological concentrations [51], [116], [120]. The effects of H_2S are achieved through a highly dynamic repertoire of signalling modalities. These include persulfidation of cysteine residues, binding to metal centres, interaction with other gasotransmitters, and scavenging of reactive oxygen species, all of which result in H_2S reacting to form other chemical species [95], [110], [153]. Additionally, H_2S is sensitive to redox and pH conditions, is labile, and many H_2S derivatives have a relatively short half-life [278]. Generally, these derivatives can be regarded as three distinct sulfide pools: free sulfides such as H_2S gas, acid-labile sulfides such as H_2S molecules coordinated to metal centres, and bound sulfane sulfides such as those found in persulfidated cysteine groups. The reactivity of sulfur atoms in these pools are distinct, and methods that measure H_2S levels will often use experimental conditions that are unable to detect sulfide levels from all three pools [281], [282]. Combined, these properties make it extremely challenging to accurately measure H_2S levels in biological samples.

This difficulty in measuring H_2S has become a crucial limitation in clarifying the role of H_2S in biological systems. To address this, in **Chapter 4** I optimised the sample preparation and mass spectrometry analysis of a novel H_2S sensing molecular probe, called MitoA. This probe molecule was designed by Prof. Richard Hartley (University of Glasgow, UK) and allows for specific and sensitive measurements of *in vivo* mitochondrial H_2S levels across tissues [269]. My work in this thesis helped improve the analytical methodology for use of this probe in the analysis of mouse liver tissue. This was achieved by improving the sample preparation method to exclude the confounding signals from phospholipid contamination and altering the mass spectrometry parameters. The methodology I developed was then applied to a transgenic mouse model of thiosulfate sulfurtransferase (TST) knock-out ($TST^{-/-}$) [232]. The expression of TST in adipocytes is correlated with lower fat mass and lower fasted blood glucose

levels [232]. It has also been shown *via* the monobromobimane method for H_2S detection that whole blood H_2S levels were greatly elevated in $TST^{-/-}$ mice compared to WT controls, however multiple other methodologies for H_2S detection have found conflicting evidence for elevated H_2S levels in liver tissue from $TST^{-/-}$ mice [232]. I applied the MitoA and lead acetate methods to provide further insight into the metabolism of H_2S in this mouse model. The results indicated a distinct regulation of mitochondrial H_2S levels compared to cytosolic H_2S production, with H_2S levels elevated in $TST^{-/-}$ mice within the cytosolic compartment but unchanged relative to WT control mice within the mitochondrial compartment. I additionally attempted to develop an imaging mass spectrometry method using MitoA. While a working method for the detection of MitoA standards on liver tissue sections was achieved, the concentration of MitoA injected into the mice was below the limit of detection of the mass spectrometer. The determination of the correct MitoA injection concentration could not be established as I did not have the required animal experiment licencing. The investigation into mitochondrial H_2S levels in TST KO mice has been published in Cell Reports ([312]) and is presented in full in **Appendix III**.

A shift has occurred over the past few decades as we have begun to reconsider the principles of ageing. While previously ageing has been considered as a distinct and incontrovertible aspect of life, we now think of ageing as a plastic process and as the umbrella term for the many diseases associated with old age such as cardiovascular disease, dementia, frailty, and cancers [34], [157], [433]. A key distinction made by this new definition of ageing is the principle that there are common underlying mechanisms that drive the onset and progression of all diseases of ageing. There have been attempts to define and categorise these underlying mechanisms of ageing, most prominently in the publishing of the ‘hallmarks of ageing’; genomic instability, telomere attrition, epigenetic alterations, loss of proteostasis, deregulated nutrient-sensing, mitochondrial dysfunction, cellular senescence, stem cell exhaustion, and altered intercellular communication [125]. It has become clear that both lifespan and healthspan of organisms can be increased by genetic, pharmacological, and environmental interventions [226], [331]. Examples of this include dietary restriction protocols, rapamycin treatment, and genetic

modification of conserved signalling pathways, most notably those pathways involving nutrient sensing.

H_2S has emerged as a molecule that that is capable of ameliorating the ageing process [66]. For instance, elevated H_2S levels are a requisite for the beneficial effects of dietary restriction (DR) and longevity is associated with elevated H_2S levels across long-lived mutant mice [166], [226], [434]. These observations have garnered interest in the role of H_2S in ageing but several pressing questions remain to be answered. Is there an exploitable overlap in the therapeutic and toxicity windows of exogenous H_2S to allow development of H_2S-boosting drugs? What are the precise molecular targets of H_2S that confer its longevity promoting effects, and can these be targeted without altering endogenous H_2S levels? In which tissues is elevated H_2S protective against ageing and in which does it become deleterious? Future research that addresses these fundamental questions will help expand our understanding of this powerful gaseous signalling molecule and perhaps bring new insight into the molecular processes that control ageing.

Dietary restriction (DR) is the most well-established intervention to promote longevity and enhance healthspan [239], [240], [275], with the beneficial effects of DR highly conserved across wide evolutionary distances [239], [240], [275]. Despite this, some studies have reported non-significant or even detrimental effects of DR on lifespan. An example of this is the ILSXISS panel of recombinant inbred mouse strains, of which only a minority displayed lifespan extension under DR [223], [224]. Additionally, while DR is a useful tool in animal models, it is unrealistic for therapeutic use in humans due to poor adherence and negative side-effects associated with long-term DR [435], [436]. Given these issues, a greater understanding of DR is required to explain the diversity of responses across ILSXISS strains, and to potentially allow for the development of DR mimicking treatments that confer lifespan and healthspan benefits without the negative consequences of DR. H_2S has emerged as a putative effector of DR and hepatic H_2S levels are elevated in C57Bl/6N and DBA/2 mice under DR [226]. However, the association between H_2S and DR has not been explored in other mouse strains. In **Chapter 3** I examined hepatic H_2S levels in female mice from three strains from the ILSXISS mouse panel: TejJ89 (which has extended lifespan

under DR), TejJ48 (which shows no effect of DR on lifespan), and TejJ114 (which has shortened lifespan under DR). I found that elevated hepatic H_2S production capacity was associated with DR only in TejJ89 mice. This finding provides additional evidence that elevated H_2S on DR is associated with longevity on DR. Additionally, this is one of very few studies to monitor H_2S production in female mice, with the majority using only male mice in their experiments. Finally, elevation of hepatic H_2S in TejJ89 mice was associated with elevated 3-mercaptopyruvate sulfurtransferase (MPST) protein levels, in contrast to most reports that find that cystathionine-γ-lyase (CSE) protein levels are what drives elevated H_2S production, which I was able to replicate in C57BL/6J mice. My findings underline the importance of employing a diversity of mouse strains when researching the molecular response to DR, as the current approach in ageing of primarily using C57BL/6J mice might obscure subtle differences in molecular processes driving DR-induced phenotypic changes for example. This work was published in Geroscience (Official Journal of the American Aging Association, [254]) in March 2020 and is presented in full in **Appendix II**.

A major limitation of this study is that the experimental design is correlational in nature, with no mechanistic explanation for the observed results. Treatment of AL and DR-fed ILSXISS mice with H_2S-donating compounds *via* injection or diet would allow determination of the causative role of H_2S in DR. Additionally, the results underline the importance of strain, phenotype, and sex differences. As such, repeating these experiments in more diverse mouse strains, such as additional ILSXISS sub-strains or male ILSXISS mice would further elucidate the diversity of responses to DR in terms of H_2S production and perhaps better frame this research in the context of human genetic diversity. This study also employed a single DR protocol (1-month 40% DR) however repeating this study using different lengths and severity of DR would help establish the exact reduction in dietary intake required to modify H_2S production in ILSXISS mice. There is also a wide variety of DR protocols beyond simple reduction in daily food intake such as amino acid restriction, methionine restriction, intermittent fasting, and time-restricted dieting. Replicating this study under these alternative DR protocols would assist in identifying the precise dietary intervention(s) that modulate H_2S production.

Progeroid syndromes are a group of rare conditions with diseases that phenotypically resemble accelerated ageing [313], [315], [318]. The most common progeroid disease is Hutchinson-Gilford progeria syndrome (HGPS) which is characterised by multi-organ accelerated ageing [334]. Treatments are critically lacking as most patients die at <15 years of age due to cardiovascular pathologies such as myocardial infarction and stroke [334]. Treatment of HGPS is a major unmet need, however some interventions are known to ameliorate some aspects of the HGPS phenotype including rapamycin, vitamin D, and sulforaphane [251], [343], [350]. Interestingly, H_2S is known to signal through the same molecular pathways as these treatments, and treatment of fibroblasts from another progeroid disease (Werner's syndrome) with exogenous H_2S was found to be protective against the protein aggregation and oxidative stress associated with the disease [251]. Despite this, no studies have directly measured H_2S levels or applied H_2S-based treatments in HGPS patients or mouse models of HGPS.

To address this lack of understanding, in **Chapter 5** I performed a preliminary study using the HGPS mouse model known as G609G. This model replicates the genetic mutation present in most human HGPS patients and results in dramatically reduced lifespan in mice [353]. G609G mice on high-fat diet (HFD) have an average lifespan twice that of G609G mice maintained on regular chow (RC) [229]. As such both diets were investigated to determine if H_2S production was reduced in G609G mice and whether diet, which is known to affect lifespan in this model, similarly impacted on H_2S production. I found a significant reduction in H_2S production capacity in G609G mice on RC compared to WT controls but no significant difference between G609G fed HFD and WT control mice as predicted. There was an elevation in protein levels of CSE in HFD fed G609G mice compared to RC fed G609G mice which might explain the difference in H_2S production capacity between these groups. These data provide preliminary evidence that hepatic H_2S production is significantly reduced in a progeroid mouse model and modulated by diet. This work is the first to examine the production of H_2S in the context of HGPS and expands our understanding of the association between H_2S and ageing.

The major limitation of this study was the number of biological replicates per group. Maintenance of mouse models of progeria syndromes such as G609G mice is extremely challenging. These mice exhibit early onset of severe multi-organ pathologies which requires attentive animal husbandry, and many mice are culled for animal welfare considerations before experimental endpoints are reached [353]. Only heterozygous G609G mice are fertile which requires larger breeding programs to generate the required number of experimental mice. As such, maintaining colonies with many G609G mice is prohibitive. Therefore, only a limited number of samples could be provided by collaborators at St. Louis University (MO, US) to support a preliminary investigation. Repeating these experiments with more mice per group, including a WT group on HFD would allow for two-way ANOVA analysis of results and enable identification of diet effects, genotype effects, and DietxGenotype interactions.

RNA polymerase III (Pol III) is one of three RNA polymerases that transcribe the cellular transcriptional machinery [416]. Pol III transcribes many non-protein coding sequences in genomic DNA including 5S ribosomal RNA (rRNA), all transfer RNAs (tRNAs), 7SL RNA, and U6 spliceosomal RNA [416]. Pol III activity is controlled by mammalian target of rapamycin (mTOR) signalling through the protein MAF1 [382], [385]. Studies in flies and worms have shown that knock down of Pol III activity extends lifespan. Longevity in a mouse model of Pol III knock down *via* heterozygous knock out of a major Pol III sub-unit called Polr3b-Polr3b Het KO mice is currently being determined in the Selman lab [405]. As the Polr3b Het KO mice are a putative long-lived mouse model (significant conservation exists across wide evolutionary distances in genetic pathways that modulate lifespan) and as H_2S production positively correlates with lifespan in long-lived mouse mutants, I investigated regulation of hepatic H_2S in these mice in **Chapter 6**. I found that while no difference was observed in H_2S production between female WT and Polr3b Het KO mice, in male mice H_2S production was elevated in Polr3b Het KO mice relative to WT controls. Dietary restriction (DR) is known to elevate hepatic H_2S levels but its effect on mTOR/Maf1/Pol III are unclear. I have previously shown that the effect of DR on H_2S production is strain-specific and it is unknown how DR affects H_2S production in C57BL/6N mice, the strain that the Polr3b Het KO mice are maintained on. Consequently, I placed male WT and Polr3b Het KO mice on 1-month 40% DR to examine if DR

increased H_2S production in this strain and whether the observed elevation in H_2S production in Polr3b Het KO mice was modulated by DR. I found that there was an additive effect of these interventions on hepatic cytosolic H_2S production which suggests that DR and reduced Pol III act in distinct pathways to increase hepatic H_2S production. The MitoA probe, described above and in **Chapter 4**, was also employed to measure mitochondrial H_2S production *in vivo*. This approach revealed that while cytosolic H_2S production was elevated by DR in both WT and Polr3b Het KO mice, mitochondrial H_2S production was reduced by DR. By contrast, Polr3b Het KO resulted in elevation of H_2S levels in both the cytosolic and mitochondrial compartments. These findings indicate that there is an uncoupling of H_2S metabolism between the cytosolic and mitochondrial compartments under DR and is the first study to report a reduction in mitochondrial H_2S under DR. However, no clear explanation for the differences in H_2S metabolism in these subcellular compartments could be established by quantification of protein and mRNA abundance of H_2S-producing or disposal enzymes.

The data presented here provide insight into the mechanisms that drive elevation of H_2S by DR and greater appreciation of the distinct response of subcellular compartments to DR. The observation that Polr3b Het KO alone is capable of elevating hepatic H_2S production capacity in male mice may be suggestive that this model may well be long-lived as has been described in other long-lived mice including Ames and Snell dwarfs and insulin receptor substrate 1 null mice [170]. However, this will not obviously be confirmed until completion of the lifespan study in these mice probably by late 2022. Repeating the DR study in female mice would further clarify the role of DR and Pol III in metabolism of H_2S and further highlight any sexual dimorphism. Cytosolic and mitochondrial H_2S levels were also found to have divergent responses to DR in Porl3b Het KO mice, with cytosolic production increasing and mitochondrial levels decreasing. No clear explanation for the differences in H_2S metabolism in these subcellular compartments could be established by quantification of protein and mRNA abundance of H_2S-producing enzymes. Mechanistic studies in fibroblasts from WT and Polr3b Het KO mice would help clarify the observed difference in H_2S production. Knockdown, inhibition, or deletion of each of the three H_2S producing enzymes and measuring H_2S production in cell culture would

directly interrogate the contribution of these enzymes to H_2S anabolism. Similarly, modifying the mitochondrial localisation sequence of *Mpst* to negate its ability to localise to mitochondria would help confirm if MPST activity drives the response in mitochondrial H_2S levels to DR and Polr3b Het KO.

7.1 Closing Remarks

It is also important to describe the extraneous circumstances that impacted on some of the original aims that initially comprised this thesis. Chief among these was the COVID-19 pandemic which has been present for 20 out of the 48 months of my PhD. Access to laboratory and animal housing facilities was suspended from March 2020 until July 2020, preventing any practical work. After July 2020 some restrictions remained in place which impacted on facilities available and training opportunities, although these have eased partially since Jan 2021. The restrictions on international travel impacted on two projects in my PhD. I had intended to visit collaborators at the Karolinska Institute (Stockholm, Sweden) for 5 months in summer 2020 to investigate the effect of RNA polymerase III knock down in mice on mitonuclear communication. I had visited the collaborators prior to this for 5 weeks in summer 2019 to learn the techniques involved and generate preliminary data. The work would have examined cytosolic and mitochondrial protein synthesis rates, ribosome and mitoribosome assembly, and imaging of mitochondria to examine mitochondrial fission and fusion. I was also scheduled to visit collaborators at St. Louis University (MO, US) to complete complementary experiments in the G609G mouse model of HGPS. With access to live G609G mice I planned to examine the administration of H_2S donor compounds and the MitoA probe to observe the effect on mouse frailty, mitochondrial respiration, and mitochondrial H_2S levels. Separate from COVID-19, I had planned to maintain a progeria mouse model cohort at the University of Glasgow (Scotland, UK). There mice were to be an alternative HGPS model with knock-out of the protein ZMPSTE24 which results in progerin protein accumulation. CRISPR gene editing of these mice to knock out the H_2S-disposal enzyme thiosulfate sulfurtransferase (TST) protein was hypothesised to result in an elevation of endogenous H_2S levels. This model would have allowed me to investigate the effect of elevated endogenous H_2S production in the context of accelerated ageing *in vivo*. Monitoring the physiology, metabolism, and frailty of these mice would reveal if elevated H_2S production ameliorated age-related pathologies. Unfortunately, the gene editing required to generate these mice was unsuccessful over 3 attempts and ultimately abandoned.

Despite these issues, the results of this thesis have furthered our knowledge of the role for H_2S in mouse longevity by studying both long-lived (DR), putatively long-lived (Polr3b Het KO) and short-lived (G609G) mouse models. The primary findings from this work highlight that genotype, sex and diet all influence H_2S metabolism in mice (**Figure 45**), but that in general H_2S production correlated with lifespan as predicted. This association helps with the growing understanding and appreciation that H_2S may play an important role in organismal lifespan. I believe that further research into the beneficial effect of H_2S might help reveal potential interventions and specific molecular targets that may help improve survival and late-life health. Given the rapidly ageing populations across the world and the increasing burden on health care services of multimorbidity in old age, development of such novel therapeutics are of extreme urgency.

	Lifespan Extension				Lifespan Shortening			
Mouse Model	TejJ89		Polr3b Het KO		TejJ114		G609G	
Diet	AL	DR	AL	DR	AL	DR	RC	HFD
Cytosolic H_2S	=	↑	↑	↑↑	=	↓	↓	=
Mitochondrial H_2S	NA	NA	↑	↓	NA	NA	NA	NA

Figure 45 Elevated H_2S is associated with longevity across mouse models and diets.

Summary of findings examining the relationship between H_2S and longevity across mouse models and diets. Two models of lifespan extension were used: the ILSXISS recombinant inbred mouse sub-strain TejJ89 which has a longer lifespan extension under dietary restriction (DR), and the putative long-lived mouse model Polr3b Het KO on *ad libitum* (AL) and DR diet. Two models of lifespan shortening were used: the ILSXISS recombinant inbred mouse sub-strain TejJ114 which is short-lived under DR, and the G609G mouse model of Hutchinson-Gilford Progeria Syndrome (HGPS) which is a disease of pathological accelerated ageing under regular chow (RC) and high fat diet (HFD). In all of these models, cytosolic hydrogen sulfide production, as measured by the lead acetate metho, is positively correlated with longevity. Mitochondrial H_2S production was also examined by the novel MitoA *in vivo* exomarker, which revealed that mitochondrial H_2S levels were positively correlated with Polr3b Het KO but negatively with DR in WT and Polr3b Het KO mice.

Appendix I: Physiological response and glucose homeostasis in Polr3b Het KO mice on 1-month 40% DR

The following experiments were performed as part of the study into the effect of heterozygous knock out of the RNA polymerase III (Pol III) sub-unit Polr3b (Polr3b Het KO) and 4-weeks 40% dietary restriction (DR) in mice (**Chapter 6**).

7.2 Polr3b Het KO mice have the same physiological response to DR as WT

I placed WT and Het mice under 4-weeks of 40% DR to examine if the expected disruption of translational machinery in Polr3b Het KO mice shared molecular mechanisms with the reduced protein synthesis of mice under DR conditions. No significant difference in body length was found when comparing diet ($F(1,28) = 0.415$, $p = 0.168$) or genotype ($F(1,28) = 0.204$, $p = 0.655$) (**Figure 46a).** Similarly, no significant difference was found in diet ($F(1,27) = 0.415$, $p = 0.525$) or genotype ($F(1,27) = 0.010$, $p = 0.921$) in terms of body temperature (**Figure 46b).**

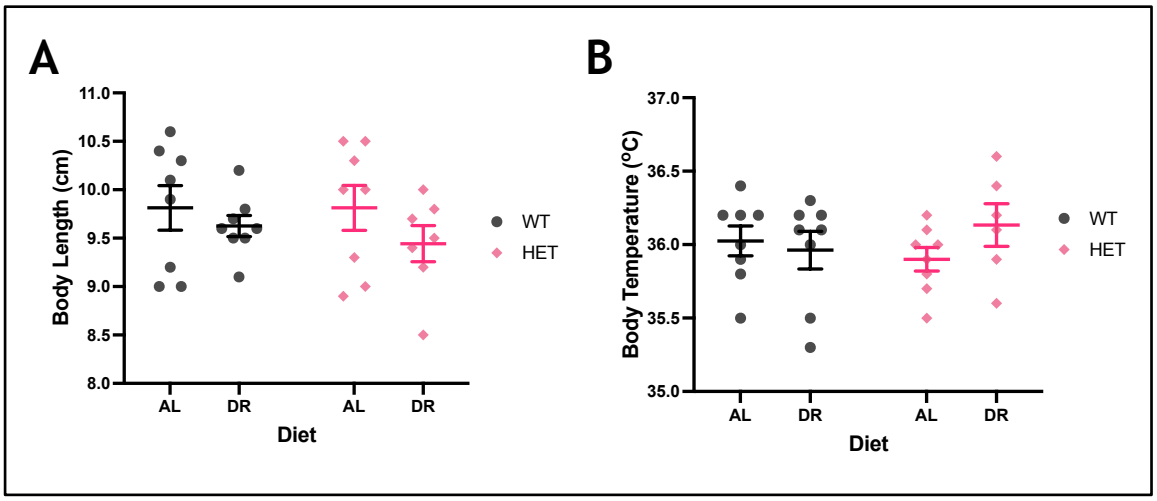

Figure 46 Changes in mouse size and thermoregulation under DR

A Mean body length as measured on scruffed animals from tip of snout to anus. **B** Mean body temperature as measured by infrared thermometer reading at gonadal region. Statistical significance determined by 2-way ANOVA with genotype and diet as factors and Tukey multiple comparisons with alpha = 0.05. Grubb's outlier test was performed with alpha = 0.05, no outliers removed. WT data in black, Het data in pink. Bars/lines/dots represent mean value and error bars represent standard error of the mean. AL: *ad libitum*, DR: Dietary restriction. * = $p < 0.05$, *** = $p < 0.001$, **** = $p < 0.0001$. D*** = two-way ANOVA main effect $p < 0.001$.

7.3 Glucose homeostasis of Polr3b Het KO mice under DR is comparable to WT controls

Fasted blood glucose was measured at cull from fresh blood samples (**Figure 47a**). Two-way ANOVA analysis determined a significant diet effect ($F(1,28) = 4.864$, $p = 0.036$), with mice on DR having reduced fasting blood glucose levels compared to AL mice. However, no genotype effect was observed ($F(1, 28) = 3.048$, $p = 0.092$). Plasma insulin levels were quantified by ELISA (**Figure 47b**). Both diet ($F(1,18) = 4.860$, $p = 0.041$) and genotype ($F(1,18) = 6.482$, $p = 0.020$) effects were detected, however these were not additive. DR reduced plasma insulin levels compared to AL and Polr3b Het KO mice had elevated fasted plasma insulin levels compared to WT mice, regardless of diet. There was a significant diet effect ($F(1,19) = 5.345$, $p = 0.032$) on insulin resistance as estimated using the homeostatic model assessment insulin resistance (HOMA-IR) method. DR fed mice had a lower average HOMA-IR levels compared to AL fed mice (**Figure 47c**). No significant genotype effect ($F(1,19) = 0.012$, $p = 0.916$) was found for this measure of insulin resistance. Western blotting of hepatic samples found no significant diet ($F(1,12) = 12.000$, $p = 0.9118$) or genotype ($F(1,12) = 0.084$, $p = 0.778$) effect on insulin receptor phosphorylation (**Figure 47d**). However, a significant genotype x diet interaction ($F(1,12) = 4.929$, $p = 0.0464$) was found for this analysis, where DR reduced insulin receptor phosphorylation in WT mice but elevated it in Het mice. Glucose homeostasis was also measured by glucose tolerance test 1 week prior to culling, with area under the curve calculated for quantification (**Figure 47e,f**). A highly significant diet effect was found ($F(1,28) = 35.750$, $p < 0.0001$) with glucose tolerance greatly improved under DR diet. No genotype effect was found ($F(1,28) = 0.595$, $p = 0.447$) in glucose tolerance.

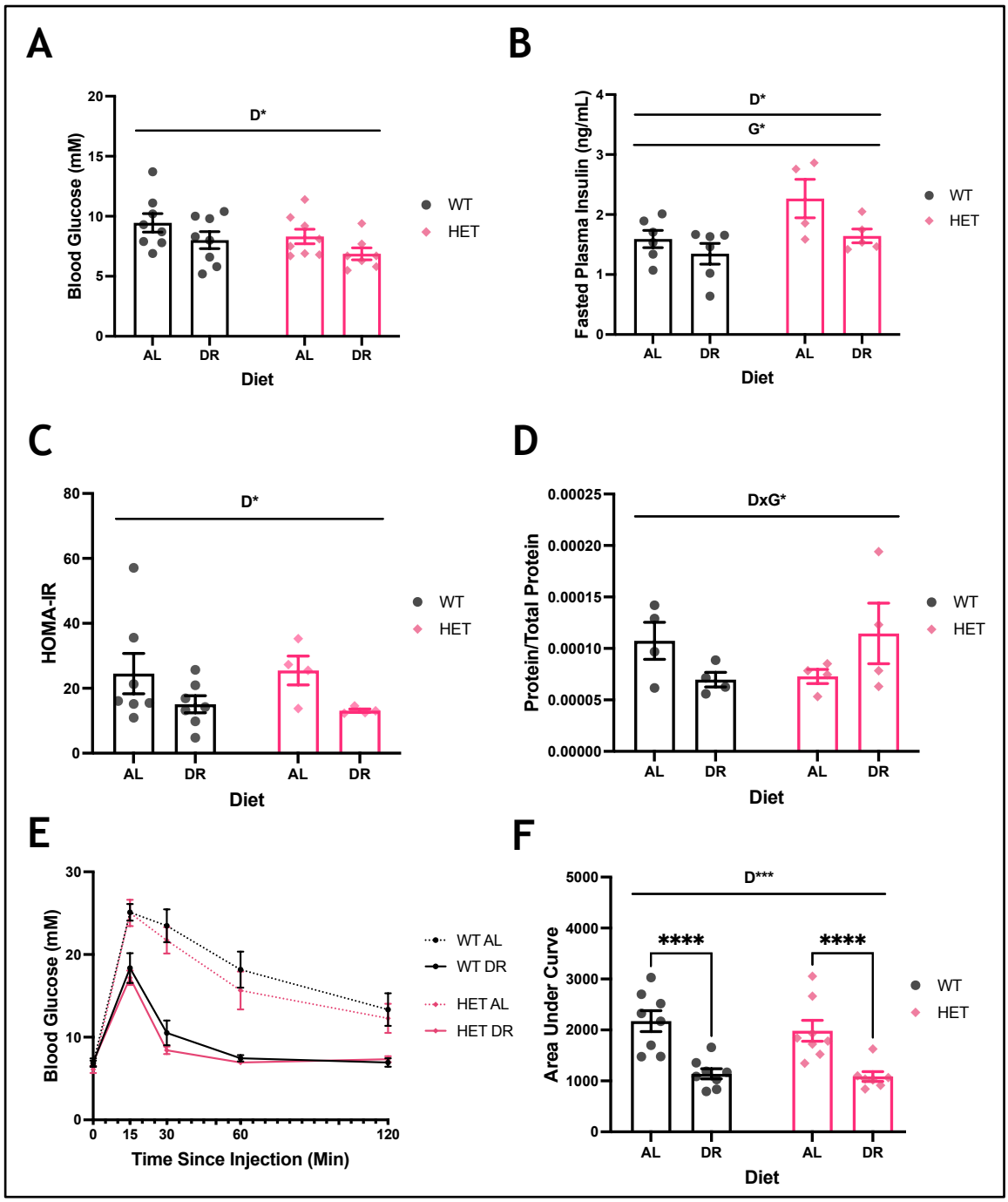

Figure 47 Glucose homeostasis in Polr3b Het KO mice under DR

A Fasted blood glucose levels from whole blood samples taken at cull. **B** Fasted blood insulin levels quantified by ELISA analysis of plasma extracted from whole blood. **C** Homeostatic model assessment (HOMA) of insulin resistance (IR) calculated from blood glucose and insulin levels. **D** Protein levels of phosphorylated insulin receptor as measured by western blot and normalised to total protein loading. **E** Mean blood glucose readings from glucose tolerance test (GTT). Blood glucose measured from tail vein samples taken at 15, 30, 60, and 120 minutes following bolus intraperitoneal injection of glucose. Dashed lines represent AL fed mice, solid lines represent DR fed mice. **F** Average area under the curve (AUC) calculated from GTT traces. Statistical significance determined by 2-way ANOVA with genotype and diet as factors and Tukey multiple comparisons with alpha = 0.05. Grubb's outlier test was performed with alpha = 0.05, no outliers removed. WT data in black, Het data in pink. Bars/dots represent mean value and error bars represent standard error of the mean. AL: *ad libitum*, DR: Dietary restriction. **** = $p < 0.0001$. D* = two-way ANOVA diet main effect $p < 0.05$, G* = two-way ANOVA genotype main effect $p < 0.05$, D*** = two-way ANOVA diet main effect $p < 0.001$, DxG* = two-way ANOVA DietxGenotype interaction effect $p < 0.05$.

7.4 Polr3b Het KO in mice does not recapitulate physiological or glucose homeostasis benefits of DR

Dietary restriction (DR) has a pronounced effect on mouse physiology and glucose homeostasis [437]. Some of these effects are mediated by reduced mammalian target of rapamycin (mTOR) signalling under DR diets, however, the precise effector of the DR/mTOR pathway remains unclear. RNA polymerase III (Pol III) is a critical mediator of cellular metabolism and controlled by mTOR signalling through the inhibitory action of Maf1 [378]. As Pol III lies downstream of mTOR signalling I hypothesised that heterozygous knock out of the second largest Pol III sub-unit Polr3b (Polr3b Het KO) would mimic the effects of DR on mouse physiology. To examine this, WT and Polr3b Het KO mice were separated into experimental groups and fed either *ad libitum* (AL) or 40% DR for 1 month. However, no significant difference was found between WT and Polr3b Het KO mice with respect to bodyweight, body length, food intake, or body temperature in AL fed mice. Further, Polr3b Het KO mice on DR were indistinguishable from WT mice on DR, and no additive effect of DR and Pol III knock-down were found for these metrics. Together, these data indicate that Polr3b Het KO did not mimic the effects of DR with regards to whole-animal physiology nor did it augment the effects of DR. Unexpectedly, phosphorylation of the mTOR signalling protein ribosomal S6 (pS6) was not found to be affected by diet or genotype in hepatic tissue lysates. This lack of elevated pS6 level on DR indicates that DR does not signal through mTORC1 in male WT C57BL/6N mice, and this is unaffected by Polr3b Het KO. Additionally, H_2S production capacity was found to be elevated under DR in both WT and Polr3b Het mice. As H_2S is capable of inhibiting mTOR and promoting autophagy [183], [184], [185], this may account for the lack of pS6 observed here and the elevation of *Ulk1* gene expression in DR groups compared to AL groups. These data could indicate strain-specificity in the physiological response of C57BL/6J mice (which are used in the majority of studies on DR in mice), and C57BL/6N (which is the background strain of the Polr3b Het KO mice). Irrespective, it appears that DR in WR and Polr3b Het KO mice does not alter mTOR signalling.

I also examined glucose homeostasis in Polr3b Het KO mice under DR. DR is known to reduce fasted blood glucose levels and improve insulin sensitivity across mouse strains [227], [259], [438]. There was no improvement in Polr3b

Het KO mice on AL when compared to WT AL mice with respect to fasted blood glucose levels or glucose tolerance. Polr3b Het KO mice were found to have higher fasted plasma insulin levels, but this did not result in higher insulin resistance in the Het mice as calculated by HOMA. Additionally, Polr3b Het KO mice on DR did not exhibit any additive beneficial effect of DR and Polr3b Het KO on measures of glucose homeostasis. Both WT and Het mice under DR displayed the expected beneficial effects of DR, with fasted blood glucose, fasted blood insulin, insulin resistance, and glucose intolerance all improved compared to their respective AL-fed control. Together, these data once again indicate that Polr3b Het KO does not act as a DR mimetic for improved glucose homeostasis. Future studies could examine other aspects of physiology such as lean body mass, energy expenditure, or motor function. Additionally, given that both DR and Pol III exhibit control over cellular metabolism, it would be useful to measure autophagy and protein synthesis rates in these mice.

Appendix II: Published first-author paper of data from Chapter 3

GeroScience (2020) 42:801–812
https://doi.org/10.1007/s11357-020-00168-2

ORIGINAL ARTICLE

Strain-specificity in the hydrogen sulphide signalling network following dietary restriction in recombinant inbred mice

Stephen E. Wilkie · Lorna Mulvey · William A. Sands · Diana E. Marcu · Roderick N. Carter · Nicholas M. Morton · Christopher Hine · James R. Mitchell · Colin Selman

Received: 4 October 2019 / Accepted: 11 February 2020 / Published online: 11 March 2020

Abstract Modulation of the ageing process by dietary restriction (DR) across multiple taxa is well established. While the exact mechanism through which DR acts remains elusive, the gasotransmitter hydrogen sulphide (H_2S) may play an important role. We employed a comparative-type approach using females from three ILSXISS recombinant inbred mouse strains previously reported to show differential lifespan responses following 40% DR. Following long-term (10 months) 40% DR, strain TejJ89—reported to show lifespan extension under DR—exhibited elevated hepatic H_2S production relative to its strain-specific ad libitum (AL) control. Strain TejJ48 (no reported lifespan effect following 40% DR) exhibited significantly reduced hepatic H_2S production, while H_2S production was unaffected by DR in strain TejJ114 (shortened lifespan reported following 40% DR). These differences in H_2S production were reflected in highly divergent gene and protein expression profiles of the major H_2S production and disposal enzymes across strains. Increased hepatic H_2S production in TejJ89 mice was associated with elevation of the mitochondrial H_2S-producing enzyme 3-mercaptopyruvate sulfurtransferase (MPST). Our findings further support the potential role of H_2S in DR-induced longevity and indicate the presence of genotypic-specificity in the production and disposal of hepatic H_2S in response to 40% DR in mice.

Keywords Caloric restriction · Ageing · ILSXISS · Longevity · Sulphide · Dietary restriction · 3-mercaptopyruvate sulfurtransferase

Electronic supplementary material The online version of this article (https://doi.org/10.1007/s11357-020-00168-2) contains supplementary material, which is available to authorized users.

S. E. Wilkie · L. Mulvey · W. A. Sands · D. E. Marcu · C. Selman (✉)
Glasgow Ageing Research Network (GARNER), Institute of Biodiversity, Animal Health and Comparative Medicine, College of Medical, Veterinary and Life Sciences, University of Glasgow, Glasgow G12 8QQ, UK
e-mail: Colin.Selman@glasgow.ac.uk

R. N. Carter · N. M. Morton
Molecular Metabolism Group, University/BHF Centre for Cardiovascular Sciences, Queens Medical Research Institute, University of Edinburgh, Edinburgh EH16 4TJ, UK

C. Hine
Department of Cardiovascular and Metabolic Sciences, Cleveland Clinic Lerner Research Institute, Cleveland, OH 44195, USA

J. R. Mitchell
Department of Genetics and Complex Diseases, Harvard T.H. Chan School of Public Health, Boston, MA 02115, USA

Introduction

Empirical evidence has existed for over a century that dietary restriction (DR) increases lifespan and healthspan across multiple species (Fontana and Partridge 2015; Picca et al. 2017; Weindruch and Walford 1988). In mice, significant strain-specific differences in lifespan exist (Turturro et al. 1999; Yuan et al. 2009) and genetic background may consequently play an important but under-appreciated role in how particular strains respond to DR (Hempenstall et al.

2010; Ingram and de Cabo 2017; Mitchell et al. 2016; Mulvey et al. 2014; Selman and Swindell 2018; Swindell 2012). For example, two independent studies have reported that recombinant inbred ILSXISS mice show significant strain-specificity in longevity following 40% DR (Liao et al. 2010; Rikke et al. 2010), and phenotypic parameters linked to the ageing process, such as in mitochondrial function and adiposity, have been shown to differ between ILSXISS strains under 40% DR (Liao et al. 2011; Mulvey et al. 2016).

Precisely how DR facilitates its beneficial effects on lifespan and healthspan has proved challenging to elucidate, although many mechanisms have been proposed (Fontana and Partridge 2015; Hine and Mitchell 2015; Kennedy et al. 2007; Mair and Dillin 2008; Masoro 2005). One such putative mechanism is the gasotransmitter hydrogen sulphide (H_2S). Direct manipulation of H_2S levels through genetic, pharmacological or environmental means can modulate lifespan in invertebrate models (Hine and Mitchell 2015; Miller and Roth 2007; Qabazard et al. 2013; Shaposhnikov et al. 2018; Wei and Kenyon 2016) and elevated hepatic H_2S production appears to be a conserved phenotype in long-lived mouse models, including DR and various genetic mutants (Hine et al. 2017; Mitchell et al. 2016). Pharmacological elevation of H_2S has also been shown to ameliorate age-associated atherosclerosis, fibrosis, cognitive decline and kidney dysfunction in rodents (Das et al. 2018; Lee et al. 2018; Zhan et al. 2018), and partially rescued a progeroid phenotype in Werner syndrome fibroblasts (Talaei et al. 2013) and senescence in endothelial cells (Latorre et al. 2018). Furthermore, DR-induced protection from ischemia-reperfusion injury was abrogated in mice treated with an inhibitor of cystathionase-γ-lyase (CSE), the major hepatic H_2S-producing enzyme (Hine et al. 2015), and longevity in mice following methionine restriction was associated with increased H_2S production and a reduction in various senescence markers within the kidney (Wang et al. 2019). Consequently, it has been proposed that elevation of endogenous H_2S may play a prominent role in the lifespan and healthspan effects of DR (Hine and Mitchell 2015).

Here, we employed a comparative-type approach (Mulvey et al. 2016) in which we determined hepatic and kidney H_2S production, and hepatic transcript and protein levels of key enzymes involved in H_2S metabolism in female mice from three genetically distinct recombinant inbred ILSXISS strains exposed to long-term (10 months) 40% DR. These strains have previously been reported to show variable lifespan responses to 40% DR ranging from life extension to life shortening relative to strain-specific ad libitum controls (Liao et al. 2010; Rikke et al. 2010).

Methods

Animals

The ILSXISS strains TejJ89, TejJ48 and TejJ114 were purchased from the Jackson Laboratory (Bar Harbour, Maine, URL: http://www.informatics.jax.org) as breeding pairs and experimental cohorts subsequently bred at The University of Glasgow. As previously discussed (Mulvey et al. 2016), female mice from strains TejJ89, TejJ48 and TejJ114 showed repeatable directional effects (TejJ89 lifespan extension under dietary restriction (DR), TejJ48 lifespan unaffected under DR, TejJ114 lifespan shortening under DR) on lifespan following 40% DR across 2 independent studies, but that no strain-specific differences in lifespan were reported when these mice were maintained on an ad libitum (AL) diet (Liao et al. 2010; Rikke et al. 2010). It should be noted that several potential shortcomings to the experimental design of these original studies have been raised (Selman and Swindell 2018), not least that 40% DR may simply be sub-optimal in TejJ48 and TejJ114, and that lifespan extension in these strains is likely to be seen at a higher or lower level of DR; these dose-response experiments are still to be undertaken (Selman and Swindell 2018). However, for the purposes of this study, we were interested in whether there was a relationship between H_2S production and reported lifespan following 40% DR. Female mice were used for all experiments because lifespan was only determined in female mice across both original studies (Liao et al. 2010; Rikke et al. 2010). In addition, we also examined components of the H_2S signalling network in female C57BL/6J mice that followed a similar long-term 40% DR protocol, to further examine potential strain-specific effects. It has previously been shown that hepatic H_2S production is increased female C57BL/6J mice under 40% DR (Mitchell et al. 2016).

All mice were maintained from weaning onwards at 22 ± 2 °C and on a 12L/12D cycle (lights on 0700–1900 h) in groups of 4 mice within shoebox cages (48 cm × 15 cm × 13 cm), with AL access to water

and standard chow (CRM(P), Research Diets Services, LBS Biotech, UK; Atwater Fuel Energy-protein 22%, carbohydrate 69%, fat 9%). 10% DR was introduced in a graded fashion from 10 weeks of age and then held at 40% DR from 12 weeks onwards, with the food intake of the DR cohorts adjusted each week relative to the average weekly AL food intake of the appropriate age-matched and strain-specific AL controls (Hempenstall et al. 2010; Mulvey et al. 2016). Following 10 months of 40% DR (13 months of age) female mice were fasted overnight and culled using cervical dislocation under a UK Home Office Project Licence (60/4504) and following the "principles of laboratory animal care" (NIH Publication No. 86-23, revised 1985). Tissues were immediately dissected out, snap-frozen in liquid nitrogen and stored at − 80 °C until use.

Hydrogen sulphide (H_2S) production

Measurement of H_2S production was performed in liver and kidney homogenates according to a previously described protocol (Hine and Mitchell 2017). Briefly, 100 mg of flash-frozen liver and kidney were lysed in passive lysis buffer. Protein concentration was determined by BCA assay (G Biosciences, MO, USA) and 100 μg of protein lysate was loaded into 96-well plate. A 150-μL reaction solution containing 10 mM L-cysteine and 1 mM pyridoxal-5′-phosphate was added to the protein lysate. Filter paper that had previously been cut to the size of the plate, soaked in 20 mM lead(II)acetate trihydrate for 20 min, then dried under vacuum, was then securely attached to the plate. The assembled plate was incubated at 37 °C for 1 h. H_2S sulphide gas produced during this time collects in the head space between the top of the solution in the well and the lead(II)acetate paper, forming a brown-black substrate on the paper. The amount of H_2S present in each sample was subsequently quantified by densitometry analysis (ImageJ) of the brown-black substrate.

RNA extraction

RNA was isolated from liver tissue by addition of 500 μL of TRIzol (Life Technologies, USA) and subsequently homogenised using a glass-glass homogeniser. Samples were transferred to screw top Eppendorf tubes and 150 μL of chloroform added. Samples were then spun by centrifuge at 8000*g* and the supernatant containing the RNA isolate was taken to a fresh Eppendorf. RNA cleanup was performed according to instructions provided in RNAeasy Mini Kit (Qiagen, Germany), including the optional DNase digestion step.

Reverse transcriptase quantitative-PCR

First strand synthesis of cDNA was performed by incubating 2 μg of RNA (quantified by spectrophotometry using Nanodrop 1000 UV-Vis spectrophotometer, ThermoScientific, MA, US) with 1 μg Random Primer Mix (Invitrogen) in a total volume of 15 μL with RNAse-free water at 70 °C for 5 min using a MJ research PTC-200 Peltier Thermal Cycler (Biorad, CA, US). Synthesis of cDNA was then performed by adding 10 μL of master mix (1 μL Promega M-MLV reverse transcriptase, 2μL Promega M-MLV 5x buffer, 5 μL pooled 10 mM dNTPs, 0.625 μL RNAseOUT 40 units/μL and 1.375 μL nuclease free water) to the first stand sample and heating to 37 °C for 1 h. Samples were then diluted 1:1 with PCR-grade water and used directly for RT-qPCR. RT-qPCR was performed in a 384-well PCR plate. Each well contained 1 μl of cDNA, 0.25 μL 10 mM upper primer, 0.25 μL 10 mM lower primer, 3.5 μL of PCR-grade water and 5 μL of QuantiFast SYBR green PCR 2x master mix (Qiagen, UK). PCR reaction was performed using a 7900HT Fast Real-Time PCR System (Applied Biosystems, CA, US). PCR profile was as follows: 95 °C for 5 min; 94 °C for 30 s, 60 °C for 30 s, 72 °C for 30 s for 40 cycles; 72 °C for 5 min. The endogenous control gene was β2M, which has been previously shown to be an appropriate housekeeping control gene for mouse dietary restriction studies (Gong et al. 2016). Gene expression was calculated by subtracting the Ct value for β2M from the Ct value pertaining to the gene of interest in each sample. As such, a lower ΔCt indicates a higher relative gene expression of mRNA transcripts and vice versa. Primer sequences are provided in Table S1.

Western blotting

Protein lysate was obtained by homogenisation of liver tissue in 1 mL of ice cold RIPA buffer (Radio Immunoprecipitation Assay Buffer; 150 mM sodium chloride, 1% NP-40 or Triton X-100, 0.5% sodium deoxycholate, 0.1% sodium dodecyl sulphate,

50 mM Tris, pH 8) containing protease and phosphatase inhibitors (Halt™ Protease and Phosphatase Inhibitor Cocktail, Thermo Fisher Scientific, UK; phenylmethylsulfonyl fluoride, Sigma Life Sciences, Germany; Complete Mini EDTA-free protease inhibitor cocktail, Merck, NJ, US) using a glass-glass homogeniser. Homogenates were kept on ice for 40 min and then spun by centrifuge at 8000*g* for 10 min at 4 °C. The supernatant was collected and used as protein lysate. Protein concentration was assessed by BCA assay (G Biosciences, MO, USA) and 20 μg of protein was loaded per well into homemade 4–12% bis-tris polyacrylamide gels. Precision Plus Protein™ Dual Xtra Standards protein marker (BioRad, CA, US) were added to a well on each gel. Proteins were separated by electrophoresis at 90 V for 90 min and then transferred onto nitrocellulose membrane at 0.25 V for 1 h. Membranes were stained with Ponceau-S (Sigma Life Sciences, Germany), briefly washed in deionised water and the resulting total protein stain was captured using a Chemidoc™ XRS System (BioRad, CA, US). The Ponceau-S stain was removed by using 1xTBST (Tris-Buffered Saline Tween[20]) and the membrane was blocked with 5% milk in 1xTBST for 40 min. The membrane was washed 5 times with 1xTBST for 5 min under constant shaking. Primary antibodies (AbCam, Cambridge, UK) were added to the membrane in 5% BSA in 1xTBST. CSE (ab151769) primary antibody was used at 1:1000 dilution; CBS (ab135626) and MPST (ab85377) were used at 1:100. Primary antibodies were allowed to incubate with the membrane overnight at 4 °C, under constant shaking. HRP-linked anti-rabbit antibody (#7074; Cell Signalling Technology, London, UK) was used at 1:2000 dilution in 5% BSA in 1xTBST as the secondary antibody for all blots. The secondary antibody was allowed to incubate with the membrane for 1 h, under constant shaking. The membrane was washed 5 times with 1xTBST for 5 min, under constant shaking before addition of all antibodies and before imaging. For imaging, membranes were coated with Clarity™ Western ECL substrate (BioRad, CA, US) reagent and left to react for approx. 3 min before an image was developed under chemiluminescent conditions using a ChemiDoc™XRS System. Protein signals were quantified using densitometry software (ImageStudio; LiCor, NE, US) and normalised to the total protein signal of their respective lane.

3-Mercaptopyruvate sulfurtransferase activity assay

3-Mercaptopyruvate sulfurtransferase (MPST) activity was determined in liver by measuring thiocyanate production capacity as described previously for thiosulfate sulfurtransferase (TST) rhodanese activity (Morton et al. 2016), except that sodium 3-mercaptopyruvate (3-MP) was used as a substrate instead of sodium thiosulfate. In a 96-well plate, 20 μg of protein lysate in RIPA was mixed with 10 μL 200 mM 3-MP (Santa-Cruz, UK) and taken to 90 μL with 500 mM potassium phosphate pH 5.5 buffer. Samples were incubated at 37 °C for 2 min before addition of 10 μL 500 mM potassium cyanide. A calibration curve of 50, 25, 10, 5, 2.5, 1, 0.5, 0.25 and 0.1 mM potassium thiocyanate solutions was also prepared and exposed to the same conditions as above, excluding the addition of potassium cyanide. The reaction was allowed to occur for 5 min at 37 °C before termination by addition of 11 μL of 38% formaldehyde to all wells. Thiocyanate production was visualised by addition of 125 μL $Fe(NO_3)_3$/26% HNO_3 where an orange-brown solution formed. Results were quantified by measuring absorbance for 460 nm light in a spectrophotometer (Multiscan GO Microplate Spectrophotometer, Thermo Scientific, MA, USA). All samples were performed in duplicate and the average 460 nm absorbance was calculated.

Statistical analysis

All statistical analyses were performed using SPSS® Version 25 (IBM®, New York, USA) and Prism 6 (GraphPad Inc., La Jolla, USA) software. All data were analysed using a general linear modelling approach with treatment (AL or DR) and genotype (TejJ89, TejJ48 and TejJ114 (and where indicated, C57BL/6J)) introduced as fixed factors, and a post hoc Bonferroni test used for multiple comparisons. In all cases, non-significant interactions ($p > 0.05$) within the GLM analyses were removed in order to obtain the best-fitting model, with only significant interactions reported. All data were analysed by Grubbs outlier test with alpha set to 5%. Unless otherwise described, all results are presented as mean ± standard error of the mean (SEM), with $p < 0.05$ regarded as statistically significant. * denotes $p < 0.05$, ** denotes $p < 0.01$ and *** denotes $p < 0.001$.

Results

Genotype-specific hepatic H_2S production following 40% DR in female ILSXISS mice

Using the lead acetate method to determine H_2S production (Hine et al. 2015; Hine et al. 2017), we observed a significant genotype effect ($F = 12.243$, $p < 0.001$) but no treatment effect ($F = 0.150$, $p = 0.701$) in the liver. However, a significant genotype by treatment interaction was detected ($F = 13.833$, $p < 0.001$). Post hoc analysis indicated that H_2S production was significantly elevated by 40% DR in strain TejJ89 ($p = 0.005$), but significantly reduced by 40% DR in strain TejJ48 ($p = 0.031$) relative to their strain-appropriate AL controls (Fig. 1a, b). In addition, H_2S production was significantly elevated in strain TejJ89 relative to strains TejJ48 ($p = 0.022$) and TejJ114 ($p < 0.001$). This genotype effect was primarily driven by significantly elevated H_2S production in TejJ89 under 40% DR compared with all other groups, with no differences in H_2S production detected between ILSXISS strains under AL feeding (Fig. 1a, b). We also determined kidney H_2S production (Fig. S1). No significant treatment effect was detected ($F = 1.540$, $p = 0.0221$), but a significant genotype effect on kidney H_2S production was seen ($F = 3.294$, $p = 0.047$), being significantly elevated in strain TejJ89 relative to strain TejJ48 ($p = 0.050$).

Transcript levels of H_2S-production and -elimination proteins in ILSXISS mice following 40% DR

In order to better understand the enzymatic pathways regulating hepatic endogenous H_2S (see Fig. 2) across different ILSXISS strains maintained under AL or 40% DR, we determined gene expression levels of a suite of H_2S-producing and -eliminating proteins (Fig. 3a–i). *Cse*, *Cbs* and *Mpst* transcript levels (Fig. 3a–c) were unaffected by both genotype and treatment (see Table S2 for all statistical output). However, a significant genotype by treatment interaction effect was observed for both *Cbs* (Fig. 3b, $F = 4.737$, $p = 0.017$) and *Mpst* (Fig. 3c, $F = 6.734$, $p = 0.004$), with lower expression in strain TejJ89 under AL feeding relative to strain TejJ114 under AL feeding ($p = 0.008$ and $p = 0.024$ for *Cbs* and *Mpst* respectively). *Got1* (Fig. 3d) and *Ethe1* expression (Fig. 3e) differed by genotype ($F = 7.185$, $p = 0.003$ and $F = 10.445$, $p < 0.001$ for *Got1* and *Ethe1* respectively) but not by treatment, with strain TejJ48 having significantly lower *Got1* and *Ethe1* expression relative to strains TejJ89 and TejJ114 ($p < 0.01$, in all cases). *Tst* expression levels (Fig. 3f) showed a significant genotype effect ($F = 6.659$, $p = 0.004$), with reduced expression in liver of TejJ89 mice compared with TejJ114 mice ($p = 0.003$), but again no treatment effect was detected. A significant *Tst* genotype by treatment interaction was also detected ($F = 6.745$, $p = 0.004$), with AL TejJ89 mice having significantly lower *Tst* expression levels compared with AL TejJ114 mice ($p < 0.001$), and 40% DR reducing *Tst* expression in Tej114 mice ($p = 0.007$) relative to TejJ114 controls (Fig. 3f). While no significant genotype nor treatment effect on *Suox* expression was detected (Fig. 3g and Table S2), a significant genotype by treatment interaction effect was observed ($F = 5.694$, $p = 0.008$), again with AL TejJ89 mice having significantly reduced expression relative to AL TejJ114 mice ($p = 0.035$), and 40% DR significantly reducing *Suox* expression in Tej114 mice relative to AL TejJ114 mice ($p = 0.008$). *Mat1a* (Fig. 3h) did not show any significant genotype effect ($F = 1.069$, $p = 0.356$) but was the only transcript that showed a significant treatment effect ($F = 5.3183$, $p = 0.030$), being significantly decreased by 40% DR across all ILSXISS strains. No significant genotype or treatment effects were detected for *Bhmt1*, *Bhmt2* or *Sahh* (Figs. 3i–k, Table S2).

Protein levels of H_2S-production enzymes in ILSXISS and C57BL/6J mice following 40% DR

Studies in C57BL/6J mice have repeatedly shown that generation of hepatic H_2S is driven primarily through CSE and CBS, with CSE appearing to be the predominant enzymatic source (e.g. Mani et al. 2014). We subsequently compared hepatic protein levels of CSE, CBS and MPST in TejJ89, TejJ48 and TejJ114 mice with levels in C57BL/6J mice under AL feeding and 40% DR. CSE protein levels (Fig. 4a) were significantly altered by both genotype ($F = 14.845$, $p < 0.001$) and treatment ($F = 5.559$, $p = 0.024$), with a significant treatment by genotype interaction present ($F = 5.990$, $p = 0.002$). CSE levels were significantly higher in C57BL/6J mice relative to all ILSXISS strains ($p < 0.001$, in all cases), with no differences in CSE levels observed between

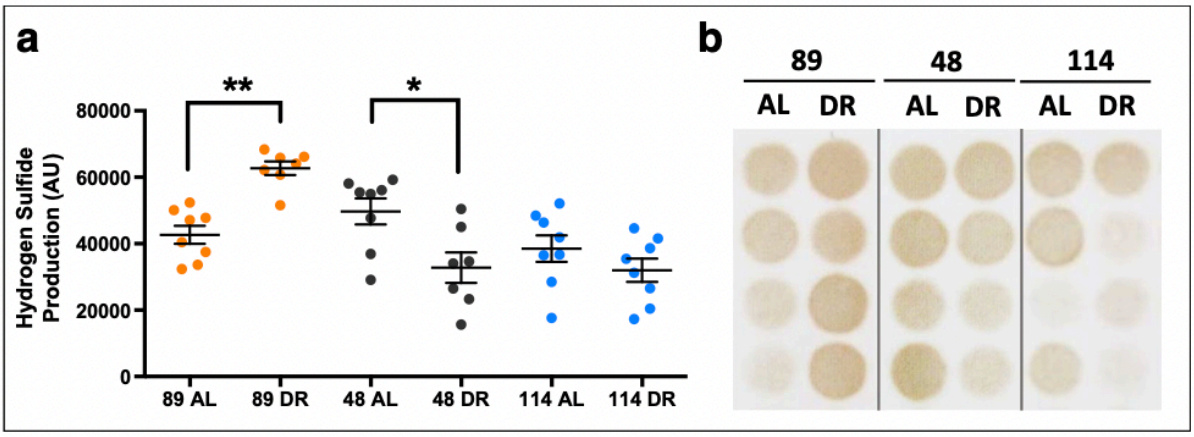

Fig. 1 Strain-specificity exists in hepatic H_2S production following 40% dietary restriction in female ILSXISS mice. **a** Hepatic H_2S production levels in TejJ89, TejJ48 and TejJ114 mice on AL or 40% DR, as quantified by densitometry analysis of lead acetate assay results. **b** Representative images of lead acetate precipitates formed in the assay; darker precipitates indicate higher hepatic H_2S production capacity. TejJ89 data in orange, TejJ48 data in black, TejJ114 data in blue. Error bars represent SEM. $*p < 0.05$, $**p < 0.01$

ILSXISS strains. CSE protein levels were elevated by 40% DR but only significantly so in C57BL/6J mice ($p = 0.002$). Hepatic CBS levels were also affected by genotype ($F = 6.451$, $p = 0.001$) but not by treatment ($F = 0.037$, $p = 0.848$), with TejJ89 mice having increased CBS levels relative to both TejJ114 ($p = 0.002$) and C57BL/6J ($p = 0.016$) mice (Fig. 4b). MPST levels were significantly altered by both genotype ($F = 12.984$, $p < 0.001$) and treatment ($F = 8.812$, $p = 0.005$), with a significant genotype by treatment interaction effect ($F = 9.848$, $p < 0.001$) also observed (Fig. 4c). Hepatic MPST levels were significantly elevated in TejJ89 mice compared with all other genotypes ($p < 0.001$, in all cases). The elevated H_2S levels observed in TejJ89 mice under 40% DR was associated with a significant elevation in hepatic MPST levels relative to TejJ89 AL mice (Fig. 4c, $p < 0.001$), but 40% DR did not alter MPST levels significantly in any other genotype compared with their appropriate AL controls. We subsequently determined hepatic MPST activity within our ILSXISS mouse strains (Fig. S2), but no genotype ($F = 0.144$, $p = 0.707$) nor treatment ($F = 2.755$, $p = 0.081$) effect was observed. Our findings indicate that significant genotype-specific differences exist in protein levels of the primary cellular H_2S generating enzymes CSE, CBS and MPST within mouse liver (Fig. 4a–c). The increased H_2S levels following 40% DR in strain TejJ89 was associated with an increase in MPST protein levels, but not in CSE (significantly elevated in C57BL/6J mice under 40% DR) or CBS levels, and that protein levels of these H_2S generating enzymes were unresponsive to 40% DR in strains TejJ48 and TejJ114.

Discussion

A reduction in the intake of calories or in the intake of macro- or micronutrients, termed here as dietary restriction (DR), is currently the most widely employed experimental intervention to modulate ageing. Indeed, DR has been shown to extend lifespan and healthspan in an evolutionary diverse group of organisms (Fontana and Partridge 2015; Speakman and Mitchell 2011), and has also been shown to provide a number of beneficial health effects in humans (Fontana et al. 2004; Fontana et al. 2007). However, it is still not understood how DR mechanistically elicits its beneficial effects. In addition, a number of studies, particularly in mice, report that the DR effect on lifespan and healthspan can vary significantly depending on genetic background (Forster et al. 2003; Goren et al. 2004; Hempenstall et al. 2010; Liao et al. 2010; Mitchell et al. 2016; Rikke et al. 2010; Swindell 2012; Turturro et al. 1999). It is believed that better understanding of the basis of this genetic variation during DR may be important if we hope to translate experimental findings from (typically) highly inbred mouse models to genetically heterogenous humans (Selman and Swindell 2018).

In this study, we investigated the potential relevance of Hydrogen sulfide (H_2S) in DR-induced lifespan by comparing genetically distinct ILSXISS recombinant inbred mouse strains that have been reported to show

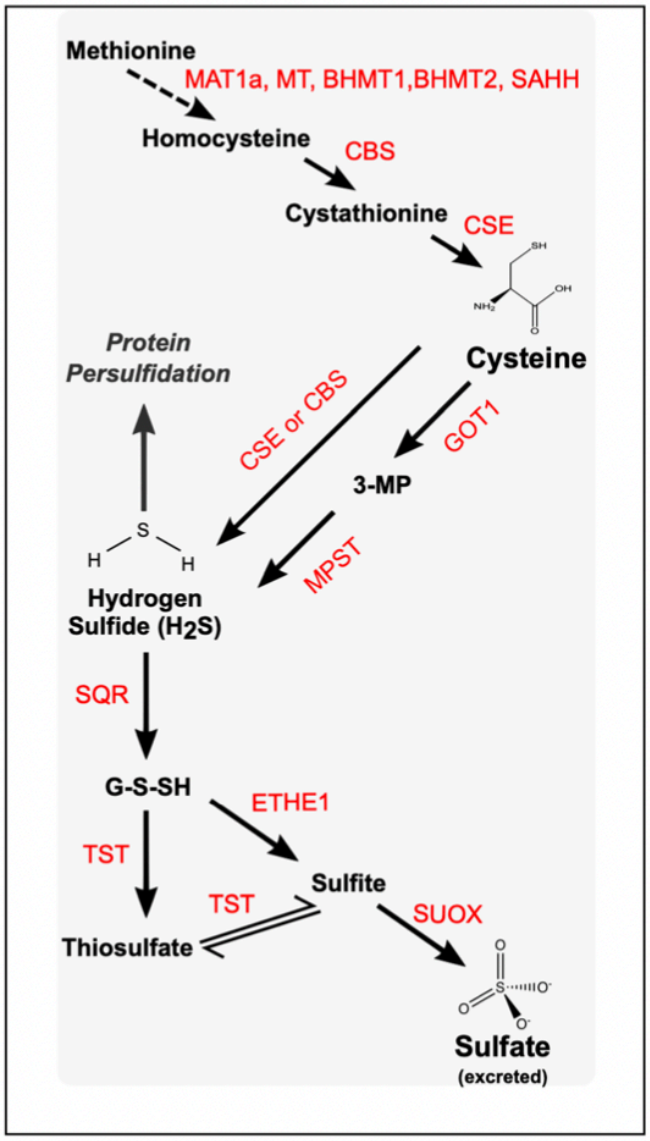

Fig. 2 Molecular pathways involved in the enzymatic production of H_2S from amino acid metabolism and subsequent elimination of H_2S by components of the sulphide disposal unit. Enzymes in red. MAT1a, methionine adenosyltransferase 1A; MT, methyl transferase; SAHH, S-adenosylhomocysteine hydrolase; BHMT1, betaine-homocysteine S-methyltransferase 1; BHMT2, betaine-homocysteine S-methyltransferase 2; CBS, cystathionine-β-synthase; CSE, cystathionine-γ-lyase; GOT1, glutamic-oxaloacetic transaminase 1; MPST, 3-mercaptopyruvate sulfurtransferase; SQR, sulphide:quinone oxidoreductase; TST, thiosulfate sulfurtransferase; ETHE1, ethylmalonic encephalopathy 1 protein; SUOX, sulfite oxidase

significant variation in their lifespan under 40% DR, ranging from life extension to no response, through to life shortening (Liao et al. 2010; Rikke et al. 2010). A number of studies have now reported genetic or pharmacological interventions that modulate H_2S levels can profoundly impact longevity in model organisms (Hine and Mitchell 2015; Miller and Roth 2007; Qabazard et al. 2013; Shaposhnikov et al. 2018; Wei and Kenyon 2016) and protect against age-associated dysfunction (Latorre et al. 2018; Wang et al. 2019; Zhan et al. 2018). In addition, increased hepatic H_2S is a conserved phenotype in long-lived genetic mouse mutants (Hine et al. 2017), is increased significantly by DR in C57BL/6J and DBA/2 mice (Hine et al. 2015; Mitchell et al. 2016) and appears essential for mediating the beneficial effects of DR (Hine et al. 2015). We found that hepatic H_2S was only elevated in female mice from strain TejJ89 under long-term 40% DR; TejJ89 is the single ILSXISS strain in our study reported to show DR-induced longevity (Liao et al. 2010; Rikke et al. 2010). In contrast, strain TejJ48 reported to be refractory to 40% DR (Liao et al. 2010; Rikke et al. 2010) showed a significant reduction in hepatic H_2S when exposed to 40% DR. In strain TejJ114 reported to show lifespan shortening under 40% DR (Liao et al. 2010; Rikke et al. 2010), we observed no DR-associated difference in hepatic H_2S production relative to AL mice. However, no treatment nor interaction effect was observed in kidney H_2S production, suggesting tissue-specificity exists in the impact of DR on H_2S production in mice, in contrast to findings (H_2S concentration) previously reported in F344 rats under DR (Wang et al. 2016). In addition, significant strain-specificity in H_2S production was also observed, being elevated in strain TejJ89 relative to both TejJ48 and TejJ114 in the liver and elevated in TejJ89 compared with TejJ48 in the kidney. Our findings indicate that TejJ89 mice show a similar association between increased hepatic H_2S production and extended lifespan under DR reported in other mouse strains such as C57BL/6J and DBA/2 (Mitchell et al. 2016). Consequently, our findings do further support the premise that elevated hepatic H_2S levels may be an important mediator of the beneficial effects of DR (Hine et al. 2015; Hine and Mitchell 2015).

To further investigate the potential processes underlying these strain-specific differences in H_2S following 40% DR, we examined a suite of H_2S-producing and -degrading enzymes at the transcript and protein level within ILSXISS mice. The predominately cytosolic enzymes cystathionine γ-lyase (CSE or CGL) and cystathionine β-synthase (CBS) are the main sources of H_2S within cells (Carter and Morton 2016), and mice carrying genetic defects in these enzymes are prone to a number of pathologies (Hine et al. 2018). In particular, elevated hepatic H_2S following DR correlates with transcript and protein levels of CSE (Derous et al. 2017;

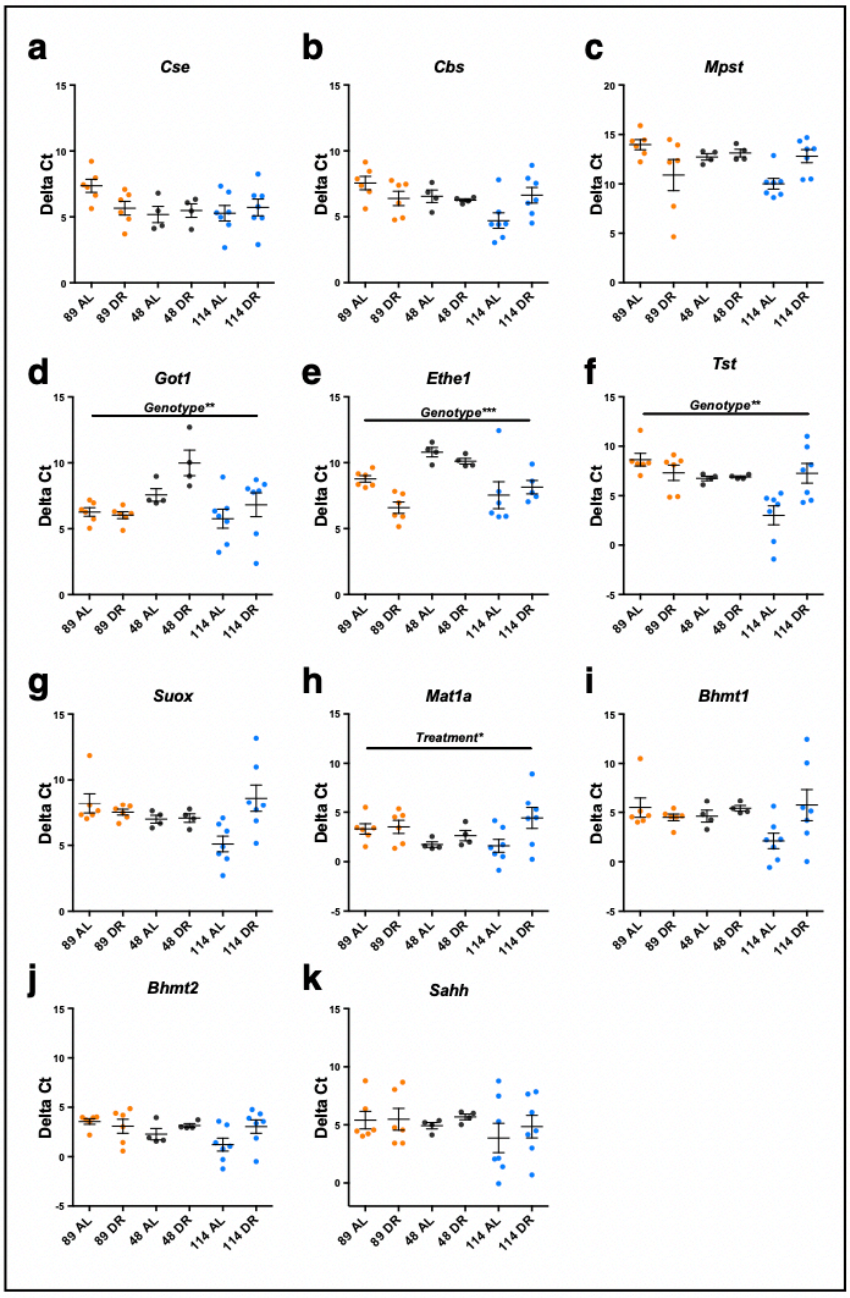

Fig. 3 ILSXISS mouse strains exhibit differential transcriptional regulation of H_2S-production and elimination enzymes following 40% DR. Hepatic mRNA gene expression (presented as Delta Ct values, a lower Delta Ct indicates a higher number of mRNA transcripts for that particular gene) of H_2S-producing (**a**–**d**), H_2S-eliminating (**e**–**g**) and methionine to cysteine conversion (**h**–**k**) genes in TejJ89, TejJ48 and TejJ114 mice under AL feeding or 40% DR. TejJ89 data in orange, TejJ48 data in black, TejJ114 data in blue. Error bars represent SEM. $*p < 0.05$, $**p < 0.01$, $***p < 0.001$. Genotype (TejJ89, TejJ48 or TejJ114) and Treatment (AL or DR). See Table S1 for statistical output. *Cse*, cystathionine-γ-lyase; *Cbs*, cystathionine-β-synthase; *Mpst*, 3-mercaptopyruvate sulfurtransferase; *Got1*, glutamic-oxaloacetic transaminase 1, *Ethe1*, ethylmalonic encephalopathy 1 protein, *Tst*, thiosulfate sulfurtransferase; *Suox*, sulfite oxidase; *Mat1a*, methionine adenosyltransferase 1A; *Bhmt1*, betaine-homocysteine S-methyltransferase 1; *Bhmt2*, betaine-homocysteine S-methyltransferase 2; *Sahh*, S-adenosylhomocysteine hydrolase

Wang et al. 2016), and similarly CSE levels are elevated in several long-lived mouse mutants (Hine et al. 2017). Perhaps surprisingly, we did not observe any genotype or treatment effects on transcript levels of *Cse*, *Cbs* or *Mpst*, although several significant genotype and genotype by treatment interaction effects (*Cbs*, *Mpst*, *Tst*, *Suox*) were detected, typically with TejJ89 AL mice having significantly reduced expression compared with TejJ114 AL mice. At the protein level, CSE was significantly elevated in C57BL/6J mice compared with all ILSXISS strains, with 40% DR further increasing CSE levels within the liver of C57BL/6J mice. However, 40% DR did not have any effect on hepatic CSE levels in ILSXISS mice. Hepatic CBS protein levels were unaffected by 40% DR across all genotypes studied. Given that both CSE and CBS levels were unaffected by 40% DR in strain TejJ89 despite the DR-associated increase in H_2S production, we subsequently investigate 3-mercaptopyruvate sulfurtransferase (MPST). This is the third H_2S-producing enzyme within cells but its role has been much less well characterised relative to both CSE and CBS, particularly in the context of ageing and DR. CSE and CBS primarily remain cytoplasmic under normal physiological conditions, whereas MPST can localise to mitochondria and exhibits a profound influence over mitochondrial-specific metabolism and H_2S

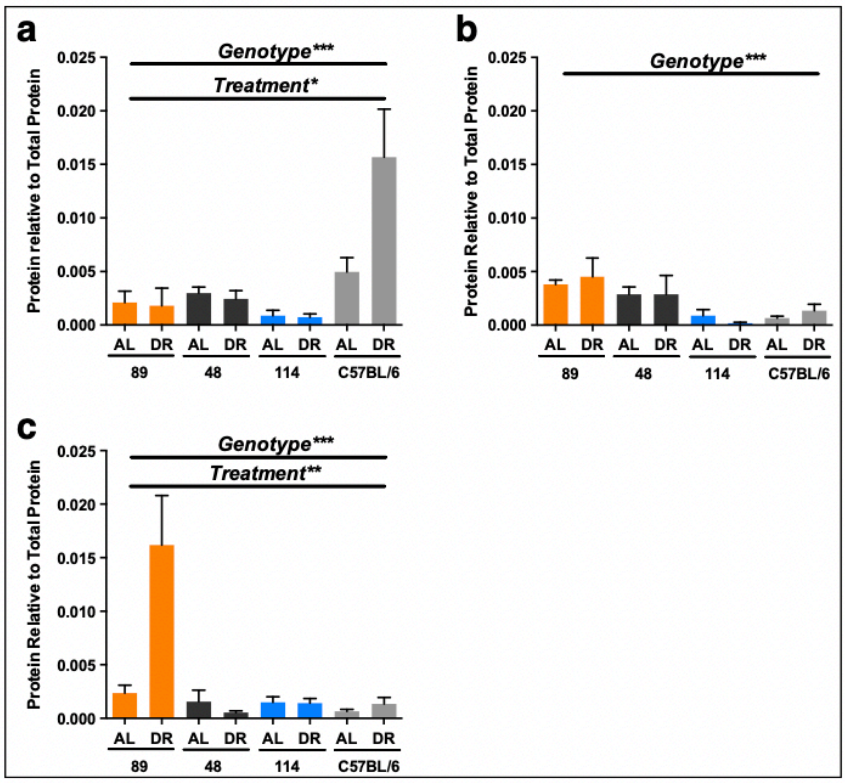

Fig. 4 40% DR significantly increases cystathionine gamma-lyase (CSE) within the liver of C57BL/6J mice but significantly increases 3-mercaptopyruvate sulfurtransferase (MPST) within the liver of TejJ89 mice. Hepatic protein levels of CSE (**a**), cystathionine-β-synthase (CBS) (**b**) and MPST (**c**) in TejJ89 ($n = 6$), TejJ48 ($n = 4$), TejJ114 ($n = 6$) and C57BL/6J ($n = 4$) AL and 40% DR mice. TejJ89 data in orange, TejJ48 data in black, TejJ114 data in blue, C57BL/6J data in light grey. Error bars represent SEM. $*p < 0.05$, $**p < 0.01$, $***p < 0.001$. Genotype (TejJ89, TejJ48, TejJ114 or C57BL/6J) and treatment (AL or DR)

levels (Kimura 2014). Furthermore, while CSE and CBS work in concert to convert homocysteine into H_2S via step-wise reactions, MPST generates H_2S from a distinct substrate, 3-mercaptopyruvate (Renga 2011; Tao et al. 2017). We found MPST to be significantly increased in the liver of TejJ89 mice under 40% DR, although it was unaffected by DR in strains TejJ48, TejJ114 or in C57BL/6J mice. Precisely why C57BL/6J mice and TejJ89 mice appear to have distinct mechanistic routes (elevated CSE or elevated MPST respectively) to achieve the same outcome of elevated hepatic H_2S under 40% DR still needs to be determined.

There are of course some caveats to our findings, not least that this work is highly correlational. As discussed elsewhere, the variation in phenotypic responses to DR across different mouse strains is quite broad (Mitchell et al. 2016; Selman and Swindell 2018; Swindell 2012). We examined females and then only in three strains of ILSXISS mice, albeit strains that represent the variety of lifespan responses reported in the original two studies (Liao et al. 2010; Rikke et al. 2010). We were vigilant in our choice of strains in this comparative study, choosing those that showed a similar direction of response across both studies. In addition, and as discussed in detail elsewhere (Selman and Swindell 2018), significant differences in experimental design and husbandry practices existed between the original studies. Consequently, a fuller investigation of the lifespan response to DR in ILSXISS mice and the potential relevance of H_2S production, particularly under graded levels of DR, is warranted, but will be a major undertaking (Selman and Swindell 2018). In addition, it will also be interesting to investigate precisely how H_2S production varies in different tissues and in different cellular locations following DR. These approaches may be made more feasible with the advent of novel chemical probes to determine H_2S in vivo (Arndt et al. 2017; Lau et al. 2019). However, irrespective of these caveats, we have shown that endogenous H_2S levels and associated signalling pathways differ significantly depending on genetic background in mice under both AL and DR conditions. Our data suggest that, similar to previous reports, increased H_2S production and/or metabolism is a conserved mechanism through which DR acts to increase lifespan in mice (Hine et al. 2017; Hine and Mitchell 2015), but the precise cellular processes that regulate H_2S production and elimination under DR appear highly strain- (and potentially tissue-) specific.

Acknowledgements We thank the animal care staff (CRF, University of Glasgow), Dr. Amy Valentine, Mrs. Kate Griffiths, Professor Lorna Harries and Dr. Ben Lee.

Authors' contributions SEW, LM, WAS, DEM, RNC and CH performed all experiments and analysed the data. SEW co-wrote

the manuscript. NMM and JRM provided critical reagents. RNC, CH, NMM and JRM edited the manuscript. CS designed the studies, co-wrote and edited the manuscript.

Funding information This work was supported through a Medical Research Council Precision Medicine Doctoral Training Program in Precision Medicine to SEW (Reference MR/N013166/1), a Wellcome Trust Biomedical Vacation Scholarship to DEM (Reference 213310/Z/18/Z), a NIH/NIA grant to CH (Reference AG050777), a Wellcome Trust Investigator award (Reference 100981/Z/13/Z) to NMM and start-up funds from the University of Glasgow (College of Medical, Veterinary and Life Sciences) to CS.

Compliance with ethical standards

Conflict of interest The authors declare that they have no conflict of interest.

https://doi.org/10.21769/BioProtoc.2382

References

Arndt S, Baeza-Garza CD, Logan A, Rosa T, Wedmann R, Prime TA, Martin JL, Saeb-Parsy K, Krieg T, Filipovic, MR, Hartley RC, Murphy MP (2017) Assessment of H_2S in vivo using the newly developed mitochondria-targeted mass spectrometry probe MitoA. J Biol Chem 292:7761–7773. https://doi.org/10.1074/jbc.M117.784678

Carter RN, Morton NM (2016) Cysteine and hydrogen sulphide in the regulation of metabolism: insights from genetics and pharmacology. J Pathol 238:321–332. https://doi.org/10.1002/path.4659

Das A, Huang GX, Bonkowski MS, Longchamp A, Li C, Schultz MB, Kim LJ, Osborne B, Joshi S, Lu Y, Treviño-Villarreal JH, Kang MJ, Hung TT, Lee B, Williams EO, Igarashi M, Mitchell JR, Wu LE, Turner N, Arany Z, Guarente L, Sinclair DA (2018) Impairment of an endothelial NAD(+)-H2S signaling network is a reversible cause of vascular aging. Cell 173:74–89 e20. https://doi.org/10.1016/j.cell.2018.02.008

Derous D, Mitchell SE, Wang L, Green CL, Wang Y, Chen L, Han JDJ, Promislow DEL, Lusseau D, Douglas A, Speakman JR (2017) The effects of graded levels of calorie restriction: XI. Evaluation of the main hypotheses underpinning the life extension effects of CR using the hepatic transcriptome. Aging (Albany NY) 9:1770–1824. https://doi.org/10.18632/aging.101269

Fontana L, Meyer TE, Klein S, Holloszy JO (2004) Long-term calorie restriction is highly effective in reducing the risk for atherosclerosis in humans. Proc Natl Acad Sci U S A 101:6659–6663

Fontana L, Partridge L (2015) Promoting health and longevity through diet: from model organisms to humans. Cell 161:106–118. https://doi.org/10.1016/j.cell.2015.02.020

Fontana L, Villareal DT, Weiss EP, Racette SB, Steger-May K, Klein S, Holloszy JO (2007) Calorie restriction or exercise: effects on coronary heart disease risk factors. A randomized, controlled trial. Am J Physiol Endocrinol Metab 293:E197–E202

Forster MJ, Morris P, Sohal RS (2003) Genotype and age influence the effect of caloric intake on mortality in mice. FASEB J 17:690–692

Gong H, Sun L, Chen B, Han Y, Pang J, Wu W, Qi R, Zhang TM (2016) Evaluation of candidate reference genes for RT-qPCR studies in three metabolism related tissues of mice after caloric restriction. Sci Rep 6:38513. https://doi.org/10.1038/srep38513

Goren HJ, Kulkarni RN, Kahn CR (2004) Glucose homeostasis and tissue transcript content of insulin signaling intermediates in four inbred strains of mice: C57BL/6, C57BLKS/6, DBA/2, and 129X1. Endocrinology 145:3307–3323

Hempenstall S, Picchio L, Mitchell SE, Speakman JR, Selman C (2010) The impact of acute caloric restriction on the metabolic phenotype in male C57BL/6 and DBA/2 mice. Mech Ageing Dev 131:111–118. https://doi.org/10.1016/j.mad.2009.12.008

Hine C, Harputlugil E, Zhang Y, Ruckenstuhl C, Lee BC, Brace L, Longchamp A, Treviño-Villarreal JH, Mejia P, Ozaki CK, Wang R, Gladyshev VN, Madeo F, Mair WB, Mitchell JR (2015) Endogenous hydrogen sulfide production is essential for dietary restriction benefits. Cell 160:132–144. https://doi.org/10.1016/j.cell.2014.11.048

Hine C, Kim H-J, Zhu Y, Harputlugil E, Longchamp A, Souza Matos M, Ramadoss P, Bauerle K, Brace L, Asara JM, Ozaki CK, Cheng S-Y, Singha S, Han Ahn K, Kimmelman A, Fisher FM, Pissios P, Withers DJ, Selman C, Wang R, Yen K, Longo VD, Cohen P, Bartke A, Kopchick JJ, Miller R, Hollenberg AN, Mitchell JR (2017) Hypothalamic-pituitary axis regulates hydrogen sulfide production. Cell Metab 25:1320–1333 e1325. https://doi.org/10.1016/j.cmet.2017.05.003

Hine C, Mitchell JR (2015) Calorie restriction and methionine restriction in control of endogenous hydrogen sulfide production by the transsulfuration pathway. Exp Gerontol 68:26–32. https://doi.org/10.1016/j.exger.2014.12.010

Hine C, Mitchell JR (2017) Endpoint or Kinetic Measurement of Hydrogen Sulfide Production Capacity in Tissue Extracts. Bio-Protoc 7(13):e2382. https://doi.org/10.21769/BioProtoc.2382

Hine C, Zhu Y, Hollenberg AN, Mitchell JR (2018) Dietary and endocrine regulation of endogenous hydrogen sulfide production: implications for longevity. Antioxid Redox Signal 28:1483–1502. https://doi.org/10.1089/ars.2017.7434

Ingram DK, de Cabo R (2017) Calorie restriction in rodents: caveats to consider. Ageing Res Rev 39:15–28. https://doi.org/10.1016/j.arr.2017.05.008

Kennedy BK, Steffen KK, Kaeberlein M (2007) Ruminations on dietary restriction and aging. Cell Mol Life Sci 64:1323–1328. https://doi.org/10.1007/s00018-007-6470-y

Kimura H (2014) Production and physiological effects of hydrogen sulfide. Antioxid Redox Signal 20:783–793. https://doi.org/10.1089/ars.2013.5309

Latorre E, Torregrossa R, Wood ME, Whiteman M, Harries LW (2018) Mitochondria-targeted hydrogen sulfide attenuates endothelial senescence by selective induction of splicing factors HNRNPD and SRSF2. Aging (Albany NY) 10: 1666–1681. https://doi.org/10.18632/aging.101500

Lau GY, Barts N, Hartley RC, Tobler M, Richards JG, Murphy MP, Arndt S (2019) Detection of changes in mitochondrial hydrogen sulfide in vivo in the fish model *Poecilia mexicana* (Poeciliidae). Biol Open:8. https://doi.org/10.1242/bio.041467

Lee HJ, Feliers D, Barnes JL, Oh S, Choudhury GG, Diaz V, Galvan V, Strong R, Nelson J, Salmon A, Kevil CG, Kasinath BS (2018) Hydrogen sulfide ameliorates aging-associated changes in the kidney. Geroscience 40:163–176. https://doi.org/10.1007/s11357-018-0018-y

Liao CY, Rikke BA, Johnson TE, Diaz V, Nelson JF (2010) Genetic variation in the murine lifespan response to dietary restriction: from life extension to life shortening. Aging Cell 9:92–95. https://doi.org/10.1111/j.1474-9726.2009.00533.x

Liao CY, Rikke BA, Johnson TE, Gelfond JA, Diaz V, Nelson JF (2011) Fat maintenance is a predictor of the murine lifespan response to dietary restriction. Aging Cell 10:629–639. https://doi.org/10.1111/j.1474-9726.2011.00702.x

Mair W, Dillin A (2008) Aging and survival: the genetics of life span extension by dietary restriction. Annu Rev Biochem 77:727–754. https://doi.org/10.1146/annurev.biochem.77.061206.171059

Mani S, Cao W, Wu L, Wang R (2014) Hydrogen sulfide and the liver. Nitric Oxide 41:62–71. https://doi.org/10.1016/j.niox.2014.02.006

Masoro EJ (2005) Overview of caloric restriction and ageing. Mech Ageing Dev 126:913–922

Miller DL, Roth MB (2007) Hydrogen sulfide increases thermotolerance and lifespan in *Caenorhabditis elegans*. Proc Natl Acad Sci U S A 104:20618–20622. https://doi.org/10.1073/pnas.0710191104

Mitchell SJ, Madrigal-Matute J, Scheibye-Knudsen M, Fang E, Aon M, González-Reyes JA, Cortassa S, Kaushik S, Gonzalez-Freire M, Patel B, Wahl D, Ali A, Calvo-Rubio M, Burón MI, Guiterrez V, Ward TM, Palacios HH, Cai H, Frederick DW, Hine C, Broeskamp F, Habering L, Dawson J, Beasley TM, Wan J, Ikeno Y, Hubbard G, Becker KG, Zhang Y, Bohr VA, Longo DL, Navas P, Ferrucci L, Sinclair DA, Cohen P, Egan JM, Mitchell JR, Baur JA, Allison DB, Anson RM, Villalba JM, Madeo F, Cuervo AM, Pearson KJ, Ingram DK, Bernier M, de Cabo R (2016) Effects of sex, Strain, and Energy Intake on Hallmarks of Aging in Mice. Cell Metab 23:1093–1112. https://doi.org/10.1016/j.cmet.2016.05.027

Morton NM, Beltram J, Carter RN, Michailidou Z, Gorjanc G, McFadden C, Barrios-Llerena ME, Rodriguez-Cuenca S, Gibbins MTG, Aird RE, Moreno-Navarrete JM, Munger SC, Svenson KL, Gastaldello A, Ramage L, Naredo G, Zeyda M, Wang ZV, Howie AF, Saari A, Sipilä P, Stulnig TM, Gudnason V, Kenyon CJ, Seckl JR, Walker BR, Webster SP, Dunbar DR, Churchill GA, Vidal-Puig A, Fernandez-Real JM, Emilsson V, Horvat S (2016) Genetic identification of thiosulfate sulfurtransferase as an adipocyte-expressed antidiabetic target in mice selected for leanness. Nat Med 22:771–779. https://doi.org/10.1038/nm.4115

Mulvey L, Sands WA, Salin K, Carr AE, Selman C (2016) Disentangling the effect of dietary restriction on mitochondrial function using recombinant inbred mice. Mol Cell Endocrinol. https://doi.org/10.1016/j.mce.2016.09.001

Mulvey L, Sinclair A, Selman C (2014) Lifespan modulation in mice and the confounding effects of genetic background. J Genet Genomics 41:497–503. https://doi.org/10.1016/j.jgg.2014.06.002

Picca A, Pesce V, Lezza AMS (2017) Does eating less make you live longer and better? An update on calorie restriction. Clin Interv Aging 12:1887–1902. https://doi.org/10.2147/CIA.S126458

Qabazard B, Ahmed S, Li L, Arlt VM, Moore PK, Stürzenbaum SR (2013) C. elegans aging is modulated by hydrogen sulfide and the sulfhydrylase/cysteine synthase cysl-2. PLoS One 8: e80135. https://doi.org/10.1371/journal.pone.0080135

Renga B (2011) Hydrogen sulfide generation in mammals: the molecular biology of cystathionine-beta- synthase (CBS) and cystathionine-gamma-lyase (CSE). Inflamm Allergy Drug Targets 10:85–91

Rikke BA, Liao CY, McQueen MB, Nelson JF, Johnson TE (2010) Genetic dissection of dietary restriction in mice supports the metabolic efficiency model of life extension. Exp Gerontol 45: 691–701. https://doi.org/10.1016/j.exger.2010.04.008

Selman C, Swindell WR (2018) Putting a strain on diversity. EMBO J 37. https://doi.org/10.15252/embj.2018100862

Shaposhnikov M, Proshkina E, Koval L, Zemskaya N, Zhavoronkov A, Moskalev A (2018) Overexpression of CBS and CSE genes affects lifespan, stress resistance and locomotor activity in Drosophila melanogaster. Aging (Albany NY) 10:3260–3272. https://doi.org/10.18632/aging.101630

Speakman JR, Mitchell SE (2011) Caloric restriction. Mol Asp Med 32:159–221. https://doi.org/10.1016/j.mam.2011.07.001

Swindell WR (2012) Dietary restriction in rats and mice: a meta-analysis and review of the evidence for genotype-dependent effects on lifespan. Ageing Res Rev 11:254–270. https://doi.org/10.1016/j.arr.2011.12.006

Talaei F, van Praag VM, Henning RH (2013) Hydrogen sulfide restores a normal morphological phenotype in Werner syndrome fibroblasts, attenuates oxidative damage and modulates mTOR pathway. Pharmacol Res 74:34–44. https://doi.org/10.1016/j.phrs.2013.04.011

Tao B, Wang R, Sun C, Zhu Y (2017) 3-Mercaptopyruvate sulfurtransferase not cystathionine beta-synthase nor cystathionine gamma-lyase, mediates hypoxia-induced migration of vascular endothelial cells. Front Pharmacol 8:657. https://doi.org/10.3389/fphar.2017.00657

Turturro A, Witt WW, Lewis S, Hass BS, Lipman RD, Hart RW (1999) Growth curves and survival characteristics of the animals used in the biomarkers of aging program. J Gerontol A Biol Sci Med Sci 54:B492–B501

Wang SY, Wang WJ, Liu JQ, Song YH, Li P, Sun XF, Cai GY, Chen XM (2019) Methionine restriction delays senescence and suppresses the senescence-associated secretory phenotype in the kidney through endogenous hydrogen sulfide. Cell Cycle 18:1573–1587. https://doi.org/10.1080/15384101.2019.1618124

Wang WJ, Cai GY, Ning YC, Cui J, Hong Q, Bai XY, Xu XM, Bu R, Sun XF, Chen XM (2016) Hydrogen sulfide mediates the protection of dietary restriction against renal senescence in aged F344 rats. Sci Rep 6:30292. https://doi.org/10.1038/srep30292

Wei Y, Kenyon C (2016) Roles for ROS and hydrogen sulfide in the longevity response to germline loss in *Caenorhabditis elegans*. Proc Natl Acad Sci U S A 113:E2832–E2841. https://doi.org/10.1073/pnas.1524727113

Weindruch R, Walford RL (1988) The retardation of aging and disease by dietary restriction. Charles C, Thomas, Springfield, Illinois

Yuan R, Tsaih SW, Petkova SB, Marin de Evsikova C, Xing S, Marion MA, Bogue MA, Mills KD, Peters LL, Bult CJ, Rosen CJ, Sundberg JP, Harrison DE, Churchill GA, Paigen B (2009) Aging in inbred strains of mice: study design and interim report on median lifespans and circulating IGF1 levels. Aging Cell 8:277–287. https://doi.org/10.1111/j.1474-9726.2009.00478.x

Zhan JQ, Zheng LL, Chen HB, Yu B, Wang W, Wang T, Ruan B, Pan BX, Chen JR, Li XF, Wei B, Yang YJ (2018) Hydrogen sulfide reverses aging-associated amygdalar synaptic plasticity and fear memory deficits in rats. Front Neurosci 12:390. https://doi.org/10.3389/fnins.2018.00390

Appendix III: Published paper containing data from Chapter 4

Cell Reports

CellPress
OPEN ACCESS

Article

The hepatic compensatory response to elevated systemic sulfide promotes diabetes

Roderick N. Carter,[1] Matthew T.G. Gibbins,[1,11] Martin E. Barrios-Llerena,[1,12] Stephen E. Wilkie,[1,2] Peter L. Freddolino,[3] Marouane Libiad,[3,13] Victor Vitvitsky,[3] Barry Emerson,[1,14] Thierry Le Bihan,[4,15] Madara Brice,[1] Huizhong Su,[5,16] Scott G. Denham,[1] Natalie Z.M. Homer,[1] Clare Mc Fadden,[1,17] Anne Tailleux,[6] Nourdine Faresse,[7,18] Thierry Sulpice,[7] Francois Briand,[7] Tom Gillingwater,[8] Kyo Han Ahn,[9] Subhankar Singha,[9,19] Claire McMaster,[10] Richard C. Hartley,[10] Bart Staels,[6] Gillian A. Gray,[1] Andrew J. Finch,[5,20] Colin Selman,[2] Ruma Banerjee,[3] and Nicholas M. Morton[1,21,*]

[1]University/British Heart Foundation Centre for Cardiovascular Science, University of Edinburgh, Queen's Medical Research Institute, Edinburgh EH16 4TJ, UK

[2]Glasgow Ageing Research Network (GARNER), Institute of Biodiversity, Animal Health and Comparative Medicine, University of Glasgow, Glasgow G12 8QQ, UK

[3]Department of Biological Chemistry, University of Michigan Medical School, Ann Arbor, MI 48109, USA

[4]SynthSys – Systems and Synthetic Biology, Edinburgh EH9 3JD, UK

[5]Cancer Research UK Edinburgh Centre, MRC Institute of Genetics & Molecular Medicine, University of Edinburgh, Western General Hospital, Edinburgh EH4 2XR, UK

[6]Université de Lille, INSERM, CHU Lille, Institut Pasteur de Lille, U101-EGID, 59000, Lille, France

[7]Physiogenex S.A.S, Prologue Biotech, 516 rue Pierre et Marie Curie, 31670 Labège, France

[8]College of Medicine & Veterinary Medicine, University of Edinburgh, Old Medical School (Anatomy), Teviot Place, Edinburgh EH8 9AG, UK

[9]Department of Chemistry, POSTECH, 77 Cheongam-Ro, Nam-Gu, Pohang, Gyungbuk 37673, South Korea

[10]School of Chemistry, Joseph Black Building, University of Glasgow, Glasgow G12 8QQ, UK

[11]Present address: Cambridge Biomedical Campus, Royal Papworth Hospital NHS Foundation Trust, Cardiology Department, Cambridge CB2 0AY, UK

[12]Present address: The International Clinical Research Centre, St. Anne's University Hospital, Brno 656 91, Czech Republic

[13]Present address: Institute for Integrative Biology of the Cell (I2BC), CEA, CNRS, Univ. Paris-Sud, Université Paris-Saclay, 91198 Gif-sur-Yvette Cedex, France

[14]Present address: BD Research Centre Ireland, Co. Limerick, Castletroy, Ireland

[15]Present address: Rapid Novor Inc., 44 Gaukel St., Kitchener, ON N2G 4P3, Canada

[16]Present address: Wellcome Trust Centre for Mitochondrial Research, Newcastle University, Newcastle NE2 4HH, UK

[17]Present address: Springer Nature Campus, London N1 9FN, UK

[18]Present address: D.I.V.A-expertise, 1 place Pierre Potier, 31100 Toulouse, France

[19]Present address: Institute of Advanced Studies and Research, JIS University, Kolkata 700091, India

[20]Present address: Cancer Research UK Barts Centre, London EC1M 6BQ, UK

[21]Lead contact

*Correspondence: nik.morton@ed.ac.uk

https://doi.org/10.1016/j.celrep.2021.109958

SUMMARY

Impaired hepatic glucose and lipid metabolism are hallmarks of type 2 diabetes. Increased sulfide production or sulfide donor compounds may beneficially regulate hepatic metabolism. Disposal of sulfide through the sulfide oxidation pathway (SOP) is critical for maintaining sulfide within a safe physiological range. We show that mice lacking the liver- enriched mitochondrial SOP enzyme thiosulfate sulfurtransferase (*Tst*$^{-/-}$ mice) exhibit high circulating sulfide, increased gluconeogenesis, hypertriglyceridemia, and fatty liver. Unexpectedly, hepatic sulfide levels are normal in *Tst*$^{-/-}$ mice because of exaggerated induction of sulfide disposal, with associated suppression of global protein persulfidation and nuclear respiratory factor 2 target protein levels. Hepatic proteomic and persulfidomic profiles converge on gluconeogenesis and lipid metabolism, revealing a selective deficit in medium-chain fatty acid oxidation in *Tst*$^{-/-}$ mice. We reveal a critical role of TST in hepatic metabolism that has implications for sulfide donor strategies in the context of metabolic disease.

INTRODUCTION

The prevalence of type 2 diabetes (T2D) continues to soar in parallel with that of obesity (World Health Organization, 2016). Increased hepatic glucose production and aberrant hepatic lipid metabolism are cardinal features of T2D (Consoli et al., 1989; Lewis et al., 2002). Dysregulation of hepatic nutrient metabolism in T2D is a promising area for therapeutic intervention because it precipitates the more severe liver pathologies that manifest along the spectrum of non-alcoholic fatty liver disease (NAFLD),

CellPress
OPEN ACCESS

Cell Reports
Article

steatosis, steatohepatitis, and hepatocellular carcinoma (Caron et al., 2011).

Hydrogen sulfide (hereafter referred to as sulfide), an endogenously produced gaseous signaling molecule (Abe and Kimura, 1996; Wang, 2012; Mishanina et al., 2015; Filipovic et al., 2017), has recently emerged as a modulator of nutrient metabolism (Desai et al., 2011; Szabo, 2011; Hine et al., 2015; Carter and Morton, 2016). Enzymatic sulfide production from sulfur amino acids is catalyzed by cystathionine beta synthase (CBS), cystathionine gamma lyase (CTH) (Chen et al., 2004; Singh et al., 2009), and 3-mercaptopyruvate sulfurtransferase (MPST) (Shibuya et al., 2009; Mikami et al., 2011; Yadav et al., 2013). Thioredoxin-mediated reduction of cysteine persulfides on proteins also regulates free sulfide and cysteine persulfide levels (Wedmann et al., 2016). Endogenously produced and exogenously administered sulfide specifically influences hepatic glucose and lipid metabolism (Mani et al., 2014; Pichette and Gagnon, 2016). Thus, *in vitro*, treatment of murine hepatocytes with sodium hydrosulfide (NaHS), or overexpression of rat *Cth* in HepG2 liver cells increased glucose production through increased gluconeogenesis and reduced glycogen storage (Zhang et al., 2013). Conversely, glucose production was lower in hepatocytes from *Cth* gene knockout ($Cth^{-/-}$) mice, which exhibit low sulfide production (Zhang et al., 2013). Elevation of sulfide with NaHS administration *in vivo* reduced cholesterol and triglyceride accumulation in the liver of high-fat diet (HFD)-fed mice (Wu et al., 2015). In contrast, inter-crossing of sulfide production-deficient $Cth^{-/-}$ mice with the hyperlipidemic $Apoe^{-/-}$ mouse strain ($Cth^{-/-}Apoe^{-/-}$) produced a phenotype of elevated plasma cholesterol following exposure to an atherogenic diet (Mani et al., 2013). Consistent with their higher cholesterol, $Cth^{-/-}Apoe^{-/-}$ mice developed fatty streak lesions earlier than $Apoe^{-/-}$ mice, and this effect was reversed by NaHS administration (Mani et al., 2013). Sulfide may also indirectly affect hepatic nutrient metabolism through its effect on hepatic artery vasorelaxation and, thus, liver perfusion (Fiorucci et al., 2005; Distrutti et al., 2008). The apparently beneficial effects of sulfide administration in multiple disease indications has led to a major drive toward development of targeted H_2S donor molecules as a therapeutic approach (Whiteman et al., 2011; Sestito et al., 2017). However, an often overlooked aspect of net sulfide exposure, key to the efficacy of therapeutic H_2S donors, is that it is regulated through its oxidative disposal. Thus, endogenous sulfide exposure is actively limited to prevent mitochondrial respiratory toxicity (Reiffenstein, 1992; Tiranti et al., 2009; Libiad et al., 2018). Sulfide is oxidized rapidly (Hildebrandt and Grieshaber, 2008; Norris et al., 2011) through the mitochondrial sulfide oxidation pathway (SOP), consisting of sulfide quinone oxidoreductase (SQOR), persulfide dioxygenase (ETHE1/PDO), and thiosulfate sulfurtransferase (TST; also known as rhodanese) (Hildebrandt and Grieshaber, 2008; Jackson et al., 2012; Libiad et al., 2014). The liver is highly abundant in SOP enzymes and is a major organ of whole-body sulfide disposal (Norris et al., 2011). Mice lacking the *Ethe1* gene ($Ethe1^{-/-}$) die of fatal sulfide toxicity (Tiranti et al., 2009), consistent with its critical role in sulfide oxidation and the severe pathological consequences of unchecked sulfide buildup in tissues. However, the importance of mitochondrial TST in the SOP *in vivo* remains obscure. In contrast to $Ethe1^{-/-}$ mice, $Tst^{-/-}$ mice were grossly normal despite exhibiting substantially elevated blood sulfide levels, as implied by qualitative measures (Morton et al., 2016). This revealed an important but distinct role of TST in the SOP *in vivo*. Nevertheless, $Tst^{-/-}$ mice showed an apparently diabetogenic impairment of glucose tolerance (Morton et al., 2016), consistent with the concept that increased sulfide promotes hepatic glucose production (Zhang et al., 2013). Because *Tst* deficiency is a model of chronic but viable sulfide elevation, determining the molecular mechanisms driving the aberrant metabolic profile can provide important insights into the optimal range for therapeutic sulfide exposure, particularly in light of the current interest in developing mitochondrially targeted sulfide donors (Gerő et al., 2016; Karwi et al., 2018). To this end, we sought to define the effect of *Tst* deficiency on the underlying molecular pathways that affect hepatic metabolism.

RESULTS

$Tst^{-/-}$ mice exhibit increased hepatic gluconeogenesis and dyslipidemia despite mild peripheral insulin sensitization

TST mRNA expression is highest in the liver (http://biogps.org/#goto=genereport&id=22117; tissue hierarchy of expression was validated in our own mouse substrain; Figure S1A). We therefore hypothesized that liver TST deficiency was the principal driver of the impaired glucose tolerance observed previously in $Tst^{-/-}$ mice (Morton et al., 2016). $Tst^{-/-}$ mice exhibited higher glucose levels than C57BL/6J controls in response to pyruvate challenge, consistent with higher hepatic glucose production (Figure 1A). We next tested phosphoenolpyruvate carboxykinase (PEPCK) activity, a key enzyme of *de novo* hepatic glucose synthesis, and found that it was higher in liver homogenates from $Tst^{-/-}$ mice (Figure 1B). Next we performed a 1-h $^{13}C_3$-pyruvate metabolite pulse incorporation experiment in isolated hepatocytes cultured in $^{12}C_3$-pyruvate-free medium. Hepatocytes from $Tst^{-/-}$ mice displayed ^{13}C labeling consistent with increased metabolism of pyruvate to oxaloacetate, a critical early step in gluconeogenesis. Specifically, aspartate, which is derived from pyruvate via oxaloacetate, was increased significantly in $Tst^{-/-}$ hepatocytes (Figure 1C). A trend toward higher $^{13}C_3$ malate and lower $^{13}C_2$ acetyl-coenzyme A (CoA) was also observed (Figures S1B and S1C). $^{13}C_3$ lactate was similar between genotypes, suggesting a similar activity of glycolytic disposal of pyruvate through lactate dehydrogenase (Figures S1B and S1C). Isotopologue distribution is shown in Figure S1C. Total pool sizes for all measured metabolites were similar between genotypes (Figure S1D). Although not a direct measure of glucose production, the data from *in vitro* hepatocytes suggested skewing of hepatocyte metabolism toward gluconeogenesis, and we therefore investigated this possibility. Indeed, consistent with increased endogenous glucose production in $Tst^{-/-}$ mice, fasting plasma glucose was higher in $Tst^{-/-}$ mice relative to 6J mice during the pre-clamp 3-^{3}H glucose tracer infusion phase (60–90 min after the tracer) of euglycemic, hyperinsulinemic (EH) clamp experiments (Figure 1D; Table S1A). Higher plasma glucose levels in $Tst^{-/-}$ mice under these conditions was not explained by lower glucose utilization in $Tst^{-/-}$ mice; glycogen synthesis and glycolysis were comparable between

Cell Reports
Article

CellPress
OPEN ACCESS

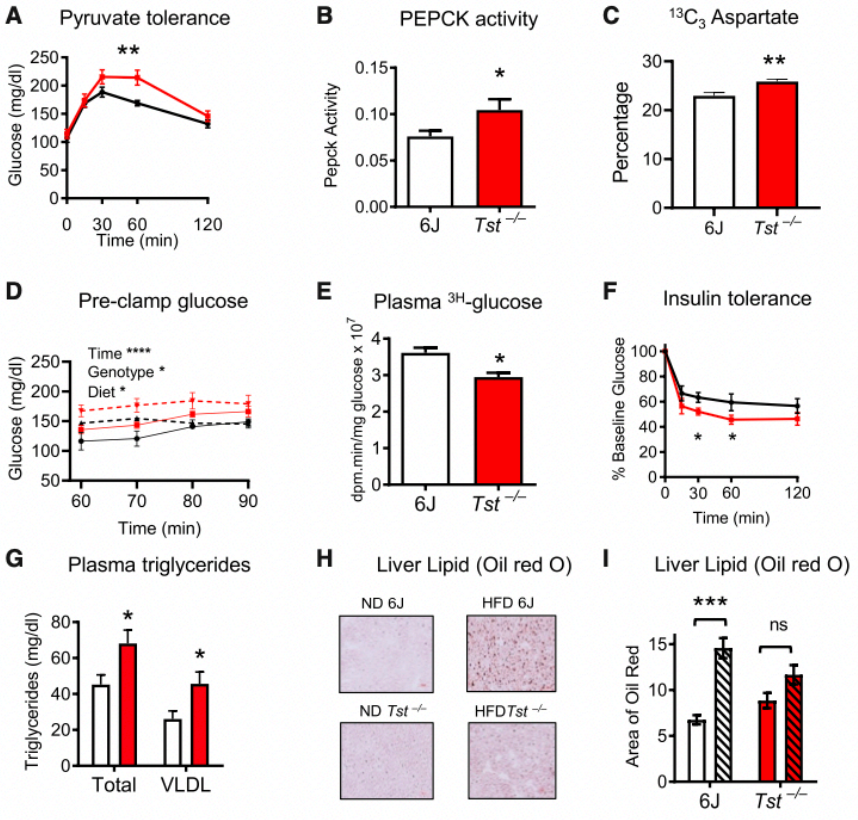

Figure 1. *Tst* deletion results in impaired glucose and lipid metabolism

(A) Plasma glucose over 120 min, following pyruvate (i.p., 1.5 mg/g) administration in overnight-fasted C57BL/6J (black line, n = 9) and *Tst*$^{-/-}$ (red line, n = 8) ND-fed mice.

(B) Extinction of NADH, measured by absorbance at 340 nm, coupled to PEPCK activity from liver homogenates taken from C57BL/6J (white bar, n = 6) and *Tst*$^{-/-}$ (red bar, n = 6) ND-fed mice.

(C) Production of ^{13}C (M+3) aspartate generated after a 1-h pulse of 1 mM 3-carbon labeled ^{13}C (M+3) pyruvate in ^{12}C pyruvate-free medium, expressed as a percentage of the total amount of detected metabolite, in primary hepatocytes from C57BL/6J (white bars, n = 6) and *Tst*$^{-/-}$ (red bars, n = 5) ND-fed mice.

(D) Blood glucose during the pre-clamp phase of the EH clamp from C57BL/6J (black lines) and *Tst*$^{-/-}$ (red lines) mice fed a control (ND, solid lines, n = 3, 6) or high-fat diet (HFD, broken lines, n = 6, 7).

(E) Mean integrated radioactive glucose (inversely related to whole-body glucose uptake) during a EH clamp from ND-fed C57BL/6J control (white, n = 3) and *Tst*$^{-/-}$ (red, n = 6) mice.

(F) Plasma glucose, expressed as percent of baseline glucose, over 120 min following insulin (i.p., 1 mU/g) administration in 4-h-fasted C57BL/6J (black line, n = 8) and *Tst*$^{-/-}$ (red line, n = 7) ND-fed mice.

(G) HPLC-quantified total and VLDL plasma triglyceride in 4-h-fasted C57BL/6J (white bar, n = 6) and *Tst*$^{-/-}$ (red bar, n = 6) ND-fed mice.

(H) Representative light microscopy images of liver sections stained with oil red O from normal diet (ND)-fed or HFD-fed C57BL/6J and *Tst*$^{-/-}$ mice. Magnification is 40X.

(I) Analysis of the area of red staining (oil red O) after thresholding, using ImageJ, from ND-fed (no pattern, n = 3–4/genotype) or HFD-fed (hatched pattern, n = 4–5/genotype) C57BL/6J (white bars) and *Tst*$^{-/-}$ (red bars) mice.

Data are represented as mean ± SEM. Significance was calculated using repeated-measures ANOVA (A and F), 2-way ANOVA (I), 3-way repeated-measures ANOVA (D), or unpaired two-tailed Student's t test (B, C, E, and G); *p < 0.05, **p < 0.01, ***p < 0.001, ****p < 0.0001. For (D), significant effects of time (****), diet (*) and genotype (*) were found. For (F), the analysis was performed on absolute glucose values and demonstrated a significant effect of time (****) and an interaction between time and genotype (*). t tests revealed that the decrement of glucose from baseline 30 and 60 min after insulin was greater in *Tst*$^{-/-}$ mice (*). For (I), no main genotype effect was found, but a significant effect of diet (***) and an interaction (*) were found. Post hoc analysis using Sidak's multiple comparison test shows an effect of diet on the 6J controls (***), whereas no effect of diet is found on *Tst*$^{-/-}$ mice. See also Figures S1 and S2 and Table S1.

genotypes across 60–90 min (Table S1A). Glucose turnover, a derived parameter used to infer glucose production, was also comparable between genotypes (Table S1A). However, derivation of glucose turnover requires that glucose levels are stable during the period in which it is calculated. In our pre-clamp baseline period, a highly significant effect of time (Figure 1D) indicated that this assumption was not met; thus, true endogenous glucose production cannot be inferred from the glucose turnover parameter in this instance. Combined with the pyruvate tolerance, PEPCK activity, and $^{13}C_3$-pyruvate pulse data, higher fasting glucose levels in *Tst*$^{-/-}$ mice, given comparable glucose utilization, are most likely due to higher endogenous glucose production.

We next wished to explore whether the changes to glucose metabolism were driven by insulin resistance. Liver glycogen, a marker of long-term carbohydrate storage typically impaired with insulin resistance, was comparable between *Tst*$^{-/-}$ and C57BL/6J control mice (Figure S2A). Despite unchanged steady-state markers of hepatic insulin sensitivity, impaired glucose tolerance, described previously in *Tst*$^{-/-}$ mice (Morton et al., 2016), suggested that whole-body, and usually hepatic, insulin resistance was present. We investigated this using the euglycemic clamp, where, unexpectedly, we observed whole-body insulin sensitization under these short-term steady-state conditions. During the clamp, when insulin was high and blood glucose levels were maintained constant, the glucose infusion rate was comparable between genotypes (Table S1B). However, an increase in whole-body glucose uptake (integral glucose) by tissues in *Tst*$^{-/-}$ mice was apparent (Figure 1E; Table S1B), supporting increased peripheral insulin sensitivity, with a directionally consistent trend for increased glucose uptake into several tissues. We confirmed this finding using standard insulin tolerance tests, where the glucose decrement in response to insulin was greater in *Tst*$^{-/-}$ mice (Figure 1F; Figure S2B). These data demonstrate a net increase in dynamic whole-body insulin sensitivity despite increased hepatic glucose output in *Tst*$^{-/-}$ mice. Finally, we assessed whole-body glucose homeostasis with the EH clamp method after chronic HFD feeding. Under these

CellPress
OPEN ACCESS

Cell Reports
Article

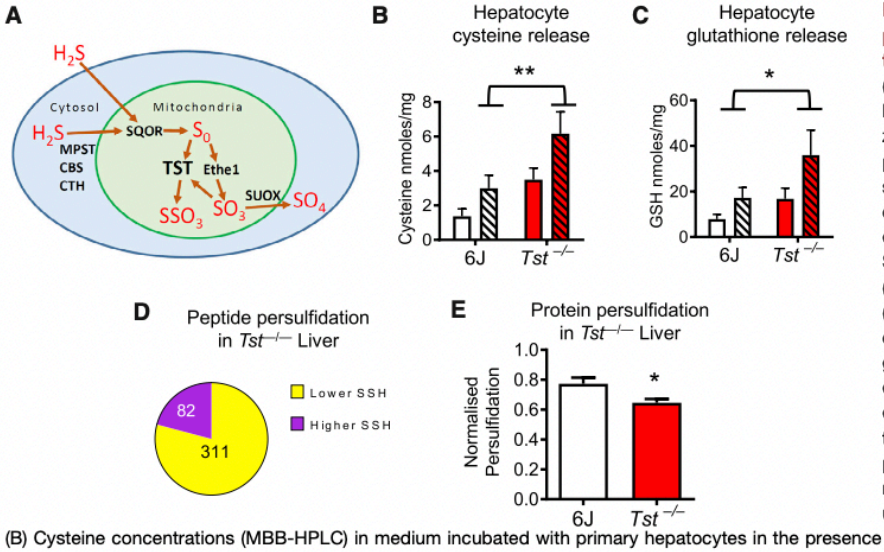

Figure 2. *Tst* deletion results in increased hepatic sulfur excretion and a reduction of protein persulfidation

(A) Schematic showing mammalian metabolism of hydrogen sulfide. The canonical production enzymes are shown in the cytosol. MPST, mercaptopyruvate sulfurtransferase; CBS, cystathionine beta synthase; CTH, cystathionine gamma lyase. Mitochondrial oxidation and disposal of hydrogen sulfide occurs through the SOP through the actions of SQOR (sulfide quinone oxidoreductase), ETHE1 (PDO), TST (thiosulfate sulfurtransferase), and SUOX (sulfite oxidase). These seven enzymes are major contributors to intracellular sulfide (and other inorganic sulfur) metabolism. For simplicity, the diagram does not include sulfide production, which can occur within mitochondria, or disposal pathways in the cytosol. The identity of oxidized sulfur species produced by SQOR remain disputed. The precise role of TST and other enzymes shown here remains under investigation.

(B) Cysteine concentrations (MBB-HPLC) in medium incubated with primary hepatocytes in the presence (hatched pattern) or absence (no pattern) of 1 mM methionine from C57BL/6J (white bars, n = 4/treatment) and *Tst*$^{-/-}$ (red bars, n = 4/treatment) mice.

(C) GSH concentrations (MBB-HPLC) in medium incubated with primary hepatocytes in the presence (hatched pattern) or absence (no pattern) of 1 mM methionine from C57BL/6J (white bars, n = 4/treatment) and *Tst*$^{-/-}$ (red bars, n = 4/treatment) mice.

(D) Pie chart depicting the proportion of liver peptides that are significantly higher (82 peptides, purple space) or lower (311 peptides, yellow space) in their persulfidation rate in *Tst*$^{-/-}$ (n = 3) relative to C57BL/6J (n = 3) mice.

(E) Total DTT-released cysteine-persulfidated liver protein as measured by REVERT total protein stain following western blotting, normalized to the total input protein of the sample from *Tst*$^{-/-}$ (red bar, n = 4) and C57BL/6J (white bar, n = 4) mice.

Data with error bars are represented as mean ± SEM. Significance was calculated using 2-way ANOVA (B and C) or Student's t test (E); *p < 0.05, **p < 0.01. For (B) and (C), the 2-way ANOVA reveals a main effect of genotype, indicated by * or ** on the histogram. A significant effect of methionine was also found for (B) and (C), not indicated on the histogram. For (D), peptides were selected as being significant at a P-diff of 0.95 or greater. See also Figure S3 and Table S2.

conditions, *Tst*$^{-/-}$ mice maintained increased hepatic glucose output (Figure 1D) but showed convergence of the insulin sensitivity profile with that of insulin-resistant C57BL/6J mice.

We also assessed whether *Tst* deficiency was associated with impaired lipid metabolism, another hallmark of diabetes. Fast protein liquid chromatography analysis of triglyceride levels and their lipoprotein distribution revealed significantly higher total plasma triglycerides in *Tst*$^{-/-}$ mice (Figure 1G). The higher triglyceride was selectively associated with an increased very low density lipoprotein (VLDL) triglyceride fraction (Figure 1G), consistent with a dominant liver-driven impairment in lipid metabolism (Mason, 1998). Total and distinct lipoprotein fraction plasma cholesterol levels were similar between genotypes (Figures S2C and S2D), suggestive of a triglyceride-selective effect of *Tst* deficiency on hepatic lipid efflux. HFD feeding significantly increased the liver lipid content of C57BL/6J mice but did not further increase the elevated lipid levels in the liver of *Tst*$^{-/-}$ mice (Figures 1H and 1I).

TST deficiency elicits compensatory hepatic sulfide disposal mechanisms that drive reduced global protein persulfidation

A role of TST in disposal of sulfide has been suggested by its participation in the SOP (Hildebrandt and Grieshaber, 2008; Libiad et al., 2014) and supported *in vivo* by the qualitatively higher blood sulfide of *Tst*$^{-/-}$ mice (Morton et al., 2016), shown schematically in Figure 2A. Here we quantified circulating sulfide, showing an approximately 10-fold elevation in the blood and plasma of *Tst*$^{-/-}$ mice (Table 1). Thiosulfate, an oxidized metabolite of sulfide (Vitvitsky et al., 2015, 2017) and a TST substrate (Banerjee et al., 2015), was approximately 20-fold higher in the plasma (Table 1) and profoundly higher (450-fold) in the urine (Table 1) of *Tst*$^{-/-}$ mice compared with C57BL/6J mice. Reduced glutathione (rGSH) levels were ~2-fold higher in the plasma of *Tst*$^{-/-}$ mice (Table 1). To determine any direct hepatic contribution to the elevated systemic sulfide *in vivo*, whole blood was sampled from the inferior vena cava (IVC) (Table 1). IVC sulfide levels tended to be higher in *Tst*$^{-/-}$ mice, but the magnitude of the increase (~3-fold) did not parallel that in trunk blood (~10-fold), suggesting that the liver was not a major source of the elevated circulating sulfide. Surprisingly, liver homogenate sulfide, thiosulfate, cysteine, and GSH levels were similar between *Tst*$^{-/-}$ and C57BL/6J mice (Table 1). Further, cultured hepatocytes from *Tst*$^{-/-}$ and C57BL/6J mice exhibited similar intracellular sulfide levels, as estimated using P3, a sulfide-selective fluorescent probe (Singha et al., 2015; Table 1). Mitochondrial sulfide levels in the liver, reported by MitoA/MitoN (Arndt et al., 2017), were similarly unchanged between genotypes (Table 1). The apparently unaltered hepatic steady-state sulfide levels, despite higher circulating sulfide, suggested that a profound homeostatic mechanism was invoked in the liver of *Tst*$^{-/-}$ mice. We assessed respiratory sulfide disposal (antimycin sensitive) and found that this was increased markedly in hepatocytes from *Tst*$^{-/-}$ mice, whereas antimycin-insensitive sulfide disposal was relatively reduced compared with hepatocytes from C57BL/6J mice (Table S2). Isolated liver mitochondria from *Tst*$^{-/-}$ hepatocytes also exhibited a higher sulfide disposal rate (Table S2). In addition, cysteine and GSH were excreted at higher

Cell Reports
Article

CellPress
OPEN ACCESS

Table 1. Sulfur species in blood, urine, tissue, and cells

C57BL/6J		$Tst^{-/-}$	$Tst^{-/-}$/6J ratio	Significance
Trunk blood (micromolar)[a]				
MBB-S (sulfide)	2.28 ± 0.43	22.18 ± 0.85	9.73	****
MBB-SSO3 (thiosulfate)	N/D	6.25 ± 3.17	n.c.	ns
Trunk plasma (micromolar)[b]				
MBB-S (sulfide)	1.88 ± 0.64	24.50 ± 2.02	13.03	****
MBB-SSO3 (thiosulfate)	3.99 ± 0.99	80.29 ± 13.6	20.12	**
MBB-GSH (reduced GSH)	48.0 ± 1.15	86.25 ± 6.27	1.80	***
Urine (micromoles/creatine/24 h)[c]				
MBB-SSO3 (thiosulfate)	4.99 ± 2.6	2374 ± 319	475.75	****
IVC (micromolar)[d]				
MBB-S (sulfide)	1.22 ± 0.20	3.58 ± 0.87	2.93	ns (0.08)
MBB-SSO3 (thiosulfate)	6.58 ± 4.51	88.3 ± 13.0	13.42	*
Liver (micromoles/kg wet liver)[e]				
MBB-S (sulfide)	13 ± 1	17 ± 3	1.31	ns
MBB-SSO3 (thiosulfate)	4 ± 1	15 ± 7	3.75	ns
DNFB-GSH (reduced GSH)	6,470 ± 380	6,850 ± 30	1.04	ns
DNFB-cysteine (cysteine)	82 ± 13	67 ± 11	0.82	ns
Sulfide P3 fluorescence (A510 nm/protein)[f]				
Hepatocyte	7.22 ± 1.00	7.89 ± 0.80	1.09	ns
Mitochondrial sulfide (MitoA)[g]				
Liver	0.78 ± 0.16	1.14 ± 0.45	1.46	ns

Tst deletion results in altered sulfur metabolites in blood and liver. Data are represented as mean ± SEM. Significance was calculated using unpaired two-tailed Student's t test. *p < 0.05, **p < 0.01, ***p < 0.001, ****p < 0.0001. MMB; monobromobimane.
[a]Sulfide dibimane and thiosulfate-MBB, measured by fluorescence detection following HPLC, from whole blood taken from trunk blood of ND-fed C57BL/6J (n = 4) and $Tst^{-/-}$ (n = 4) mice.
[b]Sulfide dibimane, thiosulfate-MBB, and rGSH-MBB, measured by fluorescence detection following HPLC, from EDTA-plasma of ND-fed C57BL/6J (n = 4) and $Tst^{-/-}$ (n = 4) mice.
[c]Thiosulfate-MBB corrected for creatinine from 24-h urine samples, taken from ND-fed C57Bl6/J (n = 4) and $Tst^{-/-}$ (n = 5) mice.
[d]Sulfide dibimane and thiosulfate-MBB from whole blood taken from the IVC downstream of the hepatic vein of ND-fed C57BL/6J (n = 3) and $Tst^{-/-}$ (n = 3) mice.
[e]Sulfide dibimane, thiosulfate-MBB, rGSH-MBB, and cysteine-MBB from whole liver (n = 4/genotype) of ND-fed C57BL/6J (n = 4) and $Tst^{-/-}$ (n = 4) mice.
[f]Fluorescence from cultured hepatocytes following incubation with P3 (sulfide reactive probe) from ND-fed C57BL/6J (n = 4) and $Tst^{-/-}$ (n = 4) mice.
[g]Ratio of MitoN/MitoA from the liver of ND-fed C57BL/6J (n = 5) and $Tst^{-/-}$ (n = 5) mice.

levels from $Tst^{-/-}$ hepatocytes under basal conditions and after stimulation of sulfur amino acid metabolism by addition of methionine (Figures 2B and 2C). Consistent with higher GSH turnover, hepatocytes from $Tst^{-/-}$ mice showed resistance to exogenous H_2O_2-mediated mitochondrial reactive oxygen species (ROS) production (Figure S3). We next determined the global hepatic protein persulfidation profile, the major post-translational modification mediated by sulfide (Krishnan et al., 2011; Kabil et al., 2014; Koike et al., 2017). Mass spectrometry analysis of maleimide-labeled liver peptides revealed a greater abundance of peptides with a lower persulfidation level (underpersulfidated) in the liver of $Tst^{-/-}$ mice (Figure 2D). We confirmed this using semiquantitative western blot analysis on pulled down maleimide-labeled proteins (Figure 2E). Gene Ontology (GO) analysis of underpersulfidated peptides (20 GO categories; Table 2) showed enrichment for "FAD-binding, methyl transferase, peroxisome, acyl-CoA dehydrogenase activity, and transaminase." Overpersulfidated peptides (8 GO categories; Table 2) were predominantly "nicotinamide metabolism." Pathway-specific peptide analysis showed a bias for over-persulfidation in gluconeogenesis proteins (Figure S4A) and a significantly higher magnitude of change (independent of direction of change) in persulfidation compared with global persulfidomic changes between C57BL/6J and $Tst^{-/-}$ mice (Figure S4B).

The hepatic proteome of $Tst^{-/-}$ mice reveals a distinct molecular signature of altered sulfur and mitochondrial nutrient metabolism

To gain molecular insight into the mechanisms underlying the apparently diabetogenic phenotype in $Tst^{-/-}$ mice, we compared hepatic proteomes of normal diet (ND)-fed mice. Kyoto Encyclopedia of Genes and Genomes (KEGG) analysis revealed 4 up-regulated pathways in the liver of $Tst^{-/-}$ mice related to amino acid metabolism, including sulfur amino acids, and

CellPress
OPEN ACCESS

Cell Reports
Article

Table 2. *Tst* deletion results in differential persulfidation rate of liver proteins

GO ID	Name	Direction ($Tst^{-/-}$ versus 6J)	Genes
GO terms identified by log fold change			
0050660	FAD binding	decreased	12
0008168	methyltransferase activity	decreased	9
			9
0016741	transferase activity, transferring one-carbon groups	decreased	9
0008565	protein transporter activity	decreased	8
0008238	exopeptidase activity	decreased	7
0005777	peroxisome	decreased	7
0042579	microbody	decreased	7
0003995	acyl-CoA dehydrogenase activity	decreased	6
0008483	transaminase activity	decreased	6
0016769	transferase activity, transferring nitrogenous groups	decreased	6
0008757	S-adenosylmethionine-dependent methyltransferase activity	decreased	6
0016655	oxidoreductase activity, acting on NADH/ NADPH, quinone	decreased	5
0004177	aminopeptidase activity	decreased	5
0000059	protein import into nucleus, docking	decreased	3
0005643	nuclear pore	decreased	3
0031965	nuclear membrane	decreased	3
0044453	nuclear membrane part	decreased	3
0046930	pore complex	decreased	3
0015629	actin cytoskeleton	decreased	3
0016652	oxidoreductase activity, NADH/NADPH, NAD/NADP acceptor	decreased	3
0050662	coenzyme binding	increased	5
			5
			4
			4
			4
			3
			3
0016651	oxidoreductase activity, NADH/NADPH,	increased	5
0003954	NADH dehydrogenase activity	increased	4
0008137	NADH dehydrogenase (ubiquinone) activity	increased	4
0050136	NADH dehydrogenase (quinone) activity	increased	4
0006739	NADP metabolism	increased	3
0006769	nicotinamide metabolism	increased	3
0006733	oxidoreduction coenzyme metabolism	increased	3

Shown are significant GO terms represented by peptides with different persulfidation rates in ND-fed $Tst^{-/-}$ mouse liver relative to C57BL/6J mice. "Direction" indicates whether persulfidation is decreased or increased in $Tst^{-/-}$ relative to C57BL/6J mice. "Genes" indicates the number of genes in $Tst^{-/-}$ mice that represent the changes driving the GO term.

sulfur metabolism (Table 3). GO analysis revealed 95 significantly up-regulated categories in the liver of $Tst^{-/-}$ mice (Table S3A). Among the top categories, 7 referred to amino acid metabolism and 1 referred to the organellar term "mitochondrion." KEGG analysis revealed 27 down-regulated pathways in the liver of $Tst^{-/-}$ mice (Table 3), including phase 1 and 2 detoxification pathways (cytochrome P450s, GSH, and glucuronidation) and "lysosome" and "protein processing in the endoplasmic reticulum" organellar terms. 213 GO terms were significantly down-regulated in $Tst^{-/-}$ mice (Table S4B). Among the most significant down-regulated terms were phase 2 detoxification "glutathione binding," "glutathione transferase activity," and "endoplasmic

Cell Reports
Article

CellPress
OPEN ACCESS

Table 3. Protein abundance and persulfidation in ND-fed *Tst*$^{-/-}$ liver

Entry	Name	Genes	Significance
KEGG pathways increased in ND *Tst*$^{-/-}$ liver[a]			
00250	alanine, aspartate, and glutamate metabolism	6	***
00260	glycine, serine, and threonine metabolism	5	**
00270	cysteine and methionine metabolism	4	*
04122	sulfur relay system	2	*
KEGG pathways reduced in ND *Tst*$^{-/-}$ liver[b]			
00980	metabolism of xenobiotics by cytochrome P450	12	****
00982	drug metabolism – cytochrome P450	12	****
05204	chemical carcinogenesis	12	****
00480	glutathione metabolism	8	***
00040	pentose and glucoronate interconversions	5	**
04142	lysosome	6	**
04390	Hippo signaling pathway	4	**
00500	starch and sucrose metabolism	5	**
05215	prostate cancer	3	**
04024	cAMP signaling pathway	4	*
04141	protein processing in ER	9	*
05211	renal cell carcinoma	3	*
00830	retinol metabolism	6	*
00053	ascorbate and aldarate metabolism	4	*
00860	porphyrin and chlorophyll metabolism	4	*
04722	neurotrophin signaling pathway	3	*
04670	leukocyte transendothelial migration	4	*
04010	MAPK signaling pathway	4	*
04720	long-term potentiation	2	*
04914	progesterone-mediated oocyte maturation	2	*
04062	chemokine signaling pathway	3	*
04110	cell cycle	3	*
04015	Rap1 signaling pathway	4	*
00983	drug metabolism – other enzymes	5	*
04918	thyroid hormone synthesis	3	*
04612	antigen processing and presentation	3	*
05203	viral carcinogenesis	5	*
GO terms common to persulfidome and proteome in ND *Tst*$^{-/-}$ liver[c]			
GO ID	GO term	Persulfidation (Tst−/− versus 6J)	Abundance (Tst−/− versus 6J)
0008483	transaminase activity	decreased	increased
0016769	transferase activity, transferring nitrogenous groups	decreased	increased
0003995	acyl-CoA dehydrogenase activity	decreased	decreased
0005777	peroxisome	decreased	decreased
0042579	microbody	decreased	decreased

*p < 0.05, **p < 0.01, ***p < 0.001, ****p < 0.0001.
[a]Significant KEGG pathway terms represented by proteins that are more abundant in the liver of ND-fed *Tst*$^{-/-}$ compared with ND-fed C57BL/6J mice.
[b]Significant KEGG pathway terms represented by proteins that are less abundant in the liver of ND-fed *Tst*$^{-/-}$ compared with ND-fed C57BL/6J mice. "Genes" indicates the number of genes in *Tst*$^{-/-}$ mice that represent the changes driving the KEGG pathway.
[c]GO terms that are significantly regulated at the level of cysteine persulfidation and protein abundance in the liver of ND-fed *Tst*$^{-/-}$ compared with ND-fed C57BL/6J mice.

CellPress
OPEN ACCESS

Cell Reports
Article

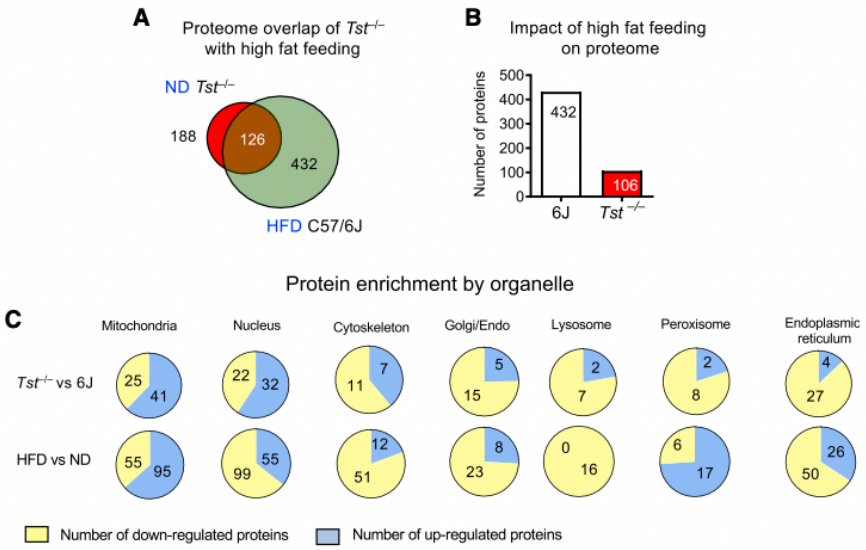

Figure 3. *Tst* deletion engenders a HFD feeding-like hepatic proteome with a distinct organellar signature

(A) Venn diagram representing the number of proteins significantly different (at $p < 0.01$) between ND-fed $Tst^{-/-}$ and C57BL/6J mice (red circle) and the number of regulated proteins between HFD-fed and ND-fed C57BL/6J (green circle) mice. The overlap (brown) represents proteins regulated in the same direction by both comparisons (n = 4/genotype).

(B) Number of proteins significantly different (at $p < 0.01$) between 58% HFD and ND in either C57BL/6J (white bar) or $Tst^{-/-}$ mice (red bar) (n = 4/genotype).

(C) Pie charts depicting the proportion of individual liver proteins that are upregulated (blue space) compared with downregulated (yellow space) after GO term categorization according to subcellular location. Top row: ND-fed $Tst^{-/-}$ relative to ND-fed C57BL/6J mice. Bottom row, HFD-fed C57BL/6J relative to ND-fed C57BL/6J mice. See also Table 3 and Figures S5 and S6.

reticulum" categories. We validated the broadly consistent direction of change in a representative subset of proteins (Figures S5A and S5D). The most robust change we observed was increased MPST protein in whole liver (Figures S5A and S5D) and mitochondrial subfractions (Figures S5B and S5D). This change was remarkable because mRNA levels for *Mpst* were lower in $Tst^{-/-}$ mice (Figure S5C), likely as a result of loss of proximal *Mpst* promoter function; *Mpst* is a paralog of *Tst* (Nagahara, 2011) juxtaposed approximately 1 kb from the *Tst* gene. Protein levels for other sulfide-producing and disposal enzymes were comparable between genotypes (Table S4). A focused comparison of canonical proteins in glucose and lipid metabolism pathways (Table S5) revealed four GO categories that were down-regulated in $Tst^{-/-}$ mice: "lipid metabolic process," "fatty acid beta-oxidation," "acyl-CoA dehydrogenase activity," and "acyl-CoA hydrolase activity" (Table S5). Canonical insulin-regulated proteins were largely comparable between genotypes (Table S6).

Hepatic protein expression in $Tst^{-/-}$ mice is consistent with lower NRF2 activation

We performed a transcription factor binding site (TFBS) enrichment analysis in the promoters of proteins that were up-regulated in the liver of $Tst^{-/-}$ mice to look for potential hub transcriptional drivers of the proteome profile (Figure S6A). This revealed a statistically significant under-representation of TFBS for the sulfide-responsive (Yang et al., 2013; Xie et al., 2016) NRF2 transcription factor (Figure S6A). Consistent with reduced hepatic NRF2 activation, 10 of 47 known NRF2-regulated proteins were lower in the liver of ND-fed $Tst^{-/-}$ mice compared with C57BL/6J mice (Figure S6B).

The proteome of TST deficiency versus HFD response in C57BL/6J mice reveals distinct regulation of lipid metabolism, sulfide metabolism, and detoxification pathways

We examined mechanistic commonalities between the diabetogenic hepatic phenotype of $Tst^{-/-}$ mice and that induced by the diabetogenic HFD feeding regimen in C57BL/6J mice. ND-fed $Tst^{-/-}$ mice were in a pre-existing diabetogenic state (Figure 1) that does not worsen with HFD feeding (Figures 1H and 1I; Table S1), suggesting gross phenotypic convergence of the two genotypes after HFD feeding. We compared the identity and direction of change of the 188 proteins differentially expressed in ND-fed $Tst^{-/-}$ mice (versus ND-fed C57BL/6J mice; Figure 3A) with proteins that were differentially expressed in response to HFD feeding in C57BL/6J mice (432 proteins; Figure 3A). There was a striking 67% overlap in individual proteins (126) in this comparison (Figure 3A). When we analyzed these two protein signatures for directionally shared pathways, one upregulated KEGG pathway, "glycine, serine and threonine metabolism" (Table S7A), and 12 downregulated KEGG pathways, including "drug metabolism" and "endoplasmic reticulum" (Table S8B), were common to the liver of ND-fed $Tst^{-/-}$ and HFD-fed C57BL/6J mice. Consistent with a pre-existing HFD-like proteome, the dynamic response to HFD in the liver of $Tst^{-/-}$ mice was muted relative to that observed in C57BL6J mice (106 proteins, a 4-fold lower response; Figure 3B). Focusing on the sulfide pathway, MPST and sulfite oxidase (SUOX) were increased by HFD feeding in C57BL/6J and $Tst^{-/-}$ mice (Table S8). The HFD-induced increase in MPST was less pronounced in the liver of $Tst^{-/-}$ mice, likely reflecting that it is already elevated in ND-fed $Tst^{-/-}$ mice. We then considered contrasting rather than congruent proteomics responses arising from TST deficiency versus HFD responses in C57BL/6J mice to illuminate potential novel pathways underlying the otherwise functionally similar diabetogenic hepatic $Tst^{-/-}$ phenotype. 5 KEGG pathways (Table S9A) and 4 GO terms (Table S9B) were regulated oppositely in this comparison. Strikingly, the GO terms were all related to lipid metabolism, which was up-regulated in the HFD response but down-regulated with TST deficiency (Tables S9A and S9B). An organelle-focused protein analysis showed shared upregulation of mitochondrial and endoplasmic reticulum pathways between TST deficiency (Figure 3C, top row) and C57BL/6J HFD responses (Figure 3C, bottom row) but a striking discordance in peroxisomal protein pathways (upregulated by HFD feeding

Cell Reports
Article

CellPress
OPEN ACCESS

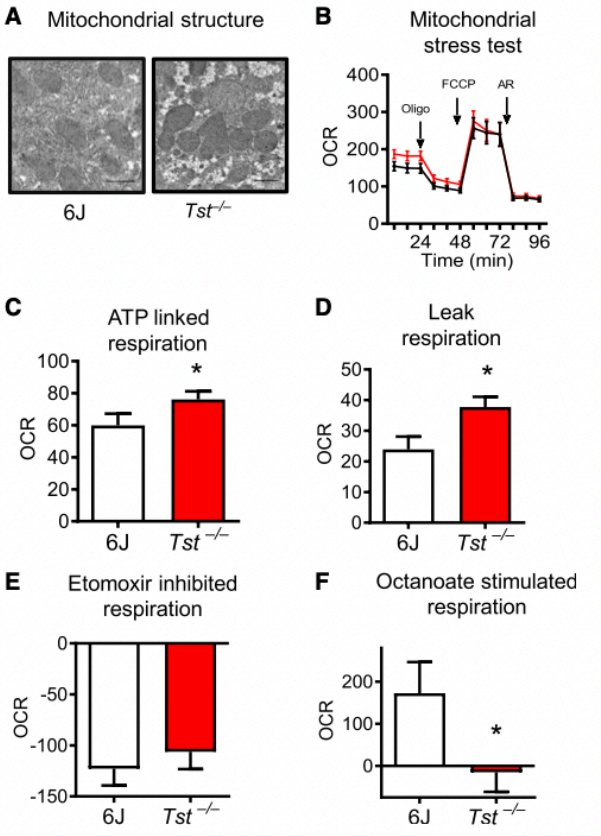

Figure 4. *Tst* deletion results in increased hepatocyte respiration but impaired medium-chain fat respiration

(A) Electron microscopy images of liver, visualizing mitochondria from ND-fed C57BL/6J (n = 4) or *Tst*$^{-/-}$ (n = 4) mice.

(B) Seahorse trace representing the mean oxygen consumption rate (OCR), normalized to protein, by hepatocytes from ND-fed C57BL/6J (n = 6) or *Tst*$^{-/-}$ (n = 6) mice during a mitochondrial stress test.

(C) Respiratory OCR linked to ATP production (oligomycin sensitive) by hepatocytes from ND-fed C57BL/6J (n = 6) or *Tst*$^{-/-}$ (n = 6) mice, calculated from (B).

(D) Respiratory OCR relating to proton leak (oligomycin insensitive) by hepatocytes from ND-fed C57BL/6J (n = 6) or *Tst*$^{-/-}$ (n = 6) mice, calculated from (B).

(E) Reduction of maximal uncoupled respiration following inhibition of LCFA mitochondrial import using etomoxir (8 μM) from ND-fed C57BL/6J (n = 4) or *Tst*$^{-/-}$ (n = 4) mice.

(F) Stimulation of maximal uncoupled respiration following addition of MCFA octanoate (250 μM) from ND-fed C57BL/6J (n = 4) or *Tst*$^{-/-}$ (n = 4) mice.

Data are represented as mean ± SEM. Significance was calculated using an unpaired two-tailed Student's t test (C–F); *p < 0.05. See also Figure S7.

and downregulated with TST deficiency) and nuclear proteins (downregulated by HFD feeding and upregulated with TST deficiency; Figure 3C).

The *Tst*$^{-/-}$ liver proteome and persulfidome converge on transamination and lipid oxidation pathways

To assess whether conservation of changes at the protein and post-translational modification levels can illuminate key regulatory hubs driving the hepatic phenotype, we ran a congruence analysis of the proteome and persulfidome. We found that the GO categories "amino acid," "lipid metabolism," and "peroxisome" were regulated significantly at the protein abundance and persulfidation levels in *Tst*$^{-/-}$ mice (Table 3).

Tst$^{-/-}$ hepatocytes exhibit elevated mitochondrial respiration and a defect in medium-chain fatty acid oxidation

Enhanced respiratory sulfide disposal was found from *Tst*$^{-/-}$ hepatocytes, and enrichment of mitochondrial proteins was suggested from the liver proteome of the *Tst*$^{-/-}$ mice (Table S4). We therefore sought to determine whether TST deficiency affected respiratory function and substrate utilization of the hepatocyte. Analysis of electron micrographs prepared from the liver of ND-fed *Tst*$^{-/-}$ mice and C57BL/6J controls showed morphologically normal mitochondria (Figure 4A). Basal respiration, comprising ATP-linked and leak respiration, was significantly higher in hepatocytes from *Tst*$^{-/-}$ mice (Figures 4B–4D). Maximal hepatocyte respiratory capacity and non-respiratory oxygen consumption were similar between genotypes (Figures S7A and S7B). In line with phenotypic convergence following HFD feeding, hepatocyte respiration was comparable between genotypes from HFD-fed mice (Figures S7C–S7H). A unique feature of the liver from *Tst*$^{-/-}$ mice was a decrease in proteins and persulfidation levels of proteins in lipid oxidation pathways. We therefore investigated hepatocyte respiration of lipids. Using a low-pyruvate (100 μM) medium to reveal respiratory dependency on other substrates, we showed that CPT1A-mediated mitochondrial oxidation of endogenous long-chain fatty acids (LCFAs; etomoxir inhibited) was similar between genotypes (Figure 4E). Next we bypassed CPT1A-mediated LCFA transfer and revealed a marked deficit in respiration stimulated by the medium-chain fatty acid octanoate in hepatocytes from *Tst*$^{-/-}$ mice (Figure 4F). A similar experiment adding back pyruvate revealed comparable stimulation of respiration between genotypes (Figure S7I). In amino acid-free medium, combined glutamine-, aspartate-, and alanine-stimulated hepatocyte respiration was comparable between genotypes (Figure S7J).

DISCUSSION

Elevated TST expression in adipose tissue has been identified as a genetic mechanism driving metabolically protective leanness in mice (Morton et al., 2016). Conversely, *Tst*$^{-/-}$ mice exhibited impaired glucose tolerance (Morton et al., 2016). However, *Tst*$^{-/-}$ mice had a subtle adipose tissue phenotype, suggesting a non-adipose origin for impaired glucose homeostasis. We found increased gluconeogenesis, steatosis, and elevated plasma VLDL triglycerides consistent with a predominantly hepatic origin for the diabetogenic phenotype. We cannot rule out a contribution of renal gluconeogenesis to the phenotype, and future work will address this limitation. Unexpectedly, and despite the markedly increased circulating sulfide levels (10-fold), the steady-state sulfide level was normal in the liver of *Tst*$^{-/-}$ mice. Moreover, we found evidence of multiple mechanisms for increased hepatic sulfide disposal, reduced downstream sulfide signaling, and associated underlying molecular links to an apparently diabetogenic phenotype. Our data suggest that the liver of *Tst*$^{-/-}$ mice has overshot in its attempt to

maximize hepatic sulfide removal, leading indirectly to detrimental metabolic consequences. This involves a combination of distinct compartmentalized cellular responses, including increased respiratory sulfide disposal and export of cysteine and GSH. Upregulation of translation and recruitment of MPST to mitochondria of *Tst*$^{-/-}$ mice is observed. This response, in the face of reduced transcription of *Mpst*, suggests a powerful post-transcriptional cellular sulfide-sensing mechanism. Interestingly, if MPST is compensating for TST-mediated sulfide disposal in this context, then it implies a subversion of normal MPST function away from sulfide production (Módis et al., 2013; Szabo et al., 2014; Kimura et al., 2017; Nagahara, 2018). Alternatively, this is a response to a perceived lower-sulfide environment. TST levels were also elevated in the liver of *Mpst*$^{-/-}$ mice, providing further support for a reciprocal compensatory mechanism between these two enzymes (Nagahara et al., 2019).

The unexpected finding of normal hepatic sulfide levels in *Tst*$^{-/-}$ mice led us to discover that the metabolic phenotype we observed was driven by the very mechanisms invoked to maintain sulfide within a normal range rather than sulfide excess per se. Several observations were consistent with this. For example, the major amino acid pathways increased in the liver of *Tst*$^{-/-}$ mice were transaminases involved in metabolism of GSH that support increased export of sulfur equivalents as GSH (and cysteine). These same transaminases support gluconeogenesis by redirecting Krebs cycle intermediates (Rui, 2014; Qian et al., 2015; Sookoian et al., 2016). Reprogramming of amino acid metabolism for sulfide disposal with knockon effects to drive hepatic glucose production are suggested, rather than any change to amino acid-linked mitochondrial respiration in hepatocytes. This is supported by the shift in hepatocyte pyruvate metabolism toward aspartate. In addition, glutathione S-transferases (GST) that inhibit gluconeogenesis (Ghosh Dastidar et al., 2018) were lower in the liver of *Tst*$^{-/-}$ mice. Further, activation of NRF2, which represses gluconeogenesis (Slocum et al., 2016) appears to be lower in the liver of *Tst*$^{-/-}$ mice. Involvement of NRF2 in the *Tst*$^{-/-}$ liver phenotype is further supported by the phenotype of *Nrf2*$^{-/-}$ mice that similarly exhibited steatohepatitis in the absence of insulin resistance (Meakin et al., 2014). However, NRF2 signaling can be complex and dependent on dietary context; *Nrf2*$^{-/-}$ mice showed improved glucose tolerance after HFD feeding (Zhang et al., 2012), suggesting that any contribution of a NRF2 signaling deficit in the liver of the *Tst*$^{-/-}$ mice changes upon HFD feeding. Beyond altered pyruvate flux, we also showed that hepatocytes of *Tst*$^{-/-}$ mice exhibited defective lipid metabolism. Specifically, medium-chain fatty acid (MCFA) oxidation was impaired, associated with selective reduction of the protein and persulfidation levels of lipid catabolic enzymes. This represents a mechanism linking altered sulfide metabolism to lipid oxidation, hepatic lipid accumulation, and dyslipidemia. Consistent with impaired MCFA oxidation defects as one driver of the phenotype, steatosis is observed in medium-chain acyl-CoA dehydrogenase (*Mcad*) $^{-/-}$ mice (Tolwani et al., 2005), and dyslipidemia is found in MCADD-deficient humans (Onkenhout et al., 1995). The data we present add to a growing understanding of the link between sulfide regulating genes and nutrient metabolism that has so far focused on the enzymes of sulfide production. Specifically, we provide support for the importance of the sulfide oxidizing pathway as a regulator of cellular sulfide exposure. Unexpectedly, the data reveal cellular mechanisms that are engaged to homeostatically regulate sulfide disposal and can affect cell energetics and nutrient metabolism.

Our findings may have implications for potentially unexpected side effects of sulfide donor therapeutic agents. In normal mice, *in vivo* sulfide administration for 4 weeks after HFD feeding partially reversed hepatic lipid accumulation invoked by chronic (16 weeks) HFD feeding (Wu et al., 2015). No evidence was provided regarding whether sulfide disposal mechanisms were altered (Wu et al., 2015). This efficacious subchronic sulfide administration regimen contrasts with our genetic model of chronic sulfide elevation as a driver of dysregulated metabolism and NAFLD. Clearly, the normal mice in the Na_2S administration studies had a fully functional SOP, suggesting that the presence of TST is required to achieve the beneficial metabolic effects of Na_2S administration. This is also consistent with the apparently low sulfide signaling status (evidenced by lower persulfidation and NRF2 target protein abundance) in the liver of the *Tst*$^{-/-}$ mice. The benefits of elevated sulfide cannot be realized, perhaps because a major mediator of those effects is missing, and the alternate mechanisms invoked do not fully compensate (e.g., MPST) or actively drive aberrant nutrient metabolism. Comparable studies of glucose and lipid metabolism after manipulation of other sulfide-regulating genes are limited. However, in a contrasting model of reduced sulfide production (*Cth*$^{-/-}$ mice), plasma triglycerides were lowered (Mani et al., 2013), opposite to what we observed with *Tst*$^{-/-}$ mice. The hepatic sulfide disposal status of the *Cth*$^{-/-}$ mouse model is unknown, but our findings predict suppression of the SOP to spare the limited endogenous sulfide produced. Intriguingly, they also predict a knockon effect on nutrient homeostasis because of reduced metabolic demand of the TST/SOP axis. A more direct model informing on the effects of impairment of the sulfide disposal pathway is deficiency of the key mitochondrial SOP enzyme ETHE1. *Ethe1*$^{-/-}$ mice suffer fatal sulfide toxicity (Tiranti et al., 2009); therefore, comparable metabolic studies are lacking. However, one notable observation is that *Ethe1*$^{-/-}$ mice have apparently 10-fold higher liver sulfide exposure than control mice (Tiranti et al., 2009), in contrast to the normalized hepatic sulfide levels of *Tst*$^{-/-}$ mice. Circulating sulfide levels were not reported for comparison, but the presumably relatively lower systemic sulfide levels of *Tst*$^{-/-}$ mice appear to have permitted an effective homeostatic sulfide disposal response in the liver to avoid toxicity, albeit with a metabolic cost. Consequently, the liver of *Tst*$^{-/-}$ mice has a functional and proteomics profile distinct from that of *Ethe1*$^{-/-}$ mice. For example, in the liver of *Tst*$^{-/-}$ and *Ethe1*$^{-/-}$ mice (Hildebrandt et al., 2013), proteins of the GST Mu type (GSTM) and peroxiredoxin (PRDX) families were altered, but sometimes in the opposite direction or with alteration of distinct protein subclasses. A notable difference is also observed in amino acid metabolism. The liver of *Ethe1*$^{-/-}$ mice exhibits increased expression of enzymes of branched-chain amino acid metabolism (Hildebrandt et al., 2013), distinct from the predominantly GSH-related amino acid pathways that are increased in the liver of *Tst*$^{-/-}$ mice. Beyond sulfide, TST may also have distinct cellular roles that affect metabolism,

such as mitoribosomal synthesis, ROS attenuation, and modulation of mitochondrial iron-sulfur clusters (Bonomi et al., 1977; Pagani and Galante, 1983; Nandi and Westley, 1998; Nandi et al., 2000; Smirnov et al., 2010).

Given the pro-diabetogenic liver phenotype in *Tst*$^{-/-}$ mice, its was surprising that insulin signaling in the liver appeared normal and peripheral insulin sensitivity was increased. There are precedents for increased hepatic glucose production independent of insulin resistance, as found in the *Nrf2*$^{-/-}$ mice (Meakin et al., 2014) and as driven by the transcription factor carbohydrate-response element-binding protein (ChREBP) (Uyeda and Repa, 2006; Kim et al., 2016). There is also evidence to support insulin-sensitizing effects of sulfide administration *in vivo* in mice and rats (Feng et al., 2009; Geng et al., 2013; Xue et al., 2013), consistent with sulfide-mediated insulin sensitization of non-hepatic tissues in *Tst*$^{-/-}$ mice. Higher circulating GSH in *Tst*$^{-/-}$ mice may also promote peripheral insulin sensitization (Jain et al., 2014; Lutchmansingh et al., 2018). Clearly, the net balance of glucose production from the liver and its peripheral disposal remain abnormal in *Tst*$^{-/-}$ mice. Indeed, the baseline metabolic phenotype of *Tst*$^{-/-}$ mice resembles in many ways that of a normal mouse fed a HFD, and we showed some overlapping pro-diabetogenic signatures between the liver proteome of *Tst*$^{-/-}$ mice and that of HFD-fed C57BL/6J mice. However, we also found distinct lipid metabolism and peroxisomal protein changes in *Tst*$^{-/-}$ mice. Unlike a HFD state, which is associated with dominant hepatic insulin resistance, the increased hepatic glucose production in ND-fed *Tst*$^{-/-}$ mice occurs despite normal hepatic insulin sensitivity. The significant changes in persulfidation of transaminase and gluconeogenesis proteins suggest that coordinated cross-talk across metabolic pathways underlies this atypical metabolic phenotype.

Sulfide donor therapeutic agents have been proposed as a clinical strategy for improving cardiovascular health (Szabó et al., 2011; Whiteman et al., 2011; Zhang et al., 2018). Elevated endogenous sulfide has also been implicated in the beneficial metabolic effects of caloric restriction (Miller et al., 2005; Hine et al., 2015, 2017, 2018; Shimokawa et al., 2015; Lee et al., 2016). Our results suggest that chronic sulfide elevation may have unintended detrimental consequences, driving liver glucose production and fat accumulation to undesirable levels. Fortunately, this may be limited to cases where SOP proteins are compromised through rare genetic effects, such as TST variants (Billaut-Laden et al., 2006; Libiad et al., 2015). More broadly, a number of drugs or supplements are known to increase cyanide, which may dominantly inhibit TST activity and result in secondary sulfide overexposure. These include nitroprusside (Morris et al., 2017) and amygdalin (Bromley et al., 2005; O'Brien et al., 2005). Indeed, the TST metabolite thiosulfate is commonly co-administered with nitroprusside to prevent cyanide toxicity (Curry et al., 1997). Furthermore, dietary and environmental exposure to cyanogenic compounds (Simeonova et al., 2004), e.g., smoking (Vinnakota et al., 2012) or cyanogenic diets (Kashala-Abotnes et al., 2019), may interfere with normal TST function and could lead to increased sensitivity to sulfide therapeutic agents. In contrast, we have shown that administration of the TST substrate thiosulfate can ameliorate diabetes (Morton et al., 2016), further underlining the potential utility of targeting the SOP in metabolic disease. As with all therapeutic strategies, a careful cost-benefit analysis is required. A comparable case of relevance are the statins, one of the most potent and widely used drugs to prevent atherosclerosis, which also carry a higher risk for diabetes (Swerdlow et al., 2015). The full effect of TST manipulation on opposing metabolic pathways requires further study. Our current study sheds light on the underlying hepatic mechanisms invoked for sulfide disposal that are relevant to current sulfide donor strategies and may inform on routes to reduce their potential metabolic side effects.

Limitations of the study

Although the liver is the site of most (~60%) post-absorptive gluconeogenesis in normal animals within physiological fasting ranges, renal/small intestinal gluconeogenesis begins to substantially contribute to circulating glucose with prolonged fasting/starvation (Sasaki et al., 2017; Mutel et al., 2011; Mithieux et al., 2003; Stumvoll 1998; Owen et al., 1969). We cannot rule out a role of renal or intestinal gluconeogenesis in the diabetogenic phenotype of *Tst*$^{-/-}$ mice. This will be an important area of future work, although liver TST is at least more than 3-fold that of the kidneys, and small intestinal TST is very low (BioGPS; Figure S1A).

STAR★METHODS

Detailed methods are provided in the online version of this paper and include the following:

- KEY RESOURCES TABLE
- RESOURCE AVAILABILITY
  - Lead contact
  - Materials availability
  - Data and code availability
- EXPERIMENTAL MODEL AND SUBJECT DETAILS
  - Experimental animals
  - Hepatocyte preparations
- METHOD DETAILS
  - Pyruvate tolerance test
  - PEPCK activity assay
  - ^{13}C Pyruvate metabolite tracing
  - Plasma lipid analysis
  - Oil Red-O lipid analysis of liver
  - Liver Glycogen measurement
  - Western blotting for protein abundance
  - Insulin tolerance test
  - Euglycemic hyperinsulinemic clamps
  - MBB derivatization of whole blood and plasma
  - Fluorometric quantification of MBB-sulfur species
  - Sulfur metabolite analysis from liver
  - P3 fluorescence detection of sulfide in hepatocytes
  - Quantification of hydrogen sulfide levels using MitoA *in vivo* exomarker
  - Preparation of hepatic mitochondria
  - Amperometric analysis of sulfide disposal
  - Mitochondrial ROS (MitoSOX) measurement in H_2O_2 treated hepatocytes
  - Persulfidation Mass Spec and GO term analysis

- GO enrichment analysis
- Focused analysis of persulfidation in gluconeogenesis proteins
- Persulfidation labeling and western blotting from frozen liver
- Mass spec analysis of liver protein
- GO and KEGG enrichment analysis of proteome data
- Transcription factor enrichment analysis
- NRF2 target identification and proteome analysis
- Electron micrograph imaging
- Seahorse respiratory analysis
- Mitochondrial stress test (MST)
- Octanoate rescue test
- Real time for mRNA analysis

● QUANTIFICATION AND STATISTICAL ANALYSIS

SUPPLEMENTAL INFORMATION

Supplemental information can be found online at https://doi.org/10.1016/j.celrep.2021.109958.

ACKNOWLEDGMENTS

This work was funded by a Wellcome Trust New Investigator Award (100981/Z/13/Z to N.M.M.) and a Diabetes UK grant (17/0005697). R.C.H. was funded by a Medical Research Council Discovery Award (MC-PC-15076). We would like to thank Prof. Ken Olsen and Eric DeLeon (Notre Dame) for advice regarding establishing sulfide measurement by probe.

AUTHOR CONTRIBUTIONS

N.M.M. and R.N.C. conceived the experiments. R.N.C., M.T.G.G., M.E.B.-L., M.L., V.V., B.E., T.L.B., M.B., H.S., S.G.D., N.Z.M.H., C.M., A.T., N.F., and T.G., performed the experiments. R.N.C., M.E.B.-L., P.L.F., V.V., T.L.B., N.Z.M.H., T.S., F.B., T.G., R.C.H., B.S., G.A.G., A.J.F., C.S., R.B., and N.M.M. analyzed and interpreted data and commented on the manuscript. K.H.A. and S.S. generated reagents. C.M. and R.C.H. generated reagents. R.N.C. and N.M.M. wrote the manuscript.

DECLARATION OF INTERESTS

The authors declare no competing interests.

Received: December 16, 2020
Revised: July 6, 2021
Accepted: October 15, 2021
Published: November 9, 2021

REFERENCES

Abe, K., and Kimura, H. (1996). The possible role of hydrogen sulfide as an endogenous neuromodulator. J. Neurosci. *16*, 1066–1071.

Arndt, S., Baeza-Garza, C.D., Logan, A., Rosa, T., Wedmann, R., Prime, T.A., Martin, J.L., Saeb-Parsy, K., Krieg, T., Filipovic, M.R., et al. (2017). Assessment of H_2S *in vivo* using the newly developed mitochondria-targeted mass spectrometry probe MitoA. J. Biol. Chem. *292*, 7761–7773.

Banerjee, R., Chiku, T., Kabil, O., Libiad, M., Motl, N., and Yadav, P.K. (2015). Assay methods for H2S biogenesis and catabolism enzymes. Methods Enzymol. *554*, 189–200.

Billaut-Laden, I., Allorge, D., Crunelle-Thibaut, A., Rat, E., Cauffiez, C., Chevalier, D., Houdret, N., Lo-Guidice, J.M., and Broly, F. (2006). Evidence for a functional genetic polymorphism of the human thiosulfate sulfurtransferase (Rhodanese), a cyanide and H2S detoxification enzyme. Toxicology *225*, 1–11.

Bonomi, F., Pagani, S., Cerletti, P., and Cannella, C. (1977). Rhodanese-Mediated sulfur transfer to succinate dehydrogenase. Eur. J. Biochem. *72*, 17–24.

Bromley, J., Hughes, B.G., Leong, D.C., and Buckley, N.A. (2005). Life-threatening interaction between complementary medicines: cyanide toxicity following ingestion of amygdalin and vitamin C. Ann. Pharmacother. *39*, 1566–1569.

Caron, S., Verrijken, A., Mertens, I., Samanez, C.H., Mautino, G., Haas, J.T., Duran-Sandoval, D., Prawitt, J., Francque, S., Vallez, E., et al. (2011). Transcriptional activation of apolipoprotein CIII expression by glucose may contribute to diabetic dyslipidemia. Arterioscler. Thromb. Vasc. Biol. *31*, 513–519.

Carter, R.N., and Morton, N.M. (2016). Cysteine and hydrogen sulphide in the regulation of metabolism: insights from genetics and pharmacology. J. Pathol. *238*, 321–332.

Chen, X., Jhee, K.H., and Kruger, W.D. (2004). Production of the neuromodulator H2S by cystathionine beta-synthase via the condensation of cysteine and homocysteine. J. Biol. Chem. *279*, 52082–52086.

Consoli, A., Nurjhan, N., Capani, F., and Gerich, J. (1989). Predominant role of gluconeogenesis in increased hepatic glucose production in NIDDM. Diabetes *38*, 550–557.

Cuadrado, A., Rojo, A.I., Wells, G., Hayes, J.D., Cousin, S.P., Rumsey, W.L., Attucks, O.C., Franklin, S., Levonen, A.L., Kensler, T.W., and Dinkova-Kostova, A.T. (2019). Therapeutic targeting of the NRF2 and KEAP1 partnership in chronic diseases. Nat. Rev. Drug Discov. *18*, 295–317.

Curry, S.C., Carlton, M.W., and Raschke, R.A. (1997). Prevention of fetal and maternal cyanide toxicity from nitroprusside with coinfusion of sodium thiosulfate in gravid ewes. Anesth. Analg. *84*, 1121–1126.

Desai, K.M., Chang, T., Untereiner, A., and Wu, L. (2011). Hydrogen sulfide and the metabolic syndrome. Expert Rev. Clin. Pharmacol. *4*, 63–73.

Distrutti, E., Mencarelli, A., Santucci, L., Renga, B., Orlandi, S., Donini, A., Shah, V., and Fiorucci, S. (2008). The methionine connection: homocysteine and hydrogen sulfide exert opposite effects on hepatic microcirculation in rats. Hepatology *47*, 659–667. https://doi.org/10.1002/hep.22037.

Feng, X., Chen, Y., Zhao, J., Tang, C., Jiang, Z., and Geng, B. (2009). Hydrogen sulfide from adipose tissue is a novel insulin resistance regulator. Biochem. Biophys. Res. Commun. *380*, 153–159. https://doi.org/10.1016/j.bbrc.2009.01.059.

Filipovic, M.R., Zivanovic, J., Alvarez, B., and Banerjee, R. (2017). Chemical Biology of H2S Signaling through Persulfidation. Chem. Rev. *118*, 1253–1337.

Fiorucci, S., Antonelli, E., Mencarelli, A., Orlandi, S., Renga, B., Rizzo, G., Distrutti, E., Shah, V., and Morelli, A. (2005). The third gas: H2S regulates perfusion pressure in both the isolated and perfused normal rat liver and in cirrhosis. Hepatology *42*, 539–548.

Gao, X.H., Krokowski, D., Guan, B.J., Bederman, I., Majumder, M., Parisien, M., Diatchenko, L., Kabil, O., Willard, B., Banerjee, R., et al. (2015). Quantitative H2S-mediated protein sulfhydration reveals metabolic reprogramming during the integrated stress response. eLife *4*, e10067.

Geng, B., Cai, B., Liao, F., Zheng, Y., Zeng, Q., Fan, X., Gong, Y., Yang, J., Cui, Q.H., Tang, C., and Xu, G.H. (2013). Increase or decrease hydrogen sulfide exert opposite lipolysis, but reduce global insulin resistance in high fatty diet induced obese mice. PLoS ONE *8*, e73892.

Gerő, D., Torregrossa, R., Perry, A., Waters, A., Le-Trionnaire, S., Whatmore, J.L., Wood, M., and Whiteman, M. (2016). The novel mitochondria-targeted hydrogen sulfide (H2S) donors AP123 and AP39 protect against hyperglycemic injury in microvascular endothelial cells in vitro. Pharmacol. Res. *113*, 186–198.

Ghosh Dastidar, S., Jagatheesan, G., Haberzettl, P., Shah, J., Hill, B.G., Bhatnagar, A., and Conklin, D.J. (2018). Glutathione S -transferase P deficiency induces glucose intolerance via JNK-dependent enhancement of hepatic gluconeogenesis. Am. J. Physiol. Endocrinol. Metab. *315*, E1005–E1018.

Hildebrandt, T.M., and Grieshaber, M.K. (2008). Three enzymatic activities catalyze the oxidation of sulfide to thiosulfate in mammalian and invertebrate mitochondria. FEBS J. *275*, 3352–3361.

Hildebrandt, T.M., Di Meo, I., Zeviani, M., Viscomi, C., and Braun, H.P. (2013). Proteome adaptations in Ethe1-deficient mice indicate a role in lipid catabolism and cytoskeleton organization via post-translational protein modifications. Biosci. Rep. *33*, 575–584.

Hine, C., Harputlugil, E., Zhang, Y., Ruckenstuhl, C., Lee, B.C., Brace, L., Longchamp, A., Treviño-Villarreal, J.H., Mejia, P., Ozaki, C.K., et al. (2015). Endogenous hydrogen sulfide production is essential for dietary restriction benefits. Cell *160*, 132–144.

Hine, C., Kim, H.J., Zhu, Y., Harputlugil, E., Longchamp, A., Matos, M.S., Ramadoss, P., Bauerle, K., Brace, L., Asara, J.M., et al. (2017). Hypothalamic-Pituitary Axis Regulates Hydrogen Sulfide Production. Cell Metab. *25*, 1320–1333.e5.

Hine, C., Zhu, Y., Hollenberg, A.N., and Mitchell, J.R. (2018). Dietary and Endocrine Regulation of Endogenous Hydrogen Sulfide Production: Implications for Longevity. Antioxid. Redox Signal. *28*, 1483–1502.

Jackson, M.R., Melideo, S.L., and Jorns, M.S. (2012). Human sulfide:quinone oxidoreductase catalyzes the first step in hydrogen sulfide metabolism and produces a sulfane sulfur metabolite. Biochemistry *51*, 6804–6815.

Jain, S.K., Micinski, D., Huning, L., Kahlon, G., Bass, P.F., and Levine, S.N. (2014). Vitamin D and L-cysteine levels correlate positively with GSH and negatively with insulin resistance levels in the blood of type 2 diabetic patients. Eur. J. Clin. Nutr. *68*, 1148–1153.

Kabil, O., Motl, N., and Banerjee, R. (2014). H2S and its role in redox signaling. Biochim. Biophys. Acta *1844*, 1355–1366.

Karwi, Q.G., Bice, J.S., and Baxter, G.F. (2018). Pre- and postconditioning the heart with hydrogen sulfide (H_2S) against ischemia/reperfusion injury in vivo: a systematic review and meta-analysis. Basic Res. Cardiol. *113*, 6.

Kashala-Abotnes, E., Okitundu, D., Mumba, D., Boivin, M.J., Tylleskär, T., and Tshala-Katumbay, D. (2019). Konzo: a distinct neurological disease associated with food (cassava) cyanogenic poisoning. Brain Res. Bull. *145*, 87–91.

Kim, M.S., Krawczyk, S.A., Doridot, L., Fowler, A.J., Wang, J.X., Trauger, S.A., Noh, H.L., Kang, H.J., Meissen, J.K., Blatnik, M., et al. (2016). ChREBP regulates fructose-induced glucose production independently of insulin signaling. J. Clin. Invest. *126*, 4372–4386.

Kimura, Y., Koike, S., Shibuya, N., Lefer, D., Ogasawara, Y., and Kimura, H. (2017). 3-Mercaptopyruvate sulfurtransferase produces potential redox regulators cysteine- and glutathione-persulfide (Cys-SSH and GSSH) together with signaling molecules H_2S_2, H_2S_3 and H_2S. Sci. Rep. *7*, 10459.

Koike, S., Nishimoto, S., and Ogasawara, Y. (2017). Cysteine persulfides and polysulfides produced by exchange reactions with H_2S protect SH-SY5Y cells from methylglyoxal-induced toxicity through Nrf2 activation. Redox Biol. *12*, 530–539.

Krishnan, N., Fu, C., Pappin, D.J., and Tonks, N.K. (2011). H2S-Induced sulfhydration of the phosphatase PTP1B and its role in the endoplasmic reticulum stress response. Sci. Signal. *4*, ra86.

Lee, B.C., Kaya, A., and Gladyshev, V.N. (2016). Methionine restriction and lifespan control. Ann. N Y Acad. Sci. *1363*, 116–124.

Lewis, G.F., Carpentier, A., Adeli, K., and Giacca, A. (2002). Disordered fat storage and mobilization in the pathogenesis of insulin resistance and type 2 diabetes. Endocr. Rev. *23*, 201–229.

Libiad, M., Yadav, P.K., Vitvitsky, V., Martinov, M., and Banerjee, R. (2014). Organization of the human mitochondrial hydrogen sulfide oxidation pathway. J. Biol. Chem. *289*, 30901–30910.

Libiad, M., Sriraman, A., and Banerjee, R. (2015). Polymorphic variants of human rhodanese exhibit differences in thermal stability and sulfur transfer kinetics. J. Biol. Chem. *290*, 23579–23588.

Libiad, M., Motl, N., Akey, D.L., Sakamoto, N., Fearon, E.R., Smith, J.L., and Banerjee, R. (2018). Thiosulfate Sulfurtransferase like Domain Containing 1 Protein Interacts with Thioredoxin. J. Biol. Chem. *293*, 2675–2686.

Lutchmansingh, F.K., Hsu, J.W., Bennett, F.I., Badaloo, A.V., McFarlane-Anderson, N., Gordon-Strachan, G.M., Wright-Pascoe, R.A., Jahoor, F., and Boyne, M.S. (2018). Glutathione metabolism in type 2 diabetes and its relationship with microvascular complications and glycemia. PLoS ONE *13*, e0198626.

Mani, S., Li, H., Untereiner, A., Wu, L., Yang, G., Austin, R.C., Dickhout, J.G., Lhoták, Š., Meng, Q.H., and Wang, R. (2013). Decreased endogenous production of hydrogen sulfide accelerates atherosclerosis. Circulation *127*, 2523–2534.

Mani, S., Cao, W., Wu, L., and Wang, R. (2014). Hydrogen sulfide and the liver. Nitric Oxide *41*, 62–71.

Mason, T.M. (1998). The role of factors that regulate the synthesis and secretion of very-low-density lipoprotein by hepatocytes. Crit. Rev. Clin. Lab. Sci. *35*, 461–487.

Meakin, P.J., Chowdhry, S., Sharma, R.S., Ashford, F.B., Walsh, S.V., McCrimmon, R.J., Dinkova-Kostova, A.T., Dillon, J.F., Hayes, J.D., and Ashford, M.L. (2014). Susceptibility of Nrf2-Null Mice to Steatohepatitis and Cirrhosis upon Consumption of a High-Fat Diet Is Associated with Oxidative Stress, Perturbation of the Unfolded Protein Response, and Disturbance in the Expression of Metabolic Enzymes but Not with Insulin Resistance. Mol. Cell. Biol. *34*, 3305–3320.

Mikami, Y., Shibuya, N., Kimura, Y., Nagahara, N., Ogasawara, Y., and Kimura, H. (2011). Thioredoxin and dihydrolipoic acid are required for 3-mercaptopyruvate sulfurtransferase to produce hydrogen sulfide. Biochem. J. *439*, 479–485.

Miller, R.A., Buehner, G., Chang, Y., Harper, J.M., Sigler, R., and Smith-Wheelock, M. (2005). Methionine-deficient diet extends mouse lifespan, slows immune and lens aging, alters glucose, T4, IGF-I and insulin levels, and increases hepatocyte MIF levels and stress resistance. Aging Cell *4*, 119–125.

Mishanina, T.V., Libiad, M., and Banerjee, R. (2015). Biogenesis of reactive sulfur species for signaling by hydrogen sulfide oxidation pathways. Nat. Chem. Biol. *11*, 457–464.

Mithieux, G., Bady, I., Gautier, A., Croset, M., Rajas, F., and Zitoun, C. (2003). Induction of control genes in intestinal gluconeogenesis is sequential during fasting and maximal in diabetes. Am. J. Physiol. Endocrinol. Metab. *286*, E370–E375.

Módis, K., Coletta, C., Erdélyi, K., Papapetropoulos, A., and Szabo, C. (2013). Intramitochondrial hydrogen sulfide production by 3-mercaptopyruvate sulfurtransferase maintains mitochondrial electron flow and supports cellular bioenergetics. FASEB J. *27*, 601–611.

Moreno-Navarrete, J.M., Petrov, P., Serrano, M., Ortega, F., García-Ruiz, E., Oliver, P., Ribot, J., Ricart, W., Palou, A., Bonet, M.L., and Fernández-Real, J.M. (2013). Decreased RB1 mRNA, protein, and activity reflect obesity-induced altered adipogenic capacity in human adipose tissue. Diabetes *62*, 1923–1931.

Morris, A.A., Page, R.L., 2nd, Baumgartner, L.J., Mueller, S.W., MacLaren, R., Fish, D.N., and Kiser, T.H. (2017). Thiocyanate Accumulation in Critically Ill Patients Receiving Nitroprusside Infusions. J. Intensive Care Med. *32*, 547–553.

Morton, N.M., Nelson, Y.B., Michailidou, Z., Di Rollo, E.M., Ramage, L., Hadoke, P.W., Seckl, J.R., Bunger, L., Horvat, S., Kenyon, C.J., and Dunbar, D.R. (2011). A stratified transcriptomics analysis of polygenic fat and lean mouse adipose tissues identifies novel candidate obesity genes. PLoS ONE *6*, e23944.

Morton, N.M., Beltram, J., Carter, R.N., Michailidou, Z., Gorjanc, G., McFadden, C., Barrios-Llerena, M.E., Rodriguez-Cuenca, S., Gibbins, M.T., Aird, R.E., et al. (2016). Genetic identification of thiosulfate sulfurtransferase as an adipocyte-expressed antidiabetic target in mice selected for leanness. Nat. Med. *22*, 771–779.

Mosharov, E., Cranford, M.R., and Banerjee, R. (2000). The quantitatively important relationship between homocysteine metabolism and glutathione synthesis by the transsulfuration pathway and its regulation by redox changes. Biochemistry *39*, 13005–13011.

Mutel, E., Gautier-Stein, A., Abdul-Wahed, A., Amigó-Correig, M., Zitoun, C., Stefanutti, A., Houberdon, I., Tourette, J.A., Mithieux, G., and Rajas, F. (2011). Control of blood glucose in the absence of hepatic glucose production

during prolonged fasting in mice: induction of renal and intestinal gluconeogenesis by glucagon. Diabetes *60*, 3121–3131.

Nagahara, N. (2011). Catalytic site cysteines of thiol enzyme: sulfurtransferases. J. Amino Acids *2011*, 709404.

Nagahara, N. (2018). Multiple role of 3-mercaptopyruvate sulfurtransferase: antioxidative function, H2S and polysulfide production and possible SOx production. Br. J. Pharmacol. *175*, 577–589.

Nagahara, N., Tanaka, M., Tanaka, Y., and Ito, T. (2019). Novel Characterization of Antioxidant Enzyme, 3-Mercaptopyruvate Sulfurtransferase-Knockout Mice: Overexpression of the Evolutionarily-Related Enzyme Rhodanese. Antioxidants *8*, 116.

Nandi, D.L., and Westley, J. (1998). Reduced thioredoxin as a sulfur-acceptor substrate for rhodanese. Int. J. Biochem. Cell Biol. *30*, 973–977.

Nandi, D.L., Horowitz, P.M., and Westley, J. (2000). Rhodanese as a thioredoxin oxidase. Int. J. Biochem. Cell Biol. *32*, 465–473.

Norris, E.J., Culberson, C.R., Narasimhan, S., and Clemens, M.G. (2011). The liver as a central regulator of hydrogen sulfide. Shock *36*, 242–250.

O'Brien, B., Quigg, C., and Leong, T. (2005). Severe cyanide toxicity from 'vitamin supplements'. Eur. J. Emerg. Med. *12*, 257–258.

Onkenhout, W., Venizelos, V., van der Poel, P.F., van den Heuvel, M.P., and Poorthuis, B.J. (1995). Identification and Quantification of Intermediates of Unsaturated Fatty Acid Metabolism in Plasma of Patients with Fatty Acid Oxidation Disorders. Clin. Chem. *41*, 1467–1474.

Owen, O.E., Felig, P., Morgan, A.P., Wahren, J., and Cahill, G.F., Jr. (1969). Liver and kidney metabolism during prolonged starvation. J. Clin. Invest. *48*, 574–583.

Pagani, S., and Galante, Y.M. (1983). Interaction of rhodanese with mitochondrial NADH dehydrogenase. Biochim. Biophys. Acta *742*, 278–284.

Perez-Riverol, Y., Csordas, A., Bai, J., Bernal-Llinares, M., Hewapathirana, S., Kundu, D.J., Inuganti, A., Griss, J., Mayer, G., Eisenacher, M., et al. (2019). The PRIDE database and related tools and resources in 2019: improving support for quantification data. Nucleic Acids Res. *47* (*D1*), D442–D450.

Peters, J.M., Hennuyer, N., Staels, B., Fruchart, J.C., Fievet, C., Gonzalez, F.J., and Auwerx, J. (1997). Alterations in lipoprotein metabolism in peroxisome proliferator-activated receptor α-deficient mice. J. Biol. Chem. *272*, 27307–27312.

Pichette, J., and Gagnon, J. (2016). Implications of Hydrogen Sulfide in Glucose Regulation: How H2S Can Alter Glucose Homeostasis through Metabolic Hormones. Oxid. Med. Cell. Longev. *2016*, 3285074. https://doi.org/10.1155/2016/3285074.

Qian, K., Zhong, S., Xie, K., Yu, D., Yang, R., and Gong, D.W. (2015). Hepatic ALT isoenzymes are elevated in gluconeogenic conditions including diabetes and suppressed by insulin at the protein level. Diabetes Metab. Res. Rev. *31*, 562–571.

Reiffenstein, R. (1992). Toxicology Of Hydrogen Sulfide. Annu. Rev. Pharmacol. Toxicol. *32*, 109–134.

Rooney, J., Oshida, K., Vasani, N., Vallanat, B., Ryan, N., Chorley, B.N., Wang, X., Bell, D.A., Wu, K.C., Aleksunes, L.M., et al. (2018). Activation of Nrf2 in the liver is associated with stress resistance mediated by suppression of the growth hormone-regulated STAT5b transcription factor. PLoS ONE *13*, e0200004.

Rui, L. (2014). Energy metabolism in the liver. Compr. Physiol. *4*, 177–197.

Sasaki, M., Sasako, T., Kubota, N., Sakurai, Y., Takamoto, I., Kubota, T., Inagi, R., Seki, G., Goto, M., Ueki, K., et al. (2017). Dual regulation of gluconeogenesis by insulin and glucose in the proximal tubules of the kidney. Diabetes *66*, 2339–2350.

Sestito, S., Nesi, G., Pi, R., Macchia, M., and Rapposelli, S. (2017). Hydrogen Sulfide: A Worthwhile Tool in the Design of New Multitarget Drugs. Front Chem. *5*, 72.

Shibuya, N., Tanaka, M., Yoshida, M., Ogasawara, Y., Togawa, T., Ishii, K., and Kimura, H. (2009). 3-Mercaptopyruvate sulfurtransferase produces hydrogen sulfide and bound sulfane sulfur in the brain. Antioxid. Redox Signal. *11*, 703–714.

Shimokawa, I., Komatsu, T., Hayashi, N., Kim, S.E., Kawata, T., Park, S., Hayashi, H., Yamaza, H., Chiba, T., and Mori, R. (2015). The life-extending effect of dietary restriction requires Foxo3 in mice. Aging Cell *14*, 707–709, 10.

Simeonova, F.P., and Fishbein, L.; World Health Organization & International Programme on Chemical Safety (2004). Hydrogen cyanide and cyanides : human health aspects. https://apps.who.int/iris/handle/10665/42942.

Singh, S., Padovani, D., Leslie, R.A., Chiku, T., and Banerjee, R. (2009). Relative contributions of cystathionine beta-synthase and gamma-cystathionase to H2S biogenesis via alternative trans-sulfuration reactions. J. Biol. Chem. *284*, 22457–22466.

Singha, S., Kim, D., Moon, H., Wang, T., Kim, K.H., Shin, Y.H., Jung, J., Seo, E., Lee, S.J., and Ahn, K.H. (2015). Toward a selective, sensitive, fast-responsive, and biocompatible two-photon probe for hydrogen sulfide in live cells. Anal. Chem. *87*, 1188–1195.

Slocum, S.L., Skoko, J.J., Wakabayashi, N., Aja, S., Yamamoto, M., Kensler, T.W., and Chartoumpekis, D.V. (2016). Keap1/Nrf2 pathway activation leads to a repressed hepatic gluconeogenic and lipogenic program in mice on a high-fat diet. Arch. Biochem. Biophys. *591*, 57–65.

Smirnov, A., Comte, C., Mager-Heckel, A.M., Addis, V., Krasheninnikov, I.A., Martin, R.P., Entelis, N., and Tarassov, I. (2010). Mitochondrial enzyme rhodanese is essential for 5 S ribosomal RNA import into human mitochondria. J. Biol. Chem. *285*, 30792–30803.

Sookoian, S., Castaño, G.O., Scian, R., Fernández Gianotti, T., Dopazo, H., Rohr, C., Gaj, G., San Martino, J., Sevic, I., Flichman, D., and Pirola, C.J. (2016). Serum aminotransferases in nonalcoholic fatty liver disease are a signature of liver metabolic perturbations at the amino acid and Krebs cycle level. Am. J. Clin. Nutr. *103*, 422–434.

Steele, R., Wall, J.S., De Bodo, R.C., and Altszuler, N. (1956). Measurement of size and turnover rate of body glucose pool by the isotope dilution method. Am. J. Physiol. *187*, 15–24.

Stumvoll, M. (1998). Glucose production by the human kidney–its importance has been underestimated. Nephrol. Dial. Transplant. *13*, 2996–2999.

Swerdlow, D.I., Preiss, D., Kuchenbaecker, K.B., Holmes, M.V., Engmann, J.E., Shah, T., Sofat, R., Stender, S., Johnson, P.C., Scott, R.A., et al.; DIAGRAM Consortium; MAGIC Consortium; InterAct Consortium (2015). HMG-coenzyme A reductase inhibition, type 2 diabetes, and bodyweight: evidence from genetic analysis and randomised trials. Lancet *385*, 351–361.

Szabo, C. (2011). Roles of Hydrogen Sulfide in the Pathogenesis of Diabetes Mellitus and Its Complications. Antioxid. Redox Signal. *17*, 68–80.

Szabó, G., Veres, G., Radovits, T., Gero, D., Módis, K., Miesel-Gröschel, C., Horkay, F., Karck, M., and Szabó, C. (2011). Cardioprotective effects of hydrogen sulfide. Nitric Oxide *25*, 201–210.

Szabo, C., Ransy, C., Módis, K., Andriamihaja, M., Murghes, B., Coletta, C., Olah, G., Yanagi, K., and Bouillaud, F. (2014). Regulation of mitochondrial bioenergetic function by hydrogen sulfide. P
mechanisms. Br. J. Pharmacol. *171*, 209

Tiranti, V., Viscomi, C., Hildebrandt, T., Di Meo, I., Mineri, R., Tiveron, C., Levitt, M.D., Prelle, A., Fagiolari, G., Rimoldi, M., and Zeviani, M. (2009). Loss of ETHE1, a mitochondrial dioxygenase, causes fatal sulfide toxicity in ethylmalonic encephalopathy. Nat. Med. *15*, 200–205.

Tolwani, R.J., Hamm, D.A., Tian, L., Sharer, J.D., Vockley, J., Rinaldo, P., Matern, D., Schoeb, T.R., and Wood, P.A. (2005). Medium-chain acyl-CoA dehydrogenase deficiency in gene-targeted mice. PLoS Genet. *1*, 205–212.

Tonelli, C., Chio, I.I.C., and Tuveson, D.A. (2018). Transcriptional Regulation by Nrf2. Antioxid. Redox Signal. *29*, 1727–1745.

Uyeda, K., and Repa, J.J. (2006). Carbohydrate response element binding protein, ChREBP, a transcription factor coupling hepatic glucose utilization and lipid synthesis. Cell Metab. *4*, 107–110.

Vinnakota, C.V., Peetha, N.S., Perrizo, M.G., Ferris, D.G., Oda, R.P., Rockwood, G.A., and Logue, B.A. (2012). Comparison of cyanide exposure markers in the biofluids of smokers and non-smokers. Biomarkers *17*, 625–633.

Vitvitsky, V., Thomas, M., Ghorpade, A., Gendelman, H.E., and Banerjee, R. (2006). A functional transsulfuration pathway in the brain links to glutathione homeostasis. J. Biol. Chem. *281*, 35785–35793.

Vitvitsky, V., Yadav, P.K., Kurthen, A., and Banerjee, R. (2015). Sulfide oxidation by a noncanonical pathway in red blood cells generates thiosulfate and polysulfides. J. Biol. Chem. *290*, 8310–8320.

Vitvitsky, V., Yadav, P.K., An, S., Seravalli, J., Cho, U.S., and Banerjee, R. (2017). Structural and mechanistic insights into hemoglobincatalyzed hydrogen sulfide oxidation and the fate of polysulfide products. J. Biol. Chem. *292*, 5584–5592.

Walsh, J., Jenkins, R.E., Wong, M., Olayanju, A., Powell, H., Copple, I., O'Neill, P.M., Goldring, C.E., Kitteringham, N.R., and Park, B.K. (2014). Identification and quantification of the basal and inducible Nrf2-dependent proteomes in mouse liver: biochemical, pharmacological and toxicological implications. J. Proteomics *108*, 171–187.

Wang, R. (2012). Physiological implications of hydrogen sulfide: a whiff exploration that blossomed. Physiol. Rev. *92*, 791–896.

Wedmann, R., Onderka, C., Wei, S., Szijártó, I.A., Miljkovic, J.L., Mitrovic, A., Lange, M., Savitsky, S., Yadav, P.K., Torregrossa, R., et al. (2016). Improved tag-switch method reveals that thioredoxin acts as depersulfidase and controls the intracellular levels of protein persulfidation. Chem. Sci. (Camb.) *7*, 3414–3426.

Whiteman, M., Le Trionnaire, S., Chopra, M., Fox, B., and Whatmore, J. (2011). Emerging role of hydrogen sulfide in health and disease: critical appraisal of biomarkers and pharmacological tools. Clin. Sci. (Lond.) *121*, 459–488.

World Health Organization (2016). Global Report on Diabetes. https://www.who.int/publications/i/item/9789241565257.

Wu, D., Zheng, N., Qi, K., Cheng, H., Sun, Z., Gao, B., Zhang, Y., Pang, W., Huangfu, C., Ji, S., et al. (2015). Exogenous hydrogen sulfide mitigates the fatty liver in obese mice through improving lipid metabolism and antioxidant potential. Med. Gas Res. *5*, 1.

Xie, L., Gu, Y., Wen, M., Zhao, S., Wang, W., Ma, Y., Meng, G., Han, Y., Wang, Y., Liu, G., et al. (2016). Hydrogen sulfide induces Keap1 S-sulfhydration and suppresses diabetes-accelerated atherosclerosis via Nrf2 activation. Diabetes *65*, 3171–3184.

Xue, R., Hao, D.D., Sun, J.P., Li, W.W., Zhao, M.M., Li, X.H., Chen, Y., Zhu, J.H., Ding, Y.J., Liu, J., and Zhu, Y.C. (2013). Hydrogen sulfide treatment promotes glucose uptake by increasing insulin receptor sensitivity and ameliorates kidney lesions in type 2 diabetes. Antioxid. Redox Signal. *19*, 5–23.

Yadav, P.K., Yamada, K., Chiku, T., Koutmos, M., and Banerjee, R. (2013). Structure and kinetic analysis of H2S production by human mercaptopyruvate sulfurtransferase. J. Biol. Chem. *288*, 20002–20013.

Yang, G., Zhao, K., Ju, Y., Mani, S., Cao, Q., Puukila, S., Khaper, N., Wu, L., and Wang, R. (2013). Hydrogen sulfide protects against cellular senescence via S-sulfhydration of Keap1 and activation of Nrf2. Antioxid. Redox Signal. *18*, 1906–1919.

Zhang, Y.K.J., Wu, K.C., Liu, J., and Klaassen, C.D. (2012). Nrf2 deficiency improves glucose tolerance in mice fed a high-fat diet. Toxicol. Appl. Pharmacol. *264*, 305–314.

Zhang, L., Yang, G., Untereiner, A., Ju, Y., Wu, L., and Wang, R. (2013). Hydrogen sulfide impairs glucose utilization and increases gluconeogenesis in hepatocytes. Endocrinology *154*, 114–126.

Zhang, L., Wang, Y., Li, Y., Li, L., Xu, S., Feng, X., and Liu, S. (2018). Hydrogen sulfide (H2S)-releasing compounds: Therapeutic potential in cardiovascular diseases. Front. Pharmacol. *9*, 1066.

Appendix III: Published first-author review paper

Biochemical Journal (2021) **478** 3485–3504
https://doi.org/10.1042/BCJ20210517

PORTLAND PRESS

Review Article

Hydrogen sulfide in ageing, longevity and disease

Stephen E. Wilkie[1], Gillian Borland[1], Roderick N. Carter[2], Nicholas M. Morton[2] and Colin Selman[1]

[1]Glasgow Ageing Research Network (GARNER), Institute of Biodiversity, Animal Health and Comparative Medicine, College of Medical, Veterinary and Life Sciences, University of Glasgow, Glasgow G12 8QQ, U.K.; [2]Molecular Metabolism Group, University/BHF Centre for Cardiovascular Sciences, Queens Medical Research Institute, University of Edinburgh, Edinburgh EH16 4TJ, U.K.

Correspondence: Colin Selman (Colin.Selman@glasgow.ac.uk)

OPEN ACCESS

Hydrogen sulfide (H_2S) modulates many biological processes, including ageing. Initially considered a hazardous toxic gas, it is now recognised that H_2S is produced endogenously across taxa and is a key mediator of processes that promote longevity and improve late-life health. In this review, we consider the key developments in our understanding of this gaseous signalling molecule in the context of health and disease, discuss potential mechanisms through which H_2S can influence processes central to ageing and highlight the emergence of novel H_2S-based therapeutics. We also consider the major challenges that may potentially hinder the development of such therapies.

Biological generation of hydrogen sulfide (H_2S)

Endogenous production

Enzymatic production of H_2S in mammalian tissues requires sulfur-containing amino acids (SAAs), specifically methionine and cysteine, as substrates [1,2]. Methionine cannot be synthesised *de novo* in mammals and must be consumed in the diet. In contrast, cysteine can be synthesised from methionine via conversion to homocysteine and is also consumed through diet. Homocysteine conversion into cysteine is referred to as the transsulfuration pathway (first described in the context of plant metabolism, in which cysteine is converted to homocysteine [3]). From cysteine, H_2S is produced by two distinct canonical enzymatic pathways: directly through the activity of two pyridoxal-5′-phosphate (PLP)-dependent enzymes, cystathionine-gamma-lyase (CSE, or CGL) and cystathionine-beta-synthase (CBS), or indirectly through stepwise conversion into 3-mercaptopyruvate by L-cysteine:2-oxoglutarate aminotransferase (CAT) and then H_2S by 3-mercaptopyruvate sulfurtransferase (MPST, or TUM1) [4]. The latter pathway is referred to the PLP-independent pathway as although CAT is PLP-dependent, MPST is not. These pathways are further distinguished by their sub-cellular localisation. CSE and CBS operate predominately within the cytosol, although both can translocate to the mitochondria under certain stress conditions [5]. For instance, CSE translocates to mitochondria during hypoxia, promoting H_2S production within mitochondria and subsequently increasing ATP production [6]. Human MPST exists in two distinct isoforms, TUM1-Iso1 which is exclusively found within the cytosol and TUM1-Iso2, a splice variant encoding an additional 20 amino acid mitochondrial-targeting sequence [7]. The specific activity of mitochondrial MPST is two to three times higher than cytosolic MPST in rat liver [8]. While the pathways described above exclusively use the L-enantiomer of cysteine as a substrate, Kimura et al. [9] discovered a PLP-independent pathway for the production of H_2S from D-cysteine (mainly in the cerebellum and kidney homogenates) through the action of MPST and D-amino acid oxidase in mitochondria and peroxisomes, respectively. While L-cysteine is the predominant, naturally occurring enantiomer of cysteine, common food processing practices rapidly racemise L-cysteine through heat and alkaline treatments, resulting in up to 44% conversion to D-cysteine [9]. The biologically relevant extent of this D-cysteine pathway remains unclear but presents an interesting alternative to the canonical mammalian production of H_2S.

Received: 7 July 2021
Revised: 16 August 2021
Accepted: 18 August 2021

Version of Record published:
6 October 2021

PORTLAND PRESS

Biochemical Journal (2021) **478** 3485–3504
https://doi.org/10.1042/BCJ20210517

Endogenous disposal

Supraphysiological concentrations of H_2S can be toxic, so efficient removal of H_2S is performed by a suite of mitochondrial enzymes, collectively termed the sulfide oxidation unit (SOU) [10]. It has been shown that SOU actively catabolises H_2S when intracellular concentrations exceed 10 nM in intact cells, with more restrictive thresholds observed in proximity to mitochondria [11]. However, determining a precise definition of supraphysiological H_2S levels remains challenging due to limitations in detection methods and tissue and species specificity [12]. While the precise order of events and sulfur species involved in H_2S oxidation are still unclear, the disposal of H_2S consists of a series of oxidative reactions coupled to components of the electron transport chain within the mitochondria, ultimately yielding sulfate which is excreted in the urine. The first step in this pathway is the oxidation of H_2S by the flavoprotein sulfur:quinone oxidoreductase (SQR) [13] catalytic cycle whereby the flavin cofactor is cyclically reduced by H_2S and oxidised by ubiquinone, with coenzyme Q acting as an electron acceptor. It is through coenzyme Q that H_2S metabolism is coupled to ATP generation by oxidative phosphorylation, making H_2S a rare example of an inorganic compound capable of fuelling mammalian oxidative phosphorylation [14]. The product of this enzymatic cycle is the generation of SQR-persulfide intermediates, which are transferred primarily to glutathione (GSH) in human tissues, generating glutathione persulfide (GSSH) [15]. SQR is also capable of catabolising H_2S to produce thiosulfate from sulfite, although low tissue levels of sulfite makes it unclear whether this reaction accounts for a substantial proportion of physiological SQR activity in mammals, despite orders of magnitude greater reactivity with persulfidated SQR compared with GSH [16,17]. GSSH is oxidised by ethylmalonic encephalopathy 1 (ETHE1) or thiosulfate sulfurtransferase (TST) to form sulfite or thiosulfate, respectively. ETHE1 is a sulfur dioxygenase, consuming O_2 and water as substrates to oxidise H_2S [18]. TST may then reversibly convert thiosulfate to sulfite which is irreversibly oxidised into sulfate by sulfite oxidase (SUOX). Both sulfate and thiosulfate are removed via the circulatory system and then ultimately excreted in the urine [19]. Overall, disposal of 1 H_2S molecule requires the consumption of 0.75 O_2 molecules; 0.5 by ETHE1 and 0.25 by Complex III [10]. The enzymatic generation of H_2S from SAAs and its subsequent removal are detailed in Figure 1. Of note, as mature red blood cells (RBCs) typically lack mitochondria, they utilise a methaemoglobin pathway for the disposal of H_2S by conversion of H_2S into thiosulfate and polysulfides [20]. It remains an open question as to whether the methaemoglobin pathway for H_2S oxidation found within RBCs is utilised in other tissues in mammals.

Bacterial production

Putrefaction of decaying organic matter in anaerobic conditions results in the production of H_2S [21]. This is due to the action of a wide range of sulfate-reducing bacteria (SRB) which utilise sulfate as a terminal electron acceptor for respiration, with the concomitant production of H_2S [22]. There is a wide range of such SRB within the microbiome of the human colon, primarily of the genus *Desulfovibrio* in the class d-Proteobacteria [23]. Endogenous production of H_2S in bacteria is catalysed by orthologs of CSE, CBS, and MPST [24]. The interactions between groups of bacteria are complex and poorly understood. SRB use a wide range of substrates including lactate, hydrogen, short-chain fatty acids, and amino acids, which places them in direct competition with other bacterial species such as hydrogenotrophic bacteria, methanogens, and acetogens. However, SRB appears to dominate the use of hydrogen in the microbiome as they are capable of catabolizing hydrogen at concentrations far lower than other hydrogenotrophic species [25]. It is currently difficult to directly measure the proportion of H_2S produced by bacteria compared with endogenous enzymatic production in tissues. Germ-free mice have 50% less measurable H_2S in faecal samples compared with control mice and are capable of altering SRB-activity to compensate for the impairment in enzymatic H_2S production following a PLP-deficient diet [26]. H_2S gas produced by the microbiome in the gut can enter proximal human tissues or the bloodstream [27]. For instance, high levels of SRB-derived H_2S inhibits butyrate oxidation, the major source of energy production in intestinal colonocytes [28]. Furthermore, there is evidence that bacterial-derived H_2S can reduce arterial blood pressure in rats [29], and contradictory evidence points to either a therapeutic or causative role of H_2S in inflammatory bowel disease and colorectal cancer [30]. Additionally, there is potential for diet to influence the relative abundance of SRB, as diet has been shown to modify microbiome composition in general [31]. However, no significant effect of short-term adoption of diets either enriched for or deficient in SAAs was observed on relative SRB populations in stool samples from healthy human volunteers [32]; future studies employing longer-term dietary interventions and greater statistical power are required to further clarify this question. Finally, it has been proposed that bacterial production of H_2S protects the bacteria against

Biochemical Journal (2021) **478** 3485–3504
https://doi.org/10.1042/BCJ20210517

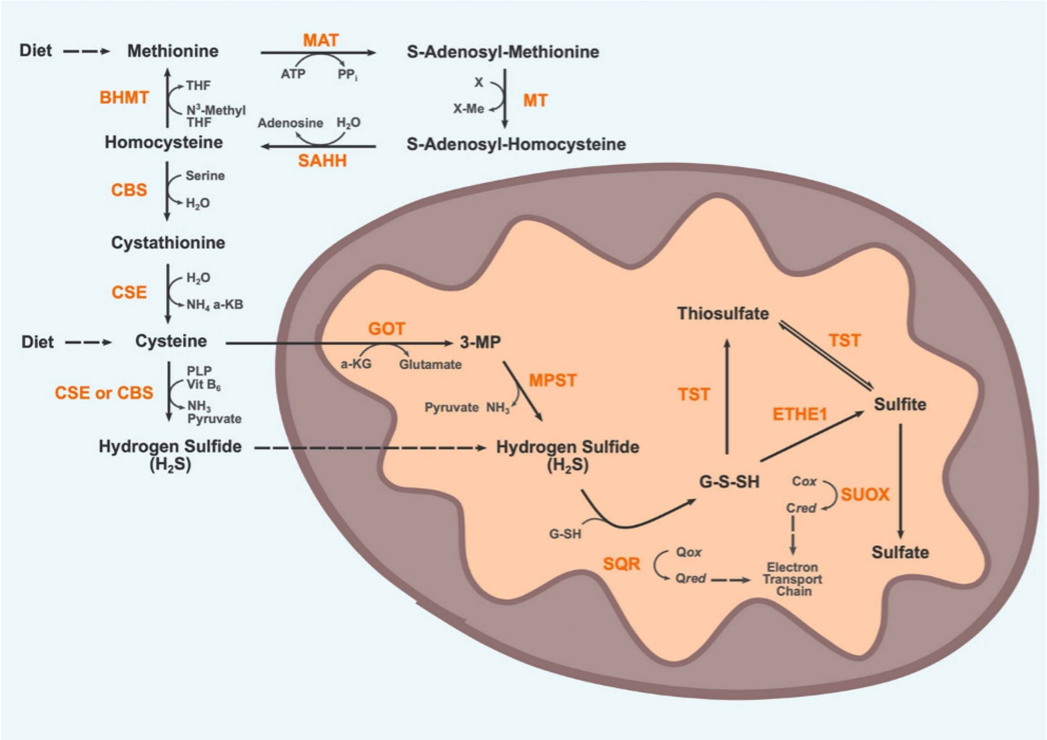

Figure 1. Substrate, intermediates and enzymes involved in the endogenous production and disposal of H_2S.
The blue region represents the cytosol, the orange region represents the matrix of a mitochondrion. The transsulfuration pathway cycles methionine into homocysteine first followed by enzymatic conversion of homocysteine into cysteine. From cysteine H_2S is generated in the cytosol by CSE and CSE. H_2S can also be generated within mitochondria by the action of MPST on 3-MP, a metabolite of cysteine. H_2S can freely permeate membranes including the mitochondrial membranes. H_2S disposal is carried out in mitochondria by several enzymes that comprise the sulfide oxidation unit (SOU). The precise mechanism of the SOU remains a subject of active research, the species and steps shown here represent just one proposed mechanism. Ultimately H_2S is oxidised into sulfate which is subsequently excreted in the urine. MAT, Methionine adenosyl-transferase; ATP, Adenosine triphosphate; PPi, Inorganic pyrophosphate; X, Methyl group acceptor; MT, Methyltransferase; SAHH, S-adenosyl homocysteine hydrolase; BHMT, Betaine-Homocysteine S-methyltransferase; N3-Methyl THF, Trimethylglycine betaine; THF, Betaine; CBS, Cystathionine-β-synthase; CSE, Cystathionine-γ-lyase; NH_3, Amine; a-KB, alpha ketobutyrate; PLP, pyridoxal 5′-phosphate; Vit B_6, Vitamin B_6; GOT, Glutamic-Oxaloacetic Transaminase; a-KG, alpha ketoglutarate; 3-MP, 3-Mercaptopyruvate; MPST, 3-Mercaptopyruvate Sulfurtransferase; SQR, Sulfur-Quinone oxidoreductase; Qox, Oxidised coenzyme Q; Qred, Reduced coenzyme Q; G-S-SH, Glutathione persulfide; ETHE1, Ethylmalonic encephalopathy 1 protein; TST, Thiosulfate Sulfurtransferase; SUOX, Sulfite Oxidase; Cox, Oxidised cytochrome C; Cred, Reduced cytochrome C.

oxidative stress and may contribute to antibacterial resistance [33]. For example, Shatalin et al. [33] developed novel small molecule inhibitors of bacterial CSE and found these inhibitors improved antibiotic potency against *Staphylococcus aureus* and *Pseudomonas aeruginosa in vitro* and in mice, supporting the theory that endogenous production of H_2S in bacteria might contribute to antibacterial resistance. We believe research using germ-free mice is one approach that may help provide more information regarding the relevance of SRB-derived H_2S in whole-animal metabolism and physiology.

Signalling modalities of H_2S

Post-translational modification (persulfidation)

Protein modification by H_2S is a reversible post-translational modification that can occur on any cysteine residue. Overall, the thiol group (R-SH) present in cysteine is indirectly changed to a persulfide group

PORTLAND PRESS

Biochemical Journal (2021) **478** 3485–3504
https://doi.org/10.1042/BCJ20210517

(R-S-SH), a process known as persulfidation or sulfhydration. The thiol group must first be oxidised to form thiol derivatives such as sulfenic acid (R-SOH), a disulfide (R-S-S-R), or S-nitrosothiol (R-SNO), which can then react with H_2S to create a persulfidated protein residue. A schematic showing the various thiol derivatives H_2S can react with and their subsequent products are shown in Figure 2, adapted from [34]. Persulfides are highly reactive, with a neucleophilic terminal sulfur atom and an electrophilic inner sulfane sulfur atom [35]. Persulfidation of cysteine residues causes conformational changes in protein structure that alter protein activity such as the regulation of Kelch-like ECH-associated protein 1 (Keap1), which has well-characterised conformational regulation through alterations of cysteine residues [36,37]. Keap1 is the major inhibitor of the nuclear factor erythroid 2-related factor 2 (NRF2)-mediated antioxidant response mechanism. *In vitro* approaches have shown alteration of cysteine residues on Keap1 following exposure to H_2S leading to inactivation of KEAP1, but currently, there is no agreement on the precise residue(s) persulfidated in this process [36,37]. Another established persulfidation target is the Kir6.1 subunit of K_{ATP} channels which confers cardioprotective effects when activated by H_2S [38]. An extensive review of the chemistry of persulfides, their molecular targets, and role in various tissues and diseases was compiled by Filipovic and colleagues in 2017 [39]. Persulfides decay under biologically relevant conditions, which poses a challenge in the identification, measurement, and characterisation of persulfidated species in biological contexts. The half-life of Cys-S-SH is ∼35 min at 37°C [40]. Spontaneous removal of persulfides is caused by a disproportionation reaction between two persulfides to form many sulfur-containing species including: elemental sulfur, thiols, polysulfanes, and/or H_2S [40–42]. Additional

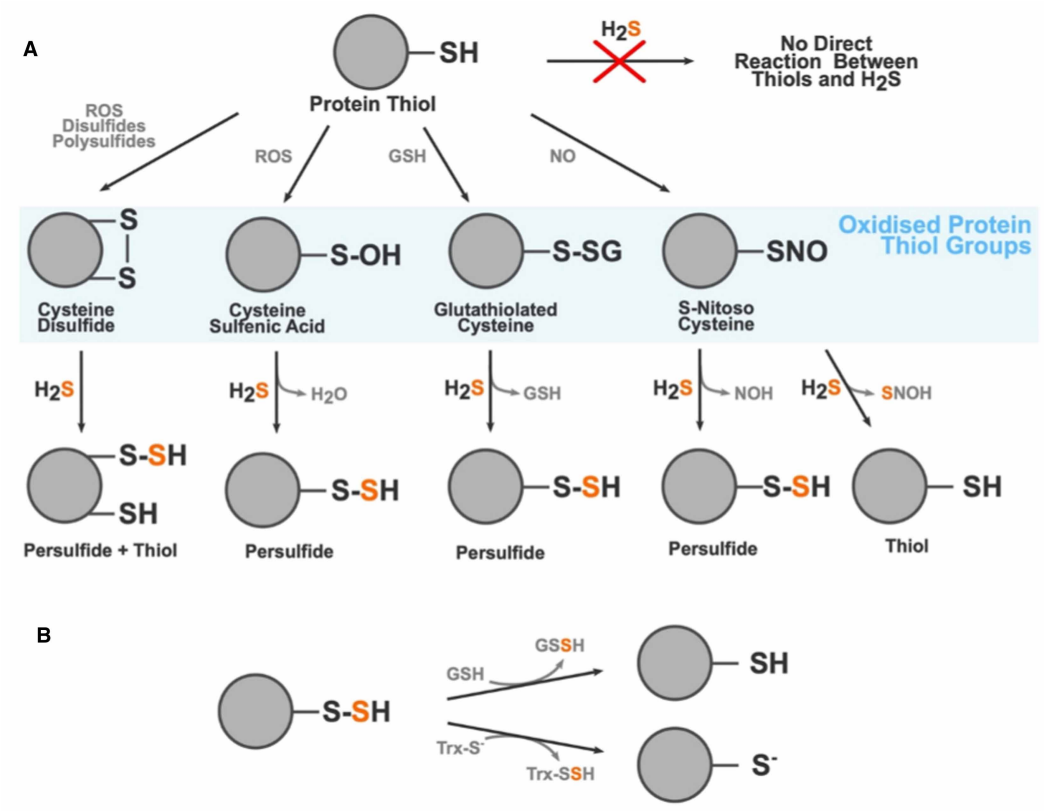

Figure 2. Formation of protein persulfides by H2S.

(**A**) Modification of cysteine residues by H_2S. H_2S cannot directly modify thiol groups (i.e. cysteine residues). The thiol group must first be must first be oxidised into a disulfide (disulfide bond formation), sulfenic acid (S-Sulfenylation), glutathiolated cysteine (S-Glutathiolation), or a S-Nitroso Cysteine (S-Nitrosation). From these oxidised thiol groups H_2S can react to form persilfides, thiols, and a variety of by-products dependent on the type of oxidised thiol it is reacting with. The sulfur atom from the H_2S molecule is highlighted in orange to show where in the product it incorporates. (**B**) Persulfidation is a reversible post-translational modification and can be readily removed by the action of glutathione and thioredoxin. ROS, Reactive oxygen species; GSH, Glutathione; NO, Nitric oxide; NOH, Nitroxyl; SNOH, Thionitrous acid; GSSH, Glutathione persulfide; Trx-S^-, Thioredoxin.

Biochemical Journal (2021) **478** 3485–3504
https://doi.org/10.1042/BCJ20210517

processes that can break down persulfides include homolysis by heat or light and enzymatic removal by the thioredoxin system. Given these constraints, it is difficult to achieve a full understanding of the dynamics of protein persulfidation as most methods take a 'snap-shot' of global persulfidation at one time. Despite these limitations, our understanding of the extent of protein modification by persulfidation, collectively termed the persulfidome, is growing. In *Arabidopsis thaliana*, for example, 5% of the proteome was found to be persulfidated using modified tag-switching protocol that employed methylsufonylbenzothiazole (MSBT) to block both thiol and persulfide groups within the sample [43]. This was then followed by the addition of CN-biotin which does not react with MSBT adducts of thiol origin and therefore allows for streptavidin-based pull-down of persulfidated proteins [43]. Additionally, proteomic studies in wild-type mice have found 10–25% of hepatic proteins to be persulfidated under physiological homeostasis [44]. Comprehensive work by Zivanovic et al. [45] showed that a high degree of hepatic protein persulfidation is associated with an extended lifespan, augmented by dietary restriction (DR), and diminished with age; these trends were conserved across model organisms. Bithi et al. [46] described tissue-specific changes in the persulfidome of mice exposed to 50% DR and in mice homozygous null for CSE. As persulfidation can in principle occur on any cysteine residue, and is a highly dynamic, reversible post-translational modification, there is enormous scope for H_2S to modify proteins in a variety of biological settings.

Binding with metal centres

H_2S is capable of binding to multiple metal ions, the most direct signalling modality in its repertoire. Upon binding, the coordination, charge, and oxidation states of the metal ion may be altered [47]. Such reactions become biologically relevant in the context of metalloproteins which contain metal centres in their quaternary structure. Metalloproteins represent a significant percentage of all mammalian proteins, with recent estimates suggesting that approximately 6600 human proteins are metalloproteins [48], or approximately a third of all protein products. H_2S reaction with haemoproteins is well established, particularly with ferric haemoglobins but also metmyoglobins, methaemoglobins, and peroxidases [49]. In fact, the much-discussed toxicity of H_2S is a result of its highly efficient inhibition of cytochrome c oxidase (COX, also known as Complex IV in the electron transport chain). COX is a dimer formed of subunits that include two heme, two copper, one magnesium, and one zinc centre [50]. Inhibition of COX by H_2S occurs in a biphasic manner under a complex series of reactions with the haem and copper centres, forming intermediates that are currently unresolved [51]. Furthermore, H_2S inhibits angiotensin-converting enzyme by binding to a zinc atom at the active site, with dose-dependent inhibition of this enzyme demonstrated in protein lysates from human endothelial cells [52]. Interestingly, binding with haem centres in haemoglobin may be the major H_2S clearance pathway in RBCs [20]. It is established that RBCs do produce endogenous H_2S, primarily through MPST, but as they lack mitochondria in most mammals they do not possess the canonical clearance mechanisms (see section Endogenous disposal). Unchecked, H_2S production in the trillions of RBCs within the circulation would inevitably result in a lethal build-up of H_2S. However, it appears that a cycle of reactions between H_2S species and haemoglobin results in the oxidation of H_2S into reactive sulfur species (RSS) such as thiosulfate and hydropolysulfides [20]. A similar process appears to occur between H_2S and myoglobin in cardiac and skeletal muscle [53].

Interaction with other gasotransmitters

H_2S is not alone as a gasotransmitter. Other compounds with similar properties are carbon monoxide (CO) and nitric oxide (NO). These gases are also toxic at high concentrations, are produced endogenously, and can freely permeate plasma membranes to exert biological effects. All three gasotransmitters are highly reactive producing various metabolites that are collectively termed RSS, reactive oxygen species (ROS), and reactive nitrogen species (RNS). It has become clear that these reactive chemical species can react with metabolites and derivatives of the other gasotransmitter molecules to form a densely interconnected web of products sometimes collectively termed the reactive species interactome. For instance; H_2S, NO and their derivatives react to form a family of nitrothiol compounds, resulting in modulation of signalling pathways [54]. Furthermore, each gasotransmitter is capable of regulating the production of the other two gasotransmitters (Figure 3). H_2S stimulates NO production through transcriptional, translational, and post-translational interventions in the NO synthesis pathway, with reports of both elevation and suppression of NO production [55]. The mechanism by which H_2S elevates CO production is still an area of active research but appears to involve activation of the Nrf2-mediated response (see section Post-translational modification (persulfidation)) up-regulating heme oxygenase isoforms which generate CO [56]. These chemical species and intermediates are highly dynamic which makes measuring and understanding the

PORTLAND PRESS

Biochemical Journal (2021) **478** 3485–3504
https://doi.org/10.1042/BCJ20210517

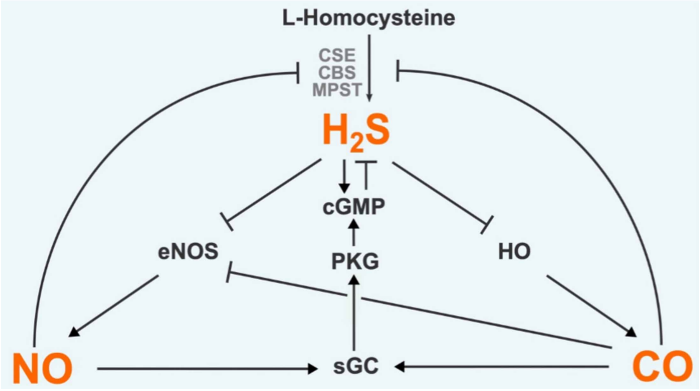

Figure 3. Known interactions between H_2S, CO, and NO signalling pathways.
Each gasotransmitter is capable of regulating the other two. Pointed arrows represent a stimulatory effect. Flat-headed arrows indicate an inhibitory effect. H_2S, Hydrogen sulfide; NO, Nitric oxide; CO, Carbon monoxide; CBS, Cystathionine-β-synthase; CSE, Cystathionine-γ-lyase; MPST, 3-Mercaptopyruvate sulfurtransferase; eNOS, Endothelial NO synthase; HO, Heme oxygenase; sGC, Soluble guanylyl cyclase; PKG, Protein kinase G; cGMP, Cyclic guanosine monophosphate.

exact processes involved in H_2S-NO-CO cross-talk challenging. What is clear is that such cross-talk is an important signalling modality across a diverse range of organisms, influencing plant growth and ripening for example [57,58]. In mammals, the dynamics and functions of H_2S-NO-CO cross-talk are best understood in the cardiovascular system where they exert control over inflammation, angiogenesis, vasodilation, and protection from ischaemia-reperfusion injury (IRI) [59,60]. An interesting case study in the complexity of gasotransmitter cross-talk is demonstrated by the regulation of the activity of soluble guanylate cyclase (sGC), a hemeprotein. Overall, the three gasotransmitters all increase sGC activity but the biochemistry involved in this outcome are distinct. NO is an exceptionally strong activator of sGC, augmenting sGC activity over 100-fold [61]; in contrast, CO is a far weaker activator of sGC [62]. Due to this disparity in potency and binding strength, NO and CO compete for dominance in their interaction with sGC: when NO concentrations are low CO is the predominant activator of sGC; but when NO concentrations are high CO actually inhibits NO-induced elevation of sGC activity [60]. Distinct from this, H_2S does not directly activate sGC but instead has been shown to reduce the heme moiety from Fe^{3+} to Fe^{2+} in human recombinant sGC. CO and NO only interact with Fe^{2+} sGC, thus H_2S facilitates the activity of the other two gases by increasing the available pool of Fe^{2+} sGC [63]. Thus, all three gases work to elevate sGC activity but there is considerable nuance in how this is achieved. The remainder of this review will focus on the effects of just one gasotransmitter, H_2S, in health, disease, and ageing. However, in light of the intricate and overlapping effects of all three gasotransmitters, we must be mindful of the possibility that any effects attributed to H_2S may in reality belong to the unity of all three gasotransmitters.

H_2S and ageing

Role of H_2S in normative ageing

Exploration of the processes that underlie ageing is most easily understood under the guidance of the hallmarks of ageing [64], a landmark review that proposed nine discrete categories of biological processes that are conserved in organismal ageing. A recent review by Perridon et al. [4] considered the impact of H_2S on each of these hallmarks in turn and collected evidence showing direct, H_2S-mediated protection from all ageing hallmarks except for telomere attrition, for which no studies had been published. This review will not aim to repeat the work previously published but instead assess subsequent publications concerning the effect of H_2S on specific tissue ageing. Whilst it is probable that the dynamics of H_2S production and activity are altered throughout age in most tissues of the body, recent papers have focussed on a few select organ systems including the heart, brain, and kidneys.

Cardiovascular ageing

The typical progression of cardiovascular ageing is initiated by endothelial dysfunction, leading to vascular dysfunction, increased severity of atherosclerosis, and subsequently cardiovascular diseases (CVDs) including

Biochemical Journal (2021) **478** 3485–3504
https://doi.org/10.1042/BCJ20210517

PORTLAND PRESS

stroke, hypertension, and coronary heart disease [65]. Key molecular mechanisms that drive this pathological progression are under the influence of H_2S including: signalling through Nrf2, SIRT1, and AMPK/mTOR; activation of potassium channels; and regulation of mitochondrial biogenesis by PGC-1a [66]. Furthermore, exposing cells and mice to H_2S can ameliorate age-associated vascular ageing [67]. Treatment of cultured endothelial cells with nicotinamide mononucleotide (NMN, an NAD^+-elevating supplement) improves vascular remodelling in response to ischaemic injury and enhances endurance and capillary density in old mice, effects that are augmented by co-treatment with H_2S-donating compounds [67]. The augmentation of vascular health by NAD^+ and H_2S boosting treatment is proposed to be due to the convergence of these signalling pathways through SIRT1. However, the same authors also reported that treatment with H_2S in isolation enhanced basal mitochondrial respiration levels in HUVEC cultures, an effect not seen when using NMN [67]. This indicates that H_2S has protective effects independent of NAD. Other evidence for a protective role for H_2S in cardiac cell culture models include improved glucose utilisation, improved metabolic efficiency of glycolysis and the citric acid cycle, and protection against induced cardiomyocyte hypertrophy [68]. Furthermore, CSE expression and H_2S production were found to be reduced in a model of aged primary rat cardiomyocytes [69]. Treatment of these cells with sodium hydrosulfide (NaHS, a H_2S-donating compound) improved cardioprotection in response to ischaemia-reperfusion events via inhibition of mitochondrial permeability transition pore opening and improved mitochondrial membrane potential [69]. Peleli et al. [70] used a mouse model with knock-out (KO) of MPST, one of the three enzymatic producers of H_2S (see section Endogenous production), to study the effect on sulfur-containing chemical species. In these MPST KO mice there was no significant effect on H_2S, polysulfides, or sulfane sulfur level in heart tissue, nor did it affect blood pressure or vascular reactivity relative to wild-type controls, but did elevate several cardiac ROS markers [70]. However, while some positive cardioprotective phenotypes were observed in these mice at 2–3 months of age (including protection from IRI), deleterious phenotypes (including hypertension, cardiac hypertrophy, and reduced myocardial nitric oxide production) were reported at 18 months of age [70]. The authors suggest that the cardioprotective effects in young mice could be explained by increased cardiac ROS levels providing a pre-conditioning against IRI, whereas at old age it appears that ablation of MPST is deleterious to heart function. This study is the first to investigate the cardiovascular phenotype in MPST KO mice and further studies should aim to extend understanding in the role and pathophysiology of MPST in the onset of age-related heart disease.

Neurological ageing

As neuromodulation was the first functional role described for endogenous H_2S in humans [71], it is unsurprising that H_2S has been implicated as a key player in brain ageing. One conduit for multiple neuropathological processes is the receptor for advanced glycation end-products (RAGE). RAGE is among several receptors that bind to advanced glycation end-products, proteins and lipids that have been modified by reaction with sugar molecules in a non-enzymatic manner that accumulate in tissue with age, including the brain [72]. It should be noted that while the transmembrane forms of RAGE are implicated in neurotoxic signalling, soluble forms of RAGE have instead been shown to confer neuroprotective effects, in part due to inhibition of membrane-associated RAGE [73]. RAGE also binds to beta-amyloid, engendering deleterious effects and, as such, has drawn interest as a potential target in the treatment of Alzheimer's disease [74]. Treatment with exogenous H_2S in cells has been shown to inhibit stabilisation of membrane-associated RAGE dimers and the modality for this inhibition was direct persulfidation of a cysteine residue on RAGE [75]. Beyond RAGE signalling, other ageing processes are subject to H_2S regulation in neural cell systems. In a cell culture model of hyperglycaemia-induced hippocampal senescence, treatment of cells with a H_2S donor resulted in a reduction in senescence markers and improved autophagic flux in a SIRT1-dependent manner [76]. H_2S also influences synaptic plasticity, as shown by Abe and Kimura's work on H_2S-facilitated long-term potentiation (LTP) [71]. Thus, stimulation of *N*-methyl-D-aspartic acid (NMDA) receptors in active rat hippocampal synapses was augmented by AdoMet, a CBS-activating compound [71]. More recently, Lu et al. [77] screened a group of aged mice on cognitive ability and showed CBS protein levels were significantly lower in mice with impaired cognition and that the cognitive impairment in these mice was rescued following administration of a H_2S donor (NaHS). These effects were associated with altered sensitivity of metabotropic glutamate receptors to local calcium levels [77], likely due to H_2S modulation of neuronal calcium homeostasis [78]. Similarly, the ability of rats to learn an adaptive associative response to fear conditioning was dependent on endogenous H_2S production by CBS [79]. When CBS was inhibited by hydroxylamine or amino-oxyacetate, amygdalar and hippocampal H_2S levels were reduced, NMDA-receptor mediated LTP was significantly impaired, and fear conditioning

PORTLAND PRESS

Biochemical Journal (2021) **478** 3485–3504
https://doi.org/10.1042/BCJ20210517

responses were dampened. All these effects were rescued by the application of H_2S donor compounds, even in the presence of CBS inhibitors, indicating that the loss of H_2S production is what mediates these effects. In agreement, a similar reduction in fear conditioning-stimulated LTP due to reduced tissue H_2S production and reversal of this effect by application of a sulfide donor was observed in synaptic plasticity in aged rats [80]. H_2S also modulates the biological response to ischaemic stroke, which accounts for over 80% of all strokes [81]. Both endogenous and exogenous sources of H_2S confer neuroprotective effects at low doses and deleterious effects at higher doses. For instance, H_2S production via CBS is greatly elevated following stroke and inhibitors of CBS activity reduced infarct volume in rat models of stroke, whereas administration of H_2S-donating compounds increased infarct volume [82]. However, elevated H_2S activity ameliorated deleterious pro-inflammatory response co-ordinated by microglia, a major contributor to the cerebral IRI pathology. Inhalation of a low dose of H_2S for 3 h immediately after induced cerebral IRI in rats resulted in suppression of this inflammation response through protein kinase C-dependent reduction in aquaporin 4 protein expression, resulting in a reduction in ischaemia infarct size and improved neurobehavioral outcomes [83].

Renal ageing

H_2S production in the kidney is driven by CSE and CBS activity with expression of these enzymes concentrated particularly within the proximal tubule [84]. As H_2S production through these enzymes is part of the transsulfuration pathway there is overlap with homocysteine metabolism which is associated with mortality in late-stage kidney disease [85]. Given the kidney's role in filtering blood content, it is unsurprising that they are sensitive to nutritional intake. Various studies demonstrated a link between diet composition and renal ageing, with amino acid content emerging as a key driver. Dietary restriction (DR) is the most well-characterised intervention for improving health and lifespan (see section H2S in dietary restriction) and typically involves a reduction in gross calories consumed within a set period [86]. However, recent studies have highlighted a specific requirement for restriction of essential amino acids (EAA) in DR protocols for renal protective effects to occur [87]. In a study by Yoshida et al. [88] mice were placed under 'simple DR' (40% reduction in calorie intake) and DR with supplementation of EAAs (DR + EAA) or non-EAA (DR + NEAA). They found that while DR and DR + NEAAs groups displayed extended lifespan and protection from tubulointerstitial lesions, these effects were lost in groups subjected to DR + EAA supplementation. More specifically, they found that excluding methionine from the EAA supplementation was sufficient to restore DR-induced benefits on longevity, kidney function and oxidative stress, and was correlated with an increase in tissue H_2S levels and increased CSE gene expression. Wang et al. similarly found that methionine restriction alone was sufficient to extend lifespan and improve markers of renal ageing in mice. Their mechanistic investigations suggest that AMPK-dependent H_2S signalling protected kidney tissue from the onset of senescence [89]. Additionally, various histological and functional markers of renal ageing were described in both male and female marmosets between ∼3 and 16 years of age, with these changes correlating with an age-associated reduction in CBS protein levels across both sexes, although a significant age-associated reduction in H_2S production was observed only in male marmosets [90]. Another major consequence of renal ageing is acute kidney injury (AKI), which is driven in part by IRI [91]. A single incidence of AKI has profound implications for mortality; hospital patients with AKI commonly have 30–40% mortality rates and as high as 60% for AKI patients admitted to intensive care units [92]. Renal IRI can be ameliorated by the action of H_2S and NO signalling which improve blood flow by causing local vasodilation, inhibiting inflammatory cytokines, and reducing ROS production [93].

H_2S in lifespan extension

Ageing is plastic and modifiable by a variety of environmental, genetic, and pharmaceutical interventions [86]. This section will consider established lifespan extension interventions and assess the potential mechanistic role of H_2S in their modulation of biological ageing.

H_2S in dietary restriction

DR is an umbrella term for a panel of interventions that have been known to consistently improve longevity across taxa for more than 100 years [94–96]. The conservation of this response suggests an evolutionary origin of longevity through DR, best understood through the framework of the disposable soma, mutation accumulation, and antagonistic pleiotropy theories of ageing, among others [97,98]. DR typically confers significant health benefits, and improves late-life health by reducing the incidence and/or trajectory of many age-related pathologies, including cognitive decline, metabolic syndrome, CVD and many cancers [94,99]. Many of these health benefits are also observed in non-human primates exposed to life-long DR [99]. However, cognitive

Biochemical Journal (2021) **478** 3485–3504
https://doi.org/10.1042/BCJ20210517

defects under DR have been reported in rats and atrophy of grey matter volume in DR fed primates [100,101]. Critically, many of the positive health benefits found in model organisms under DR are replicated in humans under DR protocols that carefully supply 100% of essential daily nutrients, but the impact on lifespan is currently unknown [94,95]. The application of DR as a preventive therapeutic tool in humans is promising [102] but remains a challenge, largely due to the difficulty in avoiding accidental malnutrition. Additionally, DR in humans has several reported drawbacks including infertility, sarcopenia, osteoporosis, and reduced immunity [103]. As such, the challenges of applying DR in the wider human population are prohibitive and we may be better served by gaining an understanding of the mechanisms that underlie DR and designing therapeutics targeting them more selectively.

Our understanding of the mechanisms that underpin the effect of DR on lifespan remain imprecise despite decades of investigations. What is certain is a major contribution to DR-induced longevity is from reduced nutrient signalling and improved insulin sensitivity through modulation of signalling pathways including mTOR, insulin/insulin-like signalling (IIS), and NAD metabolism. Murine models with compromised TOR or IIS signalling molecules (such as global loss of ribosomal S6 protein kinase 1 or insulin receptor substrate 1, respectively) showed marked increases in lifespan and a delay in age-related physiological decline [104,105]. Several studies identified H_2S as a potentially conserved mechanism underlying DR-induced longevity and healthspan improvements. In a series of seminal papers led by Dr James Mitchell, the positive effects of multiple DR regimes were dependent on elevated H_2S production in yeast, worms, fruit flies, and mice [106–110]. It is also clear that the effects attributed to DR can largely be recapitulated by the removal of specific dietary components from the diet, even if total calorie intake is maintained [111]. Such interventions include restriction of total protein or tryptophan intake, but perhaps the best studied is methionine restriction, which appears to be closely tied to the transsulfuration pathway and H_2S homeostasis [94]. Life-long methionine restriction in mice protected against renal senescence and elevated endogenous H_2S production, with complementary *in vitro* assays indicating a mechanistic role for H_2S in this protection [89]. Given that the SAAs (methionine and cysteine) are the canonical sources for endogenous *de novo* H_2S production, it is perhaps unsurprising that restriction of methionine modulates H_2S production. However, it is counterintuitive that restriction of the dietary source for *de novo* H_2S synthesis ultimately results in elevation of H_2S levels; a conundrum that has several possible solutions but no concrete answer to date [107]. One resolution to this apparent contradiction is that DR reduces hypothalamic–pituitary signalling, which functions partly through the inhibition of H_2S production by growth hormone and thyroid hormone at the transcriptional and protein levels, respectively [112]. As such, DR-mediated reduction in growth and thyroid hormone release may reduce inhibition of H_2S production enzymes. One alternative explanation for the observation that reduced calorie intake elevates H_2S levels despite reduced pools of SAAs is that elevation of autophagic processes under nutrient-limiting conditions generates the substrate pool for H_2S biogenesis. DR and fasting interventions have been shown to elevate autophagy processes across tissues in mice and humans [113]. Indeed, induction of H_2S biogenesis under DNA damage stress has been demonstrated to be a autophagy-dependent response *in vitro* [114], and cysteine pools are maintained through autophagic processes in pancreatic cancer [115]. Methionine has also been shown to indirectly inhibit the induction of autophagy by elevating S-adenosylmethioine (SAM) levels, which in turn promotes methylation of protein phosphatase 2A, leading to autophagy inhibition [116]. Together, these studies support the premise that elevated autophagy replenishes the cellular cysteine pool, allowing for the generation of H_2S under nutrient-limiting conditions. More studies that directly measure H_2S levels under such conditions are required to definitively support this.

H_2S in dwarf mouse models

Beyond dietary interventions, various mutations in model organisms confer significant longevity benefits. In fact, the Ames dwarf mouse has the longest extension in lifespan achieved by genetic, dietary, or pharmaceutical intervention with mean and maximal lifespan increase in over 45% in both sexes [117]. The dwarf mouse models have genetic disruption of anterior pituitary gland function either through mutations in transcription factors like Pit1 and Prop1 (as in the Snell and Ames dwarf mice models, respectively) or in growth hormone signalling receptors such as growth hormone receptor and growth hormone-releasing hormone receptor, both of which result in long-lived dwarf mice [117–119]. There have been relatively few studies that link the reduced pituitary signalling phenotype to the action of H_2S, with the notable exception of Hine et al. [112] who showed that both the Snell and Ames dwarf models had up-regulation of H_2S production pathways. This is in part due to ablation of the transcriptional regulation of CSE and CBS expression by thyroid hormone signalling and

PORTLAND PRESS

Biochemical Journal (2021) **478** 3485–3504
https://doi.org/10.1042/BCJ20210517

through substrate availability control by autophagic processes, respectively, in dwarf mice [112]. This correlates well with previous research that used labelled metabolites to demonstrate an increase in the flux of methionine through the transsulfuration pathway in Ames mice [120]. These studies unveiled a rerouting of metabolism through transsulfuration in the liver, brain, and kidneys of the mice with a concomitant, but non-significant, increase in hepatic CSE gene expression compared with wild-type controls [120]. Hepatic CSE specific activity is also elevated in Ames mice [121]. The expected result of this altered metabolism is that the Ames mice will have an elevated pool of cysteine from which H_2S can be generated, which may contribute to the findings of Hine et al. [112] that these mice have improved H_2S production capacity. Interestingly, while restriction of dietary methionine extended lifespan and increased hepatic H_2S levels in many models, the Ames models showed no increased lifespan on a methionine-restricted diet [122]. H_2S levels have not been measured in Ames mice under methionine-restricted conditions, however, Brown-Borg et al. [123] showed that much of the rerouting of metabolic processes through transsulfuration observed in Ames mice was unaffected by methionine restriction. This was opposed to the expected up-regulation of transsulfuration as seen in wild-type animals on methionine restriction [123]. From this, we could infer that intact growth hormone signalling is essential for 'sensing' dietary amino acid abundance and plays an important role in coordinating altered metabolism in response to differential methionine abundance. Further work is required to assess if H_2S plays a role in this proposed mechanism for growth hormone regulation of methionine metabolism as well as in the extraordinary lifespan extension of growth hormone mutant mice.

H_2S in longevity through pharmaceutical intervention

Longevity is plastic in response to a variety of pharmaceutical interventions, and chief among these are inhibitors of nutrient-sensing pathways such as Rapamycin (targets mTOR signalling), and the anti-diabetic drugs Metformin (targets AMPK signalling) and Acarbose (targets IIS signalling) [94]. H_2S signalling overlaps with all of these mechanisms.

Rapamycin and mTOR signalling

Within the context of mTOR signalling, H_2S can be either stimulatory or inhibitory, as recently reviewed [124]. This is counterintuitive as both H_2S and Rapamycin were implicated as pro-longevity molecules and therefore we might anticipate they would both act upon the mTOR pathway in a similar manner, i.e. suppression of mTOR activity. This is the case in some instances, such as a study in brain tissue from diabetic mice where treatment with a H_2S donor reduced protein synthesis by inhibiting mTOR signalling and increasing autophagic processes [125]. Furthermore, exogenously increased H_2S concentration induces autophagy in cells and is associated with inhibition of TOR activity [126,127]. However, contradictory studies showed an anti-autophagic role for H_2S via mTOR signalling with myriad effects ranging from rescuing high-fat diet-induced liver disease, protecting against diabetic myopathy, stimulating angiogenesis, and stimulating osteoclastogenesis [128–131]. Along with conflicting results in mTOR signalling, we lack a full appreciation of the effect of Rapamycin on H_2S production pathways. To date only one study has investigated this, using Rapamycin in *Saccharomyces cerevisiae* and human cells [132]. The authors found that Rapamycin inhibited H_2S production through the depression of CSE and CBS gene transcription in both cell models, indicating a conserved role of Rapamycin in regulating H_2S generation [132]. More work is required to test how conserved this response to Rapamycin treatment is across tissues and species. There also remains a lack of studies that combine Rapamycin and H_2S donors. Such approaches offer an additional understanding of how these compounds co-interact with mTOR signalling. One example of such an approach used a human hepatocellular carcinoma cell line and treatment with Rapamycin and a H_2S-donor separately or in combination [133]. Wang et al. also found that both treatments inhibited mTOR signalling and stimulated anti-tumour autophagic and pro-apoptotic pathways and were additive when used in combination. The sum of work performed by researchers has confirmed the theory that longevity through Rapamycin inhibition of mTOR is subject to regulation by H_2S. However, further studies are required to dissect out the precise conditions where H_2S modulates mTOR in alignment with Rapamycin, in opposition, or whether there is a more nuanced interaction between these molecules.

Metformin and AMPK signalling

Metformin is another putative lifespan-extending drug that interacts with H_2S signalling. Metformin's mechanism of action remains only partially resolved, but appears to operate largely through activation of AMPK (which in turn inhibits mTOR and IIS signalling pathways) [134]. Early studies showed that there was a

Biochemical Journal (2021) **478** 3485–3504
https://doi.org/10.1042/BCJ20210517

correlational link between metformin treatment in mice and the elevation of H_2S levels in the brain, heart, kidney, and liver tissues [135]. Following this discovery, the role of H_2S in the pharmacological activity of AMPK signalling and metformin treatment was studied in earnest and this body of work was collected in a 2017 review [136]. How metformin increases H_2S levels is becoming increasingly apparent and appears related to the ability of metformin to remodel DNA methylation patterns [137]. Work by Ma et al. [138] showed that a high methionine diet (methionine forming 2% of diet) resulted in the elevation of plasma homocysteine levels and a reduction in plasma H_2S levels, effects that were rescued by metformin treatment. Complementary cell culture assays suggest that metformin treatment removes homocysteine-stimulated hypermethylation of the *CSE* promotor region, resulting in greater mRNA and protein expression of CSE and elevation of H_2S production [138]. Similarly, a metabolomics study in rats found that metformin treatment ameliorated oxidative liver damage caused by exposure to bisphenol A through elevation of CSE and CBS levels [139]. Our emerging understanding of the transcriptional control of H_2S producing genes presents a clear connection between metformin and H_2S production. However, as the modes of action of metformin remain only partially understood, more work is required to fully understand the interplay between H_2S, AMPK signalling, and metformin.

Acarbose and IIS signalling

Acarbose inhibits carbohydrate digestion and glucose absorption and is known to extend maximum lifespan in male and female mice, but only extends median lifespan in males [140]. There is currently a scarcity of studies interrogating the interaction of Acarbose with H_2S. This presents a potentially fruitful area of novel research as H_2S is already known to modulate insulin signalling and whole-animal glucose metabolism across tissues, cellular processes that appear intimately linked with longevity [141]. As with other signalling pathways, the effects of H_2S are complex, with independent studies reporting either protective or deleterious effects [142]. The endogenous production of H_2S in adipose cells was first described by Feng et al. [143] who showed that elevated CSE expression and H_2S production was correlated with insulin resistance in rats, suggestive of a deleterious diabetic phenotype associated with H_2S expression in adipocytes. Similar results were found in a hepatocyte cell line and primary mouse hepatocytes which showed that supraphysiological levels of H_2S, either through H_2S donor compounds or adenovirus-induced overexpression of CSE, negatively impacted glucose uptake and storage as glycogen [144]. These effects were attributed in part to inhibition of both the AMPK and IIS signalling pathways [144]. Finally, pancreatic beta-cells under chronic exogenous H_2S treatment exhibited suppression of insulin secretion and were protected against oxidative stress-induced apoptosis via elevated glutathione content and reduced ROS [145]. The authors suggest that this cytoprotection may constitute a homeostatic response to maintain islet beta-cell numbers in the presence of cytotoxic extracellular glucose concentrations (which is common in patients with uncontrolled Type 1 diabetes), but at the cost of reduced insulin secretion [145]. However, many other studies implicate a protective role of H_2S in insulin signalling pathways. Studies in a mouse myoblast cell model insulin resistance reported a reduction in H_2S production, despite elevation in CSE protein levels [146]. Treatment of these cells with exogenous H_2S improved insulin sensitivity and mitochondrial function in part through phosphorylation and activation of the insulin receptor pathway [146]. CSE activity and H_2S production in adipocytes also mediated translocation of glucose transporter 4 (GLUT4), an essential step in the effective uptake and utilisation of glucose [147]. Work by Xue et al. [148] showed that H_2S donor treatment increased activation of insulin receptor and improved glucose uptake in adipocytes and myocytes and that chronic H_2S donor treatment decreased blood glucose, improved insulin sensitivity and glucose tolerance, and elevated phosphorylation of insulin signalling pathway enzymes in a diabetic rat model. However, the beneficial effect of H_2S donors on whole-animal carbohydrate metabolism is contradicted by Gheibi et al. [149] who showed that chronic administration of H_2S donor compounds in a type-II diabetic rat model resulted in dose-dependent impairment of glucose tolerance, pyruvate tolerance, and insulin secretion. These two rat studies underline the importance of H_2S donor concentration in the interpretation of the biological effects of H_2S. The Xue et al. paper used NaSH over the range of 168–670 μg/Kg/day for 10 weeks, whereas the Gheibi et al. study used a higher range of 280–5600 μg/Kg/day for 9 weeks. The majority of the deleterious effects of chronic NaHS treatment reported by Gheibi et al. were found in the highest dosage groups, indicating that their treatment range may well approach the dosage at which NaHS begins to confer deleterious or toxic side-effects. The often contradictory work compiled to date shows that the interaction between H_2S and the molecular, cellular, and physiological role of insulin signalling remains poorly understood. As such, any potential overlap between H_2S and Acarbose in improving longevity and late-life health remains unresolved and more work is required to investigate this potentially important signalling commonality.

PORTLAND PRESS

Biochemical Journal (2021) **478** 3485–3504
https://doi.org/10.1042/BCJ20210517

H_2S in lifespan shortening

Progeria syndromes

Progeroid syndromes are a set of genetic disorders characterised by a shortened lifespan and the development of phenotypes normally associated with advanced age [150]. Progeroid syndromes mimic many characteristics of normal human ageing to varying degrees, and therefore present invaluable insight into dysregulation of normal physiological ageing [151]. While all progeroid conditions are extremely rare, the most common is Hutchinson–Gilford progeria syndrome (HGPS). HGPS is an example of a laminopathy, a sub-set of progeria caused by various mutations in the LMNA gene which encodes for lamin proteins [150]. Lamins are a class of intermediate filaments, serving as scaffolds that anchor chromatin and transcription factors to the nuclear periphery [152]. Dysfunctional post-translational processing of lamin A leads to a permanently farnesylated and methylated lamin A isoform, named progerin. The expression of progerin produces disruption of the nuclear membrane, leading to premature senescence, and ageing. Progerin also accumulates in small amounts during physiological ageing due to spontaneous activation of the cryptic splice site observed in HGPS [153]. This suggests that normal and accelerated ageing share at least some common molecular basis. Moreover, many of the hallmarks of physiological ageing are observed in HGPS patients [154]. Overall, the link between progerin accumulation and hallmarks of ageing, the manifestation of age-related diseases in HGPS patients, the expression of progerin during normal ageing and the well-characterised genetic defects in HGPS make it a relevant human ageing model [155].

H_2S in progeria

Therapeutic treatments for patients with progeroid diseases remain critically lacking, with an average life expectancy in HGPS of less than 15 years [156]. Current treatments include farnesyltransferase inhibitors, rapamycin analogues, sulforaphane, and vitamin D analogues which all have clear impacts on disease symptoms but have yet to provide substantial improvements to patient lifespan or comorbidities [156]. While no studies have investigated the role of H_2S in HGPS to date, there is known overlap between H_2S and the mechanisms that underpin the effects of rapamycin (see section H2S in dwarf mouse models), sulforaphane, and vitamin D treatments. Sulforaphane is an isothiocyanate compound found naturally in cruciferous vegetables that acts as a H_2S donor. Beyond HGPS, treatment or ingestion of sulforaphane-rich vegetable homogenates is a promising treatment in Alzheimer's disease and boosts antiviral responses of natural killer cells in human clinical trials [157,158]. The mechanism through which sulforaphane operates *in vitro* appears to involve the generation of H_2S, with sulforaphane treatment elevating H_2S levels upon addition to cells and tissue homogenates [157,159]. Furthermore, sulforaphane treatment in a human prostate cancer cell lines impeded cancer cell survival via H_2S-mediated JNK and MAPK signalling [159]. Finally, the activity of sulforaphane was attributed largely to its potent activation of NRF2 by modification of KEAP1 [160] and insulin signalling [161], mechanisms that are also directly influenced by H_2S signalling (see sections Post-translational modification (persulfidation) and Acarbose and IIS signalling). Given that sulforaphane is a compound that is essentially a naturally occurring H_2S donor and has been shown to operate through biological mechanisms that are known H_2S signalling pathways, there have been a surprisingly limited number of studies that directly monitor H_2S levels following sulforaphane treatment, and none in the context of HGPS. Future studies should aim to monitor H_2S production, disposal, and activity in sulforaphane treated HGPS models to better understand the interplay between these compounds.

Vitamin D and related compounds have also been used in the treatment of HGPS [162], and while the connection to H_2S is not as immediately evident as the H_2S-donating sulforaphane, evidence exists for a commonality in their modes of action. Vitamin D treatment in mice elicits a dose-dependent elevation of tissue H_2S levels in the kidney and brain [163]. Cell culture studies found that H_2S formation was central to vitamin D-induced protection of adipocytes from inflammation and impaired glucose utilisation due to high glucose culture conditions [147]. Finally, a population study found a correlation between reduced plasma H_2S and vitamin D levels in African American type-II diabetics compared with Caucasians with type-II diabetes, and *in vitro* studies in monocyte culture also found an elevation of CSE expression and H_2S production following vitamin D treatment [164].

Together, the strong overlap between proven treatments for HGPS and established molecular mechanisms under the influence of H_2S (mTOR signalling, NRF2 response, and vitamin D signalling) it is surprising there have been so few studies addressing the role of H_2S in the management of HGPS. While there has been no

Biochemical Journal (2021) **478** 3485–3504
https://doi.org/10.1042/BCJ20210517

PORTLAND PRESS

research directly linking H_2S to HGPS, there has been work published in another progeria syndrome, Werner syndrome (WS). The study showed that the cellular morphological phenotype of human WS cells, characterised by increased protein aggregation, high levels of oxidative stress and nuclear dysmorphology, was ameliorated by treatment with NaHS [165]. The beneficial effects of NaHS treatment were due to inhibition of the mTOR pathway, as rapamycin treatment displayed similar effects to NaHS treatment. Furthermore, the enzymes involved in the endogenous production of H_2S were down-regulated in WS cells, suggesting that reduced H_2S levels may be one of the causes of WS phenotype [165]. Overall, this study hints at the importance of the TSP and H_2S production in WS progeria and stresses the importance of further research across all progeroid diseases.

The potential for H_2S therapeutics against ageing

With the accumulated evidence that H_2S is central to physiology and pathology across species and tissues, the inevitable question is whether we can leverage our understanding of H_2S to design translational interventions, potentially even as a treatment against ageing [166]. Studies that show clinically relevant roles for H_2S in age-related diseases have fuelled this discussion. One such example is critical limb ischaemia (CLI), the end stage of peripheral arterial disease which is fast becoming a major morbidity in the aging population, with incidence increasing at twice the rate of global population growth and a higher global incidence than cancer, dementia, HIV/AIDs, and heart failure [167]. Islam et al. [168] examined gastrocnemius tissues sampled from post-amputation limbs of patients with CLI to interrogate regulation and signalling of H_2S in these patients. CLI patients showed decreased transcription of CSE, CBS, and MPST mRNAs, reduced H_2S and sulfane sulfur levels, a reduction in NRF2 and transcription of its target genes such as catalase and glutathione peroxidase and an increase in markers of oxidative stress such as malondialdehydes and protein carbonyls [168]. While their study was limited by the difficulty in obtaining human control samples from amputees without CLI, the results show a potentially pathological role of dysregulated H_2S production and signalling in a clinical setting. Further work is required to develop this understanding and attempt H_2S-based therapies for this growing clinical population. Another major clinical presentation in the ageing population is the increased risk of osteoporosis. A genome-wide association study (GWAS) identified nonsynonymous single nucleotide polymorphisms in the H_2S oxidising enzyme gene SQR as a susceptibility variant in postmenopausal osteoporosis risk in Korean women [169]. Validation studies in a preosteoblast cell line found overexpression of this variant improved markers of osteoblast differentiation [169]. The study did not have a direct measure of H_2S in individuals with this variant and so could not determine for certain if the variant resulted in an increase or decrease in the H_2S oxidation activity of SQR. Nonetheless, this implicates H_2S in osteoblast maintenance. This is supported by other studies that have described conflicting roles for H_2S in bone remodelling [170,171]. Furthermore, a GWAS meta-analysis of age-related hearing impairment identified CSE as one of the seven loci that was reproducibly identified as a candidate in the onset of hearing loss [172], while another identified a variant in the promotor region of CBS in peripheral neuropathy caused by the chemotherapy treatment of multiple myeloma [173]. These studies help foster the potential for H_2S-based therapies as they suggest a role for H_2S in many age-related pathologies and provide novel targets for drug development.

The emerging understanding of how H_2S exerts influence over clinically relevant biological processes raises hopes for the development of a new class of therapeutics. However, several major obstacles prevent this from being immediately achievable. The chemical nature of H_2S itself poses the greatest challenge to its use as a therapy. The volatility of H_2S impedes its study in basic research as H_2S gas readily escapes into the air on the bench. Furthermore, as H_2S reacts so readily with a wide range of other chemical species, it would prove challenging to control off-target effects in a potential H_2S-based therapy. Of greatest concern, however, is the powerful inhibition of COX by H_2S. It has been proposed that the regulation of H_2S production and oxidation is so well conserved across species largely due to the necessity to precisely modulate intracellular H_2S levels in order to avoid toxicity by COX inhibition. There may be some hope, however, that chronic administration of H_2S need not be toxic. Reed et al. [174] investigated cognitive outcomes in the urban population of Rotorua, New Zealand where residents have been exposed to unusually high atmospheric concentrations of volcanic H_2S for decades. As H_2S is a known environmental toxin, their hypothesis was that this population would have reduced cognition compared with controls, but they found that areas of the city with lower (but still abnormally high) ambient H_2S had no significant reduction in measures of cognition while those exposed to the highest levels of ambient H_2S actually showed better performance in reaction time and in the digit symbol tests [174]. Related studies on the population of Rotorua found no association between H_2S exposure and asthma risk, peripheral neuropathy or cancer incidence, and actually indicated a potential protective effect against Parkinson's

PORTLAND PRESS

Biochemical Journal (2021) **478** 3485–3504
https://doi.org/10.1042/BCJ20210517

disease [175–178]. While these studies are indicative of safe, long-term exposure to H_2S in humans, there are limitations in their design including the difficulties in estimating the ambient H_2S levels throughout the decades, misclassification of individuals into the wrong exposure group, and it is impossible to confirm causality for any of the observed effects as the studies were epidemiological in nature. These limitations necessitate further study to best understand the therapeutic window for safe and effective H_2S exposure. The challenges of H_2S therapies and the positive and negative considerations for each of the established H_2S-donating compounds was reviewed recently [179]. Given these challenges, any progress in the development of H_2S therapies is contingent on better measurements of tissue H_2S concentrations *in vivo*, the improved resolution of flux through H_2S production, oxidation, and signalling, the establishment of the therapeutic window for H_2S compounds, and innovations in the administration and targeting of H_2S in therapies. These are not insubstantial open questions for the field but given the rapid rise in interest of H_2S biology in recent years, our understanding of these questions is likely to expand greatly.

Future directions and conclusions

Increasing evidence shows that H_2S is integral to multiple healthspan- and lifespan-extending interventions, whether dietary, pharmacological, or genetic in nature. This is due to the capability of H_2S to participate in a multitude of biological processes by virtue of its diverse signalling modalities. There is a high degree of evolutionary conservation across taxa for the production of H_2S itself through the transsulfuration pathway and in the signalling pathways it interacts with. Together, these attributes implicate H_2S as a powerful modulator of healthspan, severity of disease, and longevity. However, there are many aspects of our understanding that remain vague. Most prominently, due to the short half-life and chemical promiscuity of H_2S, it is extremely challenging to obtain accurate measures of H_2S and related chemical species *in vivo*. This limitation means that while we are increasingly certain of a correlation between H_2S and various markers of longevity and healthspan, it is difficult to ascertain which specific chemical species confers the observed effects and where these effects are occurring at the tissue, cellular or even sub-cellular level. In addition, while this review has focussed on the many beneficial effects of H_2S, it should not be forgotten that excessive levels of H_2S are extremely toxic in biological systems. As such, future research should focus on better understanding the precise mechanisms by which H_2S operates and the development of more sophisticated methods for measuring *in vivo* H_2S levels. Only once these advancements are made can we begin in earnest to work towards H_2S-based therapeutics.

Competing Interests

The authors declare that there are no competing interests associated with the manuscript.

Funding

We acknowledge support through a MRC Precision Medicine Doctoral Training Programme PhD studentship (to S.E.W., Ref: MR/N013166/1) and the BBSRC (to C.S., Ref: BB/S014330/1).

Acknowledgements

We are grateful for the support of Professor Jay Mitchell and Dr. Chris Hine, whose enthusiasm for this field of research helped stimulate our enthusiasm.

Abbreviations

AKI, acute kidney injury; AMPK, AMP-activated protein kinase; CBS, cystathionine-beta-synthase; CLI, critical limb ischaemia; COX, cytochrome c oxidase; CSE, or CGL, cystathionine-gamma-lyase; CVDs, cardiovascular diseases; DR, dietary restriction; DR, dietary restriction; EAA, essential amino acids; ETHE1, ethylmalonic encephalopathy 1; GSH, glutathione; GSSH, generating glutathione persulfide; GWAS, genome-wide association study; H_2S, hydrogen sulfide; HGPS, Hutchinson–Gilford progeria syndrome; IIS, insulin/insulin-like signalling; KO, knock-out; LTP, long-term potentiation; MPST, or TUM1, 3-mercaptopyruvate sulfurtransferase; MSBT, methylsufonylbenzothiazole; NMDA, *N*-methyl-D-aspartic acid; NMN, nicotinamide mononucleotide; NRF2, nuclear factor erythroid 2-related factor 2; PLP, pyridoxal-5′-phosphate; RAGE, receptor for advanced glycation end-products; RBCs, red blood cells; ROS, reactive oxygen species; RSS, reactive sulfur species; SAAs, sulfur-containing amino acids; sGC, soluble guanylate cyclase; SOU, sulfide oxidation unit; SQR, sulfur:quinone oxidoreductase; SRB, sulfate-reducing bacteria; TST, thiosulfate sulfurtransferase; WS, Werner syndrome.

Biochemical Journal (2021) **478** 3485–3504
https://doi.org/10.1042/BCJ20210517

Reference

1 Kabil, H., Kabil, O., Banerjee, R., Harshman, L.G. and Pletcher, S.D. (2011) Increased transsulfuration mediates longevity and dietary restriction in drosophila. *Proc. Natl Acad. Sci. U.S.A.* **108**, 16831–6 https://doi.org/10.1073/pnas.1102008108

2 Sbodio, J.I., Snyder, S.H. and Paul, B.D. (2018) Regulators of the transsulfuration pathway. *Br. J. Pharmacol.* **176**, 583–593 https://doi.org/10.1111/bph.14446

3 Giovanelli, J. and Mudd, S.H. (1971) Transsulfuration in higher plants partial purification and properties of β-cystathionase of spinach. *Biochim. Biophys. Acta* **227**, 654–670 https://doi.org/10.1016/0005-2744(71)90015-5

4 Perridon, B.W., Leuvenink, H.G.D., Hillebrands, J.-L., van Goor, H. and Bos, E.M. (2016) The role of hydrogen sulfide in aging and age-related pathologies. *Aging (Albany, NY)* **8**, 2264–2289 https://doi.org/10.18632/aging.101026

5 Stipanuk, M.H. and Beck, P.W. (1982) Characterization of the enzymic capacity for cysteine desulphhydration in liver and kidney of the rat. *Biochem. J.* **206**, 267–277 https://doi.org/10.1042/bj2060267

6 Fu, M., Zhang, W., Wu, L., Yang, G., Li, H. and Wang, R. (2012) Hydrogen sulfide (H2S) metabolism in mitochondria and its regulatory role in energy production. *Proc. Natl Acad. Sci. U.S.A.* **109**, 2943–2948 https://doi.org/10.1073/pnas.1115634109

7 Fräsdorf, B., Radon, C. and Leimkühler, S. (2014) Characterization and interaction studies of two isoforms of the dual localized 3-mercaptopyruvate sulfurtransferase TUM1 from humans. *J. Biol. Chem.* **289**, 34543–34556 https://doi.org/10.1074/jbc.M114.605733

8 Nagahara, N., Ito, T., Kitamura, H. and Nishino, T. (1998) Tissue and subcellular distribution of mercaptopyruvate sulfurtransferase in the rat: confocal laser fluorescence and immunoelectron microscopic studies combined with biochemical analysis. *Histochem. Cell Biol.* **110**, 243–250 https://doi.org/10.1007/s004180050286

9 Shibuya, N., Koike, S., Tanaka, M., Ishigami-Yuasa, M., Kimura, Y., Ogasawara, Y. et al. (2013) A novel pathway for the production of hydrogen sulfide from D-cysteine in mammalian cells. *Nat. Commun.* **4**, 1366 https://doi.org/10.1038/ncomms2371

10 Lagoutte, E., Mimoun, S., Andriamihaja, M., Chaumontet, C., Blachier, F. and Bouillaud, F. (2010) Oxidation of hydrogen sulfide remains a priority in mammalian cells and causes reverse electron transfer in colonocytes. *Biochim. Biophys. Acta Bioenerg.* **1797**, 1500–1511 https://doi.org/10.1016/j.bbabio.2010.04.004

11 Bouillaud, F. and Blachier, F. (2011) Mitochondria and sulfide: a very old story of poisoning, feeding, and signaling? *Antioxid. Redox Signal.* **15**, 379–391 https://doi.org/10.1089/ars.2010.3678

12 Furne, J., Saeed, A. and Levitt, M.D. (2008) Whole tissue hydrogen sulfide concentrations are orders of magnitude lower than presently accepted values. *Am. J. Physiol. Regul. Integr. Comp. Physiol.* **295**, 1479–1485 https://doi.org/10.1152/ajpregu.90566.2008

13 Rose, P., Moore, P.K. and Zhu, Y.Z. (2017) H2s biosynthesis and catabolism: new insights from molecular studies. *Cell Mol. Life Sci.* **74**, 1391–1412 https://doi.org/10.1007/s00018-016-2406-8

14 Goubern, M., Andriamihaja, M., Nübel, T., Blachier, F. and Bouillaud, F. (2007) Sulfide, the first inorganic substrate for human cells. *FASEB J.* **21**, 1699–1706 https://doi.org/10.1096/fj.06-7407com

15 Jackson, M.R., Melideo, S.L. and Jorns, M.S. (2012) Human sulfide:quinone oxidoreductase catalyzes the first step in hydrogen sulfide metabolism and produces a sulfane sulfur metabolite. *Biochemistry* **51**, 6804–6815 https://doi.org/10.1021/bi300778t

16 Mishanina T, V., Yadav, P.K., Ballou, D.P. and Banerjee, R. (2015) Transient kinetic analysis of hydrogen sulfide oxidation catalyzed by human sulfide quinone oxidoreductase. *J. Biol. Chem.* **290**, 25072–25080 https://doi.org/10.1074/jbc.M115.682369

17 Augustyn, K.D.C., Jackson, M.R. and Jorns, M.S. (2017) Use of tissue metabolite analysis and enzyme kinetics to discriminate between alternate pathways for hydrogen sulfide metabolism. *Biochemistry* **56**, 986–996 https://doi.org/10.1021/acs.biochem.6b01093

18 Kabil, O. and Banerjee, R. (2012) Characterization of patient mutations in human persulfide dioxygenase (ETHE1) involved in H2S catabolism. *J. Biol. Chem.* **287**, 44561–44667 https://doi.org/10.1074/jbc.M112.407411

19 Maseda, C., Hayakawa, A., Okuda, K., Asari, M., Tanaka, H., Yamada, H. et al. (2017) Liquid chromatography-tandem mass spectrometry method for the determination of thiosulfate in human blood and urine as an indicator of hydrogen sulfide poisoning. *Leg. Med.* **24**, 67–74 https://doi.org/10.1016/j.legalmed.2016.12.004

20 Vitvitsky, V., Yadav, P.K., Kurthen, A. and Banerjee, R. (2015) Sulfide oxidation by a noncanonical pathway in red blood cells generates thiosulfate and polysulfides. *J. Biol. Chem.* **290**, 8310–8320 https://doi.org/10.1074/jbc.M115.639831

21 Barton, L.L. and Hamilton, A.W. (2007) Sulphate-reducing bacteria: Environmental and engineered systems. In *Sulphate-Reducing Bacteria: Environmental and Engineered Systems* (Barton, L.L. and Hamilton, W.A., eds), pp. 1–538, Cambridge University Press, Cambridge, United Kingdom

22 Linden, D.R. (2014) Hydrogen sulfide signaling in the gastrointestinal tract. *Antioxid. Redox Signal.* **20**, 818–830 https://doi.org/10.1089/ars.2013.5312

23 Scanlan, P.D., Shanahan, F. and Marchesi, J.R. (2009) Culture-independent analysis of desulfovibrios in the human distal colon of healthy, colorectal cancer and polypectomized individuals. *FEMS Microbiol. Ecol.* **69**, 213–221 https://doi.org/10.1111/j.1574-6941.2009.00709.x

24 Shatalin, K., Shatalina, E., Mironov, A. and Nudler, E. (2011) H2s: a universal defense against antibiotics in bacteria. *Science* **334**, 986–990 https://doi.org/10.1126/science.1209855

25 Cord-Ruwisch, R., Seitz, H.J. and Conrad, R. (1988) The capacity of hydrogenotrophic anaerobic bacteria to compete for traces of hydrogen depends on the redox potential of the terminal electron acceptor. *Arch. Microbiol.* **149**, 350–357 https://doi.org/10.1007/BF00411655

26 Flannigan, K.L., McCoy, K.D. and Wallace, J.L. (2011) Eukaryotic and prokaryotic contributions to colonic hydrogen sulfide synthesis. *Am. J. Physiol. Liver Physiol.* **301**, G188–G193 https://doi.org/10.1152/ajpgi.00105.2011

27 Tomasova, L., Konopelski, P. and Ufnal, M. (2016) Gut bacteria and hydrogen sulfide: the new old players in circulatory system homeostasis. *Molecules* **21**, 1558 https://doi.org/10.3390/molecules21111558

28 Roediger, W.E.W., Duncan, A., Kapaniris, O. and Millard, S. (1993) Reducing sulfur compounds of the colon impair colonocyte nutrition: implications for ulcerative colitis. *Gastroenterology* **104**, 802–809 https://doi.org/10.1016/0016-5085(93)91016-B

29 Tomasova, L., Dobrowolski, L., Jurkowska, H., Wróbel, M., Huc, T., Ondrias, K. et al. (2016) Intracolonic hydrogen sulfide lowers blood pressure in rats. *Nitric Oxide* **60**, 50–58 https://doi.org/10.1016/j.niox.2016.09.007

30 Guo, F.-F., Yu, T.-C., Hong, J. and Fang, J.-Y. (2016) Emerging roles of hydrogen sulfide in inflammatory and neoplastic colonic diseases. *Front. Physiol.* **7**, 156 https://doi.org/10.3389/fphys.2016.00156

PORTLAND PRESS

Biochemical Journal (2021) **478** 3485–3504
https://doi.org/10.1042/BCJ20210517

31 Singh, R.K., Chang, H.-W., Yan, D., Lee, K.M., Ucmak, D., Wong, K. et al. (2017) Influence of diet on the gut microbiome and implications for human health. *J. Transl. Med.* **15**, 73 https://doi.org/10.1186/s12967-017-1175-y

32 Dostal Webster, A., Staley, C., Hamilton, M.J., Huang, M., Fryxell, K., Erickson, R. et al. (2019) Influence of short-term changes in dietary sulfur on the relative abundances of intestinal sulfate-reducing bacteria. *Gut Microbes* **10**, 447–457 https://doi.org/10.1080/19490976.2018.1559682

33 Shatalin, K., Nuthanakanti, A., Kaushik, A., Shishov, D., Peselis, A., Shamovsky, I. et al. (2021) Inhibitors of bacterial H2S biogenesis targeting antibiotic resistance and tolerance. *Science* **372**, 1169–1175 https://doi.org/10.1126/science.abd8377

34 Zhang, D., Du, J., Tang, C., Huang, Y. and Jin, H. (2017) H_2S-induced sulfhydration: biological function and detection methodology. *Front. Pharmacol.* **8**, 608 https://doi.org/10.3389/fphar.2017.00608

35 Jencks, W.P. and Carriuolo, J. (1960) Reactivity of nucleophilic reagents toward esters. *J. Am. Chem. Soc.* **82**, 1778–1786 https://doi.org/10.1021/ja01492a058

36 Yang, G., Zhao, K., Ju, Y., Mani, S., Cao, Q., Puukila, S. et al. (2013) Hydrogen sulfide protects against cellular senescence via s-sulfhydration of keap1 and activation of Nrf2. *Antioxidants Redox Signal.* **18**, 1906–1919 https://doi.org/10.1089/ars.2012.4645

37 Hourihan, J.M., Kenna, J.G. and Hayes, J.D. (2013) The gasotransmitter hydrogen sulfide induces Nrf2-target genes by inactivating the keap1 ubiquitin ligase substrate adaptor through formation of a disulfide bond between Cys-226 and Cys-613. *Antioxidants Redox Signal.* **19**, 465–481 https://doi.org/10.1089/ars.2012.4944

38 Olas, B. (2015) Hydrogen sulfide in signaling pathways. *Clin. Chim. Acta* **439**, 212–218 https://doi.org/10.1016/j.cca.2014.10.037

39 Filipovic, M.R., Zivanovic, J., Alvarez, B. and Banerjee, R. (2017) Chemical biology of H2S signaling through persulfidation. *Chem. Rev.* **118**, 1253–1337 https://doi.org/10.1021/acs.chemrev.7b00205

40 Yadav, P.K., Martinov, M., Vitvitsky, V., Seravalli, J., Wedmann, R., Filipovic, M.R. et al. (2016) Biosynthesis and reactivity of cysteine persulfides in signaling. *J. Am. Chem. Soc.* **138**, 289–299 https://doi.org/10.1021/jacs.5b10494

41 Kawamura, S., Kitao, T., Nakabayashi, T., Horii, T. and Tsurugi, J. (1968) Aralkyl hydrodisulfides. VIII. alkaline decomposition and its competition with nucleophiles. *J. Org. Chem.* **33**, 1179–1181 https://doi.org/10.1021/jo01267a053

42 Bailey, T.S., Zakharov, L.N. and Pluth, M.D. (2014) Understanding hydrogen sulfide storage: probing conditions for sulfide release from hydrodisulfides. *J. Am. Chem. Soc.* **136**, 10573–10576 https://doi.org/10.1021/ja505371z

43 Aroca, A., Benito, J.M., Gotor, C. and Romero, L.C. (2017) Persulfidation proteome reveals the regulation of protein function by hydrogen sulfide in diverse biological processes in arabidopsis. *J. Exp. Bot.* **68**, 4915–4927 https://doi.org/10.1093/jxb/erx294

44 Mustafa, A.K., Gadalla, M.M., Sen, N., Kim, S., Mu, W., Gazi, S.K. et al. (2009) HS signals through protein S-Sulfhydration. *Sci. Signal.* **2**, ra72 https://doi.org/10.1126/scisignal.2000464

45 Zivanovic, J., Kouroussis, E., Kohl, J.B., Adhikari, B., Bursac, B., Schott-Roux, S. et al. (2019) Selective persulfide detection reveals evolutionarily conserved antiaging effects of S-sulfhydration. *Cell Metab.* **30**, 1152–1170.e13 https://doi.org/10.1016/j.cmet.2019.10.007

46 Bithi, N., Link, C., Henderson, Y.O., Kim, S., Yang, J., Li, L. et al. (2021) Dietary restriction transforms the mammalian protein persulfidome in a tissue-specific and cystathionine γ-lyase-dependent manner. *Nat. Commun.* **12**, 1745 https://doi.org/10.1038/s41467-021-22001-w

47 Bianco, C.L., Toscano, J.P. and Fukuto, J.M. (2017) An integrated view of the chemical biology of NO, CO, H_2S, and O_2. In *Nitric Oxide: Biology and Pathobiology: Third Edition* (Louis Ignarro Bruce Freeman, ed.), pp.9–21, Elsevier Academic Press, Amsterdam, Netherlands https://doi.org/10.1016/B978-0-12-804273-1.00002-8

48 Lothian, A., Hare, D.J., Grimm, R., Ryan, T.M., Masters, C.L. and Roberts, B.R. (2013) Metalloproteomics: principles, challenges, and applications to neurodegeneration. *Front. Aging Neurosci.* **5**, 35 https://doi.org/10.3389/fnagi.2013.00035

49 Boubeta, F.M., Bieza, S.A., Bringas, M., Palermo, J.C., Boechi, L., Estrin, D.A. et al. (2020) Hemeproteins as targets for sulfide species. *Antioxid. Redox Signal.* **32**, 247–257 https://doi.org/10.1089/ars.2019.7878

50 Tsukihara, T., Aoyama, H., Yamashita, E., Tomizaki, T., Yamaguchi, H., Shinzawa-Itoh, K. et al. (1995) Structures of metal sites of oxidized bovine heart cytochrome c oxidase at 2.8 Å. *Science* **269**, 1069–1074 https://doi.org/10.1126/science.7652554

51 Nicholls, P., Marshall, D.C., Cooper, C.E. and Wilson, M.T. (2013) Sulfide inhibition of and metabolism by cytochrome c oxidase. *Biochem. Soc. Trans.* **41**, 1312–1316 https://doi.org/10.1042/BST20130070

52 Laggner, H., Hermann, M., Esterbauer, H., Muellner, M.K., Exner, M., Gmeiner, B.M.K. et al. (2007) The novel gaseous vasorelaxant hydrogen sulfide inhibits angiotensin-converting enzyme activity of endothelial cells. *J. Hypertens.* **25**, 2100–2104 https://doi.org/10.1097/HJH.0b013e32829b8fd0

53 Bostelaar, T., Vitvitsky, V., Kumutima, J., Lewis, B.E., Yadav, P.K., Brunold, T.C. et al. (2016) Hydrogen sulfide oxidation by myoglobin. *J. Am. Chem. Soc.* **138**, 8476–8488 https://doi.org/10.1021/jacs.6b03456

54 Whiteman, M. and Moore, P.K. (2009) Hydrogen sulfide and the vasculature: a novel vasculoprotective entity and regulator of nitric oxide bioavailability? *J. Cell. Mol. Med.* **13**, 488–507 https://doi.org/10.1111/j.1582-4934.2009.00645.x

55 Kolluru, G.K., Shen, X. and Kevil, C.G. (2013) A tale of two gases: NO and H2S, foes or friends for life? *Redox Biol.* **1**, 313–318 https://doi.org/10.1016/j.redox.2013.05.001

56 Xie, L., Gu, Y., Wen, M., Zhao, S., Wang, W., Ma, Y. et al. (2016) Hydrogen sulfide induces Keap1 S-sulfhydration and suppresses diabetes-accelerated atherosclerosis via Nrf2 activation. *Diabetes* **65**, 3171–3184 https://doi.org/10.2337/db16-0020

57 Mukherjee, S. (2019) Recent advancements in the mechanism of nitric oxide signaling associated with hydrogen sulfide and melatonin crosstalk during ethylene-induced fruit ripening in plants. *Nitric Oxide* **82**, 25–34 https://doi.org/10.1016/j.niox.2018.11.003

58 Singh, S., Kumar, V., Kapoor, D., Kumar, S., Singh, S., Dhanjal, D.S. et al. (2020) Revealing on hydrogen sulfide and nitric oxide signals co-ordination for plant growth under stress conditions. *Physiol. Plant.* **168**, 301–317 https://doi.org/10.1111/ppl.13066

59 Giuffrè, A. and Vicente, J.B. (2018) Hydrogen sulfide biochemistry and interplay with other gaseous mediators in mammalian physiology. *Oxid. Med. Cell. Longev.* **2018**, 6290931 https://doi.org/10.1155/2018/6290931

60 Li, L., Hsu, A. and Moore, P.K. (2009) Actions and interactions of nitric oxide, carbon monoxide and hydrogen sulphide in the cardiovascular system and in inflammation - a tale of three gases!. *Pharmacol. Ther.* **123**, 386–400 https://doi.org/10.1016/j.pharmthera.2009.05.005

61 Dangel, O., Mergia, E., Karlisch, K., Groneberg, D., Koesling, D. and Friebe, A. (2010) Nitric oxide-sensitive guanylyl cyclase is the only nitric oxide receptor mediating platelet inhibition. *J. Thromb. Haemost.* **8**, 1343–1352 https://doi.org/10.1111/j.1538-7836.2010.03806.x

Biochemical Journal (2021) **478** 3485–3504
https://doi.org/10.1042/BCJ20210517

62 Maines, M.D. (1996) Carbon monoxide and nitric oxide homology: differential modulation of heme oxygenases in brain and detection of protein and activity. *Methods Enzymol.* **268**, 473–488 https://doi.org/10.1016/S0076-6879(96)68049-5
63 Zhou, Z., Martin, E., Sharina, I., Esposito, I., Szabo, C., Bucci, M. et al. (2016) Regulation of soluble guanylyl cyclase redox state by hydrogen sulfide. *Pharmacol. Res.* **111**, 556–562 https://doi.org/10.1016/j.phrs.2016.06.029
64 López-Otín, C., Blasco, M.A., Partridge, L., Serrano, M. and Kroemer, G. (2013) The hallmarks of aging. *Cell* **153**, 1194–1217 https://doi.org/10.1016/j.cell.2013.05.039
65 Seals, D.R., Jablonski, K.L. and Donato, A.J. (2011) Aging and vascular endothelial function in humans. *Clin. Sci.* **120**, 357–375 https://doi.org/10.1042/CS20100476
66 Testai, L., Citi, V., Martelli, A., Brogi, S. and Calderone, V. (2020) Role of hydrogen sulfide in cardiovascular ageing. *Pharmacol Res.* **160**, 105125 https://doi.org/10.1016/j.phrs.2020.105125
67 Das, A., Huang, G.X., Bonkowski, M.S., Longchamp, A., Li, C., Schultz, M.B. et al. (2018) Impairment of an endothelial NAD+-H2S signaling network Is a reversible cause of vascular aging. *Cell* **173**, 74–89.e20 https://doi.org/10.1016/j.cell.2018.02.008
68 Liang, M., Jin, S., Wu, D.D., Wang, M.J. and Zhu, Y.C. (2015) Hydrogen sulfide improves glucose metabolism and prevents hypertrophy in cardiomyocytes. *Nitric Oxide* **46**, 114–122 https://doi.org/10.1016/j.niox.2014.12.007
69 Li, H., Zhang, C., Sun, W., Li, L., Wu, B., Bai, S. et al. (2015) Exogenous hydrogen sulfide restores cardioprotection of ischemic post-conditioning via inhibition of mPTP opening in the aging cardiomyocytes. *Cell Biosci.* **5**, 43 https://doi.org/10.1186/s13578-015-0035-9
70 Peleli, M., Bibli, S.I., Li, Z., Chatzianastasiou, A., Varela, A., Katsouda, A. et al. (2020) Cardiovascular phenotype of mice lacking 3-mercaptopyruvate sulfurtransferase. *Biochem. Pharmacol.* **176**, 113833 https://doi.org/10.1016/j.bcp.2020.113833
71 Abe, K. and Kimura, H. (1996) The possible role of hydrogen sulfide as an endogenous neuromodulator. *J. Neurosci.* **16**, 1066–1071 https://doi.org/10.1523/JNEUROSCI.16-03-01066.1996
72 Li, J.J., Surini, M., Catsicas, S., Kawashima, E. and Bouras, C. (1995) Age-dependent accumulation of advanced glycosylation end products in human neurons. *Neurobiol. Aging* **16**, 69–76 https://doi.org/10.1016/0197-4580(95)80009-G
73 Ghidoni, R., Benussi, L., Glionna, M., Franzoni, M., Geroldi, D., Emanuele, E. et al. (2008) Decreased plasma levels of soluble receptor for advanced glycation end products in mild cognitive impairment. *J. Neural Transm.* **115**, 1047–1050 https://doi.org/10.1007/s00702-008-0069-9
74 Walker, D., Lue, L.F., Paul, G., Patel, A. and Sabbagh, M.N. (2015) Receptor for advanced glycation endproduct modulators: a new therapeutic target in Alzheimer's disease. *Expert Opin. Investig. Drugs* **24**, 393–399 https://doi.org/10.1517/13543784.2015.1001490
75 Zhou, H., Ding, L., Wu, Z., Cao, X., Zhang, Q., Lin, L. et al. (2017) Hydrogen sulfide reduces RAGE toxicity through inhibition of its dimer formation. *Free Radic. Biol. Med.* **104**, 262–271 https://doi.org/10.1016/j.freeradbiomed.2017.01.026
76 Wu, L., Chen, Y., Wang, C.Y., Tang, Y.Y., Huang, H.L., Kang, X. et al. (2019) Hydrogen sulfide inhibits high glucose-induced neuronal senescence by improving autophagic flux via up-regulation of SIRT1. *Front. Mol. Neurosci.* **12**, 194 https://doi.org/10.3389/fnmol.2019.00194
77 Lu, Z., Zhao, T., Tao, L., Yu, Q., Yang, Y., Cheng, J. et al. (2019) Cystathionine β-synthase-derived hydrogen sulfide correlates with successful aging in mice. *Rejuvenation Res.* **22**, 513–520 https://doi.org/10.1089/rej.2018.2166
78 García-Bereguiaín, M.A., Samhan-Arias, A.K., Martín-Romero, F.J. and Gutiérrez-Merino, C. (2008) Hydrogen sulfide raises cytosolic calcium in neurons through activation of L-type Ca^{2+} channels. *Antioxid. Redox Signal.* **10**, 31–41 https://doi.org/10.1089/ars.2007.1656
79 Chen, H.B., Wu, W.N., Wang, W., Gu, X.H., Yu, B., Wei, B. et al. (2017) Cystathionine-β-synthase-derived hydrogen sulfide is required for amygdalar long-term potentiation and cued fear memory in rats. *Pharmacol. Biochem. Behav.* **155**, 16–23 https://doi.org/10.1016/j.pbb.2017.03.002
80 Zhan, J.Q., Zheng, L.L., Chen, H.B., Yu, B., Wang, W., Wang, T. et al. (2018) Hydrogen sulfide reverses aging-associated amygdalar synaptic plasticity and fear memory deficits in rats. *Front. Neurosci.* **12**, 390 https://doi.org/10.3389/fnins.2018.00390
81 Go, A.S., Mozaffarian, D., Roger, V.L., Benjamin, E.J., Berry, J.D., Borden, W.B. et al. (2013) Heart disease and stroke statistics-2013 update: a report from the American heart association. *Circulation* **127**, e6–e245 https://doi.org/10.1161/CIR.0b013e31828124ad
82 Qu, K., Chen, C.P.L.H., Halliwell, B., Moore, P.K. and Wong, P.T.H. (2006) Hydrogen sulfide is a mediator of cerebral ischemic damage. *Stroke* **37**, 889–893 https://doi.org/10.1161/01.STR.0000204184.34946.41
83 Wei, X., Zhang, B., Cheng, L., Chi, M., Deng, L., Pan, H. et al. (2015) Hydrogen sulfide induces neuroprotection against experimental stroke in rats by down-regulation of AQP4 via activating PKC. *Brain Res.* **1622**, 292–299 https://doi.org/10.1016/j.brainres.2015.07.001
84 Yamamoto, J., Sato, W., Kosugi, T., Yamamoto, T., Kimura, T., Taniguchi, S. et al. (2013) Distribution of hydrogen sulfide (H2S)-producing enzymes and the roles of the H2S donor sodium hydrosulfide in diabetic nephropathy. *Clin. Exp. Nephrol.* **17**, 32–40 https://doi.org/10.1007/s10157-012-0670-y
85 Ostrakhovitch, E.A. and Tabibzadeh, S. (2015) Homocysteine in chronic kidney disease. *Adv. Clin. Chem.* **72**, 77–106 https://doi.org/10.1016/bs.acc.2015.07.002
86 Selman, C. (2014) Dietary restriction and the pursuit of effective mimetics. *Proc. Nutr. Soc.* **73**, 260–270 https://doi.org/10.1017/S0029665113003832
87 Cooke, D., Ouattara, A. and Ables, G.P. (2018) Dietary methionine restriction modulates renal response and attenuates kidney injury in mice. *FASEB J.* **32**, 693–702 https://doi.org/10.1096/fj.201700419R
88 Yoshida, S., Yamahara, K., Kume, S., Koya, D., Yasuda-Yamahara, M., Takeda, N. et al. (2018) Role of dietary amino acid balance in diet restriction-mediated lifespan extension, renoprotection, and muscle weakness in aged mice. *Aging Cell* **17**, e12796 https://doi.org/10.1111/acel.12796
89 Wang, S.Y., Wang, W.J., Liu, J.Q., Song, Y.H., Li, P., Sun, X.F. et al. (2019) Methionine restriction delays senescence and suppresses the senescence-associated secretory phenotype in the kidney through endogenous hydrogen sulfide. *Cell Cycle* **18**, 1573–1587 https://doi.org/10.1080/15384101.2019.1618124
90 Lee, H.J., Gonzalez, O., Dick, E.J., Donati, A., Feliers, D., Choudhury, G.G. et al. (2019) Marmoset as a model to study kidney changes associated with aging. *J. Gerontol. Ser. A Biol. Sci. Med. Sci.* **74**, 315–324 https://doi.org/10.1093/gerona/gly237
91 Malek, M. and Nematbakhsh, M. (2015) Renal ischemia/reperfusion injury; from pathophysiology to treatment. *J. Ren. Inj. Prev.* **4**, 20–27 https://doi.org/10.12861/jrip.2015.06
92 Chang, C.-H., Fan, P.-C., Chang, M.-Y., Tian, Y.-C., Hung, C.-C., Fang, J.-T. et al. (2014) Acute kidney injury enhances outcome prediction ability of sequential organ failure assessment score in critically Ill patients. *PLoS ONE* **9**, e109649 https://doi.org/10.1371/journal.pone.0109649

PORTLAND PRESS

Biochemical Journal (2021) **478** 3485–3504
https://doi.org/10.1042/BCJ20210517

93 Pieretti, J.C., Junho, C.V.C., Ramos, M.S.C. and Seabra, A.B. (2020) H_2S- and NO-releasing gasotransmitter platform: a crosstalk signaling pathway in the treatment of acute kidney injury. *Pharmacol. Res.* **161**, 105121 https://doi.org/10.1016/j.phrs.2020.105121
94 Fontana, L. and Partridge, L. (2015) Promoting health and longevity through diet: from model organisms to humans. *Cell* **161**, 106–118 https://doi.org/10.1016/j.cell.2015.02.020
95 Picca, A., Pesce, V. and Lezza, A.M.S. (2017) Does eating less make you live longer and better? An update on calorie restriction. *Clin. Interv. Aging* **12**, 1887–1902 https://doi.org/10.2147/CIA.S126458
96 Weindruch, R., Walford, R.L., Fligiel, S. and Guthrie, D. (1986) The retardation of aging in mice by dietary restriction: longevity, cancer, immunity and lifetime energy intake. *J. Nutr.* **116**, 641–654 https://doi.org/10.1093/jn/116.4.641
97 Maklakov, A.A. and Chapman, T. (2019) Evolution of ageing as a tangle of trade-offs: energy versus function. *Proc. R. Soc. B Biol. Sci.* **286**, 20191604 https://doi.org/10.1098/rspb.2019.1604
98 Kirkwood, T.B.L. and Shanley, D.P. (2005) Food restriction, evolution and ageing. *Mech. Ageing Dev.* **126**, 1011–1016 https://doi.org/10.1016/j.mad.2005.03.021
99 Balasubramanian, P., Mattison, J.A. and Anderson, R.M. (2017) Nutrition, metabolism, and targeting aging in nonhuman primates. *Ageing Res. Rev.* **39**, 29–35 https://doi.org/10.1016/j.arr.2017.02.002
100 Yanai, S., Okaichi, Y. and Okaichi, H. (2004) Long-term dietary restriction causes negative effects on cognitive functions in rats. *Neurobiol. Aging* **25**, 325–332 https://doi.org/10.1016/S0197-4580(03)00115-5
101 Pifferi, F., Terrien, J., Marchal, J., Dal-Pan, A., Djelti, F., Hardy, I. et al. (2018) Caloric restriction increases lifespan but affects brain integrity in grey mouse lemur primates. *Commun. Biol.* **1**, 30 https://doi.org/10.1038/s42003-018-0024-8
102 Most, J., Tosti, V., Redman, L.M. and Fontana, L. (2017) Calorie restriction in humans: an update. *Ageing Res. Rev.* **39**, 36–45 https://doi.org/10.1016/j.arr.2016.08.005
103 Fontana, L., Partridge, L. and Longo, V.D. (2010) Extending healthy life span-from yeast to humans. *Science* **328**, 321–326 https://doi.org/10.1126/science.1172539
104 Selman, C., Lingard, S., Choudhury, A.I., Batterham, R.L., Claret, M., Clements, M. et al. (2008) Evidence for lifespan extension and delayed age–related biomarkers in insulin receptor substrate 1 null mice. *FASEB J.* **22**, 807–818 https://doi.org/10.1096/fj.07-9261com
105 Selman, C., Tullet, J.M.A., Wieser, D., Irvine, E., Lingard, S.J., Choudhury, A.I. et al. (2009) Ribosomal protein S6 kinase 1 signaling regulates mammalian life span. *Science* **326**, 140–144 https://doi.org/10.1126/science.1177221
106 Hine, C., Harputlugil, E., Zhang, Y., Ruckenstuhl, C., Lee, B.C., Brace, L. et al. (2015) Endogenous hydrogen sulfide production is essential for dietary restriction benefits. *Cell* **160**, 132–144 https://doi.org/10.1016/j.cell.2014.11.048
107 Hine, C. and Mitchell, J.R. (2015) Calorie restriction and methionine restriction in control of endogenous hydrogen sulfide production by the transsulfuration pathway. *Exp. Gerontol.* **68**, 26–32 https://doi.org/10.1016/j.exger.2014.12.010
108 Hine, C., Zhu, Y., Hollenberg, A.N. and Mitchell, J.R. (2018) Dietary and endocrine regulation of endogenous hydrogen sulfide production: implications for longevity. *Antioxid. Redox Signal.* **28**, 1483–1502 https://doi.org/10.1089/ars.2017.7434
109 Longchamp, A., Mirabella, T., Arduini, A., MacArthur, M.R., Das, A., Treviño-Villarreal, J.H. et al. (2018) Amino acid restriction triggers angiogenesis via GCN2/ATF4 regulation of VEGF and H2S production. *Cell* **173**, 117–129.e14 https://doi.org/10.1016/j.cell.2018.03.001
110 Trocha, K.M., Kip, P., Tao, M., MacArthur, M.R., Trevinõ-Villarreal, J.H., Longchamp, A. et al. (2020) Short-term preoperative protein restriction attenuates vein graft disease via induction of cystathionine γ-lyase. *Cardiovasc. Res.* **116**, 416–428 https://doi.org/10.1093/cvr/cvz086
111 Sanz, A., Caro, P. and Barja, G. (2004) Protein restriction without strong caloric restriction decreases mitochondrial oxygen radical production and oxidative DNA damage in rat liver. *J. Bioenerg. Biomembr.* **36**, 545–552 https://doi.org/10.1007/s10863-004-9001-7
112 Hine, C., Kim, H.J., Zhu, Y., Harputlugil, E., Longchamp, A., Matos, M.S. et al. (2017) Hypothalamic-pituitary axis regulates hydrogen sulfide production. *Cell Metab.* **25**, 1320–1333.e5 https://doi.org/10.1016/j.cmet.2017.05.003
113 Bagherniya, M., Butler, A.E., Barreto, G.E. and Sahebkar, A. (2018) The effect of fasting or calorie restriction on autophagy induction: a review of the literature. *Ageing Res. Rev.* **47**, 183–197 https://doi.org/10.1016/j.arr.2018.08.004
114 Jiang, X., MacArthur, M.R., Treviño-Villarreal, J.H., Kip, P., Ozaki, C.K., Mitchell, S.J. et al. (2021) Intracellular H2S production is an autophagy-dependent adaptive response to DNA damage. *Cell Chem. Biol.* **28**, S2451-9456(21)00261-0 https://doi.org/10.1016/j.chembiol.2021.05.016
115 Mukhopadhyay, S., Biancur, D.E., Parker, S.J., Yamamoto, K., Banh, R.S., Paulo, J.A. et al. (2021) Autophagy is required for proper cysteine homeostasis in pancreatic cancer through regulation of SLC7A11. *Proc. Natl Acad. Sci. U.S.A.* **118**, e2021475118 https://doi.org/10.1073/pnas.2021475118
116 Sutter, B.M., Wu, X., Laxman, S. and Tu, B.P. (2013) Methionine inhibits autophagy and promotes growth by inducing the SAM-responsive methylation of PP2A. *Cell* **154**, 403 https://doi.org/10.1016/j.cell.2013.06.041
117 Brown-Borg, H.M., Borg, K.E., Meliska, C.J. and Bartke, A. (1996) Dwarf mice and the ageing process. *Nature* **384**, 33 https://doi.org/10.1038/384033a0
118 Flurkey, K., Papaconstantinou, J., Miller, R.A. and Harrison, D.E. (2001) Lifespan extension and delayed immune and collagen aging in mutant mice with defects in growth hormone production. *Proc. Natl Acad. Sci. U.S.A.* **98**, 6736–6741 https://doi.org/10.1073/pnas.111158898
119 Godfrey, P., Rahal, J.O., Beamer, W.G., Copeland, N.G., Jenkins, N.A. and Mayo, K.E. (1993) GHRH receptor of little mice contains a missense mutation in the extracellular domain that disrupts receptor function. *Nat. Genet.* **4**, 227–232 https://doi.org/10.1038/ng0793-227
120 Uthus, E.O. and Brown-Borg, H.M. (2006) Methionine flux to transsulfuration is enhanced in the long living Ames dwarf mouse. *Mech. Ageing Dev.* **127**, 444–450 https://doi.org/10.1016/j.mad.2006.01.00
121 Uthus, E.O. and Brown-Borg, H.M. (2003) Altered methionine metabolism in long living Ames dwarf mice. *Exp. Gerontol.* **38**, 491–498 https://doi.org/10.1016/S0531-5565(03)00008-1
122 Brown-Borg, H.M., Rakoczy, S.G., Wonderlich, J.A., Rojanathammanee, L., Kopchick, J.J., Armstrong, V. et al. (2014) Growth hormone signaling is necessary for lifespan extension by dietary methionine. *Aging Cell* **13**, 1019–1027 https://doi.org/10.1111/acel.12269

Biochemical Journal (2021) **478** 3485–3504
https://doi.org/10.1042/BCJ20210517

123 Brown-Borg, H.M., Rakoczy, S., Wonderlich, J.A., Armstrong, V. and Rojanathammanee, L. (2014) Altered dietary methionine differentially impacts glutathione and methionine metabolism in long-living growth hormone-deficient Ames dwarf and wild-type mice. *Longev. Healthspan* **3**, 1–16 https://doi.org/10.1186/2046-2395-3-10
124 Wu, D., Wang, H., Teng, T., Duan, S., Ji, A. and Li, Y. (2018) Hydrogen sulfide and autophagy: a double edged sword. *Pharmacol Res.* **131**, 120–127 https://doi.org/10.1016/j.phrs.2018.03.002
125 Talaei, F., Van Praag, V.M., Shishavan, M.H., Landheer, S.W., Buikema, H. and Henning, R.H. (2014) Increased protein aggregation in Zucker diabetic fatty rat brain: identification of key mechanistic targets and the therapeutic application of hydrogen sulfide. *BMC Cell Biol.* **15**, 1 https://doi.org/10.1186/1471-2121-15-1
126 Ji, L., Li, L., Qu, F., Zhang, G., Wang, Y., Bai, X. et al. (2016) Hydrogen sulphide exacerbates acute pancreatitis by over-activating autophagy via AMPK/mTOR pathway. *J. Cell. Mol. Med.* **20**, 2349–2361 https://doi.org/10.1111/jcmm.12928
127 Chen, J., Gao, J., Sun, W., Li, L., Wang, Y., Bai, S. et al. (2016) Involvement of exogenous H2S in recovery of cardioprotection from ischemic post-conditioning via increase of autophagy in the aged hearts. *Int. J. Cardiol.* **220**, 681–692 https://doi.org/10.1016/j.ijcard.2016.06.200
128 Wu, D., Zhong, P., Wang, Y., Zhang, Q., Li, J., Liu, Z. et al. (2020) Hydrogen sulfide attenuates high-fat diet-induced non-alcoholic fatty liver disease by inhibiting apoptosis and promoting autophagy via reactive oxygen species/phosphatidylinositol 3-kinase/AKT/MAMMALIAN target of rapamycin signaling pathway. *Front. Pharmacol.* **11**, 1965 https://doi.org/10.3389/fphar.2020.585860
129 Yang, F., Zhang, L., Gao, Z., Sun, X., Yu, M., Dong, S. et al. (2017) Exogenous H2S protects against diabetic cardiomyopathy by activating autophagy via the AMPK/mTOR pathway. *Cell. Physiol. Biochem.* **43**, 1168–1187 https://doi.org/10.1159/000481758
130 Zhou, Y., Li, X.-H., Zhang, C.-C., Wang, M.-J., Xue, W.-L., Wu, D.-D. et al. (2016) Hydrogen sulfide promotes angiogenesis by downregulating miR-640 via the VEGFR2/mTOR pathway. *Am. J. Physiol. Physiol.* **310**, C305–C317 https://doi.org/10.1152/ajpcell.00230.2015
131 Ma, J., Du, D., Liu, J., Guo, L., Li, Y., Chen, A. et al. (2020) Hydrogen sulphide promotes osteoclastogenesis by inhibiting autophagy through the PI3K/AKT/mTOR pathway. *J. Drug Target.* **28**, 176–185 https://doi.org/10.1080/1061186X.2019.1624969
132 Lyu, Z., Gao, X., Wang, W., Dang, J., Yang, L., Yan, M. et al. (2019) mTORC1-Sch9 regulates hydrogen sulfide production through the transsulfuration pathway. *Aging (Albany, NY)* **11**, 8418–8432 https://doi.org/10.18632/aging.102327
133 Wang, S.S., Chen, Y.H., Chen, N., Wang, L.J., Chen, D.X., Weng, H.L. et al. (2017) Hydrogen sulfide promotes autophagy of hepatocellular carcinoma cells through the PI3K/Akt/mTOR signaling pathway. *Cell Death Dis.* **8**, e2688 https://doi.org/10.1038/cddis.2017.18
134 Zhou, G., Myers, R., Li, Y., Chen, Y., Shen, X., Fenyk-Melody, J. et al. (2001) Role of AMP-activated protein kinase in mechanism of metformin action. *J. Clin. Invest.* **108**, 1167–1174 https://doi.org/10.1172/JCI13505
135 Wiliński, B., Wiliński, J., Somogyi, E., Piotrowska, J. and Opoka, W. (2013) Metformin raises hydrogen sulfide tissue concentrations in various mouse organs. *Pharmacol. Rep.* **65**, 737–742 https://doi.org/10.1016/S1734-1140(13)71053-3
136 Wang, M., Tang, W. and Zhu, Y.Z. (2017) An update on AMPK in hydrogen sulfide pharmacology. *Front. Pharmacol.* **8**, 810 https://doi.org/10.3389/fphar.2017.00810
137 Zhong, T., Men, Y., Lu, L., Geng, T., Zhou, J., Mitsuhashi, A. et al. (2017) Metformin alters DNA methylation genome-wide via the H19/SAHH axis. *Oncogene* **36**, 2345–2354 https://doi.org/10.1038/onc.2016.391
138 Ma, X., Jiang, Z., Wang, Z. and Zhang, Z. (2020) Administration of metformin alleviates atherosclerosis by promoting H2S production via regulating CSE expression. *J. Cell. Physiol.* **235**, 2102–2112 https://doi.org/10.1002/jcp.29112
139 Sun, Y., Wang, X., Zhou, Y., Zhang, J., Cui, W., Wang, E. et al. (2021) Protective effect of metformin on BPA-induced liver toxicity in rats through upregulation of cystathionine β synthase and cystathionine γ lyase expression. *Sci. Total Environ.* **750**, 141685 https://doi.org/10.1016/j.scitotenv.2020.141685
140 Harrison, D.E., Strong, R., Allison, D.B., Ames, B.N., Astle, C.M., Atamna, H. et al. (2014) Acarbose, 17-α-estradiol, and nordihydroguaiaretic acid extend mouse lifespan preferentially in males. *Aging Cell* **13**, 273–282 https://doi.org/10.1111/acel.12170
141 Akintola, A.A. and van Heemst, D. (2015) Insulin, aging, and the brain: mechanisms and implications. *Front. Endocrinol.* **6**, 13 https://doi.org/10.3389/fendo.2015.00013
142 Zhang, H., Huang, Y., Chen, S., Tang, C., Wang, G., Du, J. et al. (2021) Hydrogen sulfide regulates insulin secretion and insulin resistance in diabetes mellitus, a new promising target for diabetes mellitus treatment? A review. *J. Adv. Res.* **27**, 19–30 https://doi.org/10.1016/j.jare.2020.02.013
143 Feng, X., Chen, Y., Zhao, J., Tang, C., Jiang, Z. and Geng, B. (2009) Hydrogen sulfide from adipose tissue is a novel insulin resistance regulator. *Biochem. Biophys. Res. Commun.* **380**, 153–159 https://doi.org/10.1016/j.bbrc.2009.01.059
144 Zhang, L., Yang, G., Untereiner, A., Ju, Y., Wu, L. and Wang, R. (2013) Hydrogen sulfide impairs glucose utilization and increases gluconeogenesis in hepatocytes. *Endocrinology* **154**, 114–126 https://doi.org/10.1210/en.2012-1658
145 Okamoto, M., Ishizaki, T. and Kimura, T. (2015) Protective effect of hydrogen sulfide on pancreatic beta-cells. *Nitric Oxide* **46**, 32–36 https://doi.org/10.1016/j.niox.2014.11.007
146 Chen, X., Zhao, X., Lan, F., Zhou, T., Cai, H., Sun, H. et al. (2017) Hydrogen sulphide treatment increases insulin sensitivity and improves oxidant metabolism through the CaMKKbeta-AMPK pathway in PA-induced IR C2C12 cells. *Sci. Rep.* **7**, 1–13 https://doi.org/10.1038/s41598-016-0028-x
147 Manna, P. and Jain, S.K. (2012) Vitamin D up-regulates glucose transporter 4 (GLUT4) translocation and glucose utilization mediated by cystathionine-γ-lyase (CSE) activation and H2S formation in 3T3L1 adipocytes. *J. Biol. Chem.* **287**, 42324–42332 https://doi.org/10.1074/jbc.M112.407833
148 Xue, R., Hao, D.D., Sun, J.P., Li, W.W., Zhao, M.M., Li, X.H. et al. (2013) Hydrogen sulfide treatment promotes glucose uptake by increasing insulin receptor sensitivity and ameliorates kidney lesions in type 2 diabetes. *Antioxid. Redox Signal.* **19**, 5–23 https://doi.org/10.1089/ars.2012.5024
149 Gheibi, S., Jeddi, S., Kashfi, K. and Ghasemi, A. (2019) Effects of hydrogen sulfide on carbohydrate metabolism in obese type 2 diabetic rats. *Molecules* **24**, 190 https://doi.org/10.3390/molecules24010190
150 Gonzalo, S., Kreienkamp, R. and Askjaer, P. (2017) Hutchinson-Gilford progeria syndrome: a premature aging disease caused by LMNA gene mutations. *Ageing Res. Rev.* **33**, 18–29 https://doi.org/10.1016/j.arr.2016.06.007
151 Ding, S.L. and Shen, C.Y. (2008) Model of human aging: recent findings on Werner's and Hutchinson-Gilford progeria syndromes. *Clin. Interv. Aging* **3**, 431–444 https://doi.org/10.2147/CIA.S1957

PORTLAND PRESS

Biochemical Journal (2021) **478** 3485–3504
https://doi.org/10.1042/BCJ20210517

152 Graziano, S., Kreienkamp, R., Coll-Bonfill, N. and Gonzalo, S. (2018) Causes and consequences of genomic instability in laminopathies: replication stress and interferon response. *Nucleus* **9**, 289–306 https://doi.org/10.1080/19491034.2018.1454168
153 Scaffidi, P. and Misteli, T. (2006) Lamin A-dependent nuclear defects in human aging. *Science* **312**, 1059–1063 https://doi.org/10.1126/science.1127168
154 Carrero, D., Soria-Valles, C. and López-Otín, C. (2016) Hallmarks of progeroid syndromes: lessons from mice and reprogrammed cells. *Dis. Models Mech.* **9**, 719–735 https://doi.org/10.1242/dmm.024711
155 Kubben, N. and Misteli, T. (2017) Shared molecular and cellular mechanisms of premature ageing and ageing-associated diseases. *Nat. Rev. Mol. Cell Biol.* **18**, 595–609 https://doi.org/10.1038/nrm.2017.68
156 Kreienkamp, R. and Gonzalo, S. (2019) Hutchinson-Gilford progeria syndrome: challenges at bench and bedside. *Subcell. Biochem.* **91**, 435–451 https://doi.org/10.1007/978-981-13-3681-2_15
157 Sestito, S., Pruccoli, L., Runfola, M., Citi, V., Martelli, A., Saccomanni, G. et al. (2019) Design and synthesis of H2S-donor hybrids: a new treatment for Alzheimer's disease? *Eur. J. Med. Chem.* **184**, 111745 https://doi.org/10.1016/j.ejmech.2019.111745
158 Müller, L., Meyer, M., Bauer, R.N., Zhou, H., Zhang, H., Jones, S. et al. (2016) Effect of broccoli sprouts and live attenuated influenza virus on peripheral blood natural killer cells: a randomized, double-Blind study. *PLoS ONE* **11**, e0147742 https://doi.org/10.1371/journal.pone.0147742
159 Pei, Y., Wu, B., Cao, Q., Wu, L. and Yang, G. (2011) Hydrogen sulfide mediates the anti-survival effect of sulforaphane on human prostate cancer cells. *Toxicol. Appl. Pharmacol.* **257**, 420–428 https://doi.org/10.1016/j.taap.2011.09.026
160 Hong, F., Freeman, M.L. and Liebler, D.C. (2005) Identification of sensor cysteines in human Keap1 modified by the cancer chemopreventive agent sulforaphane. *Chem. Res. Toxicol.* **18**, 1917–1926 https://doi.org/10.1021/tx0502138nes
161 Qi, Z., Ji, H., Le, M., Li, H., Wieland, A., Bauer, S. et al. (2021) Sulforaphane promotes C. elegans longevity and healthspan via DAF-16/DAF-2 insulin/IGF-1 signaling. *Aging (Albany. NY* **13**, 1649–1670 https://doi.org/10.18632/aging.202512
162 Kreienkamp, R., Croke, M., Neumann, M.A., Bedia-Diaz, G., Graziano, S., Dusso, A. et al. (2016) Vitamin D receptor signaling improves hutchinson-Gilford progeria syndrome cellular phenotypes. *Oncotarget* **7**, 30018–30031 https://doi.org/10.18632/oncotarget.9065
163 Wiliński, B., Wiliński, J., Somogyi, E., Piotrowska, J. and Opoka, W. (2012) Vitamin D3 (cholecalciferol) boosts hydrogen sulfide tissue concentrations in heart and other mouse organs. *Folia Biol. (Czech Republic)* **60**, 243–247 https://doi.org/10.3409/fb60_3-4.243-247
164 Jain, S.K., Manna, P., Micinski, D., Lieblong, B.J., Kahlon, G., Morehead, L. et al. (2013) In african American type 2 diabetic patients, is vitamin d deficiency associated with lower blood levels of hydrogen sulfide and cyclic adenosine monophosphate, and elevated oxidative stress? *Antioxid. Redox Signal.* **18**, 1154–1158 https://doi.org/10.1089/ars.2012.4843
165 Talaei, F., van Praag, V.M. and Henning, R.H. (2013) Hydrogen sulfide restores a normal morphological phenotype in Werner syndrome fibroblasts, attenuates oxidative damage and modulates mTOR pathway. *Pharmacol Res.* **74**, 34–44 https://doi.org/10.1016/j.phrs.2013.04.011
166 Qabazard, B. and Stürzenbaum, S.R. (2015) H_2S: a new approach to lifespan enhancement and healthy ageing?, *Handb. Exp. Pharmacol.* **230**, 269–287 https://doi.org/10.1007/978-3-319-18144-8_14
167 Vos, T., Abajobir, A.A., Abbafati, C., Abbas, K.M., Abate, K.H., Abd-Allah, F. et al. (2017) Global, regional, and national incidence, prevalence, and years lived with disability for 328 diseases and injuries for 195 countries, 1990-2016: a systematic analysis for the global burden of disease study 2016. *Lancet* **390**, 1211–1259 https://doi.org/10.1016/S0140-6736(17)32154-2
168 Islam, K.N., Polhemus, D.J., Donnarumma, E., Brewster, L.P. and Lefer, D.J. (2015) Hydrogen sulfide levels and nuclear factor-erythroid 2-related factor 2 (NRF2) activity are attenuated in the setting of critical limb ischemia (CLI). *J. Am. Heart Assoc.* **4**, e001986 https://doi.org/10.1161/JAHA.115.001986
169 Jin, H.S., Kim, J., Park, S., Park, E., Kim, B.Y., Choi, V.N. et al. (2015) Association of the I264T variant in the sulfide quinone reductase-like (SQRDL) gene with osteoporosis in Korean postmenopausal women. *PLoS ONE* **10**, e0135285 https://doi.org/10.1371/journal.pone.0135285
170 Zavaczki, E., Jeney, V., Agarwal, A., Zarjou, A., Oros, M., Katkó, M. et al. (2011) Hydrogen sulfide inhibits the calcification and osteoblastic differentiation of vascular smooth muscle cells. *Kidney Int.* **80**, 731–739 https://doi.org/10.1038/ki.2011.212
171 Yang, M., Huang, Y., Chen, J., Chen, Y.L., Ma, J.J. and Shi, P.H. (2014) Activation of AMPK participates hydrogen sulfide-induced cyto-protective effect against dexamethasone in osteoblastic MC3T3-E1 cells. *Biochem. Biophys. Res. Commun.* **454**, 42–47 https://doi.org/10.1016/j.bbrc.2014.10.033
172 Nagtegaal, A.P., Broer, L., Zilhao, N.R., Jakobsdottir, J., Bishop, C.E., Brumat, M. et al. (2019) Genome-wide association meta-analysis identifies five novel loci for age-related hearing impairment. *Sci. Rep.* **9**, 15192 https://doi.org/10.1038/s41598-019-51630-x
173 Magrangeas, F., Kuiper, R., Avet-Loiseau, H., Gouraud, W., Guerin-Charbonnel, C., Ferrer, L. et al. (2016) A genome-wide association study identifies a novel locus for bortezomib-induced peripheral neuropathy in European patients with multiple myeloma. *Clin. Cancer Res.* **22**, 4350–4355 https://doi.org/10.1158/1078-0432.CCR-15-3163
174 Reed, B.R., Crane, J., Garrett, N., Woods, D.L. and Bates, M.N. (2014) Chronic ambient hydrogen sulfide exposure and cognitive function. *Neurotoxicol. Teratol.* **42**, 68–76 https://doi.org/10.1016/j.ntt.2014.02.002
175 Bates, M.N., Garrett, N., Graham, B. and Read, D. (1998) Cancer incidence, morbidity and geothermal air pollution in Rotorua, New Zealand. *Int. J. Epidemiol.* **27**, 10–14 https://doi.org/10.1093/ije/27.1.10
176 Cakmak, Y.O. (2017) Rotorua, hydrogen sulphide and Parkinson's disease—a possible beneficial link? *N. Z. Med. J.* **130**, 123–125 PMID:28494485
177 Pope, K., So, Y.T., Crane, J. and Bates, M.N. (2017) Ambient geothermal hydrogen sulfide exposure and peripheral neuropathy. *Neurotoxicology* **60**, 10–15 https://doi.org/10.1016/j.neuro.2017.02.006
178 Bates, M.N., Garrett, N., Crane, J. and Balmes, J.R. (2013) Associations of ambient hydrogen sulfide exposure with self-reported asthma and asthma symptoms. *Environ. Res.* **122**, 81–87 https://doi.org/10.1016/j.envres.2013.02.002
179 Mulvey, L. (2017) *Dissecting out the Mechanisms to Longevity Through Eating Less*, University of Glasgow, Glasgow, Scotland, UK

List of References

[1] chevalier de J. (biography) Louis, “Fates,” *Encycl. Diderot d’Alembert - Collab. Transl. Proj.*, Oct. 2014, Accessed: Sep. 01, 2021. [Online]. Available: http://hdl.handle.net/2027/spo.did2222.0003.132.

[2] Encyclopaedia Britannica, “Fate Greek and Roman Mythology,” 1998. https://www.britannica.com/topic/Fate-Greek-and-Roman-mythology (accessed Sep. 01, 2021).

[3] J. Lindow, *Norse Mythology: A Guide to Gods, Heroes, Rituals, and Beliefs - John Lindow - Google Books*. Oxford: Oxford University Press, 2002.

[4] S. Sturluson, *The Prose Edda: Norse Mythology*. Penguin Classics, 2006.

[5] A. J. Greimas, *Of Gods and Men: Studies in Lithuanian Mythology*. Indiana University Press, 1992.

[6] P. Lunde, “Ponce de Leon and an Arab Legend,” *Aramco World Arab Islam. Cult. Connect.*, vol. 43, no. 3, pp. 42–46, May 1992, Accessed: Sep. 01, 2021. [Online]. Available: https://archive.aramcoworld.com/issue/199203/ponce.de.leon.and.an.arab.legend.htm.

[7] Aristotle, *On Longevity and Shortness of Life - Translated by G. R. T. Ross*. Adelaide: The University of Adelaide Library, 2004.

[8] S. N. Austad, “Comparative aging and life histories in mammals,” *Exp. Gerontol.*, vol. 32, no. 1–2, pp. 23–38, Jan. 1997, doi: 10.1016/S0531-5565(96)00059-9.

[9] A. J. J. Lynch, R. W. Barnes, J. Cambecèdes, and R. E. Vaillancourt, “Genetic evidence that Lomatia tasmanica (Proteaceae) is an ancient clone,” *Aust. J. Bot.*, vol. 46, no. 1, pp. 25–33, 1998, doi: 10.1071/BT96120.

[10] A. Trembley, A. Trembley, C. Pronk, J. van der, Schley, and P. Lyonet,

Mémoires pour servir à l'histoire d'un genre de polypes d'eau douce, à bras en forme de cornes. A Leide : Chez Jean & Herman Verbeek, 1744.

[11] P. Brien, "La Pérennité Somatique," *Biol. Rev.*, vol. 28, no. 3, pp. 308–349, Aug. 1953, doi: 10.1111/j.1469-185X.1953.tb01381.x.

[12] S. Tomczyk, K. Fischer, S. Austad, and B. Galliot, "Hydra, a powerful model for aging studies," *Invertebr. Reprod. Dev.*, vol. 59, no. sup1, p. 11, Jan. 2015, doi: 10.1080/07924259.2014.927805.

[13] J. Nielsen *et al.*, "Eye lens radiocarbon reveals centuries of longevity in the Greenland shark (Somniosus microcephalus)," *Science (80-.).*, vol. 353, no. 6300, pp. 702–704, Aug. 2016, doi: 10.1126/SCIENCE.AAF1703.

[14] K. N. Lewis and R. Buffenstein, "The Naked Mole-Rat: A Resilient Rodent Model of Aging, Longevity, and Healthspan," *Handb. Biol. Aging Eighth Ed.*, pp. 179–204, Jan. 2016, doi: 10.1016/B978-0-12-411596-5.00006-X.

[15] J. G. Ruby, M. Smith, and R. Buffenstein, "Naked mole-rat mortality rates defy gompertzian laws by not increasing with age," *Elife*, vol. 7, Jan. 2018, doi: 10.7554/ELIFE.31157.

[16] J.-M. Robine and M. Allard, "Validation of Exceptional Longevity Jeanne Calment: Validation of the Duration of Her Life," 1999. Accessed: Sep. 03, 2021. [Online]. Available: https://www.demogr.mpg.de/books/odense/6/09.htm.

[17] J. Oeppen and J. W. Vaupel, "Demography: Broken limits to life expectancy," *Science*, vol. 296, no. 5570. pp. 1029–1031, May 10, 2002, doi: 10.1126/science.1069675.

[18] J. Klenk, U. Keil, A. Jaensch, M. C. Christiansen, and G. Nagel, "Changes in life expectancy 1950-2010: Contributions from age- and disease-specific mortality in selected countries," *Popul. Health Metr.*, vol. 14, no. 1, pp. 1–11, May 2016, doi: 10.1186/s12963-016-0089-x.

[19] “Ageing in the Twenty-First Century | UNFPA - United Nations Population Fund,” *United Nations Population Fund (UNFPA)*, 2012. https://www.unfpa.org/publications/ageing-twenty-first-century (accessed Sep. 03, 2021).

[20] E. M. Crimmins, “Recent trends and increasing differences in life expectancy present opportunities for multidisciplinary research on aging,” *Nat. Aging*, vol. 1, no. 1, pp. 12–13, Jan. 2021, doi: 10.1038/s43587-020-00016-0.

[21] J. Y. Ho and A. S. Hendi, “Recent trends in life expectancy across high income countries: Retrospective observational study,” *BMJ*, vol. 362, p. 2562, Aug. 2018, doi: 10.1136/bmj.k2562.

[22] M. Poulain *et al.*, “Identification of a geographic area characterized by extreme longevity in the Sardinia island: The AKEA study,” *Exp. Gerontol.*, vol. 39, no. 9, pp. 1423–1429, 2004, doi: 10.1016/j.exger.2004.06.016.

[23] D. Buettner and S. Skemp, “Blue Zones: Lessons From the World’s Longest Lived,” *American Journal of Lifestyle Medicine*, vol. 10, no. 5. SAGE Publications, pp. 318–321, Sep. 01, 2016, doi: 10.1177/1559827616637066.

[24] R. Legrand, G. Nuemi, M. Poulain, and P. Manckoundia, “Description of lifestyle, including social life, diet and physical activity, of people =90 years living in Ikaria, a longevity blue zone,” *Int. J. Environ. Res. Public Health*, vol. 18, no. 12, p. 6602, Jun. 2021, doi: 10.3390/ijerph18126602.

[25] G. M. Pes *et al.*, “Male longevity in Sardinia, a review of historical sources supporting a causal link with dietary factors,” *European Journal of Clinical Nutrition*, vol. 69, no. 4. Eur J Clin Nutr, pp. 411–418, Apr. 04, 2015, doi: 10.1038/ejcn.2014.230.

[26] B. Poljsak, V. Kovač, T. Levec, and I. Milisav, “Nature Versus Nurture: What Can be Learned from the Oldest-Old’s Claims about Longevity?,” *Rejuvenation Res.*, vol. 24, no. 4, pp. 262–273, Aug. 2021, doi: 10.1089/rej.2020.2379.

[27] W. M. Passtoors *et al.*, “Gene expression analysis of mTOR pathway: association with human longevity,” *Aging Cell*, vol. 12, no. 1, pp. 24–31, Feb. 2013, doi: 10.1111/ACEL.12015.

[28] A. M. Herskind, M. McGue, N. V. Holm, T. I. A. Sørensen, B. Harvald, and J. W. Vaupel, “The heritability of human longevity: A population-based study of 2872 Danish twin pairs born 1870-1900,” *Hum. Genet.*, vol. 97, no. 3, pp. 319–323, 1996, doi: 10.1007/BF02185763.

[29] D. Govindaraju, G. Atzmon, and N. Barzilai, “Genetics, lifestyle and longevity: Lessons from centenarians,” *Applied and Translational Genomics*, vol. 4. Elsevier, pp. 23–32, Mar. 01, 2015, doi: 10.1016/j.atg.2015.01.001.

[30] E. Dolgin, “There’s no limit to longevity, says study that revives human lifespan debate,” *Nat. 2021 5597712*, Jun. 2018, Accessed: Sep. 02, 2021. [Online]. Available: https://www.nature.com/articles/d41586-018-05582-3.

[31] F. Colchero *et al.*, “The long lives of primates and the ‘invariant rate of ageing’ hypothesis,” *Nat. Commun. 2021 121*, vol. 12, no. 1, pp. 1–10, Jun. 2021, doi: 10.1038/s41467-021-23894-3.

[32] S. J. Olshansky and B. A. Carnes, “Inconvenient Truths About Human Longevity,” *Journals of Gerontology - Series A Biological Sciences and Medical Sciences*, vol. 74, no. Supplement_1. Oxford Academic, pp. S7–S12, Nov. 13, 2019, doi: 10.1093/gerona/glz098.

[33] M. S. Ben-Haim *et al.*, “Breaking the Ceiling of Human Maximal Life span,” *Journals Gerontol. Ser. A*, vol. 73, no. 11, pp. 1465–1471, Oct. 2018, doi: 10.1093/GERONA/GLX219.

[34] E. M. Crimmins, “Lifespan and healthspan: Past, present, and promise,” *Gerontologist*, vol. 55, no. 6, pp. 901–911, Dec. 2015, doi: 10.1093/geront/gnv130.

[35] B. K. Kennedy *et al.*, “Geroscience: Linking aging to chronic disease,” *Cell*, vol. 159, no. 4. Cell Press, pp. 709–713, Nov. 06, 2014, doi: 10.1016/j.cell.2014.10.039.

[36] V. D. Longo *et al.*, “Interventions to Slow Aging in Humans: Are We Ready?,” *Aging Cell*, vol. 14, no. 4, pp. 497–510, Aug. 2015, doi: 10.1111/ACEL.12338.

[37] T. Hvitved-Jacobsen, *Sewer Processes*. CRC Press, 2001.

[38] B. Ramazzini, “De morbis artificum diatriba [diseases of workers]. 1713.,” *Am. J. Public Health*, vol. 91, no. 9, pp. 1380–1382, 2001, doi: 10.2105/AJPH.91.9.1380.

[39] M. D.-J. de Medicine and undefined 1806, “Rapport sur une espéce de mephitisme des fosses d’aisance, produite par le gas azote.”

[40] L. C. Mccabe and G. D. Clayton, “Air Pollution by Hydrogen Sulfide in Poza Rica, Mexico. An Evaluation of the Incident of Nov. 24, 1950.,” *Arch. Indust. Hyg. & Occup. Med.*, vol. 6, no. 3, pp. 199–213, 1952.

[41] R. G. Hendrickson, A. Chang, and R. J. Hamilton, “Co-Worker Fatalities from Hydrogen Sulfide,” *American Journal of Industrial Medicine*, vol. 45, no. 4. Am J Ind Med, pp. 346–350, Apr. 2004, doi: 10.1002/ajim.10355.

[42] L. R. Kump, A. Pavlov, and M. A. Arthur, “Massive release of hydrogen sulfide to the surface ocean and atmosphere during intervals of oceanic anoxia,” *Geology*, vol. 33, no. 5, pp. 397–400, May 2005, doi: 10.1130/G21295.1.

[43] P. D. Ward, “Impact from the deep,” *Scientific American*, vol. 295, no. 4. Scientific American Inc., pp. 64–71, 2006, doi: 10.1038/scientificamerican1006-64.

[44] Francis Binkley and Vincent du Vigneaud, “The Formation of Cysteine from Homocysteine and Serine by Liver Tissue of Rats,” *J. Biol. Chem*, vol. 144,

pp. 507–511, 1942, Accessed: Jun. 04, 2020. [Online]. Available: http://www.jbc.org/.

[45] K. Abe and H. Kimura, “The possible role of hydrogen sulfide as an endogenous neuromodulator.,” *J. Neurosci.*, vol. 16, no. 3, pp. 1066–71, Feb. 1996, doi: 10.1523/jneurosci.16-03-01066.1996.

[46] R. Hosoki, N. Matsuki, and H. Kimura, “The possible role of hydrogen sulfide as an endogenous smooth muscle relaxant in synergy with nitric oxide,” *Biochem. Biophys. Res. Commun.*, vol. 237, no. 3, pp. 527–531, Aug. 1997, doi: 10.1006/bbrc.1997.6878.

[47] G. Yang *et al.*, “H2S as a physiologic vasorelaxant: Hypertension in mice with deletion of cystathionine γ-lyase,” *Science (80-.).*, vol. 322, no. 5901, pp. 587–590, Oct. 2008, doi: 10.1126/science.1162667.

[48] R. C. O. Zanardo *et al.*, “Hydrogen sulfide is an endogenous modulator of leukocyte-mediated inflammation,” *FASEB J.*, vol. 20, no. 12, pp. 2118–2120, Oct. 2006, doi: 10.1096/fj.06-6270fje.

[49] A. Papapetropoulos *et al.*, “Hydrogen sulfide is an endogenous stimulator of angiogenesis,” *Proc. Natl. Acad. Sci. U. S. A.*, vol. 106, no. 51, pp. 21972–21977, Dec. 2009, doi: 10.1073/pnas.0908047106.

[50] M. Eberhardt *et al.*, “H2S and NO cooperatively regulate vascular tone by activating a neuroendocrine HNO-TRPA1-CGRP signalling pathway,” *Nat. Commun.*, vol. 5, no. 1, pp. 1–17, Jul. 2014, doi: 10.1038/ncomms5381.

[51] C. Coletta *et al.*, “Hydrogen sulfide and nitric oxide are mutually dependent in the regulation of angiogenesis and endothelium-dependent vasorelaxation,” *Proc. Natl. Acad. Sci. U. S. A.*, vol. 109, no. 23, pp. 9161–9166, Jun. 2012, doi: 10.1073/pnas.1202916109.

[52] C. Szabo, “A timeline of hydrogen sulfide (H2S) research: From environmental toxin to biological mediator,” *Biochem. Pharmacol.*, 2017, doi: 10.1016/j.bcp.2017.09.010.

[53] R. Fleisher, “Occupational Safety and Health Administration,” in *From Waiting Room to Courtroom: How Doctors can Avoid Getting Sued*, 2016, pp. 99–99.

[54] C. E. Cooper and G. C. Brown, “The inhibition of mitochondrial cytochrome oxidase by the gases carbon monoxide, nitric oxide, hydrogen cyanide and hydrogen sulfide: Chemical mechanism and physiological significance,” *Journal of Bioenergetics and Biomembranes*, vol. 40, no. 5. Springer, pp. 533–539, Oct. 07, 2008, doi: 10.1007/s10863-008-9166-6.

[55] N. N. Greenwood and A. Earnshaw, “Sulfur,” in *Chemistry of the Elements*, Elsevier, 1997, pp. 645–746.

[56] I. Navratilova *et al.*, *Organic Chemistry 2nd Edition*, vol. 55, no. 24. Oxford University Press, 2012.

[57] N. N. Greenwood and A. Earnshaw, “Selenium, Tellurium and Polonium,” in *Chemistry of the Elements*, Elsevier, 1997, pp. 747–788.

[58] R. Wang, “ Two’s company, three’s a crowd: can H 2 S be the third endogenous gaseous transmitter? ,” *FASEB J.*, vol. 16, no. 13, pp. 1792–1798, Nov. 2002, doi: 10.1096/fj.02-0211hyp.

[59] A. R. Lucheta and M. R. Lambais, “Sulfur in Agriculture,” *Rev. Bras. Ciência do Solo*, vol. 36, no. 5, pp. 1369–1379, 2012.

[60] T. Ubuka, “Assay methods and biological roles of labile sulfur in animal tissues,” *Journal of Chromatography B: Analytical Technologies in the Biomedical and Life Sciences*, vol. 781, no. 1–2. Elsevier, pp. 227–249, Dec. 05, 2002, doi: 10.1016/S1570-0232(02)00623-2.

[61] R. McBride and J. Edwards, “Lead acetate test for hydrogen sulphide in gas,” *United States Dep. Commer.*, vol. 41, pp. 4–46, 1914.

[62] E. Kuester and S. Williams, “Production of hydrogen sulfide by Streptomycetes and methods for its detection,” *J. Appl. Microbiol.*, vol.

12, pp. 46–52, 1964.

[63] H. Kabil, O. Kabil, R. Banerjee, L. G. Harshman, and S. D. Pletcher, “Increased transsulfuration mediates longevity and dietary restriction in Drosophila,” *Proc. Natl. Acad. Sci.*, vol. 108, no. 40, pp. 16831–16836, Oct. 2011, doi: 10.1073/pnas.1102008108.

[64] J. I. Sbodio, S. H. Snyder, and B. D. Paul, “Regulators of the transsulfuration pathway,” *British Journal of Pharmacology*, 2018.

[65] J. Giovanelli and S. H. Mudd, “Transsulfuration in higher plants Partial purification and properties of ß-cystathionase of spinach,” *BBA - Enzymol.*, vol. 227, no. 3, pp. 654–670, Mar. 1971, doi: 10.1016/0005-2744(71)90015-5.

[66] B. W. Perridon, H. G. D. Leuvenink, J.-L. Hillebrands, H. van Goor, and E. M. Bos, “The role of hydrogen sulfide in aging and age-related pathologies.,” *Aging (Albany. NY).*, vol. 8, no. 10, pp. 2264–2289, Sep. 2016, doi: 10.18632/aging.101026.

[67] M. H. Stipanuk and P. W. Beck, “Characterization of the enzymic capacity for cysteine desulphhydration in liver and kidney of the rat.,” *Biochem. J.*, vol. 206, no. 2, pp. 267–277, Aug. 1982, doi: 10.1042/bj2060267.

[68] M. Fu, W. Zhang, L. Wu, G. Yang, H. Li, and R. Wang, “Hydrogen sulfide (H 2S) metabolism in mitochondria and its regulatory role in energy production,” *Proc. Natl. Acad. Sci. U. S. A.*, vol. 109, no. 8, pp. 2943–2948, Feb. 2012, doi: 10.1073/pnas.1115634109.

[69] B. Fräsdorf, C. Radon, and S. Leimkühler, “Characterization and Interaction Studies of Two Isoforms of the Dual Localized 3-Mercaptopyruvate Sulfurtransferase TUM1 from Humans,” *J. Biol. Chem.*, vol. 289, no. 50, pp. 34543–34556, Dec. 2014, doi: 10.1074/jbc.M114.605733.

[70] N. Nagahara, T. Ito, H. Kitamura, and T. Nishino, “Tissue and subcellular

distribution of mercaptopyruvate sulfurtransferase in the rat: Confocal laser fluorescence and immunoelectron microscopic studies combined with biochemical analysis," *Histochem. Cell Biol.*, vol. 110, no. 3, pp. 243–250, 1998, doi: 10.1007/s004180050286.

[71] N. Shibuya *et al.*, "A novel pathway for the production of hydrogen sulfide from D-cysteine in mammalian cells," *Nat. Commun.*, vol. 4, no. 1, pp. 1–7, Jan. 2013, doi: 10.1038/ncomms2371.

[72] E. Lagoutte, S. Mimoun, M. Andriamihaja, C. Chaumontet, F. Blachier, and F. Bouillaud, "Oxidation of hydrogen sulfide remains a priority in mammalian cells and causes reverse electron transfer in colonocytes," *Biochim. Biophys. Acta - Bioenerg.*, vol. 1797, no. 8, pp. 1500–1511, Aug. 2010, doi: 10.1016/j.bbabio.2010.04.004.

[73] F. Bouillaud and F. Blachier, "Mitochondria and sulfide: A very old story of poisoning, feeding, and signaling?," *Antioxidants and Redox Signaling*, vol. 15, no. 2. Mary Ann Liebert, Inc. 140 Huguenot Street, 3rd Floor New Rochelle, NY 10801 USA , pp. 379–391, Jul. 15, 2011, doi: 10.1089/ars.2010.3678.

[74] J. Furne, A. Saeed, and M. D. Levitt, "Whole tissue hydrogen sulfide concentrations are orders of magnitude lower than presently accepted values," *https://doi.org/10.1152/ajpregu.90566.2008*, vol. 295, no. 5, pp. 1479–1485, Nov. 2008, doi: 10.1152/AJPREGU.90566.2008.

[75] P. Rose, P. K. Moore, and Y. Z. Zhu, "H2S biosynthesis and catabolism: new insights from molecular studies," *Cellular and Molecular Life Sciences*, vol. 74, no. 8. Birkhauser Verlag AG, pp. 1391–1412, Apr. 01, 2017, doi: 10.1007/s00018-016-2406-8.

[76] M. Goubern, M. Andriamihaja, T. Nübel, F. Blachier, and F. Bouillaud, "Sulfide, the first inorganic substrate for human cells," *FASEB J.*, vol. 21, no. 8, pp. 1699–1706, Jun. 2007, doi: 10.1096/fj.06-7407com.

[77] M. R. Jackson, S. L. Melideo, and M. S. Jorns, "Human sulfide:Quinone

oxidoreductase catalyzes the first step in hydrogen sulfide metabolism and produces a sulfane sulfur metabolite," *Biochemistry*, vol. 51, no. 34, pp. 6804–6815, Aug. 2012, doi: 10.1021/bi300778t.

[78] K. D. C. Augustyn, M. R. Jackson, and M. S. Jorns, "Use of Tissue Metabolite Analysis and Enzyme Kinetics To Discriminate between Alternate Pathways for Hydrogen Sulfide Metabolism," *Biochemistry*, vol. 56, no. 7, pp. 986–996, Feb. 2017, doi: 10.1021/acs.biochem.6b01093.

[79] O. Kabil and R. Banerjee, "Characterization of patient mutations in human persulfide dioxygenase (ETHE1) involved in H2S catabolism," *J. Biol. Chem.*, vol. 287, no. 53, pp. 44561–44667, Dec. 2012, doi: 10.1074/jbc.M112.407411.

[80] C. Maseda *et al.*, "Liquid chromatography-tandem mass spectrometry method for the determination of thiosulfate in human blood and urine as an indicator of hydrogen sulfide poisoning," *Leg. Med.*, vol. 24, pp. 67–74, Jan. 2017, doi: 10.1016/j.legalmed.2016.12.004.

[81] V. Vitvitsky, P. K. Yadav, A. Kurthen, and R. Banerjee, "Sulfide oxidation by a noncanonical pathway in red blood cells generates thiosulfate and polysulfides," *J. Biol. Chem.*, vol. 290, no. 13, pp. 8310–8320, Mar. 2015, doi: 10.1074/jbc.M115.639831.

[82] L. L. Barton and A. W. Hamilton, *Sulphate-reducing bacteria: Environmental and engineered systems*. Cambridge University Press University Printing House Shaftesbury Road Cambridge CB2 8BS United Kingdom: Cambridge University Press, 2007.

[83] D. R. Linden, "Hydrogen sulfide signaling in the gastrointestinal tract," *Antioxidants and Redox Signaling*, vol. 20, no. 5. Mary Ann Liebert, Inc., pp. 818–830, Feb. 10, 2014, doi: 10.1089/ars.2013.5312.

[84] P. D. Scanlan, F. Shanahan, and J. R. Marchesi, "Culture-independent analysis of desulfovibrios in the human distal colon of healthy, colorectal cancer and polypectomized individuals," *FEMS Microbiol. Ecol.*, vol. 69,

no. 2, pp. 213–221, Aug. 2009, doi: 10.1111/j.1574-6941.2009.00709.x.

[85] K. Shatalin, E. Shatalina, A. Mironov, and E. Nudler, “H2S: A Universal Defense Against Antibiotics in Bacteria,” *Science (80-.).*, vol. 334, no. 6058, pp. 986–990, Nov. 2011, doi: 10.1126/SCIENCE.1209855.

[86] R. Cord-Ruwisch, H. J. Seitz, and R. Conrad, “The capacity of hydrogenotrophic anaerobic bacteria to compete for traces of hydrogen depends on the redox potential of the terminal electron acceptor,” *Arch. Microbiol.*, vol. 149, no. 4, pp. 350–357, Feb. 1988, doi: 10.1007/BF00411655.

[87] K. L. Flannigan, K. D. McCoy, and J. L. Wallace, “Eukaryotic and prokaryotic contributions to colonic hydrogen sulfide synthesis,” *Am. J. Physiol. Liver Physiol.*, vol. 301, no. 1, pp. G188–G193, Jul. 2011, doi: 10.1152/ajpgi.00105.2011.

[88] L. Tomasova, P. Konopelski, and M. Ufnal, “Gut bacteria and hydrogen sulfide: The new old players in circulatory system homeostasis,” *Molecules*, vol. 21, no. 11. MDPI AG, Nov. 01, 2016, doi: 10.3390/molecules21111558.

[89] W. E. W. Roediger, A. Duncan, O. Kapaniris, and S. Millard, “Reducing sulfur compounds of the colon impair colonocyte nutrition: Implications for ulcerative colitis,” *Gastroenterology*, vol. 104, no. 3, pp. 802–809, Mar. 1993, doi: 10.1016/0016-5085(93)91016-B.

[90] L. Tomasova *et al.*, “Intracolonic hydrogen sulfide lowers blood pressure in rats,” *Nitric Oxide - Biol. Chem.*, vol. 60, pp. 50–58, Nov. 2016, doi: 10.1016/j.niox.2016.09.007.

[91] F.-F. Guo, T.-C. Yu, J. Hong, and J.-Y. Fang, “Emerging Roles of Hydrogen Sulfide in Inflammatory and Neoplastic Colonic Diseases,” *Front. Physiol.*, vol. 7, no. MAY, p. 156, May 2016, doi: 10.3389/fphys.2016.00156.

[92] R. K. Singh *et al.*, “Influence of diet on the gut microbiome and

implications for human health," *J. Transl. Med.*, vol. 15, no. 1, p. 73, Apr. 2017, doi: 10.1186/S12967-017-1175-Y.

[93] D. W. A *et al.*, "Influence of short-term changes in dietary sulfur on the relative abundances of intestinal sulfate-reducing bacteria," *Gut Microbes*, vol. 10, no. 4, pp. 447–457, Jul. 2019, doi: 10.1080/19490976.2018.1559682.

[94] K. Shatalin *et al.*, "Inhibitors of bacterial H2S biogenesis targeting antibiotic resistance and tolerance," *Science (80-.).*, vol. 372, no. 6547, pp. 1169–1175, Jun. 2021, doi: 10.1126/SCIENCE.ABD8377.

[95] D. Zhang, J. Du, C. Tang, Y. Huang, and H. Jin, "H2S-induced sulfhydration: Biological function and detection methodology," *Frontiers in Pharmacology*, vol. 8, no. SEP. Frontiers, p. 608, Sep. 06, 2017, doi: 10.3389/fphar.2017.00608.

[96] W. P. Jencks and J. Carriuolo, "Reactivity of Nucleophilic Reagents toward Esters," *J. Am. Chem. Soc.*, vol. 82, no. 7, pp. 1778–1786, Apr. 1960, doi: 10.1021/ja01492a058.

[97] G. Yang *et al.*, "Hydrogen sulfide protects against cellular senescence via s-sulfhydration of keap1 and activation of Nrf2," *Antioxidants Redox Signal.*, vol. 18, no. 15, pp. 1906–1919, May 2013, doi: 10.1089/ars.2012.4645.

[98] J. M. Hourihan, J. G. Kenna, and J. D. Hayes, "The gasotransmitter hydrogen sulfide induces Nrf2-target genes by inactivating the keap1 ubiquitin ligase substrate adaptor through formation of a disulfide bond between Cys-226 and Cys-613," *Antioxidants Redox Signal.*, vol. 19, no. 5, pp. 465–481, Aug. 2013, doi: 10.1089/ars.2012.4944.

[99] B. Olas, "Hydrogen sulfide in signaling pathways," *Clinica Chimica Acta*, vol. 439. pp. 212–218, Jan. 15, 2015, doi: 10.1016/j.cca.2014.10.037.

[100] M. R. Filipovic, J. Zivanovic, B. Alvarez, and R. Banerjee, "Chemical

Biology of H2S Signaling through Persulfidation," *Chem. Rev.*, vol. 118, no. 3, p. acs.chemrev.7b00205, Nov. 2017, doi: 10.1021/acs.chemrev.7b00205.

[101] P. K. Yadav *et al.*, "Biosynthesis and Reactivity of Cysteine Persulfides in Signaling," *J. Am. Chem. Soc.*, vol. 138, no. 1, pp. 289–299, Jan. 2016, doi: 10.1021/jacs.5b10494.

[102] S. Kawamura, T. Kitao, T. Nakabayashi, T. Horii, and J. Tsurugi, "Aralkyl Hydrodisulfides. VIII. Alkaline Decomposition and Its Competition with Nucleophiles," *J. Org. Chem.*, vol. 33, no. 3, pp. 1179–1181, Mar. 1968, doi: 10.1021/jo01267a053.

[103] T. S. Bailey, L. N. Zakharov, and M. D. Pluth, "Understanding hydrogen sulfide storage: Probing conditions for sulfide release from hydrodisulfides," *J. Am. Chem. Soc.*, vol. 136, no. 30, pp. 10573–10576, Jul. 2014, doi: 10.1021/ja505371z.

[104] A. Aroca, J. M. Benito, C. Gotor, and L. C. Romero, "Persulfidation proteome reveals the regulation of protein function by hydrogen sulfide in diverse biological processes in Arabidopsis," *J. Exp. Bot.*, vol. 68, no. 17, pp. 4915–4927, Oct. 2017, Accessed: Jun. 25, 2020. [Online]. Available: https://www.ncbi.nlm.nih.gov/pmc/articles/PMC5853657/.

[105] A. K. Mustafa *et al.*, "HS signals through protein S-Sulfhydration," *Sci. Signal.*, vol. 2, no. 96, Nov. 2009, doi: 10.1126/scisignal.2000464.

[106] J. Zivanovic *et al.*, "Selective Persulfide Detection Reveals Evolutionarily Conserved Antiaging Effects of S-Sulfhydration," *Cell Metab.*, vol. 30, no. 6, pp. 1152-1170.e13, Dec. 2019, doi: 10.1016/j.cmet.2019.10.007.

[107] N. Bithi *et al.*, "Dietary restriction transforms the mammalian protein persulfidome in a tissue-specific and cystathionine γ-lyase-dependent manner," *Nat. Commun.*, vol. 12, no. 1, p. 1745, Dec. 2021, doi: 10.1038/s41467-021-22001-w.

[108] C. L. Bianco, J. P. Toscano, and J. M. Fukuto, “An Integrated View of the Chemical Biology of NO, CO, H2S, and O2,” in *Nitric Oxide: Biology and Pathobiology: Third Edition*, Elsevier Inc., 2017, pp. 9–21.

[109] A. Lothian, D. J. Hare, R. Grimm, T. M. Ryan, C. L. Masters, and B. R. Roberts, “Metalloproteomics: Principles, challenges, and applications to neurodegeneration,” *Front. Aging Neurosci.*, vol. 5, no. JUL, 2013, doi: 10.3389/fnagi.2013.00035.

[110] F. M. Boubeta *et al.*, “Hemeproteins as Targets for Sulfide Species,” *Antioxid. Redox Signal.*, vol. 32, no. 4, pp. 247–257, Feb. 2020, doi: 10.1089/ars.2019.7878.

[111] T. Tsukihara *et al.*, “Structures of metal sites of oxidized bovine heart cytochrome c oxidase at 2.8 Å,” *Science (80-.).*, vol. 269, no. 5227, pp. 1069–1074, Aug. 1995, doi: 10.1126/science.7652554.

[112] P. Nicholls, D. C. Marshall, C. E. Cooper, and M. T. Wilson, “Sulfide inhibition of and metabolism by cytochrome c oxidase,” *Biochem. Soc. Trans.*, vol. 41, no. 5, pp. 1312–1316, Oct. 2013, doi: 10.1042/BST20130070.

[113] H. Laggner *et al.*, “The novel gaseous vasorelaxant hydrogen sulfide inhibits angiotensin-converting enzyme activity of endothelial cells,” *J. Hypertens.*, vol. 25, no. 10, pp. 2100–2104, 2007, doi: 10.1097/HJH.0b013e32829b8fd0.

[114] T. Bostelaar *et al.*, “Hydrogen Sulfide Oxidation by Myoglobin,” *J. Am. Chem. Soc.*, vol. 138, no. 27, pp. 8476–8488, Jul. 2016, doi: 10.1021/jacs.6b03456.

[115] M. Whiteman and P. K. Moore, “Hydrogen sulfide and the vasculature: A novel vasculoprotective entity and regulator of nitric oxide bioavailability?,” *Journal of Cellular and Molecular Medicine*, vol. 13, no. 3. J Cell Mol Med, pp. 488–507, Mar. 2009, doi: 10.1111/j.1582-4934.2009.00645.x.

[116] G. K. Kolluru, X. Shen, and C. G. Kevil, “A tale of two gases: NO and H2S, foes or friends for life?,” *Redox Biology*, vol. 1, no. 1. Elsevier B.V., pp. 313–318, Jan. 01, 2013, doi: 10.1016/j.redox.2013.05.001.

[117] L. Xie *et al.*, “Hydrogen sulfide induces Keap1 S-sulfhydration and suppresses diabetes-accelerated atherosclerosis via Nrf2 activation,” *Diabetes*, vol. 65, no. 10, pp. 3171–3184, Oct. 2016, doi: 10.2337/db16-0020.

[118] S. Mukherjee, “Recent advancements in the mechanism of nitric oxide signaling associated with hydrogen sulfide and melatonin crosstalk during ethylene-induced fruit ripening in plants,” *Nitric Oxide - Biology and Chemistry*, vol. 82. Academic Press Inc., pp. 25–34, Jan. 01, 2019, doi: 10.1016/j.niox.2018.11.003.

[119] S. Singh *et al.*, “Revealing on hydrogen sulfide and nitric oxide signals co-ordination for plant growth under stress conditions,” *Physiol. Plant.*, vol. 168, no. 2, pp. 301–317, Feb. 2020, doi: 10.1111/ppl.13002.

[120] G. A and V. JB, “Hydrogen Sulfide Biochemistry and Interplay With Other Gaseous Mediators in Mammalian Physiology,” *Oxid. Med. Cell. Longev.*, vol. 2018, 2018, doi: 10.1155/2018/6290931.

[121] L. Li, A. Hsu, and P. K. Moore, “Actions and interactions of nitric oxide, carbon monoxide and hydrogen sulphide in the cardiovascular system and in inflammation - a tale of three gases!,” *Pharmacology and Therapeutics*, vol. 123, no. 3. Pergamon, pp. 386–400, Sep. 01, 2009, doi: 10.1016/j.pharmthera.2009.05.005.

[122] O. Dangel, E. Mergia, K. Karlisch, D. Groneberg, D. Koesling, and A. Friebe, “Nitric oxide-sensitive guanylyl cyclase is the only nitric oxide receptor mediating platelet inhibition,” *J. Thromb. Haemost.*, vol. 8, no. 6, pp. 1343–1352, Jun. 2010, doi: 10.1111/j.1538-7836.2010.03806.x.

[123] M. D. Maines, “Carbon monoxide and nitric oxide homology: Differential modulation of heme oxygenases in brain and detection of protein and

activity," *Methods Enzymol.*, vol. 268, pp. 473–488, 1996, doi: 10.1016/s0076-6879(96)68049-5.

[124] Z. Zhou *et al.*, "Regulation of soluble guanylyl cyclase redox state by hydrogen sulfide," *Pharmacol. Res.*, vol. 111, pp. 556–562, Sep. 2016, doi: 10.1016/j.phrs.2016.06.029.

[125] C. López-Otín, M. A. Blasco, L. Partridge, M. Serrano, and G. Kroemer, "The hallmarks of aging," *Cell*, vol. 153, no. 6. Elsevier, pp. 1194–1217, Jun. 06, 2013, doi: 10.1016/j.cell.2013.05.039.

[126] D. R. Seals, K. L. Jablonski, and A. J. Donato, "Aging and vascular endothelial function in humans," *Clinical Science*, vol. 120, no. 9. NIH Public Access, pp. 357–375, May 2011, doi: 10.1042/CS20100476.

[127] L. Testai, V. Citi, A. Martelli, S. Brogi, and V. Calderone, "Role of hydrogen sulfide in cardiovascular ageing," *Pharmacological Research*, vol. 160. Academic Press, p. 105125, Oct. 01, 2020, doi: 10.1016/j.phrs.2020.105125.

[128] A. Das *et al.*, "Impairment of an Endothelial NAD+-H2S Signaling Network Is a Reversible Cause of Vascular Aging," *Cell*, vol. 173, no. 1, pp. 74-89.e20, Mar. 2018, doi: 10.1016/j.cell.2018.02.008.

[129] M. Liang, S. Jin, D. D. Wu, M. J. Wang, and Y. C. Zhu, "Hydrogen sulfide improves glucose metabolism and prevents hypertrophy in cardiomyocytes," *Nitric Oxide - Biol. Chem.*, vol. 46, pp. 114–122, Apr. 2015, doi: 10.1016/j.niox.2014.12.007.

[130] H. Li *et al.*, "Exogenous hydrogen sulfide restores cardioprotection of ischemic post-conditioning via inhibition of mPTP opening in the aging cardiomyocytes," *Cell Biosci.*, vol. 5, no. 1, Jul. 2015, doi: 10.1186/s13578-015-0035-9.

[131] M. Peleli *et al.*, "Cardiovascular phenotype of mice lacking 3-mercaptopyruvate sulfurtransferase," *Biochem. Pharmacol.*, vol. 176, Jun.

2020, doi: 10.1016/j.bcp.2020.113833.

[132] J. J. Li, M. Surini, S. Catsicas, E. Kawashima, and C. Bouras, “Age-dependent accumulation of advanced glycosylation end products in human neurons,” *Neurobiol. Aging*, vol. 16, no. 1, pp. 69–76, Jan. 1995, doi: 10.1016/0197-4580(95)80009-G.

[133] R. Ghidoni *et al.*, “Decreased plasma levels of soluble receptor for advanced glycation end products in mild cognitive impairment,” *J. Neural Transm.*, vol. 115, no. 7, pp. 1047–1050, Jul. 2008, doi: 10.1007/s00702-008-0069-9.

[134] D. Walker, L. F. Lue, G. Paul, A. Patel, and M. N. Sabbagh, “Receptor for advanced glycation endproduct modulators: A new therapeutic target in Alzheimer’s disease,” *Expert Opinion on Investigational Drugs*, vol. 24, no. 3. Informa Healthcare, pp. 393–399, 2015, doi: 10.1517/13543784.2015.1001490.

[135] H. Zhou *et al.*, “Hydrogen sulfide reduces RAGE toxicity through inhibition of its dimer formation,” *Free Radic. Biol. Med.*, vol. 104, pp. 262–271, Mar. 2017, doi: 10.1016/j.freeradbiomed.2017.01.026.

[136] L. Wu *et al.*, “Hydrogen Sulfide Inhibits High Glucose-Induced Neuronal Senescence by Improving Autophagic Flux via Up-regulation of SIRT1,” *Front. Mol. Neurosci.*, vol. 12, Aug. 2019, doi: 10.3389/fnmol.2019.00194.

[137] Z. Lu *et al.*, “Cystathionine ß-Synthase-Derived Hydrogen Sulfide Correlates with Successful Aging in Mice,” *Rejuvenation Res.*, vol. 22, no. 6, pp. 513–520, Dec. 2019, doi: 10.1089/rej.2018.2166.

[138] M. A. García-Bereguiaín, A. K. Samhan-Arias, F. J. Martín-Romero, and C. Gutiérrez-Merino, “Hydrogen sulfide raises cytosolic calcium in neurons through activation of L-type Ca2+ channels,” *Antioxidants Redox Signal.*, vol. 10, no. 1, pp. 31–41, Jan. 2008, doi: 10.1089/ars.2007.1656.

[139] H. B. Chen *et al.*, “Cystathionine-ß-synthase-derived hydrogen sulfide is

required for amygdalar long-term potentiation and cued fear memory in rats," *Pharmacol. Biochem. Behav.*, vol. 155, pp. 16–23, Apr. 2017, doi: 10.1016/j.pbb.2017.03.002.

[140] J. Q. Zhan *et al.*, "Hydrogen sulfide reverses aging-associated amygdalar synaptic plasticity and fear memory deficits in rats," *Front. Neurosci.*, vol. 12, no. JUN, Jun. 2018, doi: 10.3389/fnins.2018.00390.

[141] A. S. Go *et al.*, "Heart disease and stroke statistics-2013 update: A Report from the American Heart Association," *Circulation*, vol. 127, no. 1. Jan. 01, 2013, doi: 10.1161/CIR.0b013e31828124ad.

[142] K. Qu, C. P. L. H. Chen, B. Halliwell, P. K. Moore, and P. T. H. Wong, "Hydrogen sulfide is a mediator of cerebral ischemic damage," *Stroke*, vol. 37, no. 3, pp. 889–893, Mar. 2006, doi: 10.1161/01.STR.0000204184.34946.41.

[143] X. Wei *et al.*, "Hydrogen sulfide induces neuroprotection against experimental stroke in rats by down-regulation of AQP4 via activating PKC," *Brain Res.*, vol. 1622, pp. 292–299, Oct. 2015, doi: 10.1016/j.brainres.2015.07.001.

[144] J. Yamamoto *et al.*, "Distribution of hydrogen sulfide (H2S)-producing enzymes and the roles of the H2S donor sodium hydrosulfide in diabetic nephropathy," *Clin. Exp. Nephrol.*, vol. 17, no. 1, pp. 32–40, Feb. 2013, doi: 10.1007/s10157-012-0670-y.

[145] E. A. Ostrakhovitch and S. Tabibzadeh, "Homocysteine in Chronic Kidney Disease," in *Advances in Clinical Chemistry*, vol. 72, Academic Press Inc., 2015, pp. 77–106.

[146] C. Selman, "Dietary restriction and the pursuit of effective mimetics," in *Proceedings of the Nutrition Society*, 2014, vol. 73, no. 2, pp. 260–270, doi: 10.1017/S0029665113003832.

[147] D. Cooke, A. Ouattara, and G. P. Ables, "Dietary methionine restriction

modulates renal response and attenuates kidney injury in mice," *FASEB J.*, vol. 32, no. 2, pp. 693–702, Feb. 2018, doi: 10.1096/fj.201700419R.

[148] S. Yoshida *et al.*, "Role of dietary amino acid balance in diet restriction-mediated lifespan extension, renoprotection, and muscle weakness in aged mice," *Aging Cell*, vol. 17, no. 4, Aug. 2018, doi: 10.1111/acel.12796.

[149] S. Y. Wang *et al.*, "Methionine restriction delays senescence and suppresses the senescence-associated secretory phenotype in the kidney through endogenous hydrogen sulfide," *Cell Cycle*, vol. 18, no. 14, pp. 1573–1587, Jul. 2019, doi: 10.1080/15384101.2019.1618124.

[150] H. J. Lee *et al.*, "Marmoset as a model to study kidney changes associated with aging," *Journals Gerontol. - Ser. A Biol. Sci. Med. Sci.*, vol. 74, no. 3, pp. 315–324, Feb. 2019, doi: 10.1093/gerona/gly237.

[151] M. Malek and M. Nematbakhsh, "Journal of Renal Injury Prevention Renal ischemia/reperfusion injury; from pathophysiology to treatment," *J Ren. Inj Prev*, vol. 4, no. 2, pp. 20–27, Jun. 2015, doi: 10.12861/jrip.2015.06.

[152] C.-H. Chang *et al.*, "Acute Kidney Injury Enhances Outcome Prediction Ability of Sequential Organ Failure Assessment Score in Critically Ill Patients," *PLoS One*, vol. 9, no. 10, p. e109649, Oct. 2014, doi: 10.1371/journal.pone.0109649.

[153] J. C. Pieretti, C. V. C. Junho, M. S. C. Ramos, and A. B. Seabra, "H2S- and NO-releasing gasotransmitter platform: A crosstalk signaling pathway in the treatment of acute kidney injury," *Pharmacol. Res.*, vol. 161, p. 105121, Aug. 2020, doi: 10.1016/j.phrs.2020.105121.

[154] L. Fontana and L. Partridge, "Promoting health and longevity through diet: From model organisms to humans," *Cell*, vol. 161, no. 1, pp. 106–118, Mar. 2015, doi: 10.1016/j.cell.2015.02.020.

[155] A. Picca, V. Pesce, and A. M. S. Lezza, "Does eating less make you live longer and better? An update on calorie restriction.," *Clin. Interv. Aging*,

vol. 12, pp. 1887–1902, 2017, doi: 10.2147/CIA.S126458.

[156] R. Weindruch, R. L. Walford, S. Fligiel, and D. Guthrie, “The retardation of aging in mice by dietary restriction: Longevity, cancer, immunity and lifetime energy intake,” *J. Nutr.*, vol. 116, no. 4, pp. 641–654, 1986, doi: 10.1093/jn/116.4.641.

[157] A. A. Maklakov and T. Chapman, “Evolution of ageing as a tangle of trade-offs: Energy versus function,” *Proceedings of the Royal Society B: Biological Sciences*, vol. 286, no. 1911. Royal Society Publishing, Sep. 25, 2019, doi: 10.1098/rspb.2019.1604.

[158] T. B. L. Kirkwood and D. P. Shanley, “Food restriction, evolution and ageing,” *Mech. Ageing Dev.*, vol. 126, no. 9 SPEC. ISS., pp. 1011–1016, Sep. 2005, doi: 10.1016/j.mad.2005.03.021.

[159] P. Balasubramanian, J. A. Mattison, and R. M. Anderson, “Nutrition, metabolism, and targeting aging in nonhuman primates,” *Ageing Research Reviews*, vol. 39. Elsevier Ireland Ltd, pp. 29–35, Oct. 01, 2017, doi: 10.1016/j.arr.2017.02.002.

[160] S. Yanai, Y. Okaichi, and H. Okaichi, “Long-term dietary restriction causes negative effects on cognitive functions in rats,” *Neurobiol. Aging*, vol. 25, no. 3, pp. 325–332, Mar. 2004, doi: 10.1016/S0197-4580(03)00115-5.

[161] F. Pifferi *et al.*, “Caloric restriction increases lifespan but affects brain integrity in grey mouse lemur primates,” *Commun. Biol.*, vol. 1, no. 1, pp. 1–8, Dec. 2018, doi: 10.1038/s42003-018-0024-8.

[162] J. Most, V. Tosti, L. M. Redman, and L. Fontana, “Calorie restriction in humans: An update,” *Ageing Research Reviews*, vol. 39. Elsevier Ireland Ltd, pp. 36–45, Oct. 01, 2017, doi: 10.1016/j.arr.2016.08.005.

[163] L. Fontana, L. Partridge, and V. D. Longo, “Extending healthy life span-from yeast to humans,” *Science*, vol. 328, no. 5976. American Association for the Advancement of Science, pp. 321–326, Apr. 16, 2010, doi:

10.1126/science.1172539.

[164] C. Hine *et al.*, “Endogenous hydrogen sulfide production is essential for dietary restriction benefits,” *Cell*, vol. 160, no. 1–2, pp. 132–144, Jan. 2015, doi: 10.1016/j.cell.2014.11.048.

[165] C. Hine and J. R. Mitchell, “Calorie restriction and methionine restriction in control of endogenous hydrogen sulfide production by the transsulfuration pathway,” *Exp. Gerontol.*, vol. 68, pp. 26–32, Aug. 2015, doi: 10.1016/j.exger.2014.12.010.

[166] C. Hine, Y. Zhu, A. N. Hollenberg, and J. R. Mitchell, “Dietary and Endocrine Regulation of Endogenous Hydrogen Sulfide Production: Implications for Longevity,” *Antioxidants and Redox Signaling*, vol. 28, no. 16. Mary Ann Liebert Inc., pp. 1483–1502, Jun. 01, 2018, doi: 10.1089/ars.2017.7434.

[167] A. Longchamp *et al.*, “Amino Acid Restriction Triggers Angiogenesis via GCN2/ATF4 Regulation of VEGF and H2S Production,” *Cell*, vol. 173, no. 1, pp. 117-129.e14, Mar. 2018, doi: 10.1016/j.cell.2018.03.001.

[168] K. M. Trocha *et al.*, “Short-term preoperative protein restriction attenuates vein graft disease via induction of cystathionine γ-lyase,” *Cardiovasc. Res.*, vol. 116, no. 2, pp. 416–428, Feb. 2020, doi: 10.1093/cvr/cvz086.

[169] A. Sanz, P. Caro, and G. Barja, “Protein restriction without strong caloric restriction decreases mitochondrial oxygen radical production and oxidative DNA damage in rat liver,” *J. Bioenerg. Biomembr.*, vol. 36, no. 6, pp. 545–552, Dec. 2004, doi: 10.1007/s10863-004-9001-7.

[170] C. Hine *et al.*, “Hypothalamic-Pituitary Axis Regulates Hydrogen Sulfide Production,” *Cell Metab.*, vol. 25, no. 6, pp. 1320-1333.e5, Jun. 2017, doi: 10.1016/j.cmet.2017.05.003.

[171] B. M, B. AE, B. GE, and S. A, “The effect of fasting or calorie restriction on

autophagy induction: A review of the literature," *Ageing Res. Rev.*, vol. 47, pp. 183–197, Nov. 2018, doi: 10.1016/J.ARR.2018.08.004.

[172] X. Jiang *et al.*, "Intracellular H2S production is an autophagy-dependent adaptive response to DNA damage," *Cell Chem. Biol.*, Jun. 2021, doi: 10.1016/j.chembiol.2021.05.016.

[173] S. Mukhopadhyay *et al.*, "Autophagy is required for proper cysteine homeostasis in pancreatic cancer through regulation of SLC7A11," *Proc. Natl. Acad. Sci.*, vol. 118, no. 6, Feb. 2021, doi: 10.1073/PNAS.2021475118.

[174] B. M. Sutter, X. Wu, S. Laxman, and B. P. Tu, "Methionine Inhibits Autophagy and Promotes Growth by Inducing the SAM-Responsive Methylation of PP2A," *Cell*, vol. 154, no. 2, p. 403, Jul. 2013, doi: 10.1016/J.CELL.2013.06.041.

[175] H. M. Brown-Borg, K. E. Borg, C. J. Meliska, and A. Bartke, "Dwarf mice and the ageing process," *Nature*, vol. 384, no. 6604. Nature Publishing Group, p. 33, 1996, doi: 10.1038/384033a0.

[176] K. Flurkey, J. Papaconstantinou, R. A. Miller, and D. E. Harrison, "Lifespan extension and delayed immune and collagen aging in mutant mice with defects in growth hormone production," *Proc. Natl. Acad. Sci. U. S. A.*, vol. 98, no. 12, pp. 6736–6741, Jun. 2001, doi: 10.1073/pnas.111158898.

[177] P. Godfrey, J. O. Rahal, W. G. Beamer, N. G. Copeland, N. A. Jenkins, and K. E. Mayo, "GHRH receptor of little mice contains a missense mutation in the extracellular domain that disrupts receptor function," *Nat. Genet.*, vol. 4, no. 3, pp. 227–232, 1993, doi: 10.1038/ng0793-227.

[178] E. O. Uthus and H. M. Brown-Borg, "Methionine flux to transsulfuration is enhanced in the long living Ames dwarf mouse," *Mech. Ageing Dev.*, vol. 127, no. 5, pp. 444–450, May 2006, doi: 10.1016/j.mad.2006.01.001.

[179] E. O. Uthus and H. M. Brown-Borg, "Altered methionine metabolism in long

living Ames dwarf mice," *Exp. Gerontol.*, vol. 38, no. 5, pp. 491–498, May 2003, doi: 10.1016/S0531-5565(03)00008-1.

[180] H. M. Brown-Borg *et al.*, "Growth hormone signaling is necessary for lifespan extension by dietary methionine," *Aging Cell*, vol. 13, no. 6, pp. 1019–1027, Dec. 2014, doi: 10.1111/acel.12269.

[181] H. M. Brown-Borg, S. Rakoczy, J. A. Wonderlich, V. Armstrong, and L. Rojanathammanee, "Altered dietary methionine differentially impacts glutathione and methionine metabolism in long-living growth hormone-deficient Ames dwarf and wild-type mice," *Longev. Heal.*, vol. 3, no. 1, pp. 1–16, Dec. 2014, doi: 10.1186/2046-2395-3-10.

[182] D. Wu, H. Wang, T. Teng, S. Duan, A. Ji, and Y. Li, "Hydrogen sulfide and autophagy: A double edged sword," *Pharmacological Research*, vol. 131. Academic Press, pp. 120–127, May 01, 2018, doi: 10.1016/j.phrs.2018.03.002.

[183] F. Talaei, V. M. Van Praag, M. H. Shishavan, S. W. Landheer, H. Buikema, and R. H. Henning, "Increased protein aggregation in Zucker Diabetic Fatty rat brain: Identification of key mechanistic targets and the therapeutic application of hydrogen sulfide," *BMC Cell Biol.*, vol. 15, no. 1, p. 1, Jan. 2014, doi: 10.1186/1471-2121-15-1.

[184] L. Ji *et al.*, "Hydrogen sulphide exacerbates acute pancreatitis by over-activating autophagy via AMPK/mTOR pathway," *J. Cell. Mol. Med.*, vol. 20, no. 12, pp. 2349–2361, Dec. 2016, doi: 10.1111/jcmm.12928.

[185] J. Chen *et al.*, "Involvement of exogenous H2S in recovery of cardioprotection from ischemic post-conditioning via increase of autophagy in the aged hearts," *Int. J. Cardiol.*, vol. 220, pp. 681–692, Oct. 2016, doi: 10.1016/j.ijcard.2016.06.200.

[186] D. Wu *et al.*, "Hydrogen Sulfide Attenuates High-Fat Diet-Induced Non-Alcoholic Fatty Liver Disease by Inhibiting Apoptosis and Promoting Autophagy via Reactive Oxygen Species/Phosphatidylinositol 3-

Kinase/AKT/Mammalian Target of Rapamycin Signaling Pathway," *Front. Pharmacol.*, vol. 11, p. 1965, Nov. 2020, doi: 10.3389/fphar.2020.585860.

[187] F. Yang *et al.*, "Exogenous H2S Protects Against Diabetic Cardiomyopathy by Activating Autophagy via the AMPK/mTOR Pathway," *Cell. Physiol. Biochem.*, vol. 43, no. 3, pp. 1168–1187, Nov. 2017, doi: 10.1159/000481758.

[188] Y. Zhou *et al.*, "Hydrogen sulfide promotes angiogenesis by downregulating miR-640 via the VEGFR2/mTOR pathway," *Am. J. Physiol. Physiol.*, vol. 310, no. 4, pp. C305–C317, Feb. 2016, doi: 10.1152/ajpcell.00230.2015.

[189] J. Ma *et al.*, "Hydrogen sulphide promotes osteoclastogenesis by inhibiting autophagy through the PI3K/AKT/mTOR pathway," *J. Drug Target.*, vol. 28, no. 2, pp. 176–185, Feb. 2020, doi: 10.1080/1061186X.2019.1624969.

[190] Z. Lyu *et al.*, "mTORC1-Sch9 regulates hydrogen sulfide production through the transsulfuration pathway," *Aging (Albany. NY).*, vol. 11, no. 19, pp. 8418–8432, Oct. 2019, doi: 10.18632/aging.102327.

[191] S. S. Wang *et al.*, "Hydrogen sulfide promotes autophagy of hepatocellular carcinoma cells through the PI3K/Akt/mTOR signaling pathway," *Cell Death Dis.*, vol. 8, no. 3, p. e2688, 2017, doi: 10.1038/cddis.2017.18.

[192] G. Zhou *et al.*, "Role of AMP-activated protein kinase in mechanism of metformin action," *J. Clin. Invest.*, vol. 108, no. 8, pp. 1167–1174, 2001, doi: 10.1172/JCI13505.

[193] B. Wiliński, J. Wiliński, E. Somogyi, J. Piotrowska, and W. Opoka, "Metformin raises hydrogen sulfide tissue concentrations in various mouse organs," *Pharmacol. Reports*, vol. 65, no. 3, pp. 737–742, 2013, doi: 10.1016/S1734-1140(13)71053-3.

[194] M. Wang, W. Tang, and Y. Z. Zhu, "An update on AMPK in hydrogen sulfide pharmacology," *Frontiers in Pharmacology*, vol. 8, no. NOV. Frontiers Media S.A., p. 810, Nov. 08, 2017, doi: 10.3389/fphar.2017.00810.

[195] T. Zhong *et al.*, “Metformin alters DNA methylation genome-wide via the H19/SAHH axis,” *Oncogene*, vol. 36, no. 17, pp. 2345–2354, Apr. 2017, doi: 10.1038/onc.2016.391.

[196] X. Ma, Z. Jiang, Z. Wang, and Z. Zhang, “Administration of metformin alleviates atherosclerosis by promoting H2S production via regulating CSE expression,” *J. Cell. Physiol.*, vol. 235, no. 3, pp. 2102–2112, Mar. 2020, doi: 10.1002/jcp.29112.

[197] Y. Sun *et al.*, “Protective effect of metformin on BPA-induced liver toxicity in rats through upregulation of cystathionine ß synthase and cystathionine γ lyase expression,” *Sci. Total Environ.*, vol. 750, Jan. 2021, doi: 10.1016/j.scitotenv.2020.141685.

[198] D. E. Harrison *et al.*, “Acarbose, 17-α-estradiol, and nordihydroguaiaretic acid extend mouse lifespan preferentially in males,” *Aging Cell*, vol. 13, no. 2, pp. 273–282, 2014, doi: 10.1111/acel.12170.

[199] A. A. Akintola and D. van Heemst, “Insulin, aging, and the brain: Mechanisms and implications,” *Frontiers in Endocrinology*, vol. 6, no. FEB. Frontiers Media S.A., 2015, doi: 10.3389/fendo.2015.00013.

[200] H. Zhang *et al.*, “Hydrogen sulfide regulates insulin secretion and insulin resistance in diabetes mellitus, a new promising target for diabetes mellitus treatment? A review,” *Journal of Advanced Research*, vol. 27. Elsevier B.V., pp. 19–30, Jan. 01, 2021, doi: 10.1016/j.jare.2020.02.013.

[201] X. Feng, Y. Chen, J. Zhao, C. Tang, Z. Jiang, and B. Geng, “Hydrogen sulfide from adipose tissue is a novel insulin resistance regulator,” *Biochem. Biophys. Res. Commun.*, vol. 380, no. 1, pp. 153–159, Feb. 2009, doi: 10.1016/j.bbrc.2009.01.059.

[202] L. Zhang, G. Yang, A. Untereiner, Y. Ju, L. Wu, and R. Wang, “Hydrogen Sulfide Impairs Glucose Utilization and Increases Gluconeogenesis in Hepatocytes,” *Endocrinology*, vol. 154, no. 1, pp. 114–126, Jan. 2013, doi: 10.1210/en.2012-1658.

[203] M. Okamoto, T. Ishizaki, and T. Kimura, “Protective effect of hydrogen sulfide on pancreatic beta-cells,” *Nitric Oxide - Biology and Chemistry*, vol. 46. Academic Press Inc., pp. 32–36, Apr. 30, 2015, doi: 10.1016/j.niox.2014.11.007.

[204] X. Chen *et al.*, “Hydrogen Sulphide Treatment Increases Insulin Sensitivity and Improves Oxidant Metabolism through the CaMKKbeta-AMPK Pathway in PA-Induced IR C2C12 Cells,” *Sci. Rep.*, vol. 7, no. 1, pp. 1–13, Dec. 2017, doi: 10.1038/s41598-017-13251-0.

[205] P. Manna and S. K. Jain, “Vitamin D up-regulates glucose transporter 4 (GLUT4) translocation and glucose utilization mediated by cystathionine-γ-lyase (CSE) activation and H2S formation in 3T3L1 adipocytes,” *J. Biol. Chem.*, vol. 287, no. 50, pp. 42324–42332, Dec. 2012, doi: 10.1074/jbc.M112.407833.

[206] R. Xue *et al.*, “Hydrogen sulfide treatment promotes glucose uptake by increasing insulin receptor sensitivity and ameliorates kidney lesions in type 2 diabetes,” *Antioxidants Redox Signal.*, vol. 19, no. 1, pp. 5–23, Jul. 2013, doi: 10.1089/ars.2012.5024.

[207] S. Gheibi, S. Jeddi, K. Kashfi, and A. Ghasemi, “Effects of hydrogen sulfide on carbohydrate metabolism in obese type 2 diabetic rats,” *Molecules*, vol. 24, no. 1, Jan. 2019, doi: 10.3390/molecules24010190.

[208] B. Qabazard and S. R. Stürzenbaum, “H2S: A New Approach to Lifespan Enhancement and Healthy Ageing?,” in *Handbook of experimental pharmacology*, vol. 230, 2015, pp. 269–287.

[209] T. Vos *et al.*, “Global, regional, and national incidence, prevalence, and years lived with disability for 328 diseases and injuries for 195 countries, 1990-2016: A systematic analysis for the Global Burden of Disease Study 2016,” *Lancet*, vol. 390, no. 10100, pp. 1211–1259, Sep. 2017, doi: 10.1016/S0140-6736(17)32154-2.

[210] K. N. Islam, D. J. Polhemus, E. Donnarumma, L. P. Brewster, and D. J.

Lefer, “Hydrogen Sulfide Levels and Nuclear Factor-Erythroid 2-Related Factor 2 (NRF2) Activity Are Attenuated in the Setting of Critical Limb Ischemia (CLI),” *J. Am. Heart Assoc.*, vol. 4, no. 5, May 2015, doi: 10.1161/JAHA.115.001986.

[211] H. S. Jin *et al.*, “Association of the I264T variant in the sulfide quinone reductase-like (SQRDL) gene with osteoporosis in Korean postmenopausal women,” *PLoS One*, vol. 10, no. 8, p. e0135285, Aug. 2015, doi: 10.1371/journal.pone.0135285.

[212] E. Zavaczki *et al.*, “Hydrogen sulfide inhibits the calcification and osteoblastic differentiation of vascular smooth muscle cells,” *Kidney Int.*, vol. 80, no. 7, pp. 731–739, Oct. 2011, doi: 10.1038/ki.2011.212.

[213] M. Yang, Y. Huang, J. Chen, Y. L. Chen, J. J. Ma, and P. H. Shi, “Activation of AMPK participates hydrogen sulfide-induced cyto-protective effect against dexamethasone in osteoblastic MC3T3-E1 cells,” *Biochem. Biophys. Res. Commun.*, vol. 454, no. 1, pp. 42–47, Nov. 2014, doi: 10.1016/j.bbrc.2014.10.033.

[214] A. P. Nagtegaal *et al.*, “Genome-wide association meta-analysis identifies five novel loci for age-related hearing impairment,” *Sci. Rep.*, vol. 9, no. 1, pp. 1–10, Dec. 2019, doi: 10.1038/s41598-019-51630-x.

[215] F. Magrangeas *et al.*, “A genome-wide association study identifies a novel locus for bortezomib-induced peripheral neuropathy in European patients with multiple myeloma,” *Clin. Cancer Res.*, vol. 22, no. 17, pp. 4350–4355, Sep. 2016, doi: 10.1158/1078-0432.CCR-15-3163.

[216] B. R. Reed, J. Crane, N. Garrett, D. L. Woods, and M. N. Bates, “Chronic ambient hydrogen sulfide exposure and cognitive function,” *Neurotoxicol. Teratol.*, vol. 42, pp. 68–76, 2014, doi: 10.1016/j.ntt.2014.02.002.

[217] M. N. Bates, N. Garrett, B. Graham, and D. Read, “Cancer incidence, morbidity and geothermal air pollution in Rotorua, New Zealand,” *Int. J. Epidemiol.*, vol. 27, no. 1, pp. 10–14, Feb. 1998, doi: 10.1093/ije/27.1.10.

[218] Y. O. Cakmak, “Rotorua, hydrogen sulphide and parkinson’s disease—A possible beneficial link?,” *N. Z. Med. J.*, vol. 130, no. 1455, pp. 123–125, May 2017, Accessed: May 18, 2021. [Online]. Available: https://pubmed.ncbi.nlm.nih.gov/28494485/.

[219] K. Pope, Y. T. So, J. Crane, and M. N. Bates, “Ambient geothermal hydrogen sulfide exposure and peripheral neuropathy,” *Neurotoxicology*, vol. 60, pp. 10–15, May 2017, doi: 10.1016/j.neuro.2017.02.006.

[220] M. N. Bates, N. Garrett, J. Crane, and J. R. Balmes, “Associations of ambient hydrogen sulfide exposure with self-reported asthma and asthma symptoms,” *Environ. Res.*, vol. 122, pp. 81–87, Apr. 2013, doi: 10.1016/j.envres.2013.02.002.

[221] Y. Zheng, B. Yu, L. K. De La Cruz, M. Roy Choudhury, A. Anifowose, and B. Wang, “Toward Hydrogen Sulfide Based Therapeutics: Critical Drug Delivery and Developability Issues,” *Med. Res. Rev.*, vol. 38, no. 1, pp. 57–100, Jan. 2018, doi: 10.1002/med.21433.

[222] L. Mulvey, W. A. Sands, K. Salin, A. E. Carr, and C. Selman, “Disentangling the effect of dietary restriction on mitochondrial function using recombinant inbred mice,” *Mol. Cell. Endocrinol.*, vol. 455, pp. 41–53, Nov. 2017, Accessed: Jul. 31, 2018. [Online]. Available: http://www.ncbi.nlm.nih.gov/pubmed/27597651.

[223] C.-Y. Liao, B. A. Rikke, T. E. Johnson, V. Diaz, and J. F. Nelson, “Genetic variation in the murine lifespan response to dietary restriction: from life extension to life shortening,” *Aging Cell*, vol. 9, no. 1, pp. 92–95, Feb. 2010, doi: 10.1111/j.1474-9726.2009.00533.x.

[224] B. A. Rikke, C.-Y. Y. Liao, M. B. McQueen, J. F. Nelson, and T. E. Johnson, “Genetic dissection of dietary restriction in mice supports the metabolic efficiency model of life extension,” *Exp. Gerontol.*, vol. 45, no. 9, pp. 691–701, Sep. 2010, doi: 10.1016/j.exger.2010.04.008.

[225] C. Selman and W. R. Swindell, “Putting a strain on diversity,” *EMBO J.*,

vol. 37, no. 22, p. e100862, Nov. 2018, doi: 10.15252/embj.2018100862.

[226] S. J. Mitchell *et al.*, “Effects of Sex, Strain, and Energy Intake on Hallmarks of Aging in Mice,” *Cell Metab.*, vol. 23, no. 6, pp. 1093–1112, 2016, doi: 10.1016/j.cmet.2016.05.027.

[227] S. Hempenstall, L. Picchio, S. E. Mitchell, J. R. Speakman, and C. Selman, “The impact of acute caloric restriction on the metabolic phenotype in male C57BL/6 and DBA/2 mice,” *Mech. Ageing Dev.*, vol. 131, no. 2, pp. 111–118, Feb. 2010, doi: 10.1016/J.MAD.2009.12.008.

[228] F. G. Osorio *et al.*, “Hutchinson-Gilford progeria: Splicing-directed therapy in a new mouse model of human accelerated aging,” *Sci. Transl. Med.*, vol. 3, no. 106, Oct. 2011, doi: 10.1126/scitranslmed.3002847.

[229] R. Kreienkamp *et al.*, “Doubled lifespan and patient-like pathologies in progeria mice fed high-fat diet,” *Aging Cell*, vol. 18, no. 1, Feb. 2019, doi: 10.1111/acel.12852.

[230] C. Hine and J. Mitchell, “Endpoint or Kinetic Measurement of Hydrogen Sulfide Production Capacity in Tissue Extracts,” *BIO-PROTOCOL*, vol. 7, no. 13, Jul. 2017, doi: 10.21769/BioProtoc.2382.

[231] H. Gong *et al.*, “Evaluation of candidate reference genes for RT-qPCR studies in three metabolism related tissues of mice after caloric restriction,” *Sci. Rep.*, vol. 6, no. 1, p. 38513, Dec. 2016, doi: 10.1038/srep38513.

[232] N. M. Morton *et al.*, “Genetic identification of thiosulfate sulfurtransferase as an adipocyte-expressed antidiabetic target in mice selected for leanness,” *Nat. Med.*, vol. 22, no. 7, pp. 771–779, Jul. 2016, doi: 10.1038/nm.4115.

[233] N. M. Morton *et al.*, “Genetic identification of thiosulfate sulfurtransferase as an adipocyte-expressed antidiabetic target in mice selected for leanness,” *Nat. Med.*, vol. 22, no. 7, pp. 771–779, 2016, doi:

10.1038/nm.4115.

[234] T. M. Wallace, J. C. Levy, and D. R. Matthews, “Use and Abuse of HOMA Modeling,” *Diabetes Care*, vol. 27, no. 6, pp. 1487–1495, Jun. 2004, doi: 10.2337/DIACARE.27.6.1487.

[235] J. Crowe *et al.*, “The parasitic worm product ES-62 promotes health- and life-span in a high calorie diet-accelerated mouse model of ageing,” *PLoS Pathog.*, vol. 16, no. 3, 2020, doi: 10.1371/JOURNAL.PPAT.1008391.

[236] A. Turturro, W. W. Witt, S. Lewis, B. S. Hass, R. D. Lipman, and R. W. Hart, “Growth curves and survival characteristics of the animals used in the biomarkers of aging program,” *Journals Gerontol. - Ser. A Biol. Sci. Med. Sci.*, vol. 54, no. 11, 1999, doi: 10.1093/gerona/54.11.B492.

[237] R. Yuan *et al.*, “Aging in inbred strains of mice: Study design and interim report on median lifespans and circulating IGF1 levels,” *Aging Cell*, vol. 8, no. 3, pp. 277–287, 2009, doi: 10.1111/j.1474-9726.2009.00478.x.

[238] D. K. Ingram and R. de Cabo, “Calorie restriction in rodents: Caveats to consider,” *Ageing Research Reviews*, vol. 39. Ageing Res Rev, pp. 15–28, Oct. 01, 2017, doi: 10.1016/j.arr.2017.05.008.

[239] L. Mulvey, A. Sinclair, and C. Selman, “Lifespan Modulation in Mice and the Confounding Effects of Genetic Background,” *Journal of Genetics and Genomics*, vol. 41, no. 9. J Genet Genomics, pp. 497–503, Sep. 20, 2014, doi: 10.1016/j.jgg.2014.06.002.

[240] W. R. Swindell, “Dietary restriction in rats and mice: A meta-analysis and review of the evidence for genotype-dependent effects on lifespan,” *Ageing Research Reviews*, vol. 11, no. 2. pp. 254–270, Apr. 2012, doi: 10.1016/j.arr.2011.12.006.

[241] C. Y. Liao, B. A. Rikke, T. E. Johnson, J. A. L. Gelfond, V. Diaz, and J. F. Nelson, “Fat maintenance is a predictor of the murine lifespan response to dietary restriction,” *Aging Cell*, vol. 10, no. 4, pp. 629–639, Aug. 2011,

doi: 10.1111/j.1474-9726.2011.00702.x.

[242] B. K. Kennedy, K. K. Steffen, and M. Kaeberlein, “Ruminations on dietary restriction and aging,” *Cellular and Molecular Life Sciences*, vol. 64, no. 11. Cell Mol Life Sci, pp. 1323–1328, Jun. 2007, doi: 10.1007/s00018-007-6470-y.

[243] W. Mair and A. Dillin, “Aging and survival: The genetics of life span extension by dietary restriction,” *Annual Review of Biochemistry*, vol. 77. Annu Rev Biochem, pp. 727–754, 2008, doi: 10.1146/annurev.biochem.77.061206.171059.

[244] E. J. Masoro, “Overview of caloric restriction and ageing,” *Mech. Ageing Dev.*, vol. 126, no. 9 SPEC. ISS., pp. 913–922, 2005, doi: 10.1016/j.mad.2005.03.012.

[245] D. L. Miller and M. B. Roth, “Hydrogen sulfide increases thermotolerance and lifespan in Caenorhabditis elegans.,” *Proc. Natl. Acad. Sci. U. S. A.*, vol. 104, no. 51, pp. 20618–22, Dec. 2007, doi: 10.1073/pnas.0710191104.

[246] B. Qabazard, S. Ahmed, L. Li, V. M. Arlt, P. K. Moore, and S. R. Stürzenbaum, “C. elegans Aging Is Modulated by Hydrogen Sulfide and the sulfhydrylase/cysteine Synthase cysl-2,” *PLoS One*, vol. 8, no. 11, p. e80135, Nov. 2013, doi: 10.1371/journal.pone.0080135.

[247] M. Shaposhnikov, E. Proshkina, L. Koval, N. Zemskaya, A. Zhavoronkov, and A. Moskalev, “Overexpression of CBS and CSE genes affects lifespan, stress resistance and locomotor activity in Drosophila melanogaster,” *Aging (Albany. NY).*, vol. 10, no. 11, pp. 3260–3272, Nov. 2018, doi: 10.18632/aging.101630.

[248] Y. Wei and C. Kenyon, “Roles for ROS and hydrogen sulfide in the longevity response to germline loss in *Caenorhabditis elegans*,” *Proc. Natl. Acad. Sci.*, vol. 113, no. 20, pp. E2832–E2841, May 2016, doi: 10.1073/pnas.1524727113.

[249] H. J. Lee *et al.*, “Hydrogen sulfide ameliorates aging-associated changes in the kidney,” *GeroScience*, vol. 40, no. 2, pp. 163–176, Apr. 2018, doi: 10.1007/s11357-018-0018-y.

[250] J. Q. Zhan *et al.*, “Hydrogen sulfide reverses aging-associated amygdalar synaptic plasticity and fear memory deficits in rats,” *Front. Neurosci.*, vol. 12, no. JUN, Jun. 2018, doi: 10.3389/fnins.2018.00390.

[251] F. Talaei, V. M. Van Praag, and R. H. Henning, “Hydrogen sulfide restores a normal morphological phenotype in Werner syndrome fibroblasts, attenuates oxidative damage and modulates mTOR pathway,” *Pharmacol. Res.*, vol. 74, pp. 34–44, Aug. 2013, doi: 10.1016/j.phrs.2013.04.011.

[252] E. Latorre, R. Torregrossa, M. E. Wood, M. Whiteman, and L. W. Harries, “Mitochondria-targeted hydrogen sulfide attenuates endothelial senescence by selective induction of splicing factors HNRNPD and SRSF2,” *Aging (Albany. NY).*, vol. 10, no. 7, pp. 1666–1681, Jul. 2018, doi: 10.18632/aging.101500.

[253] O. Kabil, V. Vitvitsky, P. Xie, and R. Banerjee, “The quantitative significance of the transsulfuration enzymes for H 2S production in murine tissues,” *Antioxidants Redox Signal.*, vol. 15, no. 2, pp. 363–372, Jun. 2011, doi: 10.1089/ars.2010.3781.

[254] S. E. Wilkie *et al.*, “Strain-specificity in the hydrogen sulphide signalling network following dietary restriction in recombinant inbred mice,” *GeroScience*, vol. 42, no. 2, pp. 801–812, 2020, doi: 10.1007/s11357-020-00168-2.

[255] B. Bennett, M. Beeson, L. Gordon, and T. E. Johnson, “Reciprocal congenics defining individual quantitative trait loci for sedative/hypnotic sensitivity to ethanol,” *Alcohol. Clin. Exp. Res.*, vol. 26, no. 2, pp. 149–157, Feb. 2002, doi: 10.1111/j.1530-0277.2002.tb02519.x.

[256] S. Mani, W. Cao, L. Wu, and R. Wang, “Hydrogen sulfide and the liver,” *Nitric Oxide*, vol. 41, pp. 62–71, Sep. 2014, Accessed: Jul. 03, 2019.

[Online]. Available: http://www.ncbi.nlm.nih.gov/pubmed/24582857.

[257] J. R. Speakman and S. E. Mitchell, “Caloric restriction,” *Mol. Aspects Med.*, vol. 32, no. 3, pp. 159–221, Jun. 2011, doi: 10.1016/j.mam.2011.07.001.

[258] L. Fontana, T. E. Meyer, S. Klein, and J. O. Holloszy, “Long-term calorie restriction is highly effective in reducing the risk for atherosclerosis in humans,” *Proc. Natl. Acad. Sci. U. S. A.*, vol. 101, no. 17, pp. 6659–6663, Apr. 2004, doi: 10.1073/pnas.0308291101.

[259] L. Fontana *et al.*, “Calorie restriction or exercise: Effects on coronary heart disease risk factors. A randomized, controlled trial,” *Am. J. Physiol. - Endocrinol. Metab.*, vol. 293, no. 1, Jul. 2007, doi: 10.1152/ajpendo.00102.2007.

[260] M. J. Forster, P. Morris, and R. S. Sohal, “Genotype and age influence the effect of caloric intake on mortality in mice.,” *FASEB J.*, vol. 17, no. 6, pp. 690–692, 2003, doi: 10.1096/fj.02-0533fje.

[261] H. J. Goren, R. N. Kulkarni, and C. R. Kahn, “Glucose homeostasis and tissue transcript content of insulin signaling intermediates in four inbred strains of mice: C57BL/6, C57BLKS/6, DBA/2, and 129X1,” *Endocrinology*, vol. 145, no. 7, pp. 3307–3323, Jul. 2004, doi: 10.1210/en.2003-1400.

[262] C. L. Hou *et al.*, “Protective Effects of Hydrogen Sulfide in the Ageing Kidney,” *Oxid. Med. Cell. Longev.*, vol. 2016, 2016, doi: 10.1155/2016/7570489.

[263] R. N. Carter and N. M. Morton, “Cysteine and hydrogen sulphide in the regulation of metabolism: Insights from genetics and pharmacology,” *Journal of Pathology*, vol. 238, no. 2. J Pathol, pp. 321–332, Jan. 01, 2016, doi: 10.1002/path.4659.

[264] D. Derous *et al.*, “The effects of graded levels of calorie restriction: XI. Evaluation of the main hypotheses underpinning the life extension effects

of CR using the hepatic transcriptome," *Aging (Albany. NY).*, vol. 9, no. 7, pp. 1770–1824, Jul. 2017, doi: 10.18632/aging.101269.

[265] B. Wang, J. Zeng, and Q. Gu, "Exercise restores bioavailability of hydrogen sulfide and promotes autophagy influx in livers of mice fed with high-fat diet," *Can. J. Physiol. Pharmacol.*, vol. 95, no. 6, pp. 667–674, 2017, doi: 10.1139/cjpp-2016-0611.

[266] H. Kimura, "Signaling of hydrogen sulfide and polysulfides.," *Antioxid. Redox Signal.*, vol. 22, no. 5, pp. 347–9, Feb. 2015, doi: 10.1089/ars.2014.6082.

[267] B. Renga, "Hydrogen sulfide generation in mammals: the molecular biology of cystathionine-ß- synthase (CBS) and cystathionine-γ-lyase (CSE).," *Inflamm. Allergy Drug Targets*, vol. 10, no. 2, pp. 85–91, Apr. 2011, Accessed: Sep. 18, 2019. [Online]. Available: http://www.ncbi.nlm.nih.gov/pubmed/21275900.

[268] B. Tao, R. Wang, C. Sun, and Y. Zhu, "3-Mercaptopyruvate Sulfurtransferase, Not Cystathionine ß-Synthase Nor Cystathionine γ-Lyase, Mediates Hypoxia-Induced Migration of Vascular Endothelial Cells.," *Front. Pharmacol.*, vol. 8, p. 657, 2017, doi: 10.3389/fphar.2017.00657.

[269] S. Arndt *et al.*, "Assessment of H2S in vivo using the newly developed mitochondria-targeted mass spectrometry probe MitoA," *J. Biol. Chem.*, vol. 292, no. 19, pp. 7761–7773, May 2017, doi: 10.1074/jbc.M117.784678.

[270] G. Y. Lau *et al.*, "Detection of changes in mitochondrial hydrogen sulfide in vivo in the fish model Poecilia mexicana (Poeciliidae)," *Biol. Open*, vol. 8, no. 5, May 2019, doi: 10.1242/bio.041467.

[271] K. R. Olson, "A practical look at the chemistry and biology of hydrogen sulfide.," *Antioxid. Redox Signal.*, vol. 17, no. 1, pp. 32–44, Jul. 2012, doi: 10.1089/ars.2011.4401.

[272] E. Blackstone, M. Morrison, and M. B. Roth, "H2S induces a suspended

animation-like state in mice," *Science (80-.).*, vol. 308, no. 5721, p. 518, Apr. 2005, doi: 10.1126/science.1108581.

[273] C.-L. Hou *et al.*, "Protective Effects of Hydrogen Sulfide in the Ageing Kidney," *Oxid. Med. Cell. Longev.*, vol. 2016, pp. 1–13, 2016, doi: 10.1155/2016/7570489.

[274] L. T. Ng, J. Gruber, and P. K. Moore, *Is there a role of H2S in mediating health span benefits of caloric restriction?*, vol. 149. 2018, pp. 91–100.

[275] M. D. W. Piper, L. Partridge, D. Raubenheimer, and S. J. Simpson, "Dietary restriction and aging: A unifying perspective," *Cell Metabolism*, vol. 14, no. 2. Europe PMC Funders, pp. 154–160, Aug. 03, 2011, doi: 10.1016/j.cmet.2011.06.013.

[276] X. Shen, G. K. Kolluru, S. Yuan, and C. G. Kevil, "Measurement of H2S in vivo and in vitro by the monobromobimane method," in *Methods in Enzymology*, vol. 554, NIH Public Access, 2015, pp. 31–45.

[277] X. Shen, E. A. Peter, S. Bir, R. Wang, and C. G. Kevil, "Analytical measurement of discrete hydrogen sulfide pools in biological specimens.," *Free Radic. Biol. Med.*, vol. 52, no. 11–12, pp. 2276–83, 2012, doi: 10.1016/j.freeradbiomed.2012.04.007.

[278] O. Kabil and R. Banerjee, "Redox Biochemistry of Hydrogen Sulfide," *J. Biol. Chem.*, vol. 285, no. 29, p. 21903, Jul. 2010, doi: 10.1074/JBC.R110.128363.

[279] E. R. DeLeon, G. F. Stoy, and K. R. Olson, "Passive loss of hydrogen sulfide in biological experiments," *Anal. Biochem.*, vol. 421, no. 1, pp. 203–207, Feb. 2012, doi: 10.1016/j.ab.2011.10.016.

[280] H. Ibrahim, A. Serag, and M. A. Farag, "Emerging analytical tools for the detection of the third gasotransmitter H2S, a comprehensive review," *J. Adv. Res.*, vol. 27, pp. 137–153, Jan. 2021, doi: 10.1016/J.JARE.2020.05.018.

[281] T. Ditrói, A. Nagy, D. Martinelli, A. Rosta, V. Kožich, and P. Nagy, “Comprehensive analysis of how experimental parameters affect H2S measurements by the monobromobimane method,” *Free Radic. Biol. Med.*, vol. 136, pp. 146–158, May 2019, doi: 10.1016/j.freeradbiomed.2019.04.006.

[282] J. E. Doeller *et al.*, “Polarographic measurement of hydrogen sulfide production and consumption by mammalian tissues,” *Anal. Biochem.*, vol. 341, no. 1, pp. 40–51, Jun. 2005, doi: 10.1016/J.AB.2005.03.024.

[283] Y. Zheng, F. Liao, J.-B. Du, C.-S. Tang, G.-H. Xu, and B. Geng, “[Modified methylene blue method for measurement of hydrogen sulfide level in plasma].,” *Sheng Li Xue Bao*, vol. 64, no. 6, pp. 681–6, Dec. 2012, Accessed: Jul. 31, 2019. [Online]. Available: http://www.ncbi.nlm.nih.gov/pubmed/23258332.

[284] V. S. Lin and C. J. Chang, “Fluorescent probes for sensing and imaging biological hydrogen sulfide,” *Current Opinion in Chemical Biology*, vol. 16, no. 5–6. NIH Public Access, pp. 595–601, Dec. 2012, doi: 10.1016/j.cbpa.2012.07.014.

[285] K. R. Olson, *A practical look at the chemistry and biology of hydrogen sulfide*, vol. 17, no. 1. Mary Ann Liebert, Inc., 2012, pp. 32–44.

[286] R. A. J. Smith, C. M. Porteous, A. M. Gane, and M. P. Murphy, “Delivery of bioactive molecules to mitochondria in vivo,” *Proc. Natl. Acad. Sci. U. S. A.*, vol. 100, no. 9, pp. 5407–5412, Apr. 2003, doi: 10.1073/pnas.0931245100.

[287] R. Greenway *et al.*, “Convergent evolution of conserved mitochondrial pathways underlies repeated adaptation to extreme environments,” *Proc. Natl. Acad. Sci.*, vol. 117, no. 28, pp. 16424–16430, Jul. 2020, doi: 10.1073/PNAS.2004223117.

[288] E. Marutani *et al.*, “Sulfide catabolism ameliorates hypoxic brain injury,” *Nat. Commun.*, vol. 12, no. 1, Dec. 2021, doi: 10.1038/S41467-021-23363-

X.

[289] R. Cipollone, P. Ascenzi, P. Tomao, F. Imperi, and P. Visca, “Enzymatic detoxification of cyanide: Clues from Pseudomonas aeruginosa rhodanese,” *Journal of Molecular Microbiology and Biotechnology*, vol. 15, no. 2–3. Karger Publishers, pp. 199–211, Aug. 2008, doi: 10.1159/000121331.

[290] G. L. Sharp, W. G. Hill, and A. Robertson, “Effects of selection on growth, body composition and food intake in mice I. Responses in selected traits,” *Genet. Res.*, vol. 43, no. 1, pp. 75–92, 1984, doi: 10.1017/S0016672300025738.

[291] L. Bünger and W. G. Hill, “Inbred lines of mice derived from long-term divergent selection on fat content and body weight,” *Mamm. Genome*, vol. 10, no. 6, pp. 645–648, 1999, doi: 10.1007/s003359901063.

[292] F. BONOMI, S. PAGANI, P. CERLETTI, and C. CANNELLA, “Rhodanese-Mediated Sulfur Transfer to Succinate Dehydrogenase,” *Eur. J. Biochem.*, vol. 72, no. 1, pp. 17–24, 1977, doi: 10.1111/j.1432-1033.1977.tb11219.x.

[293] S. Pagani and Y. M. Galante, “Interaction of rhodanese with mitochondrial NADH dehydrogenase,” *Biochim. Biophys. Acta (BBA)/Protein Struct. Mol.*, vol. 742, no. 2, pp. 278–284, Jan. 1983, doi: 10.1016/0167-4838(83)90312-6.

[294] D. L. Nandi, P. M. Horowitz, and J. Westley, “Rhodanese as a thioredoxin oxidase,” *Int. J. Biochem. Cell Biol.*, vol. 32, no. 4, pp. 465–473, Apr. 2000, doi: 10.1016/S1357-2725(99)00035-7.

[295] A. Smirnov, N. Entelis, R. P. Martin, and I. Tarassov, “Biological significance of 5s rRNA import into human mitochondria: Role of ribosomal protein MRP-L18,” *Genes Dev.*, vol. 25, no. 12, pp. 1289–1305, 2011, doi: 10.1101/gad.624711.

[296] R. N. Carter *et al.*, “The hepatic compensatory response to elevated systemic sulfide 2 impairs medium chain fat oxidation and promotes

diabetes Competing interests statement," Cold Spring Harbor Laboratory, Apr. 2020. doi: 10.1101/2020.04.27.064287.

[297] S. V. Hoffmann Edmond de, "Mass Spectrometry: principles and applications, 3rd Edition - Edmond de Hoffmann, Vincent Stroobant." pp. 1–4, 2007.

[298] International Council for Harmonisation of Technical Requirements for Pharmaceuticals for Human Use, "IHT Guideline: Validation of analytical procedures: text and methodology," Geneva, 2008. [Online]. Available: http://www.ihc.org.

[299] W. Zhou, S. Yang, and P. G. Wang, "Matrix effects and application of matrix effect factor," *https://doi.org/10.4155/bio-2017-0214*, vol. 9, no. 23, pp. 1839–1844, Nov. 2017, doi: 10.4155/BIO-2017-0214.

[300] M. Caban, N. Migowska, P. Stepnowski, M. Kwiatkowski, and J. Kumirska, "Matrix effects and recovery calculations in analyses of pharmaceuticals based on the determination of β-blockers and β-agonists in environmental samples," *J. Chromatogr. A*, vol. 1258, pp. 117–127, Oct. 2012, doi: 10.1016/J.CHROMA.2012.08.029.

[301] T. M. Annesley, "Ion Suppression in Mass Spectrometry," *Clin. Chem.*, vol. 49, no. 7, pp. 1041–1044, Jul. 2003, doi: 10.1373/49.7.1041.

[302] T. M. Maia *et al.*, "Simple Peptide Quantification Approach for MS-Based Proteomics Quality Control," *ACS Omega*, vol. 5, no. 12, pp. 6754–6762, Mar. 2020, doi: 10.1021/acsomega.0c00080.

[303] P. Feist and A. B. Hummon, "Proteomic challenges: Sample preparation techniques for Microgram-Quantity protein analysis from biological samples," *International Journal of Molecular Sciences*, vol. 16, no. 2. Int J Mol Sci, pp. 3537–3563, Feb. 05, 2015, doi: 10.3390/ijms16023537.

[304] B. Alberts, A. Johnson, J. Lewis, M. Raff, K. Roberts, and P. Walter, *Molecular Biology of the Cell*, 4th ed. New York: Garland Science, 2002.

[305] O. A. Ismaiel, M. S. Halquist, M. Y. Elmamly, A. Shalaby, and H. T. Karnes, “Monitoring phospholipids for assessment of matrix effects in a liquid chromatography-tandem mass spectrometry method for hydrocodone and pseudoephedrine in human plasma,” *J. Chromatogr. B Anal. Technol. Biomed. Life Sci.*, vol. 859, no. 1, pp. 84–93, Nov. 2007, doi: 10.1016/j.jchromb.2007.09.007.

[306] N. D, H. R, and G. S, “Efficacy of plasma phospholipid removal during sample preparation and subsequent retention under typical UHPLC conditions,” *Bioanalysis*, vol. 4, no. 7, pp. 795–807, Apr. 2012, doi: 10.4155/BIO.12.38.

[307] R. Miyamoto, K. Otsuguro, S. Yamaguchi, and S. Ito, “Contribution of cysteine aminotransferase and mercaptopyruvate sulfurtransferase to hydrogen sulfide production in peripheral neurons,” *J. Neurochem.*, vol. 130, no. 1, pp. 29–40, Jul. 2014, doi: 10.1111/JNC.12698.

[308] R. Ma, A. S. Martínez-Ramírez, T. L. Borders, F. Gao, and B. Sosa-Pineda, “Metabolic and non-metabolic liver zonation is established non-synchronously and requires sinusoidal Wnts,” *Elife*, vol. 9, Mar. 2020, doi: 10.7554/ELIFE.46206.

[309] R. Manco and S. Itzkovitz, “Liver zonation,” *Journal of Hepatology*, vol. 74, no. 2. Elsevier, pp. 466–468, Feb. 01, 2021, doi: 10.1016/j.jhep.2020.09.003.

[310] J. Tillner *et al.*, “Faster, More Reproducible DESI-MS for Biological Tissue Imaging,” *J. Am. Soc. Mass Spectrom.*, vol. 28, no. 10, p. 2090, Oct. 2017, doi: 10.1007/S13361-017-1714-Z.

[311] J. A. Barry, M. R. Groseclose, and S. Castellino, “Quantification and assessment of detection capability in imaging mass spectrometry using a revised mimetic tissue model,” *Bioanalysis*, vol. 11, no. 11, pp. 1099–1116, Jun. 2019, doi: 10.4155/bio-2019-0035.

[312] R. N. Carter *et al.*, “The hepatic compensatory response to elevated

systemic sulfide promotes diabetes," *Cell Rep.*, vol. 37, no. 6, p. 109958, Nov. 2021, doi: 10.1016/J.CELREP.2021.109958.

[313] S. L. Ding and C. Y. Shen, "Model of human aging: Recent findings on Werner's and Hutchinson-Gilford progeria syndromes," *Clinical Interventions in Aging*, vol. 3, no. 3. Dove Press, pp. 431–444, 2008, doi: 10.2147/cia.s1957.

[314] L. Harkema, S. A. Youssef, and A. de Bruin, "Pathology of Mouse Models of Accelerated Aging," *Vet. Pathol.*, vol. 53, no. 2, pp. 366–389, Feb. 2016, doi: 10.1177/0300985815625169.

[315] J. A. Brassard, N. Fekete, A. Garnier, and C. A. Hoesli, "Hutchinson-Gilford progeria syndrome as a model for vascular aging," *Biogerontology*, vol. 17, no. 1. Springer, pp. 129–145, Sep. 01, 2016, doi: 10.1007/s10522-015-9602-z.

[316] H. Li *et al.*, "Mouse models in modeling aging and cancer," *Experimental Gerontology*, vol. 120. Exp Gerontol, pp. 88–94, Jun. 01, 2019, doi: 10.1016/j.exger.2019.03.002.

[317] F. A. Questions and F. L. B. Gordon, "The Progeria Research Foundation," pp. 1–6, 2006, Accessed: Oct. 07, 2021. [Online]. Available: https://www.progeriaresearch.org/.

[318] S. Gonzalo, R. Kreienkamp, and P. Askjaer, "Hutchinson-Gilford Progeria Syndrome: A premature aging disease caused by LMNA gene mutations," *Ageing Research Reviews*, vol. 33. Elsevier Ireland Ltd, pp. 18–29, Jan. 01, 2017, doi: 10.1016/j.arr.2016.06.007.

[319] A. Casasola *et al.*, "Prelamin A processing, accumulation and distribution in normal cells and laminopathy disorders," *Nucleus*, vol. 7, no. 1, pp. 84–102, Mar. 2016, doi: 10.1080/19491034.2016.1150397.

[320] S. Graziano, R. Kreienkamp, N. Coll-Bonfill, and S. Gonzalo, "Causes and consequences of genomic instability in laminopathies: Replication stress

and interferon response," *Nucleus*, vol. 9, no. 1. Taylor and Francis Inc., pp. 289–306, Jan. 01, 2018, doi: 10.1080/19491034.2018.1454168.

[321] B. S. J. Davies, L. G. Fong, S. H. Yang, C. Coffinier, and S. G. Young, "The posttranslational processing of prelamin A and disease," *Annual Review of Genomics and Human Genetics*, vol. 10. Annu Rev Genomics Hum Genet, pp. 153–174, Sep. 2009, doi: 10.1146/annurev-genom-082908-150150.

[322] P. Scaffidi and T. Misteli, "Lamin A-dependent nuclear defects in human aging," *Science (80-.).*, vol. 312, no. 5776, pp. 1059–1063, May 2006, doi: 10.1126/science.1127168.

[323] S. mi Kang *et al.*, "Progerinin, an optimized progerin-lamin A binding inhibitor, ameliorates premature senescence phenotypes of Hutchinson-Gilford progeria syndrome," *Commun. Biol.*, vol. 4, no. 1, pp. 1–11, Jan. 2021, doi: 10.1038/s42003-020-01540-w.

[324] D. Carrero, C. Soria-Valles, and C. López-Otín, "Hallmarks of progeroid syndromes: lessons from mice and reprogrammed cells," *Dis. Model. Mech.*, vol. 9, no. 7, pp. 719–735, Jul. 2016, doi: 10.1242/dmm.024711.

[325] R. Kreienkamp and S. Gonzalo, "Metabolic Dysfunction in Hutchinson-Gilford Progeria Syndrome," *Cells*, vol. 9, no. 2. Multidisciplinary Digital Publishing Institute (MDPI), Feb. 08, 2020, doi: 10.3390/cells9020395.

[326] J. Rivera-Torres *et al.*, "Identification of mitochondrial dysfunction in Hutchinson-Gilford progeria syndrome through use of stable isotope labeling with amino acids in cell culture," *J. Proteomics*, vol. 91, pp. 466–477, Oct. 2013, doi: 10.1016/j.jprot.2013.08.008.

[327] H. T. Kang *et al.*, "Chemical screening identifies ROCK as a target for recovering mitochondrial function in Hutchinson-Gilford progeria syndrome," *Aging Cell*, vol. 16, no. 3, pp. 541–550, Jun. 2017, doi: 10.1111/acel.12584.

[328] Z. M. Xiong *et al.*, "Methylene blue alleviates nuclear and mitochondrial

abnormalities in progeria," *Aging Cell*, vol. 15, no. 2, pp. 279–290, Apr. 2016, doi: 10.1111/acel.12434.

[329] J. Mateos *et al.*, "iTRAQ-based analysis of progerin expression reveals mitochondrial dysfunction, reactive oxygen species accumulation and altered proteostasis," *Stem Cell Res. Ther.*, vol. 6, no. 1, Jun. 2015, doi: 10.1186/s13287-015-0110-5.

[330] T. Sieprath *et al.*, "Sustained accumulation of prelamin A and depletion of lamin A/C both cause oxidative stress and mitochondrial dysfunction but induce different cell fates," *Nucleus*, vol. 6, no. 3, pp. 236–246, Jan. 2015, doi: 10.1080/19491034.2015.1050568.

[331] S. van der Rijt, M. Molenaars, R. L. McIntyre, G. E. Janssens, and R. H. Houtkooper, "Integrating the Hallmarks of Aging Throughout the Tree of Life: A Focus on Mitochondrial Dysfunction," *Frontiers in Cell and Developmental Biology*, vol. 8. Front Cell Dev Biol, Nov. 26, 2020, doi: 10.3389/fcell.2020.594416.

[332] N. Kubben and T. Misteli, "Shared molecular and cellular mechanisms of premature ageing and ageing-associated diseases," *Nat. Rev. Mol. Cell Biol.*, vol. 18, no. 10, pp. 595–609, 2017, doi: 10.1038/nrm.2017.68.

[333] X. Xu *et al.*, "Progerin accumulation in nucleus pulposus cells impairs mitochondrial function and induces intervertebral disc degeneration and therapeutic effects of sulforaphane," *Theranostics*, vol. 9, no. 8, pp. 2252–2267, 2019, doi: 10.7150/thno.30658.

[334] R. C. M. Hennekam, "Hutchinson-Gilford progeria syndrome: Review of the phenotype," in *American Journal of Medical Genetics, Part A*, Dec. 2006, vol. 140, no. 23, pp. 2603–2624, doi: 10.1002/ajmg.a.31346.

[335] G. Lo Sasso, W. K. Schlage, S. Boué, E. Veljkovic, M. C. Peitsch, and J. Hoeng, "The Apoe-/- mouse model: A suitable model to study cardiovascular and respiratory diseases in the context of cigarette smoke exposure and harm reduction," *J. Transl. Med.*, vol. 14, no. 1, p. 146, May

2016, doi: 10.1186/s12967-016-0901-1.

[336] M. R. Hamczyk *et al.*, “Vascular smooth muscle–specific progerin expression accelerates atherosclerosis and death in a mouse model of Hutchinson-Gilford progeria syndrome,” *Circulation*, vol. 138, no. 3, pp. 266–282, 2018, doi: 10.1161/CIRCULATIONAHA.117.030856.

[337] C. Bárcena *et al.*, “Methionine Restriction Extends Lifespan in Progeroid Mice and Alters Lipid and Bile Acid Metabolism,” *Cell Rep.*, vol. 24, no. 9, pp. 2392–2403, Aug. 2018, doi: 10.1016/j.celrep.2018.07.089.

[338] Progeria Research Foundation, “Nutrition: Increasing calories Healthy, high calorie snacks Making healthy food choices Shakes & smoothies,” *Progeria Research Foundation*. https://www.progeriaresearch.org/assets/files/pdf/info_sheets/6_Nutrition_0410.pdf (accessed Jun. 30, 2021).

[339] M. T. Peh *et al.*, “Effect of feeding a high fat diet on hydrogen sulfide (H2S) metabolism in the mouse,” *Nitric Oxide*, vol. 41, pp. 138–145, Sep. 2014, doi: 10.1016/j.niox.2014.03.002.

[340] D. Wu *et al.*, “Hydrogen sulfide mitigates kidney injury in high fat diet-induced obese mice,” *Oxid. Med. Cell. Longev.*, vol. 2016, 2016, doi: 10.1155/2016/2715718.

[341] R. Kreienkamp and S. Gonzalo, “Hutchinson-Gilford progeria syndrome: Challenges at bench and bedside,” in *Subcellular Biochemistry*, vol. 91, Springer New York, 2019, pp. 435–451.

[342] Y. Pei, B. Wu, Q. Cao, L. Wu, and G. Yang, “Hydrogen sulfide mediates the anti-survival effect of sulforaphane on human prostate cancer cells,” *Toxicol. Appl. Pharmacol.*, vol. 257, no. 3, pp. 420–428, Dec. 2011, doi: 10.1016/j.taap.2011.09.026.

[343] D. Gabriel, D. Roedl, L. B. Gordon, and K. Djabali, “Sulforaphane enhances progerin clearance in Hutchinson-Gilford progeria fibroblasts,” *Aging Cell*,

vol. 14, no. 1, pp. 78–91, Feb. 2015, doi: 10.1111/acel.12300.

[344] S. Sestito *et al.*, “Design and synthesis of H2S-donor hybrids: A new treatment for Alzheimer’s disease?,” *Eur. J. Med. Chem.*, vol. 184, Dec. 2019, doi: 10.1016/j.ejmech.2019.111745.

[345] L. Müller *et al.*, “Effect of Broccoli Sprouts and Live Attenuated Influenza Virus on Peripheral Blood Natural Killer Cells: A Randomized, Double-Blind Study,” *PLoS One*, vol. 11, no. 1, p. e0147742, Jan. 2016, doi: 10.1371/journal.pone.0147742.

[346] F. Hong, M. L. Freeman, and D. C. Liebler, “Identification of sensor cysteines in human Keap1 modified by the cancer chemopreventive agent sulforaphane,” *Chem. Res. Toxicol.*, vol. 18, no. 12, pp. 1917–1926, Dec. 2005, doi: 10.1021/tx0502138.

[347] Z. Qi *et al.*, “Sulforaphane promotes C. elegans longevity and healthspan via DAF-16/DAF-2 insulin/IGF-1 signaling,” *Aging (Albany. NY).*, vol. 13, no. 2, pp. 1649–1670, Jan. 2021, doi: 10.18632/aging.202512.

[348] M. Petkovic *et al.*, “Dietary supplementation with sulforaphane ameliorates skin aging through activation of the Keap1-Nrf2 pathway,” *J. Nutr. Biochem.*, vol. 98, Dec. 2021, doi: 10.1016/j.jnutbio.2021.108817.

[349] X. Huang, Y. Gao, J. Qin, and S. Lu, “The role of miR-34a in the hepatoprotective effect of hydrogen sulfide on ischemia/reperfusion injury in young and old rats,” *PLoS One*, vol. 9, no. 11, p. e113305, Nov. 2014, doi: 10.1371/journal.pone.0113305.

[350] R. Kreienkamp *et al.*, “Vitamin D receptor signaling improves Hutchinson-Gilford progeria syndrome cellular phenotypes,” *Oncotarget*, vol. 7, no. 21, pp. 30018–30031, May 2016, doi: 10.18632/oncotarget.9065.

[351] B. Wiliński, J. Wiliński, E. Somogyi, J. Piotrowska, and W. Opoka, “Vitamin D3 (cholecalciferol) boosts hydrogen sulfide tissue concentrations in heart and other mouse organs,” *Folia Biol. (Czech Republic)*, vol. 60, no. 3–4,

pp. 243–247, 2012, doi: 10.3409/fb60_3-4.243-247.

[352] S. K. Jain *et al.*, “In African American Type 2 diabetic patients, is vitamin d deficiency associated with lower blood levels of hydrogen sulfide and cyclic adenosine monophosphate, and elevated oxidative stress?,” *Antioxidants and Redox Signaling*, vol. 18, no. 10. pp. 1154–1158, Apr. 01, 2013, doi: 10.1089/ars.2012.4843.

[353] A. Zaghini *et al.*, “Long term breeding of the Lmna G609G progeric mouse: Characterization of homozygous and heterozygous models,” *Exp. Gerontol.*, vol. 130, p. 110784, Feb. 2020, doi: 10.1016/j.exger.2019.110784.

[354] M. T. Peh, A. B. Anwar, D. S. Ng, M. S. Atan, S. D. Kumar, and P. K. Moore, “Effect of feeding a high fat diet on hydrogen sulfide (H2S) metabolism in the mouse,” *Nitric Oxide*, vol. 41, pp. 138–145, 2014.

[355] B. Geng *et al.*, “Endogenous hydrogen sulfide regulation of myocardial injury induced by isoproterenol,” *Biochem. Biophys. Res. Commun.*, vol. 318, no. 3, pp. 756–763, Jun. 2004, doi: 10.1016/j.bbrc.2004.04.094.

[356] M. Wang, Z. Guo, and S. Wang, “Cystathionine gamma-lyase expression is regulated by exogenous hydrogen peroxide in the mammalian cells,” *Gene Expr.*, vol. 15, no. 5–6, pp. 235–241, 2013, doi: 10.3727/105221613X13571653093286.

[357] Z. Liu, X. Wang, L. Li, G. Wei, and M. Zhao, “Hydrogen Sulfide Protects against Paraquat-Induced Acute Liver Injury in Rats by Regulating Oxidative Stress, Mitochondrial Function, and Inflammation,” *Oxid. Med. Cell. Longev.*, vol. 2020, 2020, doi: 10.1155/2020/6325378.

[358] R. Villa-Bellosta, “Dietary magnesium supplementation improves lifespan in a mouse model of progeria,” *EMBO Mol. Med.*, vol. 12, no. 10, Oct. 2020, doi: 10.15252/emmm.202012423.

[359] M. Ristow and K. Schmeisser, “Mitohormesis: Promoting health and

lifespan by increased levels of reactive oxygen species (ROS)," *Dose-Response*, vol. 12, no. 2, pp. 288–341, 2014, doi: 10.2203/dose-response.13-035.Ristow.

[360] B. Li *et al.*, "Downregulation of the Werner syndrome protein induces a metabolic shift that compromises redox homeostasis and limits proliferation of cancer cells," *Aging Cell*, vol. 13, no. 2, pp. 367–378, Apr. 2014, doi: 10.1111/acel.12181.

[361] M. Seco-Cervera *et al.*, "Oxidative stress and antioxidant response in fibroblasts from Werner and Atypical Werner Syndromes," *Aging (Albany. NY).*, vol. 6, no. 3, pp. 231–245, 2014, doi: 10.18632/aging.100649.

[362] L. Bai *et al.*, "Angiotensin II downregulates vascular endothelial cell hydrogen sulfide production by enhancing cystathionine γ-lyase degradation through ROS-activated ubiquitination pathway," *Biochem. Biophys. Res. Commun.*, vol. 514, no. 3, pp. 907–912, Jun. 2019, doi: 10.1016/j.bbrc.2019.05.021.

[363] M. Togo *et al.*, "Effects of a high-fat diet on superoxide anion generation and membrane fluidity in liver mitochondria in rats," *J. Int. Soc. Sports Nutr.*, vol. 15, no. 1, pp. 1–8, Mar. 2018, doi: 10.1186/s12970-018-0217-z.

[364] V. T. Samuel *et al.*, "Mechanism of hepatic insulin resistance in non-alcoholic fatty liver disease," *J. Biol. Chem.*, vol. 279, no. 31, pp. 32345–32353, Jul. 2004, doi: 10.1074/jbc.M313478200.

[365] A. Görlach *et al.*, "Reactive oxygen species, nutrition, hypoxia and diseases: Problems solved?," *Redox Biology*, vol. 6. Elsevier, pp. 372–385, Dec. 01, 2015, doi: 10.1016/j.redox.2015.08.016.

[366] B. Qabazard and S. R. Stürzenbaum, "H2S: A new approach to lifespan enhancement and healthy ageing?," *Handb. Exp. Pharmacol.*, vol. 230, pp. 269–287, 2015, doi: 10.1007/978-3-319-18144-8_14.

[367] S. Srivastava, "The mitochondrial basis of aging and age-related

disorders," *Genes*, vol. 8, no. 12. MDPI AG, Dec. 19, 2017, doi: 10.3390/genes8120398.

[368] Y. Yuan *et al.*, "S-Sulfhydration of SIRT3 by Hydrogen Sulfide Attenuates Mitochondrial Dysfunction in Cisplatin-Induced Acute Kidney Injury," *Antioxidants Redox Signal.*, vol. 31, no. 17, pp. 1302–1319, Oct. 2019, doi: 10.1089/ars.2019.7728.

[369] K. Módis *et al.*, "S-Sulfhydration of ATP synthase by hydrogen sulfide stimulates mitochondrial bioenergetics," *Pharmacol. Res.*, vol. 113, no. Pt A, pp. 116–124, Nov. 2016, doi: 10.1016/j.phrs.2016.08.023.

[370] J. Y. Lee *et al.*, "GATA4-dependent regulation of the secretory phenotype via MCP-1 underlies lamin A-mediated human mesenchymal stem cell aging," *Exp. Mol. Med.*, vol. 50, no. 5, pp. 1–12, May 2018, doi: 10.1038/s12276-018-0092-3.

[371] J. Bełtowski, "Hydrogen sulfide in pharmacology and medicine - An update," *Pharmacol. Reports*, vol. 67, no. 3, pp. 647–658, 2015, doi: 10.1016/j.pharep.2015.01.005.

[372] C. Cantó and P. M. Garcia-Roves, "High-Resolution Respirometry for Mitochondrial Characterization of Ex Vivo Mouse Tissues," *Curr. Protoc. Mouse Biol.*, vol. 5, no. 2, pp. 135–153, 2015, doi: 10.1002/9780470942390.mo140061.

[373] J. Acker, C. Conesa, and O. Lefebvre, "Yeast RNA polymerase III transcription factors and effectors," *Biochim. Biophys. Acta - Gene Regul. Mech.*, vol. 1829, no. 3–4, pp. 283–295, Mar. 2013, doi: 10.1016/J.BBAGRM.2012.10.002.

[374] T. W. Turowski and D. Tollervey, "Transcription by RNA polymerase III: insights into mechanism and regulation," *Biochem. Soc. Trans.*, vol. 44, no. 5, pp. 1367–1375, Oct. 2016, doi: 10.1042/BST20160062.

[375] C. Kutter *et al.*, "Pol III binding in six mammals shows conservation among

amino acid isotypes despite divergence among tRNA genes," *Nat. Genet.*, vol. 43, no. 10, pp. 948–957, Oct. 2011, doi: 10.1038/ng.906.

[376] I. M. Willis and R. D. Moir, "Signaling to and from the RNA Polymerase III Transcription and Processing Machinery," *Annu. Rev. Biochem.*, vol. 87, no. 1, pp. 75–100, Jun. 2018, doi: 10.1146/annurev-biochem-062917-012624.

[377] R. J. White, "Transcription by RNA polymerase III: More complex than we thought," *Nat. Rev. Genet.*, vol. 12, no. 7, pp. 459–463, Jun. 2011, doi: 10.1038/nrg3001.

[378] R. Upadhya, J. H. Lee, and I. M. Willis, "Maf1 Is an Essential Mediator of Diverse Signals that Repress RNA Polymerase III Transcription," *Mol. Cell*, vol. 10, no. 6, pp. 1489–1494, Dec. 2002, doi: 10.1016/S1097-2765(02)00787-6.

[379] M. K. Vorländer *et al.*, "Structural basis for RNA polymerase III transcription repression by Maf1," *Nat. Struct. Mol. Biol. 2020 273*, vol. 27, no. 3, pp. 229–232, Feb. 2020, doi: 10.1038/s41594-020-0383-y.

[380] L. Marshall, E. J. Rideout, and S. S. Grewal, "Nutrient/TOR-dependent regulation of RNA polymerase III controls tissue and organismal growth in Drosophila," *EMBO J.*, vol. 31, no. 8, p. 1916, Apr. 2012, doi: 10.1038/EMBOJ.2012.33.

[381] A. A. Michels *et al.*, "mTORC1 Directly Phosphorylates and Regulates Human MAF1," *Mol. Cell. Biol.*, vol. 30, no. 15, p. 3749, Aug. 2010, doi: 10.1128/MCB.00319-10.

[382] A. Orioli, V. Praz, P. Lhôte, and N. Hernandez, "Human MAF1 targets and represses active RNA polymerase III genes by preventing recruitment rather than inducing long-term transcriptional arrest," *Genome Res.*, vol. 26, no. 5, pp. 624–634, May 2016, doi: 10.1101/gr.201400.115.

[383] A. Vannini, R. Ringel, A. G. Kusser, O. Berninghausen, G. A. Kassavetis,

and P. Cramer, “Molecular basis of RNA polymerase III transcription repression by Maf1,” *Cell*, vol. 143, no. 1, pp. 59–70, Oct. 2010, doi: 10.1016/j.cell.2010.09.002.

[384] Y. L. Lee, Y. C. Li, C. H. Su, C. H. Chiao, I. H. Lin, and M. T. Hsu, “MAF1 represses CDKN1A through a Pol III-dependent mechanism,” *Elife*, vol. 4, no. JUNE, Jun. 2015, doi: 10.7554/eLife.06283.

[385] J. Rollins, I. Veras, S. Cabarcas, I. Willis, and L. Schramm, “Human Maf1 negatively regulates RNA polymerase III transcription via the TFIIB family members Brf1 and Brf2,” *Int. J. Biol. Sci.*, vol. 3, no. 5, pp. 292–302, May 2007, doi: 10.7150/ijbs.3.292.

[386] A. G. Arimbasseri and R. J. Maraia, “RNA Polymerase III Advances: Structural and tRNA Functional Views,” *Trends in Biochemical Sciences*, vol. 41, no. 6. Elsevier Ltd, pp. 546–559, Jun. 01, 2016, doi: 10.1016/j.tibs.2016.03.003.

[387] K. Pluta *et al.*, “Maf1p, a Negative Effector of RNA Polymerase III in Saccharomyces cerevisiae,” *Mol. Cell. Biol.*, vol. 21, no. 15, pp. 5031–5040, Aug. 2001, doi: 10.1128/mcb.21.15.5031-5040.2001.

[388] I. Grummt, “The nucleolus - Guardian of cellular homeostasis and genome integrity,” *Chromosoma*, vol. 122, no. 6. Springer, pp. 487–497, Dec. 11, 2013, doi: 10.1007/s00412-013-0430-0.

[389] T. W. Turowski *et al.*, “Global analysis of transcriptionally engaged yeast RNA polymerase III reveals extended tRNA transcripts,” 2016, doi: 10.1101/gr.205492.116.

[390] T. W. Turowski and D. Tollervey, “Transcription by RNA polymerase III: Insights into mechanism and regulation,” *Biochem. Soc. Trans.*, vol. 44, no. 5, pp. 1367–1375, Oct. 2016, doi: 10.1042/BST20160062.

[391] Y. Kulaberoglu, Y. Malik, G. Borland, C. Selman, N. Alic, and J. M. A. Tullet, “RNA Polymerase III, Ageing and Longevity,” *Frontiers in Genetics*,

vol. 12. Frontiers, p. 1198, Jul. 06, 2021, doi: 10.3389/fgene.2021.705122.

[392] M. R, C.-B. D, R. FJ, S. LS, and K. M, “Regulation of mRNA translation as a conserved mechanism of longevity control,” *Adv. Exp. Med. Biol.*, vol. 694, pp. 14–29, 2010, doi: 10.1007/978-1-4419-7002-2_2.

[393] W. L, K. J, and J. H, “Promoting longevity by maintaining metabolic and proliferative homeostasis,” *J. Exp. Biol.*, vol. 217, no. Pt 1, pp. 109–118, 2014, doi: 10.1242/JEB.089920.

[394] P. D *et al.*, “mTOR as a central regulator of lifespan and aging,” *F1000Research*, vol. 8, 2019, doi: 10.12688/F1000RESEARCH.17196.1.

[395] D. S. Evans, P. Kapahi, W.-C. Hsueh, and L. Kockel, “TOR signaling never gets old: Aging, longevity and TORC1 activity,” *Ageing Res. Rev.*, vol. 10, no. 2, p. 225, Apr. 2011, doi: 10.1016/J.ARR.2010.04.001.

[396] J. J. Wu *et al.*, “Increased Mammalian Lifespan and a Segmental and Tissue-Specific Slowing of Aging after Genetic Reduction of mTOR Expression,” *Cell Rep.*, vol. 4, no. 5, pp. 913–920, Sep. 2013, doi: 10.1016/j.celrep.2013.07.030.

[397] S. C. Johnson, P. S. Rabinovitch, and M. Kaeberlein, “MTOR is a key modulator of ageing and age-related disease,” *Nature*, vol. 493, no. 7432. NIH Public Access, pp. 338–345, Jan. 17, 2013, doi: 10.1038/nature11861.

[398] D. E. Harrison *et al.*, “Rapamycin fed late in life extends lifespan in genetically heterogeneous mice,” *Nature*, vol. 460, no. 7253, pp. 392–395, Jul. 2009, doi: 10.1038/nature08221.

[399] M. Wei *et al.*, “Life span extension by calorie restriction depends on Rim15 and transcription factors downstream of Ras/PKA, Tor, and Sch9,” *PLoS Genet.*, vol. 4, no. 1, pp. 0139–0149, Jan. 2008, doi: 10.1371/journal.pgen.0040013.

[400] C. W. Cheng *et al.*, “Prolonged fasting reduces IGF-1/PKA to promote

hematopoietic-stem-cell- based regeneration and reverse immunosuppression," *Cell Stem Cell*, vol. 14, no. 6, pp. 810–823, Jun. 2014, doi: 10.1016/j.stem.2014.04.014.

[401] R. Tulsian, N. Velingkaar, and R. Kondratov, "Caloric restriction effects on liver mTOR signaling are time-of-day dependent," *Aging (Albany NY)*, vol. 10, no. 7, p. 1640, Jul. 2018, doi: 10.18632/AGING.101498.

[402] D. Papadopoli *et al.*, "mTOR as a central regulator of lifespan and aging," *F1000Research*, vol. 8, 2019, doi: 10.12688/F1000RESEARCH.17196.1.

[403] D. Shahbazian *et al.*, "The mTOR/PI3K and MAPK pathways converge on eIF4B to control its phosphorylation and activity," *EMBO J.*, vol. 25, no. 12, pp. 2781–2791, Jun. 2006, doi: 10.1038/sj.emboj.7601166.

[404] C. T. Warnick and H. M. Lazarus, "Effect of a Protein-Free Diet and Fasting on RNA Polymerase Activity in Mice," *J. Nutr.*, vol. 112, no. 2, pp. 293–298, Feb. 1982, doi: 10.1093/JN/112.2.293.

[405] D. Filer *et al.*, "RNA polymerase III limits longevity downstream of TORC1," *Nature*, vol. 552, no. 7684, pp. 263–267, Dec. 2017, doi: 10.1038/nature25007.

[406] N. Bonhoure *et al.*, "Loss of the RNA polymerase III repressor MAF1 confers obesity resistance," *Genes Dev.*, vol. 29, no. 9, pp. 934–947, May 2015, doi: 10.1101/gad.258350.115.

[407] I. M. Willis, R. D. Moir, and N. Hernandez, "Metabolic programming a lean phenotype by deregulation of RNA polymerase III," *Proc. Natl. Acad. Sci. U. S. A.*, vol. 115, no. 48, pp. 12182–12187, Nov. 2018, doi: 10.1073/pnas.1815590115.

[408] Y. Cai and Y. H. Wei, "Distinct regulation of Maf1 for lifespan extension by Protein kinase A and Sch9," *Aging (Albany. NY).*, vol. 7, no. 2, pp. 133–143, 2015, doi: 10.18632/aging.100727.

[409] Y. Cai and Y. H. Wei, “Stress resistance and lifespan are increased in C. elegans but decreased in S. cerevisiae by mafr-1/maf1 deletion,” *Oncotarget*, vol. 7, no. 10, pp. 10812–10826, 2016, doi: 10.18632/oncotarget.7769.

[410] A. Csiszar *et al.*, “Caloric restriction confers persistent anti-oxidative, pro-angiogenic, and anti-inflammatory effects and promotes anti-aging miRNA expression profile in cerebromicrovascular endothelial cells of aged rats,” *https://doi.org/10.1152/ajpheart.00307.2014*, vol. 307, no. 3, pp. 292–306, 2014, doi: 10.1152/AJPHEART.00307.2014.

[411] B. F. Miller *et al.*, “Calorie Restriction Does Not Increase Short-term or Long-term Protein Synthesis,” *Journals Gerontol. Ser. A Biol. Sci. Med. Sci.*, vol. 68, no. 5, p. 530, May 2013, doi: 10.1093/GERONA/GLS219.

[412] B.-S. MC, R. MS, S. J, H. JP, and R. A, “Effect of dietary restriction on liver protein synthesis in rats,” *J. Nutr.*, vol. 115, no. 7, pp. 944–950, 1985, doi: 10.1093/JN/115.7.944.

[413] W. E. Sonntag, J. E. Lenham, and R. L. Ingram, “Effects of Aging and Dietary Restriction on Tissue Protein Synthesis: Relationship to Plasma Insulin-like Growth Factor-1,” *J. Gerontol.*, vol. 47, no. 5, pp. B159–B163, Sep. 1992, doi: 10.1093/GERONJ/47.5.B159.

[414] J. E. Kieckhaefer *et al.*, “The RNA Polymerase III Subunit Polr3b Is Required for the Maintenance of Small Intestinal Crypts in Mice,” *Cell. Mol. Gastroenterol. Hepatol.*, vol. 2, no. 6, p. 783, Nov. 2016, doi: 10.1016/J.JCMGH.2016.08.003.

[415] D. Djordjevic *et al.*, “De novo variants in POLR3B cause ataxia, spasticity, and demyelinating neuropathy,” *Am. J. Hum. Genet.*, vol. 108, no. 1, pp. 186–193, Jan. 2021, doi: 10.1016/J.AJHG.2020.12.002.

[416] D. N. Roberts, A. J. Stewart, J. T. Huff, and B. R. Cairns, “The RNA polymerase III transcriptome revealed by genome-wide localization and activity-occupancy relationships,” *PNAS December*, vol. 9, pp. 14695–

14700, 2003, Accessed: Oct. 27, 2021. [Online]. Available: www.pnas.orgcgidoi10.1073pnas.2435566100.

[417] D. A. Kramerov and N. S. Vassetzky, “SINEs,” *Wiley Interdisciplinary Reviews: RNA*, vol. 2, no. 6. John Wiley & Sons, Ltd, pp. 772–786, Nov. 01, 2011, doi: 10.1002/wrna.91.

[418] Y. Quentin, “Emergence of master sequences in families of retroposons derived from 7sl RNA,” *Genetica*, vol. 93, no. 1–3, pp. 203–215, Feb. 1994, doi: 10.1007/BF01435252.

[419] K. A. Tatosyan, D. V. Stasenko, A. P. Koval, I. K. Gogolevskaya, and D. A. Kramerov, “TATA-Like Boxes in RNA Polymerase III Promoters: Requirements for Nucleotide Sequences,” *Int. J. Mol. Sci.*, vol. 21, no. 10, May 2020, doi: 10.3390/IJMS21103706.

[420] Y. O. Henderson *et al.*, “Late-life intermittent fasting decreases aging-related frailty and increases renal hydrogen sulfide production in a sexually dimorphic manner,” *GeroScience 2021*, pp. 1–28, Mar. 2021, doi: 10.1007/S11357-021-00330-4.

[421] N. Diette, J. Koo, S. Cabarcas-Petroski, and L. Schramm, “Gender Specific Differences in RNA Polymerase III Transcription,” *J. Carcinog. Mutagen.*, vol. 7, no. 1, 2016, doi: 10.4172/2157-2518.1000251.

[422] B. Pedre and T. P. Dick, “3-Mercaptopyruvate sulfurtransferase: an enzyme at the crossroads of sulfane sulfur trafficking,” *Biol. Chem.*, vol. 402, no. 3, pp. 223–237, Feb. 2021, doi: 10.1515/HSZ-2020-0249.

[423] Y. Bian *et al.*, “An enzyme assisted RP-RPLC approach for in-depth analysis of human liver phosphoproteome,” *J. Proteomics*, vol. 96, pp. 253–262, Jan. 2014, doi: 10.1016/J.JPROT.2013.11.014.

[424] K. Módis, A. Asimakopoulou, C. Coletta, A. Papapetropoulos, and C. Szabo, “Oxidative stress suppresses the cellular bioenergetic effect of the 3-mercaptopyruvate sulfurtransferase/hydrogen sulfide pathway,” *Biochem.*

Biophys. Res. Commun., vol. 433, no. 4, pp. 401–407, Apr. 2013, doi: 10.1016/J.BBRC.2013.02.131.

[425] N. Nagahara and A. Katayama, "Post-translational Regulation of Mercaptopyruvate Sulfurtransferase via a Low Redox Potential Cysteine-sulfenate in the Maintenance of Redox Homeostasis," *J. Biol. Chem.*, vol. 280, no. 41, pp. 34569–34576, Oct. 2005, doi: 10.1074/JBC.M505643200.

[426] M. Ziosi *et al.*, "Coenzyme Q deficiency causes impairment of the sulfide oxidation pathway," *EMBO Mol. Med.*, vol. 9, no. 1, pp. 96–111, 2017, doi: 10.15252/emmm.201606356.

[427] M. Libiad, P. K. Yadav, V. Vitvitsky, M. Martinov, and R. Banerjee, "Organization of the human mitochondrial hydrogen sulfide oxidation pathway," *J. Biol. Chem.*, vol. 289, no. 45, pp. 30901–30910, Nov. 2014, doi: 10.1074/jbc.M114.602664.

[428] Z. Z. Xie, Y. Liu, and J. S. Bian, "Hydrogen Sulfide and Cellular Redox Homeostasis," *Oxid. Med. Cell. Longev.*, vol. 2016, 2016, doi: 10.1155/2016/6043038.

[429] I. Dalle-Donne, R. Rossi, D. Giustarini, A. Milzani, and R. Colombo, "Protein carbonyl groups as biomarkers of oxidative stress," *Clin. Chim. Acta*, vol. 329, no. 1–2, pp. 23–38, Mar. 2003, doi: 10.1016/S0009-8981(03)00003-2.

[430] H. Kimura, "Physiological role of hydrogen sulfide and polysulfide in the central nervous system," *Neurochemistry International*, vol. 63, no. 5. Neurochem Int, pp. 492–497, 2013, doi: 10.1016/j.neuint.2013.09.003.

[431] M. E. Walsh, Y. Shi, and H. Van Remmen, "The effects of dietary restriction on oxidative stress in rodents," *Free Radic. Biol. Med.*, vol. 66, p. 88, Jan. 2014, doi: 10.1016/J.FREERADBIOMED.2013.05.037.

[432] H. Kimura, "Hydrogen sulfide: From brain to gut," *Antioxidants and Redox Signaling*, vol. 12, no. 9. Antioxid Redox Signal, pp. 1111–1123, May 01,

2010, doi: 10.1089/ars.2009.2919.

[433] E. Fabbri, M. Zoli, M. Gonzalez-Freire, M. E. Salive, S. A. Studenski, and L. Ferrucci, “Aging and Multimorbidity: New Tasks, Priorities, and Frontiers for Integrated Gerontological and Clinical Research,” *Journal of the American Medical Directors Association*, vol. 16, no. 8. Elsevier Inc., pp. 640–647, Aug. 01, 2015, doi: 10.1016/j.jamda.2015.03.013.

[434] C. Hine and J. R. Mitchell, “Calorie restriction and methionine restriction in control of endogenous hydrogen sulfide production by the transsulfuration pathway,” *Exp. Gerontol.*, vol. 68, pp. 26–32, Aug. 2015, doi: 10.1016/j.exger.2014.12.010.

[435] R. Arking, “Human Reproductive Costs and the Predicted Response to Dietary Restriction,” *Rejuvenation Res.*, vol. 10, no. 3, pp. 261–280, Sep. 2007, doi: 10.1089/rej.2007.0519.

[436] J. P. Moatt, S. Nakagawa, M. Lagisz, and C. A. Walling, “The effect of dietary restriction on reproduction: a meta-analytic perspective,” *BMC Evol. Biol.*, vol. 16, no. 1, pp. 1–9, Oct. 2016, doi: 10.1186/s12862-016-0768-z.

[437] L. Mulvey, “Dissection out the mechanisms to longevity through eating less,” Univeristy of Glasgoe, 2017.

[438] B. P. Lee *et al.*, “Dietary restriction in ILSXISS mice is associated with widespread changes in splicing regulatory factor expression levels,” *Exp. Gerontol.*, vol. 128, p. 110736, Dec. 2019, doi: 10.1016/j.exger.2019.110736.